DEVELOPMENT AND APPLICATIONS OF THE PALLADIUM-CATALYZED ENANTIOSELECTIVE OXIDATION OF SECONDARY ALCOHOLS

Thesis by

David Christopher Ebner

In Partial Fulfillment of the Requirements for the Degree of

Doctor of Philosophy

California Institute of Technology

Pasadena, California

2009

(Defended September 11, 2008)

To my family

ACKNOWLEDGEMENTS

First, I need to thank Professor Brian Stoltz, who has been a great advisor, mentor, and friend. His enthusiasm and passion for chemistry is contagious. At the end of our discussions, I have always had new ideas and felt more excitement and motivation for research. I appreciate that he has given me a fairly long leash to explore but has been there for guidance when research is not going as well. Brian has also created an amazing training environment within the lab, as his attention to detail and drive for excellence have prepared me for my future career.

I have also had an outstanding thesis committee: Professor Bob Grubbs, Professor John Bercaw, and Professor Peter Dervan. Professor Grubbs, the chair of my committee, has always had insightful questions, comments, and suggestions, and he has never complained when I run to him with last-minute recommendation letter requests. After taking two courses with Professor Bercaw, I was delighted to have him on my committee. His feedback on my research and proposals has been invaluable, and I have enjoyed our interactions during my time here. While Professor Dervan is the newest member of my committee, he has already provided beneficial guidance and support.

I am deeply indebted to Professor J. Thomas Ippoliti, my undergraduate research advisor. I probably would not be in organic chemistry if he had not taken a chance and allowed a freshman with no organic experience to join his labs. I have always been amazed at his ability to maintain a well-balanced life while supporting a thriving undergraduate research lab and committing so much to his courses, and I consider him a great role model and friend.

Thanks to Lynne Martinez, Dian Buchness, Laura Howe, and Anne Penney for keeping our lab and the department going with a smile. Tom Dunn and Scott Ross have kept the instruments running for me, and Rick Gerhart has been nice enough not to scold me too much when I show up with yet another stuck joint or broken flash column.

I have had the immense pleasure of working with a talented and creative group of coworkers in the Stoltz lab. First, I would like to acknowledge my baymates over the years: Professor Govindasamy Sekar, Mike Meyer, Kristin Finch, Dr. Kousuke Tani, Professor Andy Harned, TC Scotton, Dr. Xiaoqing Han, Allen Hong, and even the Symyx PPR machine. There have been many, and in some cases our time together has been brief, but I have had positive experiences with every one of them. Finally, I can leave the bay in Allen's capable hands.

I really appreciate the support of the older students in the lab, particularly when I was just a naïve first year. Dr. Doug Behenna was instrumental in getting those first few reactions going, and he was always so tolerant of me stopping by to pester him with all kinds of chemistry questions. Professor Neil Garg was also great for chemistry questions and just chatting about life in general. Dr. Raissa Trend is a good friend and was a vital resource for all things organometallic, especially when I was struggling to make palladium complexes or had to use a special technique.

My fellow classmates, Dr. Ryan McFadden and Dr. Dan Caspi, were a great pair of guys with which to learn the ropes in the Stoltz lab. We all started on the same project, and conversations with them my first year really helped get my chemistry working.

I also have to express my gratitude for my other project mates over the years. Professor Eric Ferreira is one of the most amazing, hardworking chemists I have known. He had a hand in getting most of the palladium oxidation projects going in the lab. Dr. Jeff Bagdanoff and Raissa were also instrumental in the oxidative kinetic resolution project, as many of their studies led to my successes in the lab. Dr. Shyam Krishnan was also indirectly on the alcohol oxidation project. He had many helpful chemistry suggestions and put an incredible amount of work to get the big paper on our syntheses of alkaloids out the door. Collaborating with Dr. Zoltán Novák, a postdoctoral scholar in the Stoltz lab, on the kinetic resolution / Claisen chemistry was a very rewarding experience, both personally and scientifically. Our collaborator at the University of York, Professor Peter O'Brien, has been very generous in sending along the latest diamine ligand from his group for us to test in the resolution, and I am happy that our combined efforts were ultimately very fruitful. Dr. Uttam Tambar was a great project mate for the amurensinine research. He taught me a lot about total synthesis and dealing with frustration with a project, and chatting with him my first year was really what convinced me that the Stoltz lab was the place to be.

JT Mohr has been a good friend and an excellent resource for information in topics ranging from pK_a's to rubik's cubes. He has also been a key player in both the weekly racquetball games and the group poker games, which have been a good distraction from the daily grind of chemistry. Thanks to everyone else involved with those too!

Thank you also to those who proofread portions of my thesis: Dr. Jan Streuff, Jenn Stockdill, Dr. Amanda Jones, and Pam Tadross. I especially owe Jan, who read

through all the chapters of my thesis and had some good comments. I also appreciate the efforts of those who read through my proposals and papers over the years. I don't remember too many specific names, but hopefully you know who you are! Nat Sherden and Hosea Nelson were also very willing to listen to my complaining and provide welcome distractions during long nights spent typing in the computer room, for which I am very grateful.

I look forward to Monday night burgers with Jenny Roizen, Jenn, Andre, and the rest of the BC folk every week. Thanks to Narae Park and Sandy Ma for getting together with me for a few beers at the end of the day once in awhile. Thomas Jensen was only here for 9 months, but I feel like I have known him much longer, and I have valued his friendship.

In addition to where she is mentioned above, Jenn Stockdill at least deserves her own paragraph (but I will try to keep it brief). She joined the lab not too long after I did, and she has been a fellow member of Crellin 264 and a dear friend ever since. I can always count on her for a chat about chemistry or life in general, lunch or late night ice cream runs, and even a few too many margaritas at Amigo's. She is one of the few people who consistently understands my strange sense of humor, for which I am ever grateful. Jenn also was kind enough to play her music loud over and over, so that I might learn the words. She is so thoughtful.

I am very privileged to have gotten to know Professor Jen Dionne more recently. She has been a good support for me while writing my thesis, spending many a day at Broad typing away. She has also been an outstanding host, and I have had many lunches and dinners at her apartment (sometimes she is even there too!).

John Keith has been a great friend over the years. Starting in first year when we fought our way through the organometallic problem sets together, chemistry discussions with him have always been enlightening. He was also a good gym buddy, keeping me motivated to do something athletic on occasion.

Dr. Gavin Murphy, Adam Dennis, Dr. Cristal Gama, and Tammy Campbell have all been close friends throughout my time at Caltech. I enjoyed spending many a night at Amigo's with them. Gavin and Adam were also always ready and willing to join an impromptu poker game.

Even though we are different in some ways, Erik Rodriguez and I have somehow gotten along really well. Wednesday night drinking (yes, it is exactly what it sounds like) was definitely a high point of the week for years. Erik has always been good for a trip to Amigo's too, and he epitomizes the 'work hard, play hard' mentality that I have yet to successfully emulate. There is never a dull moment when Erik is around, but he has also been a great listener when I have needed to do some venting.

Dr. Heather Murrey has also been a very close friend during my time at Caltech. She is an outstanding cook and could drink almost anyone under the table, especially if tequila was involved. She has really been the leader of the gang, getting everyone together and organizing the parties. I have also had many stimulating scientific discussions with her, as her talents in the lab are matched only by her intellectual brilliance.

Chad Vecitis was my roommate for most of my graduate career. I have played more games of Rikiki with him than I can count. From day I arrived in our apartment

first year, he has been a solid and dependable friend. I guess we Midwesterners just stick together.

None of this work would have been possible without the strong support of my mom, dad, and sister. I can't imagine a better environment in which to grow up. My parents have made so many sacrifices to get me where I am today, and I can't thank them enough for that. Apparently, I tried to show my appreciation by taking off halfway across the country, hardly ever visiting, and calling far too infrequently, but they have taken it all and loved me anyway.

There are so many other people to thank, but this has already gotten way too long, and I know you are anxious to get to the actual chemistry that these people made possible, so I will end here. Okay, one more: thanks for reading!

ABSTRACT

The development of new methods for the preparation of chiral alcohols is vital due to the presence of alcohols in natural products, pharmaceuticals, and a variety of synthetic materials, as well as their versatility as synthetic intermediates. Until recently, oxidative kinetic resolution has been a relatively underdeveloped strategy for obtaining enantioenriched alcohols.

The development of a palladium-catalyzed aerobic system for the enantioselective oxidation of secondary alcohols is described. This mild method utilizes (–)-sparteine as a chiral ligand to resolve a wide range of benzylic, allylic, and cyclopropylcarbinyl alcohols to high enantiomeric excesses with excellent selectivity. The resolution of pharmaceutical intermediates and the Claisen rearrangement of resolved allylic alcohols demonstrate the utility of the method.

Mechanistic insights have driven further catalyst development. Anionic ligand modification has provided more efficient catalysts for the resolution of a broader array of substrates. Neutral ligand studies have led to an enantioselective alcohol oxidation system with a diamine pseudo-enantiomeric to (–)-sparteine, allowing access to enantioenriched alcohols in either enantiomeric series.

This methodology has been applied to the enantioselective total synthesis of (–)-amurensinine via a selective C–H insertion, an aryne C–C insertion, and an oxidative kinetic resolution with (–)-sparteine. Use of an alternative diamine in the resolution results in a formal synthesis of (+)-amurensinine.

TABLE OF CONTENTS

LIST OF FIGURES

CHAPTER 4

APPENDIX 2

APPENDIX 3

LIST OF SCHEMES

CHAPTER 1

CHAPTER 2

CHAPTER 3

CHAPTER 4

CHAPTER 5

APPENDIX 6

LIST OF TABLES

CHAPTER 2

CHAPTER 3

CHAPTER 4

CHAPTER 5

APPENDIX 6

APPENDIX 8

LIST OF ABBREVIATIONS

$[\alpha]_D$	specific rotation at wavelength of sodium D line
Å	angstrom(s)
abs.	absolute
Ac	acetyl
app.	apparent
aq	aqueous
Ar	aryl, argon
atm	atmosphere(s)
B3LYP	Becke, three-parameter, Lee-Yang-Parr functional
BHT	2,6-di-*tert*-butyl-4-methylphenol
BINAP	2,2'-bis(diphenylphosphino)-1,1'-binaphthalene
BINOL	1,1'-bi(2-naphthol)
Bn	benzyl
Boc	*tert*-butoxycarbonyl
br.	broad
Bu	1-butyl
i-Bu	2-methyl-1-propyl
s-Bu	2-butyl
(*S*,*S*)-*t*-Bu-BOX	2,2'-isopropylidenebis[(4*S*)-4-*tert*-butyl-2-oxazoline]
c	concentration for optical rotation
calcd	calculated
CCDC	Cambridge Crystallographic Data Centre
cf.	compare
cm	centimeter(s)
COD	*cis,cis*-1,5-cyclooctadiene
comp.	complex
conc.	concentrated
conv	conversion
d	doublet
DABCO	1,4-diazabicyclo[2.2.2]octane
dba	dibenzylideneacetone
DBU	1,8-diazabicyclo[5.4.0]undec-7-ene

DCE	1,2-dichloroethane
dec.	decomposition
°	degrees
°C	degrees Celsius
DFT	density functional theory
$(DHQ)_2PHAL$	hydroquinine 1,4-phthalazinediyl diether
DIBAL-H	diisobutylaluminum hydride
(–)-DIOP	(–)-(4*R*,5*R*)-2,2-dimethyl-4,5-bis[(diphenylphosphino)-methyl]-1,3-dioxolane
DMAP	4-dimethylaminopyridine
DMF	*N,N*-dimethylformamide
DMP	Dess-Martin periodinane
DPPA	diphenylphosphoryl azide
e	electron
ee	enantiomeric excess
EI	electron impact
equiv	equivalent(s)
ES	electrospray ionization
Et	ethyl
FAB	fast atom bombardment
FID	flame ionization detector
g	gram(s)
GC	gas chromatography
h	hour(s)
$h\nu$	light
hNK-1	human neurokinin-1
HPLC	high performance liquid chromatography
HRMS	high resolution mass spectrometry
Hz	hertz
IR	infrared (spectroscopy)
J	coupling constant
k	reaction rate constant
L	L-type ligand
λ	wavelength
lit.	literature
M	molar, metal, or molecular ion

m	meter(s), multiplet
m/*z*	mass to charge ratio
Me	methyl
mg	milligram(s)
MHz	megahertz
μL	microliter(s)
μm	micrometer(s)
min	minute(s)
mL	milliliter(s)
mm	millimeter(s)
mmol	millimole(s)
mol	mole(s)
mp	melting point
Ms	methanesulfonyl
MS	molecular sieves
MTBE	*tert*-butyl methyl ether
N	normal
nbd	norbornadiene
NBS	*N*-bromosuccinimide
p-Nbz	*para*-nitrobenzoyl
nm	nanometer(s)
NMR	nuclear magnetic resonance (spectroscopy)
[O]	oxidation
p	*para*
p-ABSA	*para*-acetamidobenzenesulfonyl azide
Ph	phenyl
pH	hydrogen ion concentration
PhH	benzene
(*S*,*S*)-Ph-PYBOX	2,6-bis[(*S*)-4-*tert*-butyl-2-oxazolinyl]pyridine
Piv	pivaloyl
pK_a	acid dissociation constant
ppm	parts per million
i-Pr	2-propyl
n-Pr	*n*-propyl
psi	pounds per square inch
Py	pyridine

q	quartet
ref	reference
R_f	retention factor
s	selectivity factor
s	singlet
S_N1	nucleophilic substitution, unimolecular
S_N2	nucleophilic substitution, bimolecular
Sub	substrate
t	triplet
TBAF	tetrabutylammonium fluoride
TBS	*tert*-butyldimethylsilyl
TEMPO	2,2,6,6-tetramethylpiperidine 1-oxyl
Tf	trifluoromethanesulfonate
TFA	trifluoroacetate
THF	tetrahydrofuran
TIPS	triisopropylsilyl
TLC	thin-layer chromatography
TMS	trimethylsilyl
Ts	*para*-toluenesulfonyl
UV	ultraviolet light
Vis	visible light
w/v	weight to volume ratio
w/w	weight to weight ratio
X	halide, anionic ligand

CHAPTER 1

Introduction to Enantioselective Oxidation Chemistry

1.1 Oxidation in Biological Systems

The selective oxidation of organic molecules is vital to biological systems. All aerobic organisms utilize molecular oxygen to perform cellular respiration. These redox processes with oxygen are mediated by metalloenzymes and can be divided into two classes (Figure 1.1.1). Oxygenases catalyze the transfer of oxygen atoms to the organic substrate via an intermediate metal-oxo species (**1**). Oxygenation of the substrate results in a reduced metal species (**2**). Reoxidation by molecular oxygen, two protons, and two electrons reforms the metal-oxo and generates water as a byproduct. Oxidases, on the other hand, do not involve oxygen-atom transfer to the substrate. Instead, the metal oxidant (**3**) catalyzes a formal dehydrogenation, resulting in the loss of two electrons and two protons from the substrate and the formation of a reduced metal species (**2**). Molecular oxygen then acts as an electron acceptor, regenerating the oxidized metal species (**3**). Water or hydrogen peroxide is the byproduct of these oxidations.

Figure 1.1.1 Oxygenase and oxidase enzymes.

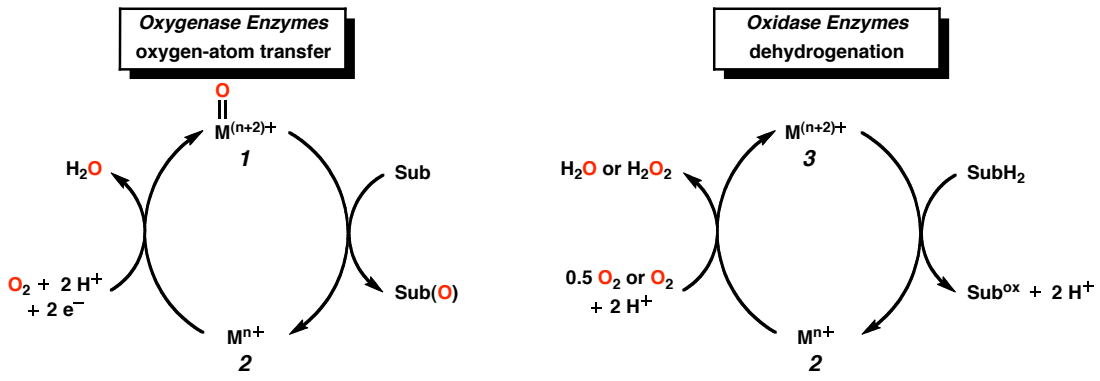

1.2 Enantioselective Oxidations in Synthetic Chemistry

1.2.1 Oxygenase-Type Reactions

Oxidation is also an essential process in synthetic chemistry. The exquisite substrate specificity and selectivity demonstrated with metalloenzymes has inspired many chemists to design synthetic catalysts to replicate nature. Recently, asymmetric oxidative processes have emerged as an important area for the construction of complex molecules.

Oxygenase-type reactions have been explored extensively, and numerous examples of catalytic asymmetric oxidations involving heteroatom transfer to the substrate have been demonstrated (Figure 1.2.1).[1] Sharpless and Katsuki developed one of the first widely applicable processes, utilizing readily available reagents to selectively epoxidize allylic alcohols with *tert*-butyl hydroperoxide as the stoichiometric oxygen atom donor (**4**→**5**).[2] Later, Sharpless was able to achieve the asymmetric dihydroxylation of olefins with an osmium catalyst and potassium ferricyanide as the terminal oxidant (**6**→**7**).[3] Jacobsen also reported an enantioselective epoxidation of olefins with manganese catalyst **9** and bleach as the oxidant (**8**→**10**).[4] Evans has shown that a copper(I) complex with bisoxazoline (*S*,*S*)-**12** catalyzes the aziridination of olefins with *N*-tosyliminobenzyliodinane (**11**→**13**).[5] Each of these oxidative systems involves heteroatom transfer to the organic substrate, though none utilize molecular oxygen as the terminal oxidant as in oxygenase enzymes.

Figure 1.2.1 Synthetic asymmetric oxygenase-type chemistry.

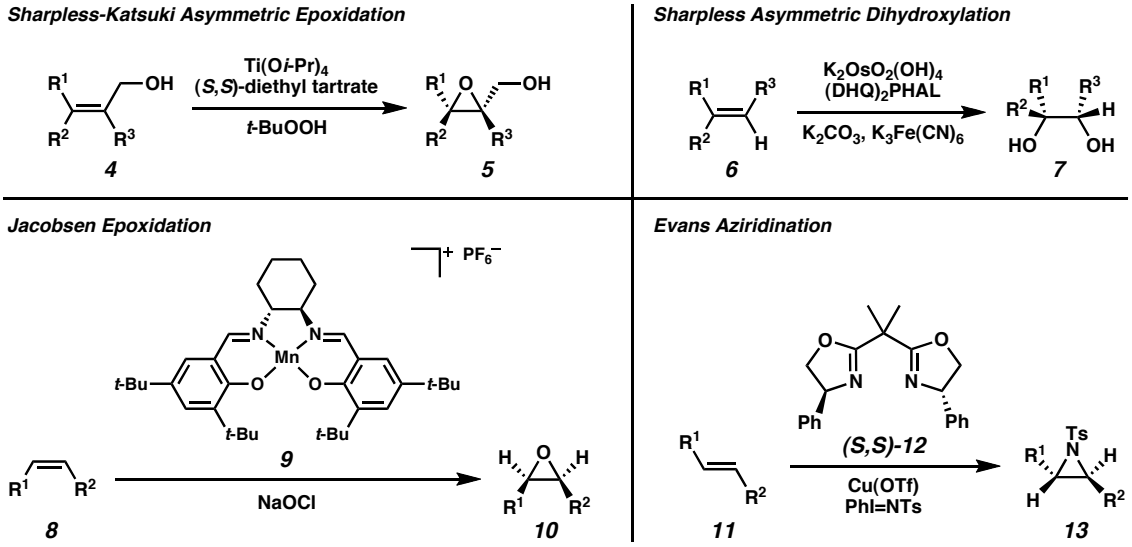

1.2.2 Oxidase-Type Reactions

Synthetic variants of oxidase-type reactions, which involve a formal dehydrogenation rather than heteroatom transfer, have also been demonstrated. Asymmetric versions, however, have been much less explored. The scarcity of these methods is somewhat understandable, as dehydrogenation is a complexity-minimizing process.[6] While enantioselective oxygenase-type transformations involve asymmetric induction in the *construction* of substrate-heteroatom bonds, oxidase-type reactions often result in the formation of unsaturated bonds through the *destruction* of stereogenic centers. Nevertheless, the Stoltz laboratory at the California Institute of Technology envisioned a number of dehydrogenative processes that could be amenable to asymmetric catalysis (Figure 1.2.2). While long-term goals included asymmetric Wacker-type cyclizations (**18**→**19**)[7] and C–C bond forming cyclizations (**20**→**21**),[8] the initial focus of the project has been the kinetic resolution of secondary alcohols (e.g., (±)-**14**→**15** + (+)-**14**) and the related desymmetrization of *meso*-diols (**16**→**17**).

Figure 1.2.2 Proposed synthetic asymmetric oxidase-type chemistry.

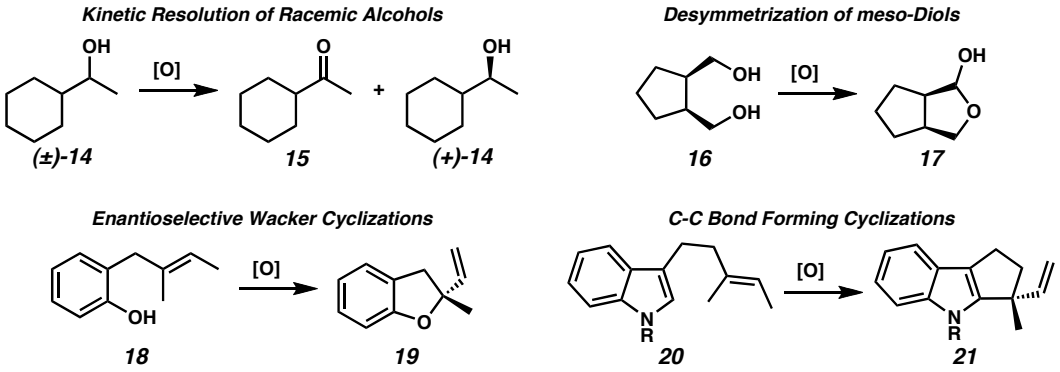

1.3 Oxidative Kinetic Resolution of Alcohols

1.3.1 Kinetic Resolutions

Of all oxidase-type dehydrogenative processes, the oxidation of alcohols to carbonyl compounds is one of the most fundamental in organic chemistry.[9] Though a wide variety of oxidants have been used for these transformations,[10] comparatively few catalytic enantioselective variants are known. These enantioselective alcohol oxidations require the selective destruction of a stereocenter in a stereoablative kinetic resolution process.[11,12]

A kinetic resolution separates the two enantiomers of a racemic mixture by exploiting their unequal rates of reaction with an enantioenriched reagent or catalyst (Figure 1.3.1).[12c] One enantiomer (e.g., (*R*)-**22**) reacts faster with the enantioenriched catalyst, with rate k_{fast}, to provide product **23**. The other enantiomer ((*S*)-**22**) reacts much more slowly (k_{slow}). Ideally, the reaction is terminated when all or most of the faster-reacting enantiomer has been converted to product **23**. The remaining enantioenriched starting material ((*S*)-**22**) and product **23** can be separated by standard techniques. The selectivity factor (*s*) of a resolution is determined by measuring the relative rates of

reaction of the two enantiomers ($k_{rel} = k_{fast} / k_{slow}$). In practice, the selectivity factor is usually determined by measuring the total conversion of starting material to product and the enantiomeric excess of the recovered starting material.[12a] For an ideal system, the chiral reagent or catalyst maintains the same relative enantiomeric preference throughout the reaction, so the selectivity factor remains constant. As shown in the graph in Figure 1.3.1, the enantiomeric excess of the starting material always increases with increasing conversion for any kinetic resolution with a selectivity factor greater than 1. Thus, kinetic resolutions have the ability to provide compounds of high enantiomeric excess for even modestly selective processes at higher levels of conversion.

Figure 1.3.1 Kinetic resolution overview.

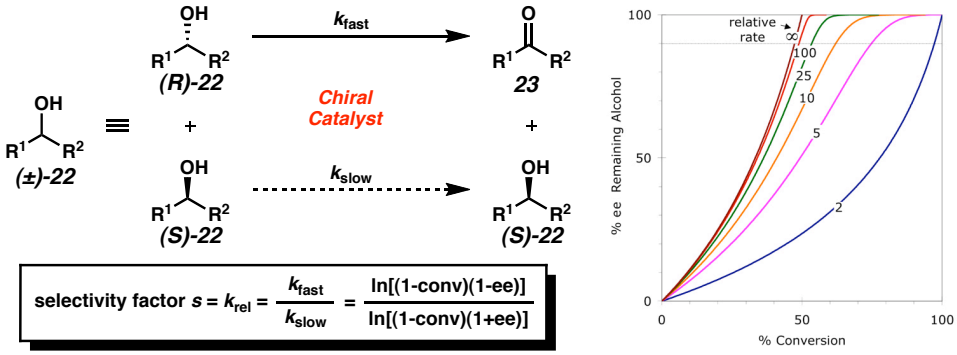

1.3.2 Previous Catalytic Enantioselective Alcohol Oxidations

At the beginning of our efforts in this area, only a few approaches to the nonenzymatic catalytic asymmetric oxidation of alcohols had been reported.[13] Several groups have utilized nitroxyl radicals for this process. Rychnovsky found that binaphthyl radical **24** catalyzes the oxidation of (±)-1-phenylethanol ((±)-**25**) to acetophenone (**26**) with bleach as the terminal oxidant, leaving enantioenriched alcohol (+)-**25** (Scheme 1.3.1).[14] Low catalyst loadings could be used, though only modest selectivity was

observed across a range of secondary alcohols ($s \leq 7.1$). Further studies with other chiral nitroxyl radicals led to even lower selectivity.[15]

Scheme 1.3.1 Rychnovsky's chiral TEMPO-based oxidation.

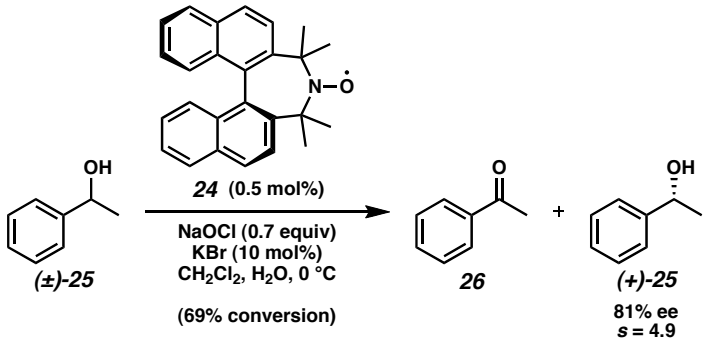

Catalytic nitroxyl radicals have also been used in electrolytic oxidation of alcohols. Kashiwagi and Bobbitt performed the enantioselective oxidation of alcohol (±)-**25** using a graphite electrode and chiral *N*-oxyl **27** (Scheme 1.3.2).[16] Again, the observed selectivity was modest for several substrates (s = 4.1–4.6). Tanaka reported a similar system utilizing Rychnovsky's *N*-oxyl **24** under electrolytic conditions that displayed improved selectivity ($s \leq 16$) at temperatures below 23 °C.[17]

Scheme 1.3.2 Chiral nitroxyl oxidation under electrolysis.

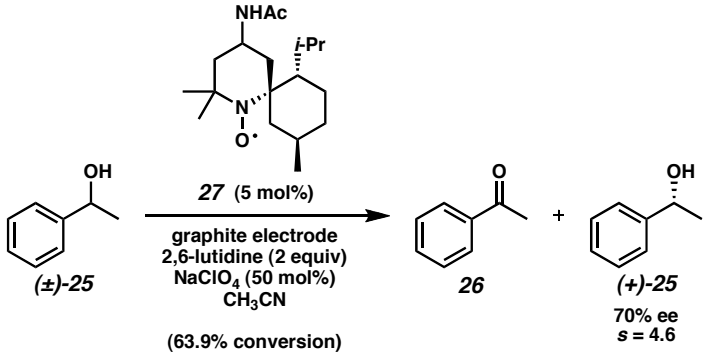

Osa and Bobbitt also demonstrated an oxidative kinetic resolution using an achiral nitroxyl radical. Utilizing a TEMPO-modified graphite electrode and the chiral diamine (–)-sparteine (**28**), highly enantioenriched alcohol (+)-**25** was recovered (Scheme 1.3.3).[18] Several other secondary alcohols also exhibited impressive selectivity factors (s = 56-184). The researchers postulated that (–)-sparteine (**28**) acts as a chiral base in the resolution. Oxidations conducted with (–)-strychnine as the chiral base were less selective.

Scheme 1.3.3 Nitroxyl oxidation with a chiral base.

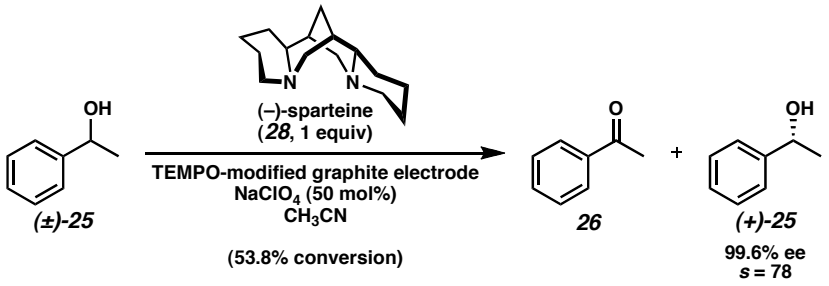

Transition metal catalysts have also been used to effect enantioselective alcohol oxidation. Ohkubo disclosed the earliest example of a nonenzymatic oxidative kinetic resolution of a secondary alcohol in 1976 (Scheme 1.3.4).[19] Extremely low levels of enantioselectivity were observed in the oxidation of (±)-1-phenylethanol ((±)-**25**) with a ruthenium catalyst and menthol-derived phosphine **29**. While not a synthetically useful transformation, this process served as an important conceptual proof for later oxidative kinetic resolutions by transfer hydrogenation. Saburi and Yoshikawa subsequently found that a rhodium hydride species with bisphosphine (–)-DIOP as a chiral ligand could catalyze the oxidative desymmetrization of a *meso*-diol by transfer hydrogenation with modest selectivity.[20]

Scheme 1.3.4 Ohkuba ruthenium-catalyzed transfer hydrogenation.

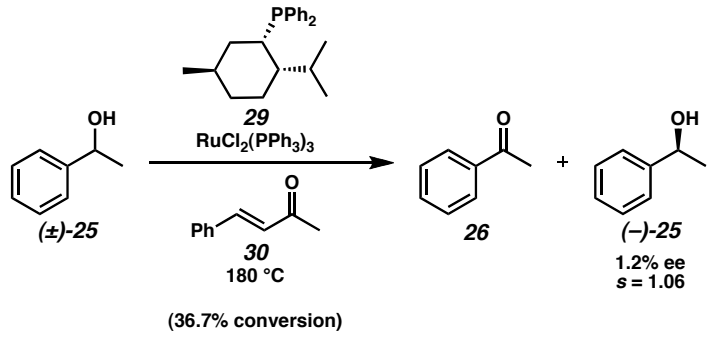

More recently, Noyori demonstrated the asymmetric oxidation of alcohol (±)-**25** with ruthenium arene complex **31** under transfer hydrogenation conditions with acetone as the terminal oxidant (Scheme 1.3.5).[21] Highly selective oxidations were observed with this system, with *s* factors for some alcohols above 100.

Scheme 1.3.5 Noyori ruthenium-catalyzed transfer hydrogenation.

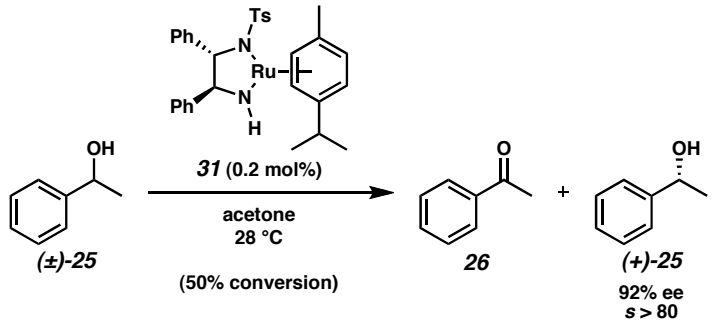

Uemura has demonstrated a similar system with a different chiral ligand (Scheme 1.3.6).[22] Ferrocenylphosphine catalyst **32** promoted transfer hydrogenation with acetone to afford alcohol (–)-**25** with outstanding selectivity. This system was active even at extremely low catalyst loadings, and a range of substrates could be resolved to high enantiomeric excesses.

Scheme 1.3.6 Uemura ruthenium-catalyzed transfer hydrogenation.

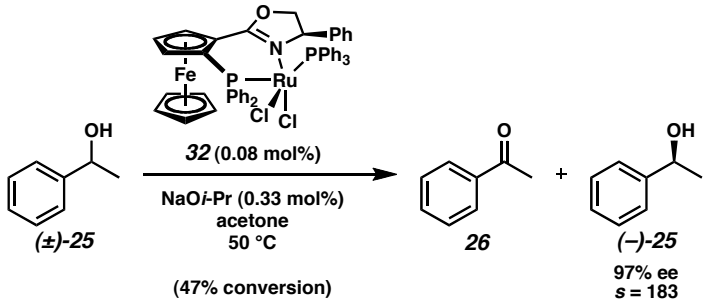

Katsuki showed that ruthenium complex **33** was a catalyst for the oxidative kinetic resolution of several alcohols (Scheme 1.3.7).[23] Under photolysis conditions, (±)-1-phenylethanol ((±)-**25**) could be resolved to high ee. This system was the first to use molecular oxygen from dry air as the terminal oxidant, representing a major advance toward catalytic systems that truly mimic aerobic oxidase enzymes. This complex was also able to perform oxidative desymmetrizations of several *meso*-diols, albeit in a modest 59-67% ee.[24] More recently, improvements in selectivity were observed with 1,3-diketone additives.[25] Finally, Gross reported a ruthenium-porphyrin-catalyzed oxidative kinetic resolution with 2,6-dichloropyridine-*N*-oxide as the terminal oxidant, though the observed enantiomeric excesses were moderate (2-28% ee).[26]

Scheme 1.3.7 Katsuki aerobic enantioselective alcohol oxidation.

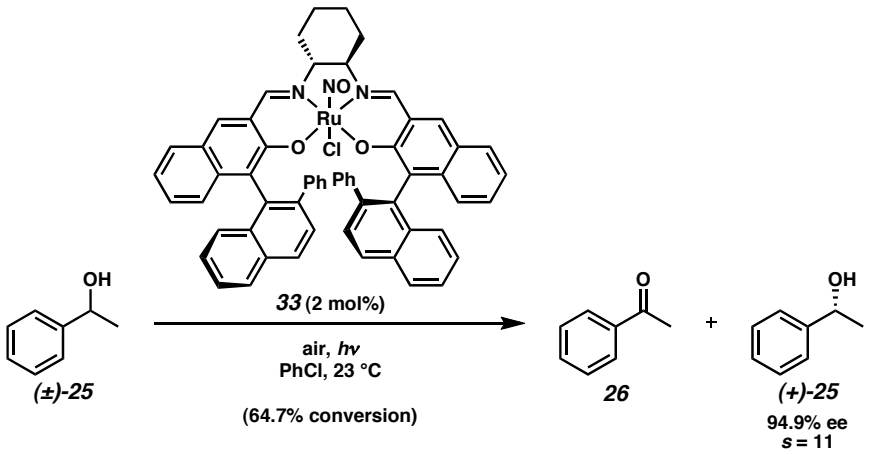

1.3.3 Subsequent Enantioselective Alcohol Oxidations

Subsequent to our initial publication on the palladium-catalyzed aerobic oxidative kinetic resolution of secondary alcohols, several other systems have been disclosed. Xia performed the enantioselective oxidation of alcohol (±)-**25** with cationic manganese(III) complex **9** and $PhI(OAc)_2$ as terminal oxidant (Scheme 1.3.8).[27] Based on an oxidation system previously reported by Katsuki,[28] water was found to be an excellent solvent for the resolutions with tetraethylammonium bromide as a phase transfer catalyst. Low to good selectivity (s = 1.1-24) was observed in the resolution of a variety of secondary alcohols. Some selectivity improvements were found with water/organic solvent mixtures.[29] A number of studies on the use of polymeric[30] and solid supported[31] catalysts for easier purification and catalyst recycling have also been reported.

Scheme 1.3.8 Manganese-catalyzed oxidation with $PhI(OAc)_2$.

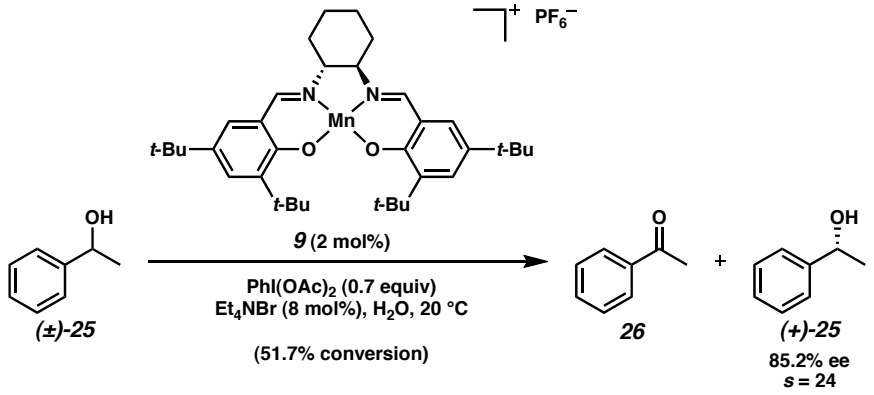

Gao has found that iridium complex **34** catalyzes the oxidative kinetic resolution of benzylic alcohols (Scheme 1.3.9).[32] (±)-1-Phenylethanol ((±)-**25**) could be resolved to high enantiomeric excess under transfer hydrogenation conditions with acetone as stoichiometric oxidant, similar to previous ruthenium-based systems (Scheme 1.3.5 and Scheme 1.3.6).

Scheme 1.3.9 Gao iridium-catalyzed transfer hydrogenation.

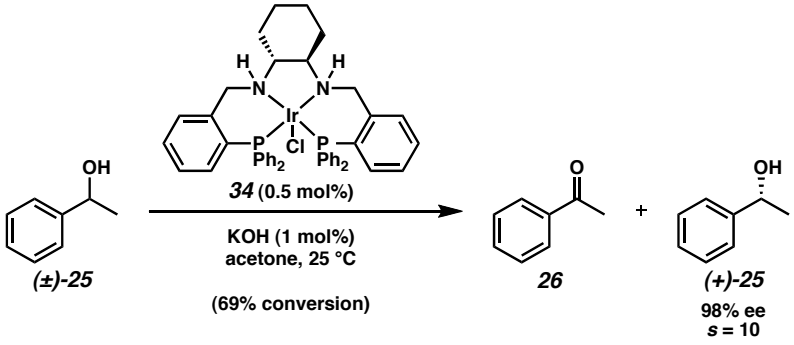

Another iridium catalyst (**35**) has demonstrated catalytic enantioselective oxidation with air as the terminal oxidant (Scheme 1.3.10).[33] Alcohol (±)-**25** was able to be resolved to high ee with excellent selectivity. Employing ligands related to the

diimido ligand in Noyori's ruthenium catalyst (**31**), several other benzylic alcohols could be resolved under aerobic conditions as well.

Scheme 1.3.10 Ikariya iridium-catalyzed aerobic oxidation.

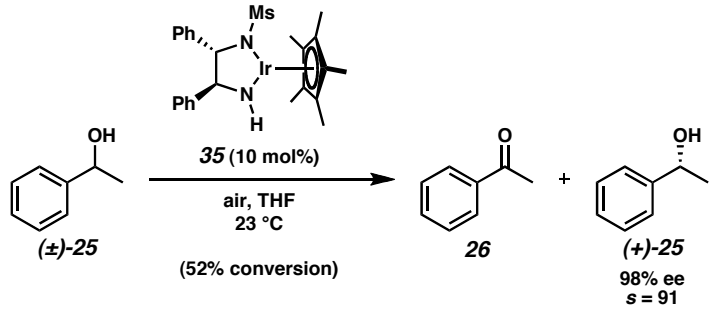

Toste has explored oxidative kinetic resolutions with vanadium catalysts.[34] salicylaldehyde-derived imine **37** proved to be an effective ligand for enantioselective oxidation of alcohols under an atmosphere of molecular oxygen as the terminal oxidant (Scheme 1.3.11). Indeed, (*R*)-ethyl mandelate ((*R*)-**36**) could be prepared with this highly selective oxidation. A number of α-hydroxyesters and also an α-hydroxyamide were resolved with good to excellent selectivity (*s* = 6-42). Interestingly, secondary alcohols without an adjacent ester or amide displayed poor reactivity with this system. Recently, Toste applied this methodology to the enantioselective total synthesis of (–)-octalactin A.[35]

Scheme 1.3.11 Toste vanadium-catalyzed aerobic oxidation.

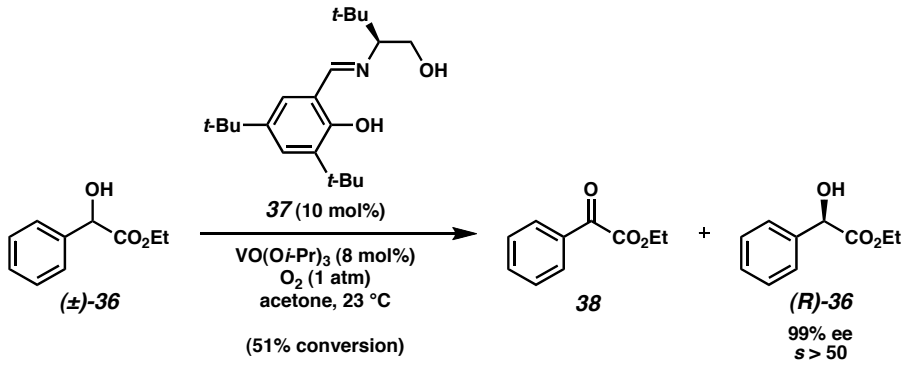

Chen subsequently reported a related system exploiting vanadium catalyst **40** with molecular oxygen as the stoichiometric oxidant to resolve phosphonate (±)-**39** with outstanding selectivity (Scheme 1.3.12).[36] Enantioselective oxidation of a range of other α-hydroxyphosphonate esters, frequently with selectivity factors over 100, was also accomplished with this aerobic system. Further developments by Chen led to a catalyst (**44**) that could resolve α-hydroxyesters and α-hydroxyamides with extremely high selectivity in some cases.[37] Vanadium clusters were found to be active catalysts for the aerobic oxidative kinetic resolution of α-hydroxythioesters.[38]

Scheme 1.3.12 Chen vanadium-catalyzed aerobic oxidations.

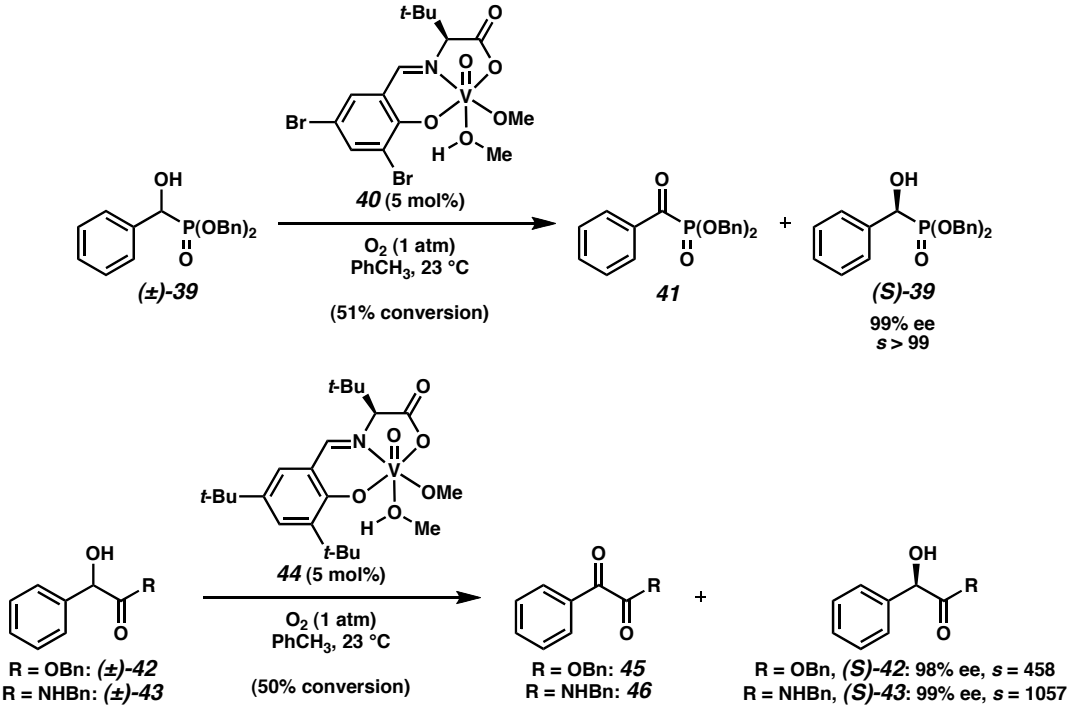

Onomura described an enantioselective oxidation with a copper catalyst and bisoxazoline (*R*,*R*)-**12** (Scheme 1.3.13).[39] This system successfully resolved a number of racemic 1,2-diols with *N*-bromosuccinimide as the terminal oxidant. Oxidation of cyclohexanediol (±)-**47** provided hydroxyketone (*S*)-**48** in 30% yield and 82% ee. Diol (*R*,*R*)-**47** was recovered in 70% yield and 28% ee, corresponding to a selectivity factor of 14. Desymmetrization of *meso*-hydrobenzoin (**49**) with low catalyst loading afforded (*R*)-benzoin ((*R*)-**50**) in 94% yield and 69% ee.

Scheme 1.3.13 Onomura copper-catalyzed enantioselective oxidations.

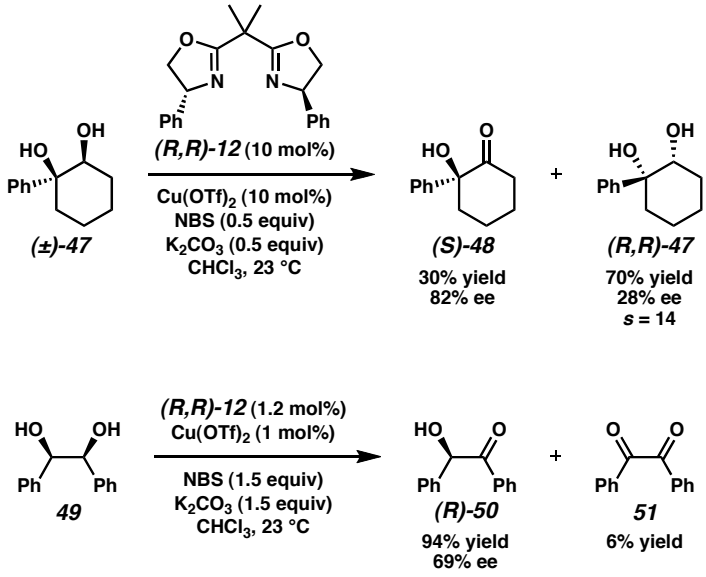

1.4 Conclusion

Inspired by biological systems, chemists have developed a number of asymmetric oxidations based on small molecule catalysis. While numerous transformations involving oxygenase-type reactivity have been reported, catalytic enantioselective oxidase-type reactivity has been relatively less explored. Even asymmetric variants of the ubiquitous alcohol oxidation have been limited. Despite efforts by a number of researchers, a mild, general, and selective method for the oxidative kinetic resolution of secondary alcohols has remained elusive. The discovery and development of a palladium-catalyzed aerobic system to achieve this goal is the subject of this thesis.

1.5 Notes and References

(1) *Asymmetric Oxidation Reactions*; Katsuki, T., Ed.; Practical Approach in Chemistry Series; Oxford Press: New York, 2001.

(2) For discussions on enantioselective epoxidation of allylic alcohols, see: (a) Katsuki, T. Epoxidation of Allylic Alcohols. In *Comprehensive Asymmetric Catalysis*; Jacobsen, E. N., Pfaltz, A., Yamamoto, H., Eds.; Springer-Verlag: Berlin, 1999; Vol. 2, Chapter 18.1, pp 621-648. (b) Johnson, R. A.; Sharpless, K. B. Catalytic Asymmetric Epoxidation of Allylic Alcohols. In *Catalytic Asymmetric Synthesis,* 2nd ed.; Ojima, I., Ed.; Wiley & Sons: New York, 2000; Chapter 6A, pp 231-280. (c) Wen, X.; Ojima, I. Chapter 6A Addendum–1999. In *Catalytic Asymmetric Synthesis,* 2nd ed.; Ojima, I., Ed.; Wiley & Sons: New York, 2000; Chapter 6A, pp 281-286.

(3) For discussions on the enantioselective dihydroxylation of alkenes, see: (a) Markó, I. E.; Svendsen, J. S. Dihydroxylation of Carbon-Carbon Double Bonds. In *Comprehensive Asymmetric Catalysis*; Jacobsen, E. N., Pfaltz, A., Yamamoto, H., Eds.; Springer-Verlag: Berlin, 1999; Vol. 2, Chapter 20, pp 713-787. (b) Johnson, R. A.; Sharpless, K. B. Catalytic Asymmetric Dihydroxylation–Discovery and Development. In *Catalytic Asymmetric Synthesis,* 2nd ed.; Ojima, I., Ed.; Wiley & Sons: New York, 2000; Chapter 6D, pp 357-398. (c) Bolm, C.; Hildebrand, J. P.; Muñiz, K. Recent Advances in Asymmetric Dihydroxylation and Aminohydroxylation. In *Catalytic Asymmetric Synthesis,* 2nd ed.; Ojima, I., Ed.; Wiley & Sons: New York, 2000; Chapter 6E, pp 399-428.

(4) For discussions on the enantioselective epoxidation of unfunctionalized alkenes, see: (a) Jacobsen, E. N.; Wu, M. H. Epoxidation of Alkenes Other than Allylic Alcohols. In *Comprehensive Asymmetric Catalysis*; Jacobsen, E. N., Pfaltz, A., Yamamoto, H., Eds.; Springer-Verlag: Berlin, 1999; Vol. 2, Chapter 18.2, pp 649-677. (b) Katsuki, T. Asymmetric Epoxidation of Unfunctionalized Olefins and Related Reactions. In *Catalytic Asymmetric Synthesis,* 2nd ed.; Ojima, I., Ed.; Wiley & Sons: New York, 2000; Chapter 6B, pp 287-326.

(5) For a discussion on enantioselective aziridination, see: Jacobsen, E. N. Aziridination. In *Comprehensive Asymmetric Catalysis*; Jacobsen, E. N., Pfaltz, A., Yamamoto, H., Eds.; Springer-Verlag: Berlin, 1999; Vol. 2, Chapter 17, pp 607-618.

(6) Stoltz, B. M. *Chem. Lett.* **2004**, *33*, 362-367.

(7) (a) Trend, R. M.; Ramtohul, Y. K.; Ferreira, E. M.; Stoltz, B. M. *Angew. Chem., Int. Ed.* **2003**, *42*, 2892-2895. (b) Trend, R. M.; Ramtohul, Y. K.; Stoltz, B. M. *J. Am. Chem. Soc.* **2005**, *127*, 17778-17788. (c) Liu, Q.; Ferreira, E. M.; Stoltz, B. M. *J. Org. Chem.* **2007**, *72*, 7352-7358.

(8) (a) Ferreira, E. M.; Stoltz, B. M. *J. Am. Chem. Soc.* **2003**, *125*, 9578-9579. (b) Garg, N. K.; Caspi, D. D.; Stoltz, B. M. *J. Am. Chem. Soc.* **2004**, *126*, 9552-9553. (c) Zhang, H.; Ferreira, E. M.; Stoltz, B. M. *Angew. Chem., Int. Ed.* **2004**, *43*, 6144-6148. (d) Garg, N. K.; Caspi, D. D.; Stoltz, B. M. *J. Am. Chem. Soc.* **2005**, *127*, 5970-5978. (e) Garg, N. K.; Caspi, D. D.; Stoltz, B. M. *Synlett* **2006**, 3081-

3087. (f) Ferreira, E. M.; Zhang, H.; Stoltz, B. M. *Tetrahedron* **2008**, *64*, 5987-6001.

(9) (a) Hudlicky, M. *Oxidations in Organic Chemistry*; ACS Monograph Series; American Chemical Society: Washington, DC, 1990. (b) Tidwell, T. T. *Org. React.* **1990**, *39*, 297-572. (c) *Comprehensive Organic Synthesis*; Trost, B. M. Fleming, I., Eds.; Pergamon: Oxford, U.K., 1991. (d) Luzzio, F. A. *Org. React.* **1998**, *53*, 1-221.

(10) Larock, R. C. *Comprehensive Organic Transformations*; Wiley & Sons: New York, 1999; pp 1234-1248.

(11) Mohr, J. T.; Ebner, D. C.; Stoltz, B. M. *Org. Biomol. Chem.* **2007**, *5*, 3571-3576.

(12) For discussions on kinetic resolution, see: (a) Kagan, H. B.; Fiaud, J. C. In *Topics in Stereochemistry*; Eliel, E. L., Ed.; Wiley & Sons: New York, 1988; Vol. 18, pp 249-330. (b) Keith, J. M.; Larrow, J. F.; Jacobsen, E. N. *Adv. Synth. Catal.* **2001**, *343*, 5-26. (c) Vedejs, E.; Jure, M. *Angew. Chem., Int. Ed.* **2005**, *44*, 3974-4001.

(13) For a monograph describing enzymatic approaches to kinetic resolution, see: Wong, C.-H.; Whitesides, G. M. *Enzymes in Synthetic Organic Chemistry*; Pergamon: Oxford, U.K., 1994.

(14) Rychnovsky, S. D.; McLernon, T. L.; Rajapakse, H. *J. Org. Chem.* **1996**, *61*, 1194-1195.

(15) Graetz, B.; Rychnovsky, S.; Leu, W.-H.; Farmer, P.; Lin, R. *Tetrahedron: Asymmetry* **2005**, *16*, 3584-3598.

(16) Kashiwagi, Y.; Kurashima, F.; Kikuchi, C.; Anzai, J.-i.; Osa, T.; Bobbitt, J. M. *Tetrahedron Lett.* **1999**, *40*, 6469-6472.

(17) Kuroboshi, M.; Yoshihisa, H.; Cortona, M. N.; Kawakami, Y.; Gao, Z.; Tanaka, H. *Tetrahedron Lett.* **2000**, *41*, 8131-8135.

(18) Kashiwagi, Y.; Yanagisawa, Y.; Kurashima, F.; Anzai, J.-i.; Osa, T.; Bobbitt, J. M. *Chem. Commun.* **1996**, 2745-2746.

(19) Ohkubo, K.; Hirata, K.; Yoshinaga, K.; Okada, M. *Chem. Lett.* **1976**, 183-184.

(20) Ishii, Y.; Suzuki, K.; Ikariya, T.; Saburi, M.; Yoshikawa, S. *J. Org. Chem.* **1986**, *51*, 2822-2824.

(21) Hashiguchi, S.; Fujii, A.; Haack, K.-J.; Matsumura, K.; Ikariya, T.; Noyori, R. *Angew. Chem., Int. Ed. Engl.* **1997**, *36*, 288-289.

(22) (a) Nishibayashi, Y.; Takei, I.; Uemura, S.; Hidai, M. *Organometallics* **1999**, *18*, 2291-2293. (b) Nishibayashi, Y.; Yamauchi, A.; Onodera, G.; Uemura, S. *J. Org. Chem.* **2003**, *68*, 5875-5880.

(23) Masutani, K.; Uchida, T.; Irie, R.; Katsuki, T. *Tetrahedron Lett.* **2000**, *41*, 5119-5123.

(24) Shimizu, H.; Nakata, K.; Katsuki, T. *Chem. Lett.* **2002**, 1080-1081.

(25) Nakamura, Y.; Egami, H.; Matsumoto, K.; Uchida, T.; Katsuki, T. *Tetrahedron* **2007**, *63*, 6383-6387.

(26) Gross, Z.; Ini, S. *Org. Lett.* **1999**, *1*, 2077-2080.

(27) Sun, W.; Wang, H.; Xia, C.; Li, J.; Zhao, P. *Angew. Chem., Int. Ed.* **2003**, *42*, 1042-1044.

(28) Hamada, T.; Irie, R.; Mihara, J.; Hamachi, K.; Katsuki, T. *Tetrahedron* **1998**, *54*, 10017-10028.

(29) Li, Z.; Tang, Z. H.; Hu, X. X.; Xia, C. G. *Chem.–Eur. J.* **2005**, *11*, 1210-1216.

(30) (a) Kureshy, R. I.; Ahmad, I.; Pathak, K.; Khan, N.-u. H.; Abdi, S. H. R.; Prathap, J. K.; Jasra, R. V. *Chirality* **2007**, *19*, 352-357. (b) Sun, W.; Wu, X.; Xia, C. *Helv. Chim. Acta* **2007**, *90*, 623-626. (c) Pathak, K.; Ahmad, I.; Abdi, S. H. R.; Kureshy, R. I.; Khan, N.-u. H.; Jasra, R. V. *J. Mol. Catal. A: Chem.* **2007**, *274*, 120-126.

(31) (a) Kantam, M. L.; Ramani, T.; Chakrapani, L.; Choudary, B. M. *J. Mol. Catal. A: Chem.* **2007**, *274*, 11-15. (b) Sahoo, S.; Kumar, P.; Lefebvre, F.; Halligudi, S. B. *Tetrahedron Lett.* **2008**, *49*, 4865-4868.

(32) Li, Y.-Y.; Zhang, X.-Q.; Dong, Z.-R.; Shen, W.-Y.; Chen, G.; Gao, J.-X. *Org. Lett.* **2006**, *8*, 5565-5567.

(33) Arita, S.; Koike, T.; Kayaki, Y.; Ikariya, T. *Angew. Chem., Int. Ed.* **2008**, *47*, 2447-2449.

(34) Radosevich, A. T.; Musich, C.; Toste, F. D. *J. Am. Chem. Soc.* **2005**, *127*, 1090-1091.

(35) Radosevich, A. T.; Chan, V. S.; Shih, H.-W.; Toste, F. D. *Angew. Chem., Int. Ed.* **2008**, *47*, 3755-3758.

(36) Pawar, V. D.; Bettigeri, S.; Weng, S.-S.; Kao, J.-Q.; Chen, C.-T. *J. Am. Chem. Soc.* **2006**, *128*, 6308-6309.

(37) Weng, S.-S.; Shen, M.-W.; Kao, J.-Q.; Munot, Y. S.; Chen, C.-T. *Proc. Natl. Acad. Sci. U.S.A.* **2006**, *103*, 3522-3527.

(38) Chen, C.-T.; Bettigeri, S.; Weng, S.-S.; Pawar, V. D.; Lin, Y.-H.; Liu, C.-Y.; Lee, W.-Z. *J. Org. Chem.* **2007**, *72*, 8175-8185.

(39) Onomura, O.; Arimoto, H.; Matsumura, Y.; Demizu, Y. *Tetrahedron Lett.* **2007**, *48*, 8668-8672.

CHAPTER 2

The Development of the Palladium-Catalyzed Oxidative Kinetic Resolution of Secondary Alcohols

2.1 Background and Introduction

Chiral alcohols are present in many natural products, pharmaceutical agents, and useful synthetic materials, and are highly versatile as synthetic intermediates in the construction of other functional groups. The ready availability of a wide range of racemic alcohols and the potential for recycling the product ketone by a simple reduction makes oxidative kinetic resolution a practical process for the preparation of enantioenriched alcohols. Thus, a general catalytic system for enantioselective alcohol oxidation would be of great benefit to the synthetic organic community.[1-6]

Because of its prevalence in a variety of enantioselective transformations[7] and known utility in the aerobic oxidation of alcohols, we chose to pursue palladium(II) as a catalytic metal for the oxidative kinetic resolution of secondary alcohols.[8,9] Particularly intriguing was a report by Uemura of racemic alcohol oxidation utilizing a palladium(II) catalyst and pyridine in toluene (Scheme 2.1.1).[10] Employing molecular oxygen as the sole stoichiometric oxidant, high yields of aldehydes and ketones were obtained for a variety of alcohols. These conditions were attractive for a number of reasons. Molecular oxygen, essential for cellular respiration in all aerobic organisms, is an inexpensive, abundant, and environmentally benign oxidant. The lack of additional co-oxidants reduces reaction complexity. Hydrogen peroxide, the sole byproduct of the oxidation, decomposes to water and molecular oxygen under the reaction conditions. Also, pyridine was found to be critical to the reaction as both ligand and base. Uemura reported no

catalytic activity in the absence of pyridine, indicating a strong ligand acceleration effect. We anticipated that the use of chiral ligands in the place of pyridine would lead to significant enantiodiscrimination in the oxidation, while the ligand acceleration could minimize racemic background oxidation by other Pd(II) species that might be present in the reaction. Finally, the non-coordinating nature of toluene should limit solvent displacement of a chiral ligand from the palladium center.

Scheme 2.1.1 Uemura oxidation conditions.

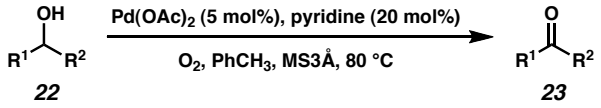

The proposed mechanism for the oxidation involves ligand substitution by the alcohol (**22**) and deprotonation of a palladium(II) complex to generate intermediate palladium alkoxide **52** (Scheme 2.1.2). Subsequent β-hydride elimination from this complex forms the product ketone (**23**) and palladium hydride **53**, which then reacts with oxygen and another equivalent of alcohol **22** to reform **52**. Efforts by a number of researchers have further clarified this mechanism.[11-13]

Scheme 2.1.2 Uemura oxidation proposed mechanism.

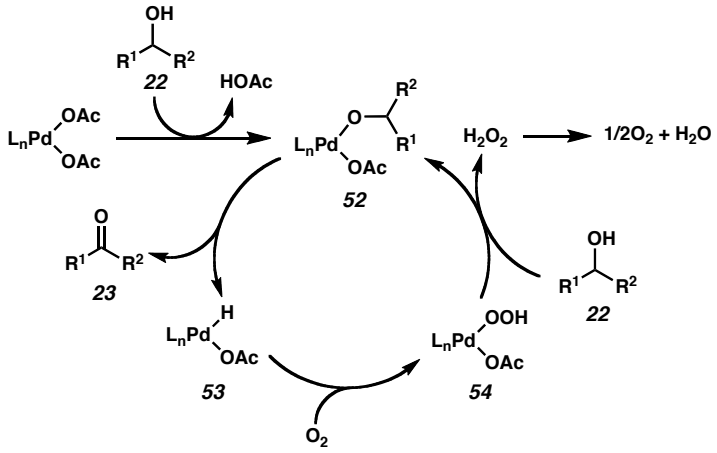

2.2 Reaction Development[†]

2.2.1 Original Conditions[14,15]

We initially focused on substituting an appropriate chiral ligand for pyridine in the oxidation. While many of the compounds evaluated as ligands led to little or no alcohol oxidation, some provided moderately reactive palladium complexes. (–)-Sparteine (**28**) rapidly emerged as a uniquely effective ligand for this transformation, providing modest levels of selectivity[16] in the oxidation of (±)-1-phenylethanol ((±)-**25**, Table 2.2.1).[17]

Table 2.2.1 Initial ligand screen for the oxidative kinetic resolution.

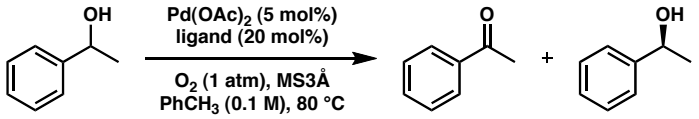

(±)-25 ***26*** ***(–)-25***

entry	ligand[a]	time	conversion[b]	alcohol ee[c]	*s*
1	(*S*,*S*)-Ph-PYBOX (***55***)	72 h	2%	–	–
2	(*S*)-*t*-Bu-BOX (***56***)	24 h	3%	–	–
3	cinchonidine (***57***)	72 h	2%	–	–
4	quinine (***58***)	24 h	0%	–	–
5	(*R*,*R*)-Jacobsen ligand (***59***)	24 h	3%	–	–
6	(–)-isopinocampheylamine (***60***)	24 h	0%	–	–
7	(*R*)-BINAP (***61***)	24 h	29.0%	0%	1.0
8	brucine (***62***)	24 h	77.0%	0%	1.0
9	$(DHQ)_2PHAL$ (***63***)	24 h	31.6%	8.7%	1.6
10	(–)-sparteine (***28***)	24 h	15.1%	13.7%	8.8

[a] For structures, see Figure 2.2.1. [b] Measured by GC. [c] Measured by chiral HPLC.

[†] This work was primarily performed by Eric M. Ferreira (Ph.D. 2005) and Jeffrey T. Bagdanoff (Ph.D. 2005), graduate students in the Stoltz group at California Institute of Technology.

Figure 2.2.1 Stuctures of ligands in Table 2.2.1.

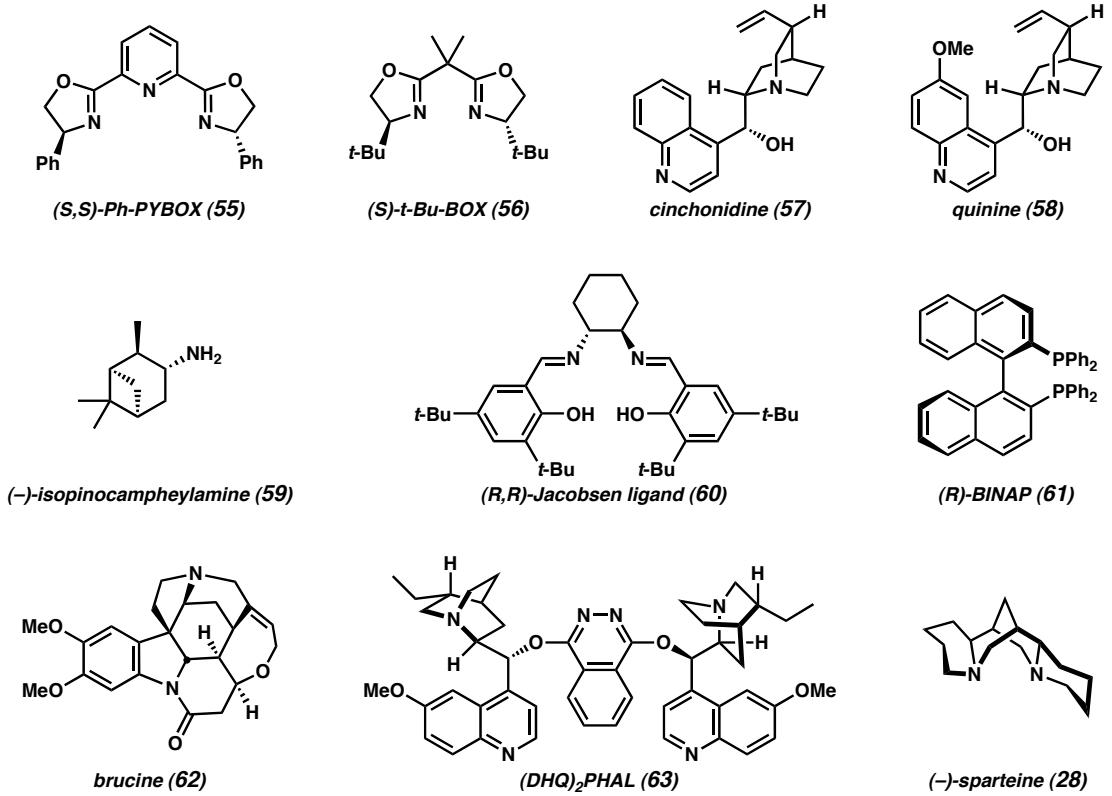

Reexamination of the general mechanism proposed by Uemura was critical for optimization of the reaction. Notably, an acetate is coordinated to the palladium center throughout the catalytic cycle, indicating the possible importance of the Pd(II) counterion in the resolution. Investigation of a number of palladium sources permitted counterion modification, resulting in greatly improved reactivity and selectivity in the oxidation employing palladium chloride complexes. $Pd(nbd)Cl_2$ proved to be the most effective precatalyst, providing good selectivity in the oxidation of a number of benzylic alcohols (Scheme 2.2.1).

Scheme 2.2.1 Original resolution conditions.

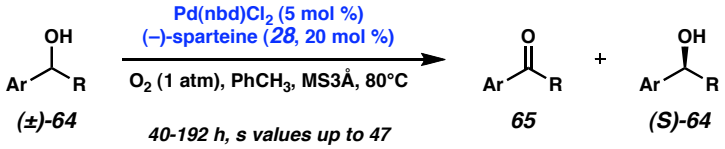

2.2.2 Rate Acceleration with Exogenous Base and a Non-Oxidizing Alcohol[18]

Although useful in principle, a major limitation of this resolution was the sluggish reaction rates. Usually, 4 days or more were required to provide alcohols in high enantiomeric excess. The high operating temperature (80 °C) further demonstrates the low activity of the system. During the course of studies to improve the reaction rate, the discrete complex Pd(sparteine)Cl_2 (**66**) was prepared. The reactivity of this complex was substantially decreased relative to the complex generated in situ with a 4:1 sparteine:Pd loading (Table 2.2.2).[15a]

Table 2.2.2 Catalyst activity versus (–)-sparteine loading.

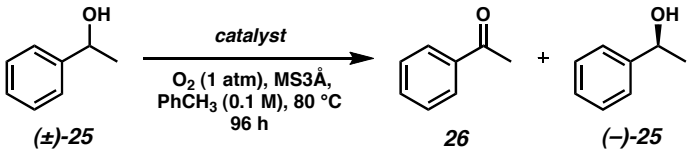

entry	catalyst	conversion[a]	alcohol ee[b]	*s*
1	Pd(nbd)Cl_2 (5 mol%) (–)-sparteine (***28***, 20 mol%)	59.9%	98.7%	23
2	Pd(sparteine)Cl_2 (***66***, 5 mol%)	4.6%	3.4%	6.0
3	Pd(sparteine)Cl_2 (***66***, 5 mol%) (–)-sparteine (***28***, 15 mol%)	60.6%	99.2%	24

[a] Measured by GC. [b] Measured by chiral HPLC.

Interestingly, we found that reactivity could be restored by adding 3 equivalents of (–)-sparteine (**28**) relative to complex **66**. The excess (–)-sparteine was suspected to act as a general base, neutralizing the hydrogen chloride byproduct generated during

palladium alkoxide formation. Indeed, kinetic studies have confirmed the role of sparteine as base.[13a] Without this added (–)-sparteine, palladium alkoxide formation is much less favorable. Thus, it was anticipated that the addition of a stoichiometric base would promote palladium alkoxide formation, facilitating alcohol oxidation.

We initiated studies to supplant (–)-sparteine (**28**) as a base in the oxidative kinetic resolution. Early experiments centered on the addition of achiral amines (Table 2.2.3). After 13 h, triethylamine seemed promising (entry 3), but rapid catalyst deactivation led to little further conversion (entry 4). Use of additional equivalents proved more detrimental (entries 5 and 6). The more nucleophilic base DABCO was even poorer. However, carbonate bases were effective at accelerating the oxidations. Cesium carbonate was found to be optimal, leading to the greatest reactivity enhancement.[19]

Table 2.2.3 Base screening studies with amines and carbonates.

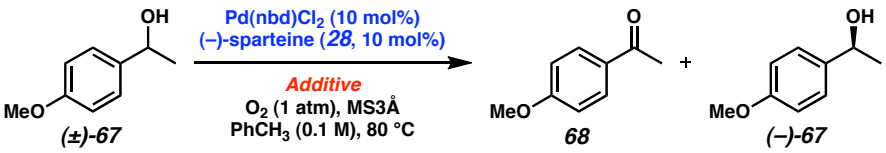

entry	additive	time	conversion[a]	alcohol ee[b]	*s*
1	(–)-sparteine (***28***, 30 mol%)	13 h	29%	34%	15
2	none	13 h	2%	<2%	–
3	Et_3N (0.4 equiv)	13 h	26%	31%	22
4	Et_3N (0.4 equiv)	26 h	29%	33%	13
5	Et_3N (2.0 equiv)	13 h	19%	19%	11
6	Et_3N (4.0 equiv)	13 h	14%	11%	6
7	DABCO (0.4 equiv)	13 h	7%	8%	20
8	Na_2CO_3 (1.0 equiv)	13 h	27%	31%	15
9	K_2CO_3 (1.0 equiv)	13 h	56%	84%	13
10	Cs_2CO_3 (1.0 equiv)	13 h	68%	99%	13

[a] Measured by ^{1}H NMR. [b] Measured by chiral HPLC.

The loss of reactivity with excess achiral amine bases is presumably due to competition between the amine and sparteine for coordination to the palladium center. We have demonstrated that monodentate amines do not generate catalytically active systems for alcohol oxidation with $Pd(nbd)Cl_2$ (Table 2.2.4).[10b] While (–)-sparteine (**28**) promotes rapid alcohol oxidation (entry 3), little oxidation occurs with either pyridine (entry 1) or quinuclidine (entry 2).

Table 2.2.4 Catalyst activity with (–)-sparteine and other amines.

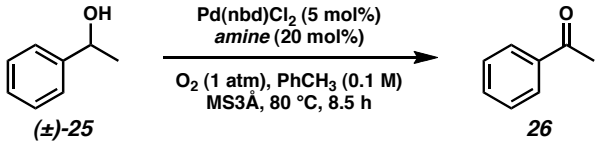

entry	amine	conversion[a]
1	pyridine	1.2%
2	quinuclidine	3.8%
3	(–)-sparteine (***28***)	36.6%

[a] Measured by GC. Conversion is the average of two experiments.

Even with added cesium carbonate, excess (–)-sparteine (**28**) relative to the palladium precursor is still beneficial. The solubility of cesium carbonate in toluene is minimal, even at elevated temperatures. Also, finely milled cesium carbonate performs much better than the granular base of lower surface area.[20] These observations suggest cesium carbonate is acting as a heterogeneous base. (–)-Sparteine (**28**), which is much more soluble in toluene, may act as a better kinetic base than the heterogeneous cesium carbonate for neutralizing hydrogen chloride generated in the formation of the palladium alkoxide (Scheme 2.2.2). While the pK_a values of sparteine•HCl[21] and cesium bicarbonate[22] are similar, the excess carbonate base could minimize sparteine•HCl concentration,[23] reducing the extent of protonation of the palladium alkoxide and accelerating the reaction.[24]

Scheme 2.2.2 Potential role of excess (–)-sparteine.

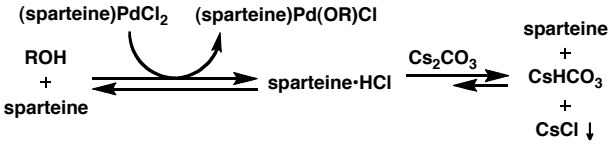

Another key development arose fortuitously from early investigations of the substrate scope. The inclusion of *tert*-butyl alcohol proved to be an excellent exogenous alcohol additive, providing more active catalytic systems for alcohol oxidation.[25] We optimized the process to maintain high selectivity across a range of secondary alcohols, while dramatically decreasing reaction times (Table 2.2.5, cf. entries 1 and 2). Furthermore, we found ambient air to be a competent replacement for molecular oxygen as the stoichiometric oxidant in these resolutions, providing a comparable reaction rate and selectivity (entry 3).

Table 2.2.5 Comparison of various conditions in toluene.

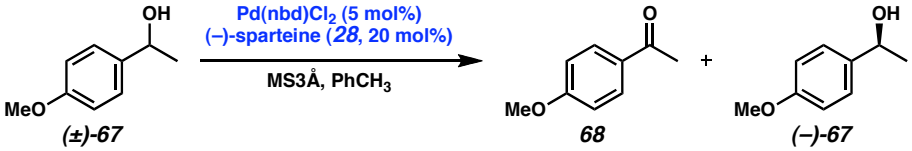

entry	conditions	time	conversion[a]	alcohol ee[b]	*s*
1	O_2 (1 atm) $PhCH_3$ (0.1 M) 80 °C	96 h	66.6%	98.1%	12
2	*O_2 (1 atm)* Cs_2CO_3 (50 mol%) *t*-BuOH (1.5 equiv) $PhCH_3$ (0.25 M), 60 °C	9.5 h	67.4%	99.5%	15
3[c]	*ambient air (1 atm)* Cs_2CO_3 (40 mol%) *t*-BuOH (1.5 equiv) $PhCH_3$ (0.25 M), 60 °C	7 h	64.0%	99.1%	17

[a] Measured by GC. [b] Measured by chiral HPLC. [c] Pd(sparteine)Cl_2 (**66**, 5 mol%) and (–)-sparteine (**28**, 15 mol%) were used.

While the purpose of the carbonate base fit well with our mechanistic model for the oxidative kinetic resolution, the role of *tert*-butyl alcohol was less clear. One possibility was that the modified reaction conditions were transforming Pd(sparteine)Cl_2 into a more reactive complex. In order to test this theory, we exposed dichloride complex **66** to *tert*-butyl alcohol and cesium carbonate. After 4 days at 60 °C, carbonate **69** was isolated in 94% yield (Scheme 2.2.3). Carbonate complex **69** displayed neither catalytic nor even stoichiometric activity under kinetic resolution conditions. This finding suggests carbonate **69** is a catalyst deactivation product. While these additives provide dramatic rate enhancement, they could also detrimentally affect catalyst longevity.[26]

Scheme 2.2.3 Synthesis of palladium carbonate **69**.

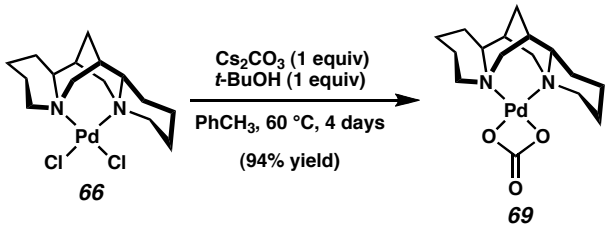

An alternative explanation for the beneficial effect of *tert*-butyl alcohol involves the formation of trace amounts of CsO*t*-Bu in situ. We have examined the addition of several *tert*-butoxide salts to these resolutions (Table 2.2.6, entries 2-4). These oxidations maintain the high reactivity observed with the *tert*-butyl alcohol conditions (entry 1). However, the recovered alcohol is nearly racemic with any of these bases. Thus, it is unlikely that CsO*t*-Bu is forming in oxidative kinetic resolution conditions with *tert*-butyl alcohol and cesium carbonate.

Table 2.2.6 Evaluation of tert-butoxide additives.

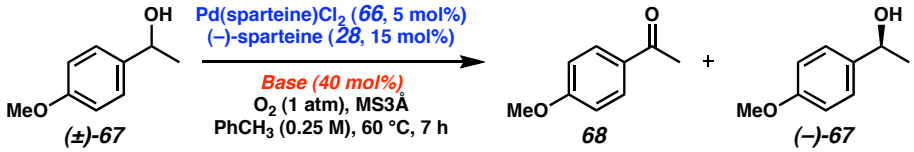

entry	base	conversion[a]	alcohol ee[b]	*s*
1	Cs_2CO_3 *t*-BuOH (1.5 equiv)	62.1%	98.6%	18
2	CsO*t*-Bu	48.1%	0.6%	1.0
3	KO*t*-Bu	61.3%	0.6%	1.0
4	NaO*t*-Bu	65.7%	2.3%	1.0

[a] Measured by GC. [b] Measured by chiral HPLC.

It is possible that these alkoxides modify the catalyst such that all selectivity is lost in the oxidation. Alternatively, a competing Meerwein-Ponndorf-Verley reduction[27] could be occurring (Scheme 2.2.4). Selective, Pd(sparteine)Cl_2-catalyzed alcohol oxidation and deprotonation of secondary alcohol (–)-**67** could provide ketone **68** and alkoxide (*S*)-**70**. Non-selective, metal-promoted Meerwein-Ponndorf-Verley reduction of the ketone could then afford product ketone **68** and racemized alkoxide (±)-**70**.

Scheme 2.2.4 Possible racemization mechanism with *tert*-butoxide.

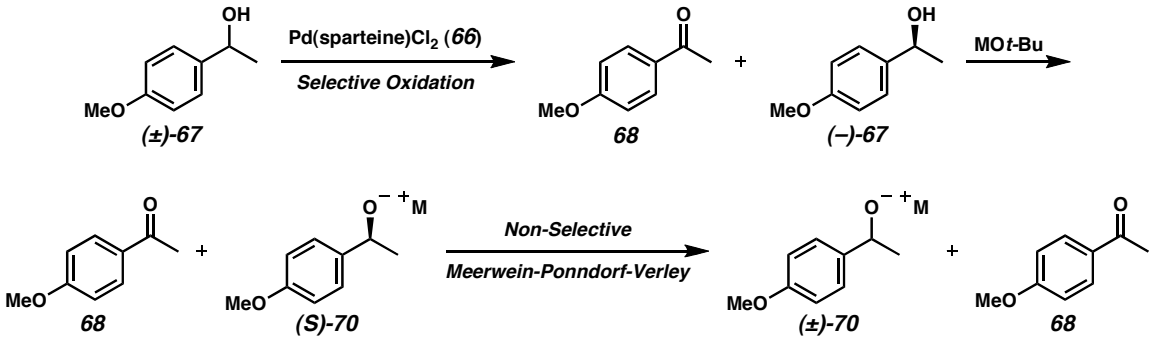

2.2.3 Chloroform as Solvent in the Resolution[28]

Having eliminated several potential roles for a non-oxidizing alcohol in the resolution, we hypothesized that the observed rate enhancement could be due to the

hydrogen bonding potential of *tert*-butyl alcohol. While hydrogen bonding plays an essential and well-documented role in the catalysis of a number of biological[29] and synthetic processes,[30] less is known about its function in organometallic transformations. A hydrogen-bond donor may enhance reactivity by stabilizing and solubilizing polar or charged intermediates in the nonpolar solvent toluene. In particular, cationic palladium complexes generated as the immediate products of alcohol coordination and β-hydride elimination result in the formation of chloride anions, which could be solubilized by hydrogen-bond donors.[13b,d]

Based on this hypothesis, we performed a more rigorous solvent screen, with an emphasis on solvents capable of hydrogen-bond donation and solubilization of polar or charged intermediates (Table 2.2.7). Surprisingly, while common organic solvents led to little oxidation (entries 12, 15, 16, 19, and 20), halogenated solvents that could act as weak hydrogen-bond donors provided rapid reactions (entries 1-6). Oxidations conducted in the hydrogen-bond donating solvent dichloromethane are the fastest (entry 1), but catalyst selectivity in kinetic resolutions suffers.[31] Chloroform, on the other hand, emerges as an outstanding nonflammable solvent for rapid and selective oxidation, even at 23 °C (entry 2). Strikingly, chlorinated solvents lacking the ability to donate a hydrogen bond (entries 13, 14, 17, and 21) are less effective. Other factors do not appear to explain the observed trends. Oxygen solubility is fairly similar in many of the solvents.[32] Also, there is no clear trend between reaction rate and dielectric constant, a measure of solvent polarity.[33]

Table 2.2.7 Solvent screen with Pd(sparteine)Cl_2.

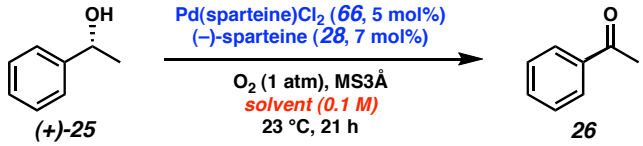

entry	solvent	dielectric constant	conversion[a]
1	CH_2Cl_2	8.9	83%
2	***$CHCl_3$***	***4.8***	***74%***
3	CH_2Br_2	7.8	73%
4	$CHCl_3$/1 equiv *t*-BuOH	4.8/12.5	72%
5	$CHBr_3$	4.4	68%
6	$ClCH_2CH_2Cl$	10.4	46%
7	$PhCH_3$/1 equiv *t*-BuOH	2.4/12.5	39%
8	$PhCH_3$/*t*-BuOH (1:1)	2.4/12.5	29%
9	$PhCH_3$	2.4	23%
10	pinacolone	12.7	21%
11	*tert*-amyl alcohol	5.8	21%
12	THF	7.5	14%
13	$Cl_2C{=}CHCl$	3.4	10%
14	Cl_3CCH_3	7.2	9%
15	EtOAc	6.1	8%
16	2-propanol	20.2	7%
17	$Cl_2C{=}CCl_2$	2.3	6%
18	H_2O/2-propanol	80.1/20.2	3%
19	CH_3CN	36.6	3%
20	CH_3NO_2	37.3	2%
21	CCl_4	2.2	2%

[a] Measured by GC.

Spectroscopic evidence for hydrogen-bond formation between chloroform and catalytic species was found in IR spectra of $CDCl_3$ solutions (Table 2.2.8).[34] A significant shift in the C–D stretching frequency of $CDCl_3$ occurred in the presence of either (–)-sparteine (**28**, entry 2) or Pd(sparteine)Cl_2 (**66**, entry 3).[35,36] The observed decrease in λ_{max} corresponds to a lower energy C–D stretching frequency due to a weaker C–D bond over free $CDCl_3$ when hydrogen-bond accepting species are present. Notably, no shift in the C–D stretch was observed with the catalytically inactive carbonate **69**, suggesting little or no hydrogen bonding occurs.

Table 2.2.8 IR data supporting hydrogen-bond donation.

entry	concentration	$CDCl_3$ solution	λ_{max} (cm^{-1})	predicted D-X bond
1	–	neat	2258	–
2	0.25 M	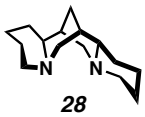 ***28***	2175	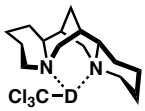
3	0.25 M	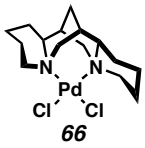 ***66***	2230	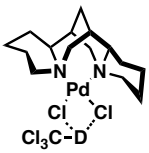
4	0.10 M[a]	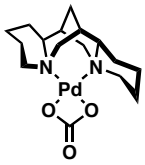 ***69***	2258	–

[a] Near saturation concentration at 23 °C.

Based on these findings of discrete interactions between chloroform and a catalytically active species, we anticipated that chloroform, like *tert*-butyl alcohol, could provide a beneficial role in the oxidative kinetic resolution as an additive. As shown in Table 2.2.9, a 1:1 ratio of chloroform and toluene (entry 2) performs as well as pure chloroform (entry 1) as solvent. There is a clear difference in rate between the stoichiometric (entry 3) and substoichiometric (entry 4) chloroform additions, indicating that the function of chloroform in these resolutions is not exclusively a bulk solvent polarity effect.

Table 2.2.9 Chloroform:toluene ratio variation.

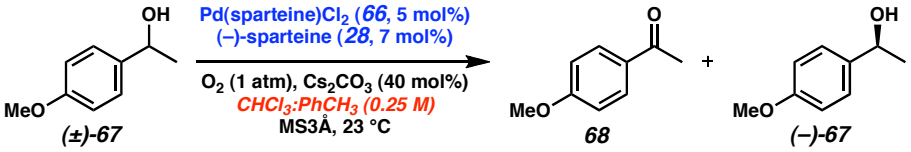

entry	$CHCl_3$:$PhCH_3$	time	conversion[a]	alcohol ee[b]	*s*
1	1:0	21 h	55.9%	92.0%	20
2	1:1	21 h	55.1%	91.0%	21
3	1:50 (1 equiv $CHCl_3$)	66 h	54.8%	91.3%	22
4	1:125 (40 mol% $CHCl_3$)	109 h	55.7%	87.5%	16

[a] Measured by GC. [b] Measured by chiral HPLC.

The change in solvent to chloroform also allows decreased amounts of (–)-sparteine (**28**) to be used with little effect on rate. Performing the reactions at 23 °C provides a dramatic increase in the catalyst selectivity (cf. Table 2.2.10, entry 1 and Table 2.2.5). Furthermore, as little as 5% O_2 atmosphere is sufficient for oxidation, enabling the use of ambient air as the terminal oxidant (entry 2). These milder conditions greatly improve the operational simplicity and safety of the oxidation, avoiding the use of flammable solvents at elevated temperatures under an oxygen atmosphere.

Table 2.2.10 Chloroform conditions with O_2 or ambient air.

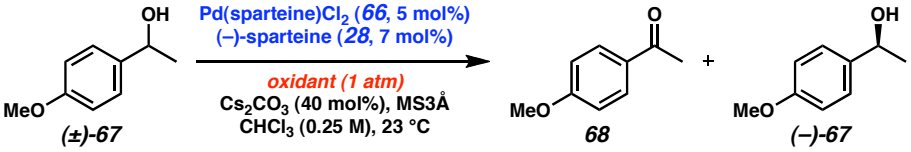

entry	oxidant	time	conversion[a]	alcohol ee[b]	*s*
1	O_2	48 h	62.6%	99.9%	27
2	ambient air	24 h	62.3%	99.8%	25

[a] Measured by GC. [b] Measured by chiral HPLC.

2.3 Conclusion

The first palladium-catalyzed enantioselective oxidation of secondary alcohols has been developed, utilizing the readily available diamine (–)-sparteine as chiral ligand and molecular oxygen as the sole stoichiometric oxidant. Mechanistic insights regarding the role of base and hydrogen bond donors have resulted in several improvements to the original system. Namely, addition of cesium carbonate and *tert*-butyl alcohol greatly enhances reaction rates, promoting accelerated resolutions. The use of chloroform as solvent allows resolutions to be conducted at 23 °C, resulting in enhanced catalyst selectivity. Finally, the use of ambient air as the terminal oxidant for reactions in either toluene or chloroform further increases the operational simplicity and safety of the process. These developments have led to a process with a broad substrate scope[37] and many practical applications, including the desymmetrization of *meso*-diols,[14] the preparation of synthetically useful molecules,[38] and the total synthesis of complex natural products.[39] Our efforts in these areas are reported in Chapters 3 and 5. Further studies in catalyst development are disclosed in Chapter 4.

2.4 Experimental Section

2.4.1 Materials and Methods

Pd(sparteine)Cl_2 (**66**) was prepared as previously reported.[13c] Cesium *tert*-butoxide was prepared by the method of Chisholm.[40] (+)-1-Phenylethanol ((+)-**25**) was purchased from Acros Organics. Pyridine was distilled over CaH_2. Solvents were dried by passage through an activated alumina column under argon. Powdered 3Å molecular sieves were stored in a 120 °C drying oven until immediately prior to use. Other chemicals were purchased from the Sigma-Aldrich Chemical Company and used as received. Liquids and solutions were transferred via syringe. Reaction temperatures were controlled using an IKAmag temperature modulator. Thin-layer chromatography (TLC) was conducted with E. Merck silica gel 60 F254 pre-coated plates (0.25 mm) and visualized using a combination of UV at 254 nm and *p*-anisaldehyde staining. Analytical achiral GC was performed on an Agilent 6850 GC with FID detector using an Agilent DB-WAX (30.0 m x 0.25 mm) column at 1.0 mL/min He carrier gas flow. Analytical chiral HPLC was performed with an Agilent 1100 Series HPLC utilizing a Chiralcel OD-H or Chiralcel OJ column (each is 4.6 mm x 25 cm) obtained from Daicel Chemical Industries, Ltd with visualization at 254 nm at 1.0 mL/min mobile phase. IR spectra were recorded on a Perkin Elmer Paragon 1000 spectrometer and are reported in terms of frequency of absorption (cm^{-1}). The absolute configurations of resolved alcohols were assigned based on comparisons of optical rotations to literature values or by analogy.

2.4.2 General Oxidative Kinetic Resolution Conditions

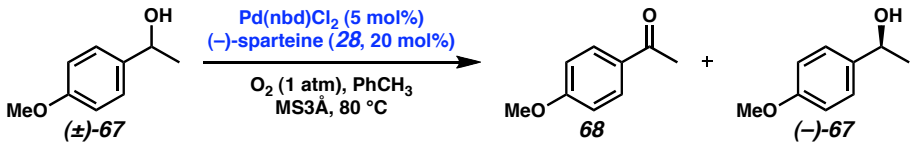

Original Resolution Conditions in $PhCH_3$ with No Achiral Base.[14] To an oven dried reaction tube with stir bar was added 3Å molecular sieves (250 mg). After cooling, $Pd(nbd)Cl_2$ (6.7 mg, 0.025 mmol, 0.05 equiv) followed by toluene (2.5 mL) and then (–)-sparteine (**28**, 23.0 μL, 0.10 mmol, 0.20 equiv) were added.[41] The reaction tube was then cooled to –78 °C, then vacuum evacuated and purged with O_2 (3x). Then, the tube was heated to 80 °C with vigorous stirring under O_2 atmosphere (1 atm, balloon) for 20 min. A solution of alcohol (±)-**67** (76.1 mg, 0.50 mmol, 1.0 equiv) and tridecane (36.6 μL, 0.15 mmol, 0.30 equiv) in toluene (2.5 mL) was added, and the reaction was allowed to proceed under O_2 atmosphere at 80 °C. Aliquots were filtered through a small plug of silica gel (Et_2O eluent), evaporated, and analyzed by GC for conversion and chiral HPLC for alcohol ee.

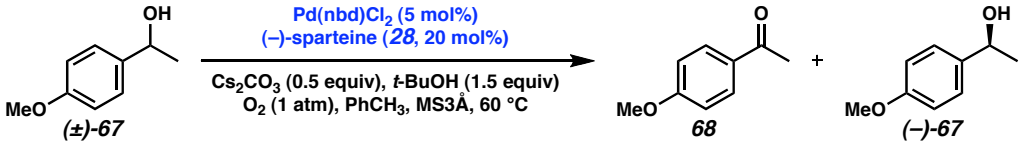

Rate Accelerated Resolution Conditions in $PhCH_3$ under O_2.[18] To an oven dried reaction tube with stir bar was added 3Å molecular sieves (250 mg). After cooling, $Pd(nbd)Cl_2$ (6.7 mg, 0.025 mmol, 0.05 equiv), followed by toluene (1 mL) and then (–)-sparteine (**28**, 23.0 μL, 0.10 mmol, 0.20 equiv) were added.[41] The reaction tube was cooled to –78 °C, then vacuum evacuated and purged with O_2 (3x). The tube was heated

to 60 °C with vigorous stirring under O_2 atmosphere (1 atm, balloon) for 20 min. Finely powdered Cs_2CO_3 (81.5 mg, 0.25 mmol, 0.50 equiv) was added, followed by a solution of alcohol (±)-**67** (76.1 mg, 0.5 mmol, 1.0 equiv), anhydrous *t*-BuOH (71.5 μL, 0.75 mmol, 1.5 equiv), and tridecane (36.6 μL, 0.15 mmol, 0.30 equiv) in toluene (1 mL). The reaction was allowed to proceed under O_2 atmosphere at 60 °C. Aliquots were filtered through a small plug of silica gel (Et_2O eluent), evaporated, and analyzed by GC for conversion and chiral HPLC for alcohol ee.

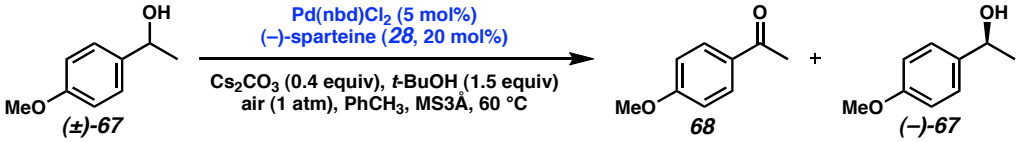

Rate Accelerated Resolution Conditions in $PhCH_3$ under Ambient Air. To an oven dried reaction tube with stir bar was added 3Å molecular sieves (250 mg). After cooling, $Pd(nbd)Cl_2$ (6.7 mg, 0.025 mmol, 0.05 equiv), followed by toluene (1 mL) and then (–)-sparteine (**28**, 23.0 μL, 0.10 mmol, 0.20 equiv) were added.[41] A short tube containing Drierite was attached to the reaction tube. The tube was heated to 60 °C with vigorous stirring under O_2 atmosphere (1 atm, balloon) for 20 min. Finely powdered Cs_2CO_3 (81.5 mg, 0.25 mmol, 0.50 equiv) was added, followed by a solution of alcohol (±)-**67** (76.1 mg, 0.5 mmol, 1.0 equiv), anhydrous *t*-BuOH (71.5 μL, 0.75 mmol, 1.5 equiv), and tridecane (36.6 μL, 0.15 mmol, 0.30 equiv) in toluene (1 mL). The reaction was allowed to proceed under air atmosphere at 60 °C. Aliquots were filtered through a small plug of silica gel (Et_2O eluent), evaporated, and analyzed by GC for conversion and chiral HPLC for alcohol ee.

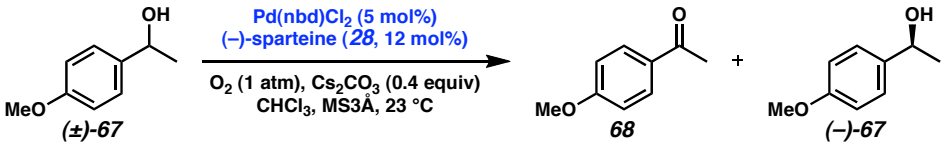

$CHCl_3$ Conditions with O_2.[28] To an oven dried reaction tube with stir bar was added 3Å molecular sieves (250 mg). After cooling, $Pd(nbd)Cl_2$ (6.7 mg, 0.025 mmol, 0.05 equiv), followed by $CHCl_3$ (1 mL)[42] and then (–)-sparteine (**28**, 13.8 μL, 0.06 mmol, 0.12 equiv) were added.[43] The reaction tube was cooled to –78 °C, then vacuum evacuated and purged with O_2 (3x). The reaction was allowed to warm to 23 °C and stirred vigorously under O_2 atmosphere (1 atm, balloon) for 15 min. Finely powdered Cs_2CO_3 (65.2 mg, 0.20 mmol, 0.40 equiv) was added, followed by a solution of alcohol (±)-**67** (76.1 mg, 0.5 mmol, 1.0 equiv) and tridecane (36.6 μL, 0.15 mmol, 0.30 equiv) in $CHCl_3$ (1 mL). The reaction was allowed to proceed under O_2 atmosphere at 23 °C. Aliquots were filtered through a small plug of silica gel (Et_2O eluent), evaporated, and analyzed by GC for conversion and chiral HPLC for alcohol ee.

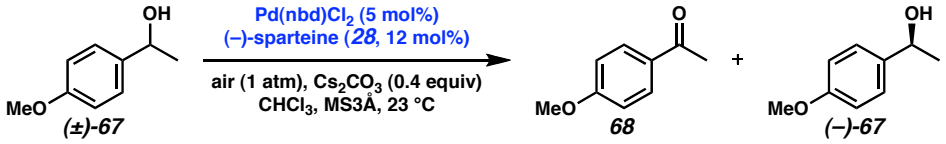

$CHCl_3$ Conditions with Ambient Air.[28] To an oven dried reaction tube with stir bar was added 3Å molecular sieves (250 mg). After cooling, $Pd(nbd)Cl_2$ (6.7 mg, 0.025 mmol, 0.05 equiv), followed by $CHCl_3$ (1 mL)[42] and then (–)-sparteine (**28**, 13.8 μL, 0.06 mmol, 0.12 equiv) were added.[43] A short tube containing Drierite was attached to the reaction tube. The reaction was stirred vigorously at 23 °C for 15 min. Finely powdered Cs_2CO_3 (65.2 mg, 0.20 mmol, 0.40 equiv) was added, followed by a solution of alcohol

(±)-**67** (76.1 mg, 0.5 mmol, 1.0 equiv) and tridecane (36.6 μL, 0.15 mmol, 0.30 equiv) in $CHCl_3$ (1 mL). The reaction was allowed to proceed under an ambient air atmosphere at 23 °C. Aliquots were filtered through a small plug of silica gel (Et_2O eluent), evaporated, and analyzed by GC for conversion and chiral HPLC for alcohol ee.

2.4.3 Screening and Optimization Studies

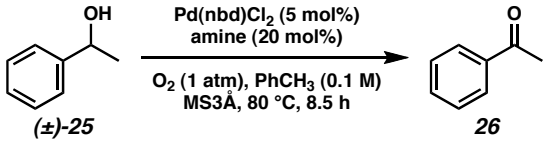

Amine Screening Procedure with $Pd(nbd)Cl_2$. To an oven dried reaction tube with stir bar was added 3Å molecular sieves (250 mg). After cooling, $Pd(nbd)Cl_2$ (6.7 mg, 0.025 mmol, 0.05 equiv) followed by toluene (2.5 mL) and the amine (0.10 mmol, 0.20 equiv) were added. The reaction tube was cooled to –78 °C, then vacuum evacuated and purged with O_2 (3x). The tube was heated to 80 °C with vigorous stirring under O_2 atmosphere (1 atm, balloon) for 20 min. A solution of (±)-1-phenylethanol ((±)-**25**, 60.3 μL, 0.50 mmol, 1.0 equiv) and tridecane (36.6 μL, 0.15 mmol, 0.30 equiv) in toluene (2.5 mL) was added, and the reaction was allowed to proceed under O_2 atmosphere at 80 °C. Aliquots were filtered through a small plug of silica gel (Et_2O eluent), evaporated, and analyzed by GC for conversion to acetophenone (**26**). Conversions given are the mean of two experiments.

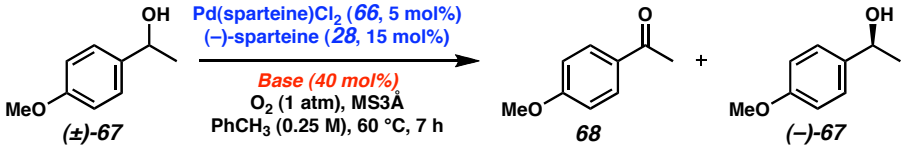

Alkoxide Base Screen in $PhCH_3$. To an oven dried reaction tube with stir bar was added 3Å molecular sieves (250 mg). After cooling, Pd(sparteine)Cl_2 (**66**, 10.3 mg, 0.025 mmol, 0.05 equiv), followed by toluene (1 mL) and then (–)-sparteine (**28**, 17.2 μL, 0.075 mmol, 0.15 equiv) were added. The reaction tube was cooled to –78 °C, then vacuum evacuated and purged with O_2 (3x). The tube was heated to 60 °C with vigorous stirring under O_2 atmosphere (1 atm, balloon) for 20 min. The alkoxide base (0.20 mmol, 0.40 equiv) was added, followed by a solution of (±)-**67** (76.1 mg, 0.5 mmol, 1.0 equiv) and tridecane (36.6 μL, 0.15 mmol, 0.30 equiv) in toluene (1 mL). The reaction was allowed to proceed under O_2 atmosphere at 60 °C. Aliquots were filtered through a small plug of silica gel (Et_2O eluent), evaporated, and analyzed by GC for conversion and chiral HPLC for alcohol ee. Conversions and enantiomeric excesses given are the mean of two experiments.

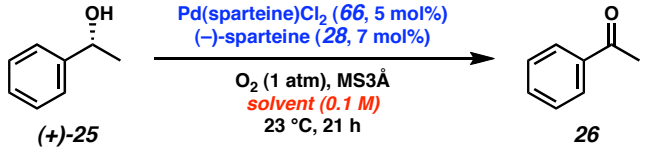

Single Enantiomer Solvent Screens with Pd(sparteine)Cl_2 (66). To an oven dried reaction tube with stir bar was added 3Å molecular sieves (250 mg). After allowing the tube to cool, Pd(sparteine)Cl_2 (**66**, 10.3 mg, 0.025 mmol, 0.05 equiv) was added, followed by the solvent (1 mL) and then **28** (8.0 μL, 0.035 mmol, 0.07 equiv). The reaction tube was cooled to –78 °C, then vacuum evacuated and purged with O_2 (3x).

The reaction was allowed to warm to 23 °C and stirred vigorously under a balloon of O_2 (1 atm) for 15 min. A solution of (+)-**25** (60.4 μL, 0.50 mmol, 1.0 equiv) and tridecane (36.6 μL, 0.15 mmol, 0.30 equiv) in the solvent (1 mL) was added. The reaction was allowed to proceed under O_2 atmosphere at 23 °C. Aliquots were filtered through a small plug of silica gel (Et_2O eluent), evaporated, and analyzed by GC for conversion to acetophenone (**26**).

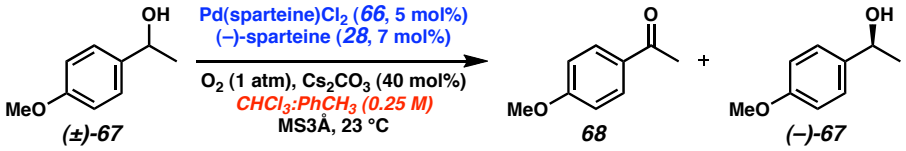

$CHCl_3$:$PhCH_3$ Ratio Screens with Pd(sparteine)Cl_2 (66). To an oven dried reaction tube with stir bar was added 3Å molecular sieves (250 mg). After allowing the tube to cool, Pd(sparteine)Cl_2 (**66**, 10.3 mg, 0.025 mmol, 0.05 equiv) was added, followed by the solvent mixture (1 mL) and then **28** (8.0 μL, 0.035 mmol, 0.07 equiv). The reaction tube was cooled to –78 °C, then vacuum evacuated and purged with O_2 (3x). The reaction was allowed to warm to 23 °C and stirred vigorously under a balloon of O_2 (1 atm) for 15 min. Finely powdered Cs_2CO_3 (65.2 mg, 0.20 mmol, 0.40 equiv) was added, followed by a solution of alcohol (±)-**67** (76.1 mg, 0.5 mmol, 1.0 equiv) and tridecane (36.6 μL, 0.15 mmol, 0.30 equiv) in the solvent mixture (1 mL). The reaction was allowed to proceed under O_2 atmosphere at 23 °C. Aliquots were filtered through a small plug of silica gel (Et_2O eluent), evaporated, and analyzed by GC for conversion and chiral HPLC for alcohol ee.

2.4.4 Methods for Determination of Conversion

All conversions were determined by GC (Table 2.4.1) relative to internal standard (tridecane), unless otherwise noted in the text.

Table 2.4.1 Methods for determination of conversion.

entry	alcohol	ketone	GC conditions	alcohol retention time (min)	ketone retention time (min)
1	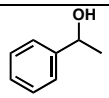 (±)-25	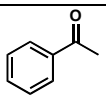 26	100 °C, 5 min; Ramp 13 °C/min	10.6	8.9
2	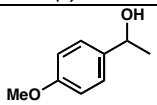 (±)-67	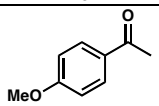 68	100 °C, 5 min; Ramp 13 °C/min	14.4	13.9

2.4.5 Methods for Determination of Enantiomeric Excess

Table 2.4.2 Methods for determination of enantiomeric excess.

entry	compound (major enantiomer)	ee assay and column	assay conditions	(*S*) enantiomer retention time (min)	(*R*) enantiomer retention time (min)
1	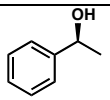 (–)-25	HPLC OJ	4% *i*PrOH/hexanes	17.8	20.8
2	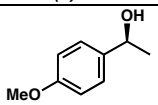 (–)-67	HPLC OD-H	3% EtOH/hexanes	15.7	16.7

2.5 Notes and References

(1) For a discussion of previous methods for catalytic asymmetric alcohol oxidation, see Chapter 1.

(2) For a general discussion of nonenzymatic kinetic resolutions, including resolutions of alcohols, see: (a) Keith, J. M.; Larrow, J. F.; Jacobsen, E. N. *Adv. Synth. Catal.* **2001**, *343*, 5-26. (b) Vedejs, E.; Jure, M. *Angew. Chem., Int. Ed.* **2005**, *44*, 3974-4001.

(3) For examples of alcohol kinetic resolutions involving acylation, see: (a) Vedejs, E.; Daugulis, O.; Diver, S. T. *J. Org. Chem.* **1996**, *61*, 430-431. (b) Vedejs, E.; Daugulis, O.; MacKay, J. A.; Rozners, E. *Synlett* **2001**, 1499-1505. (c) Vedejs, E.; Daugulis, O. *J. Am. Chem. Soc.* **2003**, *125*, 4166-4173. (d) Kawabata, T.; Nagato, M.; Takasu, K.; Fuji, K. *J. Am. Chem. Soc.* **1997**, *119*, 3169-3170. (e) Kawabata, T.; Yamamoto, K.; Momose, Y.; Yoshida, H.; Nagaoka, Y.; Fuji, K. *Chem. Commun.* **2001**, 2700-2701. (f) Ruble, J. C.; Fu, G. C. *J. Org. Chem.* **1996**, *61*, 7230-7231. (g) Ruble, J. C.; Latham, H. A.; Fu, G. C. *J. Am. Chem. Soc.* **1997**, *119*, 1492-1493. (h) Ruble, J. C.; Tweddell, J.; Fu, G. C. *J. Org. Chem.* **1998**, *63*, 2794-2795. (i) Tao, B.; Ruble, J. C.; Hoic, D. A.; Fu, G. C. *J. Am. Chem. Soc.* **1999**, *121*, 5091-5092. (j) Bellemin-Laponnaz, S.; Tweddell, J.; Ruble, J. C.; Breitling, F. M.; Fu, G. C. *Chem. Commun.* **2000**, 1009-1010. (k) Sano, T.; Imai, K.; Ohashi, K.; Oriyama, T. *Chem. Lett.* **1999**, 265-266. (l) Miller, S. J.; Copeland, G. T.; Papaioannou, N.; Horstmann, T. E.; Ruel, E. M. *J. Am. Chem. Soc.* **1998**, *120*, 1629-1630. (m) Jarvo, E. R.; Copeland, G. T.;

Papaioannou, N.; Bonitatebus, P. J., Jr.; Miller, S. J. *J. Am. Chem. Soc.* **1999**, *121*, 11638-11643.

(4) For alcohol kinetic resolutions involving S_N2 displacement, see: (a) Chandrasekhar, S.; Kulkarni, G. *Tetrahedron: Asymmetry* **2002**, *13*, 615-619. (b) Sekar, G.; Nishiyama, H. *J. Am. Chem. Soc.* **2001**, *123*, 3603-3604.

(5) For alcohol kinetic resolutions involving allylic epoxidation, see: (a) Martin, V. S.; Woodard, S. S.; Katsuki, T.; Yamada, Y.; Ikeda, M.; Sharpless, K. B. *J. Am. Chem. Soc.* **1981**, *103*, 6237-6240. (b) Carlier, P. R.; Mungall, W. S.; Schröder, G.; Sharpless, K. B. *J. Am. Chem. Soc.* **1988**, *110*, 2978-2979.

(6) For alcohol kinetic resolution involving allylic hydrogenation, see: Kitamura, M.; Kasahara, I.; Manabe, K.; Noyori, R.; Takaya, H. *J. Org. Chem.* **1988**, *53*, 708-710.

(7) (a) Trost, B. M.; Van Vranken, D. L. *Chem. Rev.* **1996**, *96*, 395-422. (b) Sodeoka, M.; Shibasaki, M. *Pure Appl. Chem.* **1998**, *70*, 411-414. (c) Hayashi, T. *J. Organomet. Chem.* **1999**, *576*, 195-202. (d) Helmchen, G. *J. Organomet. Chem.* **1999**, *576*, 203-214. (e) Trost, B. M. *Chem. Pharm. Bull.* **2002**, *50*, 1-14. (f) RajanBabu, T. V. *Chem. Rev.* **2003**, *103*, 2845-2860. (g) Graening, T.; Schmalz, H.-G. *Angew. Chem., Int. Ed.* **2003**, *42*, 2580-2584. (h) Dounay, A. B.; Overman, L. E. *Chem. Rev.* **2003**, *103*, 2945-2963. (i) Tietze, L. F.; Ila, H.; Bell, H. P. *Chem. Rev.* **2004**, *104*, 3453-3516. (j) Trost, B. M. *J. Org. Chem.* **2004**, *69*, 5813-5837. (k) Sodeoka, M.; Hamashima, Y. *Bull. Chem. Soc. Jpn.* **2005**, *78*,

941-956. (l) Hii, K. K. *Pure Appl. Chem.* **2006**, *78*, 341-349. (m) Sodeoka, M.; Hamashima, Y. *Pure Appl. Chem.* **2006**, *78*, 477-494. (n) Hamashima, Y.; Sodeoka, M. *Synlett* **2006**, 1467-1478.

(8) (a) Lloyd, W. G. *J. Org. Chem.* **1967**, *32*, 2816-2819. (b) Blackburn, T. F.; Schwartz, J. *J. Chem. Soc., Chem. Commun.* **1977**, 157-158. (c) Gómez-Bengoa, E.; Noheda, P.; Echavarren, A. M. *Tetrahedron Lett.* **1994**, *35*, 7097-7098. (d) Aït-Mohand, S.; Hénin, F.; Muzart, J. *Tetrahedron Lett.* **1995**, *36*, 2473-2476. (e) Peterson, K. P.; Larock, R. C. *J. Org. Chem.* **1998**, *63*, 3185-3189. (f) ten Brink, G.-J.; Arends, I. W. C. E.; Sheldon, R. A. *Science* **2000**, *287*, 1636-1639. (g) Hallman, K.; Moberg, C. *Adv. Synth. Catal.* **2001**, *343*, 260-263. (h) Sheldon, R. A.; Arends, I. W. C. E.; ten Brink, G.-J.; Dijksman, A. *Acc. Chem. Res.* **2002**, *35*, 774-781. (i) Schultz, M. J.; Park, C. C.; Sigman, M. S. *Chem. Commun.* **2002**, 3034-3035. (j) ten Brink, G.-J.; Arends, I. W. C. E.; Hoogenraad, M.; Verspui, G.; Sheldon, R. A. *Adv. Synth. Catal.* **2003**, *345*, 497-505. (k) Jensen, D. R.; Schultz, M. J.; Mueller, J. A.; Sigman, M. S. *Angew. Chem., Int. Ed.* **2003**, *42*, 3810-3813. (l) ten Brink, G.-J.; Arends, I. W. C. E.; Hoogenraad, M.; Verspui, G.; Sheldon, R. A. *Adv. Synth. Catal.* **2003**, *345*, 1341-1352. (m) Paavola, S.; Zetterberg, K.; Privalov, T.; Csöregh, I.; Moberg, C. *Adv. Synth. Catal.* **2004**, *346*, 237-244. (n) Iwasawa, T.; Tokunaga, M.; Obora, Y.; Tsuji, Y. *J. Am. Chem. Soc.* **2004**, *126*, 6554-6555.

(9) For reviews of palladium-catalyzed aerobic oxidations, see: (a) Muzart, J. *Tetrahedron* **2003**, *59*, 5789-5816. (b) Stahl, S. S. *Angew. Chem., Int. Ed.* **2004**,

43, 3400-3420. (c) Sigman, M. S.; Schultz, M. J. *Org. Biomol. Chem.* **2004**, *2*, 2551-2554. (d) Stoltz, B. M. *Chem. Lett.* **2004**, *33*, 362-367.

(10) (a) Nishimura, T.; Onoue, T.; Ohe, K.; Uemura, S. *Tetrahedron Lett.* **1998**, *39*, 6011-6014. (b) Nishimura, T.; Onoue, T.; Ohe, K.; Uemura, S. *J. Org. Chem.* **1999**, *64*, 6750-6755. (c) Nishimura, T.; Maeda, Y.; Kakiuchi, N.; Uemura, S. *J. Chem. Soc., Perkin Trans. 1* **2000**, 4301-4305. (d) Nishimura, T.; Uemura, S. *Synlett* **2004**, 201-216.

(11) (a) Steinhoff, B. A.; Stahl, S. S. *Org. Lett.* **2002**, *4*, 4179-4181. (b) Steinhoff, B. A.; Guzei, I. A.; Stahl, S. S. *J. Am. Chem. Soc.* **2004**, *126*, 11268-11278. (c) Privalov, T.; Linde, C.; Zetterberg, K.; Moberg, C. *Organometallics* **2005**, *24*, 885-893. (d) Schultz, M. J.; Adler, R. S.; Zierkiewicz, W.; Privalov, T.; Sigman, M. S. *J. Am. Chem. Soc.* **2005**, *127*, 8499-8507. (e) Steinhoff, B. A.; King, A. E.; Stahl, S. S. *J. Org. Chem.* **2006**, *71*, 1861-1868.

(12) For mechanistic studies of other non-enantioselective palladium-catalyzed alcohol oxidations, see: (a) Stahl, S. S.; Thorman, J. L.; Nelson, R. C.; Kozee, M. A. *J. Am. Chem. Soc.* **2001**, *123*, 7188-7189. (b) Steinhoff, B. A.; Fix, S. R.; Stahl, S. S. *J. Am. Chem. Soc.* **2002**, *124*, 766-767. (c) ten Brink, G.-J.; Arends, I. W. C. E.; Sheldon, R. A. *Adv. Synth. Catal.* **2002**, *344*, 355-369. (d) Mueller, J. A.; Goller, C. P.; Sigman, M. S. *J. Am. Chem. Soc.* **2004**, *126*, 9724-9734. (e) Konnick, M. M.; Guzei, I. A.; Stahl, S. S. *J. Am. Chem. Soc.* **2004**, *126*, 10212-10213. (f) Landis, C. R.; Morales, C. M.; Stahl, S. S. *J. Am. Chem. Soc.* **2004**, *126*, 16302-16303. (g) Zierkiewicz, W.; Privalov, T. *Organometallics* **2005**, *24*,

6019-6028. (h) Arends, I. W. C. E.; ten Brink, G.-J.; Sheldon, R. A. *J. Mol. Catal. A: Chem.* **2006**, *251*, 246-254. (i) Steinhoff, B. A.; Stahl, S. S. *J. Am. Chem. Soc.* **2006**, *128*, 4348-4355. (j) Nielsen, R. J.; Goddard, W. A., III. *J. Am. Chem. Soc.* **2006**, *128*, 9651-9660.

(13) For enantioselective palladium-catalyzed alcohol oxidation mechanistic studies, see: (a) Mueller, J. A.; Jensen, D. R.; Sigman, M. S. *J. Am. Chem. Soc.* **2002**, *124*, 8202-8203. (b) Mueller, J. A.; Sigman, M. S. *J. Am. Chem. Soc.* **2003**, *125*, 7005-7013. (c) Trend, R. M.; Stoltz, B. M. *J. Am. Chem. Soc.* **2004**, *126*, 4482-4483. (d) Nielsen, R. J.; Keith, J. M.; Stoltz, B. M.; Goddard, W. A., III. *J. Am. Chem. Soc.* **2004**, *126*, 7967-7974. (e) Keith, J. M.; Nielsen, R. J.; Oxgaard, J.; Goddard, W. A., III. *J. Am. Chem. Soc.* **2005**, *127*, 13172-13179. (f) Mueller, J. A.; Cowell, A.; Chandler, B. D.; Sigman, M. S. *J. Am. Chem. Soc.* **2005**, *127*, 14817-14824. (g) Popp, B. V.; Stahl, S. S. *J. Am. Chem. Soc.* **2007**, *129*, 4410-4422. (h) Keith, J. M.; Goddard, W. A., III.; Oxgaard, J. *J. Am. Chem. Soc.* **2007**, *129*, 10361-10369.

(14) Ferreira, E. M.; Stoltz, B. M. *J. Am. Chem. Soc.* **2001**, *123*, 7725-7726.

(15) Concurrent with our publication, a related system was reported, see: (a) Jensen, D. R.; Pugsley, J. S.; Sigman, M. S. *J. Am. Chem. Soc.* **2001**, *123*, 7475-7476. (b) Mandal, S. K.; Jensen, D. R.; Pugsley, J. S.; Sigman, M. S. *J. Org. Chem.* **2003**, *68*, 4600-4603. (c) Mandal, S. K.; Sigman, M. S. *J. Org. Chem.* **2003**, *68*, 7535-7537. (d) Sigman, M. S.; Jensen, D. R. *Acc. Chem. Res.* **2006**, *39*, 221-229.

(16) The selectivity factor (*s*) was determined using the following equation: $s = \frac{\ln[(1-conv)(1-ee_{alc})]}{\ln[(1-conv)(1+ee_{alc})]}$, where ee_{alc} is the ee of the recovered alcohol and *conv* is the total conversion of alcohol to ketone, see: Kagan, H. B.; Fiaud, J. C. In *Topics in Stereochemistry*; Eliel, E. L., Ed.; Wiley & Sons: New York, 1988; Vol. 18, pp 249-330.

(17) Recently, similar palladium-catalyzed systems utilizing different ligands for enantioselective alcohol oxidation have been developed, see: (a) Jensen, D. R.; Sigman, M. S. *Org. Lett.* **2003**, *5*, 63-65. (b) Chen, T.; Jiang, J.-J.; Xu, Q.; Shi, M. *Org. Lett.* **2007**, *9*, 865-868. (c) Lesma, G.; Pilati, T.; Sacchetti, A.; Silvani, A. *Tetrahedron: Asymmetry* **2008**, *19*, 1363-1366.

(18) Bagdanoff, J. T.; Ferreira, E. M.; Stoltz, B. M. *Org. Lett.* **2003**, *5*, 835-837.

(19) The beneficial role of carbonates as exogenous bases in the kinetic resolution was subsequently reported by Sigman, see ref 15c.

(20) A significant effect of cesium carbonate structure and particle size has been found for palladium-catalyzed aryl halide aminations in toluene, consistent with a heterogeneous process, see: Meyers, C.; Maes, B. U. W.; Loones, K. T. J.; Bal, G.; Lemiere, G. L. F.; Dommisse, R. A. *J. Org. Chem.* **2004**, *69*, 6010-6017.

(21) Crow, W. D. *Aust. J. Chem.* **1959**, *12*, 474-482.

(22) *CRC Handbook of Chemistry and Physics*, 76th ed.; Lide, D. R., Frederikse, H. P. R., Eds.; New York, 1995; Section 8, p 43.

(23) Addition of sparteine•HCl inhibits alcohol oxidation, see ref 13a.

(24) Sigman has proposed that excess chloride ion in solution may inhibit displacement of chloride by alcohol in Pd(sparteine)Cl_2. Thus, formation of insoluble CsCl may sequester excess chloride and promote alcohol coordination. For details, see ref 13f.

(25) *tert*-Butyl alcohol was found to be a competent solvent for this oxidation, see ref 15b.

(26) Palladium carbonate complex **69** was also observed on prolonged exposure of dichloride complex **66** to cesium carbonate in chloroform at 23 °C.

(27) de Graauw, C. F.; Peters, J. A.; van Bekkum, H.; Huskens, J. *Synthesis* **1994**, 1007-1017.

(28) Bagdanoff, J. T.; Stoltz, B. M. *Angew. Chem., Int. Ed.* **2004**, *43*, 353-357.

(29) *Comprehensive Biological Catalysis*; Sinnott, M., Ed.; Academic Press: San Diego, CA, 1998; Vol. 1-3.

(30) For a recent review, see: Taylor, M. S.; Jacobsen, E. N. *Angew. Chem., Int. Ed.* **2006**, *45*, 1520-1543.

(31) Goddard has proposed that the solubilization of charged intermediates by dichloromethane may be so great as to nearly completely separate the chloride anion from the palladium complex in the β-hydride elimination transition state,

improving the oxidation rate but limiting a key interaction for selectivity, see ref 13d.

(32) Fischer, F.; Pfleiderer, G. *Z. Anorg. Allg. Chem.* **1922**, *124*, 61-69.

(33) For dielectric constant tables, see: *CRC Handbook of Chemistry and Physics*, 76th ed.; Lide, D. R., Frederikse, H. P. R., Eds.; New York, 1995; Section 6, pp 159-192.

(34) The IR spectrum of $CHCl_3$ was also investigated. However, the C-H stretch was not well resolved. $CDCl_3$ performs identically to $CHCl_3$ as reaction solvent.

(35) For a discussion of the hydrogen bonding of chloroform and its effect on IR vibrational frequencies, see: Green, R. D. *Hydrogen Bonding by C–H Groups*; John Wiley & Sons: New York, 1974.

(36) A molecule of chloroform is also within hydrogen bonding distance in the solid-state structure of dichloride complex **66**.

(37) For a brief discussion of the substrate scope of the oxidative kinetic resolution, see: Stoltz, B. M.; Ebner, D. C. Kinetic Resolution by Enantioselective Aerobic Oxidation of Alcohols. In *Handbook of C–H Transformation*, Dyker, G., Ed.; Wiley-VCH: New York, 2005; Vol. 2, pp 393-401.

(38) (a) Caspi, D. D.; Ebner, D. C.; Bagdanoff, J. T.; Stoltz, B. M. *Adv. Synth. Catal.* **2004**, *346*, 185-189. (b) Ebner, D. C.; Novák, Z.; Stoltz, B. M. *Synlett* **2006**, 3533-3539.

(39) (a) Tambar, U. K.; Ebner, D. C.; Stoltz, B. M. *J. Am. Chem. Soc.* **2006**, *128*, 11752-11753. (b) Krishnan, S.; Ramtohul, Y. K.; Bagdanoff, J. T.; Ebner, D. C.; Tambar, U. K.; Stoltz, B. M. *J. Am. Chem. Soc.* in press.

(40) Chisholm, M. H.; Drake, S. R.; Naiini, A. A.; Streib, W. E. *Polyhedron* **1991**, *10*, 337-345.

(41) Alternatively, 5 mol% Pd(sparteine)Cl_2 (**66**) and 15 mol% (–)-sparteine (**28**) can be used.

(42) $CHCl_3$ stabilized with amylenes. $CHCl_3$ stabilized with EtOH must be distilled prior to use.

(43) Alternatively, 5 mol% Pd(sparteine)Cl_2 (**66**) and 7 mol% (–)-sparteine (**28**) can be used.

CHAPTER 3

Scope and Applications of the Oxidative Kinetic Resolution of Secondary Alcohols

3.1 Background and Introduction

The previously described methodology for the palladium-catalyzed oxidative kinetic resolution of secondary alcohols has led to the development of four distinct sets of conditions for this process (Table 3.1.1): the original conditions (A) in toluene with no exogenous base,[1] the rate enhanced conditions (B) that take advantage of cesium carbonate and *tert*-butyl alcohol additives,[2] and the chloroform conditions at 23 °C under an atmosphere of either molecular oxygen (C) or ambient air (D).[3,4] In general, resolutions performed without added carbonate base have slower rates but greater catalyst longevity. The rate enhanced (B) conditions are the fastest, often achieving highly enantioenriched alcohols in a small fraction of the time required for the original (A) conditions. Reactions performed in chloroform at 23 °C (C and D) are the most selective, nearly doubling the *s* factor for the resolution of some alcohols. Typically, both molecular oxygen and ambient air can be used in oxidations in chloroform with similar rates and selectivities. The development of four distinct sets of conditions provides the opportunity to resolve the widest range of alcohol substrates in order to maximize the selectivity of the process while maintaining reactivity and minimizing side reactions. The benefit of this flexibility is evident in the broad scope of this system.[5]

Table 3.1.1 Various conditions for enantioselective alcohol oxidation.

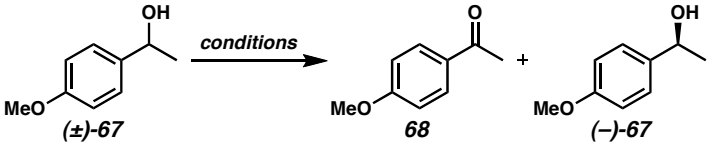

entry	conditions	time	conversion[a]	ee[b]	*s*
A	**$Pd(nbd)Cl_2$ (5 mol%)** **(–)-sparteine (*28*, 20 mol%)** $PhCH_3$ (0.1 M), O_2 MS3Å, 80 °C	96 h	66.6%	98.1%	12
B	**$Pd(nbd)Cl_2$ (5 mol%)** **(–)-sparteine (*28*, 20 mol%)** Cs_2CO_3 (0.5 equiv) *t*-BuOH (1.5 equiv) $PhCH_3$ (0.25 M), O_2 MS3Å, 60 °C	9.5 h	67.4%	99.5%	15
C	**$Pd(nbd)Cl_2$ (5 mol%)** **(–)-sparteine (*28*, 12 mol%)** Cs_2CO_3 (0.4 equiv) $CHCl_3$ (0.25 M), **O_2** MS3Å, 23 °C	48 h	62.6%	99.9%	27
D	**$Pd(nbd)Cl_2$ (5 mol%)** **(–)-sparteine (*28*, 12 mol%)** Cs_2CO_3 (0.4 equiv) $CHCl_3$ (0.25 M), **Air** MS3Å, 23 °C	24 h	62.3%	99.8%	25

[a] Measured by GC. [b] Measured by chiral HPLC.

Initially, the investigated scope of this reaction was limited. A broad survey of secondary alcohols was undertaken in order to evaluate the generality of the conditions toward oxidation and successful resolution. Furthermore, these studies were intended to test the developed selectivity models of the catalyst.[6] Finally, substrate scope exploration would demonstrate the utility of the process, leading to practical applications.

3.2 Substrate Scope of the Palladium-Catalyzed Enantioselective Oxidation

3.2.1 Benzylic Alcohols[†]

Early substrate scope investigations focused on benzylic alcohols.[1-3] Many members of this class of alcohols are commercially available or readily prepared as

[†] This work was performed in collaboration with Eric M. Ferreira (Ph.D. 2005), Jeffrey T. Bagdanoff (Ph.D. 2005), Daniel D. Caspi (Ph.D. 2008), and Ryan M. McFadden (Ph.D. 2007), graduate students in the Stoltz group at California Institute of Technology.

racemates. In particular, 1-arylethanols are easily accessible. Furthermore, the aryl and methyl groups are sterically and electronically quite different. Thus, the palladium catalyst is highly successful in distinguishing enantiomers in the oxidation, leading to high selectivity across a range of aryl groups (Table 3.2.1). Substrates with electron-rich aromatic rings are the most successful in this transformation. Substitution on the aryl ring at the 3- and 4-positions (entries 1-12, 18, 22-25) is well tolerated. Ortho-substitution leads to much slower rates of oxidation (entries 13-15, 26 and 27), although reactivity improves if the substituent is constrained in a ring (entries 16 and 17). 3,5-substituted aromatic rings, even with bulky substituents, are resolved with excellent *s* factors. Some heteroaromatic substrates (entries 28 and 29) can be resolved to high enantiomeric excesses as well.

Table 3.2.1 Resolution of 1-arylethanols.

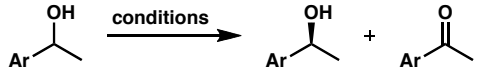

entry	alcohol, major enantiomer		conditions[a]	time	conversion[b]	alcohol ee[c]	*s*
1	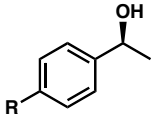	***(–)-25***: R = H	A	96 h	59.9%	98.7%	23
2			B	12.5 h	63.9%	99.6%	20
3			C	48 h	59.9%	99.7%	31
4			D	24 h	54.0%	93.3%	30
5		***(–)-67***: R = OMe	A	96 h	66.6%	98.1%	12
6			B	9.5 h	67.4%	99.5%	15
7			C	48 h	62.6%	99.9%	27
8			D	24 h	62.3%	99.8%	25
9		***(–)-71***: R = F	A	54 h	63.3%	97.4%	14
10			B	12.5 h	65.7%	97.4%	12
11			C	48 h	59.3%	98.0%	23
12			D	24 h	56.7%	93.0%	20
13	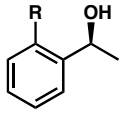	***(–)-72***: R = Me	A	144 h	48.4%	68.7%	13
14			C	63 h	40.1%	49.2%	11
15		***(–)-73***: R = OMe	C	114 h	58.4%	83.9%	10
16	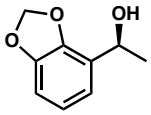	***(–)-74***	B	15 h	56.5%	99.7%	47
17			C	12 h	55.0%	95.0%	29
18	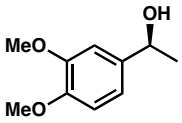	***(–)-75***	B[d]	18 h	63.8%	98.3%	15
19	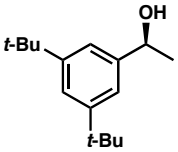	***(–)-76***	A	28 h	51.9%	92.7%	44
20			C	24 h	54.3%	98.0%	47
21			D	22 h	53.9%	98.3%	54
22	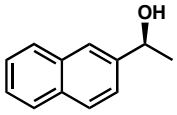	***(–)-77***	A	112 h	55.2%	99.0%	47
23			B	12 h	66.1%	99.4%	16
24			C	48 h	59.3%	99.6%	31
25			D	24 h	55.5%	98.0%	37
26		***(–)-78***: Ar = 1-Naphthyl	A	192 h	55.9%	78.4%	9.8
27			C	97 h	51.2%	65.9%	8.5
28		***(–)-79***: Ar = 2-Furyl	A	120 h	66.9%	93.8%	8.3
29		***(–)-80***: Ar = 3-Furyl	A	120 h	67.4%	93.5%	8.8

[a] For conditions, see Table 3.1.1. [b] Measured by GC or NMR. [c] Measured by chiral HPLC or chiral GC. [d] Conducted at 40 °C.

Benzylic alcohols with other structural variations are also tolerated by the catalyst system (Table 3.2.2). Cyclic benzylic alcohols are able to be resolved successfully. 1-Indanol (**81**, entries 1-3) is oxidized rapidly, albeit with decreased selectivity, compared to 1-tetralol (**82**, entries 4-7). Alcohols with a variety of β-heteroatom substituents, such as ethers (entries 12 and 13) and protected amines (entries 16-20),[7,8] can be resolved with good selectivity. Other functional groups on the alcohol substrate, including alkyl chains (entries 8-11, 21), a methyl ester (**86**, entry 14), a tertiary alcohol (**87**, entry 15), and even aryl bromides (entries 14 and 15), are tolerated under the reaction conditions.

Table 3.2.2 Resolution of other benzylic alcohols.

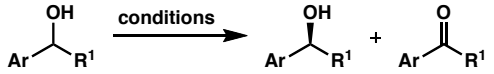

entry	alcohol, major enantiomer	conditions[a]	time	conversion[b]	alcohol ee[c]	*s*
1	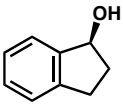 ***(+)-81***	A[d]	54 h	67.5%	93.4%	8.3
2		B[e]	12 h	74.0%	99.5%	10
3		C	24 h	68.5%	97.5%	10
4	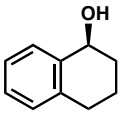 ***(+)-82***	A	40 h	68.6%	99.8%	16
5		B[e]	12 h	61.5%	99.0%	21
6		C	24 h	57.5%	98.0%	28
7		D	16 h	60.2%	99.6%	28
8	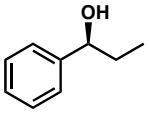 ***(–)-83***	A	192 h	59.3%	93.1%	15
9		B[f]	4.5 h	62.8%	98.0%	16
10		C	72 h	62.6%	98.2%	24
11		D	48 h	56.8%	94.9%	22
12	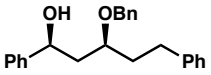 ***(1S,3S)-84***	C[e]	72 h	57.7%	99.0%	32
13	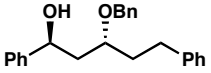 ***(1S,3R)-85***	C[e]	72 h	53.0%	88.2%	24
14	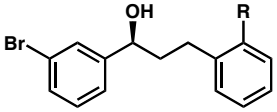 ***(S)-86***: R = CO_2Me	B[f]	4.5 h	62.5%	92.9%	11
15	***(–)-87***: R = $C(OH)Me_2$	B[f]	4.5 h	70.6%	99.9%	15
16	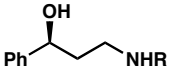 ***(–)-88***: R = Ac	A	14.5 h	70.0%	97.0%	9.0
17	***(–)-89***: R = Boc	A	24 h	57.5%	93.1%	18
18	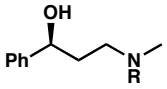 ***(S)-90***: R = Ac	C	24 h	52.3%	82.1%	18
19	***(S)-91***: R = Boc	C	24 h	57.5%	95.1%	21
20	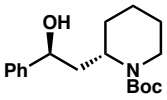 ***(–)-92***	D	60 h	53.8%	94.2%	33
21	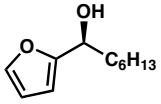 ***(S)-93***	C	122 h	55.4%	75.4%	9.0

[a-c] See Table 3.2.1 footnotes. [d] Conducted at 60 °C. [e] Conducted at 40 °C. [f] Conducted at 80 °C.

3.2.2 Allylic Alcohols

The broad utility of chiral allylic alcohols in organic synthesis led to an investigation of this important class of molecules next. Conditions in chloroform are particularly effective for these substrates, providing enhanced selectivity over the other

methods (Table 3.2.3). These studies demonstrate the importance of steric factors in determining catalyst selectivity. Cyclohexenols with relatively small substituents (entries 1-4) are oxidized rapidly but with low selectivity. However, the enantiomers of alcohols with larger substituents (entries 5-7) are better distinguished by the catalyst, leading to higher *s* factors. Cyclopentenols (entries 14-24) undergo faster oxidation with lower selectivity than their cyclohexenol counterparts (entries 2-13). Of particular note are vinyl bromides (entries 8-10, 18-20), which decompose rapidly with darkening of the reaction mixture at elevated temperatures, indicating the formation of aggregated Pd(0). Under conditions at 23 °C, on the other hand, little catalyst decomposition is observed and reactions proceed to desirable (50-70%) conversion values. While cyclopentenol **101** is oxidized fast enough to allow moderate resolution at 60 °C with cesium carbonate and *tert*-butyl alcohol (entry 19), cyclohexenol **97** is resolved successfully only at lower temperatures (entries 9 and 10). Alkyl enol ethers are stable in the reactions and are resolved to high enantiomeric excess (entries 11-13, 21-24), providing access to enantioenriched α-hydroxyketone derivatives. The catalyst is also tolerant of a variety of alkene substitution patterns (entries 25-40), again generally displaying higher enantiomer preference in chloroform at 23 °C than in toluene at higher temperatures. Resolution of acyclic allylic alcohols has proven more challenging, though Eric Ferreira and Jeffrey Bagdanoff, graduate students in these laboratories, found that allylic alcohol **104** could be obtained with good selectivity at 23 °C in chloroform (entries 31 and 32).

Table 3.2.3 Resolution of cyclic allylic alcohols.

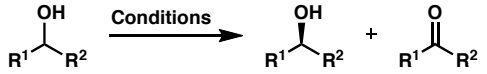

entry	alcohol, major enantiomer	conditions[a]	time	conversion[b]	alcohol ee[c]	*s*
1	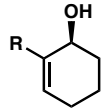 ***(–)-94***: R = H	A	4 h	63.5%	8.1%	1.2
2	***(–)-95***: R = Me	A	7 h	59.1%	36.6%	2.3
3		B	8 h	78.6%	95.8%	5.4
4		C	24 h	69.3%	84.5%	5.4
5	***(–)-96***: R = *i*-Pr	A	28.5 h	65.9%	95.9%	11
6		B	50 h	64.8%	84.2%	6.7
7		C	31 h	51.2%	74.0%	13
8	***(–)-97***: R = Br	A	73 h	25.7%	30.0%	19
9		C	33 h	63.9%	96.1%	12
10		D	25 h	54.7%	86.3%	16
11	***(S)-98***: R = O*i*-Bu	A	94 h	56.2%	73.1%	7.8
12		B	50 h	34.0%	34.5%	7.1
13		C	74 h	52.2%	85.9%	23
14	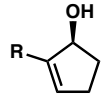 ***(S)-99***: R = Me	C	8 h	66.1%	65.8%	3.7
15	***(–)-100***: R = *i*-Pr	A	25 h	66.6%	76.0%	4.8
16		B	21 h	71.9%	93.0%	6.5
17		C	31 h	76.0%	93.7%	5.5
18	***(S)-101***: R = Br	A	24 h	42.5%	29.4%	3.0
19		B	4 h	75.1%	97.2%	7.0
20		C	24 h	63.6%	75.6%	5.4
21	***(S)-102***: R = O*i*-Bu	A	69 h	68.3%	90.9%	7.1
22		B	50 h	69.8%	99.0%	11
23		C	45 h	65.4%	99.0%	15
24		D	24 h	57.4%	96.9%	17
25	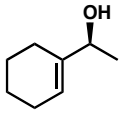 ***(–)-103***	A	13 h	45.5%	57.4%	9.5
26		B	7.5 h	63.5%	74.1%	5.2
27		C	43 h	63.7%	96.5%	13
28		D	42.5 h	60.5%	91.4%	12
29	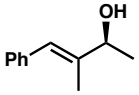 ***(+)-104***	A	120 h	70.4%	91.8%	6.6
30		B	12 h	65.1%	87.9%	7.5
31		C	48 h	62.6%	98.7%	18
32		D	44 h	64.7%	98.9%	16
33	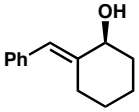 ***(–)-105***	A	25 h	51.6%	69.1%	9.5
34		B	21 h	57.0%	79.7%	9.5
35		C	45 h	56.8%	90.9%	17
36		D	24 h	62.7%	98.4%	17
37	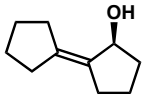 ***(+)-106***	A	48 h	53.7%	80.9%	14
38		B	10 h	62.3%	84.2%	7.7
39		C	75 h	57.4%	93.8%	19
40		D	24 h	58.0%	78.0%	8.2

[a-c] See Table 3.2.1 footnotes.

The successful resolution of benzylic alcohols prompted an exploration of aryl substituents on cyclic allylic alcohols. These substrates are readily prepared via Suzuki coupling of arylboronate esters and iodoenones[9] followed by Luche reduction (Scheme 3.2.1).[10] Gratifyingly, subjection of these alcohols to any of our developed kinetic resolution conditions affords highly enantioenriched allylic alcohols (Table 3.2.4).[11] Both electron-rich (entries 9-12) and electron-poor (entries 17-19) 2-aryl substituents lead to excellent selectivity. The lack of a large electronic influence on these resolutions suggests selectivity is primarily due to steric factors. Reactivity, on the other hand, is not adversely affected by the arene substituent. In many cases, these alcohols are oxidized as fast as 2-alkyl substituted alcohols (e.g., **95**, **96**, **99**, and **100**). Even heteroaromatic substitution (entries 28-31) and a larger ring size (entries 32-34) are tolerated, in some cases with exceptionally high selectivity (entry 32, s = 122), albeit with somewhat longer reaction times.

Scheme 3.2.1 Synthesis of 2-arylcycloalkenols.

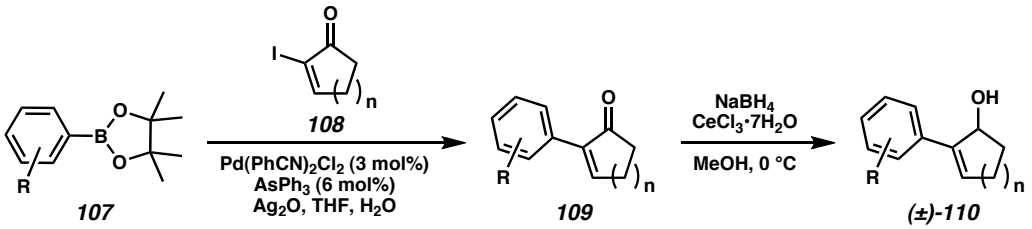

Table 3.2.4 Resolution of 2-arylcycloalkenols.

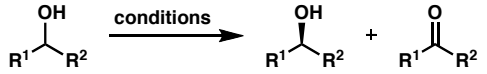

entry	alcohol, major enantiomer	conditions[a]	time	conversion[b]	alcohol ee[c]	*s*
1	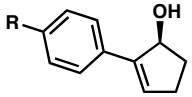 ***(+)-111***: R = H	A	7 h	57.0%	99.7%	44
2		B	1.5 h	52.8%	99.0%	85
3		C	12 h	57.4%	99.0%	33
4		D	10 h	55.8%	99.0%	42
5	***(+)-112***: R = Me	A	10 h	54.8%	92.4%	24
6		B	3.5 h	57.6%	98.8%	31
7		C	11 h	58.8%	99.1%	28
8		D	10 h	55.7%	98.5%	39
9	***(+)-113***: R = OMe	A	31 h	58.0%	99.0%	30
10		B	1.5 h	53.9%	97.3%	46
11		C	24 h	55.0%	92.1%	23
12		D	28.5 h	55.5%	89.0%	17
13	***(+)-114***: R = F	A	10 h	57.4%	99.0%	33
14		B	3.5 h	60.1%	99.0%	24
15		C	11 h	57.9%	98.9%	30
16		D	10 h	58.2%	97.8%	25
17	***(+)-115***: R = CF_3	A	10 h	59.2%	99.0%	26
18		B	1.5 h	62.9%	99.0%	18
19		C	10 h	56.5%	93.6%	21
20	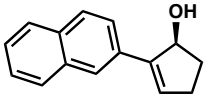 ***(+)-116***	A	10 h	58.6%	99.0%	28
21		B	1.5 h	53.1%	93.6%	37
22		C	11 h	60.8%	99.0%	22
23		D	10 h	56.1%	99.0%	40
24	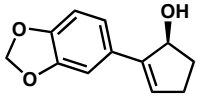 ***(+)-117***	A	24 h	54.1%	99.0%	59
25		B	1.5 h	60.6%	98.8%	22
26		C	10 h	59.4%	98.9%	25
27		D	6 h	56.8%	96.9%	27
28	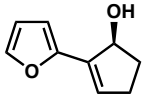 ***(+)-118***	A	49 h	54.0%	87.3%	19
29		B	3 h	51.6%	92.1%	45
30		C	72 h	57.0%	95.8%	23
31		D	42.5 h	57.2%	97.6%	27
32	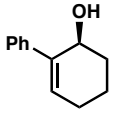 ***(–)-119***	A	17 h	51.9%	99.0%	122
33		B	3 h	56.9%	97.1%	27
34		C	24 h	55.4%	96.8%	33

[a-c] See Table 3.2.1 footnotes.

Substitution at the 3-position of cyclic allylic alcohols was also explored (Table 3.2.5). Again, allylic alcohols with 2-aryl substituents are oxidized rapidly and with exceptionally high selectivity (entries 1-8). These resolutions have some of the highest

selectivities seen with this catalyst system. 3-Substituted alcohols with 2-alkyl substituents are resolved to high enantiomeric excess as well (entries 9-19). Interestingly, analogous 2-alkyl allylic alcohols unsubstituted at the 3-position oxidize with poor selectivity (cf. Table 3.2.5, entries 9-16 and Table 3.2.3, entries 2-4 and 14).

Table 3.2.5 Resolution of 3-substituted allylic alcohols.

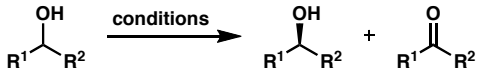

entry	alcohol, major enantiomer	conditions[a]	time	conversion[b]	alcohol ee[c]	*s*
1	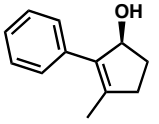 ***(–)-120***	A	4 h	52.9%	99.0%	83
2		B	1 h	53.0%	97.9%	64
3		C	9 h	57.9%	96.9%	23
4		D	6 h	55.4%	94.3%	26
5	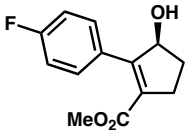 ***(–)-121***	A	4 h	55.6%	99.5%	44
6		B	1 h	55.5%	99.5%	45
7		C	9 h	50.8%	94.7%	83
8		D	20 h	52.8%	98.1%	70
9	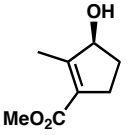 ***(–)-122***	A	8 h	73.3%	98.4%	8.6
10		B	1 h	60.7%	85.2%	9.0
11		C	8 h	74.8%	99.0%	8.7
12		D	8 h	67.6%	93.8%	8.4
13	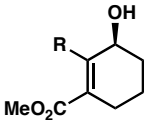 ***(–)-123***: R = Me	A	15 h	58.6%	88.4%	12
14		B	7.5 h	65.0%	99.0%	16
15		C	48 h	62.0%	95.1%	13
16		D	42.5 h	64.4%	96.9%	13
17	***(–)-124***: R = Bn	A	24 h	59.5%	87.2%	11
18		C	72 h	61.0%	90.9%	11
19		D	72 h	62.1%	92.5%	11

[a-c] See Table 3.2.1 footnotes.

3.2.3 Cyclopropylcarbinyl Alcohols

Other activated racemic alcohols were also explored, such as α-cyclopropylcarbinyl alcohols. A number of substrates were exposed to our oxidative kinetic resolution conditions (Table 3.2.6). Again, the chloroform conditions are especially effective in providing highly selective oxidation (cf. entries 2 and 3, entries 6

and 7). Even 1-cyclopropylethanol (**125**, entries 1-4), with relatively little steric differentiation between alcohol substituents, is able to be resolved to high enantiomeric excess. From the appropriate diastereomerically pure racemates, these resolutions also produce alcohols with three contiguous stereocenters (entries 5-15), including a quaternary stereocenter adjacent to the alcohol (entries 9-11). Furthermore, for entries 5-15, the product ketones are also enantioenriched (Figure 3.2.1). Importantly, these molecules have the opposite configuration at C(3) and C(4) relative to the resolved alcohol, opening the door to enantiodivergent opportunities in synthesis.

Table 3.2.6 Resolution of cyclopropylcarbinyl alcohols.

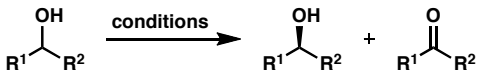

entry	alcohol, major enantiomer	conditions[a]	time	conversion[b]	alcohol ee[c]	*s*
1	 *(+)-125*	A	48 h	69.0%	99.0%	12
2		B	22 h	76.4%	96.3%	6.1
3		C	72 h	67.2%	99.0%	13
4		D	68 h	65.9%	95.5%	10
5	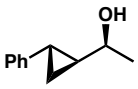 *(+)-126*	A	24 h	68.1%	99.0%	13
6		B	3 h	58.2%	90.5%	14
7		C	25 h	58.6%	99.0%	28
8		D	10.5 h	47.1%	67.4%	14
9	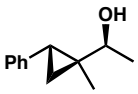 *(+)-127*	A	23 h	61.5%	77.9%	6.5
10		C	71 h	55.4%	99.0%	45
11		D	38 h	57.3%	89.2%	15
12	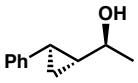 *(–)-128*	A	17 h	65.5%	99.0%	15
13		B	9 h	71.4%	99.0%	10
14		C	24 h	50.8%	76.3%	15
15		D	14.5 h	46.5%	64.3%	13

[a-c] See Table 3.2.1 footnotes.

Figure 3.2.1 Enantioenriched ketones obtained from the resolution.

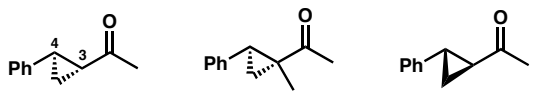

(–)-129 up to 87% ee

(–)-130 up to 85% ee

(+)-129 up to 74% ee

3.2.4 General Trends and Limitations

Though a broad range of secondary alcohols is successfully resolved with this system, limitations to the methodology exist. A number of alcohols display limited rates of oxidation, preventing their resolution (Figure 3.2.2). Benzylic alcohols with ortho-substituents (e.g., (±)-**78** and (±)-**72**) and sterically hindered alcohols such as (±)-**131** and (±)-**132** have dramatically decreased reaction rates. The presence of vicinal heteroatoms (e.g., (±)-**133** and (±)-**134**) impedes the oxidation, presumably through catalyst coordination and deactivation.[12] Finally, unactivated alcohols (e.g., (±)-**135** and (±)-**136**), particularly primary alcohols, are slow to oxidize under any of our developed conditions.[13]

Figure 3.2.2 Alcohols of low reactivity in the oxidation.

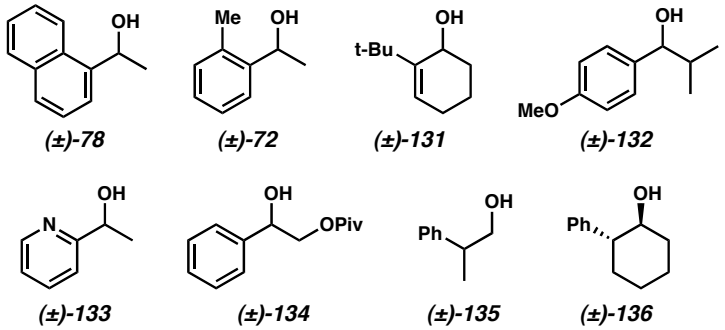

In addition to unreactive alcohols, certain classes of alcohols are resolved with poor selectivity (Figure 3.2.3). In some cases, the steric difference between the two alcohol substituents seems too small for the catalyst to adequately distinguish between enantiomers (e.g., (±)-**95**, (±)-**137**, and (±)-**138**). Benzylic alcohols with electron-poor aromatic substituents are much less selectively resolved than their electron-rich counterparts (cf. (±)-**139** and (±)-**140** with Table 3.2.1, entries 5-8 and 19-21, respectively). At least in the case of benzylic alcohols, steric effects alone do not fully

account for these selectivity differences. Saturated alcohols, such as (±)-**14** also tend to display lower selectivity factors in the resolution.

Figure 3.2.3 Alcohols oxidized with low selectivity.

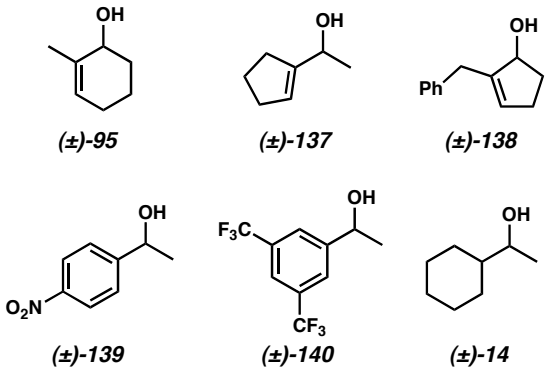

3.2.5 Selectivity Model

Theoretical calculations of the oxidative kinetic resolution by the Goddard group[14] and X-ray crystallographic analysis of a number of palladium complexes by Raissa Trend, a graduate student in these laboratories,[6] have led to a better understanding of the major factors involved in determining the preference of the catalyst for oxidation of one enantiomer of alcohol over the other. Key to high selectivity is a substrate-counterion interaction in the transition state for β-hydride elimination (Scheme 3.2.2). For a racemic mixture of alcohols (±)-**111**, poorly selective alcohol complexation forms a diastereomeric mixture of palladium alkoxides (**141** and **144**). Complex **141** is able to proceed through the β-hydride elimination transition state (**142**) by displacement of the coordinated chloride ion into an apical position of the complex to subsequently generate product ketone **143**. Diastereomeric complex **144**, on the other hand, develops an unfavorable steric interaction in the transition state (**145**), increasing the energy barrier for this process. Substrates such as cyclopentenol (±)-**111** are conformationally restricted

such that the projecting aryl ring is forced into the apical position of the resulting palladium alkoxide. Thus, the *S*-enantiomer has a significantly higher barrier to β-hydride elimination than the *R*-enantiomer, leading to the observed high selectivity factors. Similar steric effects can explain the observed selectivity for other classes of secondary alcohols as well.

Scheme 3.2.2 Model for selectivity of the resolution.

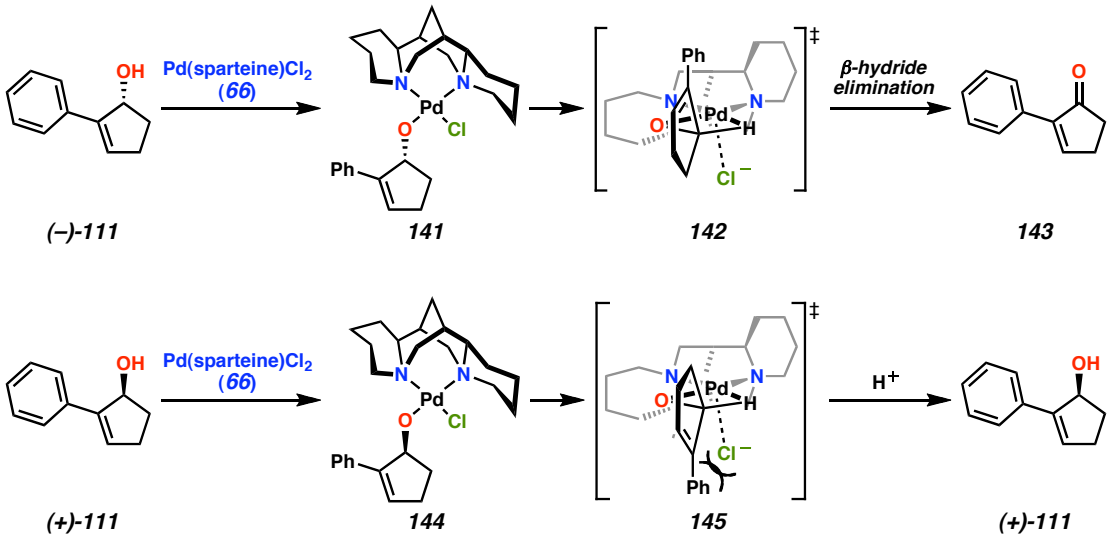

3.3 Applications

3.3.1 *meso*-Diol Desymmetrizations

In addition to kinetic resolution, the catalyst system is well suited for selective oxidation of *meso*-diols to hydroxyketones. These reactions have the potential to provide highly enantioenriched products in greater than 50% yield. Eric Ferreira has demonstrated one example of this process with the initially developed resolution conditions (Scheme 3.3.1). Selective oxidation of diol **146** provides hydroxyketone (+)-**147** in 72% yield and 95% ee.[1]

Scheme 3.3.1 Desymmetrization of *meso*-diol **146**.

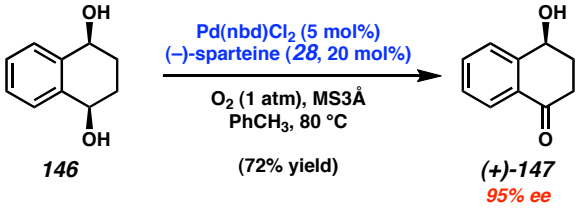

To further demonstrate the utility of the palladium-catalyzed enantioselective alcohol oxidation, Jeffrey Bagdanoff investigated several *meso*-diol arrays. Exploiting a bidirectional chain synthesis approach,[15,16] four diastereomerically pure *meso*-diols were prepared in a small number of steps. Exposure of these *meso*-diols to catalytic quantities of Pd(sparteine)Cl_2 (**66**) and (–)-sparteine (**28**) under a balloon of oxygen in chloroform provides highly enantioenriched hydroxyketones in excellent yields (Scheme 3.3.2). These reactions establish the absolute configuration of four stereocenters in a single catalytic asymmetric operation, allowing the construction of stereodefined 1,2- and 1,3-bis-ether arrays in high enantiomeric excesses.

Scheme 3.3.2 Desymmetrization of polyether *meso*-diols.

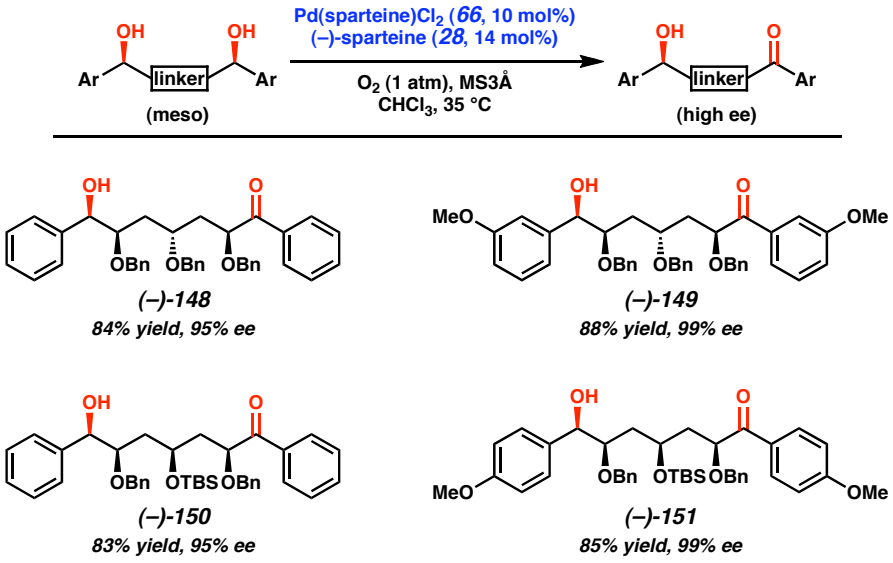

3.3.2 Kinetic Resolution / Claisen Sequence[‡]

To further highlight the utility of the enantioselective alcohol oxidation, the conversion of resolved alcohols into other synthetically useful building blocks was explored. The Claisen rearrangement of 2-aryl allylic alcohols was pursued (Table 3.3.1).[11] Both Ireland-Claisen[17] and Johnson orthoester Claisen conditions[18] did not provide the desired rearrangement products. However, the allylic alcohols can be transformed into the corresponding vinyl ethers by a Hg-catalyzed vinylation procedure. Although yields for this vinylation process are modest, the remainder of the mass balance is predominantly recovered allylic alcohol. Modification of the protocol, including the use of stoichiometric $Hg(OAc)_2$ and variations in temperature and reaction time, do not improve yields.

[‡] This work was performed in collaboration with Dr. Zoltán Novák, a postdoctoral researcher in the Stoltz group at California Institute of Technology.

Table 3.3.1 Claisen rearrangement of allylic alcohols.

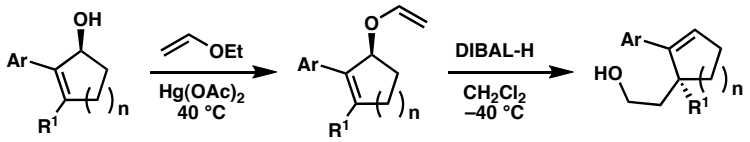

entry	vinyl ether	vinyl ether yield	Claisen product	yield
1	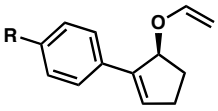	***152***: R = H	43%	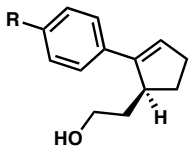	***161***: R = H	36%
2		***153***: R = Me	42%		***162***: R = Me	77%
3		***154***: R = OMe	36%		***163***: R = OMe	91%
4		***155***: R = CF_3	37%		***164***: R = CF_3	82%
5	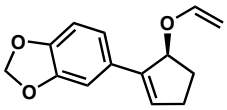	***156***	56%	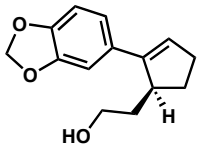	***165***	76%
6	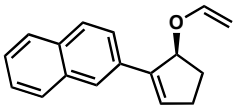	***157***	47%	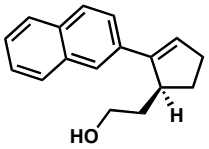	***166***	86%
7	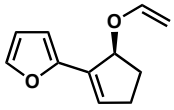	***158***	31%	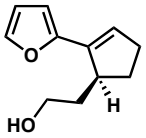	***167***	87%
8	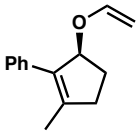	***159***	61%	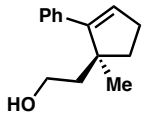	***168***	82%
9	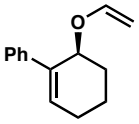	***160***	16%	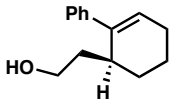	***169***	83%

Next, the Claisen rearrangement of these vinyl ethers was investigated. Thermal conditions and treatment with a number of Lewis acids at low temperature lead to competing Claisen and 1,3-rearrangement products. Gratifyingly, exposure of vinyl ethers to DIBAL-H at low temperature induces Claisen rearrangement and subsequent reduction to form the desired primary alcohols in good to excellent yields in most cases. Importantly, because the kinetic resolution is able to produce the starting allylic alcohols

in high enantiomeric excess, the product alcohols are also highly enantioenriched. Even the Claisen rearrangement of vinyl ether **159** to form a quaternary carbon center proceeds in good yield and high enantiomeric excess. Furthermore, alcohol **168** can undergo a second palladium-catalyzed oxidative process developed in our laboratories[19] to form highly enantioenriched tetrahydrofuran **170** containing vicinal, fully substituted stereocenters in 85% yield (Scheme 3.3.3).

Scheme 3.3.3 Oxidative cyclization of a Claisen product.

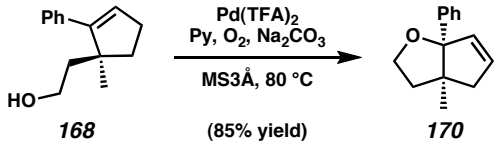

168 **(85% yield)** ***170***

3.3.3 Resolution of Pharmaceutical Intermediates

The wide use of enantioenriched alcohols in synthesis provides numerous applications for the kinetic resolution. A number of alcohols successfully resolved are intermediates in the synthesis of a variety of pharmaceuticals (Scheme 3.3.4).[7,20] Daniel Caspi, a graduate student in these laboratories, successfully resolved Boc-protected γ-aminoalcohol (–)-**89** and bromoarene (–)-**87** to high enantiomeric excess with good corresponding selectivity. Aminoalcohol (–)-**89** can be transformed into an intermediate in the synthesis of a number of antidepressants, including fluoxetine•HCl (Prozac, **171**).[21] Bromoarene (–)-**87** can be converted into a known intermediate in the synthesis of the leukotriene receptor antagonist montelukast sodium (Singulair, **172**).[22] Finally, allylic alcohol (–)-**121**, resolved with an outstanding *s* factor of 83, is an intermediate in the enantioselective synthesis of hNK-1 receptor antagonist **173**.[23]

Scheme 3.3.4 Resolved alcohols as pharmaceutical intermediates.

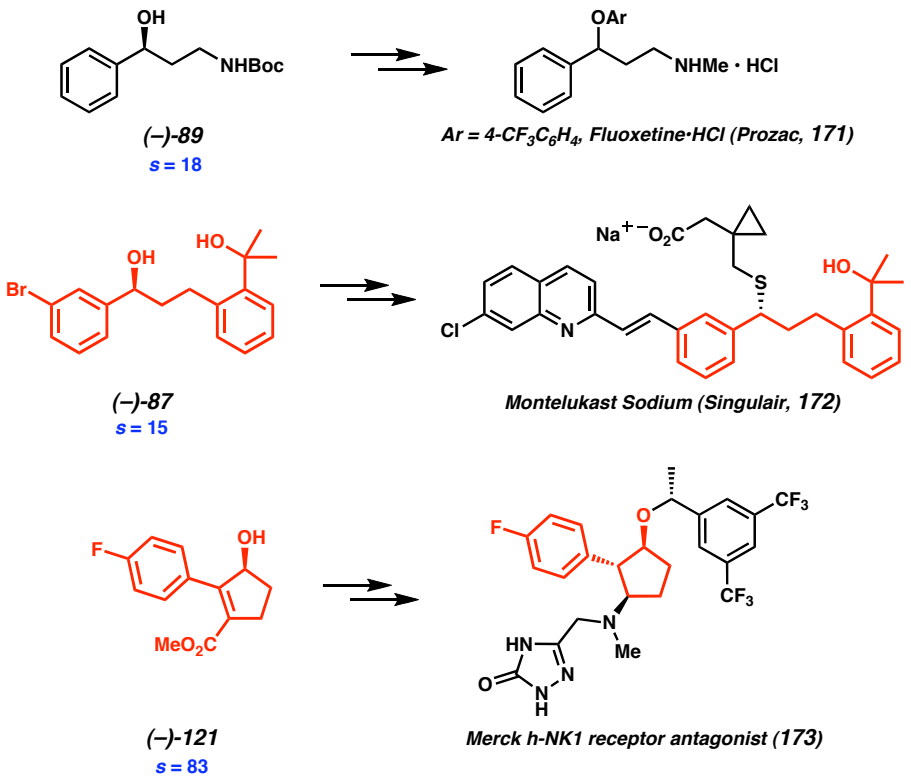

3.3.4 Resolution of Intermediates in Natural Product Syntheses

The palladium-catalyzed oxidative kinetic resolution has also been applied to the construction of enantioenriched secondary alcohols in the context of natural product total synthesis. Michael Meyer, a graduate student in these laboratories, has prepared 2-arylcyclopentenol (±)-**175** en route to the complex gorgonian-derived diterpene bielschowskysin (**176**).[24] Oxidative kinetic resolution of this more functionalized analogue of furan **118** proceeds with excellent selectivity (s = 23) to provide enantioenriched ketone (*S*)-**174** and resolved alcohol (*1S*, *4R*)-**175**. The product ketone maps onto the stereochemically rich cyclopentane and dihydrofuran of bielschowskysin, potentially providing access to this anticancer natural product as a single enantiomer. Furthermore, the alcohol obtained from the resolution has the opposite configuration at

C(4), opening the door to stereodivergent approaches to both enantiomers of bielschowskysin (**176** and **177**) from a single enantioselective oxidation.

Scheme 3.3.5 Enantioselective oxidations for natural product synthesis.

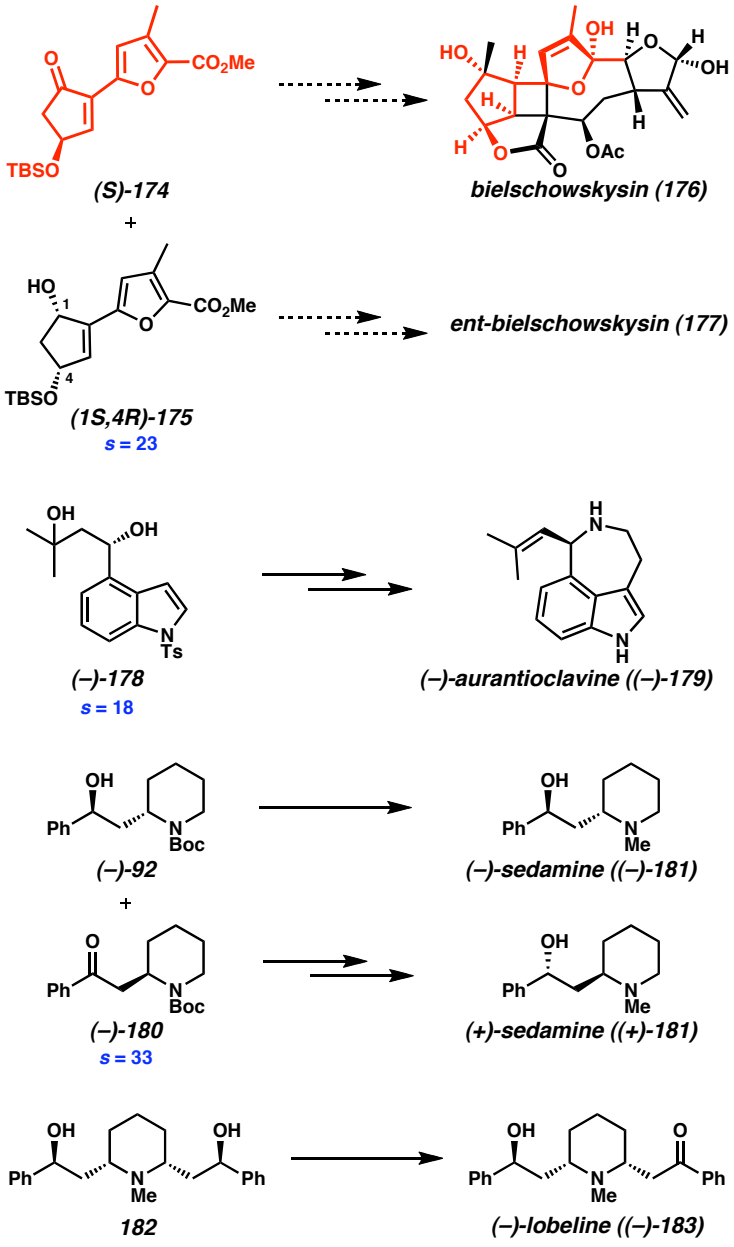

Efforts within these laboratories by postdoctoral researchers Dr. Yeeman Ramtohul and Dr. Shyam Krishnan have demonstrated a successful oxidative kinetic

resolution of indole (±)-**178** using slightly modified conditions in *tert*-butyl alcohol as solvent. Highly enantioenriched indole (–)-**178** has been advanced to the first enantioselective total synthesis of the ergot alkaloid (–)-aurantioclavine ((–)-**179**).[8]

Jeffrey Bagdanoff has prepared piperidine (–)-**92** by enantioselective oxidation of the diastereomerically pure racemate. Boc group reduction affords the natural product (–)-sedamine ((–)-**181**). Enantioenriched ketone (–)-**180** is also obtained from the oxidative kinetic resolution. Diastereoselective ketone reduction and subsequent Boc group reduction provides (+)-sedamine ((+)-**181**). Finally, *meso*-diol **182** undergoes a palladium-catalyzed oxidative desymmetrization to directly afford the nicotinic acetylcholine receptor antagonist alkaloid (–)-lobeline ((–)-**183**).[8]

3.4 Conclusion

Palladium-catalyzed aerobic oxidation is a powerful method for the preparation of enantioenriched secondary alcohols. The development of a number of distinct reaction protocols has allowed the kinetic resolution of a wide range of substrates under mild conditions. Benzylic, allylic, and α-cyclopropyl alcohols can be resolved to high enantiomeric excesses, in many cases with excellent selectivity. Extensive substrate scope studies have revealed general trends in the reactivity and selectivity of the oxidative kinetic resolution, providing a better understanding of this transformation. When diastereomerically pure racemic alcohols are exposed to oxidative kinetic resolution conditions, both enantioenriched alcohols and ketones can be obtained, allowing for enantiodivergent synthetic strategies. These studies have also led to numerous practical applications, including *meso*-diol desymmetrizations, subsequent transformations via Claisen rearrangement, preparation of enantioenriched

pharmaceutically-relevant structures, and intermediates in the total synthesis of a number of natural products. Further efforts to utilize this enantioselective oxidation in complex molecule synthesis are ongoing.

3.5 Experimental Section

3.5.1 Materials and Methods

Pd(sparteine)Cl_2 (**66**) was prepared as previously reported.[6] $Pd(PhCN)_2Cl_2$ and $Pd(TFA)_2$ were purchased from Strem Chemicals, Inc., Newburyport, MA. (±)-2-Methylcyclohex-2-enol ((±)-**95**) was prepared by the method of Minehan.[25] (±)-2-Bromocyclohex-2-enol ((±)-**97**) and (±)-2-bromocyclopent-2-enol ((±)-**101**) were prepared by the method of Murphy.[26] (±)-2-Methylcyclopent-2-enol ((±)-**99**) was prepared by the method of Bunnelle.[27] Authentic samples of ketones not commercially available were prepared as for ketone **186** from the corresponding alcohol, unless otherwise noted. Pyridine and Et_3N were distilled over CaH_2. Solvents were dried by passage through an activated alumina column under argon. Powdered 3Å molecular sieves were stored in a 120 °C drying oven until immediately prior to use. Other chemicals were prepared as described below or purchased from the Sigma-Aldrich Chemical Company and used as received. Unless stated otherwise, reactions were performed in flame-dried glassware sealed with rubber septa under a nitrogen atmosphere using dry, deoxygenated solvents. Liquids and solutions were transferred via syringe. Reaction temperatures were controlled using an IKAmag temperature modulator. Thin-layer chromatography (TLC) and preparative TLC were conducted with E. Merck silica gel 60 F254 pre-coated plates (0.25 mm) and visualized using a combination of UV at 254 nm, *p*-anisaldehyde, and potassium permanganate staining. ICN silica gel (particle size 32-63 μm) or SiliCycle Silia*Flash* P60 Academic silica gel (particle size 40-63 μm; pore diameter 60 Å) was used for flash column chromatography. Bulb-to-bulb distillations were performed with a Büchi Glass Oven B-585 Kugelrohr. Analytical

achiral GC was performed on an Agilent 6850 GC with FID detector using an Agilent DB-WAX (30.0 m x 0.25 mm) column at 1.0 mL/min He carrier gas flow. Chiral GC was performed on an Agilent 6850 GC with FID detector using a Chiraldex GTA column (30.0 m x 0.25 mm, purchased from Bodman Industries) at 1.0 mL/min He carrier gas flow. Analytical chiral HPLC was performed with an Agilent 1100 Series HPLC utilizing a Chiralpak AD, Chiralcel OD-H, Chiralcel OJ, Chiralpak AS, or Chiralcel OB-H column (each is 4.6 mm x 25 cm) obtained from Daicel Chemical Industries, Ltd with visualization at 254 nm at 1.0 mL/min mobile phase. ^{1}H NMR spectra were recorded on a Varian Mercury 300 instrument (at 300 MHz) and are reported relative to Me_4Si (δ 0.0). Data for ^{1}H NMR spectra are reported in terms of chemical shift (δ ppm), multiplicity, coupling constant (Hz), and integration. ^{13}C NMR spectra were recorded on a Varian Mercury 300 instrument (at 75 MHz) and are reported relative to Me_4Si (δ 0.0). Data for ^{13}C NMR spectra are reported in terms of chemical shift (δ ppm), multiplicity, and coupling constant (^{19}F, Hz). ^{19}F NMR spectra were recorded on a Varian Mercury 300 instrument (at 282 MHz) and are reported relative to external F_3CCO_2H standard (δ –76.53). Data for ^{19}F NMR spectra are reported in terms of chemical shift (δ ppm). IR spectra were recorded on a Perkin Elmer Paragon 1000 or Spectrum BX II spectrometer and are reported in terms of frequency of absorption (cm^{-1}). High resolution mass spectra were obtained from the California Institute of Technology Mass Spectral Facility. Optical rotations were measured with a Jasco P-1010 polarimeter at 589 nm using a 100 mm path-length cell. The absolute configurations of resolved alcohols were assigned based on comparisons of optical rotations to literature values or by analogy.

3.5.2 General Oxidative Kinetic Resolution Conditions

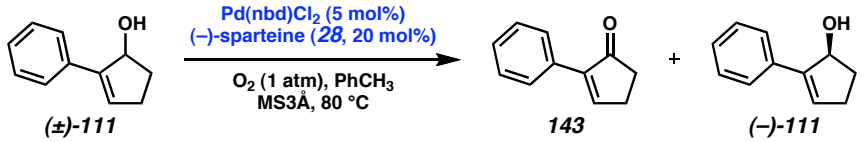

Kinetic Resolution Conditions A.[1] To an oven dried reaction tube with stir bar was added 3Å molecular sieves (250 mg). After cooling, $Pd(nbd)Cl_2$ (6.7 mg, 0.025 mmol, 0.05 equiv) followed by toluene (2.5 mL) and then (–)-sparteine (**28**, 23.0 μL, 0.10 mmol, 0.20 equiv) were added.[28] The reaction tube was then cooled to –78 °C, then vacuum evacuated and purged with O_2 (3x). Then, the tube was heated to 80 °C with vigorous stirring under O_2 atmosphere (1 atm, balloon) for 20 min. A solution of (±)-**111** (80.1 mg, 0.50 mmol, 1.0 equiv) and tridecane (36.6 μL, 0.15 mmol, 0.30 equiv) in toluene (2.5 mL) was added, and the reaction was allowed to proceed under O_2 atmosphere at 80 °C. Aliquots were filtered through a small plug of silica gel (Et_2O eluent), evaporated, and analyzed by GC for conversion and chiral HPLC for alcohol ee. Purification of ketone **143** and alcohol (–)-**111** was accomplished by direct chromatography of the crude reaction mixture.

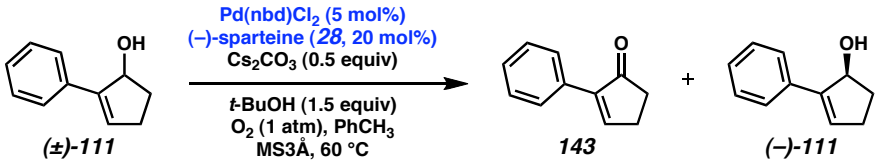

Kinetic Resolution Conditions B.[2] To an oven dried reaction tube with stir bar was added 3Å molecular sieves (500 mg). After cooling, $Pd(nbd)Cl_2$ (13.5 mg, 0.050 mmol, 0.05 equiv), followed by toluene (2 mL) and then (–)-sparteine (**28**, 46.0 μL, 0.20 mmol, 0.20 equiv) were added.[28] The reaction tube was cooled to –78 °C, then vacuum

evacuated and purged with O_2 (3x). The tube was heated to 60 °C with vigorous stirring under O_2 atmosphere (1 atm, balloon) for 20 min. Finely powdered Cs_2CO_3 (163 mg, 0.50 mmol, 0.50 equiv) was added, followed by a solution of (±)-**111** (160 mg, 1.0 mmol, 1.0 equiv), anhydrous *t*-BuOH (143 μL, 1.5 mmol, 1.5 equiv), and tridecane (73.2 μL, 0.30 mmol, 0.30 equiv) in toluene (2 mL). The reaction was allowed to proceed under O_2 atmosphere at 60 °C. Aliquots were filtered through a small plug of silica gel (Et_2O eluent), evaporated, and analyzed by GC for conversion and chiral HPLC for alcohol ee. Purification of ketone **143** and alcohol (–)-**111** was accomplished by direct chromatography of the crude reaction mixture.

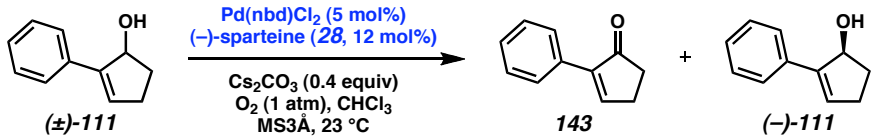

Kinetic Resolution Conditions C.[3] To an oven dried reaction tube with stir bar was added 3Å molecular sieves (250 mg). After cooling, $Pd(nbd)Cl_2$ (6.7 mg, 0.025 mmol, 0.05 equiv), followed by $CHCl_3$ (1 mL)[29] and then (–)-sparteine (**28**, 13.8 μL, 0.06 mmol, 0.12 equiv) were added.[30] The reaction tube was cooled to –78 °C, then vacuum evacuated and purged with O_2 (3x). The reaction was allowed to warm to 23 °C and stirred vigorously under O_2 atmosphere (1 atm, balloon) for 15 min. Finely powdered Cs_2CO_3 (65.2 mg, 0.20 mmol, 0.40 equiv) was added, followed by a solution of (±)-**111** (80.1 mg, 0.5 mmol, 1.0 equiv) and tridecane (36.6 μL, 0.15 mmol, 0.30 equiv) in $CHCl_3$ (1 mL). The reaction was allowed to proceed under O_2 atmosphere at 23 °C. Aliquots were filtered through a small plug of silica gel (Et_2O eluent), evaporated, and analyzed by GC for conversion and chiral HPLC for alcohol ee. Purification of ketone **143** and

alcohol (–)-**111** was accomplished by direct chromatography of the crude reaction mixture.

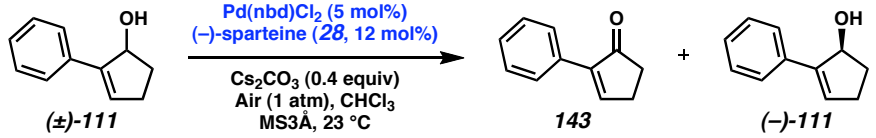

Kinetic Resolution Conditions D.[3] To an oven dried reaction tube with stir bar was added 3Å molecular sieves (250 mg). After cooling, $Pd(nbd)Cl_2$ (6.7 mg, 0.025 mmol, 0.05 equiv), followed by $CHCl_3$ (1 mL)[29] and then (–)-sparteine (**28**, 13.8 μL, 0.06 mmol, 0.12 equiv) were added.[30] A short tube containing Drierite was attached to the reaction tube. The reaction was stirred vigorously at 23 °C for 15 min. Finely powdered Cs_2CO_3 (65.2 mg, 0.20 mmol, 0.40 equiv) was added, followed by a solution of (±)-**111** (80.1 mg, 0.5 mmol, 1.0 equiv) and tridecane (36.6 μL, 0.15 mmol, 0.30 equiv) in chloroform (1 mL). The reaction was allowed to proceed under an ambient air atmosphere at 23 °C. Aliquots were filtered through a small plug of silica gel (Et_2O eluent), evaporated, and analyzed by GC for conversion and chiral HPLC for alcohol ee. Purification of ketone **143** and alcohol (–)-**111** was accomplished by direct chromatography of the crude reaction mixture.

3.5.3 Preparative Procedures

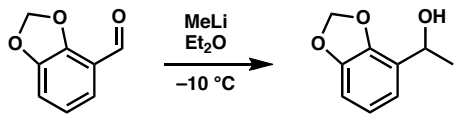

184 *(±)-74*

(±)-1-(Benzo[1,3]dioxol-4-yl)ethanol ((±)-74). A solution of 2,3-(methylenedioxy)benzaldehyde (**184**, 500 mg, 3.05 mmol, 1.0 equiv) in Et_2O (30 mL) was cooled to –10 °C. A solution of methyllithium (1.6 M in Et_2O, 2.48 mL, 3.96 mmol, 1.3 equiv) was added dropwise and the reaction was allowed to warm to 23 °C. The reaction was quenched by addition of crushed ice (10 g) and then saturated aq NH_4Cl (20 mL). The phases were separated, and the aqueous phase was extracted with Et_2O (2 x 30 mL). The combined organic extracts were washed with H_2O (20 mL) and saturated aq NaCl (20 mL), dried over $MgSO_4$, and filtered. The filtrate was concentrated under reduced pressure and purified by flash chromatography (9:1→4:1 hexanes:EtOAc) to afford (±)-**74** as an off-white solid: R_f 0.39 (7:3 hexanes:EtOAc); ^{1}H NMR (300 MHz, $CDCl_3$) δ 6.88 (dd, J = 7.9, 1.7 Hz, 1H), 6.82 (t, J = 7.5 Hz, 1H), 6.76 (dd, J = 7.2, 1.8 Hz, 1H), 5.97 (d, J = 1.6 Hz, 1H), 5.96 (d, J = 1.5 Hz, 1H), 5.00 (q, J = 6.5 Hz, 1H), 2.11 (br. s, 1H), 1.53 (d, J = 6.4 Hz, 3H); ^{13}C NMR (75 MHz, $CDCl_3$) δ 147.4, 143.9, 127.3, 121.8, 118.7, 107.7, 100.9, 66.2, 23.3; IR (thin film/NaCl): 3369, 1460, 1250, 1044 cm^{-1}; HRMS-FAB (*m/z*): $[M]^+$ calcd for $[C_9H_{10}O_3]^+$, 166.0630; found, 166.0630; $[\alpha]_D^{24}$ –26.8° (*c* 1.0, $CDCl_3$; for *S* enantiomer at 99% ee).

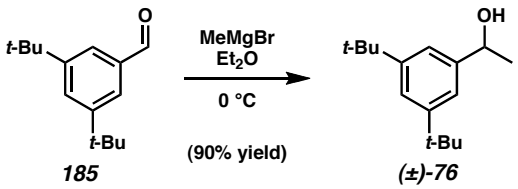

(±)-1-(3,5-Di-*tert*-butylphenyl)ethanol ((±)-76). A solution of 3,5-di-*tert*-butylbenzaldehyde (**185**, 1.09 g, 5.0 mmol, 1.0 equiv) in Et_2O (20 mL) was cooled to 0 °C. A solution of methylmagnesium bromide (3.0 M in Et_2O, 2.5 mL, 7.5 mmol, 1.5 equiv) was added dropwise. The reaction was then quenched by slow addition of saturated aq NH_4Cl (20 mL) and H_2O (10 mL). After warming to 23 °C, the mixture was extracted with EtOAc (3 x 30 mL). The combined organic extracts were dried over $MgSO_4$ and filtered. The filtrate was concentrated under reduced pressure and purified by passage through a short plug of silica gel (2:1 hexanes:EtOAc) to afford (±)-**76** (1.05 g, 90% yield) as a white solid: R_f 0.45 (4:1 hexanes:EtOAc); ^{1}H NMR (300 MHz, $CDCl_3$) δ 7.36 (t, J = 1.9 Hz, 1H), 7.24 (d, J = 1.9 Hz, 1H), 7.24 (d, J = 1.9 Hz, 1H), 4.90 (dq, J = 6.4, 3.2 Hz, 1H), 1.81 (d, J = 3.3 Hz, 1H), 1.52 (d, J = 6.5 Hz, 3H), 1.34 (s, 18H); ^{13}C NMR (75 MHz, $CDCl_3$) δ 151.0, 145.0, 121.7, 119.6, 71.2, 34.9, 31.5, 25.1; IR (thin film/NaCl): 3335, 2965, 1600, 1363 cm^{-1}; HRMS-FAB (m/z): $[M]^+$ calcd for $[C_{16}H_{26}O]^+$, 234.1984; found, 234.1989; $[\alpha]_D^{24}$ –30.6° (c 0.85, $CHCl_3$; for *S* enantiomer at 98% ee).

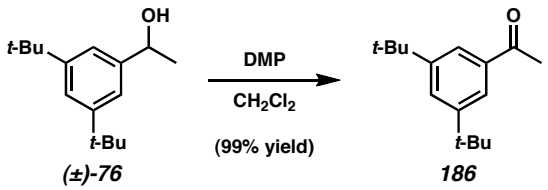

General Procedure for the Non-Asymmetric Oxidation of Alcohols to Ketones: 3',5'-Di-*tert*-butylacetophenone (186). To a solution of alcohol (±)-**76** (23.4

mg, 0.10 mmol, 1.0 equiv) in CH_2Cl_2 (1 mL) at 23 °C was added DMP[31] (84.8 mg, 0.20 mmol, 2.0 equiv). After 1 h, the reaction was complete by TLC. The reaction mixture was diluted with 4:1 hexanes:EtOAc (2 mL) and allowed to stir vigorously 20 min to precipitate white solid. Filtration through a short plug of silica gel (4:1 hexanes:EtOAc) afforded ketone **186** (22.9 mg, 99% yield) as a colorless oil. The characterization data matched the data in the literature.[32]

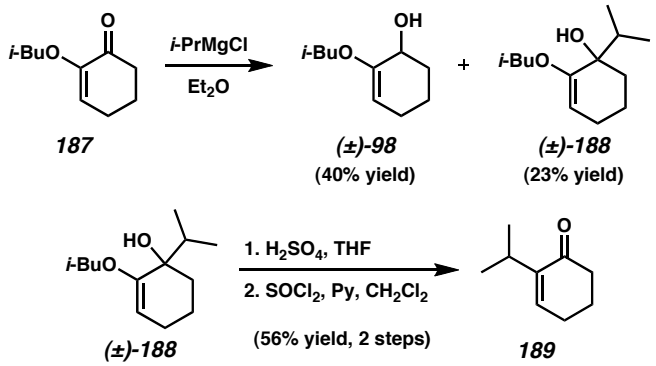

(±)-2-Isobutoxycyclohex-2-enol ((±)-98) and 2-Isopropylcyclohex-2-enone (189). To a solution of isopropylmagnesium chloride (2.0 M in Et_2O, 35.7 mL, 71.3 mmol, 2.0 equiv) in Et_2O (95 mL) was added a solution of 2-isobutoxycyclohex-2-enone[33] (**187**, 6.0 g, 35.7 mmol, 1.0 equiv) in Et_2O (29 mL) over 10 min, such that a gentle reflux was maintained. The reaction was allowed to stir for 45 min, after which it was poured slowly into a mixture of saturated aq NH_4Cl (50 mL), H_2O (50 mL), and crushed ice (50 g). After the ice melted, the phases were separated. The aqueous phase was extracted with Et_2O (3 x 100 mL). The combined organic extracts were dried over $MgSO_4$ and filtered, and the filtrate was concentrated under reduced pressure. Purification by flash chromatography (194:5:1 hexanes:EtOAc:Et_3N) afforded 2-isobutoxy-1-isopropylcyclohex-2-enol ((±)-**188**, 1.72 g, 23% yield) as a colorless oil,

which was carried on immediately to the next step, and 2-isobutoxycyclohex-2-enol ((±)-**98**, 2.45 g, 40% yield) as a colorless oil. The characterization data for (±)-**98** matched the data in the literature.[34]

To a solution of (±)-**188** (1.13 g, 5.33 mmol, 1.0 equiv) in THF (53 mL) was added conc. H_2SO_4 (400 μL). After 30 min, the reaction was quenched by slow addition of saturated aq $NaHCO_3$ (40 mL). The mixture was allowed to stir 20 min (until bubbling ceased) and then was extracted with Et_2O (3 x 40 mL). The combined organic extracts were dried over $MgSO_4$ and filtered. The filtrate was concentrated under reduced pressure. To this crude α-hydroxyketone in CH_2Cl_2 (53 mL) was added pyridine (2.15 mL, 26.6 mmol, 5.0 equiv) and $SOCl_2$ (777 μL, 10.7 mmol, 2.0 equiv). The reaction was allowed to stir at 23 °C for 7 h, after which it was quenched by addition of aq 1 N HCl (40 mL) and allowed to stir a further 10 min. The phases were separated, and the aqueous phase was extracted with Et_2O (3 x 50 mL). The combined organic extracts were dried over $MgSO_4$ and filtered. Concentration of the filtrate under reduced pressure followed by flash chromatography (49:1 hexanes:EtOAc) and bulb-to-bulb distillation (25 torr, 160-164 °C) afforded 2-isopropylcyclohex-2-enone (**189**, 412 mg, 56% yield from (±)-**188**) as a slightly yellow oil. The characterization data for **189** matched the data in the literature.[35]

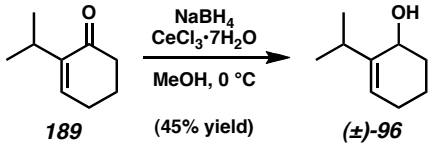

General Procedure for the Reduction of Enones: (±)-2-Isopropylcyclohex-2-enol ((±)-96).[10] To a solution of enone **189** (783 mg, 5.66 mmol, 1.0 equiv) in MeOH (57

mL) at 0 °C was added $CeCl_3 \bullet 7H_2O$ (2.32 g, 6.23 mmol, 1.1 equiv). After allowing the solid to dissolve, $NaBH_4$ (643 mg, 17.0 mmol, 3.0 equiv) was added in small portions over 5 min. After allowing the reaction mixture to warm to 23 °C, the solvent was removed under reduced pressure. H_2O (50 mL) was added, and the slurry was stirred vigorously for 20 min. The mixture was then extracted with EtOAc (4 x 60 mL). The combined organic layers were dried over $MgSO_4$ and filtered. The filtrate was concentrated and purified by flash chromatography (37:3 hexanes:EtOAc) to afford (±)-**96** (356 mg, 45% yield) as a colorless oil: R_f 0.40 (7:3 hexanes:EtOAc); ^{1}H NMR (300 MHz, $CDCl_3$) δ 5.56 (t, J = 3.9 Hz, 1H), 4.15 (t, J = 3.6 Hz, 1H), 2.52-2.35 (m, 1H), 2.14-1.88 (comp. m, 2H), 1.85-1.50 (comp. m, 4H), 1.06 (d, J = 6.9 Hz, 3H), 1.03 (d, J = 6.9 Hz, 3H); ^{13}C NMR (75 MHz, $CDCl_3$) δ 145.3, 122.7, 66.0, 32.5, 31.4, 25.5, 23.0, 21.7, 17.8; IR (thin film/NaCl): 3340, 2936, 1461, 1382, 982 cm^{-1}; HRMS-FAB (*m/z*): $[M]^+$ calcd for $[C_9H_{16}O]^+$, 140.1201; found, 140.1198; $[\alpha]_D^{25}$ –24.6° (*c* 1.8, $CHCl_3$; for *S* enantiomer at 96% ee).

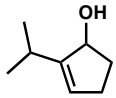

(±)-100

(±)-2-Isopropylcyclopent-2-enol ((±)-100). Prepared as for (±)-**96** from 2-isopropylcyclopent-2-enone[36] (**190**, 2.48 g, 20.0 mmol) to afford, after flash chromatography (94:5:1 hexanes:EtOAc:Et_3N), (±)-**100** (1.08 g, 43% yield) as a slightly yellow oil. The characterization data matched the data in the literature.[37] $[\alpha]_D^{24}$ –27.5° (*c* 0.48, $CHCl_3$; for *S* enantiomer at 92% ee).

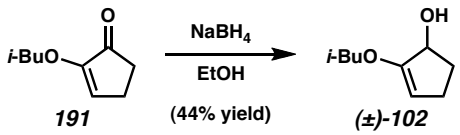

191 *(±)-102*

(±)-2-Isobutoxycyclopent-2-enol ((±)-102). To a solution of 2-isobutoxycyclopent-2-enone[36] (**191**, 1.54 g, 10.0 mmol, 1.0 equiv) in EtOH (absolute, 100 mL) was added $NaBH_4$ (1.14 g, 30.0 mmol, 3.0 equiv). After 2.5 h at 23 °C, the solvent was removed under reduced pressure and H_2O (100 mL) was added. After stirring for 30 min, this mixture was extracted with EtOAc (3 x 100 mL). The combined organic extracts were dried over Na_2SO_4 and filtered. The filtrate was concentrated under reduced pressure and purified by flash chromatography (96:3:1 hexanes:EtOAc:Et_3N) to afford (±)-**102** (688 mg, 44% yield) as a colorless oil: R_f 0.46 (7:3 hexanes:EtOAc); ^{1}H NMR (300 MHz, $CDCl_3$) δ 4.70-4.62 (m, 1H), 4.59 (t, J = 2.4 Hz, 1H), 3.57-3.47 (comp. m, 2H), 2.45-2.14 (comp. m, 3H), 2.08-1.93 (m, 1H), 1.79-1.68 (m, 1H), 0.96 (d, J = 6.7 Hz, 6H); ^{13}C NMR (75 MHz, $CDCl_3$) δ 159.9, 96.9, 76.2, 74.8, 31.2, 28.2, 26.0, 19.5, 19.4; IR (thin film/NaCl): 3392, 2958, 2909, 2871, 1648, 1055 cm^{-1}; HRMS-FAB (m/z): $[M]^+$ calcd for $[C_9H_{16}O_2]^+$, 156.1150; found, 156.1152.

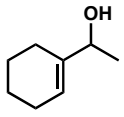

(±)-103

(±)-1-Cyclohexenyl-1-ethanol ((±)-103). Prepared as for (±)-**96** from 1-acetyl-1-cyclohexene (**192**, 3.45 g, 27.8 mmol) to afford, after distillation (22 torr, 86-88 °C) (±)-**103** (2.69 g, 77% yield) as a colorless oil. The characterization data matched the data in the literature.[38] $[\alpha]_D^{25}$ –12.1° (*c* 0.75, $CHCl_3$; for *S* enantiomer at 91% ee) [lit.[39] $[\alpha]_D$ –11.2° (*c* 0.36, $CHCl_3$; *S* enantiomer)].

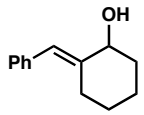

(±)-105

(±)-(*E*)-2-Benzylidenecyclohexanol ((±)-105). Prepared as for (±)-**96** from (*E*)-2-benzylidenecyclohexanone[40] (5.03 g, 27.0 mmol) to afford, after flash chromatography (9:1→17:3→4:1 hexanes:EtOAc), (±)-**105** (4.13 g, 81% yield) as a white solid. The characterization data matched the data in the literature.[41] $[\alpha]_D^{25}$ –36.0° (*c* 1.2, $CHCl_3$; for *S* enantiomer at 96% ee) [lit.[42] $[\alpha]_D^{20}$ –35.2° (*c* 1.2, $CHCl_3$; *S* enantiomer)].

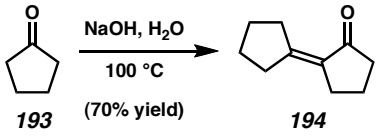

193 *194*

2-Cyclopentylidenecyclopentanone (194). Cyclopentanone (**193**, 10.0 mL, 113 mmol, 2.0 equiv) was added to aq 1 N NaOH (113 mL). The mixture was heated to reflux for 7 h, then cooled to 23 °C and saturated with solid NaCl. After the NaCl dissolved, the mixture was extracted with Et_2O (3 x 100 mL). The combined organic extracts were dried over $MgSO_4$ and filtered. The filtrate was concentrated under reduced pressure. Distillation (30 torr, 140-142 °C) afforded **194** (5.92 g, 70% yield) as a colorless oil. The characterization data matched the data in the literature.[43]

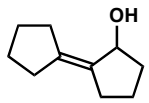

(±)-106

(±)-2-Cyclopentylidenecyclopentanol ((±)-106). Prepared as for (±)-**96** from **194** (1.10 g, 7.32 mmol) to afford, after flash chromatography (9:1 hexanes:EtOAc), (±)-**106** (881 mg, 79% yield) as a white solid. The characterization data matched the data in the literature.[44] $[\alpha]_D^{26}$ +85.3° (*c* 0.99, $CHCl_3$; for *S* enantiomer at 94% ee).

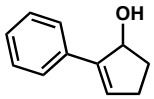

(±)-111

(±)-2-Phenylcyclopent-2-enol ((±)-111). Prepared as for (±)-**96** from 2-phenylcyclopent-2-enone[45,46] (**143**, 218 mg, 1.38 mmol) to afford, after flash chromatography (9:1→4:1→7:3 hexanes:EtOAc), (±)-**111** (196 mg, 89% yield) as a white solid: R_f 0.20 (4:1 hexanes:EtOAc); ^{1}H NMR (300 MHz, $CDCl_3$) δ 7.60-7.54 (comp. m, 2H), 7.39-7.22 (comp. m, 3H), 6.32 (t, *J* = 2.5 Hz, 1H), 5.29-5.21 (m, 1H), 2.74-2.60 (m, 1H), 2.51-2.34 (m, 2H), 2.02-1.90 (m, 1H); ^{13}C NMR (75 MHz, $CDCl_3$) δ 144.8, 135.1, 130.2, 128.8, 127.8, 126.4, 77.4, 34.3, 30.7; IR (thin film/NaCl): 3220, 2883, 1496, 1322, 1050, 759, 691 cm^{-1}; HRMS-FAB (*m*/*z*): $[M + H]^+$ calcd for $[C_{11}H_{13}O]^+$, 160.0888; found, 160.0881; $[\alpha]_D^{25}$ +14.0° (*c* 1.4, $CHCl_3$; for *S* enantiomer at 99% ee).

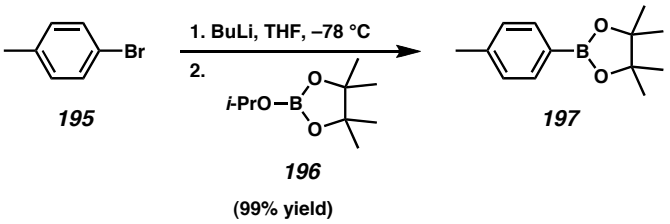

General Procedure for the Preparation of Boronate Esters: 4-(4,4,5,5-Tetramethyl-1,3,2-dioxaborolan-2-yl)toluene (197).[47] A solution of 4-bromotoluene (**195**, 1.23 mL, 10.0 mmol, 1.0 equiv) in THF (67 mL) was cooled to –78 °C. A solution of *n*-butyllithium (2.5 M in hexanes, 4.40 mL, 11.0 mmol, 1.1 equiv) was added dropwise. After stirring 10 min at –78 °C, 2-isopropoxy-4,4,5,5-tetramethyl-1,3,2-dioxaborolane (**196**, 2.65 mL, 13.0 mmol, 1.3 equiv) was added dropwise. After 10 min, the reaction was quenched at –78 °C with saturated aq NH_4Cl (35 mL) and H_2O (10 mL). After warming to 23 °C, the biphasic mixture was extracted with Et_2O (3 x 60 mL). The combined organic extracts were washed with saturated aq NaCl (30 mL), dried over $MgSO_4$, and filtered. The filtrate was concentrated under reduced pressure and purified by flash chromatography (17:3:1 hexanes:EtOAc:Et_3N) to afford **197** (2.17 g, 99% yield) as a slightly yellow oil, which solidified on standing. The characterization data matched the data in the literature.[48]

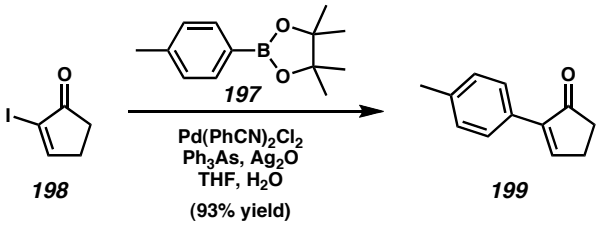

General Procedure for the Arylation of 2-Iodoenones: 2-(4-Tolyl)cyclopent-2-enone (199).[45] 2-Iodocyclopent-2-enone[49] (**198**, 1.46 g, 7.0 mmol, 1.0 equiv), boronic

ester **197** (1.83 g, 8.4 mmol, 1.2 equiv), Ag_2O (2.60 g, 11.2 mmol, 1.6 equiv), Ph_3As (129 mg, 0.42 mmol, 0.06 equiv), and $Pd(PhCN)_2Cl_2$ (81 mg, 0.21 mmol, 0.03 equiv) were added to a solution of THF (18 mL) and H_2O (2.3 mL). A vigorous exothermic reaction occurred. Once the reaction was complete as determined by TLC, it was filtered through Celite (140 mL EtOAc eluent). The filtrate was concentrated under reduced pressure and purified by flash chromatography (9:1 hexanes:EtOAc) to afford enone **199** (1.12 g, 93% yield) as a white solid. The characterization data matched the data in the literature.[50]

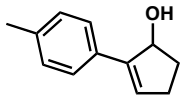

(±)-112

(±)-2-(4-Tolyl)cyclopent-2-enol ((±)-112). Prepared as for (±)-**96** from **199** (1.07 g, 6.18 mmol) to afford, after flash chromatography (9:1→4:1 hexanes:EtOAc), (±)-**112** (827 mg, 77% yield) as a white solid: R_f 0.35 (7:3 hexanes:EtOAc); ^{1}H NMR (300 MHz, $CDCl_3$) δ 7.46 (d, *J* = 8.0 Hz, 2H), 7.16 (d, *J* = 8.1 Hz, 2H), 6.26 (t, *J* = 2.5 Hz, 1H), 5.22 (m, 1H), 2.73-2.59 (m, 1H), 2.49-2.32 (m, 2H), 2.34 (s, 3H), 2.01-1.88 (m, 1H); ^{13}C NMR (75 MHz, $CDCl_3$) δ 144.7, 137.3, 132.2, 129.5, 129.2, 126.3, 77.4, 34.2, 30.7, 21.4; IR (thin film/NaCl): 3337, 2921, 1512, 1043, 813 cm^{-1}; HRMS-FAB (*m*/*z*): $[M + H]^+$ calcd for $[C_{12}H_{15}O]^+$, 174.1045; found, 174.1042; $[\alpha]_D^{25}$ +4.5° (*c* 1.6, $CHCl_3$; for *S* enantiomer at 98.5% ee).

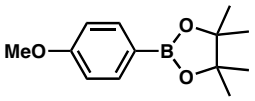

200

4-(4,4,5,5-Tetramethyl-1,3,2-dioxaborolan-2-yl)anisole (200). Prepared as for **197** to afford, after flash chromatography (79:20:1 hexanes:EtOAc:Et_3N), **200** (2.25 g, 80% yield) as a slightly yellow oil. The characterization data matched the data in the literature.[48]

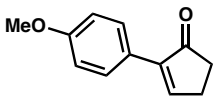

201

2-(4-Methoxyphenyl)cyclopent-2-enone (201). Prepared as for **199** from **200** to afford, after flash chromatography (4:1 hexanes:EtOAc), **201** (1.05 g, 93%) as a white solid. The characterization data matched the data in the literature.[50]

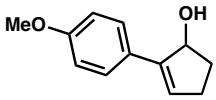

(±)-113

(±)-2-(4-Methoxyphenyl)cyclopent-2-enol ((±)-113). Prepared as for (±)-**96** from **201** (840 mg, 4.46 mmol) to afford, after flash chromatography (9:1→4:1→3:1 hexanes:EtOAc), (±)-**113** (685 mg, 81% yield) as a white solid: R_f 0.30 (7:3 hexanes:EtOAc); ^{1}H NMR (300 MHz, $CDCl_3$) δ 7.51 (d, J = 8.8 Hz, 2H), 6.88 (d, J = 8.8 Hz, 2H), 6.18 (t, J = 2.4 Hz, 1H), 5.19 (m, 1H), 3.81 (s, 3H), 2.72-2.56 (m, 1H), 2.48-2.31 (m, 2H), 2.00-1.87 (m, 1H); ^{13}C NMR (75 MHz, $CDCl_3$) δ 159.1, 144.2, 128.1, 127.8, 127.6, 114.2, 77.5, 55.5, 34.3, 30.6; IR (thin film/NaCl): 3249, 2958, 2892, 2846,

1052, 1033, 824 cm^{-1}; HRMS-FAB (*m/z*): $[M + H]^+$ calcd for $[C_{12}H_{14}O_2]^+$, 190.0994; found, 190.0995; $[\alpha]_D^{25}$ +10.6° (*c* 1.9, $CHCl_3$; for *S* enantiomer at 99% ee).

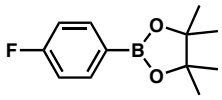

202

4-(4,4,5,5-Tetramethyl-1,3,2-dioxaborolan-2-yl)fluorobenzene (202). Prepared as for **197** to afford, after flash chromatography (17:3:1 hexanes:EtOAc:Et_3N), **202** (2.24 g, 84% yield) as a colorless oil: R_f 0.49 (4:1 hexanes:EtOAc); ^1H NMR (300 MHz, $CDCl_3$) δ 7.93 (m, 2H), 6.78 (m, 2H), 1.05 (s, 12H); ^{13}C NMR (75 MHz, $CDCl_3$) δ 165.6 (d, *J* = 250.2 Hz), 137.6 (d, *J* = 8.2 Hz), 115.2 (d, *J* = 20.2 Hz), 83.8, 24.9; ^{19}F NMR (282 MHz, $CDCl_3$) δ –108.4; IR (thin film/NaCl): 2979, 1603, 1400, 1362, 1144, 1088 cm^{-1}; HRMS-EI (*m/z*): $[M]^+$ calcd for $[C_{12}H_{16}BFO_2]^+$, 222.1227; found, 222.1236.

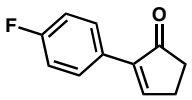

203

2-(4-Fluorophenyl)cyclopent-2-enone (203). Prepared as for **199** from **202** to afford, after flash chromatography (9:1→4:1 hexanes:EtOAc), **203** (1.03 g, 90% yield) as a white solid: R_f 0.30 (7:3 hexanes:EtOAc); ^1H NMR (300 MHz, $CDCl_3$) δ 7.79 (t, *J* = 2.9 Hz, 1H), 7.73-7.65 (m, 2H), 7.11-7.02 (m, 2H), 2.75-2.66 (m, 2H), 2.63-2.55 (m, 2H); ^{13}C NMR (75 MHz, $CDCl_3$) δ 207.8, 163.0 (d, *J* = 247.8 Hz), 158.8 (d, *J* = 1.4 Hz), 142.6, 129.1 (d, *J* = 8.0 Hz), 128.0 (d, *J* = 3.2 Hz), 115.6 (d, *J* = 21.4 Hz), 35.9, 26.4; ^{19}F NMR (282 MHz, $CDCl_3$) δ –114.1; IR (thin film/NaCl): 1701, 1507, 1224, 834 cm^{-1}; HRMS-FAB (*m/z*): $[M]^+$ calcd for $[C_{11}H_9FO]^+$, 176.0637; found, 176.0631.

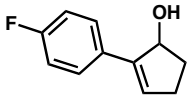

(±)-114

(±)-2-(4-Fluorophenyl)cyclopent-2-enol ((±)-114). Prepared as for (±)-**96** from **203** (933 mg, 5.29 mmol) to afford, after flash chromatography (9:1→4:1 hexanes:EtOAc), (±)-**114** (792 mg, 84% yield) as a white solid: R_f 0.31 (7:3 hexanes:EtOAc); ^{1}H NMR (300 MHz, $CDCl_3$) δ 7.58-7.50 (m, 2H), 7.07-6.98 (m, 2H), 6.24 (t, *J* = 2.5 Hz, 1H), 5.20 (m, 1H), 2.73-2.59 (m, 1H), 2.50-2.34 (comp. m, 2H), 2.01-1.88 (m, 1H); ^{13}C NMR (75 MHz, $CDCl_3$) δ 162.4 (d, *J* = 246.6 Hz), 143.7, 131.3 (d, *J* = 3.1 Hz), 129.9 (d, *J* = 1.8 Hz), 128.0 (d, *J* = 8.0 Hz), 115.6 (d, *J* = 21.5 Hz), 77.6, 34.4, 30.6; ^{19}F NMR (282 MHz, $CDCl_3$) δ –115.8; IR (thin film/NaCl): 3218, 1510, 1237, 1050, 834 cm^{-1}; HRMS-FAB (*m*/*z*): $[M]^+$ calcd for $[C_{11}H_{11}FO]^+$, 178.0794; found, 178.0786; $[\alpha]_D^{25}$ +12.8° (*c* 2.2, $CHCl_3$; for *S* enantiomer at 99% ee).

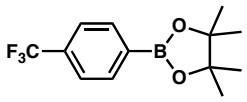

204

4-(4,4,5,5-Tetramethyl-1,3,2-dioxaborolan-2-yl)benzotrifluoride (204). Prepared as for **197** to afford, after flash chromatography (17:3:1 hexanes:EtOAc:Et_3N), **204** (3.13 g, 96% yield) as an off-white solid. The characterization data matched the data in the literature.[51]

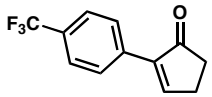

205

2-(4-Trifluoromethylphenyl)cyclopent-2-enone (205). Prepared as for **199** from **204** to afford, after flash chromatography (9:1 hexanes:EtOAc), **205** (1.14 g, 84% yield) as a white solid: R_f 0.37 (7:3 hexanes:EtOAc); ^{1}H NMR (300 MHz, $CDCl_3$) δ 7.92 (t, *J* = 2.9 Hz, 1H), 7.81 (d, *J* = 8.0 Hz, 2H), 7.62 (d, *J* = 7.9 Hz, 2H), 2.79-2.72 (m, 2H), 2.66-2.60 (m, 2H); ^{13}C NMR (75 MHz, $CDCl_3$) δ 207.0, 160.5, 142.4, 135.1, 130.2 (q, *J* = 32.5 Hz), 127.3, 125.3 (q, *J* = 3.8 Hz), 124.1 (q, *J* = 272.1 Hz), 35.7, 26.4; ^{19}F NMR (282 MHz, $CDCl_3$) δ –63.7; IR (thin film/NaCl): 3066, 1692, 1332, 1112, 847 cm^{-1}; HRMS-FAB (*m*/*z*): $[M]^+$ calcd for $[C_{12}H_9F_3O]^+$, 226.0606; found, 226.0608.

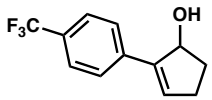

(±)-115

(±)-2-(4-Trifluoromethylphenyl)cyclopent-2-enol ((±)-115). Prepared as for (±)-**96** from **205** (1.14 g, 5.00 mmol) to afford, after flash chromatography (9:1→4:1 hexanes:EtOAc), (±)-**115** (887 mg, 77% yield) as a white solid: R_f 0.34 (7:3 hexanes:EtOAc); ^{1}H NMR (300 MHz, $CDCl_3$) δ 7.67 (d, *J* = 8.5 Hz, 2H), 7.58 (d, *J* = 8.5 Hz, 2H), 6.43 (t, *J* = 2.6 Hz, 1H), 5.24 (m, 1H), 2.77-2.62 (m, 1H), 2.54-2.37 (m, 2H), 2.02-1.86 (m, 1H); ^{13}C NMR (75 MHz, $CDCl_3$) δ 143.4, 138.4, 132.6, 127.7, 126.3, 125.4 (q, *J* = 3.8 Hz), 77.1, 34.1, 30.5; ^{19}F NMR (282 MHz, $CDCl_3$) δ –63.5; IR (thin film/NaCl): 3239, 1326, 1112, 827 cm^{-1}; HRMS-FAB (*m*/*z*): $[M + H]^+$ calcd for $[C_{12}H_{12}OF_3]^+$, 228.0762; found, 228.0752; $[\alpha]_D^{25}$ +16.0° (*c* 2.5, $CHCl_3$; for *S* enantiomer at 99% ee).

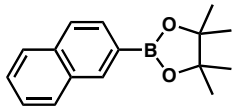

206

2-(4,4,5,5-Tetramethyl-1,3,2-dioxaborolan-2-yl)naphthalene (206). Prepared as for **197** to afford, after flash chromatography (17:3:1 hexanes:EtOAc:Et_3N), **206** (2.87 g, 94% yield) as an off-white solid. The characterization data matched the data in the literature.[48]

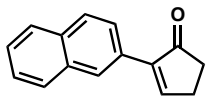

207

2-(2-Naphthyl)cyclopent-2-enone (207). Prepared as for **199** from **206** to afford, after flash chromatography (9:1 hexanes:EtOAc), **207** (180 mg, 86% yield) as an off-white solid: R_f 0.33 (7:3 hexanes:EtOAc); ^{1}H NMR (300 MHz, $CDCl_3$) δ 8.37 (s, 1H), 7.96 (t, J = 3.0 Hz, 1H), 7.93-7.78 (comp. m, 3H), 7.71 (dd, J = 8.6, 1.7 Hz, 1H), 7.52-7.44 (comp. m, 2H), 2.80-2.73 (m, 2H), 2.69-2.63 (m, 2H); ^{13}C NMR (75 MHz, $CDCl_3$) δ 208.0, 159.4, 143.3, 133.5, 133.4, 129.2, 128.8, 128.3, 127.8, 126.6, 126.5, 126.4, 125.0, 36.2, 26.5; IR (thin film/NaCl): 1690, 1311, 748, 475 cm^{-1}; HRMS-FAB (m/z): $[M]^+$ calcd for $[C_{15}H_{12}O]^+$, 208.0888; found, 208.0889.

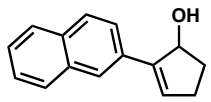

(±)-116

(±)-2-(2-Naphthyl)cyclopent-2-enol ((±)-116). Prepared as for (±)-**96** from **207** (1.90 g, 9.14 mmol) to afford, after flash chromatography (9:1→4:1 hexanes:EtOAc), (±)-**116** (1.67 g, 87% yield) as a white solid: R_f 0.37 (7:3 hexanes:EtOAc); ^{1}H NMR (300 MHz, $CDCl_3$) δ 8.00 (s, 1H), 7.87-7.67 (comp. m, 4H), 7.50-7.40 (comp. m, 2H), 6.45 (t, J = 2.5 Hz, 1H), 5.37 (m, 1H), 2.80-2.65 (m, 1H), 2.56-2.38 (m, 2H), 2.07-1.95 (m, 1H); ^{13}C NMR (75 MHz, $CDCl_3$) δ 144.7, 133.9, 133.0, 132.4, 130.9, 128.5, 128.4, 127.9, 126.4, 126.1, 125.0, 124.8, 77.4, 34.4, 30.9; IR (thin film/NaCl): 3385, 1044, 819, 476 cm^{-1}; HRMS-FAB (m/z): $[M + H]^+$ calcd for $[C_{15}H_{15}O]^+$, 210.1045; found, 210.1043; $[\alpha]_D^{25}$ +46.4° (c 2.0, $CHCl_3$; for S enantiomer at 99% ee).

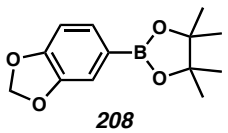

208

5-(4,4,5,5-Tetramethyl-1,3,2-dioxaborolan-2-yl)-1,3-benzodioxole (208). Prepared as for **197** to afford, after flash chromatography (17:3:1 hexanes:EtOAc:Et_3N), **208** (2.43 g, 99% yield) as an off-white solid. The characterization data matched the data in the literature.[52]

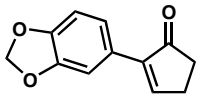

209

2-(Benzo[1,3]dioxol-5-yl)cyclopent-2-enone (209). Prepared as for **199** from **208** to afford, after flash chromatography (17:3→4:1→7:3 hexanes:EtOAc), **209** (1.37 g,

90% yield) as a white solid: R_f 0.30 (7:3 hexanes:EtOAc); ^{1}H NMR (300 MHz, $CDCl_3$) δ 7.71 (t, *J* = 2.9 Hz, 1H), 7.27-7.19 (comp. m, 2H), 6.82 (d, *J* = 8.0 Hz, 1H), 5.96 (s, 2H), 2.71-2.65 (m, 2H), 2.61-2.55 (m, 2H); ^{13}C NMR (75 MHz, $CDCl_3$) δ 207.8, 157.8, 147.8, 143.0, 125.8, 121.1, 108.5, 107.6, 101.2, 36.0, 26.2; IR (thin film/NaCl): 1695, 1488, 1240, 1035, 806 cm^{-1}; HRMS-FAB (*m/z*): $[M]^+$ calcd for $[C_{12}H_{10}O_3]^+$, 202.0630; found, 202.0623.

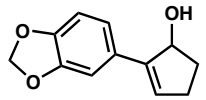

(±)-117

(±)-2-(Benzo[1,3]dioxol-5-yl)cyclopent-2-enol ((±)-117). Prepared as for (±)-(±)-**96** from **209** (1.21 g, 6.00 mmol) to afford, after flash chromatography (9:1→17:3→4:1 hexanes:EtOAc), (±)-**117** (1.03 g, 84% yield) as a white solid: R_f 0.27 (7:3 hexanes:EtOAc); ^{1}H NMR (300 MHz, $CDCl_3$) δ 7.08-7.03 (comp. m, 2H), 6.82-6.76 (m, 1H), 6.16 (t, *J* = 2.5, 1H), 5.95 (s, 2H), 5.15 (m, 1H), 2.71-2.57 (m, 1H), 2.47-2.30 (m, 2H), 1.99-1.87 (m, 1H); ^{13}C NMR (75 MHz, $CDCl_3$) δ 148.1, 147.1, 144.3, 129.5, 128.8, 120.0, 108.5, 106.8, 101.2, 77.5, 34.3, 30.6; IR (thin film/NaCl): 3354, 2894, 1490, 1503, 1226, 1041, 937 cm^{-1}; HRMS-FAB (*m/z*): $[M + H]^+$ calcd for $[C_{12}H_{13}O_3]^+$, 204.0787; found, 204.0793; $[\alpha]_D^{25}$ +9.6° (*c* 1.6, $CHCl_3$; for *S* enantiomer at 99% ee).

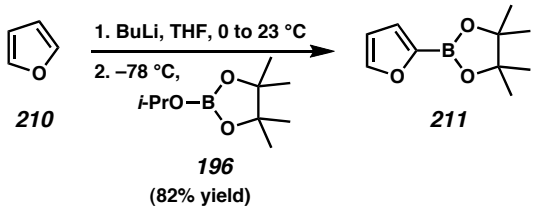

2-(4,4,5,5-Tetramethyl-1,3,2-dioxaborolan-2-yl)-furan (211). A solution of furan (**210**, 1.75 mL, 24.0 mmol, 1.2 equiv) in THF (120 mL) was cooled to 0 °C. A solution of *n*-butyllithium (2.26 M in hexanes, 8.84 mL, 20.0 mmol, 1.0 equiv) was added dropwise. The reaction was allowed to stir 30 min at 0 °C and 30 min at 23 °C, after which it was cooled to –78 °C. Borolane **196** (6.36 mL, 31.2 mmol, 1.3 equiv) was added dropwise. After stirring 10 min, the reaction was allowed to warm to 23 °C and was quenched by addition of saturated aq NH_4Cl (50 mL) and H_2O (10 mL). The mixture was extracted with Et_2O (3 x 100 mL). The combined organic layers were dried over $MgSO_4$ and filtered, and the filtrate was concentrated under reduced pressure. Bulb-to-bulb distillation (0.1 torr, 90-95 °C) afforded **211** (3.17 g, 82% yield) as a colorless oil. The characterization data matched the data in the literature.[53]

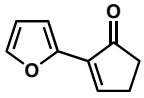

212

2-(2-Furyl)cyclopent-2-enone (212). Prepared as for **199** from **211** to afford, after flash chromatography (19:1→17:3 hexanes:EtOAc), **212** (1.09 g, 55% yield) as an off-white solid: R_f 0.51 (7:3 hexanes:EtOAc); ^{1}H NMR (300 MHz, $CDCl_3$) δ 7.79 (t, J = 3.1 Hz, 1H), 7.41 (d, J = 1.7 Hz, 1H), 7.04 (d, J = 3.5 Hz, 1H), 6.44 (dd, J = 3.5, 1.7 Hz, 1H), 2.77-2.71 (m, 2H), 2.56-2.51 (m, 2H); ^{13}C NMR (75 MHz, $CDCl_3$) δ 205.8, 154.2,

147.1, 142.5, 134.9, 111.6, 109.4, 35.5, 26.9; IR (thin film/NaCl): 1706, 1326, 1132, 747 cm^{-1}; HRMS-FAB (*m/z*): $[M]^+$ calcd for $[C_9H_8O_2]^+$, 148.0524; found, 148.0521.

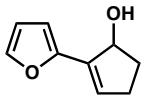

(±)-118

(±)-2-(2-Furyl)cyclopent-2-enol ((±)-118). Prepared as for (±)-**96** from **212** (961 mg, 6.49 mmol) to afford, after flash chromatography (19:1→9:1→4:1 hexanes:EtOAc), (±)-**118** (793 mg, 81% yield) as an off-white solid: R_f 0.26 (7:3 hexanes:EtOAc); ^{1}H NMR (300 MHz, $CDCl_3$) δ 7.38 (d, *J* = 1.6 Hz, 1H), 6.43 (d, *J* = 3.4 Hz, 1H), 6.40 (dd, *J* = 3.3, 1.7 Hz, 1H), 5.11 (m, 1H), 2.74-2.60 (m, 1H), 2.49-2.30 (m, 2H), 1.95-1.84 (m, 1H); ^{13}C NMR (75 MHz, $CDCl_3$) δ 151.2, 142.0, 135.7, 128.4, 111.4, 106.8, 77.3, 55.9, 30.8; IR (thin film/NaCl): 3344, 2934, 2849, 1044, 928, 733 cm^{-1}; HRMS-FAB (*m/z*): $[M + H]^+$ calcd for $[C_9H_{11}O_2]^+$, 150.0681; found, 150.0680; $[\alpha]_D^{25}$ +30.9° (*c* 1.1, $CHCl_3$; for *S* enantiomer at 99% ee).

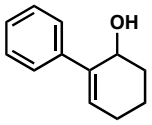

(±)-119

(±)-2-Phenylcyclohex-2-enol ((±)-119). Prepared as for (±)-**96** from 2-phenylcyclohex-2-enone[45] (**213**, 2.70 g, 15.7 mmol) to afford, after filtration through a short plug of silica gel (1:1 hexanes:EtOAc), (±)-**119** (2.22 g, 81% yield) as an off-white solid. The characterization data matched the data in the literature.[54] $[\alpha]_D^{25}$ –109.5° (*c* 1.3, $CHCl_3$; for *S* enantiomer at 99% ee) [lit.[55] $[\alpha]_D$ +114.5° (*c* 1.6, $CHCl_3$; *R* enantiomer)].

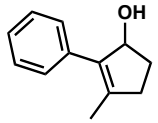

(±)-120

(±)-2-Phenyl-3-methylcyclopent-2-enol ((±)-120). Prepared as for (±)-**96** from 2-phenyl-3-methylcyclopent-2-enone[56] (**214**, 3.82 g, 22.2 mmol) to afford, after flash chromatography (9:1→4:1 hexanes:EtOAc), (±)-**120** (3.25 g, 84% yield) as a slightly yellow oil, which solidified to a white solid on standing: R_f 0.24 (4:1 hexanes:EtOAc); ^{1}H NMR (300 MHz, $CDCl_3$) δ 7.41-7.22 (comp. m, 5H), 5.16 (br. d, J = 5.5 Hz, 1H), 2.74-2.58 (m, 1H), 2.44-2.30 (m, 2H), 1.87-1.75 (m, 1H), 1.85 (d, J = 1.1 Hz, 3H); ^{13}C NMR (75 MHz, $CDCl_3$) δ 139.8, 138.5, 136.7, 128.6, 128.5, 126.9, 80.5, 36.9, 32.7, 15.9; IR (thin film/NaCl): 3370, 2930, 1442, 699 cm^{-1}; HRMS-FAB (m/z): $[M + H]^+$ calcd for $[C_{10}H_{15}O]^+$, 174.1045; found, 174.1037; $[\alpha]_D^{25}$ –2.4° (*c* 1.2, $CHCl_3$; for *S* enantiomer at 99% ee).

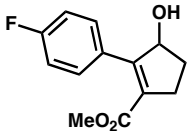

(±)-121

Fluorophenylcarboxylate (±)-121. Prepared as for (±)-**96** from methyl 2-(4-fluorophenyl)-3-oxocyclopent-1-enecarboxylate[23a] (**215**, 125 mg, 0.53 mmol) to afford, after flash chromatography (4:1 hexanes:EtOAc), (±)-**121** (103 mg, 82% yield) as a slightly yellow oil: R_f 0.11 (4:1 hexanes:EtOAc). The characterization data matched the data in the literature.[23a] $[\alpha]_D^{22}$ –37.2° (*c* 0.1, MeOH; for *S* enantiomer at 99% ee) [lit.[23a] $[\alpha]_D$ –186.6° (*c* 0.01, MeOH; *S* enantiomer)].

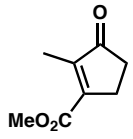

216

Methyl 2-Methyl-3-oxocyclopent-1-enecarboxylate (216). Prepared according to the procedure of Kuethe:[23a] R_f 0.26 (4:1 hexanes:EtOAc); ^{1}H NMR (300 MHz, $CDCl_3$) δ 3.90 (s, 3H), 2.84-2.76 (m, 2H), 2.55-2.48 (m, 2H), 2.09 (t, J = 2.2 Hz, 3H); ^{13}C NMR (75 MHz, $CDCl_3$) δ 209.9, 166.1, 154.4, 147.7, 52.3, 34.1, 26.6, 10.0; IR (thin film/NaCl): 1713, 1438, 1226, 1076 cm^{-1}; HRMS-FAB (*m*/*z*): $[M]^+$ calcd for $[C_8H_{10}O_3]^+$, 154.0630; found, 154.0626.

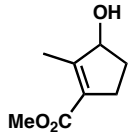

(±)-122

(±)-Methyl 3-Hydroxy-2-methylcyclopent-1-enecarboxylate ((±)-122). Prepared as for (±)-**96** from **216** (2.35 g, 15.2 mmol) to afford, after flash chromatography (7:3 hexanes:EtOAc), (±)-**122** (2.06 g, 87% yield) as a colorless oil: R_f 0.10 (4:1 hexanes:EtOAc); ^{1}H NMR (300 MHz, $CDCl_3$) δ 4.66 (t, J = 6.9 Hz, 1H), 3.75 (s, 3H), 2.75-2.62 (m, 1H), 2.53-2.25 (comp. m, 2H), 2.13 (s, 3H), 1.71-1.59 (m, 1H); ^{13}C NMR (75 MHz, $CDCl_3$) δ 167.0, 155.2, 128.9, 81.2, 51.4, 32.2, 30.4, 36.9, 13.5; IR (thin film/NaCl): 3419, 2951, 1715, 1436, 1220, 1054 cm^{-1}; HRMS-FAB (*m*/*z*): $[M]^+$ calcd for $[C_8H_{12}O_3]^+$, 156.0787; found, 156.0780; $[\alpha]_D^{25}$ –57.0° (*c* 0.82, $CHCl_3$; for *S* enantiomer at 99% ee).

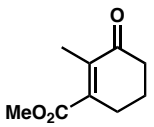

217

Methyl 2-Methyl-3-oxocyclohex-1-enecarboxylate (217). Prepared according to the procedure of Kuethe:[23a] R_f 0.24 (4:1 hexanes:EtOAc); ^{1}H NMR (300 MHz, $CDCl_3$) δ 3.82 (s, 3H), 2.61-2.53 (m, 2H), 2.51-2.44 (m, 2H), 2.07-1.97 (m, 2H), 1.94 (t, J = 2.1 Hz, 3H); ^{13}C NMR (75 MHz, $CDCl_3$) δ 199.6, 169.0, 144.4, 137.4, 52.2, 38.0, 27.5, 22.4, 12.8; IR (thin film/NaCl): 2954, 1727, 1682, 1435, 1232, 1052 cm^{-1}; HRMS-FAB (*m*/*z*): $[M]^+$ calcd for $[C_9H_{12}O_3]^+$, 168.0787; found, 168.0786.

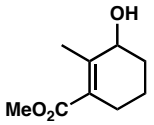

(±)-123

(±)-Methyl 3-Hydroxy-2-methylcyclohex-1-enecarboxylate ((±)-123). Prepared as for (±)-**96** from **217** (4.66 g, 27.7 mmol) to afford, after filtration through a short plug of silica gel (1:1 hexanes:EtOAc), (±)-**123** (4.71 g, 99% yield) as a colorless oil: R_f 0.12 (4:1 hexanes:EtOAc); ^{1}H NMR (300 MHz, $CDCl_3$) δ 4.06 (t, J = 4.5 Hz, 1H), 3.74 (s, 3H), 2.41-2.12 (comp. m, 2H), 2.07 (t, J = 2.1 Hz, 3H), 1.82-1.60 (comp. m, 4H); ^{13}C NMR (75 MHz, $CDCl_3$) δ 169.8, 144.0, 127.8, 69.8, 51.6, 31.6, 27.0, 18.7, 18.1; IR (thin film/NaCl): 3424, 2945, 1718, 1435, 1215, 1061 cm^{-1}; HRMS-FAB (*m*/*z*): $[M]^+$ calcd for $[C_9H_{14}O_3]^+$, 170.0943; found, 170.0938; $[\alpha]_D^{25}$ –72.3° (*c* 0.95, $CHCl_3$; for *S* enantiomer at 97% ee).

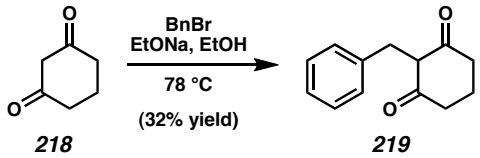

2-Benzylcyclohexane-1,3-dione (219). Prepared by modification of a procedure from Hewett.[57] Na (3.45 g, 150 mmol, 1.5 equiv) was added to EtOH (absolute, 200 mL). After all of the metal dissolved, cyclohexane-1,3-dione (**218**, 11.2 g, 100 mmol, 1.0 equiv) was added, followed by benzyl bromide (23.8 mL, 200 mmol, 2.0 equiv). The reaction was heated to reflux for 13 h. After cooling to 23 °C, the volatiles were removed under reduced pressure. Et_2O (100 mL) was added, and the mixture was extracted with 1 N NaOH (2 x 100 mL). The combined aqueous extracts were cooled to 0 °C and acidified to pH 1.5 by dropwise addition of conc. H_2SO_4. After addition of saturated aq NaCl (50 mL), the mixture was allowed to stand at 0 °C for 5 min. The solid was filtered to afford **219** (6.51 g, 32% yield) as a tan solid. The characterization data matched the data in the literature.[58]

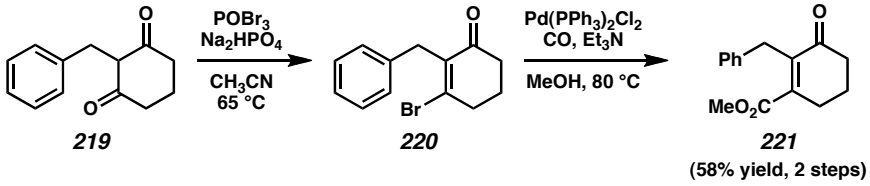

Methyl 2-Benzyl-3-oxocyclohex-1-enecarboxylate (221). Prepared according to the procedure of Kuethe.[23a] To a mixture of **219** (2.02 g, 10.0 mmol, 1.0 equiv) and Na_2HPO_4 (710 mg, 5.0 mmol, 0.5 equiv) in CH_3CN (15 mL) was added a solution of $POBr_3$ (2.15 g, 7.5 mmol, 0.75 equiv) in CH_3CN (5 mL). The reaction was heated to 65 °C for 24 h. After cooling to 23 °C, H_2O (6 mL) was added slowly to quench the reaction. After evaporation of CH_3CN under reduced pressure, H_2O (40 mL) and

saturated aq NaCl (20 mL) were added. The mixture was extracted with EtOAc (4 x 50 mL). The combined organic extracts were dried over $MgSO_4$ and filtered. The filtrate was concentrated under reduced pressure and purified by flash chromatography (9:1→17:3 hexanes:Et_2O) to afford 2-benzyl-3-bromocyclohex-2-enone (**220**), which was used directly in the next step.

To a solution of this bromide in MeOH (12.5 mL) was added $Pd(PPh_3)_2Cl_2$ (132 mg, 0.19 mmol, 0.03 equiv) followed by Et_3N (1.75 mL, 1.27 g, 12.5 mmol, 2.0 equiv) in a steel bomb. The reaction was pressurized with carbon monoxide (100 psi) and heated to 80 °C behind a blast shield for 21 h. After cooling to 23 °C and venting the carbon monoxide, the reaction was diluted with Et_2O (70 mL) and filtered through a short plug of Celite (Et_2O eluent). The filtrate was concentrated under reduced pressure and purified by flash chromatography (17:3 hexanes:Et_2O) to afford **221** (1.42 g, 58% yield from **219**) of an off-white solid: R_f 0.45 (7:3 hexanes:EtOAc); ^{1}H NMR (300 MHz, $CDCl_3$) δ 7.25-7.10 (comp. m, 5H), 3.81 (br. s, 2H), 3.78 (s, 3H), 2.63 (t, J = 6.0 Hz, 2H), 2.47 (app. t, J = 6.7 Hz, 2H), 2.04 (tt, J = 6.7, 6.1 Hz, 2H); ^{13}C NMR (75 MHz, $CDCl_3$) δ 198.7, 168.7, 145.6, 139.4, 129.6, 128.7, 128.2, 126.0, 52.2, 38.0, 31.9, 27.7, 22.0; IR (thin film/NaCl): 2951, 1726, 1681, 1255, 1238 cm^{-1}; HRMS-FAB (m/z): $[M]^+$ calcd for $[C_{15}H_{16}O_3]^+$, 244.1100; found, 244.1100.

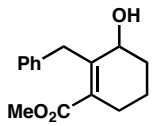

(±)-124

(±)-Methyl 3-Hydroxy-2-benzylcyclohex-1-enecarboxylate ((±)-124). Prepared as for (±)-**96** from **221** (2.02 g, 8.3 mmol) to afford, after flash chromatography (3:2

hexanes:Et_2O), (±)-**124** (1.42 g, 70% yield) as a colorless oil: R_f 0.29 (7:3 hexanes:EtOAc); ^{1}H NMR (300 MHz, $CDCl_3$) δ 7.33-7.17 (comp. m, 5H), 4.03 (br. s, 1H), 4.00 (d, *J* = 14.3 Hz, 1H), 3.75 (s, 3H), 3.69 (dt, *J* = 14.4, 2.0 Hz, 1H), 2.50-2.38 (m, 1H), 2.34-2.20 (m, 1H), 1.81-1.57 (comp. m, 4H); ^{13}C NMR (75 MHz, $CDCl_3$) δ 169.8, 143.9, 139.4, 129.7, 128.9, 128.5, 126.2, 66.2, 51.7, 36.9, 31.2, 27.1, 17.5; IR (thin film/NaCl): 3412, 2943, 1715, 1234 cm^{-1}; HRMS-FAB (*m/z*): $[M]^+$ calcd for $[C_{15}H_{18}O_3]^+$, 246.1256; found, 246.1251; $[\alpha]_D^{24}$ –226.3° (*c* 1.83, $CHCl_3$; for *S* enantiomer at 96% ee).

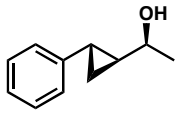

(±)-126

(±)-*syn,trans*-1-(2-Phenylcyclopropyl)ethanol ((±)-126). Prepared by the method of Charette.[59] The characterization data matched the data in the literature.[60] $[\alpha]_D^{24}$ +44.1° (*c* 1.1, $CHCl_3$; for (1*S*, 1'*S*, 2'*S*) enantiomer at 90% ee).

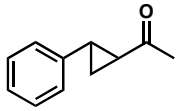

(±)-129

(±)-*trans*-1-(2-Phenylcyclopropyl)ethanone ((±)-129). Prepared as for **186** from (±)-**126** (16.5 mg, 0.10 mmol) to afford (±)-**129** (15.9 mg, 97% yield) as a colorless oil. The characterization data matched the data in the literature.[61] $[\alpha]_D^{24}$ –275.5° (*c* 0.59, $CHCl_3$; for (1'*R*, 2'*R*) enantiomer at 57% ee) [lit.[61] $[\alpha]_D^{20}$ +116.2° (*c* 0.785, $CHCl_3$; for (1'*S*, 2'*S*) enantiomer)].

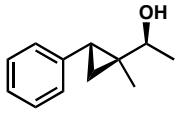

(±)-127

(±)-*syn,trans*-1-(1-Methyl-2-phenylcyclopropyl)ethanol ((±)-127). Prepared by the method of Charette.[59] The characterization data matched the data in the literature. $[\alpha]_D^{24}$ +2.1° (*c* 1.5, $CHCl_3$; for (1*S*, 1'*S*, 2'*R*) enantiomer at 89% ee).

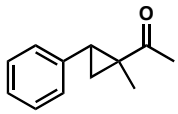

(±)-130

(±)-*trans*-1-(1-Methyl-2-phenylcyclopropyl)ethanone ((±)-130). Prepared as for **186** from (±)-**127** (17.6 mg, 0.10 mmol) to afford (±)-**130** (6.2 mg, 36% yield) as a colorless oil. The characterization data matched the data in the literature.[62] $[\alpha]_D^{25}$ –152.1° (*c* 1.59, abs. EtOH; for (1'*R*, 2'*S*) enantiomer at 74% ee) [lit.[62] $[\alpha]_D^{25}$ +173.3° (*c* 2, abs. EtOH; for (1'*S*, 2'*R*) enantiomer)].

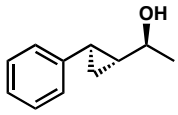

(±)-128

(±)-*anti,trans*-1-(2-Phenylcyclopropyl)ethanol ((±)-128). Prepared by the method of Charette.[63] The characterization data matched the data in the literature.[64] $[\alpha]_D^{24}$ –60.1° (*c* 1.0, $CHCl_3$; for (1*S*, 1'*R*, 2'*R*) enantiomer at 94% ee) [lit.[64] $[\alpha]_D$ +64.2° (*c* 1.0, $CHCl_3$; for (1*R*, 1'*S*, 2'*S*) enantiomer)].

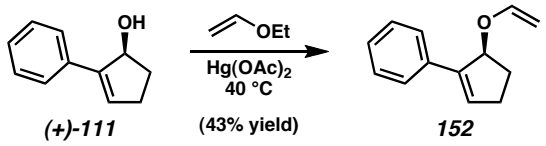

General Procedure for the Vinylation of Allylic Alcohols: Vinyl Ether 152. To a solution of cyclopentenol (+)-**111** (36.5 mg, 0.23 mmol, 1.0 equiv) in freshly distilled ethyl vinyl ether (3 mL) was added $Hg(OAc)_2$ (20.3 mg, 0.064 mmol, 0.28 equiv). The reaction was sealed with a teflon cap and heated to 40 °C for 120 h. The reaction was cooled to 23 °C, and K_2CO_3 (anhydrous, 173 mg, 1.25 mmol, 5.5 equiv) was added. The suspension was stirred for 30 min then filtered. The filtrate was concentrated under reduced pressure and purified by flash chromatography (250:7→10:1 hexanes:EtOAc) to afford recovered cyclopentenol (+)-**111** (20.1 mg, 55% yield) and vinyl ether **152** (18.5 mg, 43% yield) as a colorless oil: R_f 0.55 (10:1 hexanes:EtOAc); ^{1}H NMR (300 MHz, $CDCl_3$) δ 7.49-7.46 (comp. m, 2H), 7.35-7.22 (comp. m, 3H), 6.50-6.43 (m, 2H), 5.37 (dt, J = 6.9, 2.4 Hz, 1H), 4.35 (dd, J = 14.4, 1.8 Hz, 1H), 4.11 (dd, J = 6.6, 1.5 Hz, 1H), 2.76-2.64 (m, 1H), 2.54-2.26 (m, 2H), 2.15-2.12 (m, 1H); ^{13}C NMR (75 MHz, $CDCl_3$) δ 150.1, 141.1, 134.6, 132.0, 128.4, 127.3, 125.9, 88.3, 83.1, 31.0, 30.1; IR (thin film/NaCl): 3057, 2934, 2846, 1632, 1610, 1496, 1447, 1358, 1318, 1188, 1048, 1032, 962, 822 cm^{-1}; HRMS-ES (m/z): $[M]^+$ calcd for $[C_{13}H_{14}O]^+$, 186.1045; found, 186.1042; $[\alpha]_D^{25}$ +32.5° (c 0.38, CH_2Cl_2).

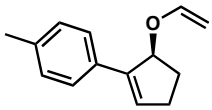

153

Vinyl Ether 153. Prepared as for **152** from (+)-**112** (100 mg, 0.57 mmol) to afford, after flash chromatography (125:2→10:1 hexanes:EtOAc), cyclopentenol (+)-**112** (48 mg, 48% yield) and **153** (48 mg, 42% yield) as a colorless oil: R_f 0.57 (10:1 hexanes:EtOAc); ^{1}H NMR (300 MHz, $CDCl_3$) δ 7.41 (d, *J* = 6.3 Hz, 2H), 7.17 (d, *J* = 8.1 Hz, 2H), 6.52 (dd, *J* = 14.4, 6.9 Hz, 1H), 6.42 (t, *J* = 2.4 Hz, 1H), 5.37 (dt, *J* = 7.2, 2.4 Hz, 1H), 4.37 (dd, *J* = 14.4, 1.8 Hz, 1H), 4.12 (dd, *J* = 6.6, 1.8 Hz, 1H), 2.74-2.65 (m, 1H), 2.54-2.43 (m, 1H), 2.36 (s, 3H), 2.39-2.27 (m, 1H), 2.16-2.09 (m, 1H); ^{13}C NMR (75 MHz, $CDCl_3$) δ 150.1, 141.0, 137.0, 131.8, 131.0, 129.1, 125.9, 88.3, 83.1, 31.0, 30.1, 21.2; IR (thin film/NaCl): 2921, 2849, 1631, 1609, 1513, 1449, 1352, 1317, 1187, 1048, 1030, 963, 813 cm^{-1}; HRMS-ES (*m*/*z*): $[M]^+$ calcd for $[C_{14}H_{16}O]^+$, 200.1201; found, 200.1201; $[\alpha]_D^{25}$ +20.8° (*c* 0.16, CH_2Cl_2).

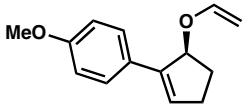

154

Vinyl Ether 154. Prepared as for **152** from (+)-**113** (100 mg, 0.53 mmol) to afford, after flash chromatography (60:1→10:1 hexanes:EtOAc), cyclopentenol (+)-**113** (61 mg, 61% yield) and **154** (41 mg, 36% yield) as a colorless oil: R_f 0.52 (10:1 hexanes:EtOAc); ^{1}H NMR (300 MHz, $CDCl_3$) δ 7.44 (d, *J* = 8.7 Hz, 2H). 6.89 (d, *J* = 9.0 Hz, 2H), 6.51 (dd, *J* = 14.4, 6.9 Hz, 1H), 6.33 (t, *J* = 2.7 Hz, 1H), 5.37 (dt, *J* = 7.2, 2.1 Hz, 1H), 4.36 (dd, *J* = 14.4, 2.1 Hz, 1H), 4.11 (dd, *J* = 6.6, 1.8 Hz, 1H), 3.81 (s, 3H),

2.75-2.62 (m, 1H), 2.52-2.42 (m, 1H), 2.38-2.56 (m, 1H), 2.14-2.05 (m, 1H); ^{13}C NMR (75 MHz, $CDCl_3$) δ 158.9, 150.1, 140.5, 129.9, 127.4, 127.2, 113.8, 88.3, 83.3, 55.2, 30.9, 30.1; IR (thin film/NaCl): 2918, 2848, 2359, 2340, 1632, 1609, 1512, 1463, 1353, 1317, 1269, 1257, 1180, 1112, 1036, 963, 891, 824 cm^{-1}; HRMS-ES (*m*/*z*): $[M]^+$ calcd for $[C_{14}H_{16}O_2]^+$, 216.1150; found, 216.1155; $[\alpha]_D^{26}$ +18.8° (*c* 0.43, CH_2Cl_2).

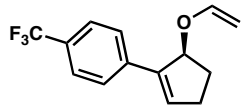

155

Vinyl Ether 155. Prepared as for **152** from (+)-**115** (100 mg, 0.44 mmol) to afford, after preparative TLC (10:1 hexanes:EtOAc), cyclopentenol (+)-**115** (57 mg, 57% yield) and **155** (41.7 mg, 37% yield) as a colorless oil: R_f 0.59 (10:1 hexanes:EtOAc); ^{1}H NMR (300 MHz, $CDCl_3$) δ 7.58 (m, 4H), 6.58 (t, *J* = 2.7 Hz, 1H), 6.50 (dd, *J* = 14.4, 6.6 Hz, 1H), 5.37 (dt, *J* = 7.2, 2.1 Hz, 1H), 4.37 (dd, *J* = 14.1, 1.8 Hz, 1H), 4.15 (dd, *J* = 6.6, 1.8 Hz, 1H), 2.80-2.67 (m, 1H), 2.58-2.47 (m, 1H), 2.42-2.30 (m, 1H), 2.17-2.08 (m, 1H); ^{13}C NMR (75 MHz, $CDCl_3$) δ 149.9, 140.2, 134.6, 126.2, 125.5, 125.4, 125.3, 125.3, 88.8, 82.9, 31.2, 30.0; IR (thin film/NaCl): 2917, 2846, 2141, 1731, 1660, 1633, 1614, 1507, 1414, 1365, 1317, 1246, 1190, 1164, 1122, 1071, 1033, 1016, 963, 829, 733 cm^{-1}; HRMS-ES (*m*/*z*): $[M]^+$ calcd for $[C_{14}H_{13}OF_3]^+$, 254.0919; found, 254.0913; $[\alpha]_D^{26}$ +31.0° (*c* 0.32, CH_2Cl_2).

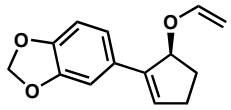

156

Vinyl Ether 156. Prepared as for **152** from (+)-**117** (100 mg, 0.49 mmol) to afford, after flash chromatography (125:2→10:1 hexanes:EtOAc), cyclopentenol (+)-**117** (36.6 mg, 37% yield) and **156** (63.3 mg, 56% yield) as a colorless oil: R_f 0.61 (10:1 hexanes:EtOAc); ^{1}H NMR (300 MHz, $CDCl_3$) δ 7.00 (d, *J* = 1.8 Hz, 1H), 6.97 (dd, *J* = 13.8, 1.5 Hz, 1H), 6.79 (d, *J* = 7.8 Hz, 1H), 6.49 (q, *J* = 6.9 Hz, 1H), 6.30 (t, *J* = 2.4 Hz, 1H), 5.94 (s, 2H), 5.29 (dt, *J* = 7.2, 2.4 Hz, 1H), 4.35 (dd, *J* = 14.4, 2.1 Hz, 1H), 4.11 (dd, *J* = 6.9, 1.8 Hz, 1H), 2.73-2.61 (m, 1H), 2.51-2.40 (m, 1H), 2.37-2.25 (m, 1H), 2.13-2.04 (m, 1H); ^{13}C NMR (75 MHz, $CDCl_3$) δ 150.0, 147.7, 146.9, 140.6, 130.6, 119.7, 108.2, 106.4, 100.9, 88.4, 83.2, 30.9, 30.0; IR (thin film/NaCl): 2898, 2849, 2359, 2340, 1632, 1610, 1503, 1490, 1447, 1366, 1317, 1227, 1187, 1106, 1040, 969, 936, 889, 808 cm^{-1}; HRMS-ES (*m*/*z*): $[M]^+$ calcd for $[C_{14}H_{14}O_3]^+$, 230.0943; found, 230.0933. $[\alpha]_D^{26}$ +20.8° (*c* 0.075, CH_2Cl_2).

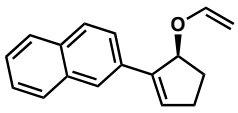

157

Vinyl Ether 157. Prepared as for **152** from (+)-**116** (100 mg, 0.48 mmol) to afford, after preparative TLC (10:1 hexanes:EtOAc), cyclopentenol (+)-**116** (47.5 mg, 48% yield) and **157** (53 mg, 47% yield) as a colorless oil: R_f 0.71 (10:1 hexanes:EtOAc); ^{1}H NMR (300 MHz, $CDCl_3$) δ 7.87-7.80 (comp. m, 4H), 7.70-7.67 (m, 1H), 7.51-7.43 (comp. m, 2H), 6.61 (t, *J* = 2.7 Hz, 1H), 6.58 (dd, *J* = 14.4, 6.9 Hz, 1H), 5.51 (dt, *J* = 7.2,

2.7 Hz, 1H), 4.43 (dd, *J* = 14.1, 1.8 Hz, 1H), 4.18 (dd, *J* = 6.9, 1.8 Hz, 1H), 2.83-2.71 (m, 1H), 2.60-2.49 (m, 1H), 2.44-2.32 (m, 1H), 2.23-2.13 (m, 1H); ^{13}C NMR (75 MHz, $CDCl_3$) δ 150.1, 141.1, 133.5, 1327, 131.9, 128.3, 127.9, 127.5, 126.0, 125.8, 124.7, 124.3, 88.5, 83.1, 31.2, 30.1; IR (thin film/NaCl): 3282, 3055, 2929, 2848, 1632, 1610, 1507, 1449, 1317, 1187, 1048, 1030, 963, 947, 894, 815, 746, 665 cm^{-1}; HRMS-ES (*m*/*z*): $[M]^+$ calcd for $[C_{17}H_{16}O]^+$, 236.1201; found, 236.1207; $[\alpha]_D^{26}$ +48.7° (*c* 0.53, CH_2Cl_2).

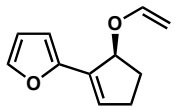

158

Vinyl Ether 158. Prepared as for **152** from (+)-**118** (82.3 mg, 0.55 mmol) to afford, after flash chromatography (125:2→10:1 hexanes:EtOAc), cyclopentenol (+)-**118** (53.2 mg, 65% yield) and **158** (30.3 mg, 31% yield) as a colorless oil: R_f 0.72 (10:1 hexanes:EtOAc); ^{1}H NMR (300 MHz, $CDCl_3$) δ 7.38 (d, *J* = 1.8 Hz, 1H), 6.49 (q, *J* = 6.6 Hz, 1H), 6.39 (dd, *J* = 3.6, 2.1 Hz, 1H), 6.36 (t, *J* = 3.0 Hz, 1H), 6.30 (d, *J* = 3.3 Hz, 1H), 5.23 (dt, *J* = 7.2, 2.7 Hz, 1H), 4.34 (dd, *J* = 14.4, 1.8 Hz, 1H), 4.10 (dd, *J* = 6.9, 1.8 Hz, 1H), 2.75-2.63 (m, 1H), 2.53-2.42 (m, 1H), 2.37-2.25 (m, 1H), 2.09-1.99 (m, 1H). ^{13}C NMR (75 MHz, $CDCl_3$) δ 150.5, 150.2, 141.9, 132.2, 130.1, 111.1, 106.9, 88.5, 83.3, 31.1, 30.1; IR (thin film/NaCl): 2924, 2850, 1633, 1611, 1487, 1349, 1317, 1189, 1153, 1051, 1028, 962, 916, 884, 806 cm^{-1}; HRMS-ES (*m*/*z*): $[M]^+$ calcd for $[C_{11}H_{12}O_2]^+$, 176.0837; found, 176.0842; $[\alpha]_D^{25}$ +39.1° (*c* 0.35, CH_2Cl_2).

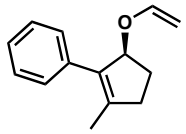

159

Vinyl Ether 159. Prepared as for **152** from (–)-**120** (428 mg, 2.47 mmol) to afford, after flash chromatography (200:1→100:1→10:1 hexanes:EtOAc), cyclopentenol (–)-**120** (140 mg, 33% yield) and **159** (301 mg, 61% yield) as a colorless oil: R_f 0.69 (10:1 hexanes:EtOAc); ^{1}H NMR (300 MHz, $CDCl_3$) δ 7.38-7.36 (comp. m, 4H), 7.31-7.24 (m, 1H), 6.45 (dd, *J* = 13.8, 6.3 Hz, 1H), 5.25 (br. d, *J* = 6.9 Hz, 1H), 4.31 (dd, *J* = 14.4, 1.8 Hz, 1H), 4.04 (dd, *J* = 6.6, 1.5 Hz, 1H), 2.79-2.68 (m, 1H), 2.48-2.22 (m, 2H), 2.06-1.97 (m, 1H); ^{13}C NMR (75 MHz, $CDCl_3$) δ 150.5, 142.3, 136.4, 134.7, 128.2, 128.1, 126.6, 88.0, 87.1, 37.1, 28.9, 15.7; IR (thin film/NaCl): 3055, 3029, 2975, 2938, 2912, 2845, 1631, 1608, 1492, 1444, 1379, 1350, 1317, 1189, 1099, 1058, 1016, 989, 964, 872, 816 cm^{-1}. HRMS-ES (*m*/*z*): $[M]^+$ calcd for $[C_{14}H_{16}O]^+$, 200.1201; found, 200.1213; $[\alpha]_D^{26}$ +6.1° (*c* 0.80, CH_2Cl_2).

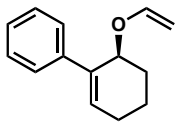

160

Vinyl Ether 160. Prepared as for **152** from (–)-**119** (174.1 mg, 1.00 mmol) to afford, after flash chromatography (125:2→10:1 hexanes:EtOAc), cyclopentenol (–)-**119** (98 mg, 56% yield) and **160** (31 mg, 16% yield) as a colorless oil: R_f 0.72 (10:1 hexanes:EtOAc); ^{1}H NMR (300 MHz, $CDCl_3$) δ 7.43-7.22 (comp. m, 5H), 6.43 (dd, *J* = 14.1, 6.6 Hz, 1H), 6.35 (t, *J* = 3.3 Hz, 1H), 4.78 (t, *J* = 3.0 Hz, 1H), 4.41 (dd, *J* = 14.1, 1.5 Hz, 1H), 4.08 (dd, *J* = 6.6, 1.8 Hz, 1H), 2.40-2.30 (m, 1H), 2.25-2.14 (m, 2H), 1.91-1.64

(comp. m, 3H); ^{13}C NMR (75 MHz, $CDCl_3$) δ 150.5, 140.4, 135.6, 130.6, 128.3, 126.9, 125.6, 88.5, 72.5, 27.6, 25.9, 16.8; IR (thin film/NaCl): 3023, 2933, 2865, 2829, 2359, 2340, 1632, 1610, 1496, 1445, 1376, 1355, 1330, 1312, 1260, 1185, 1094, 1062, 1011, 977, 946, 917, 870, 813, 756, 695 cm^{-1}; HRMS-ES (*m*/*z*): $[M]^+$ calcd for $[C_{14}H_{16}O]^+$, 200.1201; found, 200.1207; $[\alpha]_D^{25}$ –115.8° (*c* 0.17, CH_2Cl_2).

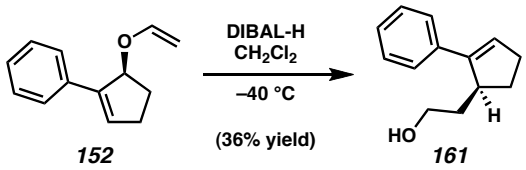

General Procedure for Claisen Rearrangement: Primary Alcohol 161. To a solution of vinyl ether **152** (7.6 mg, 0.041 mmol, 1.0 equiv) in CH_2Cl_2 (0.5 mL) at –40 °C was added DIBAL-H (1 M in $PhCH_3$, 45 μL, 0.045 mmol, 1.1 equiv) dropwise. The reaction mixture was allowed to warm to 23 °C and to stir 2 h, after which it was quenched with excess Na_2SO_4•$10H_2O$. The suspension was stirred 30 min and filtered, and the filtrate was concentrated under reduced pressure. Purification by preparative TLC (9:2 hexanes:EtOAc) to afford primary alcohol **161** (2.8 mg, 36% yield): R_f 0.16 (10:1 hexanes:EtOAc); ^{1}H NMR (300 MHz, $CDCl_3$) δ 7.35-7.20 (comp. m, 5H), 5.80 (t, *J* = 2.4 Hz, 1H), 3.75-3.58 (m, 2H), 2.42-2.35 (m, 2H), 2.10-2.01 (m, 1H), 1.89-1.77 (comp. m, 3H), 1.34 (s, 1H), 1.25 (s, 3H); ^{13}C NMR (75 MHz, $CDCl_3$) δ 150.6, 137.9, 128.9, 128.1, 127.3, 126.6, 60.7, 48.7, 48.5, 39.2, 30.1, 26.8; IR (thin film/NaCl): 3369, 3054, 2951, 2866, 1598, 1492, 1453, 1376, 1099, 1054, 1020, 759, 700 cm^{-1}; HRMS-ES (*m*/*z*): $[M]^+$ calcd for $[C_{14}H_{18}O]^+$, 202.1358; found, 202.1355; $[\alpha]_D^{25}$ +27.5° (*c* 0.66, CH_2Cl_2; for *S* enantiomer at 87% ee).

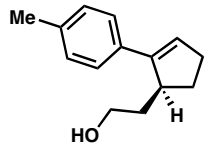

162

Primary Alcohol 162. Prepared as for **161** from **153** (40.9 mg, 0.21 mmol) to afford, after preparative TLC (9:2 hexanes:EtOAc), primary alcohol **162** (32 mg, 77% yield) as a colorless oil: R_f 0.15 (10:1 hexanes:EtOAc); ^{1}H NMR (300 MHz, $CDCl_3$) δ 7.32 (d, J = 7.8 Hz, 2H), 7.14 (d, J = 8.1 Hz, 2H), 6.02-6.00 (m, 1H), 3.73-3.65 (m, 2H), 3.26 (m, 1H), 2.52-2.44 (m, 2H), 2.34 (s, 3H), 2.26-2.13 (m, 1H), 1.94-1.74 (m, 2H), 1.55-1.43 (m, 1H), 1.34 (s, 1H); ^{13}C NMR (75 MHz, $CDCl_3$) δ 146.1, 136.6, 129.1, 126.0, 125.8, 61.7, 41.5, 36.5, 31.5, 29.8, 21.1; IR (thin film/NaCl): 3337, 3048, 3023, 2936, 2844, 1901, 1617, 1566, 1511, 1437, 1379, 1335, 1307, 1185, 1111, 1056, 1019, 981, 879, 803 cm^{-1}; HRMS-ES (m/z): $[M]^+$ calcd for $[C_{14}H_{18}O]^+$, 202.1358; found, 202.1353; $[\alpha]_D^{24}$ +51.5° (c 0.075, CH_2Cl_2; for *S* enantiomer at 96.8% ee).

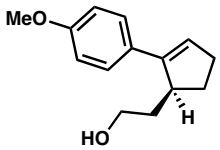

163

Primary Alcohol 163. Prepared as for **161** from **154** (38.5 mg, 0.18 mmol) to afford, after preparative TLC (9:2 hexanes:EtOAc), primary alcohol **163** (35.2 mg, 91% yield) as a colorless oil: R_f 0.15 (10:1 hexanes:EtOAc); ^{1}H NMR (300 MHz, $CDCl_3$) δ 7.36 (d, J = 8.7 Hz, 2H), 6.87 (d, J = 8.7 Hz, 2H), 5.94 (s, 1H), 3.80 (s, 3H), 3.72-3.64 (m, 2H), 3.26 (br. s, 1H), 2.50-2.44 (m, 2H), 2.24-2.11 (m, 1H), 1.92-1.73 (m, 2H), 1.54-1.42 (m, 1H), 1.44 (s, 1H); ^{13}C NMR (75 MHz, $CDCl_3$) δ 158.5, 145.6, 128.9, 127.2, 124.7, 113.7, 61.7, 55.2, 41.6, 36.4, 31.4, 29.8; IR (thin film/NaCl): 3392, 2934, 2836,

1607, 1510, 1462, 1441, 1294, 1252, 1178, 1037, 804 cm^{-1}; HRMS-ES (*m*/*z*): $[M]^+$ calcd for $[C_{14}H_{18}O_2]^+$, 218.1307; found, 218.1299; $[\alpha]_D^{25}$ +66.9° (*c* 0.27, CH_2Cl_2; for *S* enantiomer at 98.6% ee).

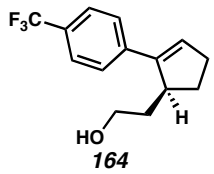

164

Primary Alcohol 164. Prepared as for **161** from **155** (41.1 mg, 0.16 mmol) to afford, after preparative TLC (9:2 hexanes:EtOAc), primary alcohol **164** (34.0 mg, 82% yield) as a colorless oil: R_f 0.18 (10:1 hexanes:EtOAc); ^{1}H NMR (300 MHz, $CDCl_3$) δ 7.58 (dd, *J* = 8.4, 21.6 Hz, 4H), 6.17 (s, 1H), 3.72-3.67 (m, 2H), 3.30 (br. s, 1H), 2.52-2.50 (m, 2H), 2.29-2.16 (m, 1H), 1.90-1.78 (m, 2H), 1.52-1.42 (m, 1H), 1.37 (s, 1H); ^{13}C NMR (75 MHz, $CDCl_3$) δ 145.3, 139.8, 129.4, 126.3, 125.4, 125.4, 125.3, 61.5, 41.5, 36.3, 31.6, 29.7; IR (thin film/NaCl): 3368, 2937, 2846, 1615, 1412, 1326, 1164, 1123, 1110, 1069, 1015, 850, 831, 815 cm^{-1}; HRMS-ES (*m*/*z*): $[M]^+$ calcd for $[C_{14}H_{15}OF_3]^+$, 256.1075; found, 256.1073; $[\alpha]_D^{26}$ +48.5° (*c* 0.20, CH_2Cl_2; for *S* enantiomer at 97.1% ee).

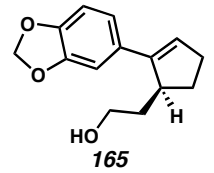

165

Primary Alcohol 165. Prepared as for **161** from **156** (63.4 mg, 0.28 mmol) to afford, after preparative TLC (9:2 hexanes:EtOAc), primary alcohol **165** (49 mg, 76% yield) as a colorless oil: R_f 0.22 (10:1 hexanes:EtOAc); ^{1}H NMR (300 MHz, $CDCl_3$) δ 6.92 (s, 1H), 6.89 (dd, *J* = 8.4, 1.2 Hz, 1H), 6.78 (d, *J* = 8.4 Hz), 5.94 (s, 2H), 5.93 (s,

1H), 3.72-3.64 (m, 2H), 3.32 (br. s, 1H), 2.49-2.43 (m, 2H), 2.23-2.11 (m, 1H), 1.92-1.73 (m, 2H), 1.54-1.42 (m, 1H), 1.49 (s, 1H); ^{13}C NMR (75 MHz, $CDCl_3$) δ 147.7, 146.5, 145.8, 130.6, 125.4, 119.6, 108.1, 106.6, 100.9, 61.6, 41.7, 36.3, 31.3, 29.7; IR (thin film/NaCl): 3350, 3041, 2935, 2888, 2777, 2063, 1850, 1604, 1503, 1489, 1443, 1356, 1223, 1126, 1104, 1040, 986, 937, 862, 806 cm^{-1}; HRMS-ES (*m*/*z*): $[M]^+$ calcd for $[C_{14}H_{16}O_3]^+$, 232.1100; found, 232.1091; $[\alpha]_D^{24}$ +62.2° (*c* 0.27, CH_2Cl_2; for *S* enantiomer at 93.1% ee).

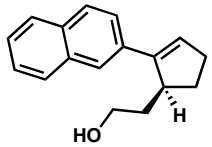

166

Primary Alcohol 166. Prepared as for **161** from **157** (45.3 mg, 0.19 mmol) to afford, after preparative TLC (9:2 hexanes:EtOAc), primary alcohol **166** (39.0 mg, 86% yield) as a colorless oil: R_f 0.24 (10:1 hexanes:EtOAc); ^{1}H NMR (300 MHz, $CDCl_3$) δ 7.83-7.78 (comp. m, 4H), 7.63 (d, *J* = 8.7 Hz, 1H), 7.49-7.41 (m, 1H), 6.22 (s, 1H), 3.80 (s, 3H), 3.72 (t, *J* = 5.1 Hz, 2H), 3.41 (br. s, 1H), 2.62-2.46 (m, 2H), 2.31-2.18 (m, 1H), 2.10-1.81 (m, 2H), 1.61-1.49 (m, 1H), 1.44 (s, 1H); ^{13}C NMR (75 MHz, $CDCl_3$) δ 146.2, 133.6, 133.5, 132.5, 128.0, 127.9, 127.52, 127.46, 126.1, 125.6, 124.8, 124.5, 61.7, 41.5, 36.4, 31.6, 29.8; IR (thin film/NaCl): 3369, 3055, 2933, 2847, 1627, 1595, 1505, 1435, 1354, 1273, 1197, 1145, 1128, 1056, 989, 962, 946, 893, 858, 812, 747 cm^{-1}; HRMS-ES (*m*/*z*): $[M]^+$ calcd for $[C_{17}H_{18}O]^+$, 238.1358; found, 238.1354; $[\alpha]_D^{25}$ +25.4° (*c* 0.47, CH_2Cl_2; for *S* enantiomer at 98.8% ee).

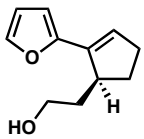

167

Primary Alcohol 167. Prepared as for **161** from **158** (27.0 mg, 0.15 mmol) to afford, after preparative TLC (9:2 hexanes:EtOAc), primary alcohol **167** (23.8 mg, 87% yield) as a colorless oil: R_f 0.21 (10:1 hexanes:EtOAc); ^{1}H NMR (300 MHz, $CDCl_3$) δ 7.35 (d, J = 1.5 Hz), 6.38 (dd, J = 3.3, 1.8 Hz, 1H), 6.26 (d, J = 3.3 Hz), 6.07 (s, 2H), 3.77-3.67 (m, 2H), 3.09 (br. s, 1H), 2.60-2.37 (m, 2H), 2.19-2.09 (m, 1H), 2.02-1.91 (m, 1H), 1.83-1.74 (m, 1H), 1.68-1.54 (m, 2H), 1.49 (s, 1H); ^{13}C NMR (75 MHz, $CDCl_3$) δ 151.9, 141.4, 136.6, 125.4, 110.9, 105.8, 61.6, 41.6, 36.7, 31.3, 29.8; IR (thin film/NaCl): 3368, 2938, 2873, 1654, 1487, 1459, 1329, 1056, 1008, 920, 885, 800, 733, 681 cm^{-1}; HRMS-ES (*m*/*z*): $[M]^+$ calcd for $[C_{11}H_{14}O_2]^+$, 178.0994; found, 178.0995; $[\alpha]_D^{24}$ +23.4° (*c* 0.29, CH_2Cl_2; for *S* enantiomer at 48.6% ee).[65]

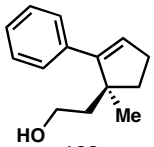

168

Primary Alcohol 168. Prepared as for **161** from **159** (39.9 mg, 0.20 mmol) to afford, after preparative TLC (4:1 hexanes:EtOAc), primary alcohol **168** (32.9 mg, 82% yield) as a colorless oil: R_f 0.12 (10:1 hexanes:EtOAc); ^{1}H NMR (300 MHz, $CDCl_3$) δ 7.35-7.20 (comp. m, 5H), 5.80 (t, J = 2.4 Hz, 1H), 3.75-3.58 (m, 2H), 2.42-2.35 (m, 2H), 2.10-2.01 (m, 1H), 1.89-1.77 (comp. m, 3H), 1.34 (s, 1H), 1.25 (s, 3H); ^{13}C NMR (75 MHz, $CDCl_3$) δ 150.6, 137.9, 128.9, 128.1, 127.3, 126.6, 60.7, 48.7, 48.5, 39.2, 30.1, 26.8; IR (thin film/NaCl): 3369, 3054, 2951, 2866, 1598, 1492, 1453, 1376, 1099, 1054,

1020, 759, 700 cm^{-1}; HRMS-ES (*m*/*z*): $[M]^+$ calcd for $[C_{14}H_{18}O]^+$, 202.1358; found, 202.1355; $[\alpha]_D^{25}$ +27.5° (*c* 0.66, CH_2Cl_2; for *S* enantiomer at 87% ee).

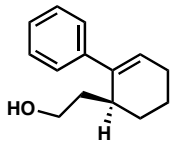

169

Primary Alcohol 169. Prepared as for **161** from **160** (32.4 mg, 0.16 mmol) to afford, after preparative TLC (9:2 hexanes:EtOAc), primary alcohol **169** (27.1 mg, 83% yield) as a colorless oil: R_f 0.29 (10:1 hexanes:EtOAc); ^{1}H NMR (300 MHz, $CDCl_3$) δ 7.32-7.21 (comp. m, 5H), 5.92 (t, *J* = 4.2 Hz, 1H), 3.59 (t, *J* = 6.0 Hz, 2H), 2.89 (br. s, 1H), 2.21-2.15 (m, 2H), 1.87-1.43 (comp. m, 7H); ^{13}C NMR (75 MHz, $CDCl_3$) δ 142.6, 141.7, 128.3, 126.5, 126.5, 126.2, 61.2, 36.5, 30.0, 27.3, 26.0, 18.5; IR (thin film/NaCl): 3351, 3021, 2930, 2861, 2832, 1639, 1598, 1493, 1443, 1430, 1058, 1032, 1013, 986, 757, 698 cm^{-1}; HRMS-ES (*m*/*z*): $[M]^+$ calcd for $[C_{14}H_{18}O]^+$, 202.1358; found, 202.1358; $[\alpha]_D^{25}$ +107.2° (*c* 0.050, CH_2Cl_2; for *S* enantiomer at 97.0% ee).

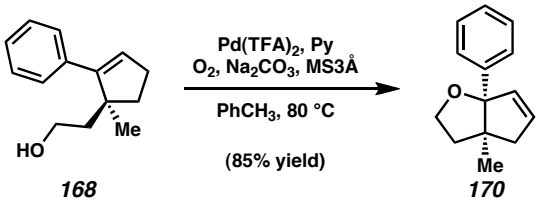

168 ***170***

Tetrahydrofuran 170. To an oven-dried reaction tube with stir bar was added oven-dried powdered 3 Å molecular sieves (120 mg). After cooling, $Pd(TFA)_2$ (4.1 mg, 0.012 mmol, 0.10 equiv), anhydrous Na_2CO_3 (52.6 mg, 0.50 mmol, 4.0 equiv), followed by $PhCH_3$ (2.5 mL), pyridine (4.0 μL, 0.050 mmol, 0.40 equiv), and alcohol **168** (25.1

mg, 0.12 mmol, 1.0 equiv). The reaction vessel was then cooled to –78 °C, vacuum evacuated, and purged with O_2 (3 x). The reaction was then heated to 80 °C with vigorous stirring under O_2 (1 atm). After 15.5 h, the reaction was complete by TLC analysis. The reaction was cooled to 23 °C, filtered through a short plug of silica gel (EtOAc eluent), and concentrated under reduced pressure to afford tetrahydrofuran **170** (21.0 mg, 85% yield) as a colorless oil. Further purification by preparative TLC (4:1 hexanes:EtOAc) afforded an analytically pure sample: R_f 0.62 (4:1 hexanes:EtOAc); ^{1}H NMR (300 MHz, $CDCl_3$) δ 7.34-7.20 (comp. m, 5H), 6.07 (ddd, *J* = 5.8, 2.4, 2.4 Hz, 1H), 5.65 (ddd, *J* = 5.8, 2.1, 2,1 Hz, 1H), 4.07 (ddd, *J* = 8.6, 6.8, 4.3 Hz, 1H), 3.82 (ddd, *J* = 8.6, 8,6, 6.2 Hz, 1H), 2.53 (ddd, *J* = 17.3, 2.2, 2.2 Hz, 1H), 2.34 (ddd, *J* = 17.3, 2.2, 2.2 Hz, 1H), 1.96 (ddd, *J* = 12.0, 6.1, 4.4 Hz, 1H), 1.89 (ddd, *J* = 11.9, 8.6, 6.8 Hz, 1H), 0.69 (s, 3H); ^{13}C NMR (75 MHz, $CDCl_3$) δ 142.7, 134.6, 133.4, 128.0, 127.0, 126.2, 100.0, 65.9, 51.4, 47.6, 43.6, 25.5; IR (thin film/NaCl): 2956, 1722, 1492, 1448, 1047 cm^{-1}; HRMS-EI (*m*/*z*): $[M]^+$ calcd for $[C_{14}H_{16}O]^+$, 200.1201; found, 200.1203; $[\alpha]_D^{26}$ –16.1° (*c* 1.6, CH_2Cl_2; for (*S*, *S*) enantiomer at 86% ee).

3.5.4 Methods for Determination of Conversion

Conversion values for **105**, **113**, **114**, and **124** were determined by ^{1}H NMR of a reaction aliquot after filtration through a short plug of silica gel. All other conversions were determined by GC (Table 3.5.1 or Chapter 2) relative to internal standard (tridecane).

Table 3.5.1 Methods for determination of conversion.

entry	alcohol	ketone	GC conditions	alcohol retention time (min)	ketone retention time (min)
1	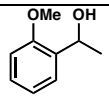 (±)-73	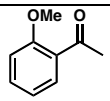 222	100 °C, 5 min; Ramp 13 °C/min	13.5	12.7
2	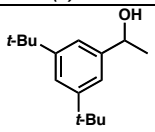 (±)-76	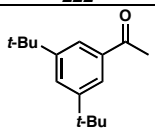 186	100 °C, 5 min; Ramp 13 °C/min	13.5	12.6
3	 (±)-94	 223	70 °C, 15 min; Ramp 7 °C/min	21.8	20.4
4	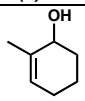 (±)-95	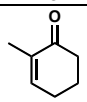 224	70 °C, 15 min; Ramp 7 °C/min	23.4	20.5
5	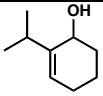 (±)-96	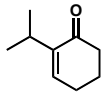 189	100 °C, 5 min; Ramp 13 °C/min	9.0	7.8
6	 (±)-97	 225	70 °C, 15 min; Ramp 7 °C/min	28.7	31.2
7	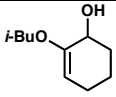 (±)-98	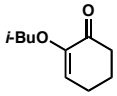 187	100 °C, 5 min; Ramp 13 °C/min	10.6	12.2
8	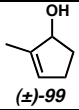 (±)-99	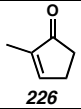 226	70 °C, 15 min; Ramp 7 °C/min	19.8	17.8
9	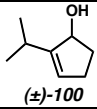 (±)-100	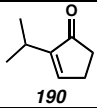 190	100 °C, 5 min; Ramp 13 °C/min	8.0	7.4

Table 3.5.1 continued

entry	alcohol	ketone	GC conditions	alcohol retention time (min)	ketone retention time (min)
10	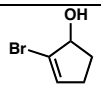 (±)-101	 227	70 °C, 15 min; Ramp 7 °C/min	28.6	30.6
11	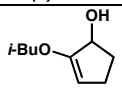 (±)-102	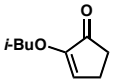 191	100 °C, 5 min; Ramp 13 °C/min	10.3	11.8
12	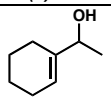 (±)-103	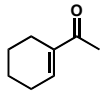 192	100 °C, 5 min; Ramp 13 °C/min	9.3	8.7
13	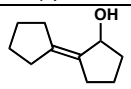 (±)-106	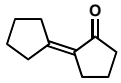 194	70 °C, 15 min; Ramp 7 °C/min	29.5	29.7
14	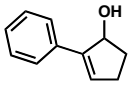 (±)-111	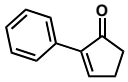 143	100 °C, 5 min; Ramp 13 °C/min to 240 °C; 240 °C, 5 min	15.8	16.1
15	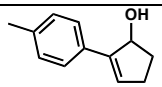 (±)-112	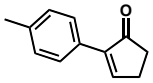 199	70 °C, 15 min; Ramp 7 °C/min	37.2	37.7
16	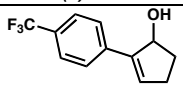 (±)-115	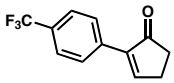 205	70 °C, 15 min; Ramp 7 °C/min	35.8	35.3
17	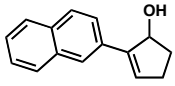 (±)-116	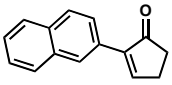 207	70 °C, 15 min; Ramp 7 °C/min to 240 °C; 240 °C, 20 min	53.3	55.4
18	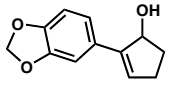 (±)-117	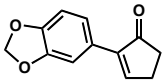 209	70 °C, 15 min; Ramp 7 °C/min to 240 °C; 240 °C, 20 min	46.9	48.6
19	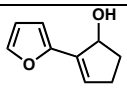 (±)-118	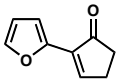 212	70 °C, 15 min; Ramp 7 °C/min	33.4	32.8
20	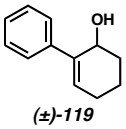 (±)-119	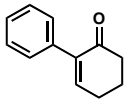 213	100 °C, 5 min; Ramp 13 °C/min to 240 °C; 240 °C, 5 min	15.8	16.1
21	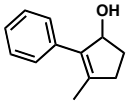 (±)-120	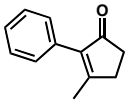 214	100 °C, 5 min; Ramp 13 °C/min to 240 °C; 240 °C, 5 min	15.1	16.6

Table 3.5.1 continued

entry	alcohol	ketone	GC conditions	alcohol retention time (min)	ketone retention time (min)
22	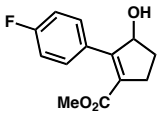 ***(±)-121***	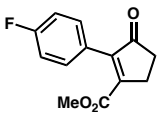 ***215***	70 °C, 15 min; Ramp 7 °C/min to 240 °C; 240 °C, 20 min	42.3	40.3
23	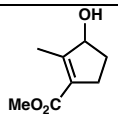 ***(±)-122***	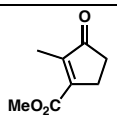 ***216***	100 °C, 5 min; Ramp 13 °C/min	14.0	12.0
24	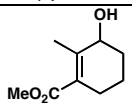 ***(±)-123***	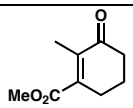 ***217***	100 °C, 5 min; Ramp 13 °C/min	15.1	13.2
25	 ***(±)-125***	 ***228***	50 °C; Ramp 3 °C/min	7.4	5.0
26	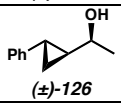 ***(±)-126***	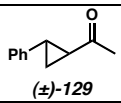 ***(±)-129***	100 °C, 5 min; Ramp 13 °C/min	14.2	13.1
27	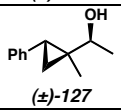 ***(±)-127***	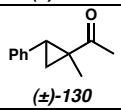 ***(±)-130***	70 °C, 15 min; Ramp 7 °C/min	33.2	31.3
28	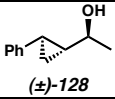 ***(±)-128***	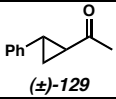 ***(±)-129***	100 °C, 5 min; Ramp 13 °C/min	14.1	13.1

3.5.5 Methods for Determination of Enantiomeric Excess

Table 3.5.2 Methods for determination of enantiomeric excess.

entry	compound (major enantiomer)	ee assay and column	assay conditions	(*S*) enantiomer retention time (min)	(*R*) enantiomer retention time (min)
1	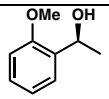 *(–)-73*	HPLC OB-H	3% EtOH/hexanes	11.5	21.4
2	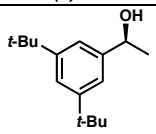 *(–)-76*	HPLC AD	0.25% *i*PrOH/hexanes	16.8	15.1
3[a]	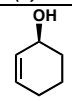 *(–)-94*	HPLC OJ	2% EtOH/hexanes	14.0	12.2
4[a]	 *(–)-95*	HPLC AD	1% EtOH/hexanes	9.7	8.9
5	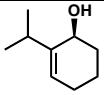 *(–)-96*	GC GTA	50 °C Ramp 1 °C/min	34.6	37.0
6[a]	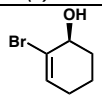 *(–)-97*	HPLC AD	1% EtOH/hexanes	16.7	15.3
7	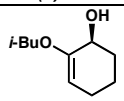 *(S)-98*	GC GTA	80 °C isothermal	53.4	52.5
8[a]	 *(S)-99*	HPLC OJ	1% EtOH/hexanes	12.0	13.2
9	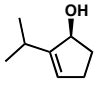 *(–)-100*	GC GTA	70 °C Ramp 1 °C/min	15.8	17.8
10[a]	 *(S)-101*	HPLC OJ	1% EtOH/hexanes	26.2	28.8
11	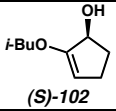 *(S)-102*	GC GTA	80 °C isothermal	27.6	25.7
12	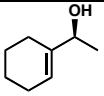 *(–)-103*	GC GTA	50 °C Ramp 3 °C/min	18.7	19.0

[a] Assayed as the *p*-NBz derivative by treatment of the aliquot with *p*-NBzCl and DMAP in CH_2Cl_2.

Table 3.5.2 continued

entry	compound (major enantiomer)	ee assay and column	assay conditions	(*S*) enantiomer retention time (min)	(*R*) enantiomer retention time (min)
13	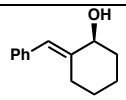 *(–)-105*	HPLC OD-H	4% EtOH/hexanes	12.4	10.3
14	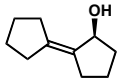 *(+)-106*	GC GTA	70 °C Ramp 1 °C/min	36.3	35.7
15	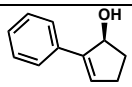 *(+)-111*	HPLC OD-H	3% EtOH/hexanes	23.3	18.5
16	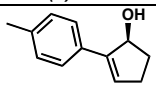 *(+)-112*	HPLC OB-H	8% EtOH/hexanes	14.4	7.5
17	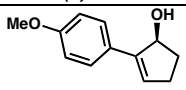 *(+)-113*	HPLC AS	4% EtOH/hexanes	11.5	15.9
18	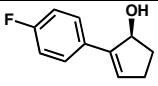 *(+)-114*	HPLC OB-H	4% EtOH/hexanes	11.0	9.1
19	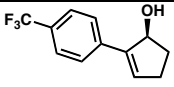 *(+)-115*	HPLC OD-H	2% EtOH/hexanes	15.3	14.0
20	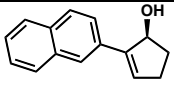 *(+)-116*	HPLC AS	3% EtOH/hexanes	11.4	13.2
21	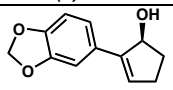 *(+)-117*	HPLC OB-H	10% EtOH/hexanes	26.8	11.0
22	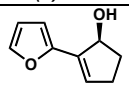 *(+)-118*	HPLC AD	4% EtOH/hexanes	21.3	17.7
23	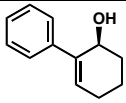 *(–)-119*	HPLC AD	3% EtOH/hexanes	21.9	16.4
24	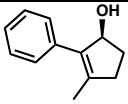 *(–)-120*	HPLC OB-H	3% EtOH/hexanes	9.6	7.9
25	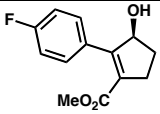 *(–)-121*	HPLC OB-H	5% EtOH/hexanes	18.2	22.3

Table 3.5.2 continued

entry	compound (major enantiomer)	ee assay and column	assay conditions	(*S*) enantiomer retention time (min)	(*R*) enantiomer retention time (min)
26	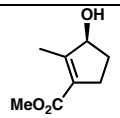 *(−)-122*	HPLC AD	3% EtOH/hexanes	23.0	26.0
27	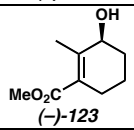 *(−)-123*	HPLC OB-H	2% *i*PrOH/hexanes	20.8	22.9
28	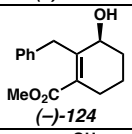 *(−)-124*	HPLC OD-H	4% EtOH/hexanes	10.2	11.5
29	 *(+)-125*	GC GTA	40 °C isothermal	10.8	11.3
30	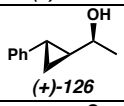 *(+)-126*	HPLC OD-H	2% EtOH/hexanes	15.1[b]	17.8
31	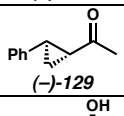 *(−)-129*	HPLC OD-H	2% EtOH/hexanes	7.9	8.5[c]
32	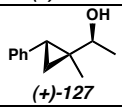 *(+)-127*	HPLC OD-H	3% EtOH/hexanes	8.8[d]	10.1
33	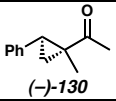 *(−)-130*	HPLC OD-H	3% EtOH/hexanes	6.9	7.5[e]
34	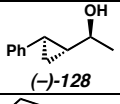 *(−)-128*	HPLC OD-H	2% EtOH/hexanes	20.7[f]	14.6
35	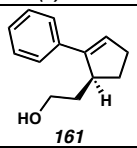 *161*	HPLC OJ	2% EtOH/hexanes	32.6	22.8
36	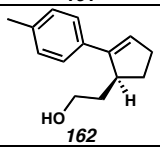 *162*	HPLC OJ	2% EtOH/hexanes	13.4	15.3
37	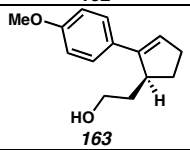 *163*	HPLC OJ	4% EtOH/hexanes	13.6	16.2

[b] Retention time for the (1*S*, 1'*S*, 2'*S*) enantiomer (shown). [c] Retention time for the (1'*R*, 2'*R*) enantiomer (shown). [d] Retention time for the (1*S*, 1'*S*, 2'*R*) enantiomer (shown). [e] Retention time for the (1'*R*, 2'*S*) enantiomer (shown). [f] Retention time for the (1*S*, 1'*R*, 2'*R*) enantiomer (shown).

Table 3.5.2 continued

entry	compound (major enantiomer)	ee assay and column	assay conditions	(*S*) enantiomer retention time (min)	(*R*) enantiomer retention time (min)
38	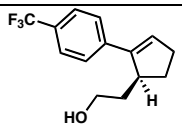 **164**	HPLC OJ	2% *i*PrOH/hexanes	21.6	18.5
39	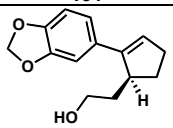 **165**	HPLC OJ	4% EtOH/hexanes	17.8	21.1
40	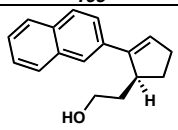 **166**	HPLC OJ	4% EtOH/hexanes	12.7	14.1
41	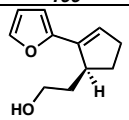 **167**	HPLC OJ	4% EtOH/hexanes	12.3	10.9
42	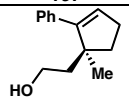 **168**	HPLC OD-H	3% EtOH/hexanes	13.1	10.7
43	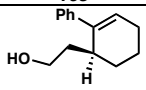 **169**	HPLC OJ	2% EtOH/hexanes	14.2	19.2
44	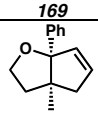 **170**	GC GTA	100 °C Ramp 1 °C/min	28.8[g]	29.2

[g] Retention time for the (*S*, *S*) enantiomer (shown).

3.6 Notes and References

(1) Ferreira, E. M.; Stoltz, B. M. *J. Am. Chem. Soc.* **2001**, *123*, 7725-7726.

(2) Bagdanoff, J. T.; Ferreira, E. M.; Stoltz, B. M. *Org. Lett.* **2003**, *5*, 835-837.

(3) Bagdanoff, J. T.; Stoltz, B. M. *Angew. Chem. Int. Ed.* **2004**, *43*, 353-357.

(4) The selectivity factor (*s*) was determined using the following equation: $s = \frac{\ln[(1-conv)(1-ee_{alc})]}{\ln[(1-conv)(1+ee_{alc})]}$, where ee_{alc} is the ee of the recovered alcohol and *conv* is the total conversion of alcohol to ketone, see: Kagan, H. B.; Fiaud, J. C. In *Topics in Stereochemistry*; Eliel, E. L., Ed.; Wiley & Sons: New York, 1988; Vol. 18, pp 249-330.

(5) For a brief discussion of the substrate scope of the oxidative kinetic resolution, see: Stoltz, B. M.; Ebner, D. C. Kinetic Resolution by Enantioselective Aerobic Oxidation of Alcohols. In *Handbook of C–H Transformation*, Dyker, G., Ed.; Wiley-VCH: New York, 2005; Vol. 2, pp 393-401.

(6) Trend, R. M.; Stoltz, B. M. *J. Am. Chem. Soc.* **2004**, *126*, 4482-4483.

(7) Caspi, D. D.; Ebner, D. C.; Bagdanoff, J. T.; Stoltz, B. M. *Adv. Synth. Catal.* **2004**, *346*, 185-189.

(8) Krishnan, S.; Ramtohul, Y. K.; Bagdanoff, J. T.; Ebner, D. C.; Tambar, U. K.; Stoltz, B. M. *J. Am. Chem. Soc.* in press.

(9) Ruel, F. S.; Braun, M. P.; Johnson, W. S. *Organic Syntheses*; Wiley & Sons: New York, 2004; Collect. Vol. X, pp 467-471.

(10) Luche, J. L.; Gemal, A. L. *J. Chem. Soc., Chem. Commun.* **1978**, 601-602.

(11) Ebner, D. C.; Novák, Z.; Stoltz, B. M. *Synlett* **2006**, 3533-3539.

(12) Low reactivity was also observed in a related system, see: Sayyed, I. A.; Kumar, N. S. C. R.; Sudalai, A. *Indian J. Chem., Sect. B* **2005**, *44B*, 1533-1535.

(13) For palladium-catalyzed alcohol oxidation conditions that allow the resolution of some saturated alkyl alcohols, see: Mandal, S. K.; Jensen, D. R.; Pugsley, J. S.; Sigman, M. S. *J. Org. Chem.* **2003**, *68*, 4600-4603.

(14) Nielsen, R. J.; Keith, J. M.; Stoltz, B. M.; Goddard, W. A., III. *J. Am. Chem. Soc.* **2004**, *126*, 7967-7974.

(15) For discussions on synthetic approaches based on bidirectional chain synthesis, see: (a) Poss, C. S.; Schreiber, S. L. *Acc. Chem. Res.* **1994**, *27*, 9-17. (b) Schreiber, S. L.; Goulet, M. T.; Schulte, G. *J. Am. Chem. Soc.* **1987**, *109*, 4718-4720.

(16) For examples of bidirectional synthesis/terminus differentiation in natural products synthesis, see: (a) Harada, T.; Kagamihara, Y.; Tanaka, S.; Sakamoto, K.; Oku, A. *J. Org. Chem.* **1992**, *57*, 1637-1639. (b) Poss, C. S.; Rychnovsky, S. D.; Schreiber, S. L. *J. Am. Chem. Soc.* **1993**, *115*, 3360-3361. (c) Schreiber, S.

L.; Sammakia, T.; Uehling, D. E. *J. Org. Chem.* **1989**, *54*, 15-16. (d) Ikemoto, N.; Schreiber, S. L. *J. Am. Chem. Soc.* **1990**, *112*, 9657-9659.

(17) Ireland, R. E.; Mueller, R. H.; Willard, A. K. *J. Am. Chem. Soc.* **1976**, *98*, 2868-2877.

(18) Johnson, W. S.; Werthemann, L.; Bartlett, W. R.; Brocksom, T. J.; Li, T.-t.; Faulkner, D. J.; Petersen, M. R. *J. Am. Chem. Soc.* **1970**, *92*, 741-743.

(19) (a) Trend, R. M.; Ramtohul, Y. K.; Ferreira, E. M.; Stoltz, B. M. *Angew. Chem., Int. Ed.* **2003**, *42*, 2892-2895. (b) Trend, R. M.; Ramtohul, Y. K.; Stoltz, B. M. *J. Am. Chem. Soc.* **2005**, *127*, 17778-17788.

(20) Related oxidative kinetic resolutions en route to pharmaceutical agents have been reported, see: (a) Ali, I. S.; Sudalai, A. *Tetrahedron Lett.* **2002**, *43*, 5435-5436. (b) Thakur, V. V.; Sudalai, A. *Indian J. Chem., Sect. B* **2005**, *44B*, 557-562.

(21) (a) Mitchell, D.; Koenig, T. M. *Synth. Commun.* **1995**, *25*, 1231-1238. (b) Kumar, A.; Ner, D. H.; Dike, S. Y. *Tetrahedron Lett.* **1991**, *32*, 1901-1904. (c) Koenig, T. M.; Mitchell, D. *Tetrahedron Lett.* **1994**, *35*, 1339-1342. (d) Ali, I. S.; Sudalai, A. *Tetrahedron Lett.* **2002**, *43*, 5435-5436. (e) Kumar, A.; Ner, D. H.; Dike, S. *Ind. J. Chem. B* **1992**, *31*, 803-809, and references therein.

(22) (a) Larsen, R. D.; Corley, E. G.; King, A. O.; Carroll, J. D.; Davis, P.; Verhoeven, T. R.; Reider, P. J.; Labelle, M; Gauthier, J. Y.; Xiang, Y. B.; Zamboni, R. J. *J. Org. Chem.* **1996**, *61*, 3398-3405. (b) King, A. O.; Corley, E. G.; Anderson, R.

K.; Larsen, R. D.; Verhoeven, T. R.; Reider, P. J.; Xiang, Y. B.; Belley, M.; Leblanc, Y.; Labelle, M.; Prasit, P.; Zamboni, R. J. *J. Org. Chem.* **1993**, *58*, 3731-3735. (c) Bhupathy, M.; McNamara, J. M.; Sidler, D. R.; Volante, R. P.; Bergan, J. J. (Merck & Co., Inc.). World Patent 95/18107, 1995. (d) Bhupathy, M.; McNamara, J. M.; Sidler, D. R.; Volante, R. P.; Bergan, J. J. (Merck & Co., Inc.). U. S. Patent 5,614,632, 1997, and references therein.

(23) (a) Kuethe, J. T.; Wong, A.; Wu, J.; Davies, I. W.; Dormer, P. G.; Welch, C. J.; Hillier, M. C.; Hughes, D. L.; Reider, P. J. *J. Org. Chem.* **2002**, *67*, 5993-6000. (b) Desai, R. C.; Cicala, P.; Meurer, L. C.; Finke, P. E. *Tetrahedron Lett.* **2002**, *43*, 4569-4570, and references therein.

(24) Marrero, J.; Rodríguez, A. D.; Baran, P.; Raptis, R. G.; Sánchez, J. A.; Ortega-Barria, E.; Capson, T. L. *Org. Lett.* **2004**, *6*, 1661-1664.

(25) Baker, L.; Minehan, T. *J. Org. Chem.* **2004**, *69*, 3957-3960.

(26) Murphy, J. A.; Scott, K. A.; Sinclair, R. S.; Martin, C. G.; Kennedy, A. R.; Lewis, N. *J. Chem. Soc., Perkin Trans. 1* **2000**, 2395-2408.

(27) Bunnelle, W. H.; Isbell, T. A. *J. Org. Chem.* **1992**, *57*, 729-740.

(28) Alternatively, 5 mol% Pd(sparteine)Cl_2 (**66**) and 15 mol% (–)-sparteine (**28**) can be used.

([29]) $CHCl_3$ stabilized with amylenes. $CHCl_3$ stabilized with EtOH must be distilled prior to use.

(30) Alternatively, 5 mol% Pd(sparteine)Cl_2 (**66**) and 7 mol% (–)-sparteine (**28**) can be used.

(31) Dess, D. B.; Martin, J. C. *J. Org. Chem.* **1983**, *48*, 4155-4156.

(32) Zhang, L.; Nadzan, A. M.; Heyman, R. A.; Love, D. L.; Mais, D. E.; Croston, G.; Lamph, W. W.; Boehm, M. F. *J. Med. Chem.* **1996**, *39*, 2659-2663.

(33) Pattenden, G.; Whybrow, D. *J. Chem. Soc., Perkin Trans. 1* **1981**, 3147-3149.

(34) Begley, M. J.; Ladlow, M.; Pattenden, G. *J. Chem. Soc., Perkin Trans. 1* **1988**, 1095-1106.

(35) Birch, A. J.; Slobbe, J. *Aust. J. Chem.* **1977**, *30*, 1045-1049.

(36) Ansell, M. F.; Ducker, J. W. *J. Chem. Soc.* **1959**, 329-331.

(37) Little, R. D.; Brown, L. M.; Masjedizadeh, M. R. *J. Am. Chem. Soc.* **1992**, *114*, 3071-3075.

(38) Hansson, S.; Heumann, A.; Rein, T.; Åkermark, B. *J. Org. Chem.* **1990**, *55*, 975-984.

(39) Yun, J.; Buchwald, S. L. *J. Am. Chem. Soc.* **1999**, *121*, 5640-5644.

(40) Billimoria, J. D. *J. Chem. Soc.* **1955**, 1126-1129.

(41) Grau-Martinez, A.; Curran, D. P. *Tetrahedron* **1997**, *53*, 5679-5698.

(42) Fogliato, G.; Fronza, G.; Fuganti, C.; Lanati, S.; Rallo, R.; Rigoni, R.; Servi, S. *Tetrahedron* **1995**, *51*, 10231-10240.

(43) Schick, H.; Mahrwald, R. *Synthesis* **1990**, 592-595.

(44) Dang, H.-S.; Davies, A. G.; Davison, I. G. E.; Schiesser, C. H. *J. Org. Chem.* **1990**, *55*, 1432-1438.

(45) Ruel, F. S.; Braun, M. P.; Johnson, W. S. *Organic Syntheses*; Wiley & Sons: New York, 2004; Collect. Vol. X, pp 467-471.

(46) Felpin, F. X. *J. Org. Chem.* **2005**, *70*, 8575-8578.

(47) Garg, N. K.; Sarpong, R.; Stoltz, B. M. *J. Am. Chem. Soc.* **2002**, *124*, 13179-13184.

(48) Murata, M.; Oyama, T.; Watanabe, S.; Masuda, Y. *J. Org. Chem.* **2000**, *65*, 164-168.

(49) Negishi, E.-i.; Tan, Z.; Liou, S.-Y.; Liao, B. *Tetrahedron* **2000**, *56*, 10197-10207.

(50) Pour, M; Spulák, M; Balsánek, V.; Kunes, J.; Kubanová, P.; Buchta, V. *Bioorg. Med. Chem.* **2003**, *11*, 2843-2866.

(51) Fürstner, A.; Seidel, G. *Org. Lett.* **2002**, *4*, 541-543.

(52) Steinke, N.; Frey, W.; Baro, A.; Laschat, S.; Drees, C.; Nimtz, M.; Hägele, C.; Giesselmann, F. *Chem.–Eur. J.* **2006**, *12*, 1026-1035.

(53) Boller, T. M.; Murphy, J. M.; Hapke, M.; Ishiyama, T.; Miyaura, N.; Hartwig, J. F. *J. Am. Chem. Soc.* **2005**, *127*, 14263-14278.

(54) Kraus, G. A.; Frazier, K. *J. Org. Chem.* **1980**, *45*, 2579-2581.

(55) Ito, S.; Kasai, M.; Ziffer, H.; Silverton, J. V. *Can. J. Chem.* **1987**, *65*, 574-582.

(56) Padwa, A.; Blacklock, T. J.; Getman, D.; Hatanaka, N.; Loza, R. *J. Org. Chem.* **1978**, *43*, 1481-1492.

(57) Hewett, C. L. *J. Chem. Soc.* **1936**, 50-52.

(58) Correa, J.; Mainero, R. M. *J. Org. Chem.* **1969**, *34*, 2192-2195.

(59) Charette, A. B.; Lebel, H. *J. Org. Chem.* **1995**, *60*, 2966-2967.

(60) Charette, A. B.; Molinaro, C.; Brochu, C. *J. Am. Chem. Soc.* **2001**, *123*, 12160-12167.

(61) Barluenga, J.; Bernad, P. L., Jr.; Concellón, J. M.; Piñera-Nicolás, A.; García-Granda, S. *J. Org. Chem.* **1997**, *62*, 6870-6875.

(62) DePuy, C. H.; Breitbeil, F. W.; DeBruin, K. R. *J. Am. Chem. Soc.* **1966**, *88*, 3347-3354.

(63) Charette, A. B.; Lacasse, M.-C. *Org. Lett.* **2002**, *4*, 3351-3353.

(64) Charette, A. B.; Lebel, H.; Gagnon, A. *Tetrahedron* **1999**, *55*, 8845-8856.

(65) The decreased enantiomeric excess for this substrate is presumably due to competing 1,3-rearrangement, leading to partial racemization.

APPENDIX 1

Spectra Relevant to Chapter 3

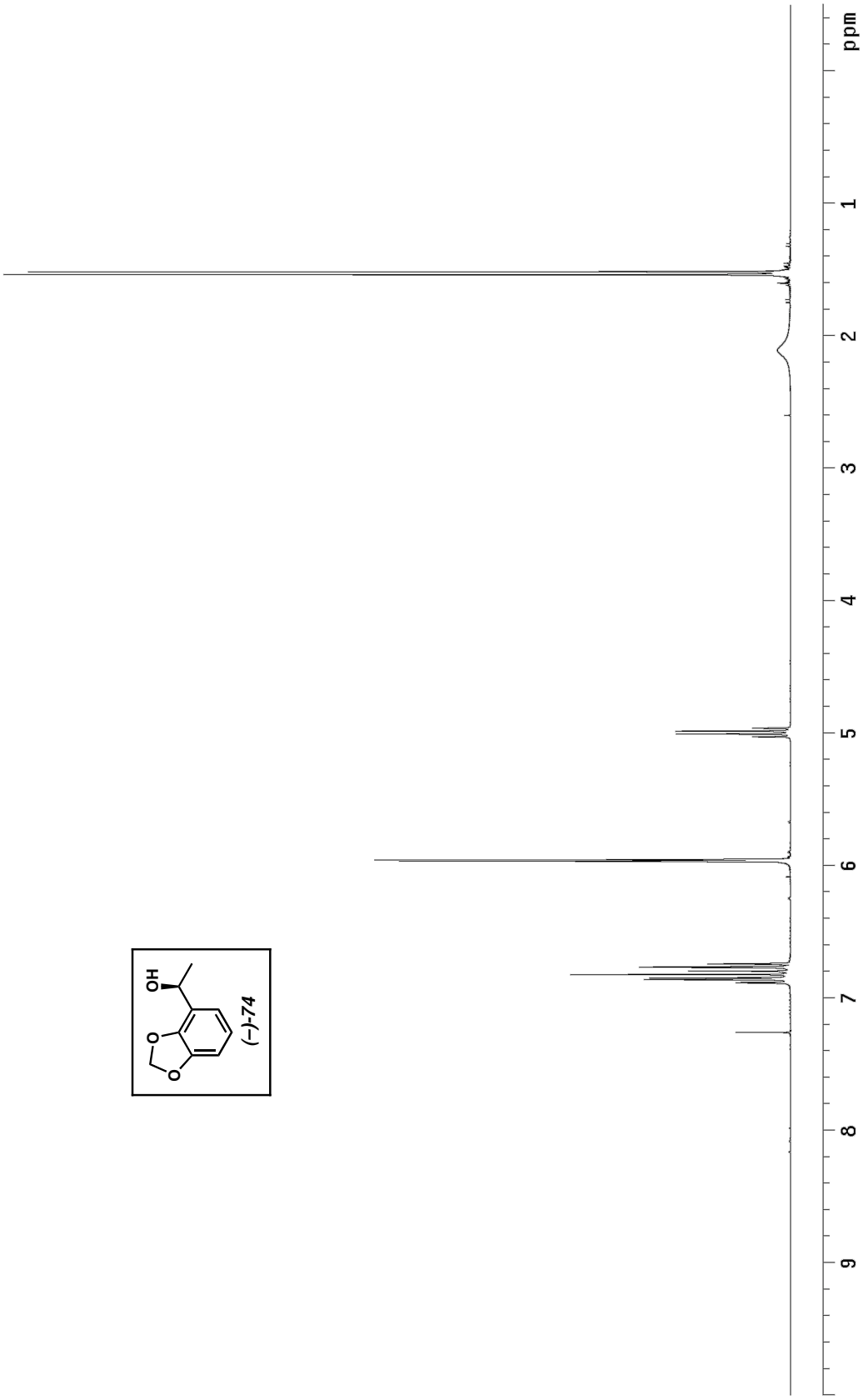

Figure A1.1 ^{1}H NMR (300 MHz, $CDCl_3$) of compound (–)-**74**.

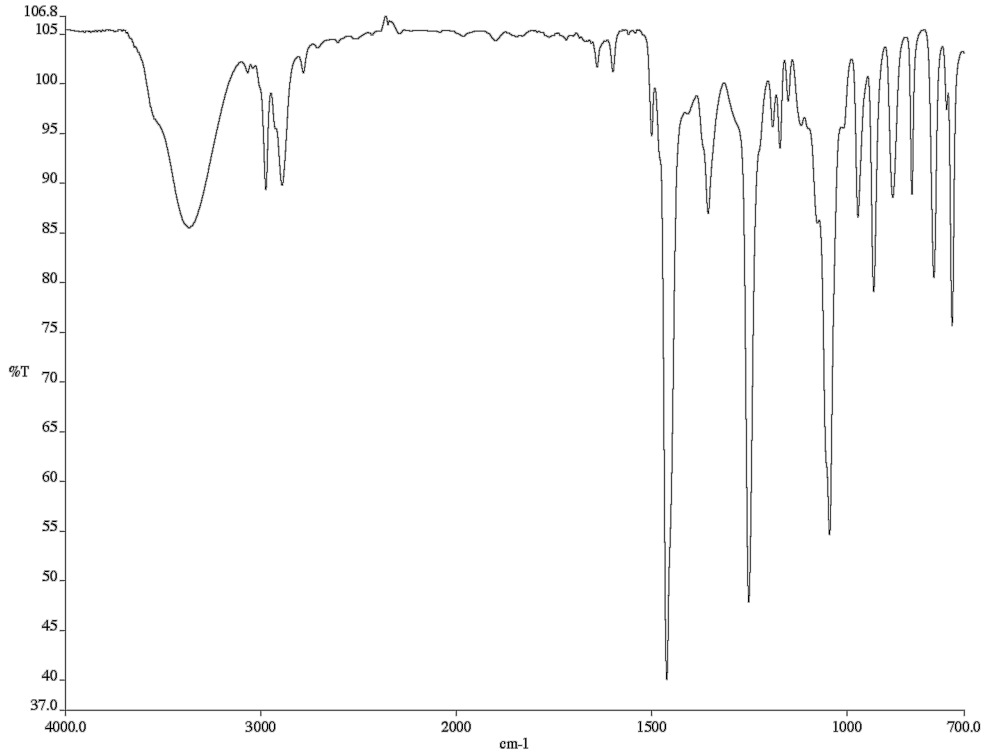

Figure A1.2 Infrared spectrum (thin film/NaCl) of compound (–)-**74**.

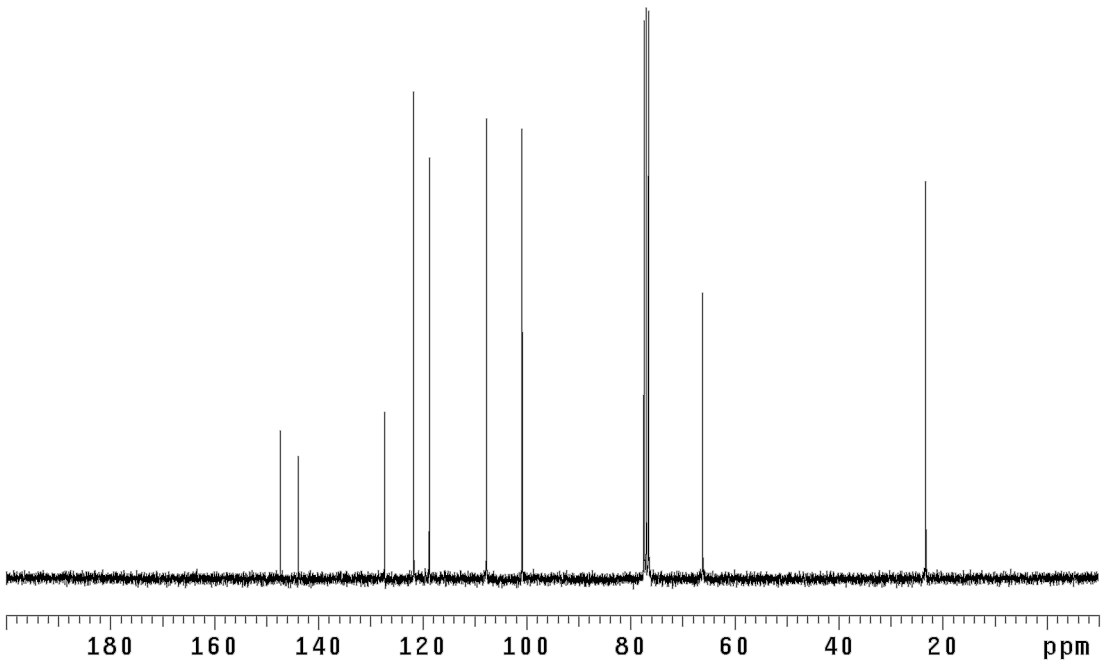

Figure A1.3 ^{13}C NMR (75 MHz, $CDCl_3$) of compound (–)-**74**.

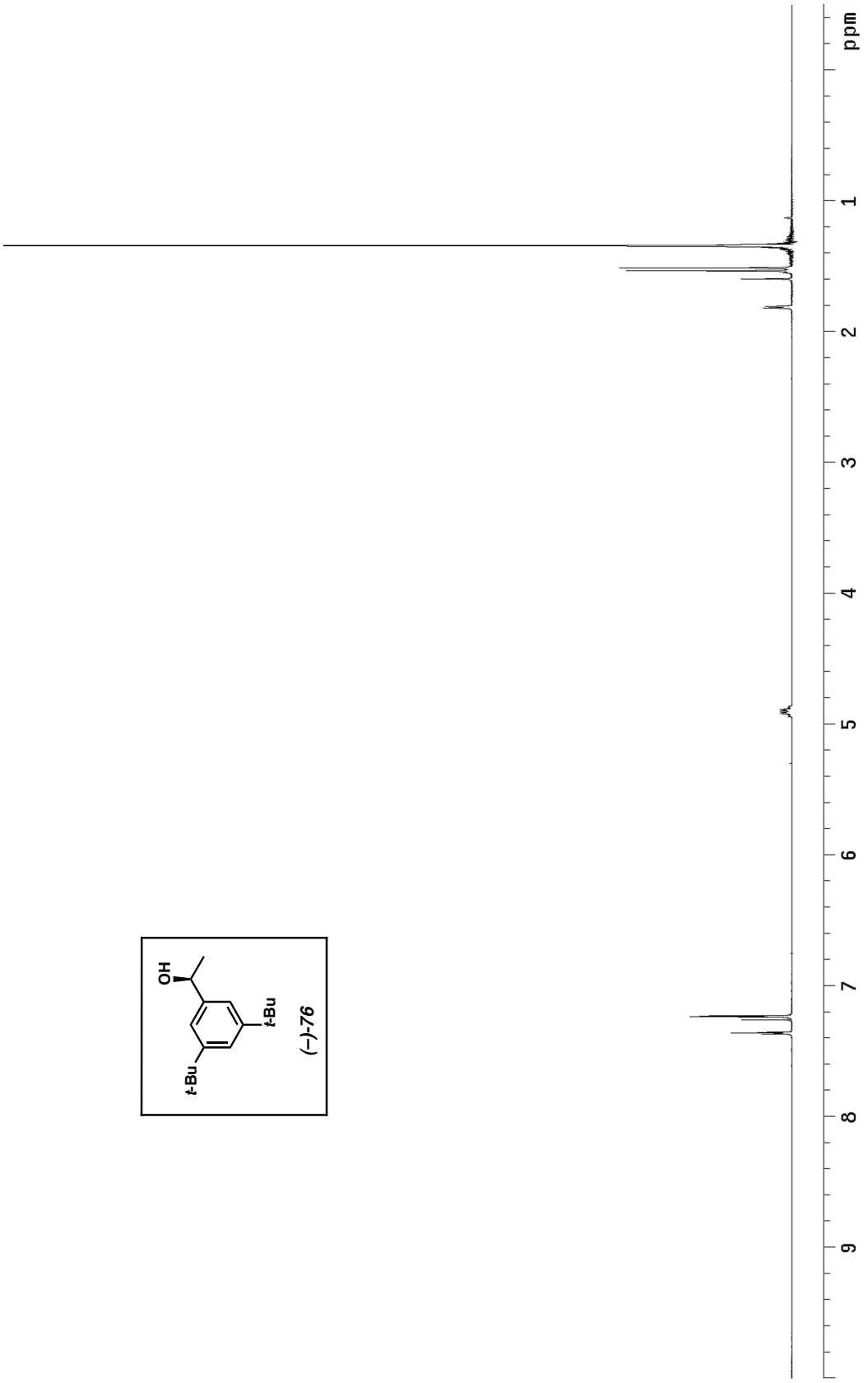

Figure A1.4 ^{1}H NMR (300 MHz, $CDCl_3$) of compound (–)-**76**.

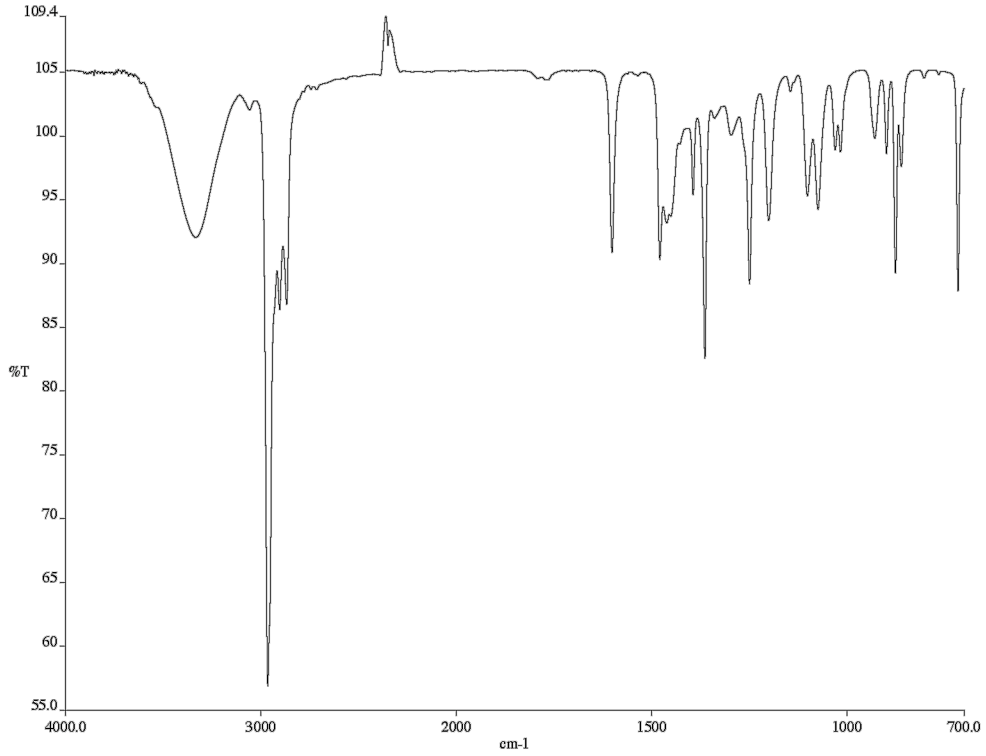

Figure A1.5 Infrared spectrum (thin film/NaCl) of compound (–)-**76**.

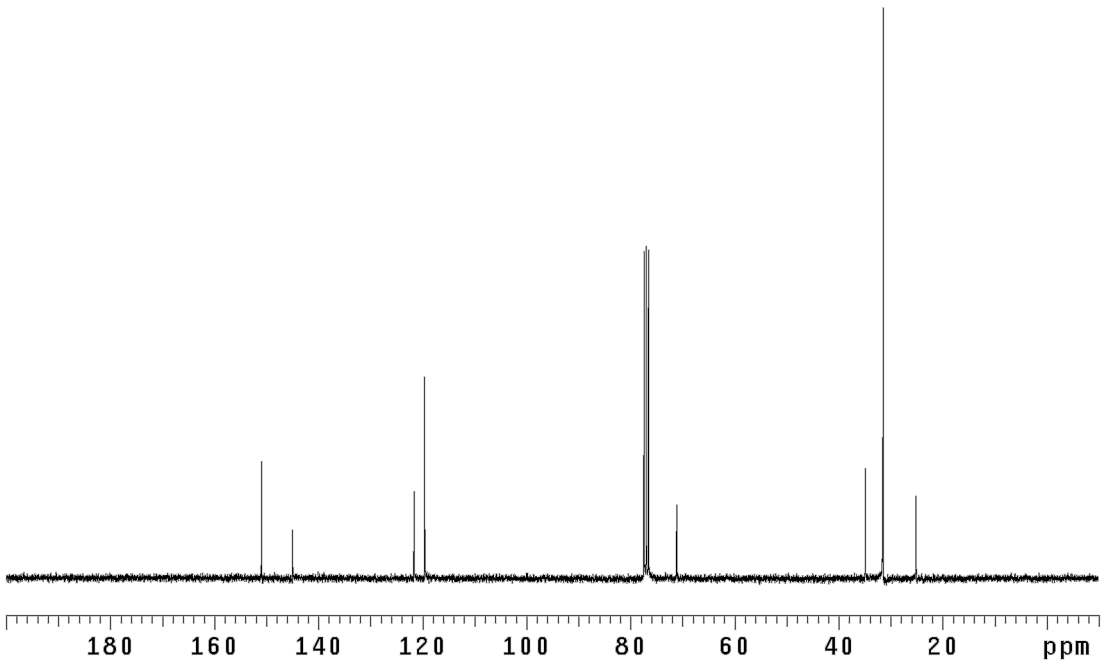

Figure A1.6 ^{13}C NMR (75 MHz, $CDCl_3$) of compound (–)-**76**.

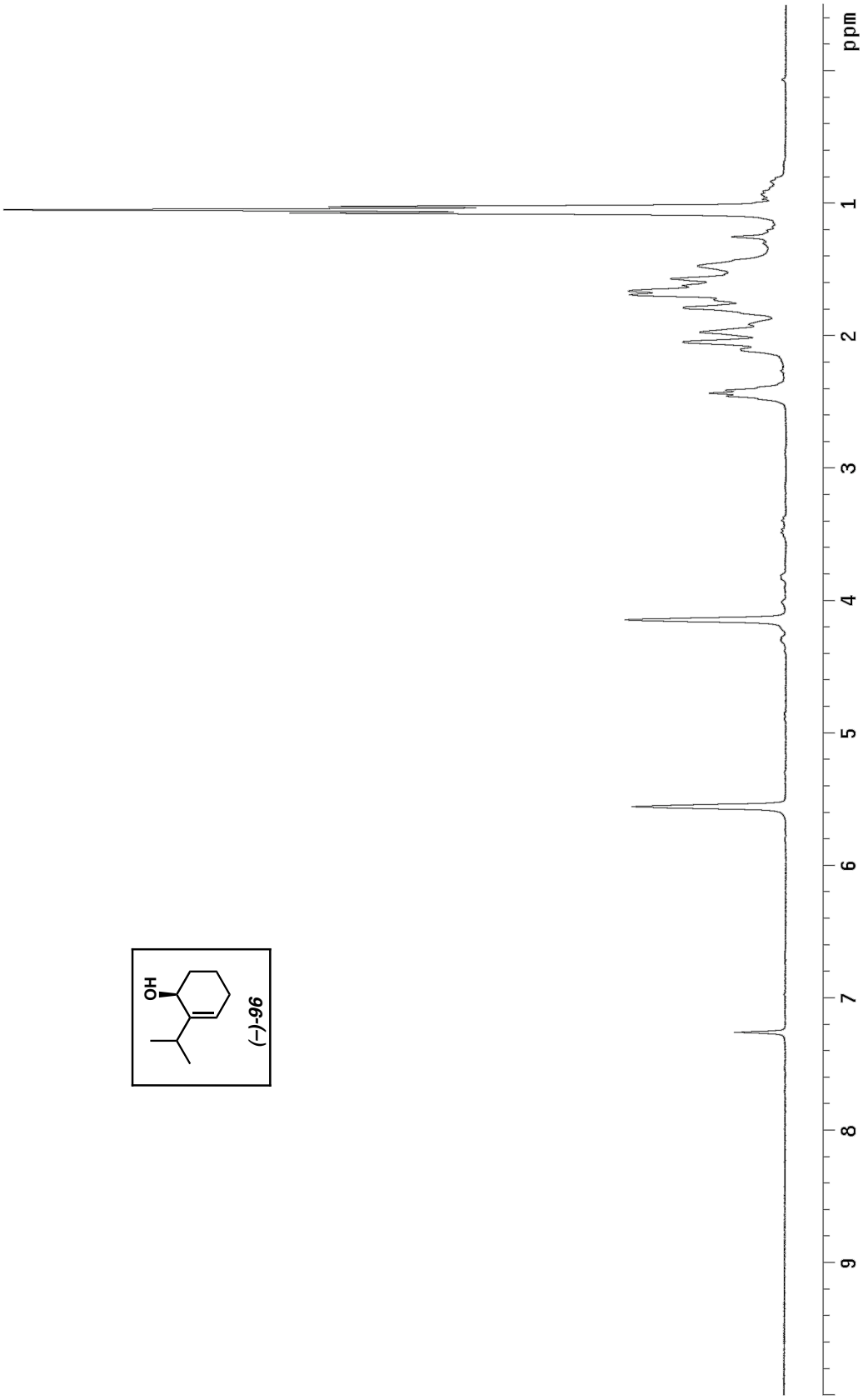

Figure A1.7 ^{1}H NMR (300 MHz, $CDCl_3$) of compound (–)-**96**.

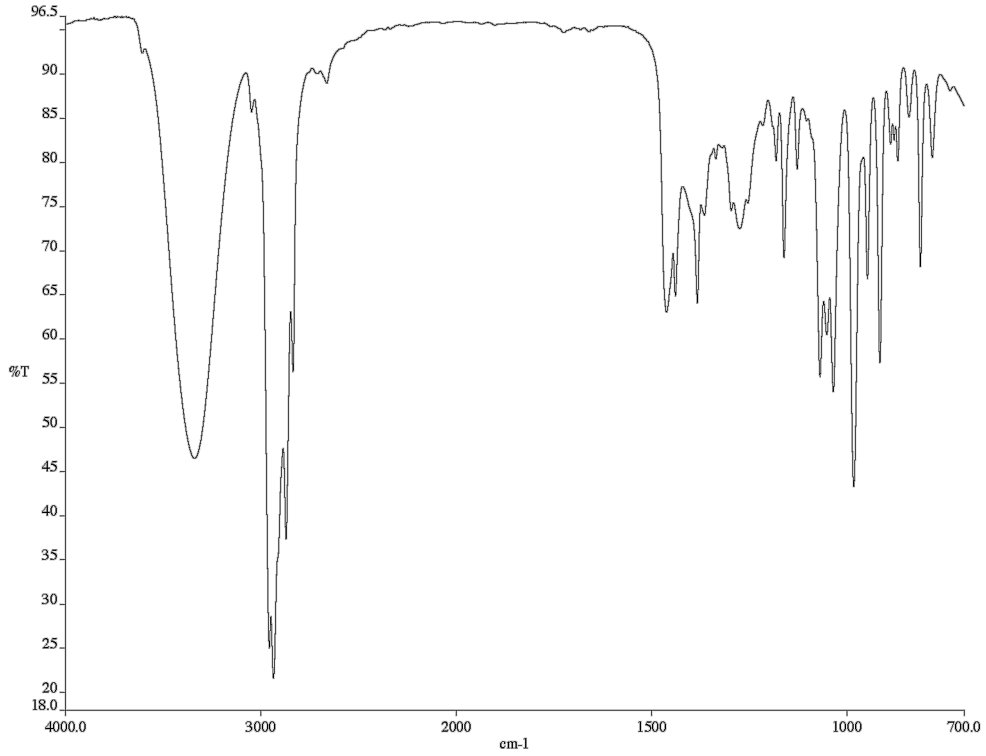

Figure A1.8 Infrared spectrum (thin film/NaCl) of compound (–)-**96**.

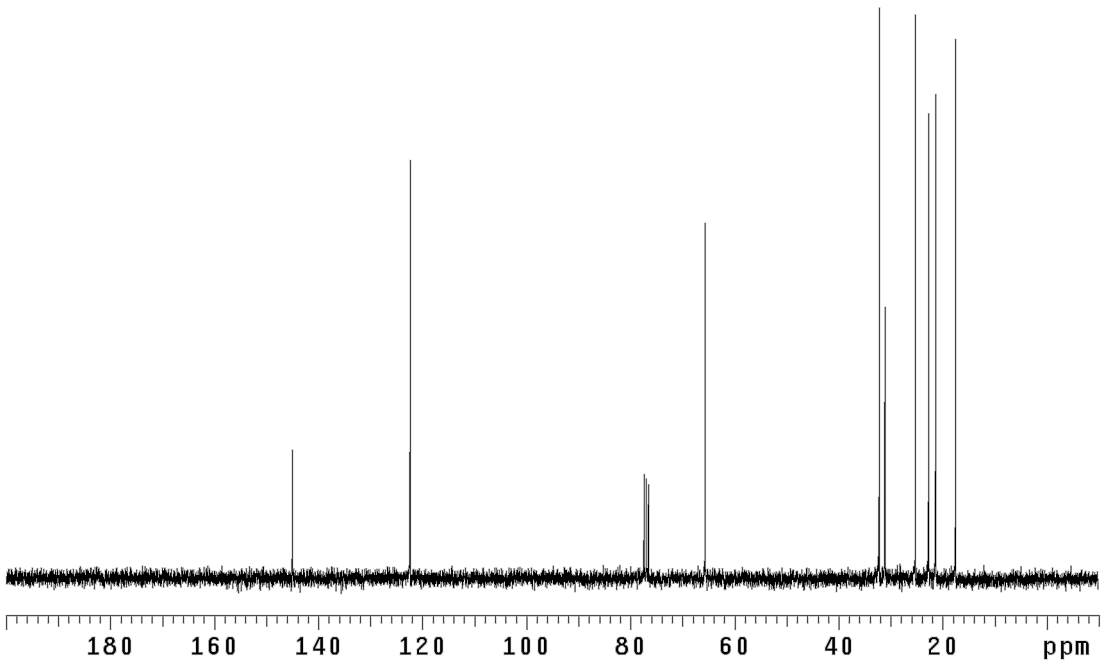

Figure A1.9 ^{13}C NMR (75 MHz, $CDCl_3$) of compound (–)-**96**.

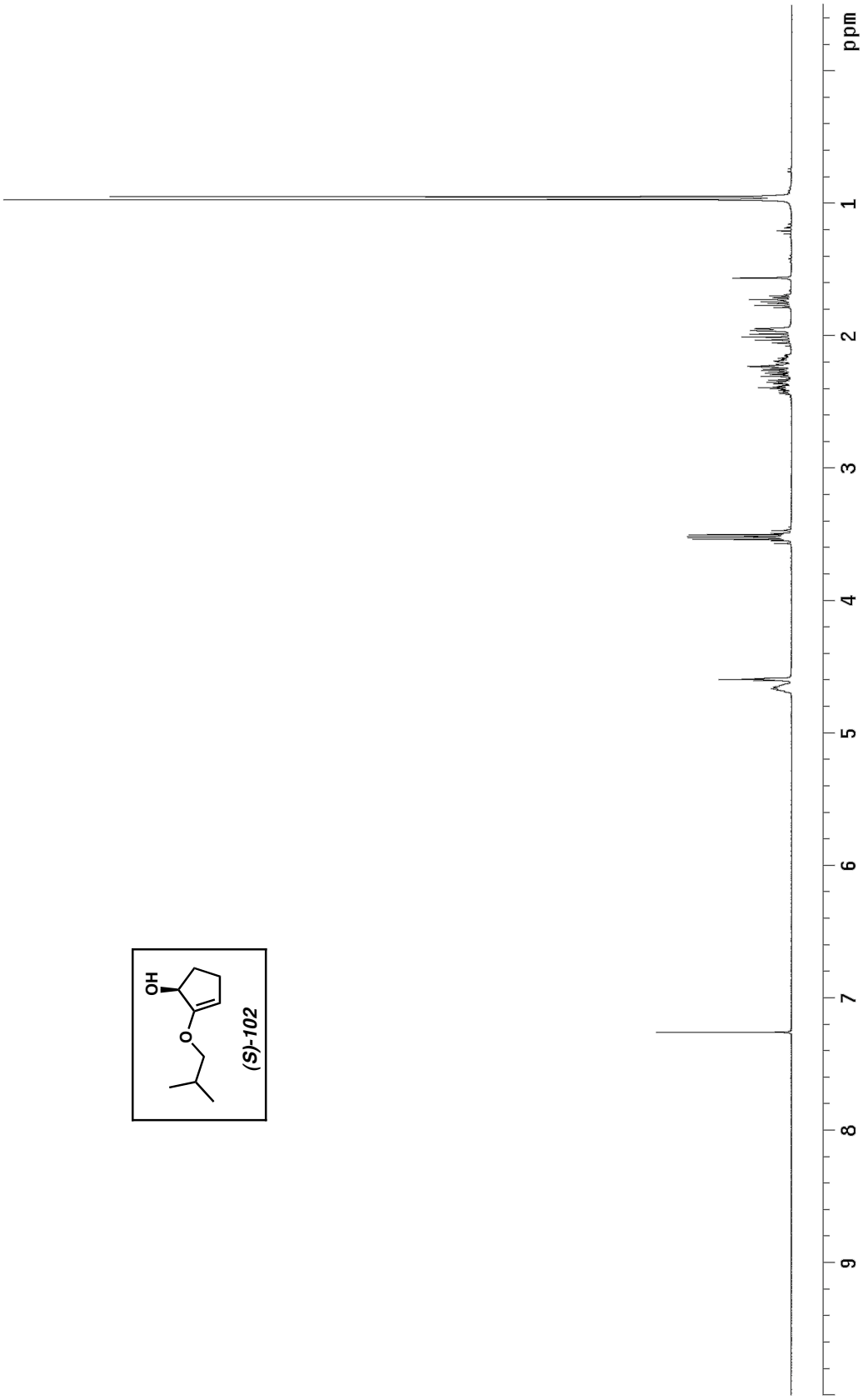

Figure A1.10 ^{1}H NMR (300 MHz, $CDCl_3$) of compound (*S*)-**102**.

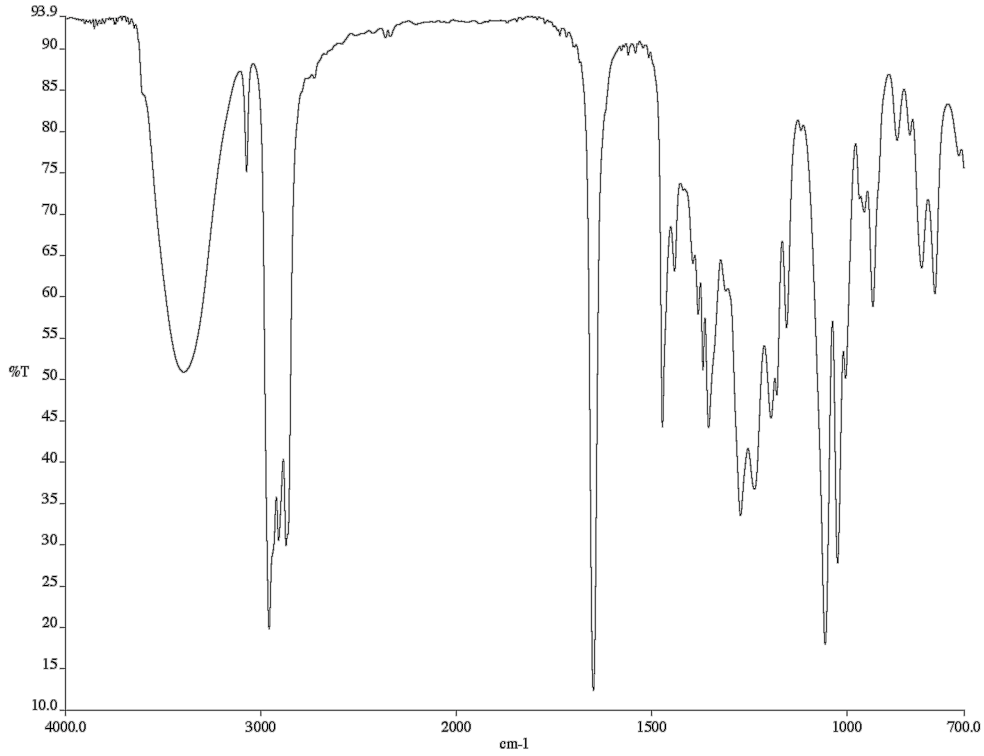

Figure A1.11 Infrared spectrum (thin film/NaCl) of compound (*S*)-**102**.

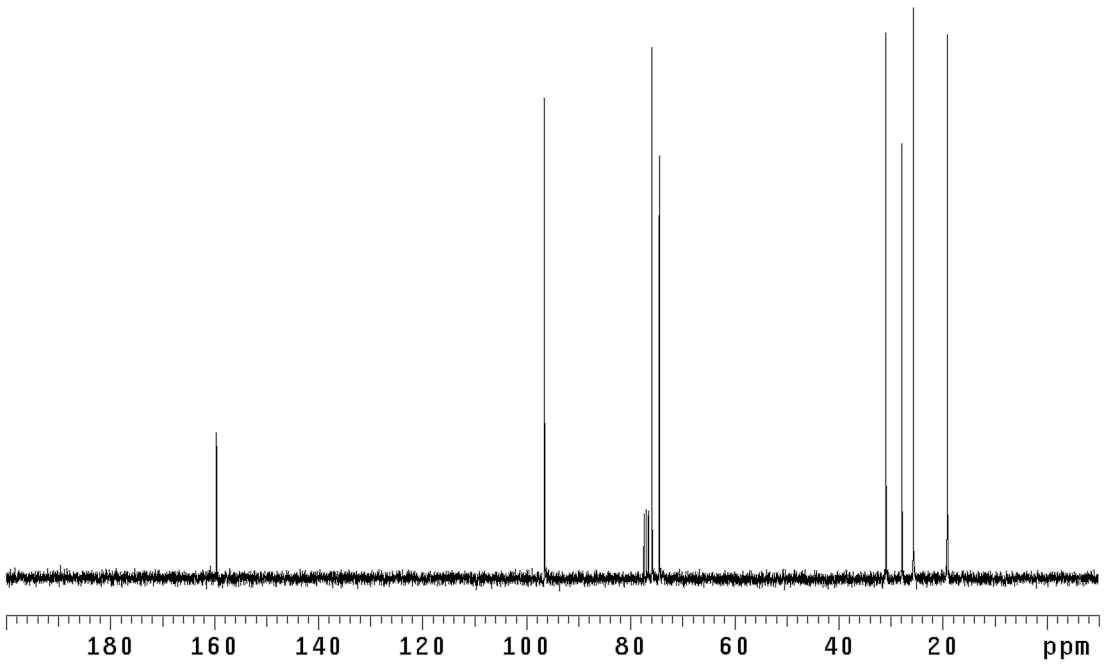

Figure A1.12 ^{13}C NMR (75 MHz, $CDCl_3$) of compound (*S*)-**102**.

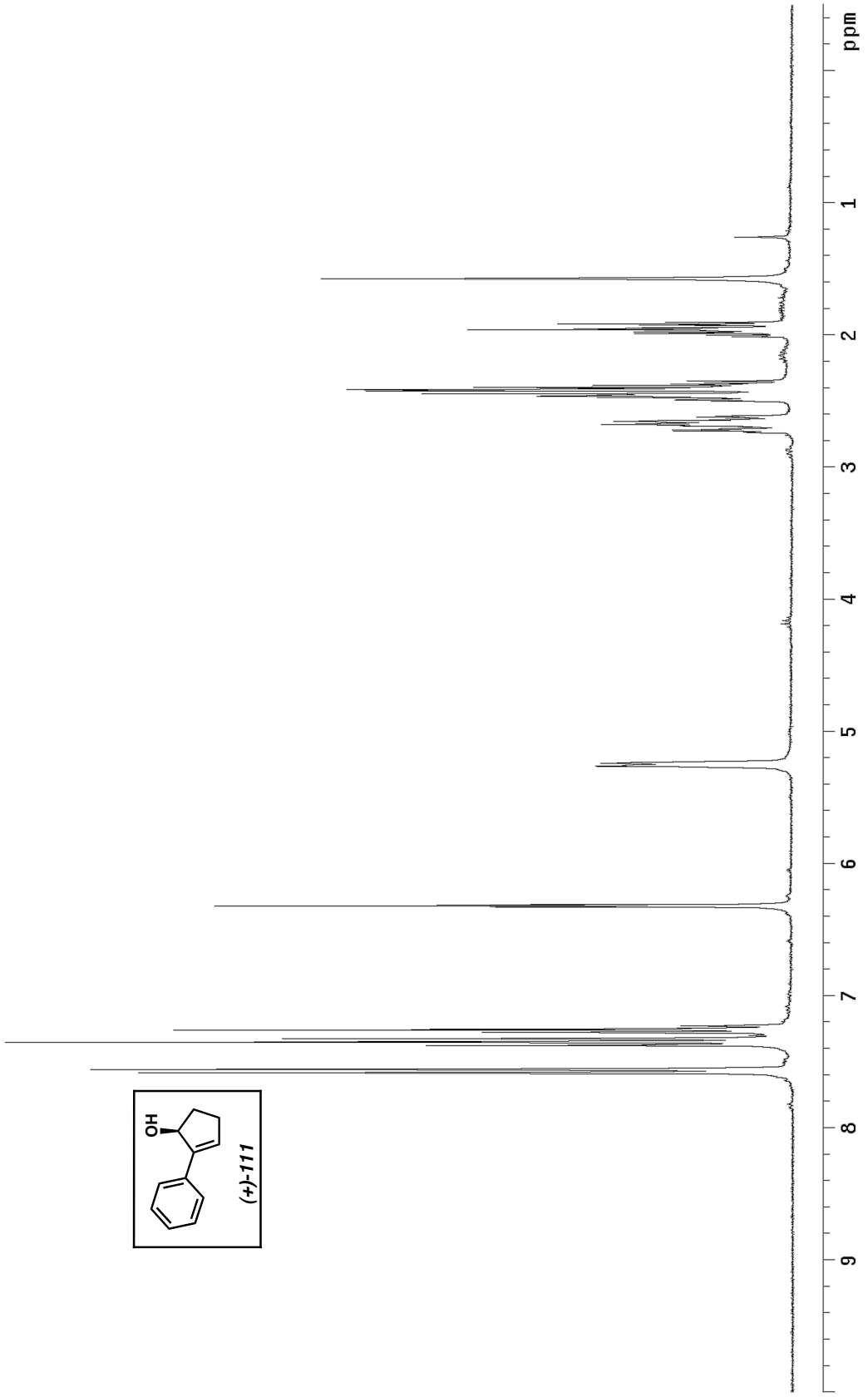

Figure A1.13 ^{1}H NMR (300 MHz, $CDCl_3$) of compound (+)-**111**.

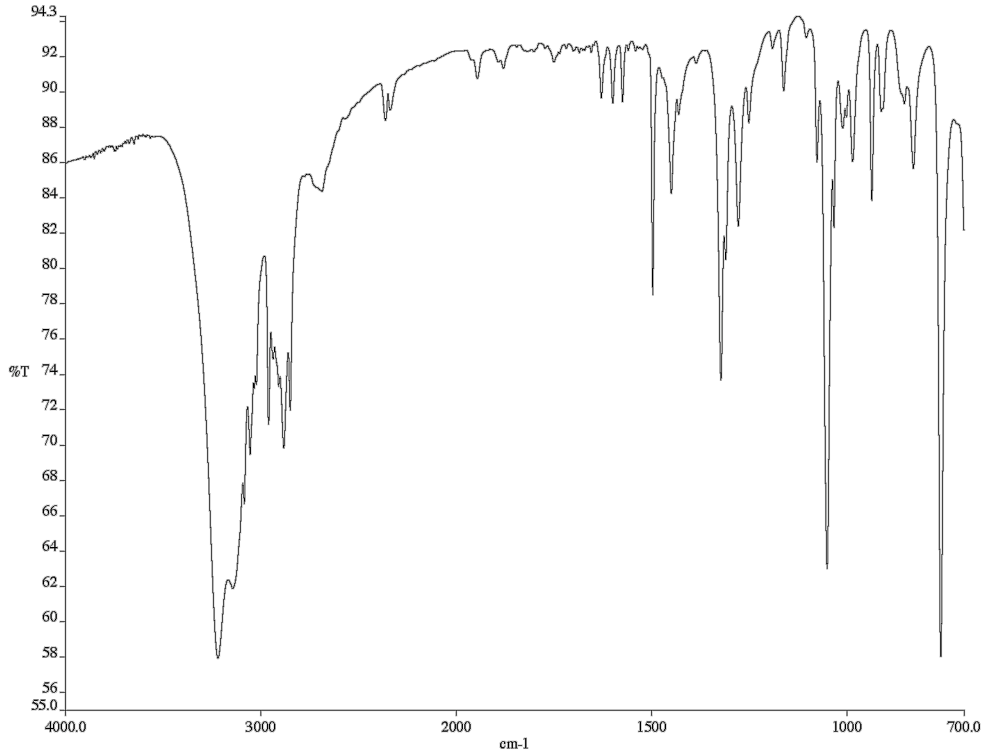

Figure A1.14 Infrared spectrum (thin film/NaCl) of compound (+)-**111**.

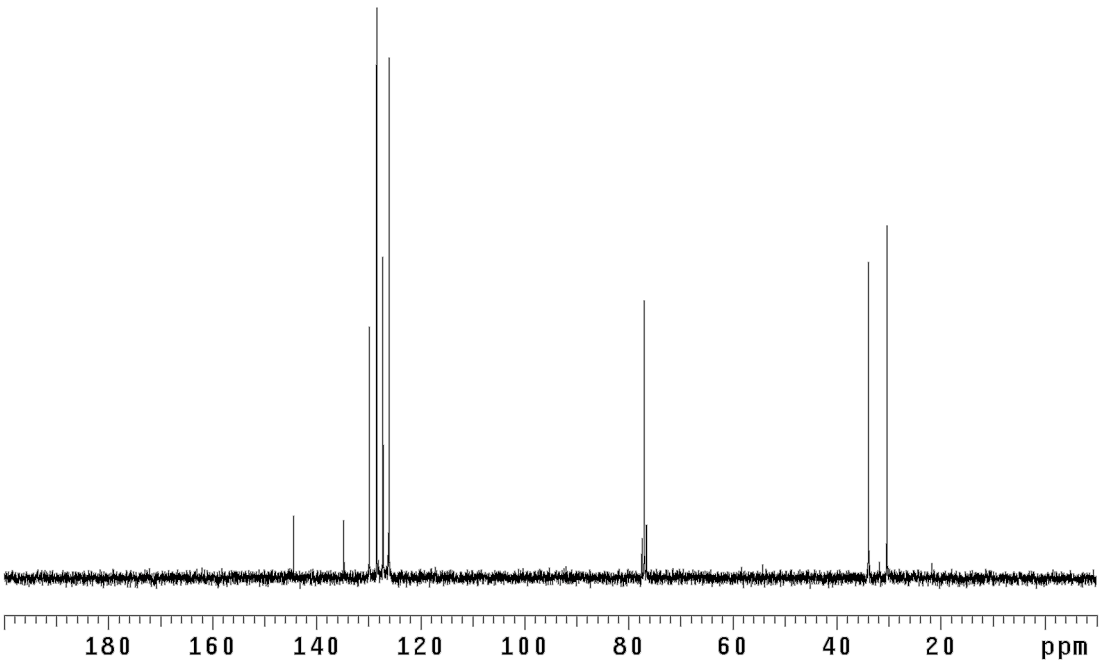

Figure A1.15 ^{13}C NMR (75 MHz, $CDCl_3$) of compound (+)-**111**.

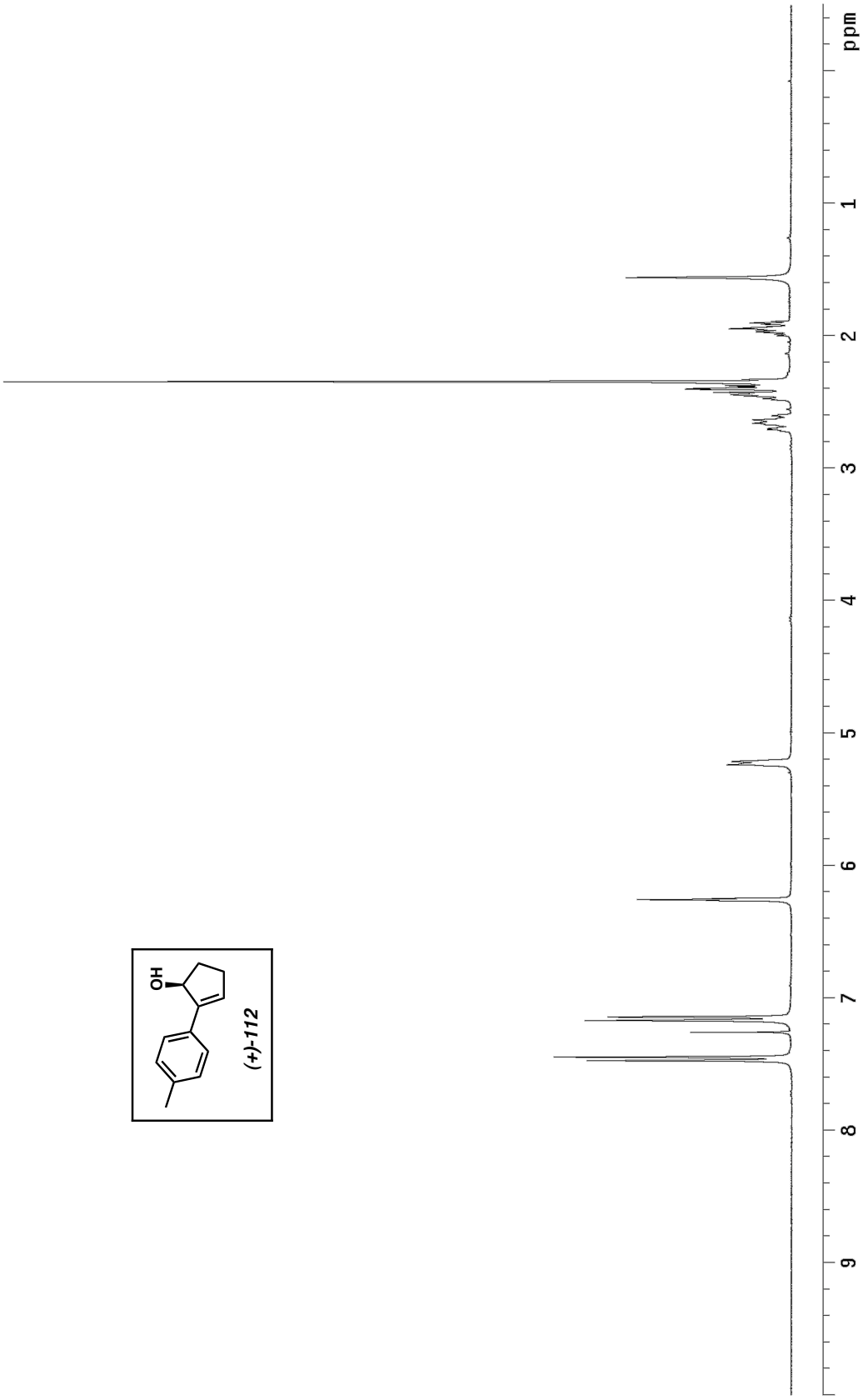

Figure A1.16 ^{1}H NMR (300 MHz, $CDCl_3$) of compound (+)-**112**.

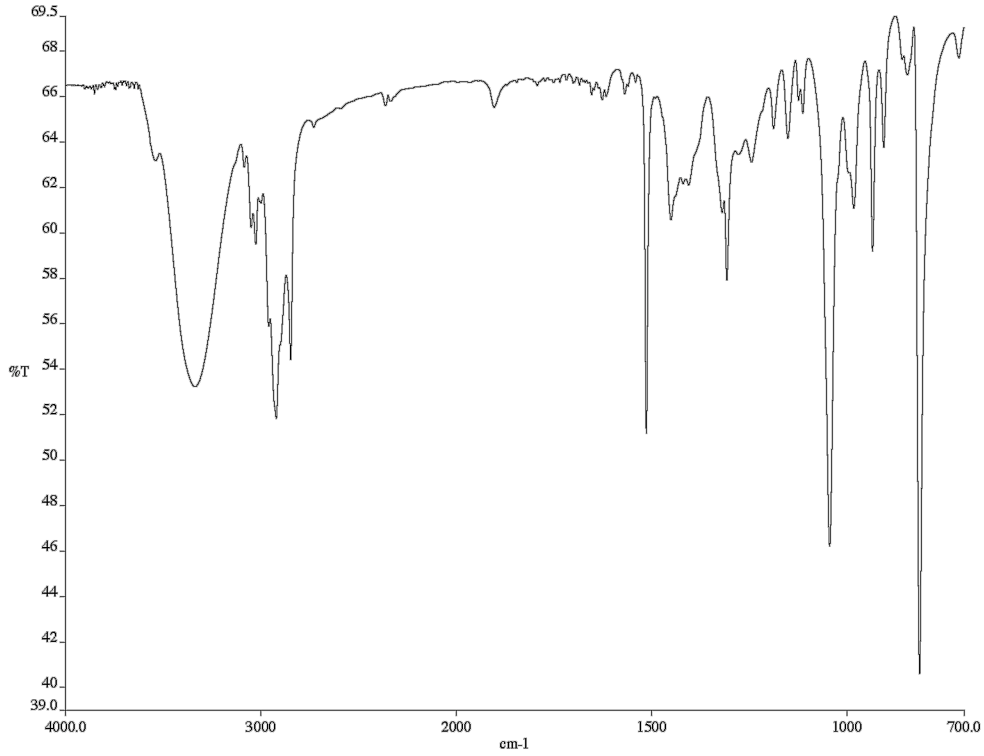

Figure A1.17 Infrared spectrum (thin film/NaCl) of compound (+)-**112**.

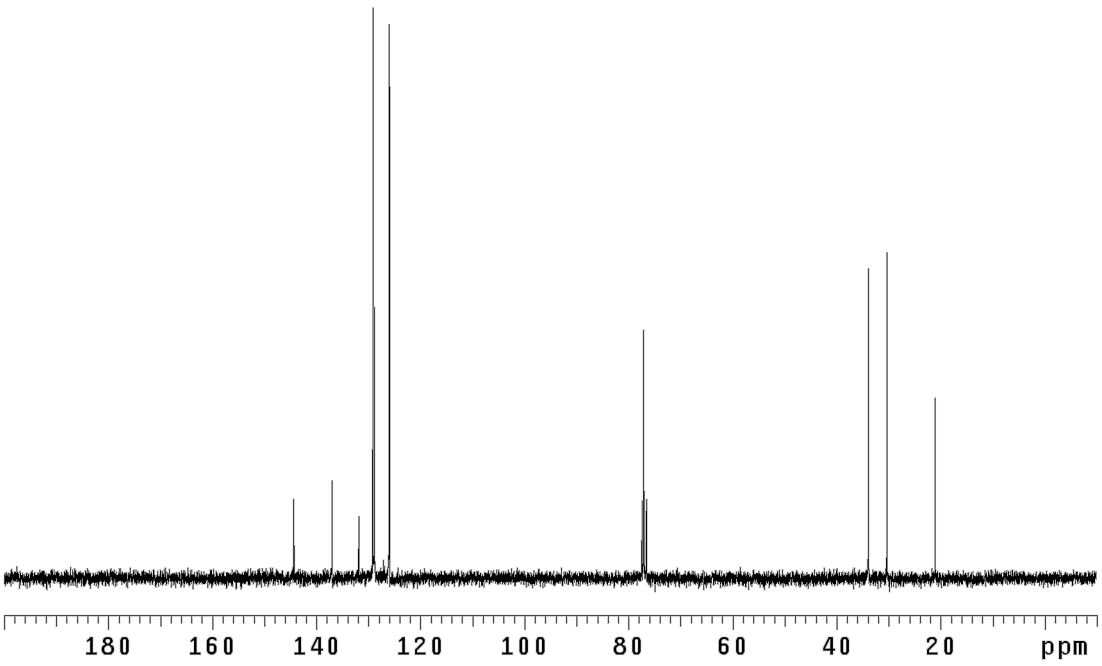

Figure A1.18 ^{13}C NMR (75 MHz, $CDCl_3$) of compound (+)-**112**.

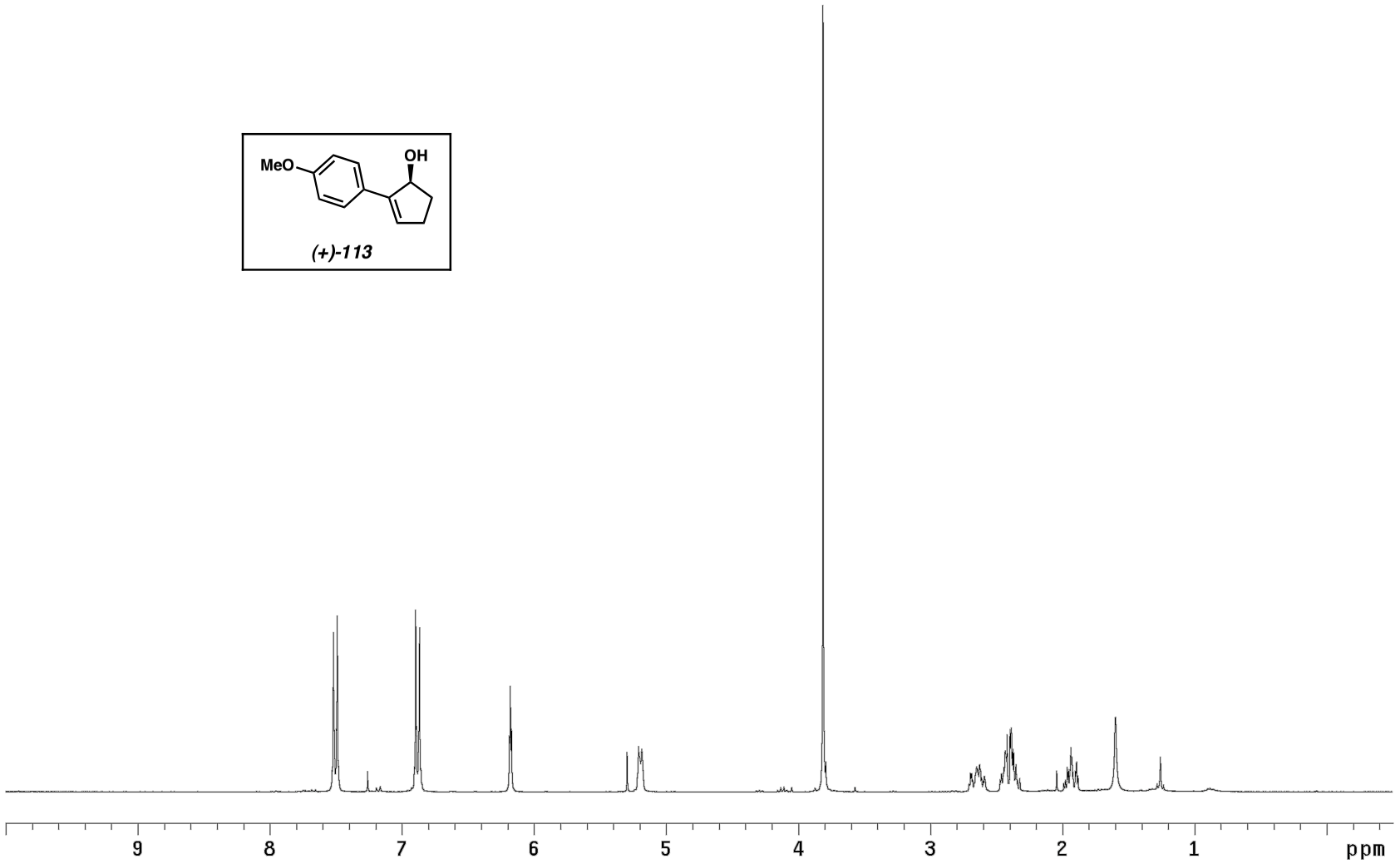

Figure A1.19 ^{1}H NMR (300 MHz, $CDCl_3$) of compound (+)-**113**.

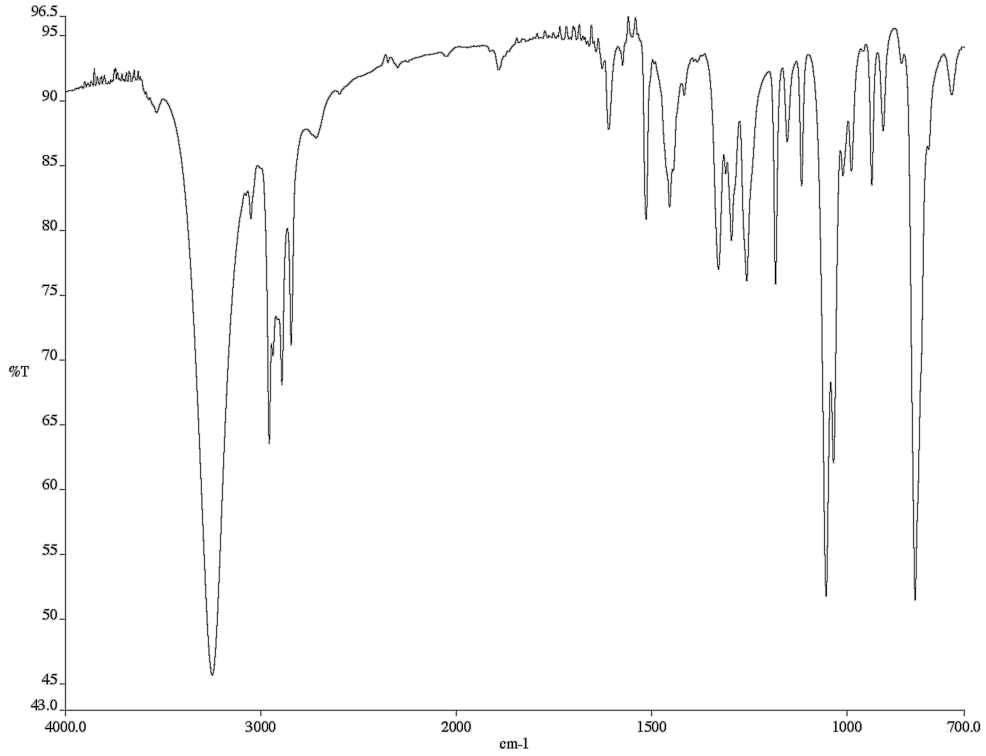

Figure A1.20 Infrared spectrum (thin film/NaCl) of compound (+)-**113**.

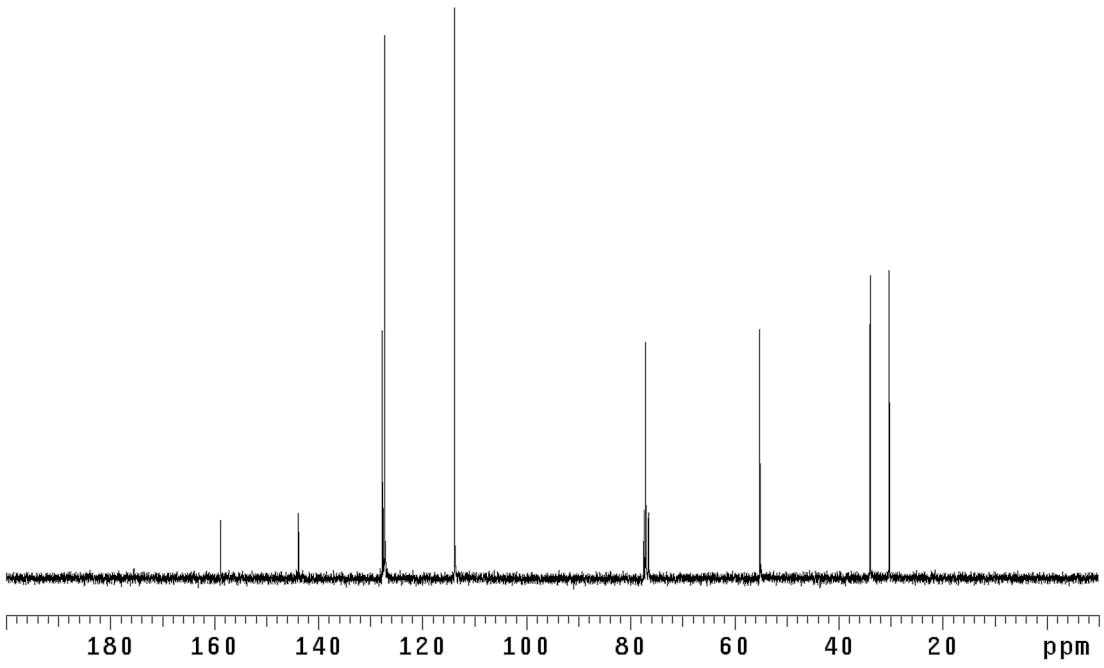

Figure A1.21 ^{13}C NMR (75 MHz, $CDCl_3$) of compound (+)-**113**.

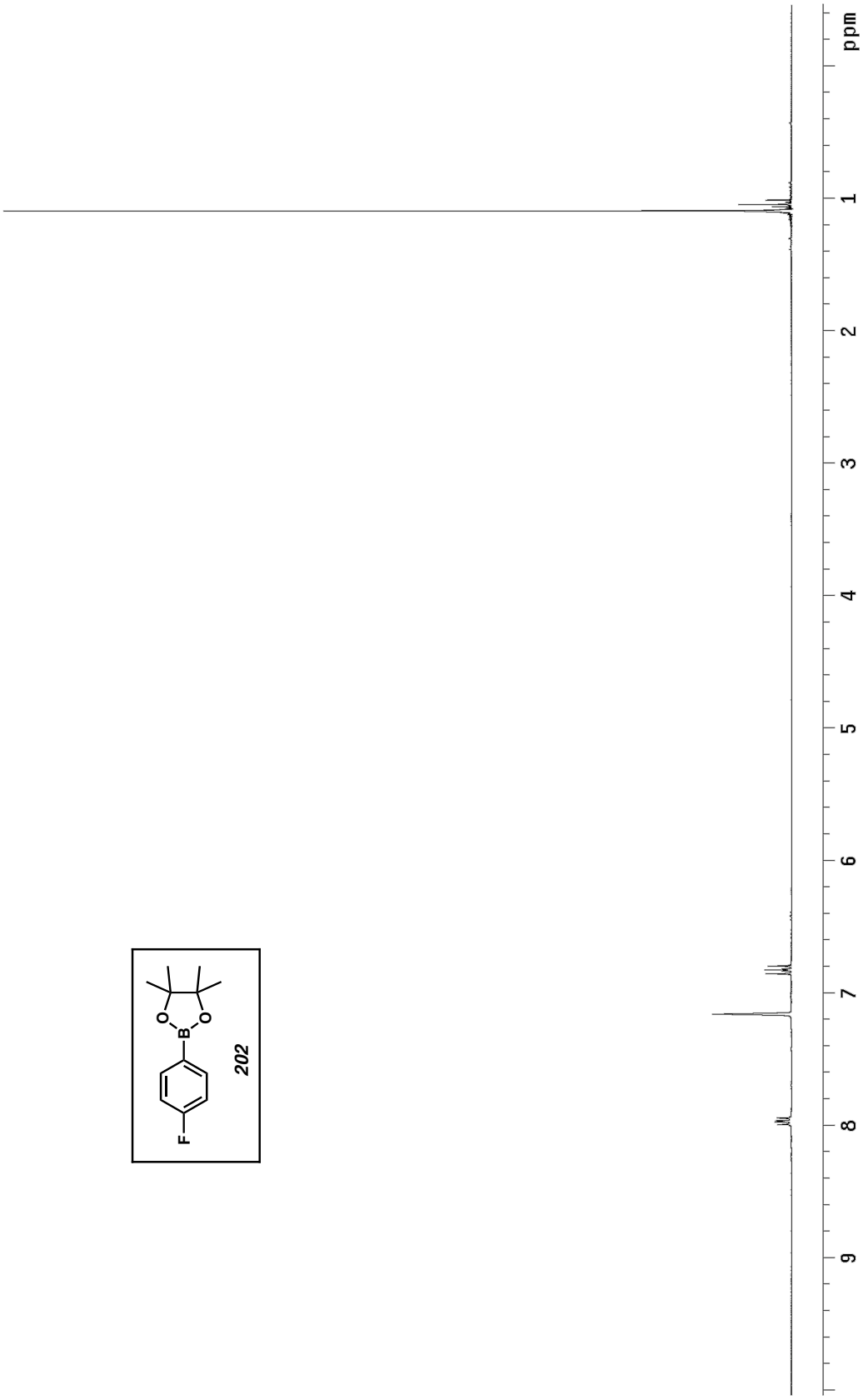

Figure A1.22 ^{1}H NMR (300 MHz, C_6D_6) of compound **202**.

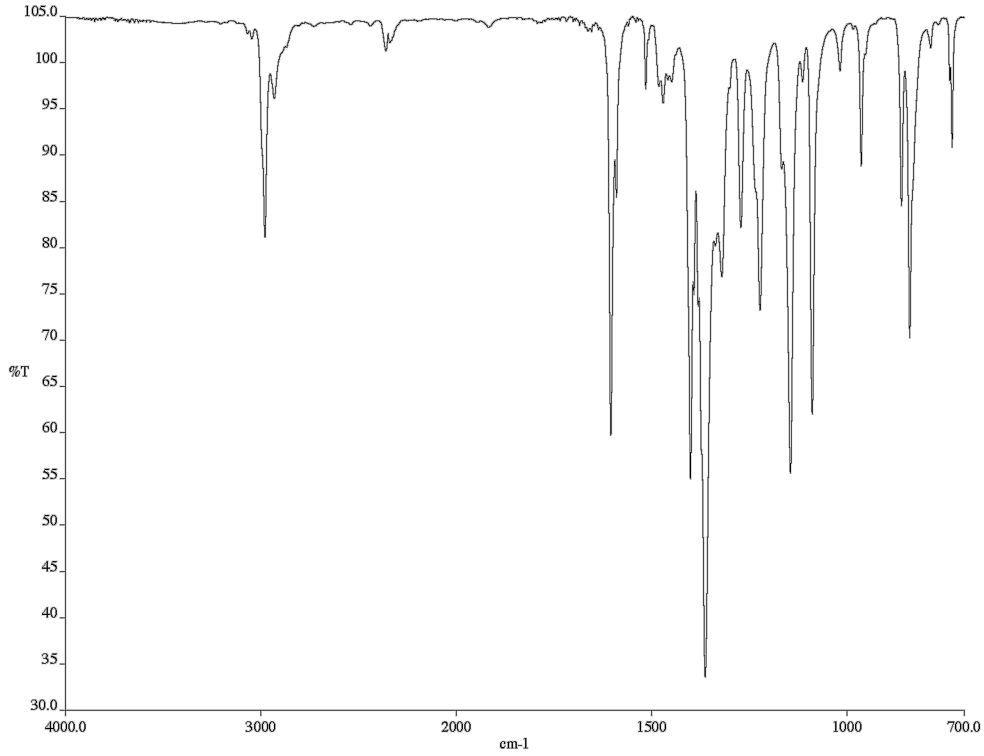

Figure A1.23 Infrared spectrum (thin film/NaCl) of compound **202**.

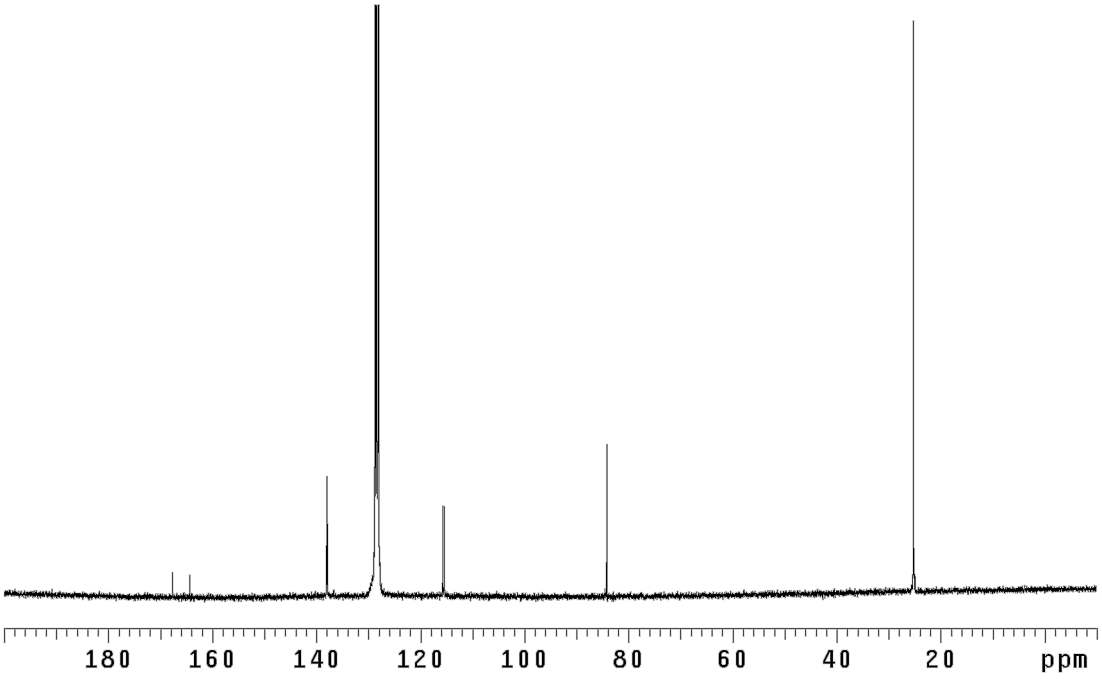

Figure A1.24 ^{13}C NMR (75 MHz, C_6D_6) of compound **202**.

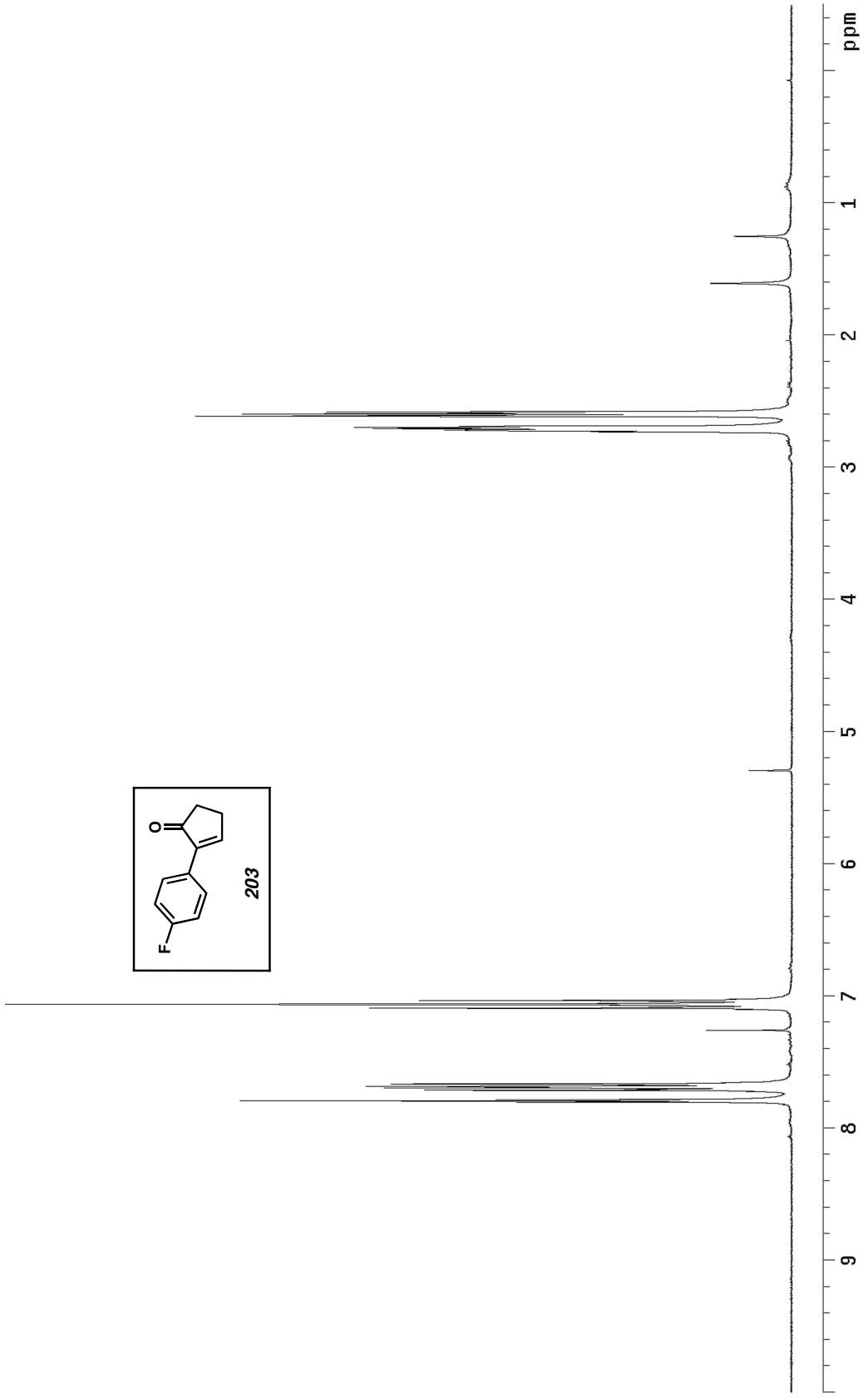

Figure A1.25 ^{1}H NMR (300 MHz, $CDCl_3$) of compound **203**.

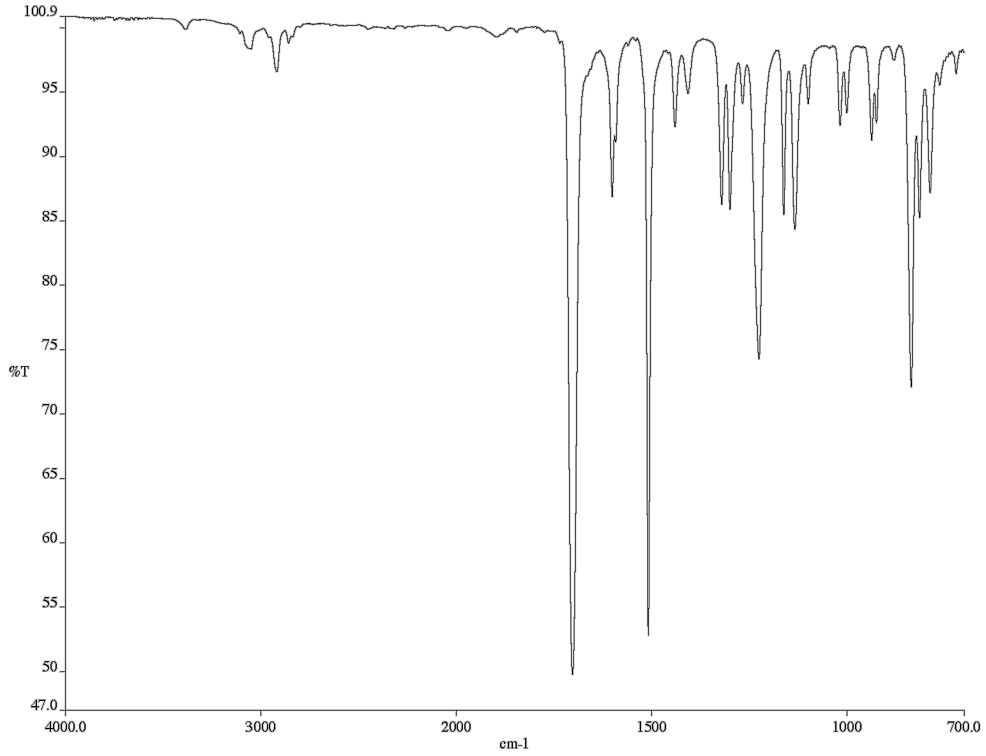

Figure A1.26 Infrared spectrum (thin film/NaCl) of compound **203**.

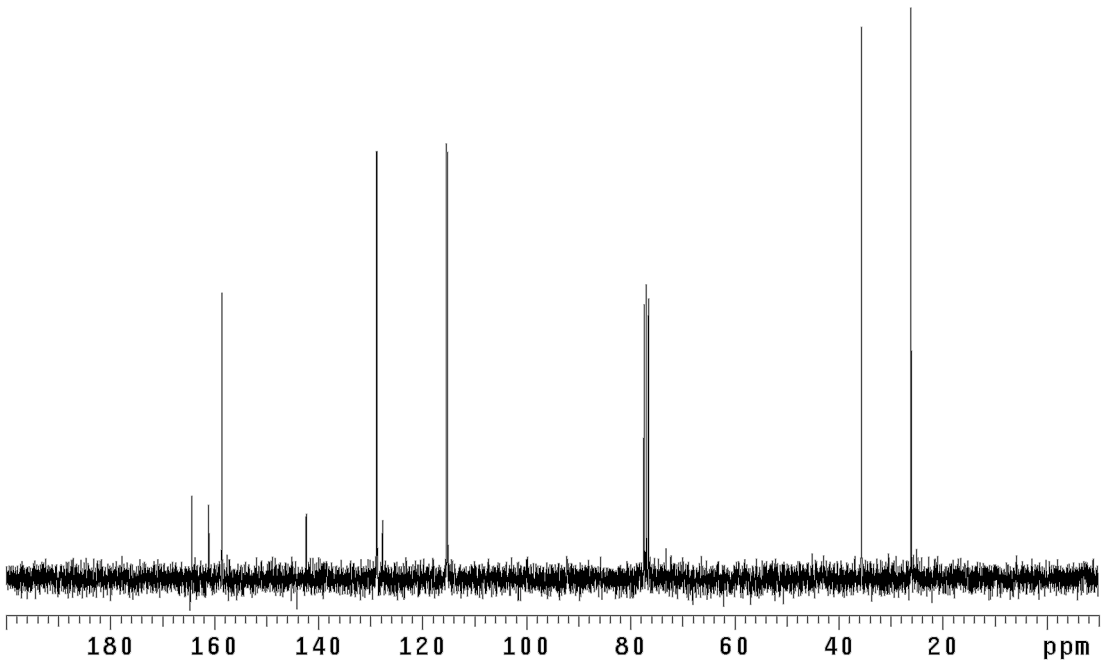

Figure A1.27 ^{13}C NMR (75 MHz, $CDCl_3$) of compound **203**.

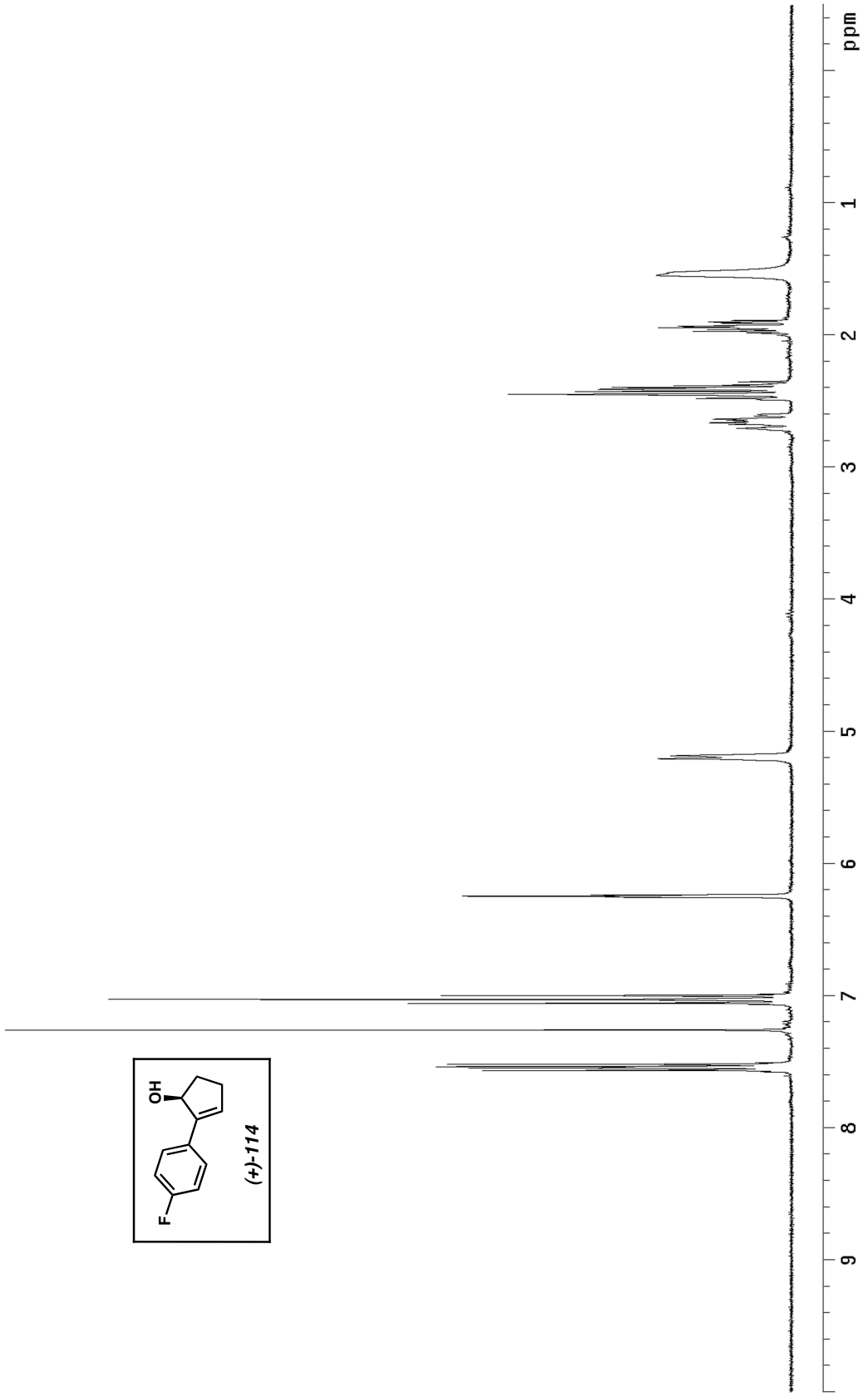

Figure A1.28 ^{1}H NMR (300 MHz, $CDCl_3$) of compound (+)-**114**.

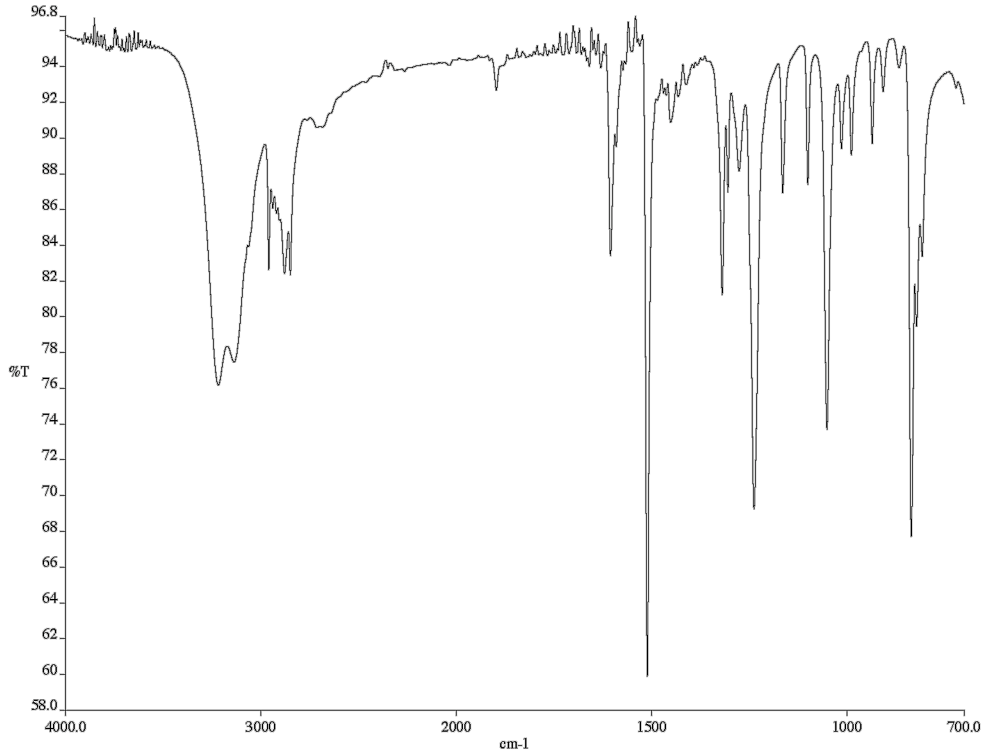

Figure A1.29 Infrared spectrum (thin film/NaCl) of compound (+)-**114**.

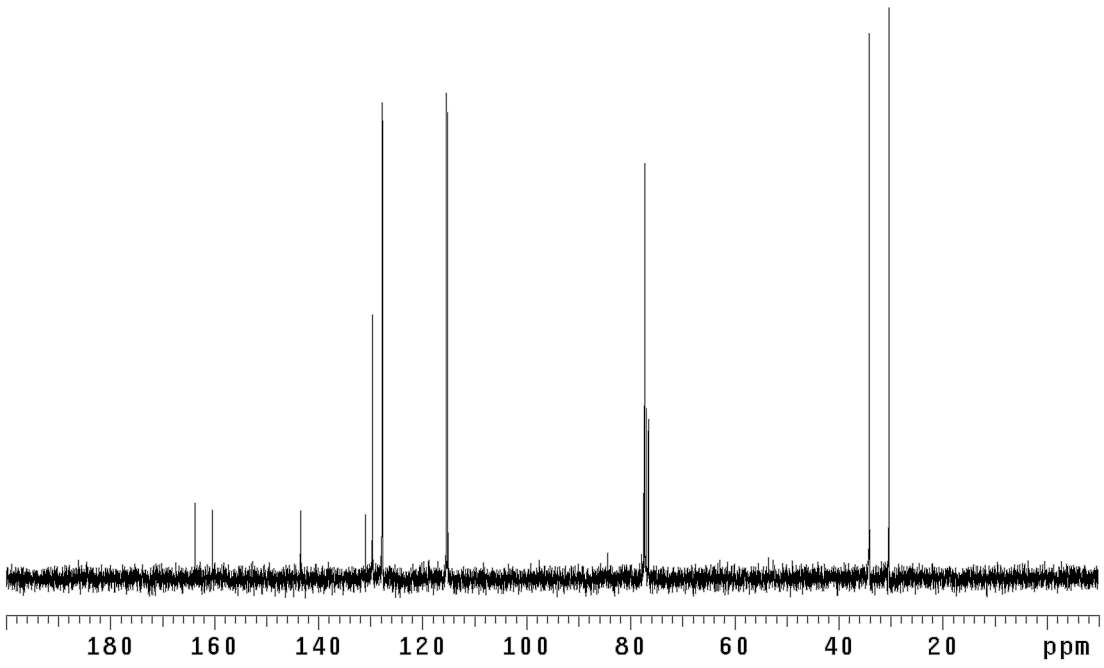

Figure A1.30 ^{13}C NMR (75 MHz, $CDCl_3$) of compound (+)-**114**.

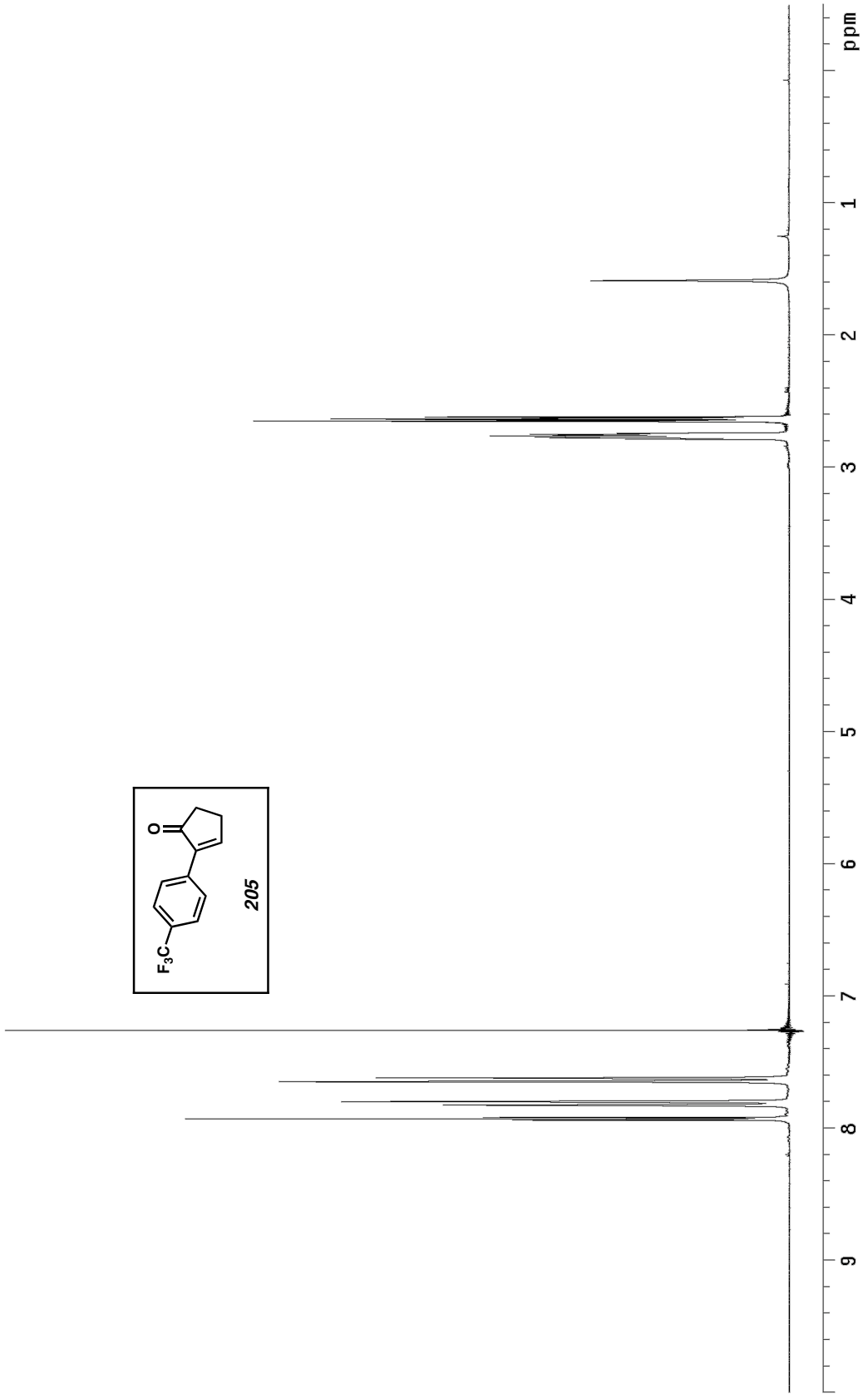

Figure A1.31 ^{1}H NMR (300 MHz, $CDCl_3$) of compound **205**.

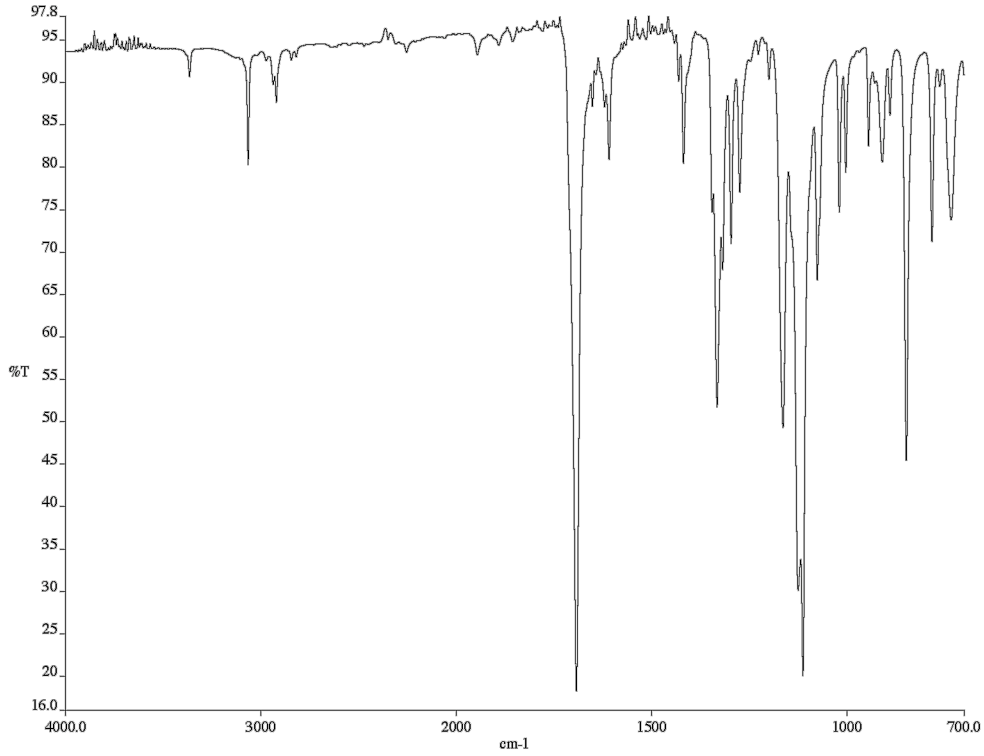

Figure A1.32 Infrared spectrum (thin film/NaCl) of compound **205**.

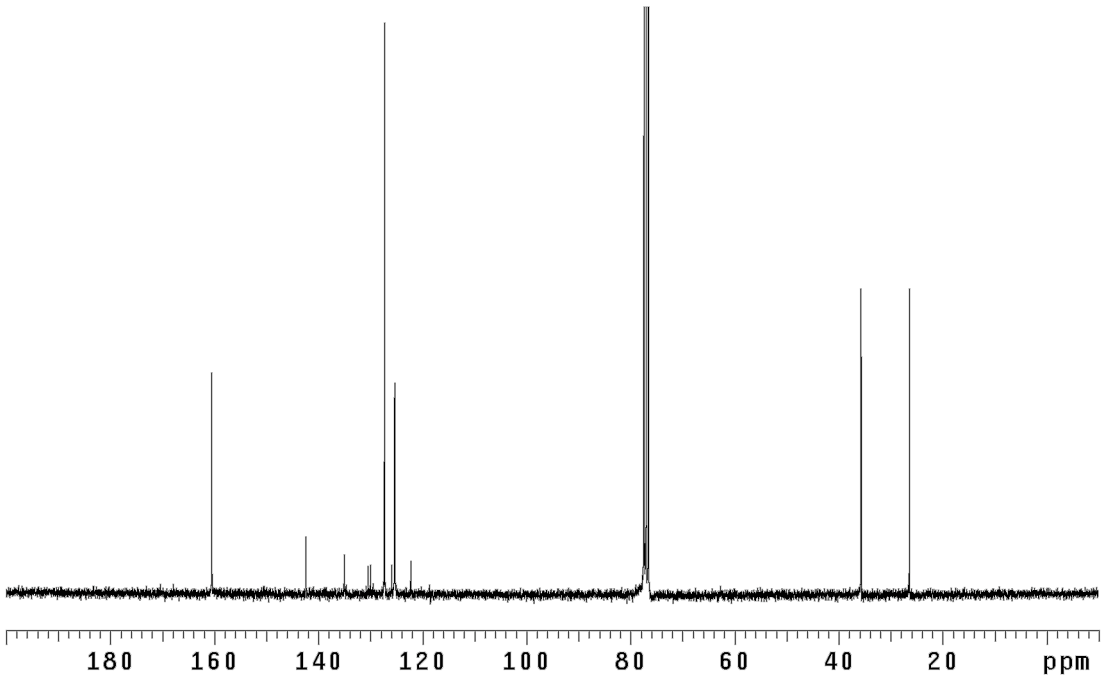

Figure A1.33 ^{13}C NMR (75 MHz, $CDCl_3$) of compound **205**.

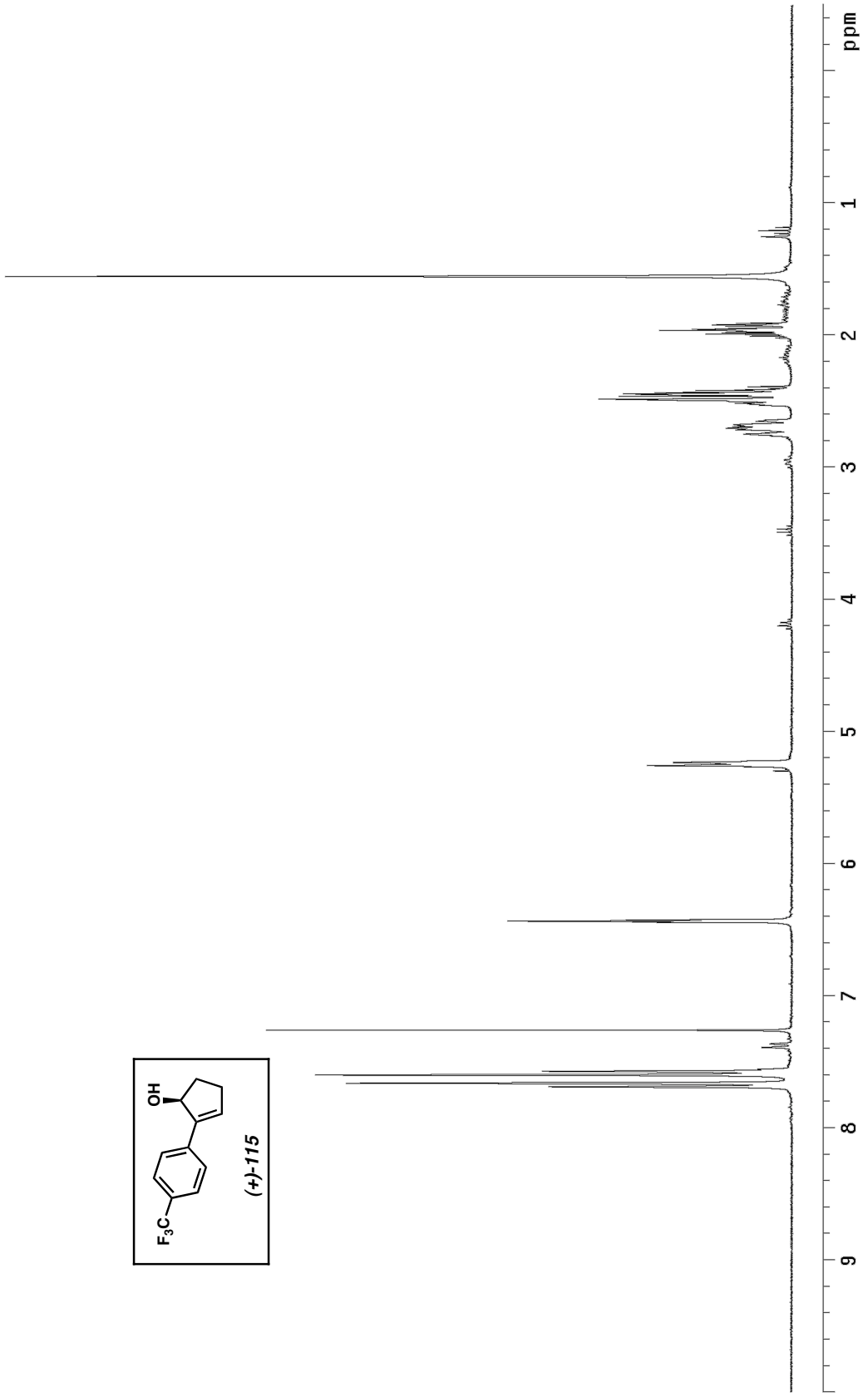

Figure A1.34 ^{1}H NMR (300 MHz, $CDCl_3$) of compound (+)-**115**.

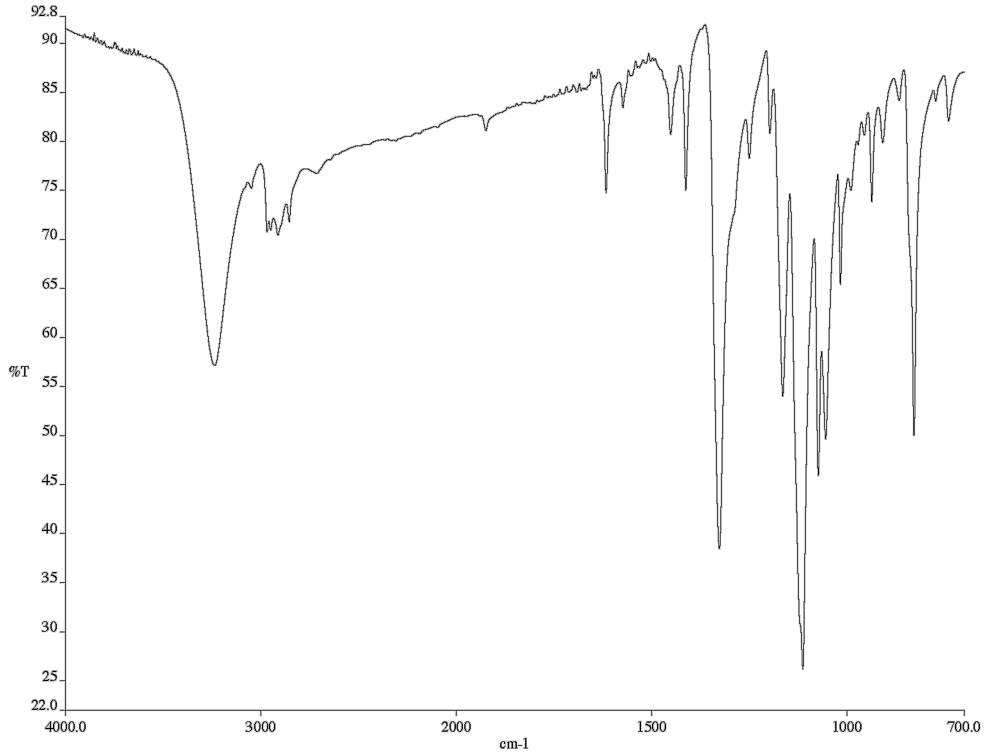

Figure A1.35 Infrared spectrum (thin film/NaCl) of compound (+)-**115**.

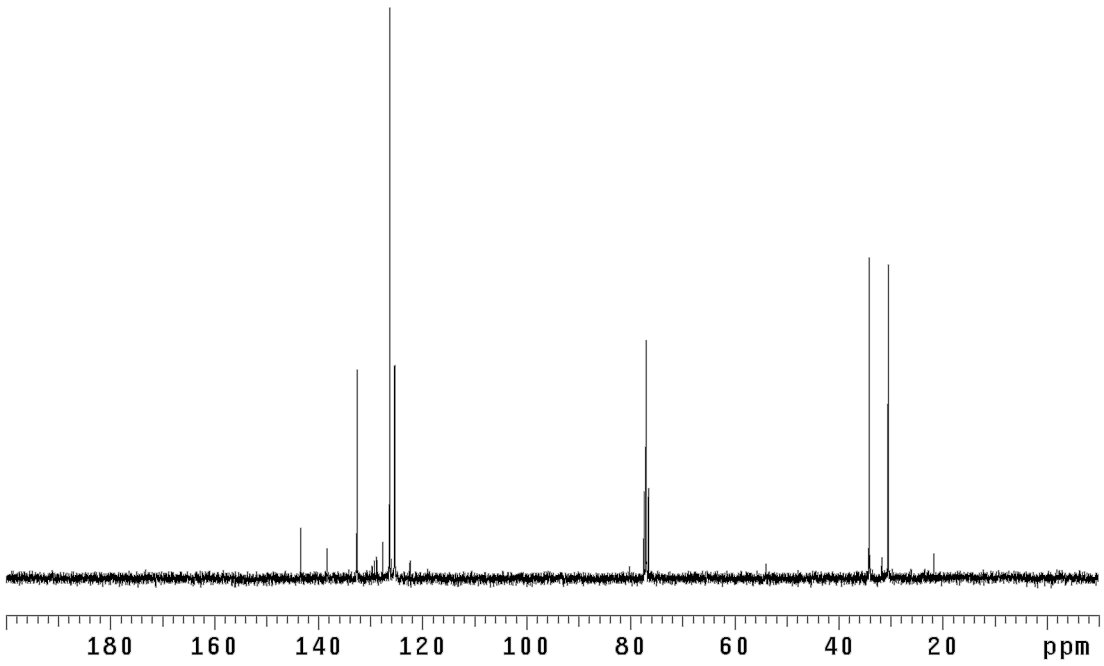

Figure A1.36 ^{13}C NMR (75 MHz, $CDCl_3$) of compound (+)-**115**.

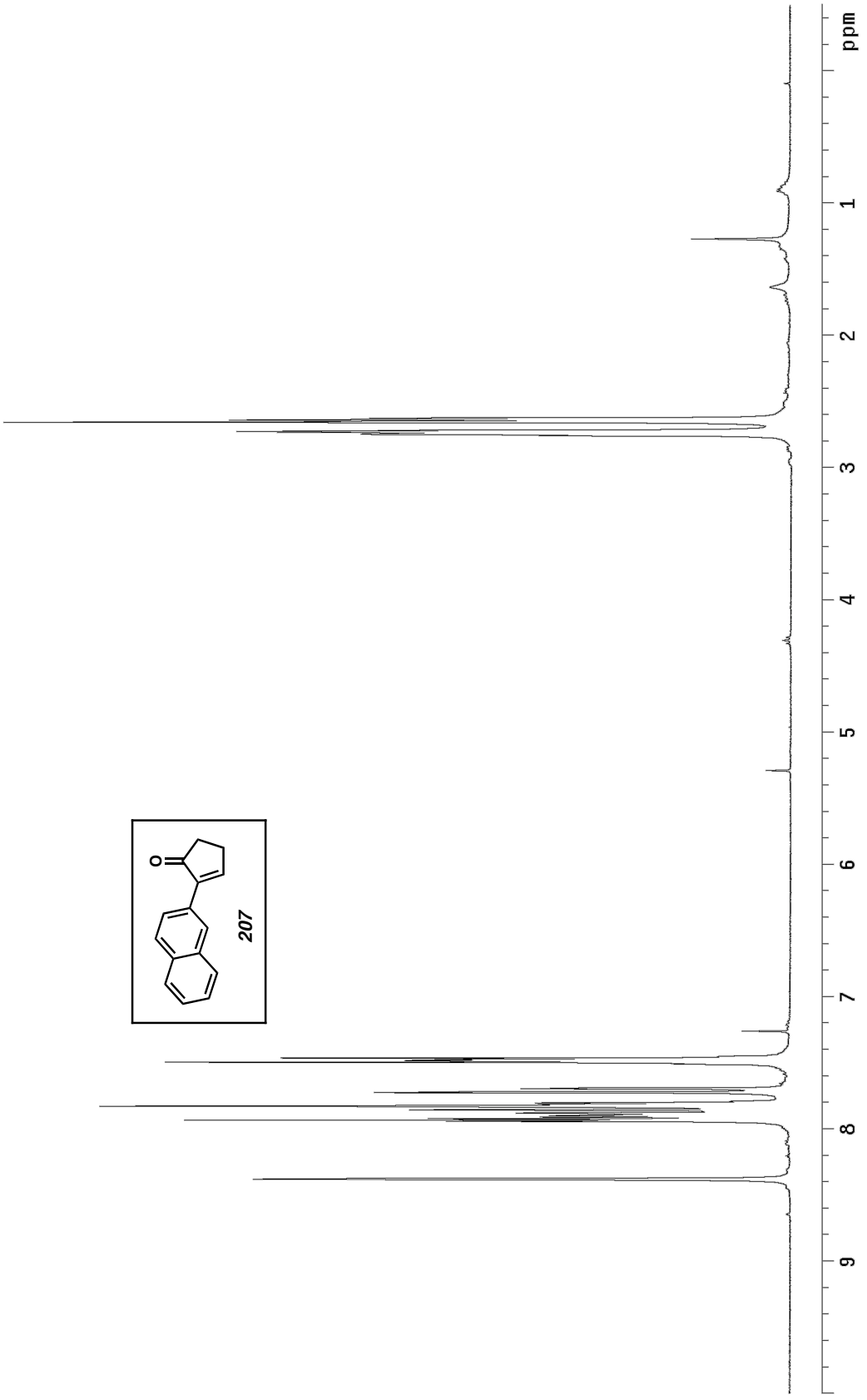

Figure A1.37 ^{1}H NMR (300 MHz, $CDCl_3$) of compound **207**.

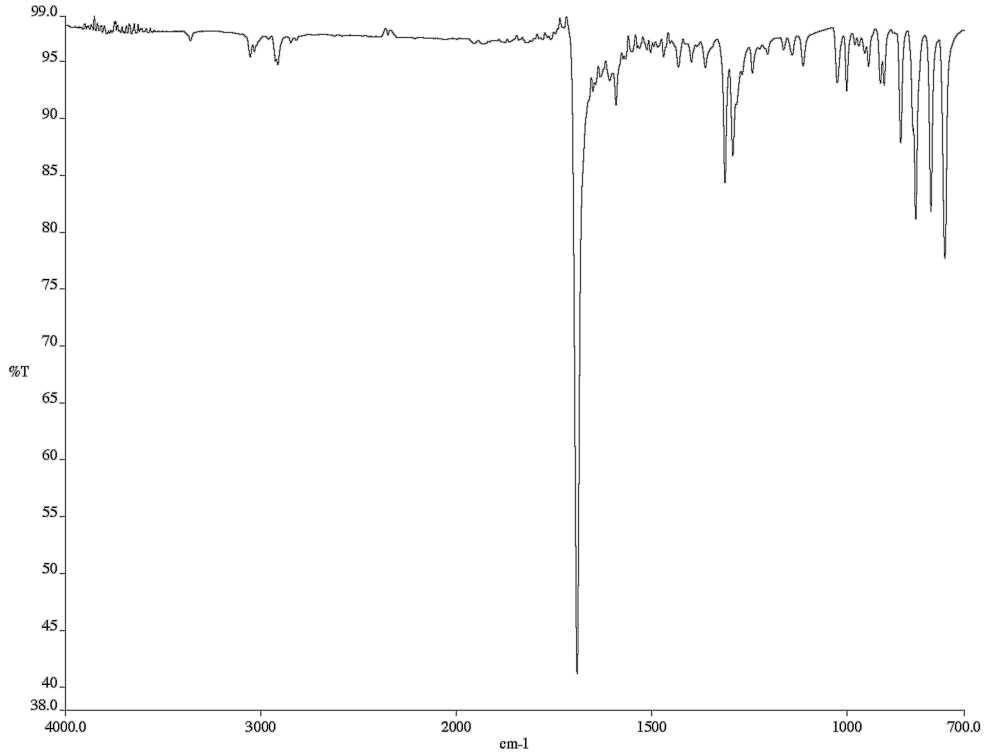

Figure A1.38 Infrared spectrum (thin film/NaCl) of compound **207**.

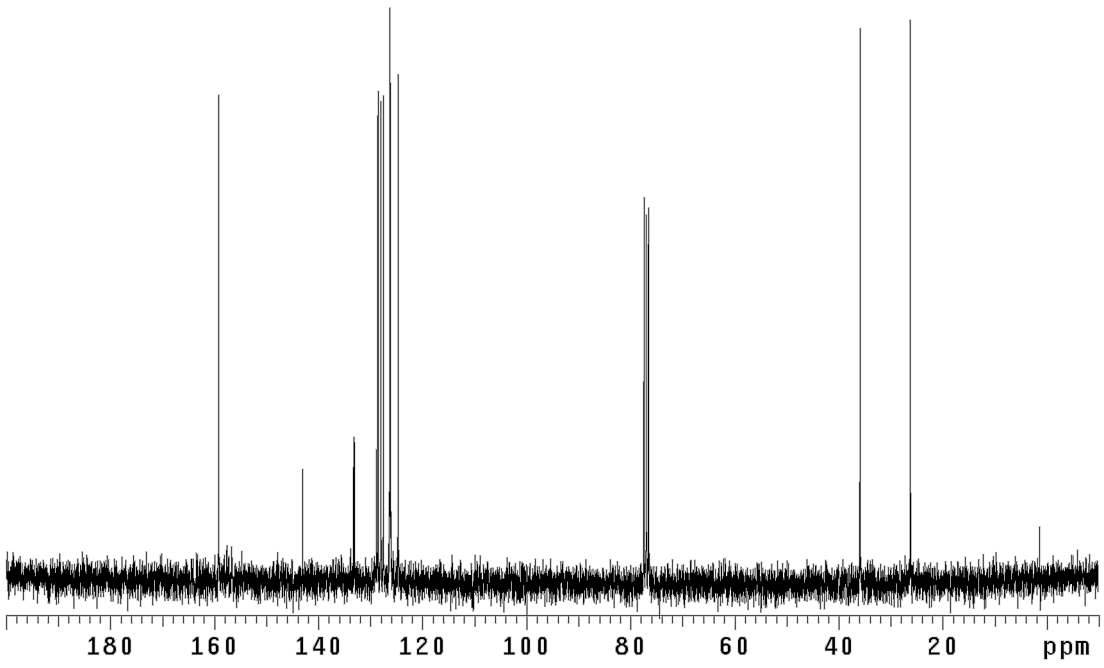

Figure A1.39 ^{13}C NMR (75 MHz, $CDCl_3$) of compound **207**.

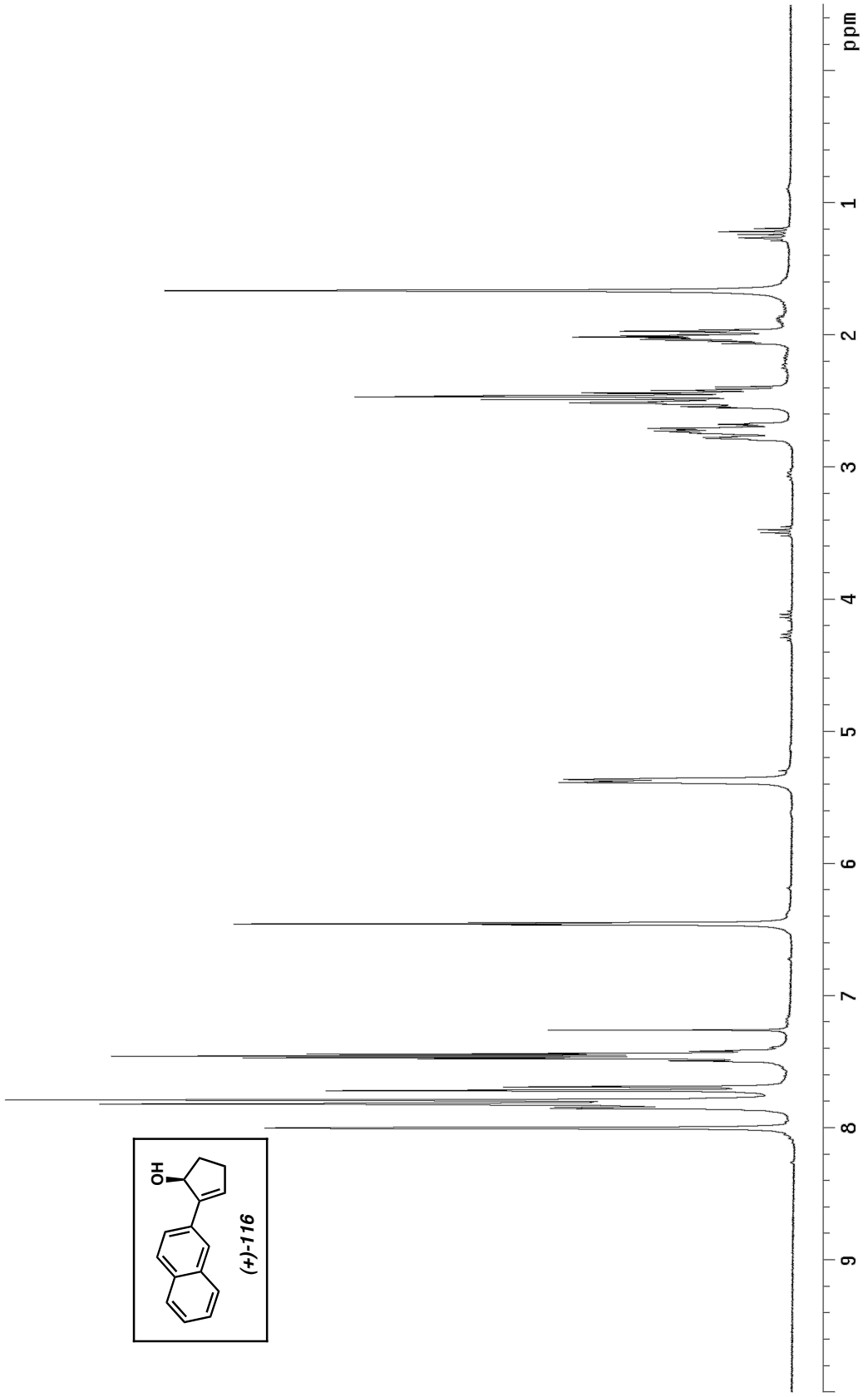

Figure A1.40 ^{1}H NMR (300 MHz, $CDCl_3$) of compound (+)-**116**.

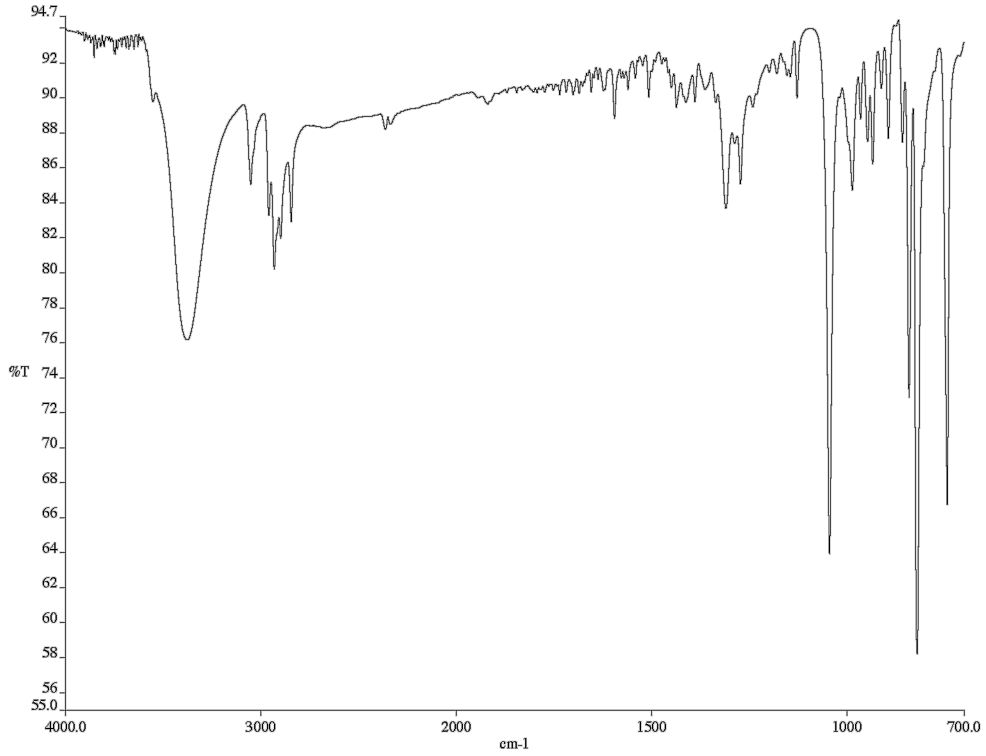

Figure A1.41 Infrared spectrum (thin film/NaCl) of compound (+)-**116**.

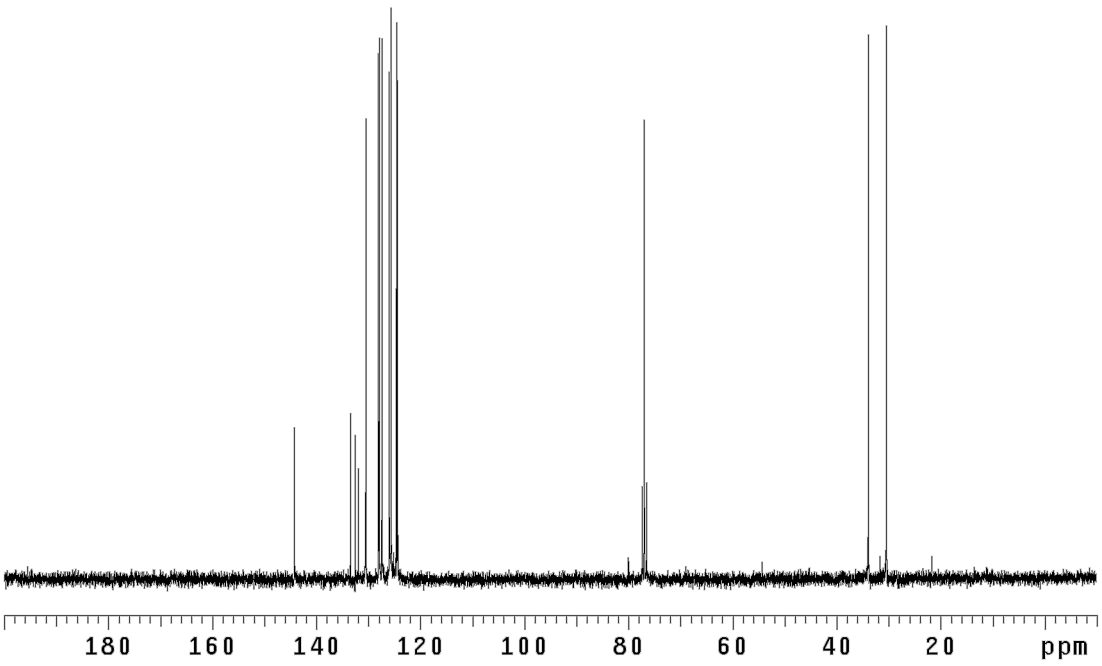

Figure A1.42 ^{13}C NMR (75 MHz, $CDCl_3$) of compound (+)-**116**.

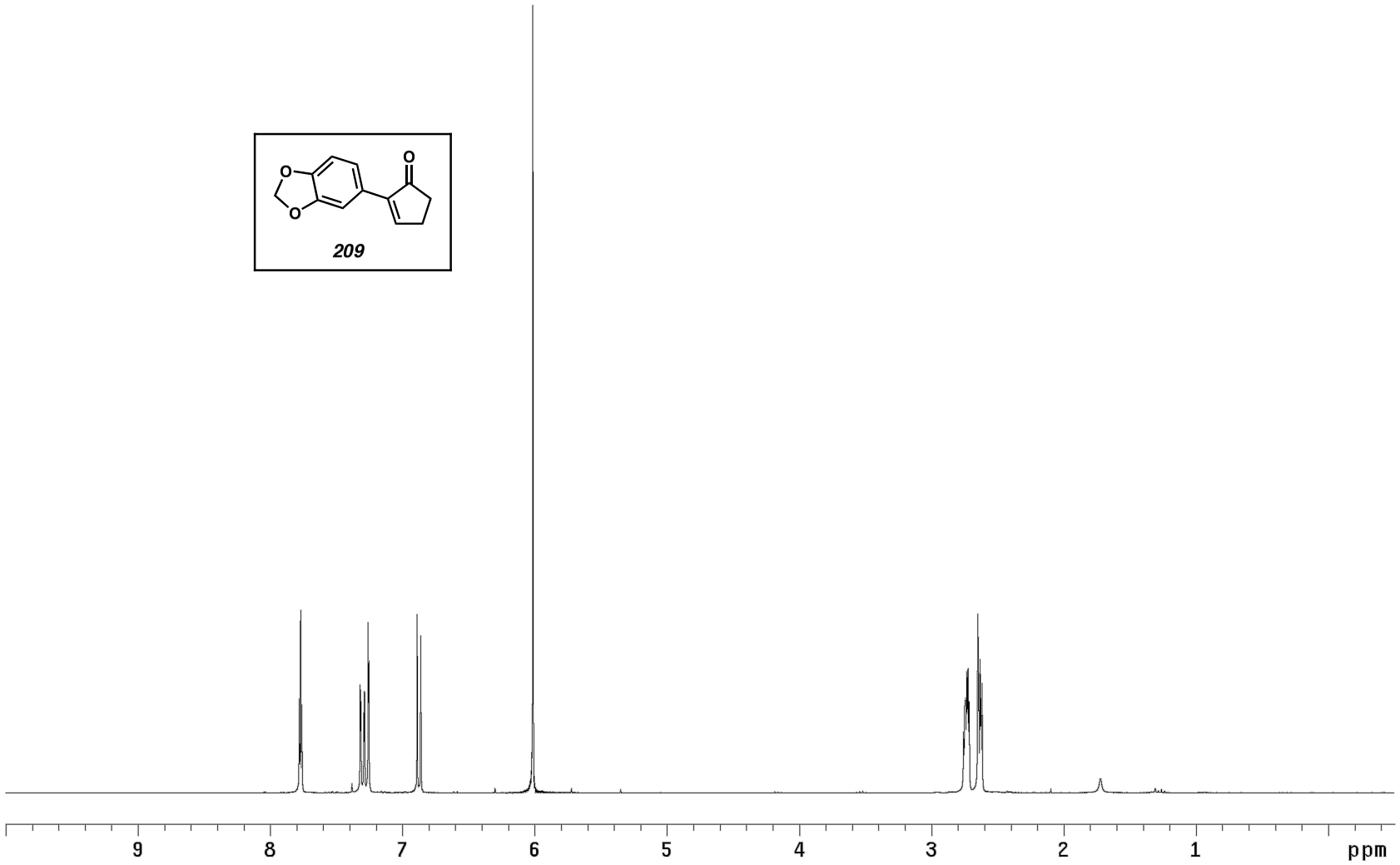

Figure A1.43 ^{1}H NMR (300 MHz, $CDCl_3$) of compound **209**.

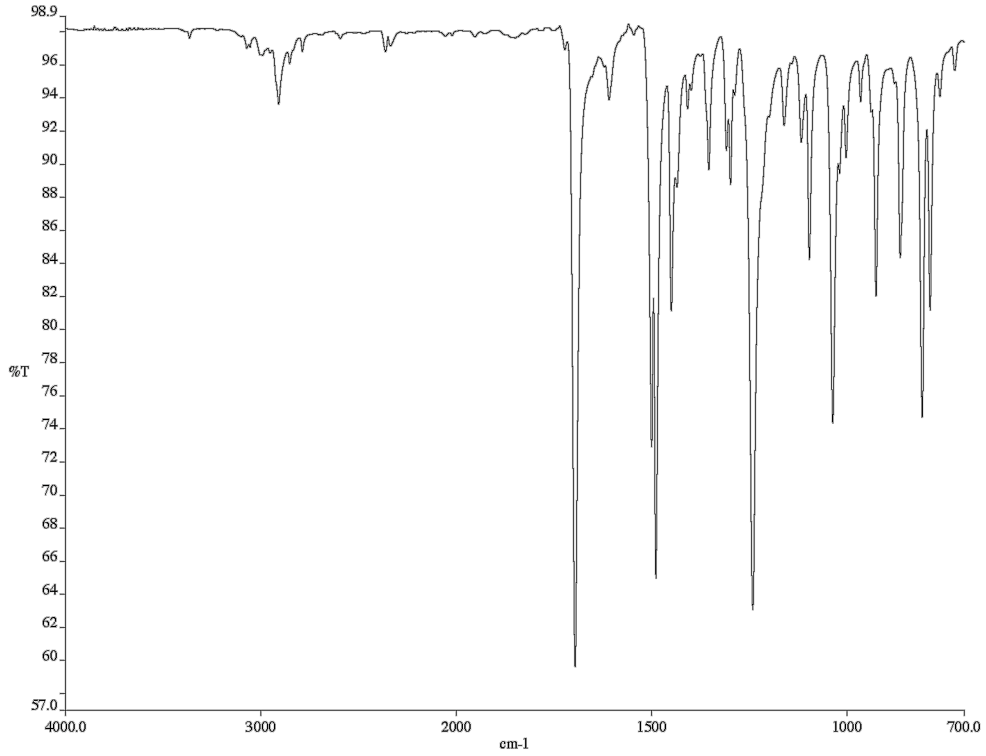

Figure A1.44 Infrared spectrum (thin film/NaCl) of compound **209**.

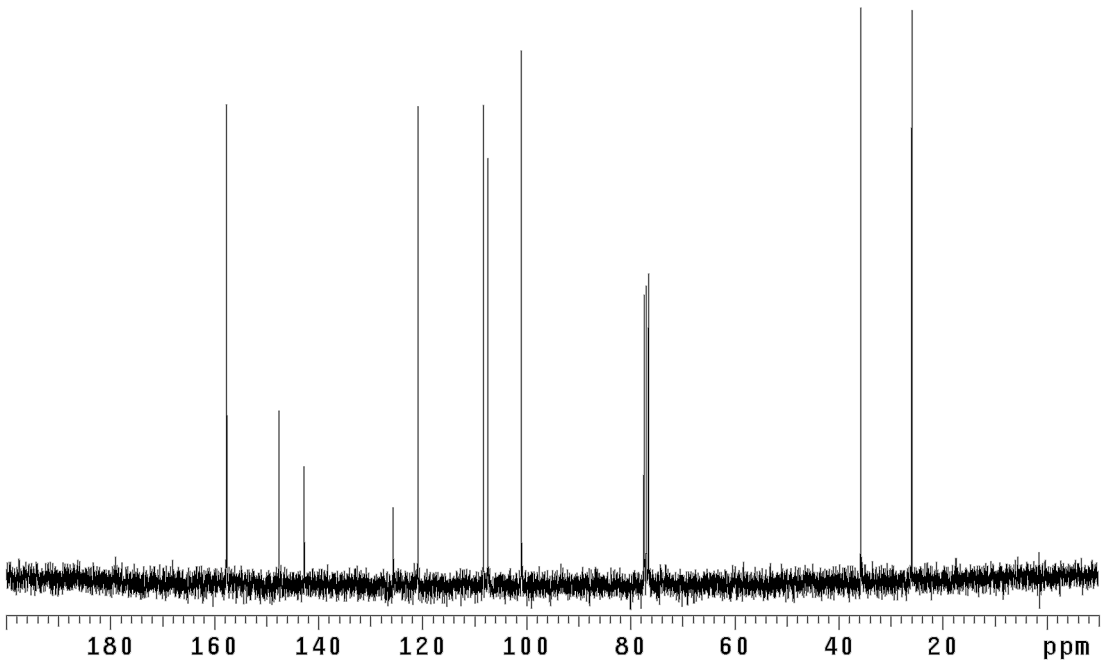

Figure A1.45 ^{13}C NMR (75 MHz, $CDCl_3$) of compound **209**.

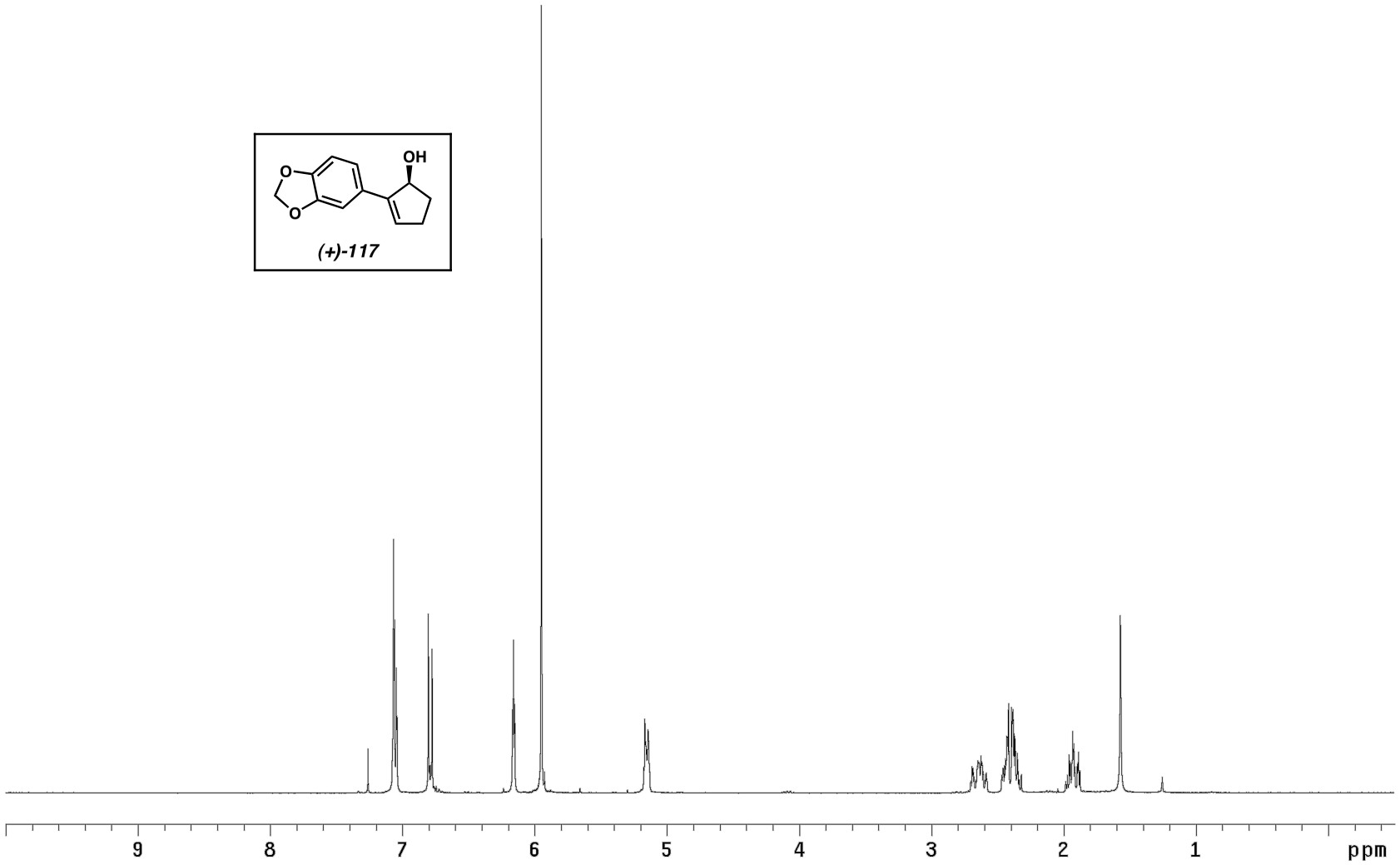

Figure A1.46 ^{1}H NMR (300 MHz, $CDCl_3$) of compound (+)-**117**.

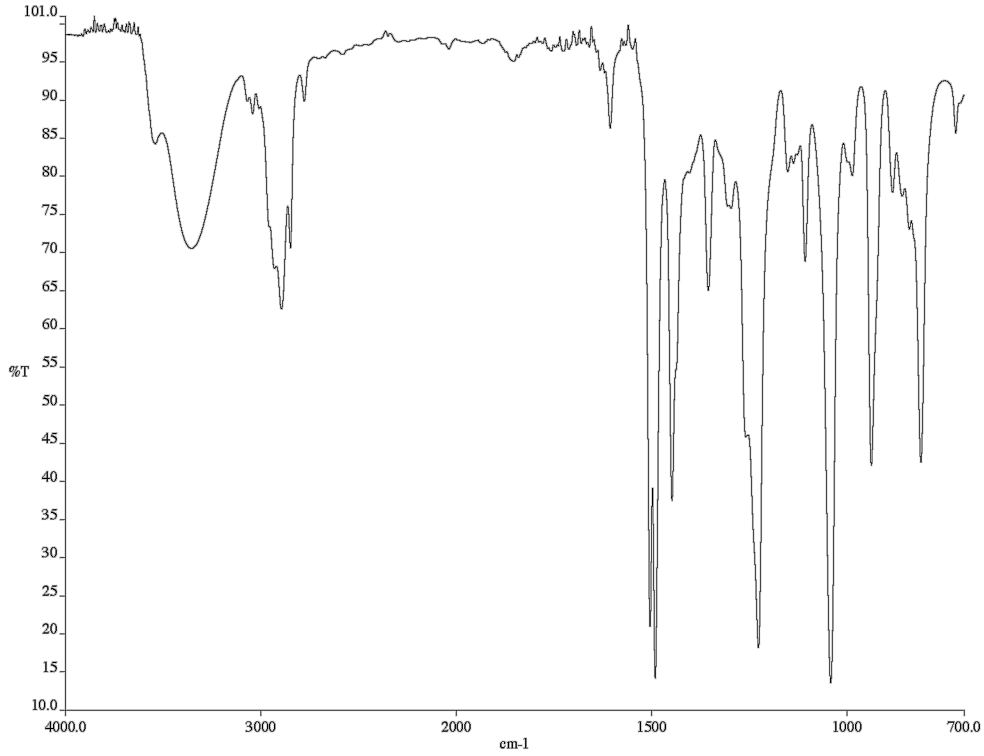

Figure A1.47 Infrared spectrum (thin film/NaCl) of compound (+)-**117**.

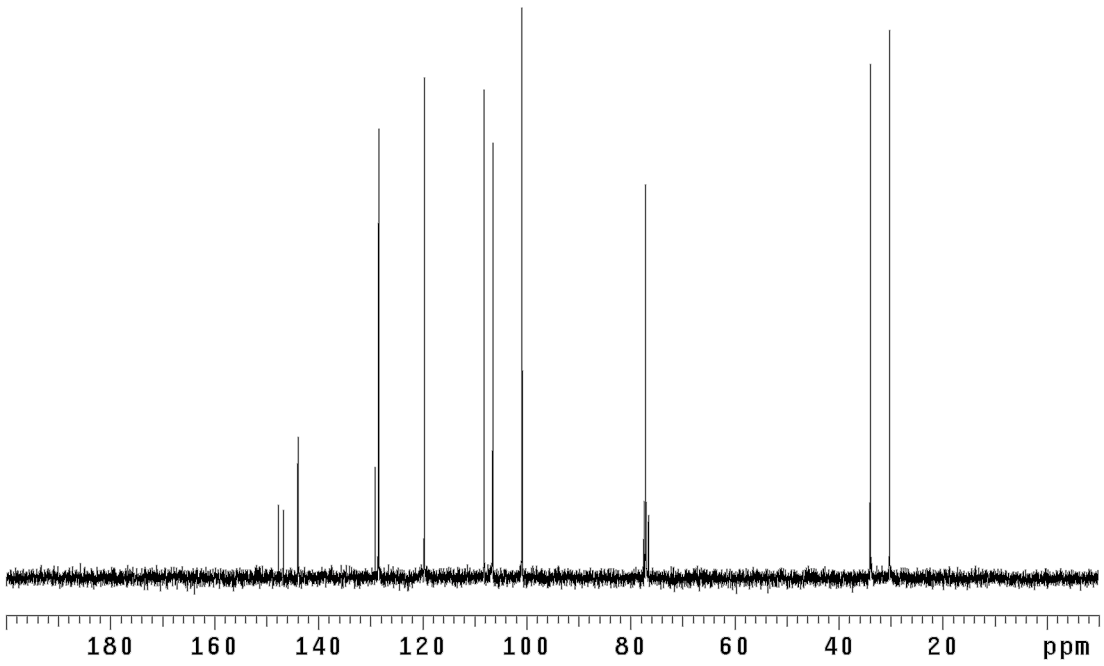

Figure A1.48 ^{13}C NMR (75 MHz, $CDCl_3$) of compound (+)-**117**.

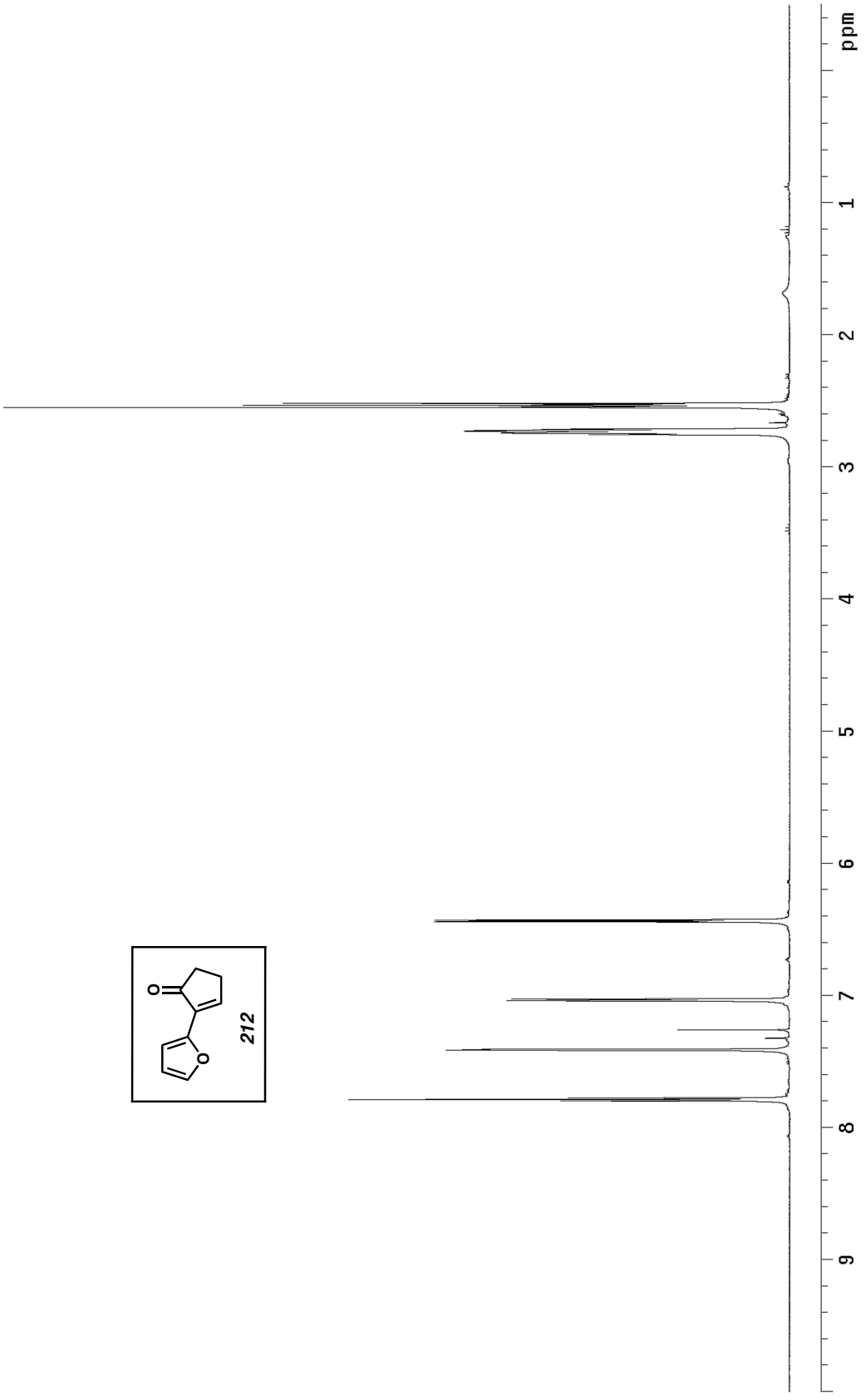

Figure A1.49 ^{1}H NMR (300 MHz, $CDCl_3$) of compound **212**.

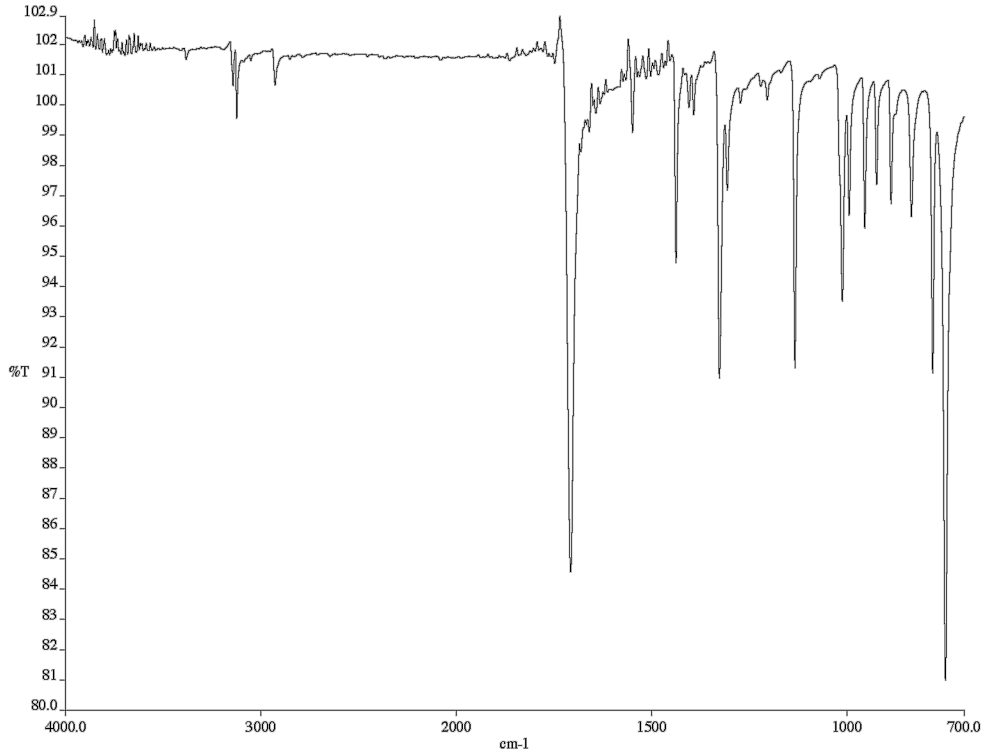

Figure A1.50 Infrared spectrum (thin film/NaCl) of compound **212**.

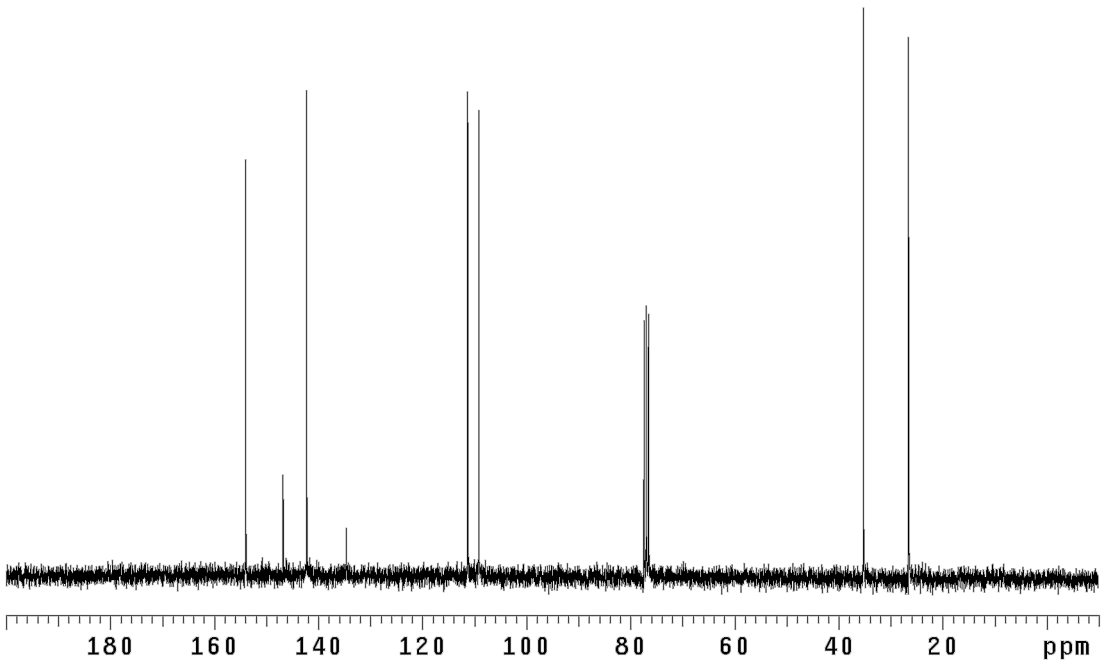

Figure A1.51 ^{13}C NMR (75 MHz, $CDCl_3$) of compound **212**.

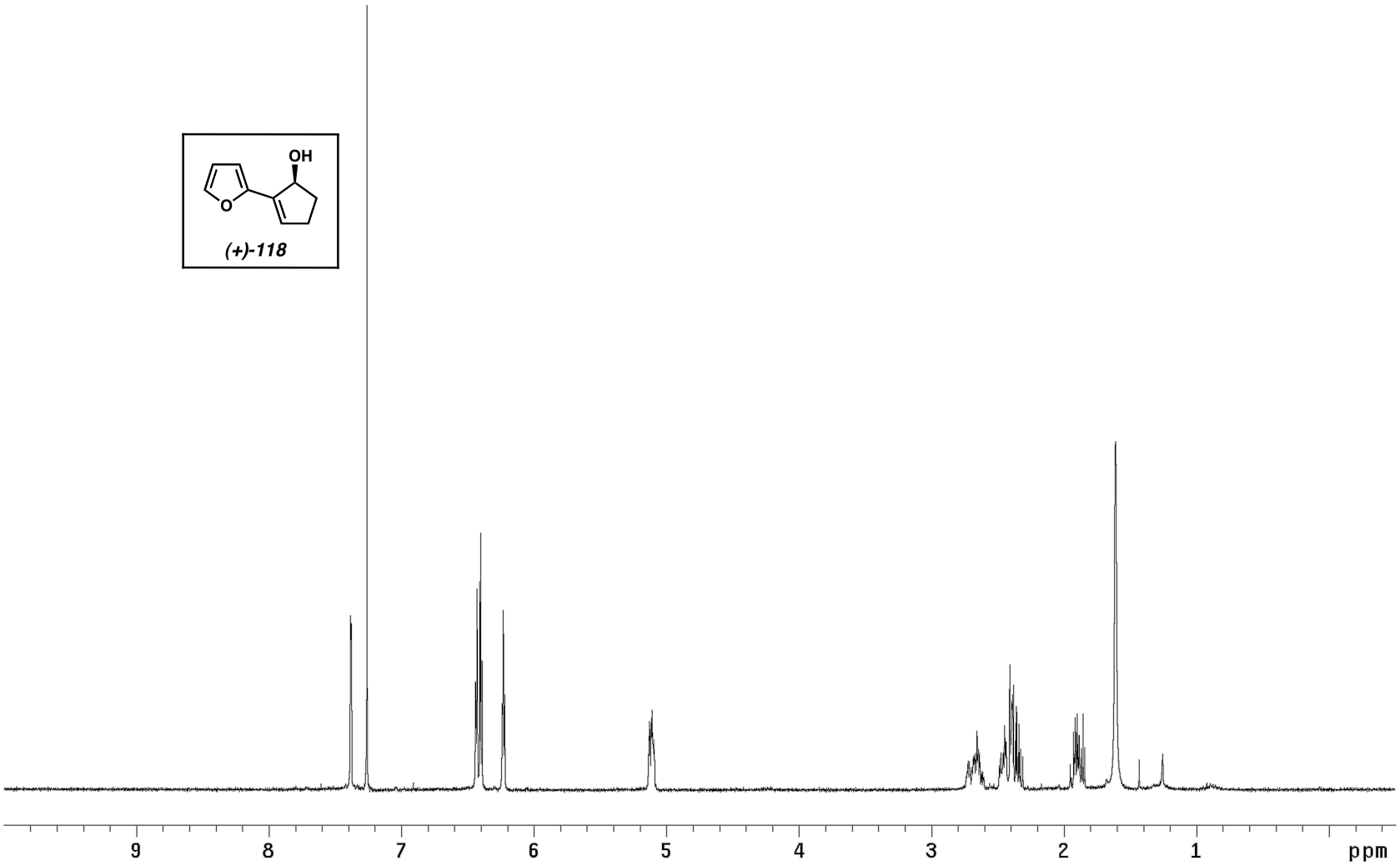

Figure A1.52 ^{1}H NMR (300 MHz, $CDCl_3$) of compound (+)-**118**.

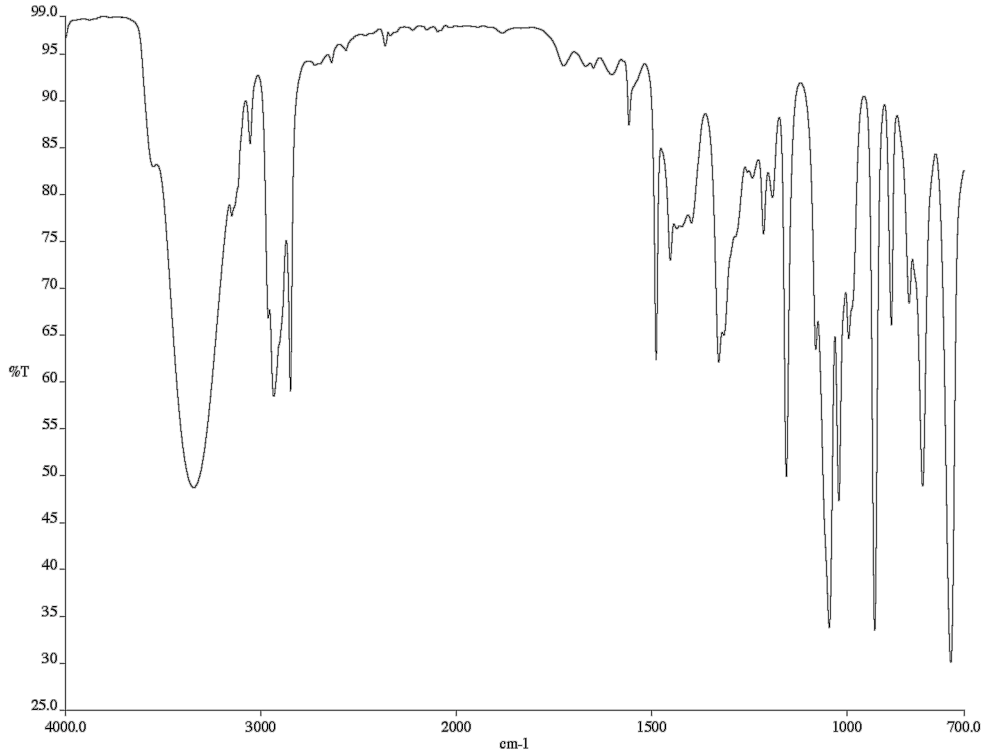

Figure A1.53 Infrared spectrum (thin film/NaCl) of compound (+)-**118**.

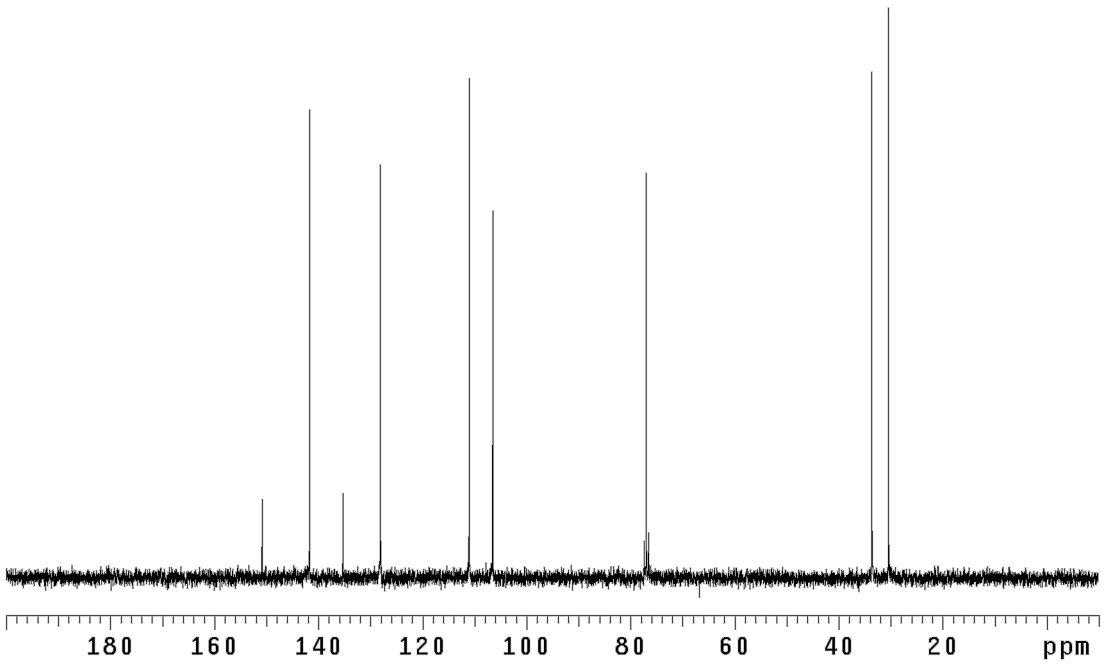

Figure A1.54 ^{13}C NMR (75 MHz, $CDCl_3$) of compound (+)-**118**.

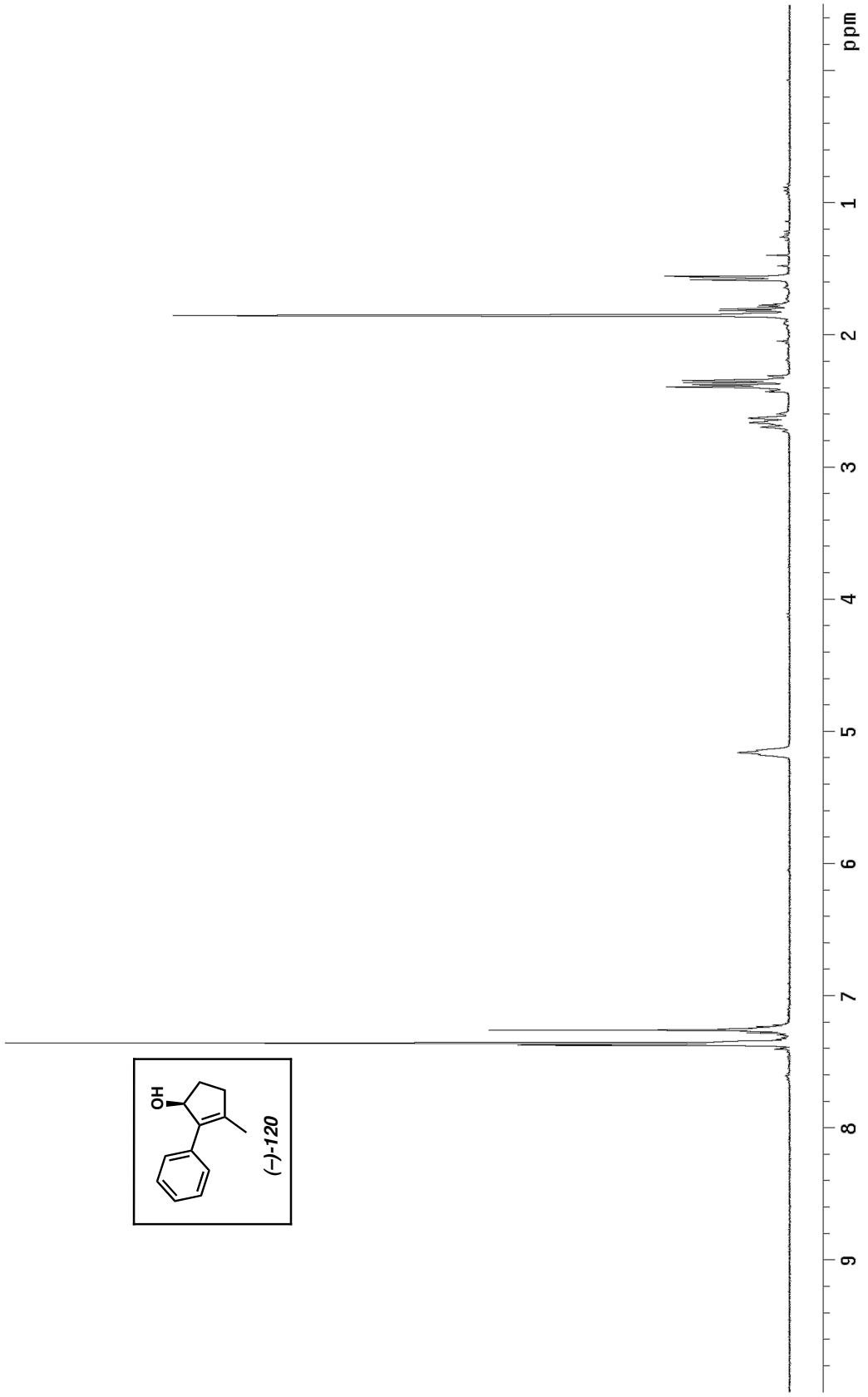

Figure A1.55 ^{1}H NMR (300 MHz, $CDCl_3$) of compound (–)-**120**.

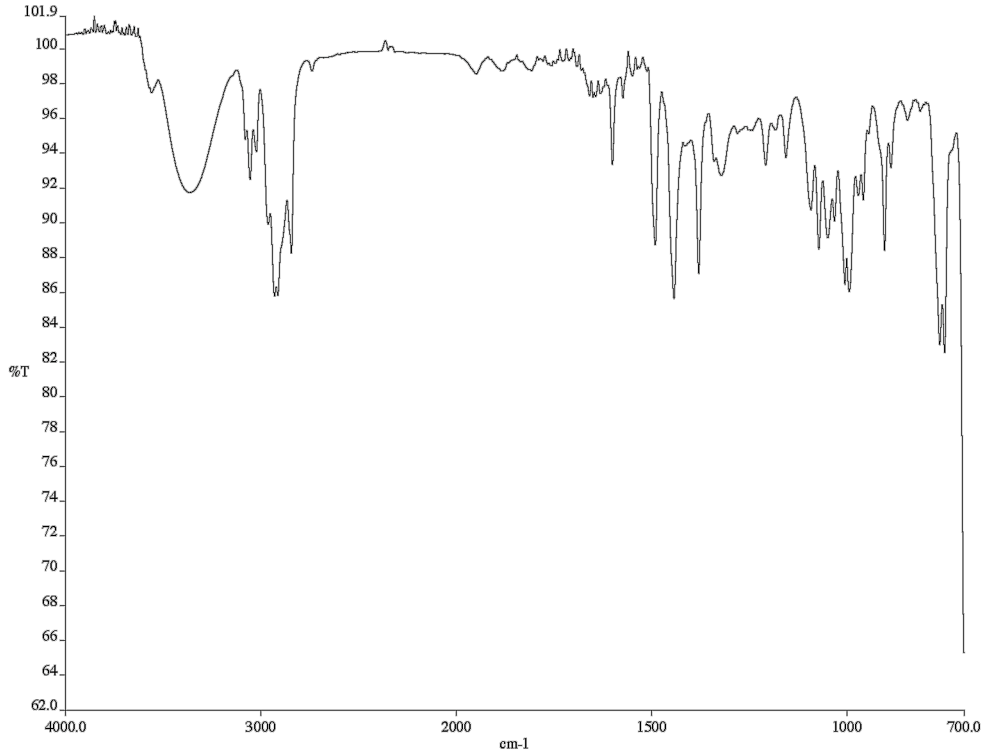

Figure A1.56 Infrared spectrum (thin film/NaCl) of compound (–)-**120**.

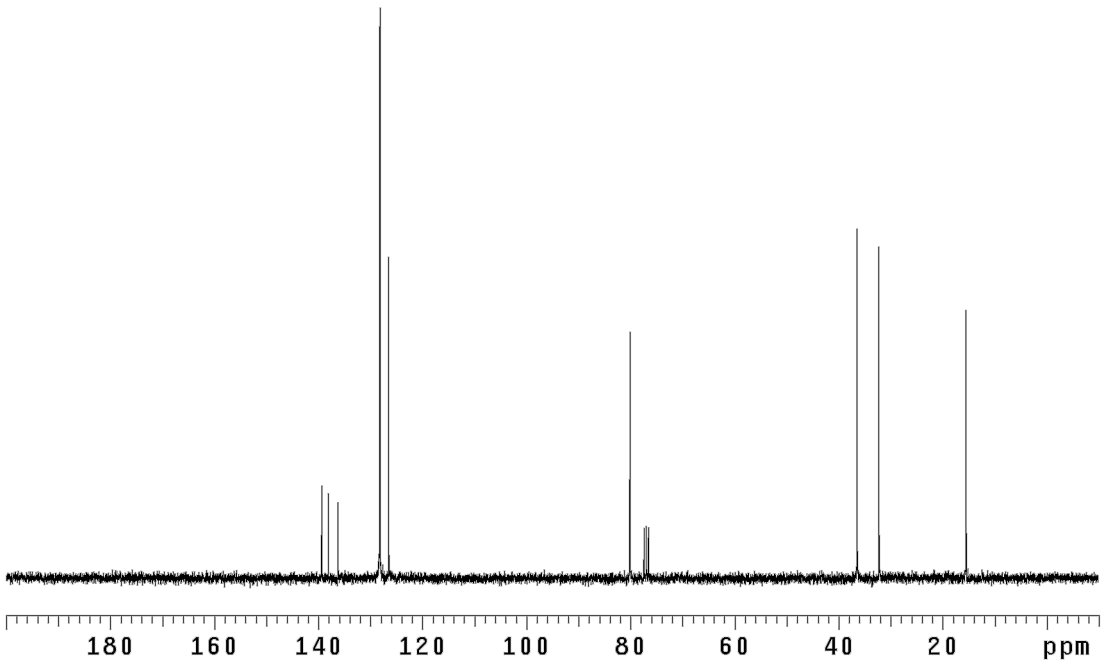

Figure A1.57 ^{13}C NMR (75 MHz, $CDCl_3$) of compound (–)-**120**.

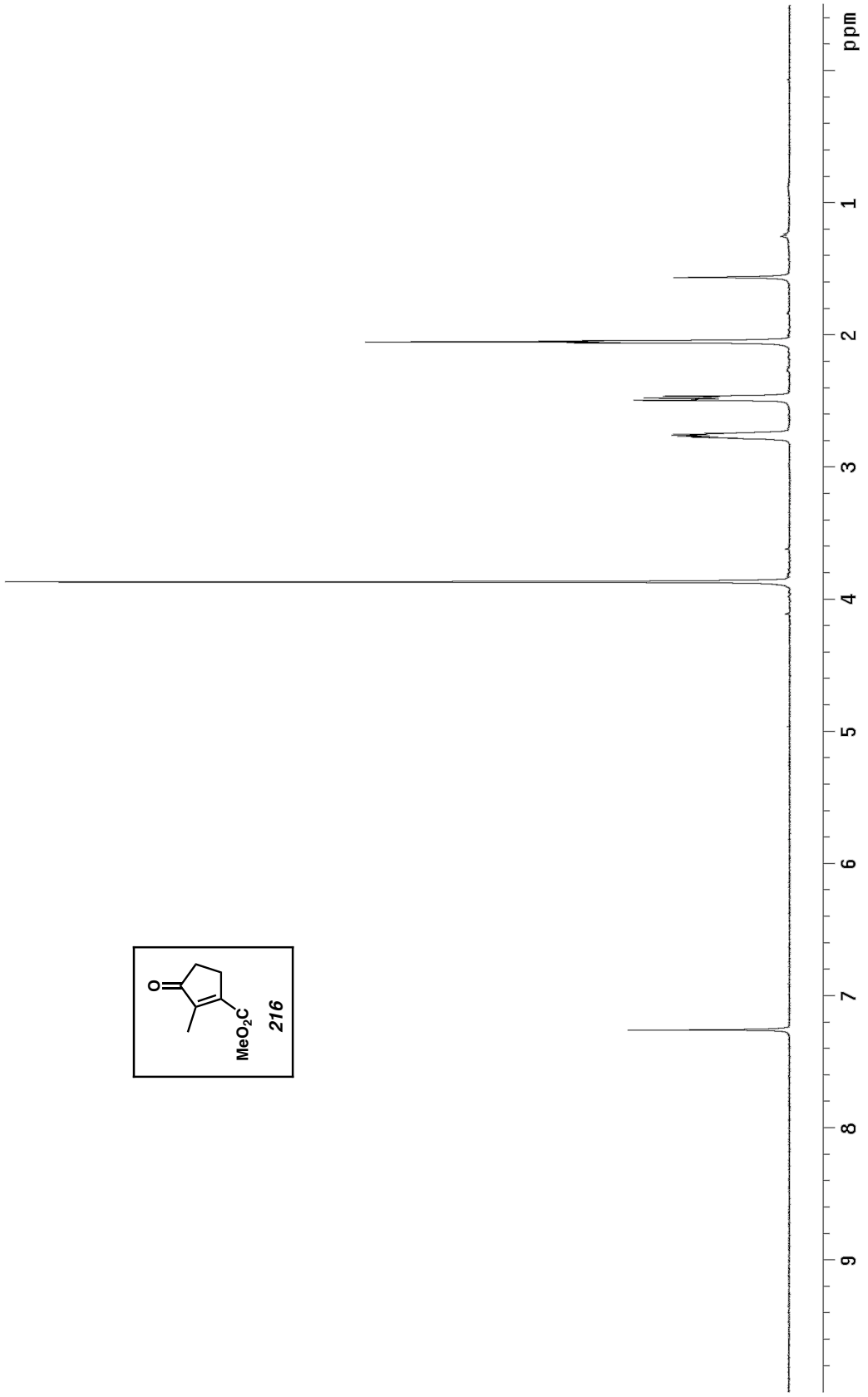

Figure A1.58 ^{1}H NMR (300 MHz, $CDCl_3$) of compound **216**.

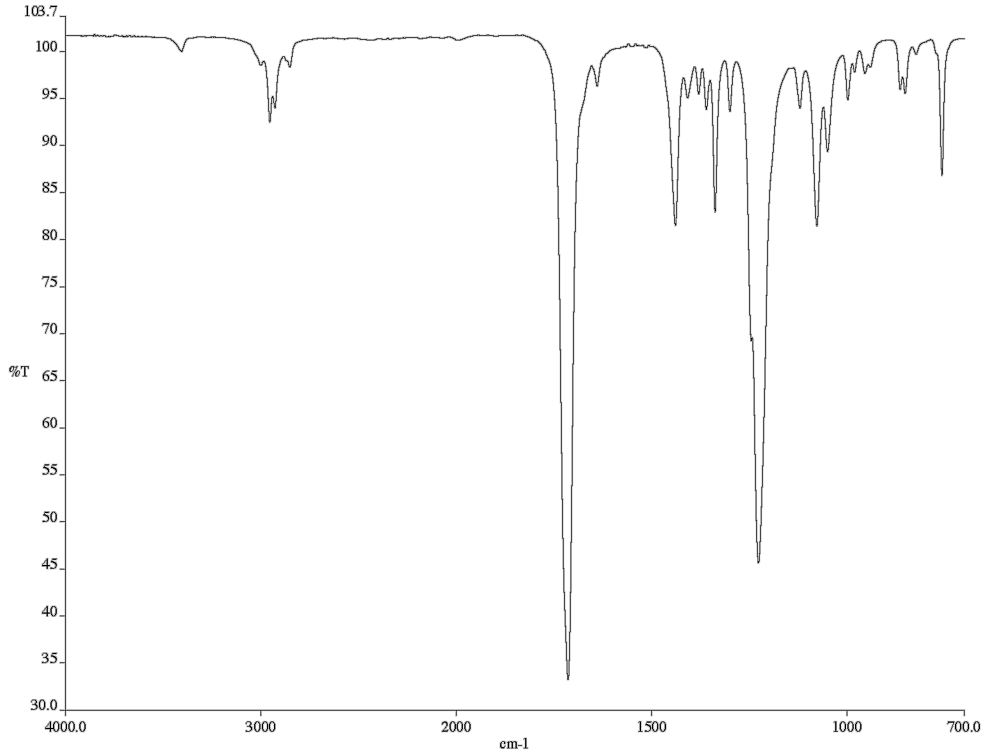

Figure A1.59 Infrared spectrum (thin film/NaCl) of compound **216**.

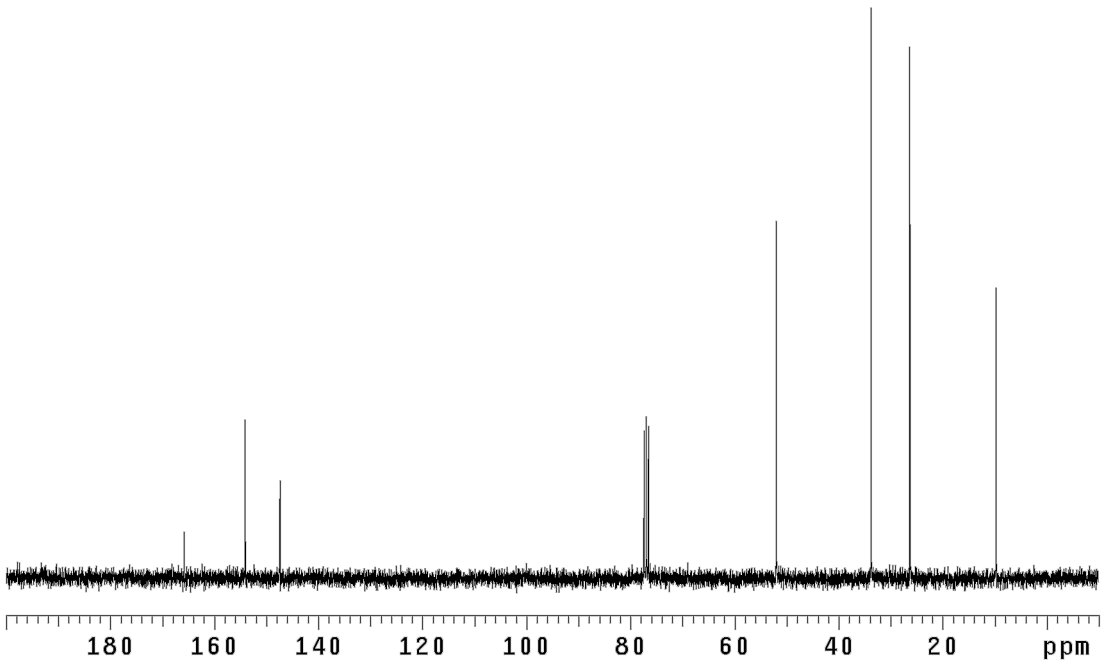

Figure A1.60 ^{13}C NMR (75 MHz, $CDCl_3$) of compound **216**.

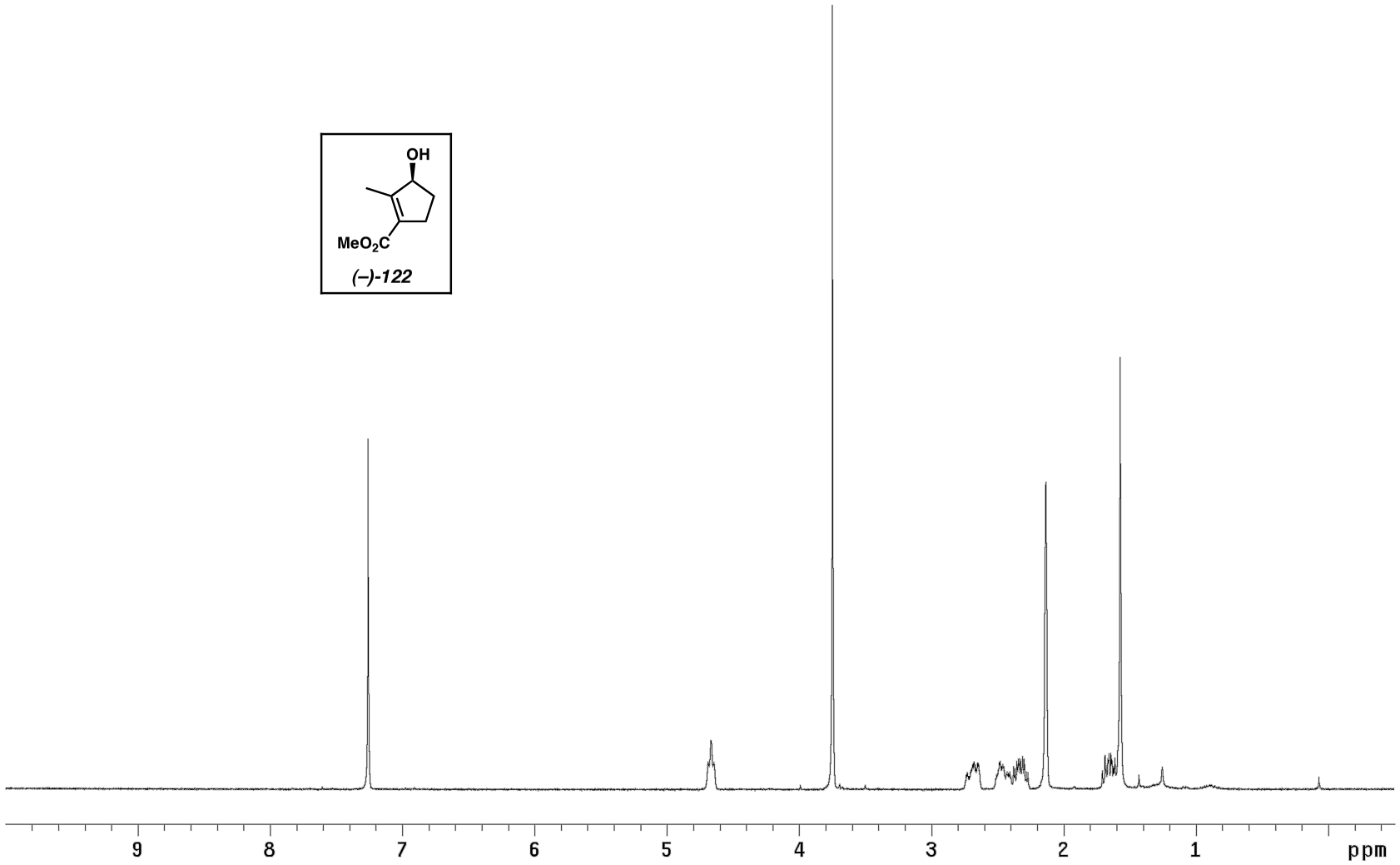

Figure A1.61 ^{1}H NMR (300 MHz, $CDCl_3$) of compound (–)-**122**.

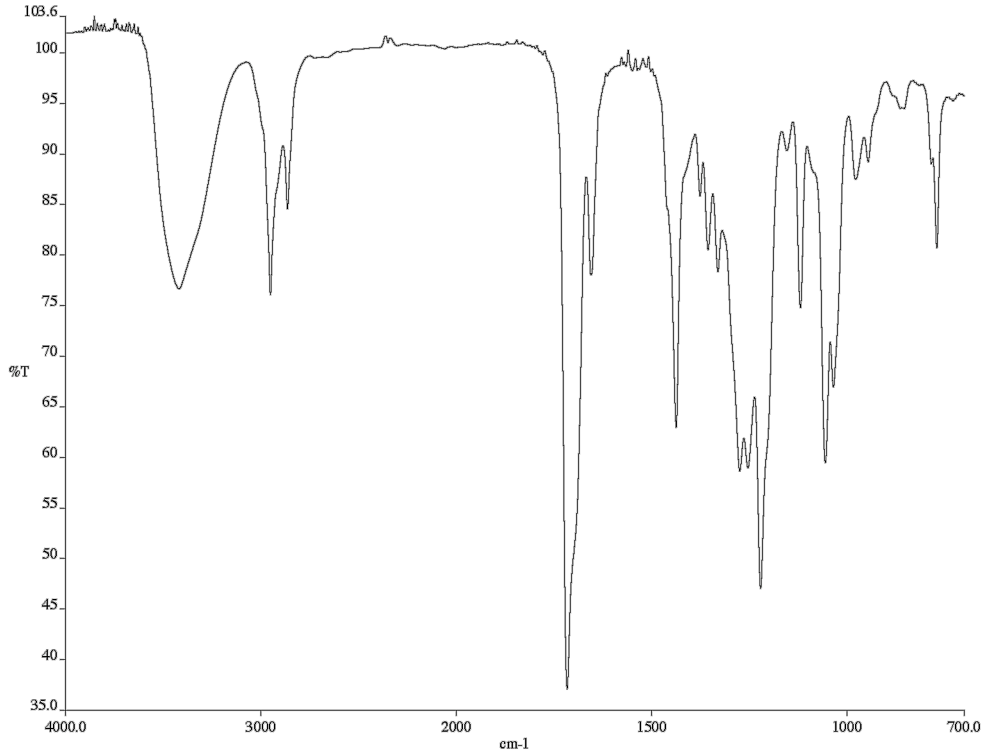

Figure A1.62 Infrared spectrum (thin film/NaCl) of compound (–)-**122**.

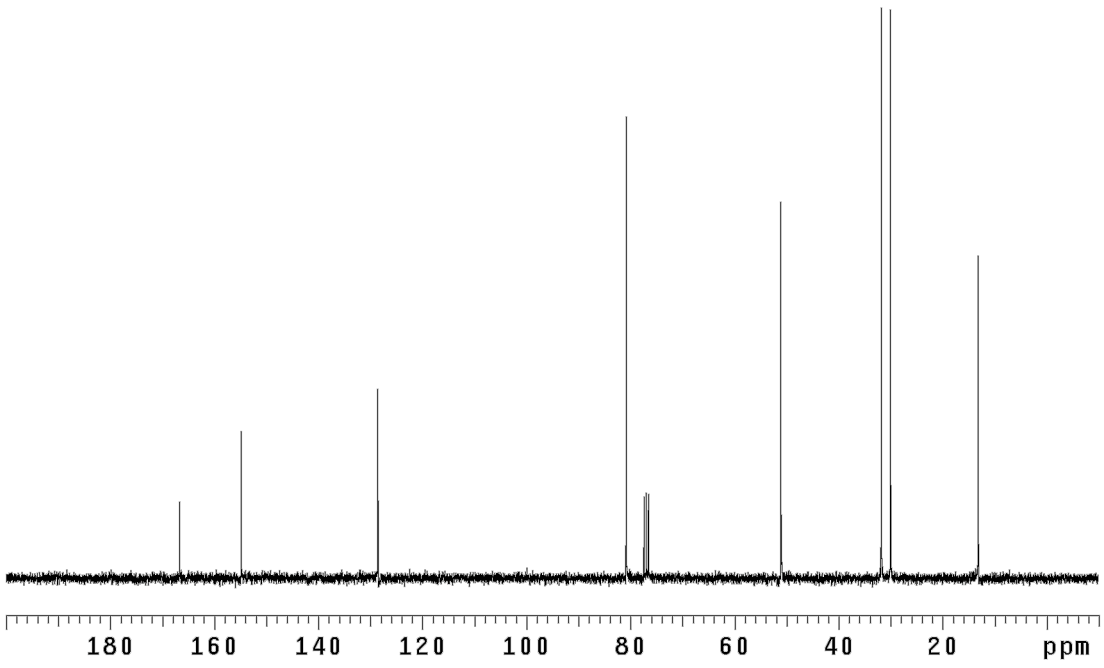

Figure A1.63 ^{13}C NMR (75 MHz, $CDCl_3$) of compound (–)-**122**.

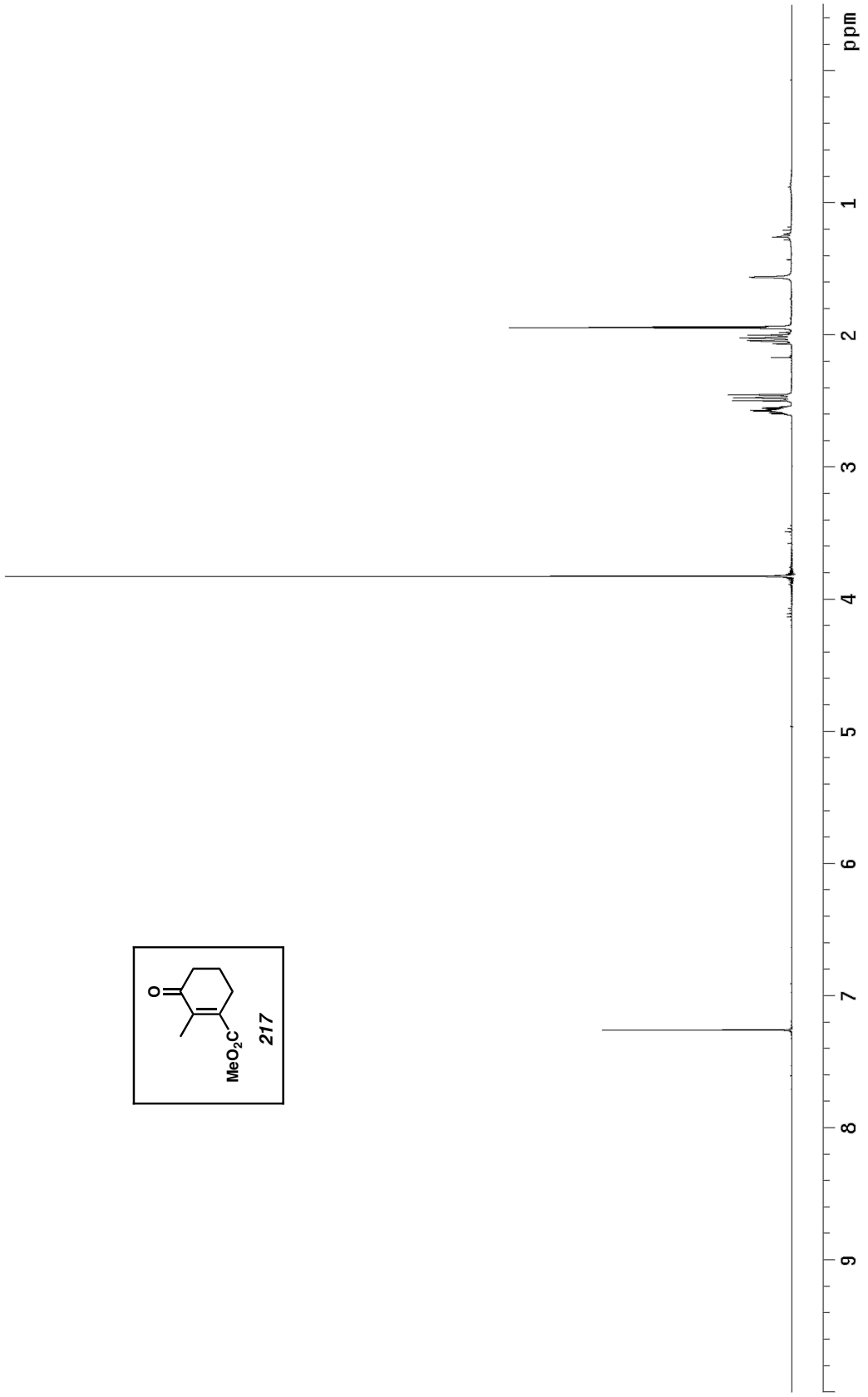

Figure A1.64 ^{1}H NMR (300 MHz, $CDCl_3$) of compound **217**.

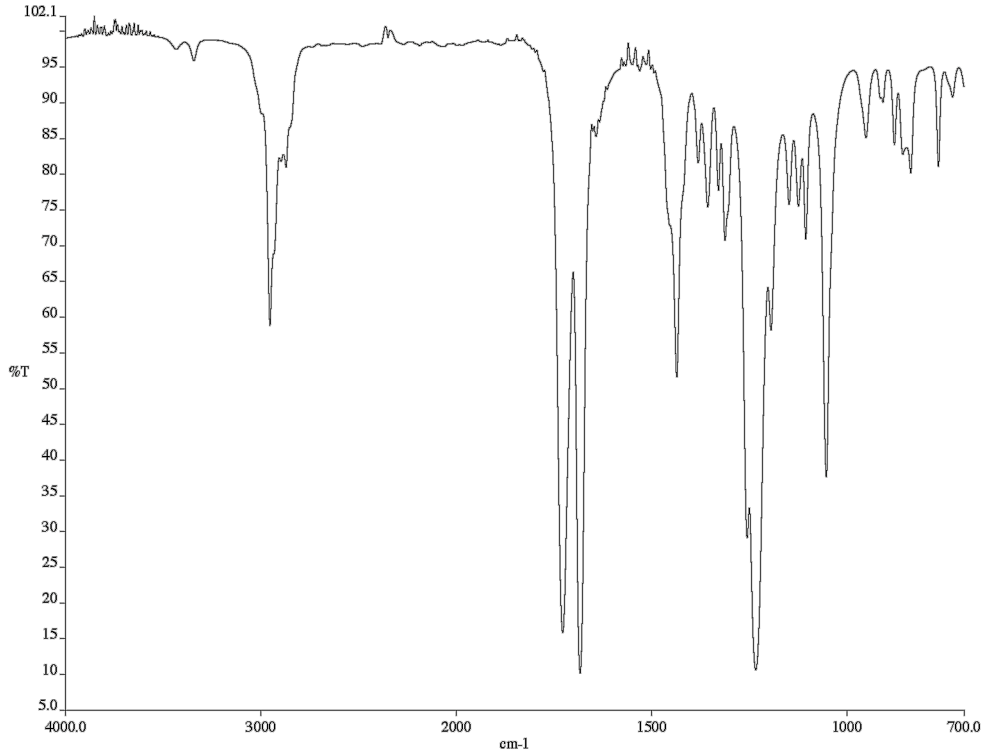

Figure A1.65 Infrared spectrum (thin film/NaCl) of compound **217**.

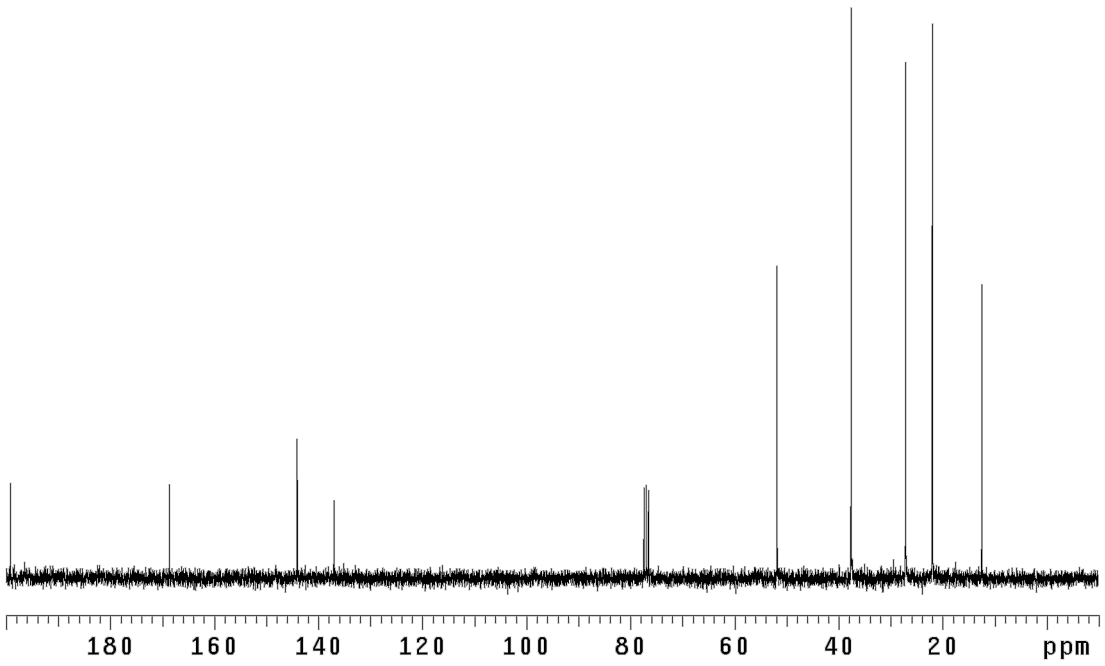

Figure A1.66 ^{13}C NMR (75 MHz, $CDCl_3$) of compound **217**.

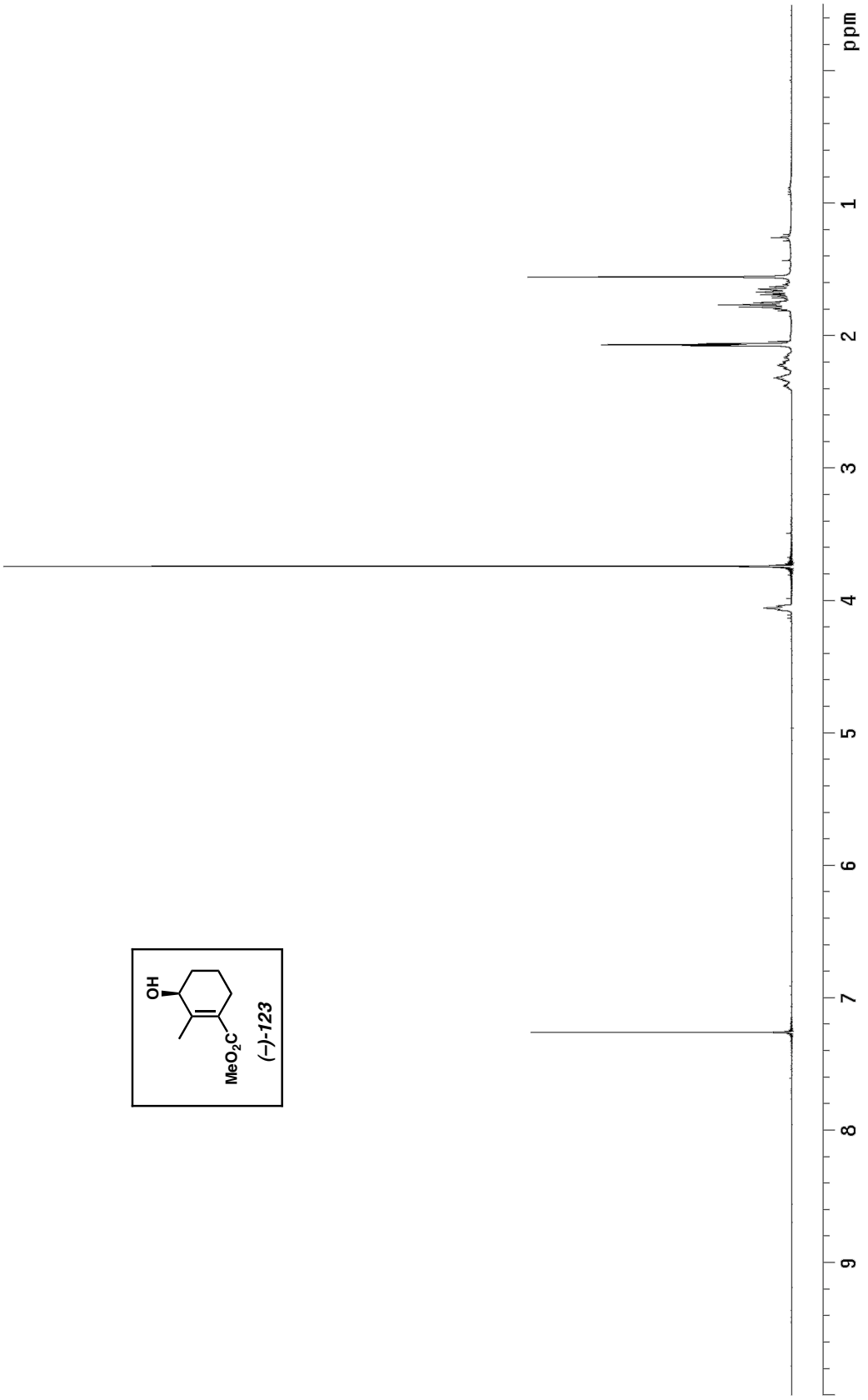

Figure A1.67 ^{1}H NMR (300 MHz, $CDCl_3$) of compound (–)-**123**.

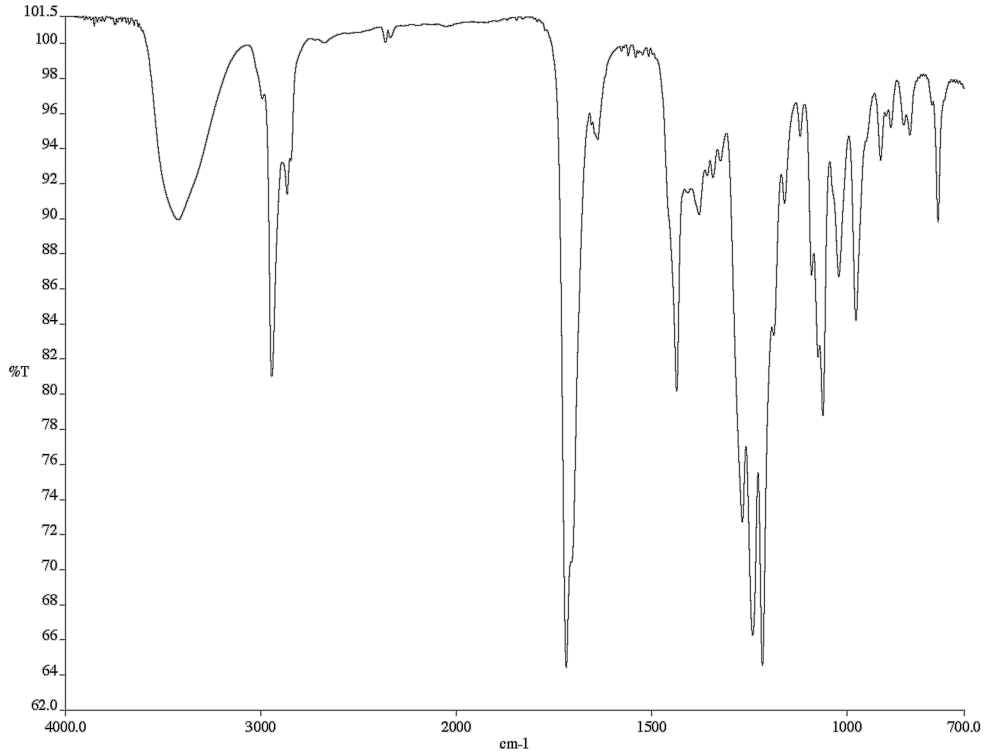

Figure A1.68 Infrared spectrum (thin film/NaCl) of compound (–)-**123**.

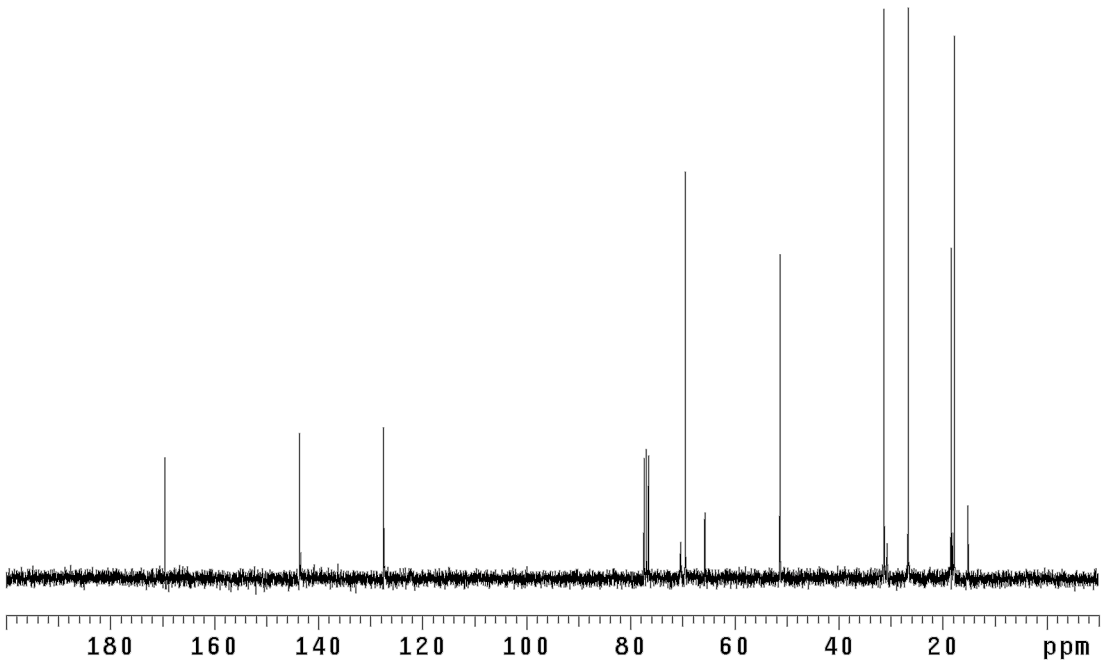

Figure A1.69 ^{13}C NMR (75 MHz, $CDCl_3$) of compound (–)-**123**.

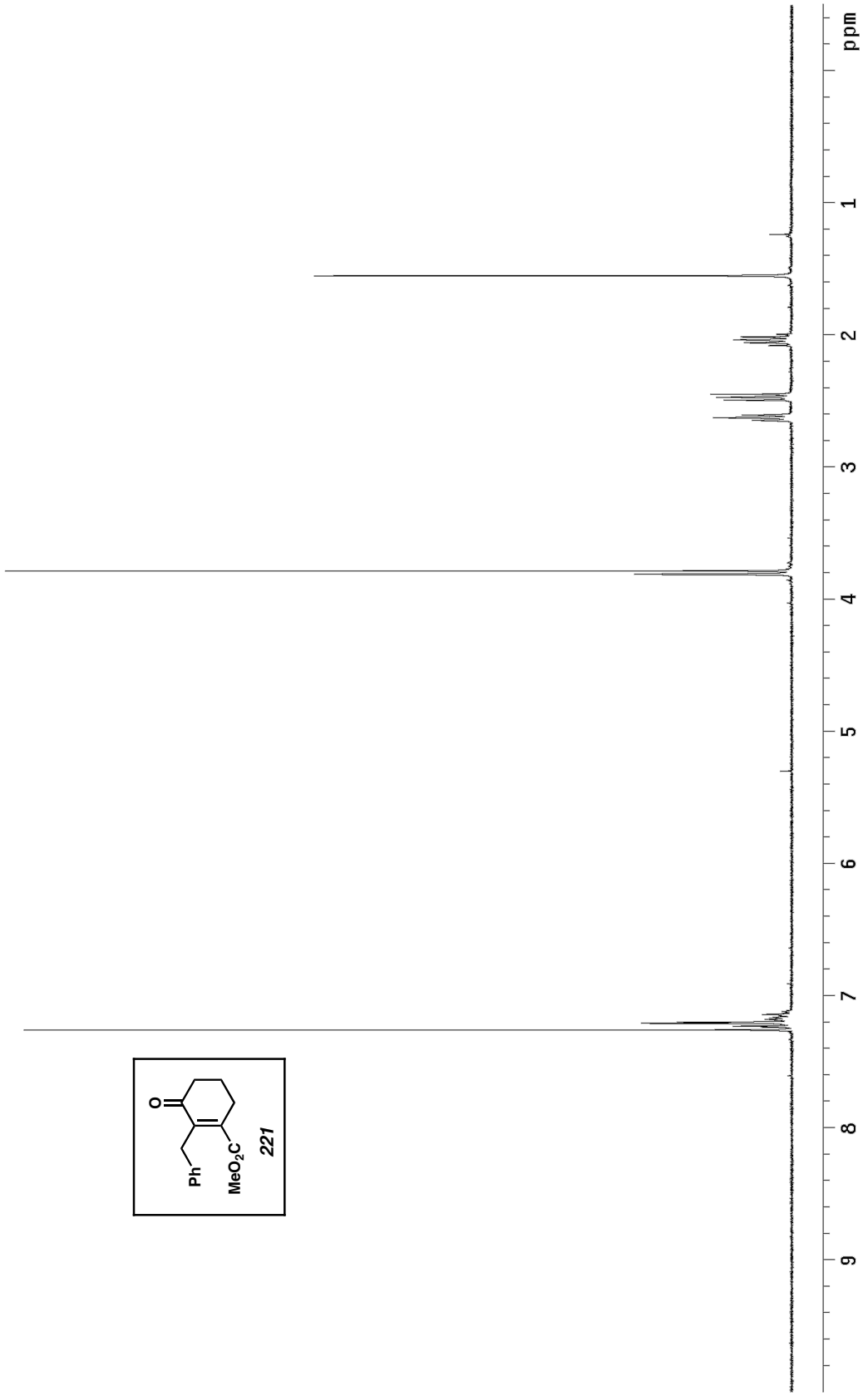

Figure A1.70 ^{1}H NMR (300 MHz, $CDCl_3$) of compound **221**.

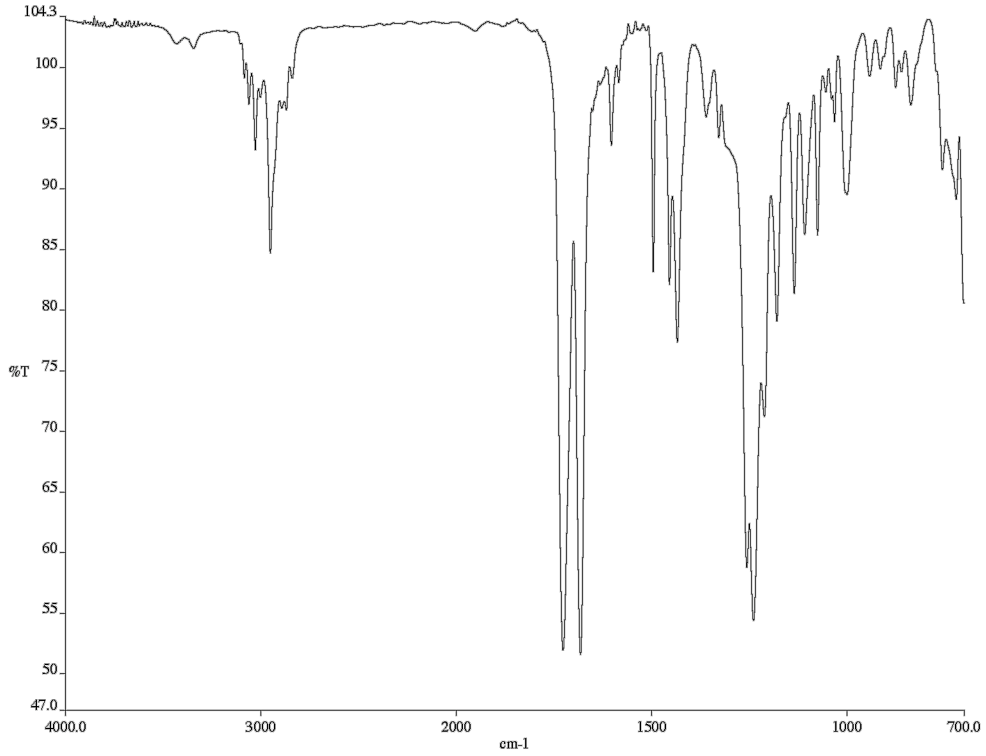

Figure A1.71 Infrared spectrum (thin film/NaCl) of compound **221**.

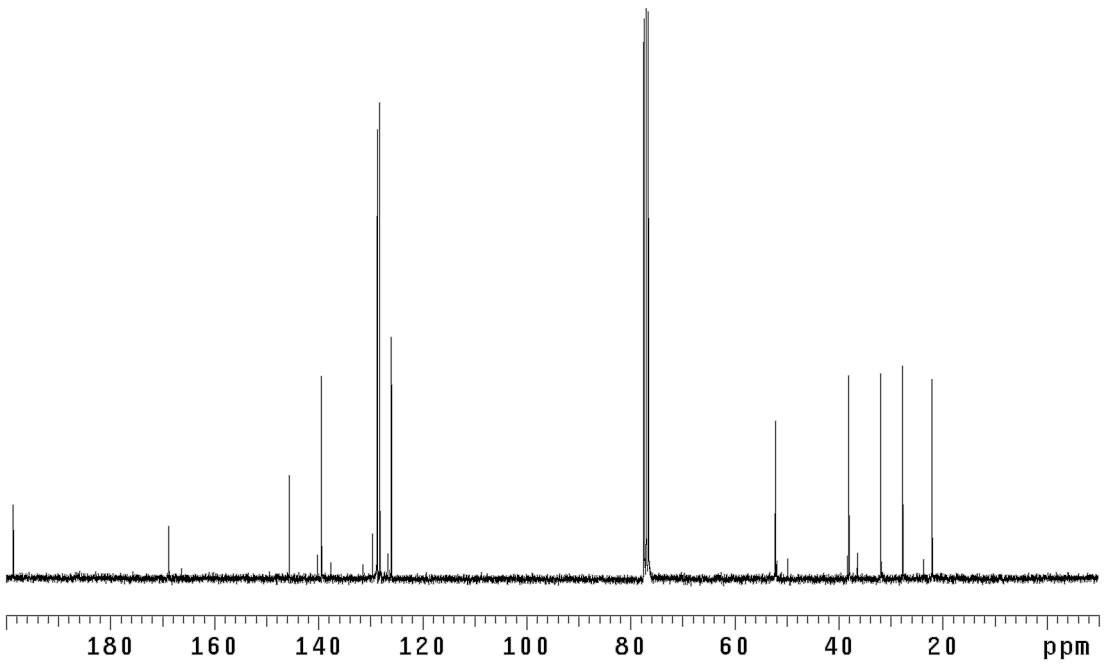

Figure A1.72 ^{13}C NMR (75 MHz, $CDCl_3$) of compound **221**.

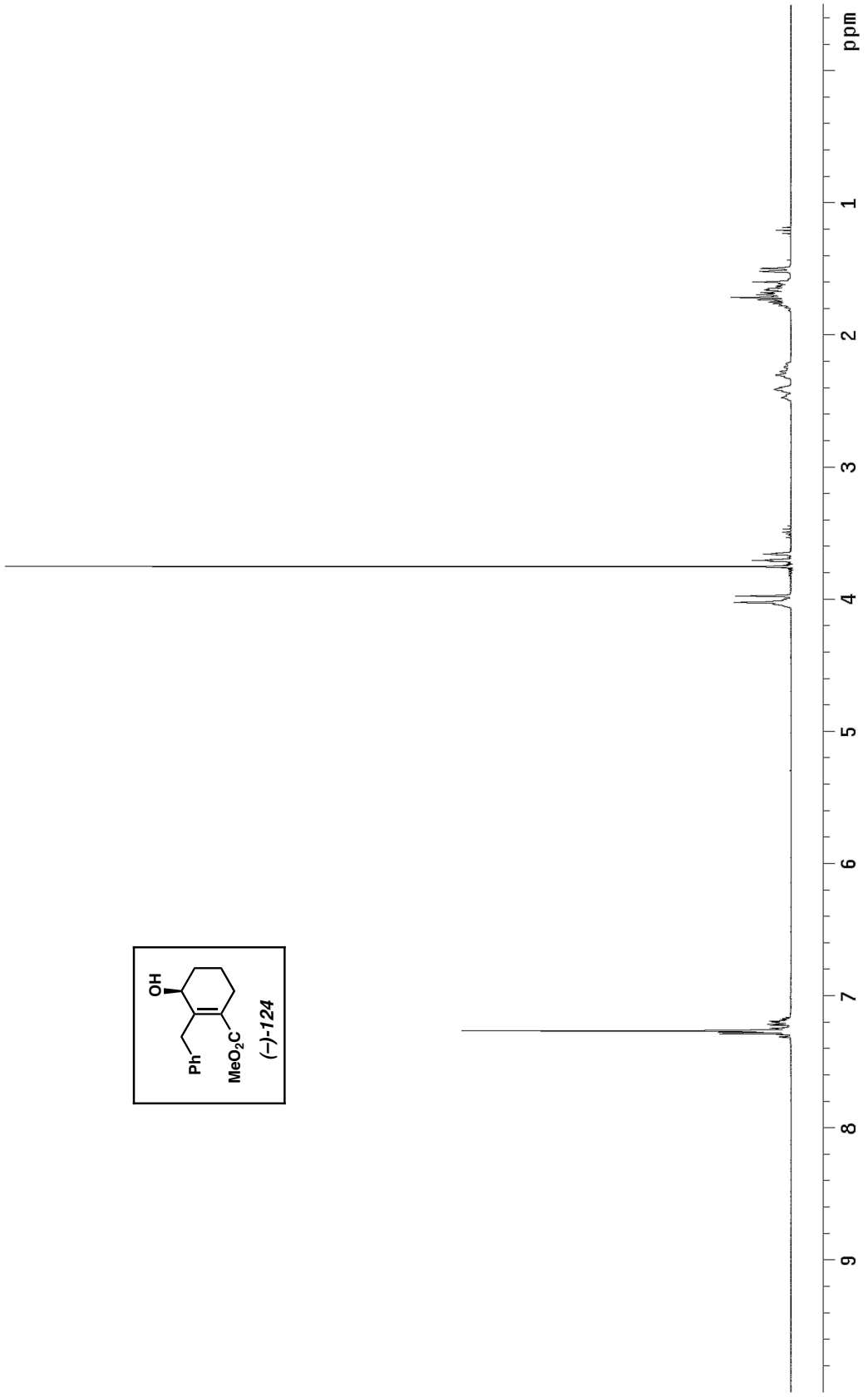

Figure A1.73 ^{1}H NMR (300 MHz, $CDCl_3$) of compound (–)-**124**.

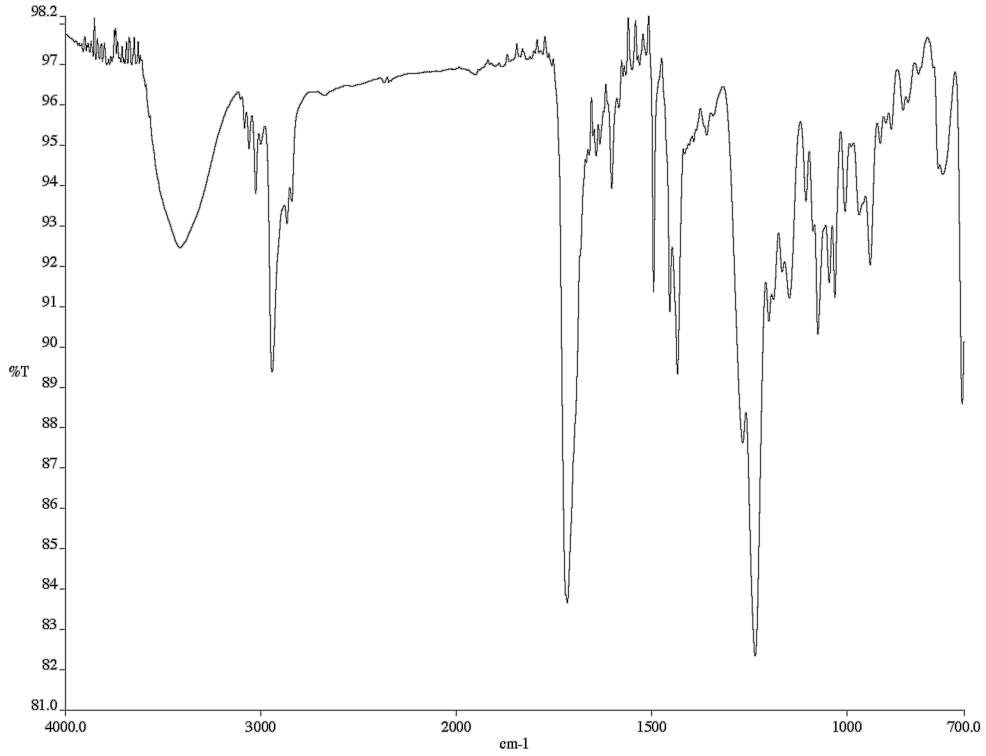

Figure A1.74 Infrared spectrum (thin film/NaCl) of compound (–)-**124**.

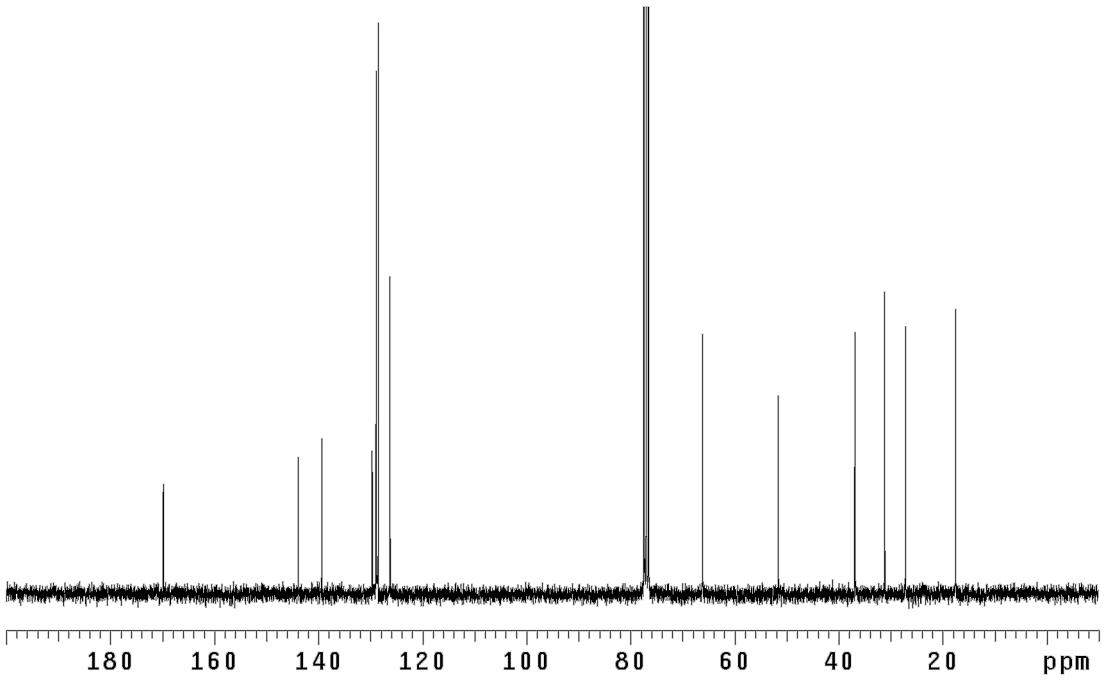

Figure A1.75 ^{13}C NMR (75 MHz, $CDCl_3$) of compound (–)-**124**.

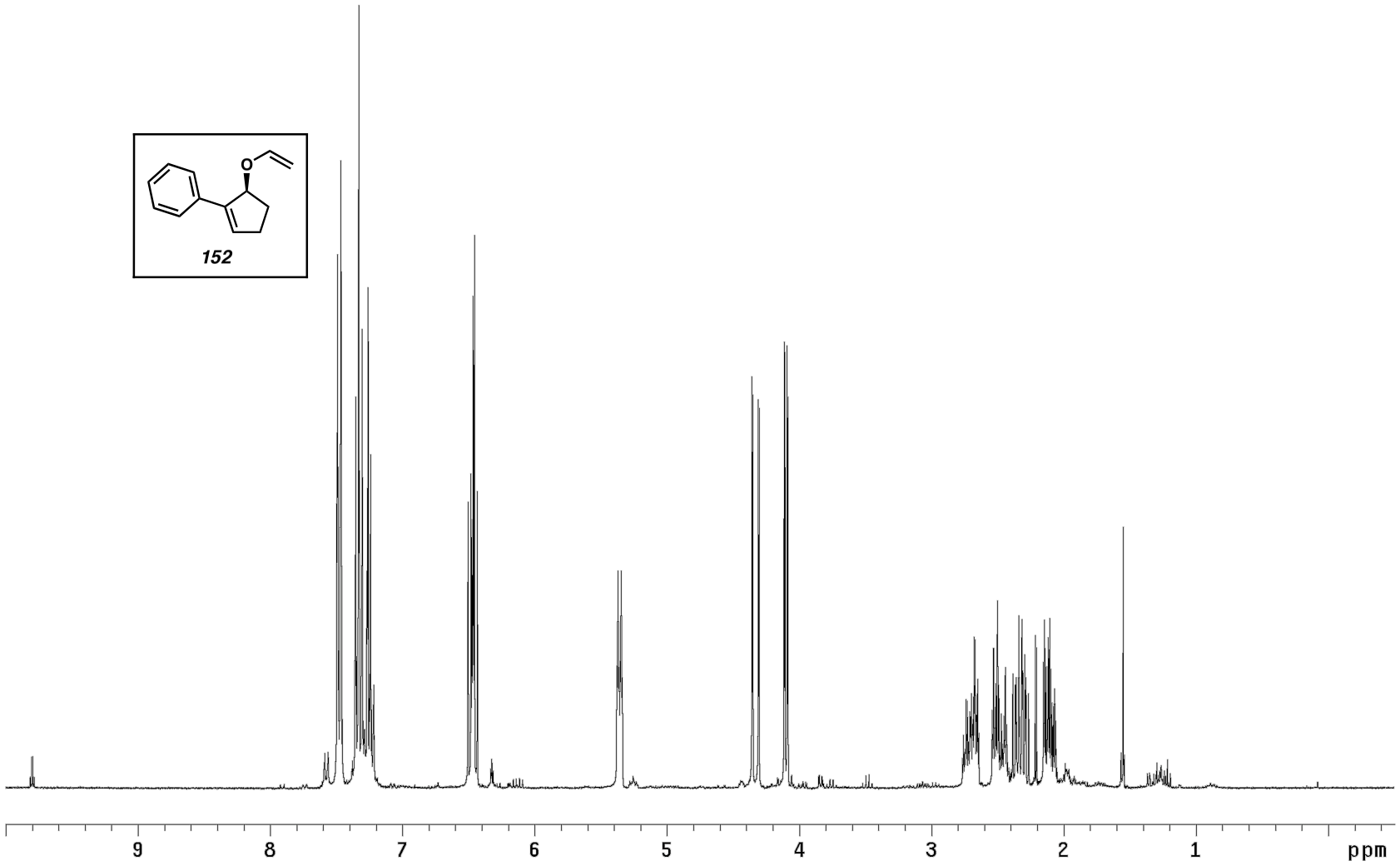

Figure A1.76 ^{1}H NMR (300 MHz, $CDCl_3$) of compound **152**.

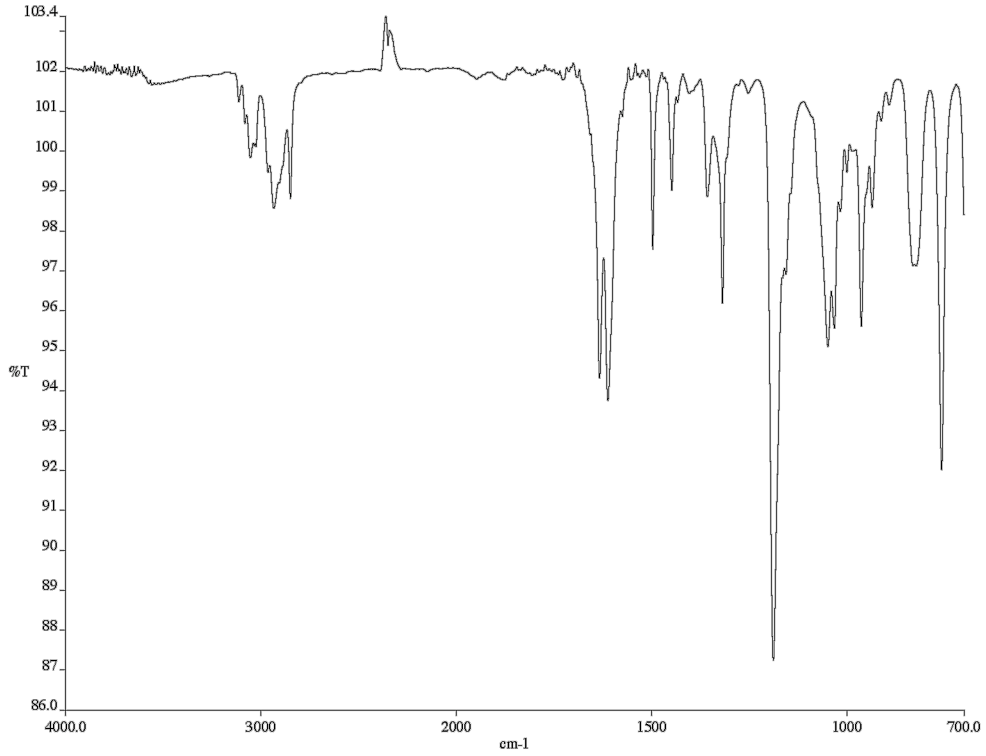

Figure A1.77 Infrared spectrum (thin film/NaCl) of compound **152**.

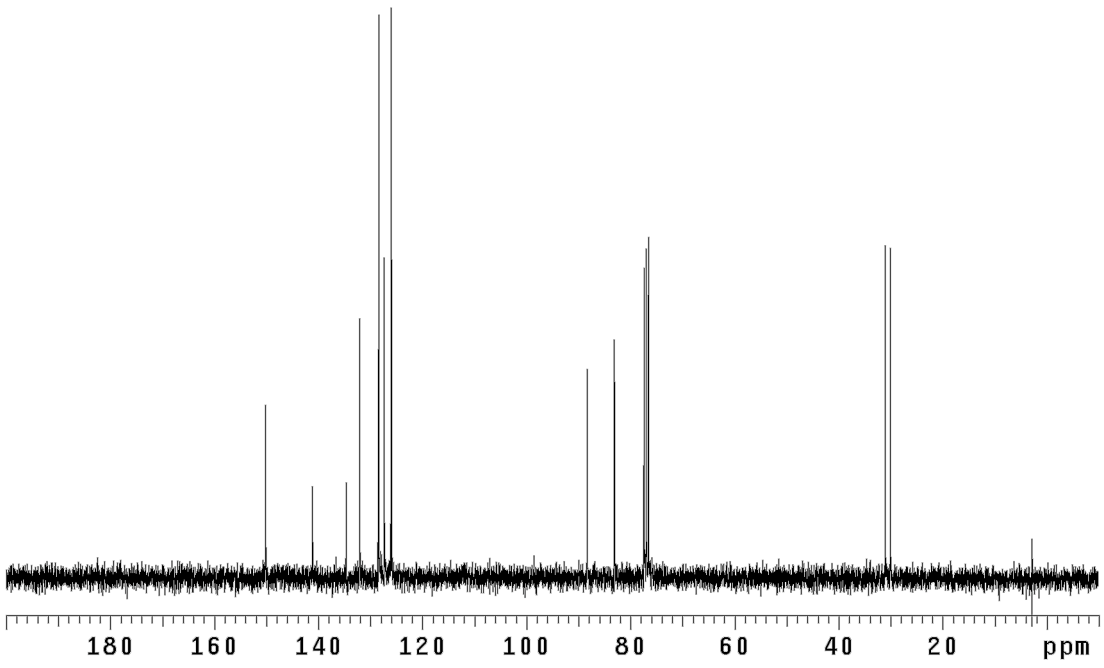

Figure A1.78 ^{13}C NMR (75 MHz, $CDCl_3$) of compound **152**.

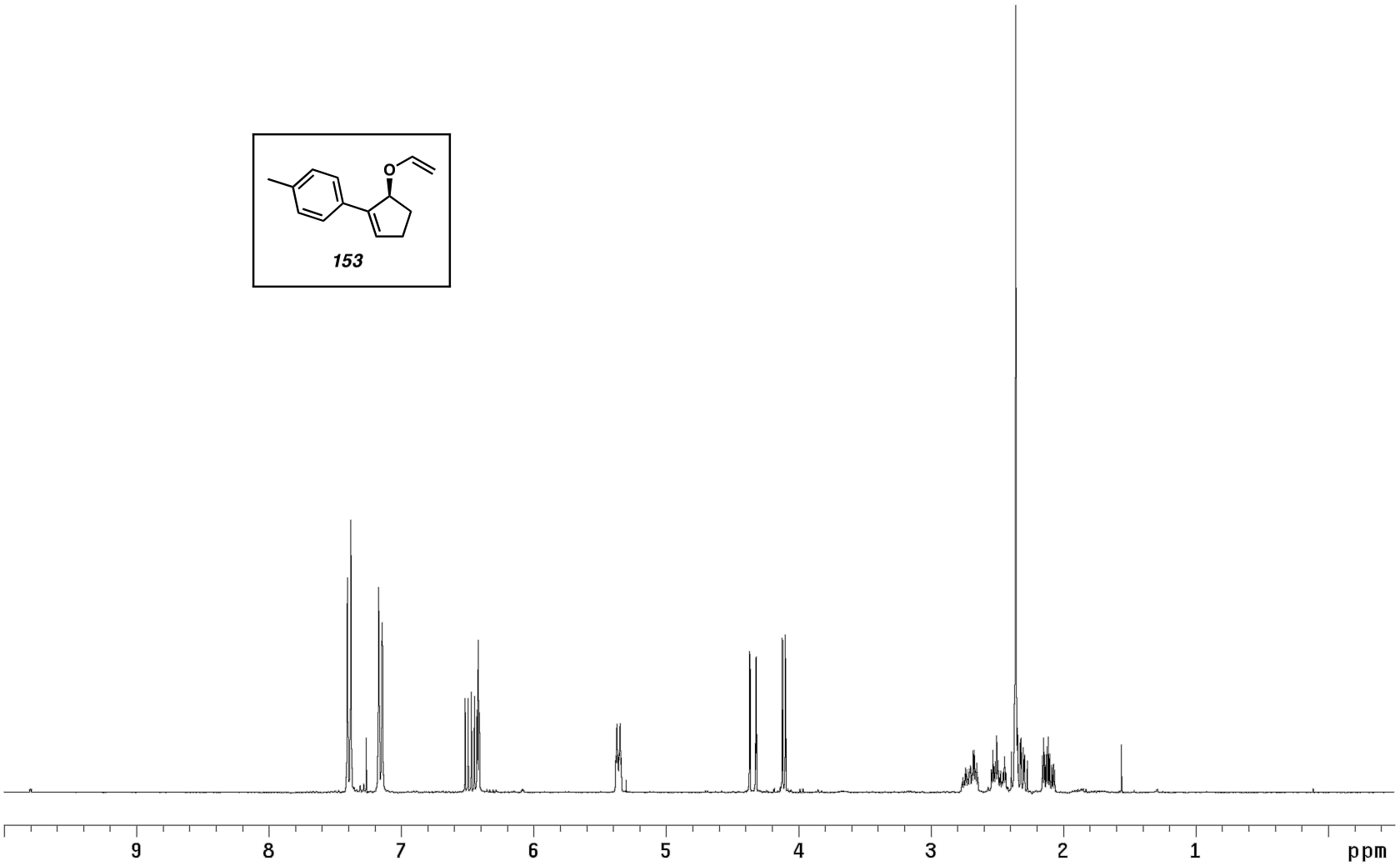

Figure A1.79 ^{1}H NMR (300 MHz, $CDCl_3$) of compound **153**.

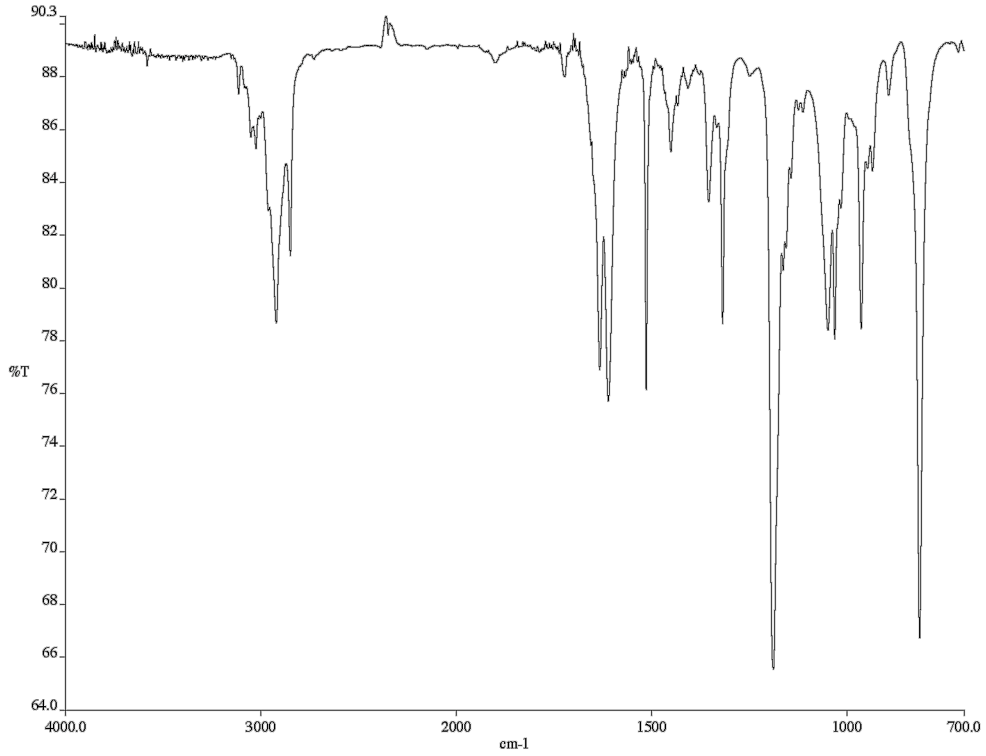

Figure A1.80 Infrared spectrum (thin film/NaCl) of compound **153**.

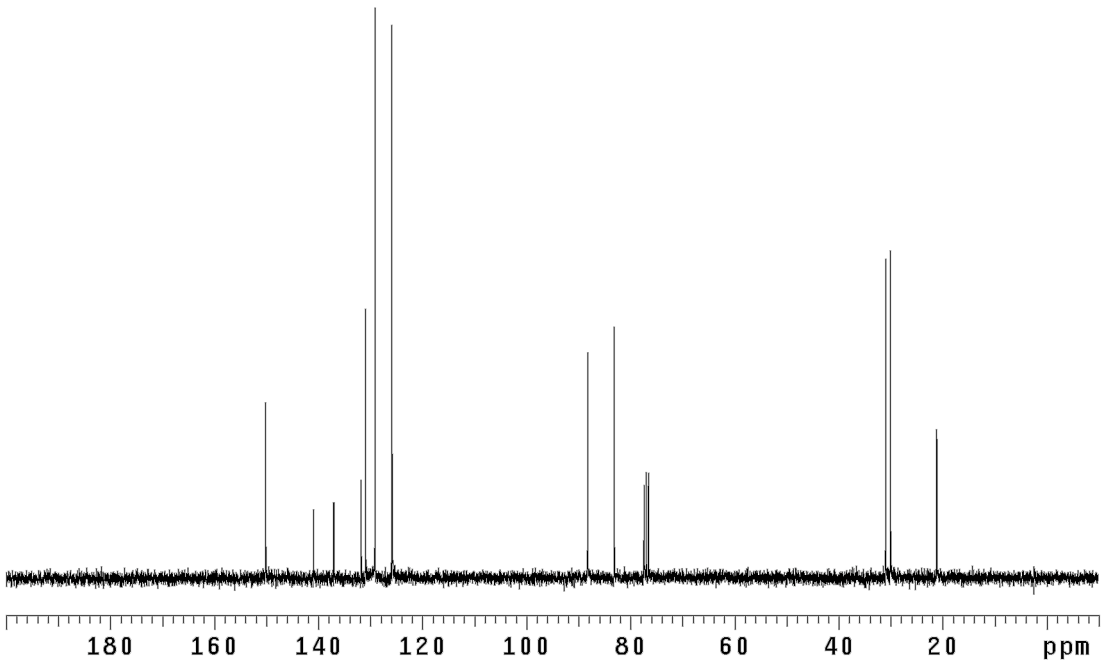

Figure A1.81 ^{13}C NMR (75 MHz, $CDCl_3$) of compound **153**.

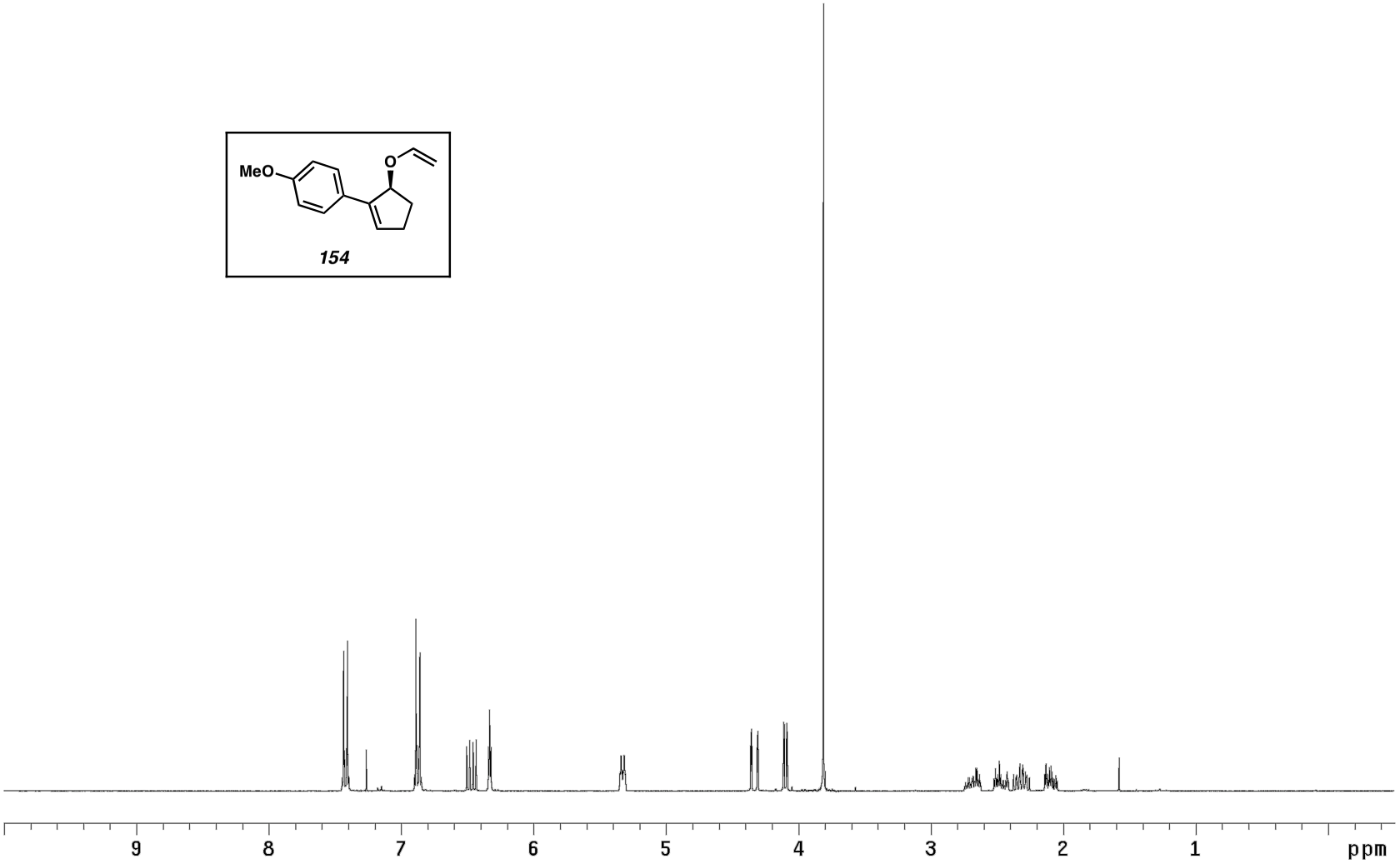

Figure A1.82 ^{1}H NMR (300 MHz, $CDCl_3$) of compound **154**.

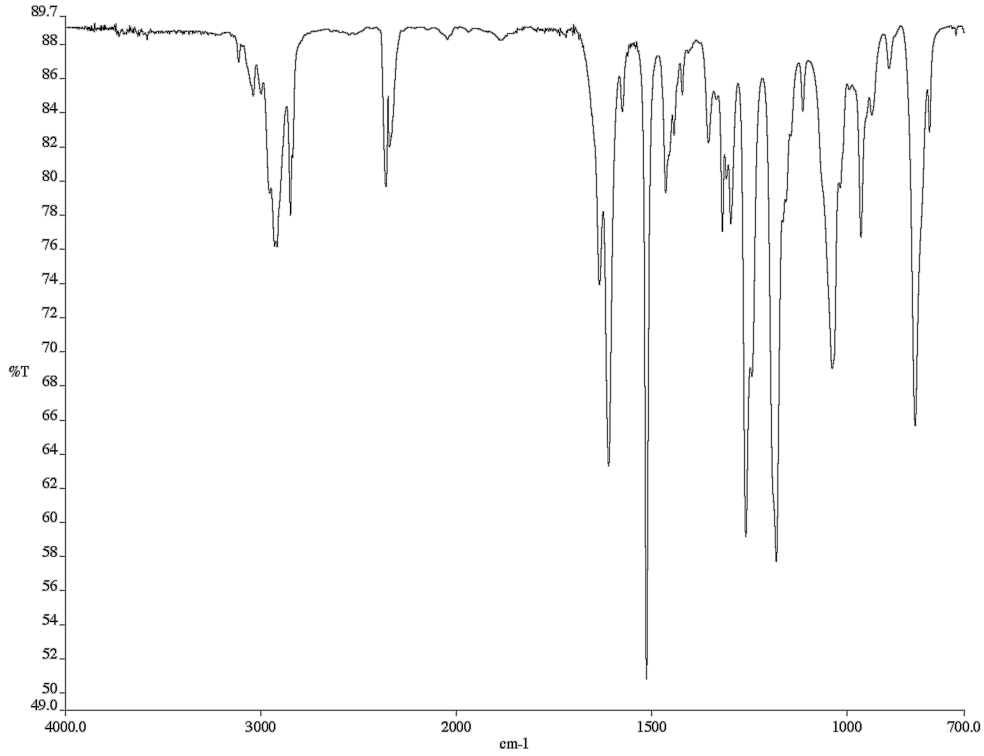

Figure A1.83 Infrared spectrum (thin film/NaCl) of compound **154**.

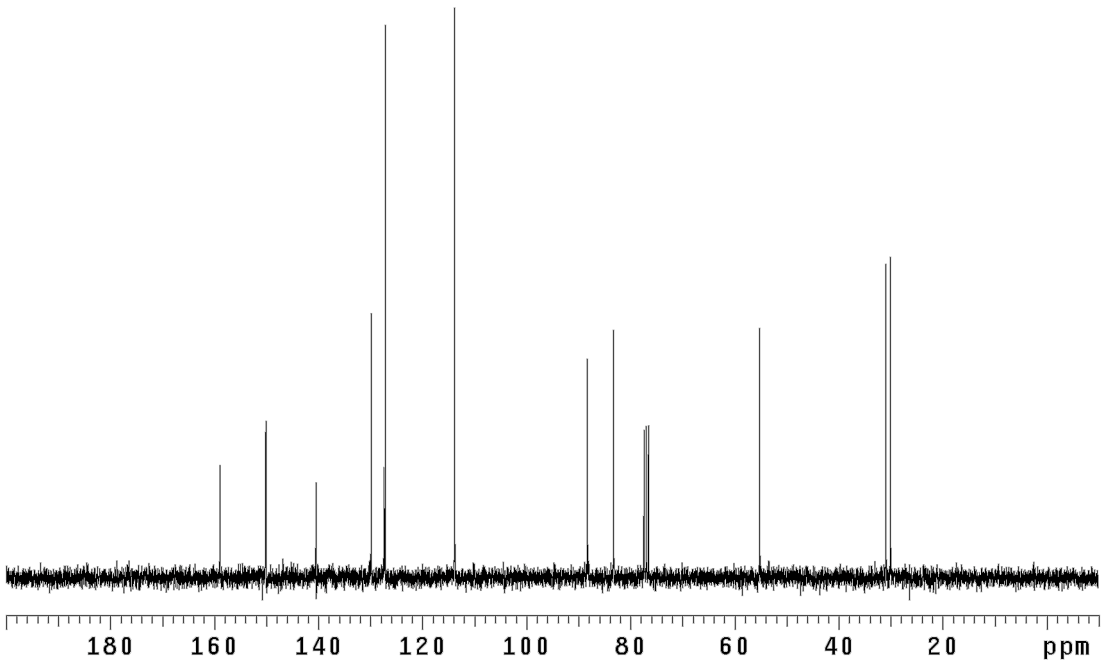

Figure A1.84 ^{13}C NMR (75 MHz, $CDCl_3$) of compound **154**.

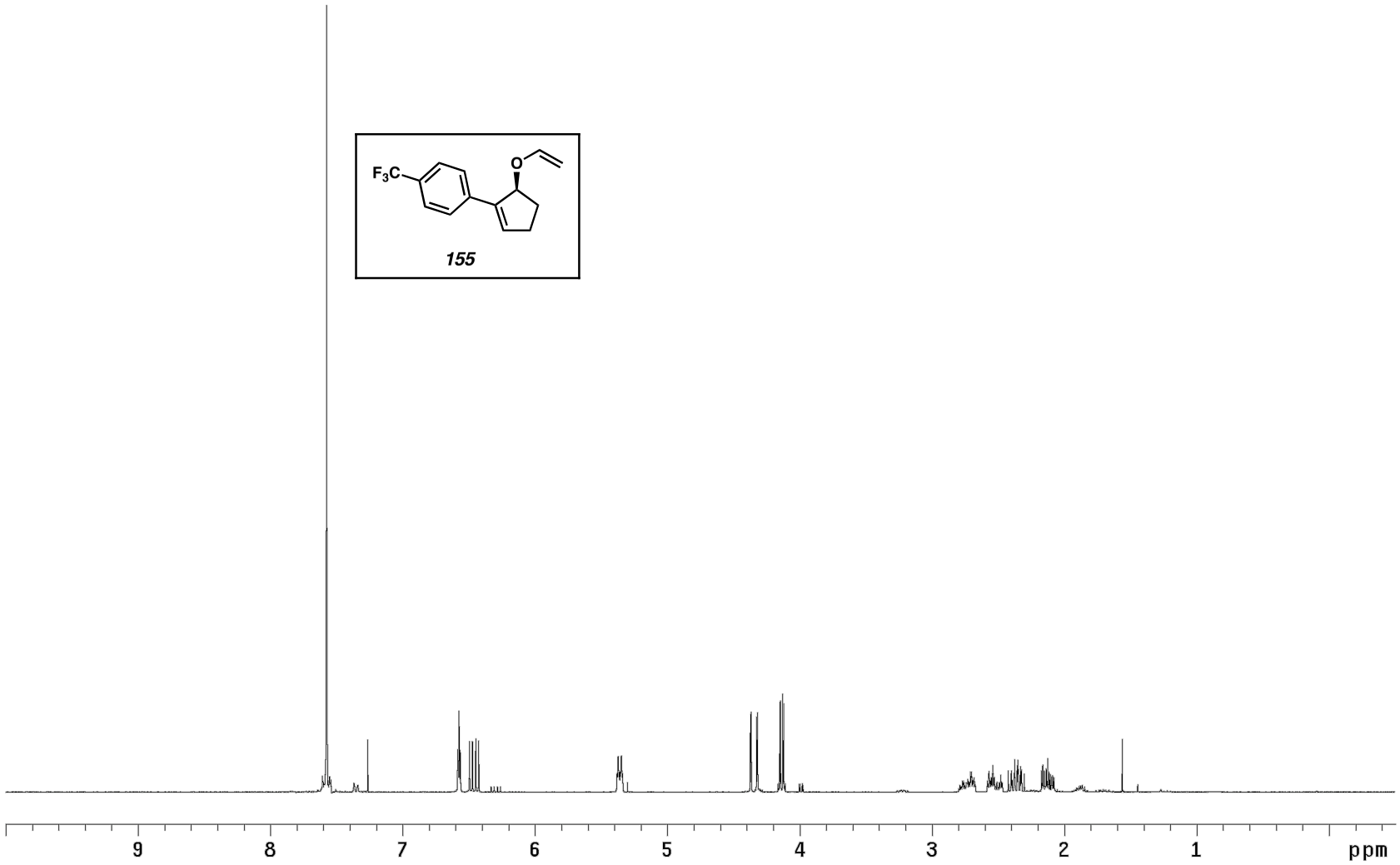

Figure A1.85 ^{1}H NMR (300 MHz, $CDCl_3$) of compound **155**.

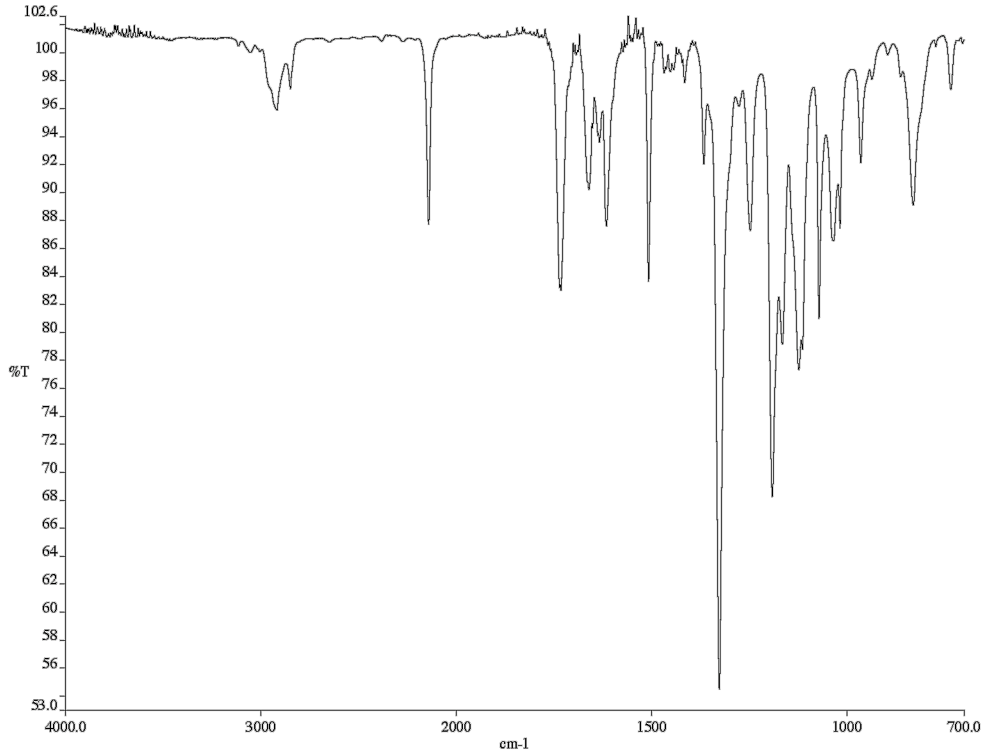

Figure A1.86 Infrared spectrum (thin film/NaCl) of compound **155**.

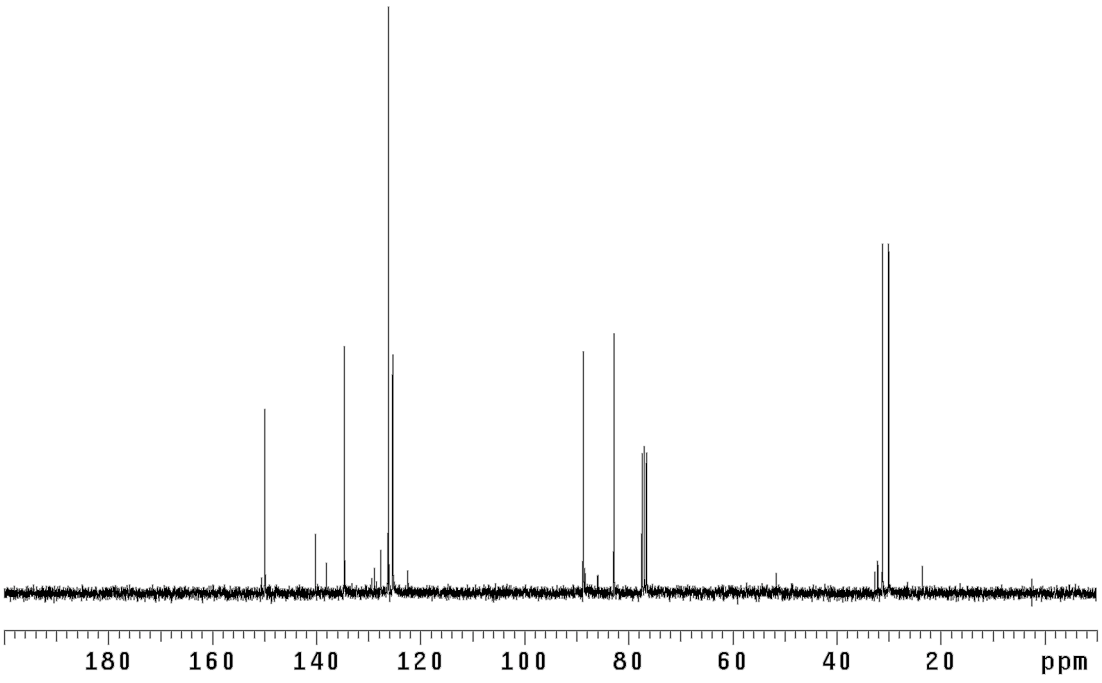

Figure A1.87 ^{13}C NMR (75 MHz, $CDCl_3$) of compound **155**.

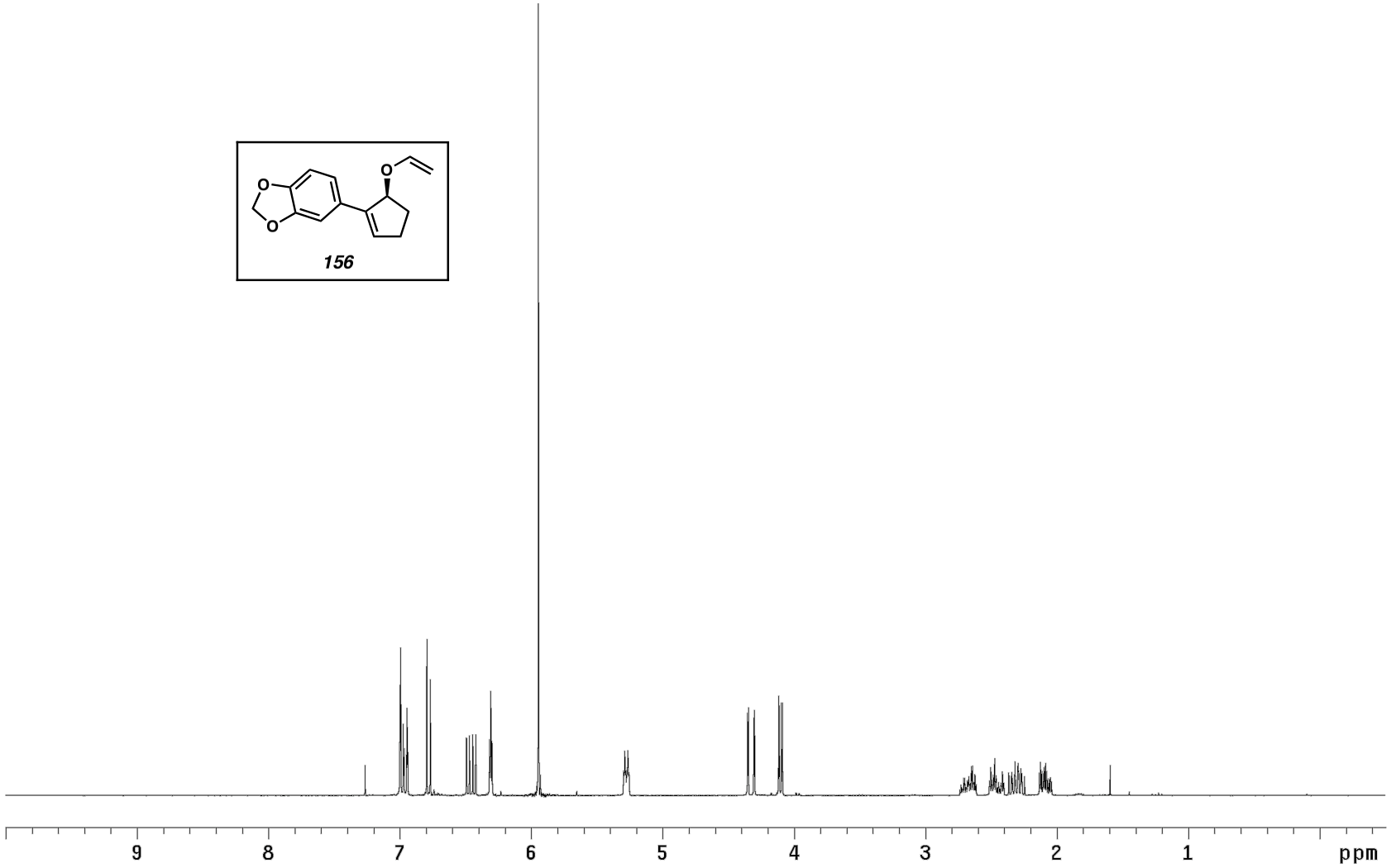

Figure A1.88 ^{1}H NMR (300 MHz, $CDCl_3$) of compound **156**.

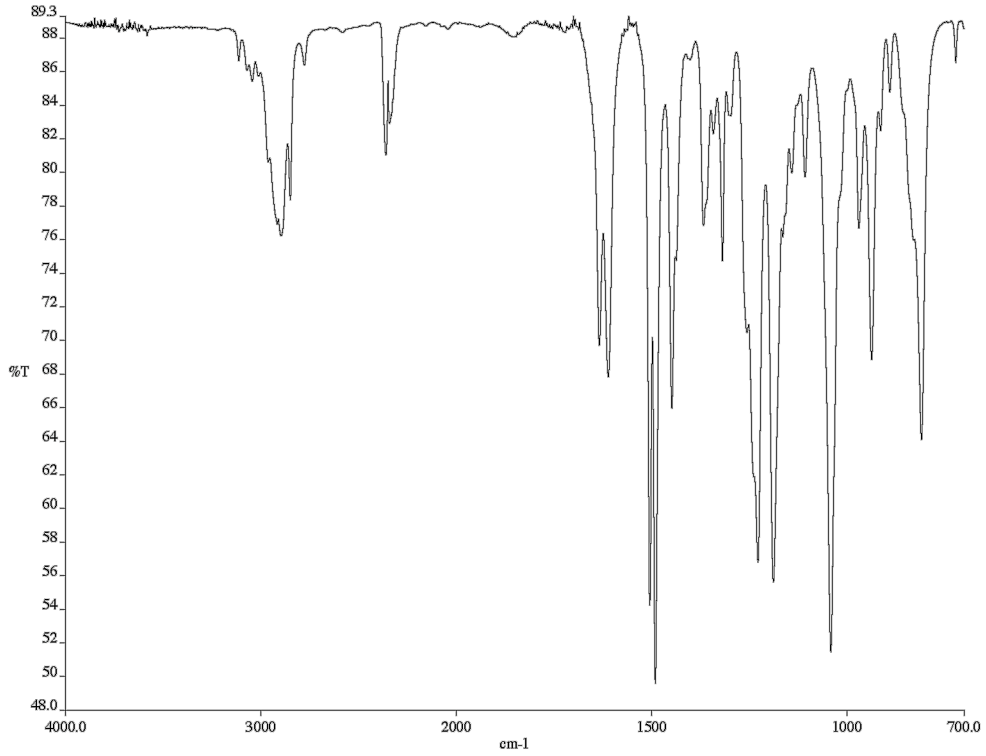

Figure A1.89 Infrared spectrum (thin film/NaCl) of compound **156**.

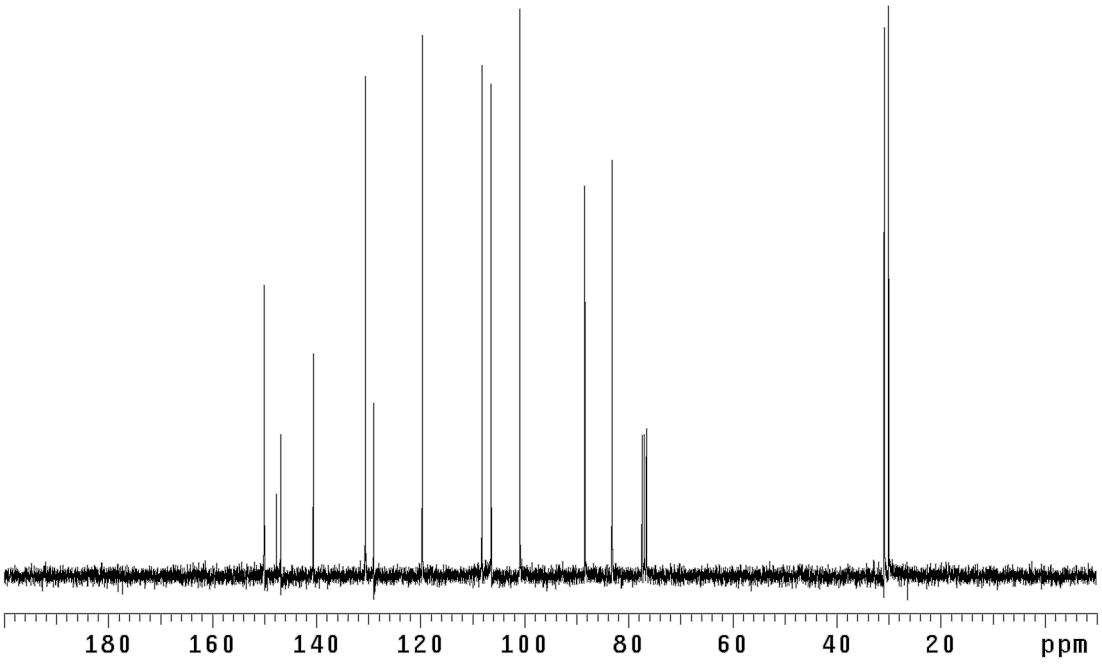

Figure A1.90 ^{13}C NMR (75 MHz, $CDCl_3$) of compound **156**.

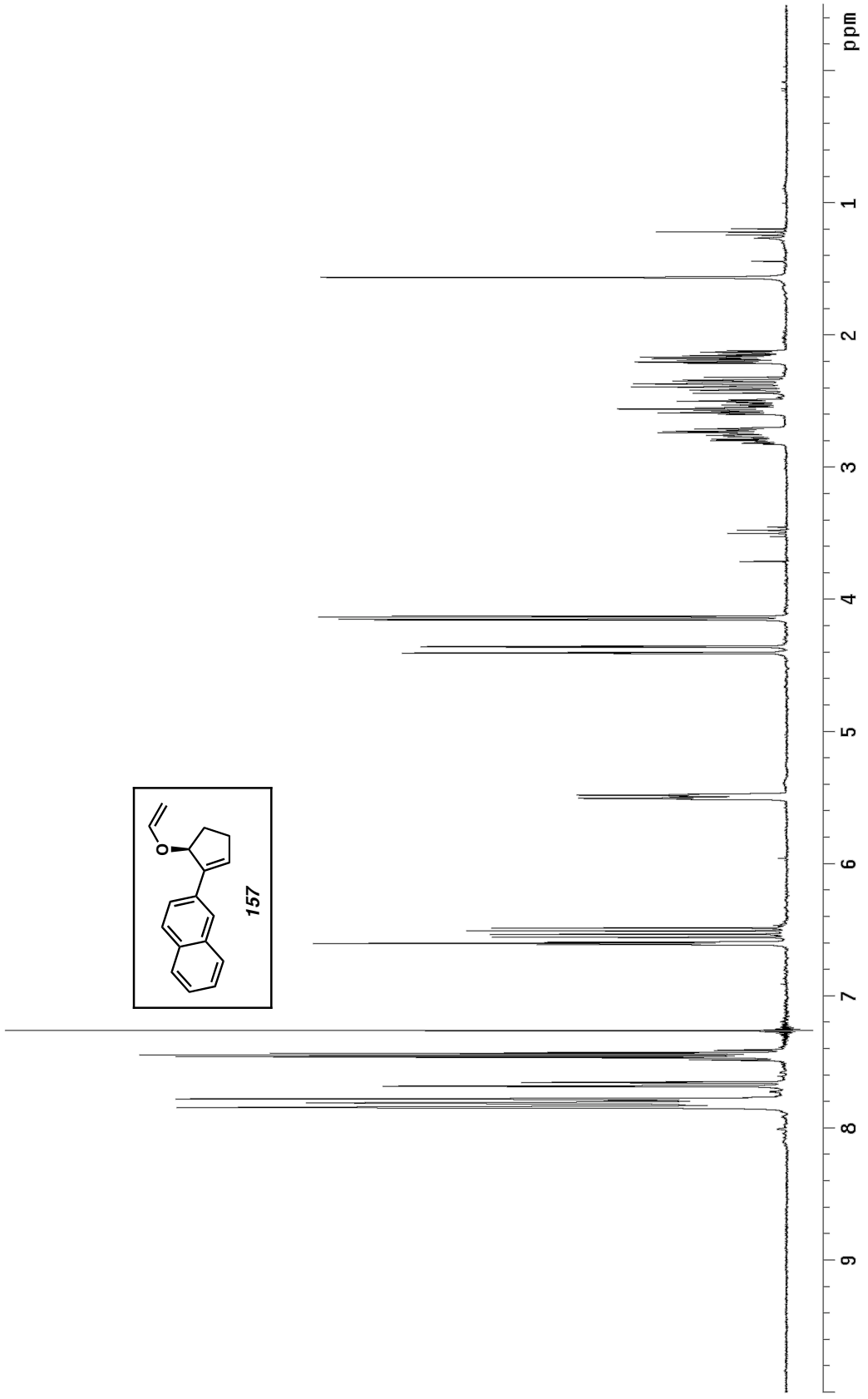

Figure A1.91 ^{1}H NMR (300 MHz, $CDCl_3$) of compound **157**.

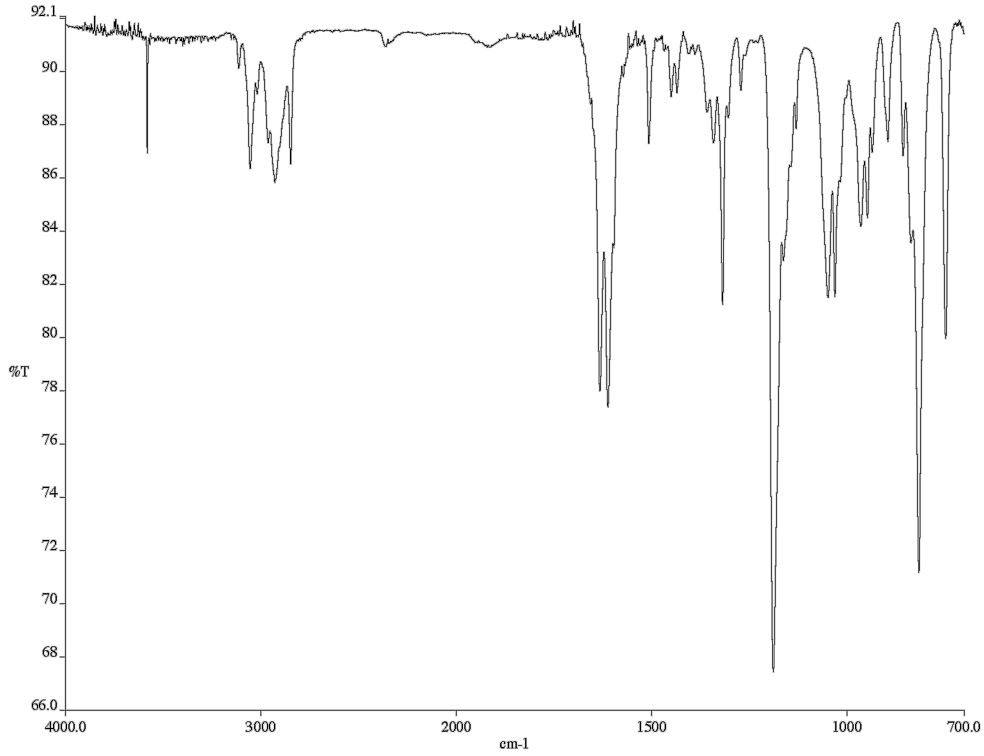

Figure A1.92 Infrared spectrum (thin film/NaCl) of compound **157**.

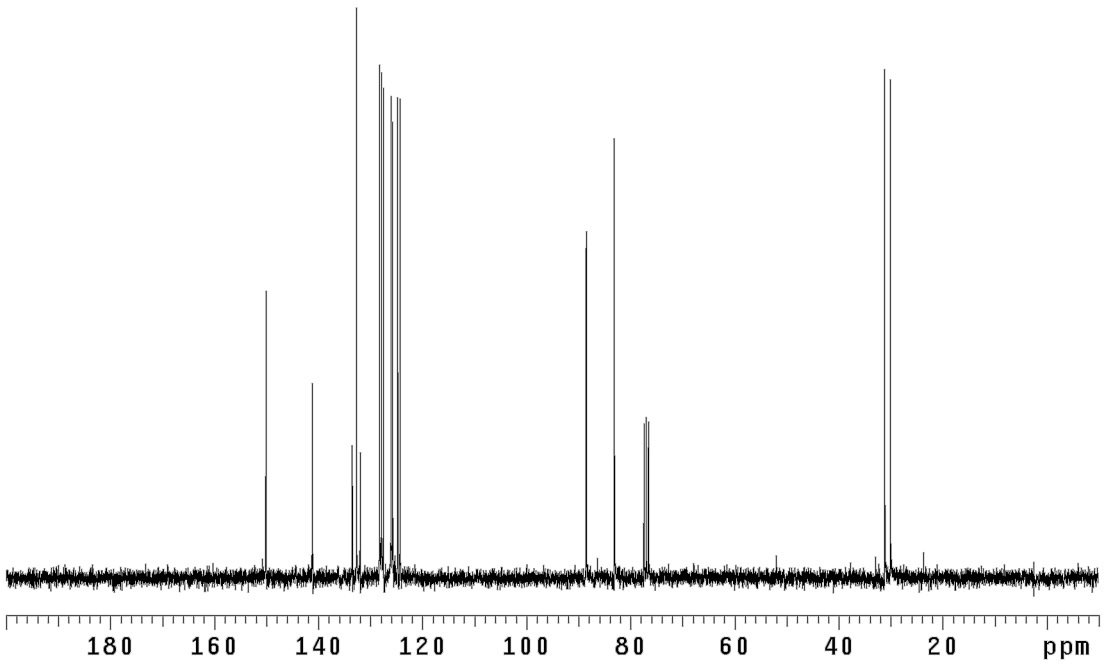

Figure A1.93 ^{13}C NMR (75 MHz, $CDCl_3$) of compound **157**.

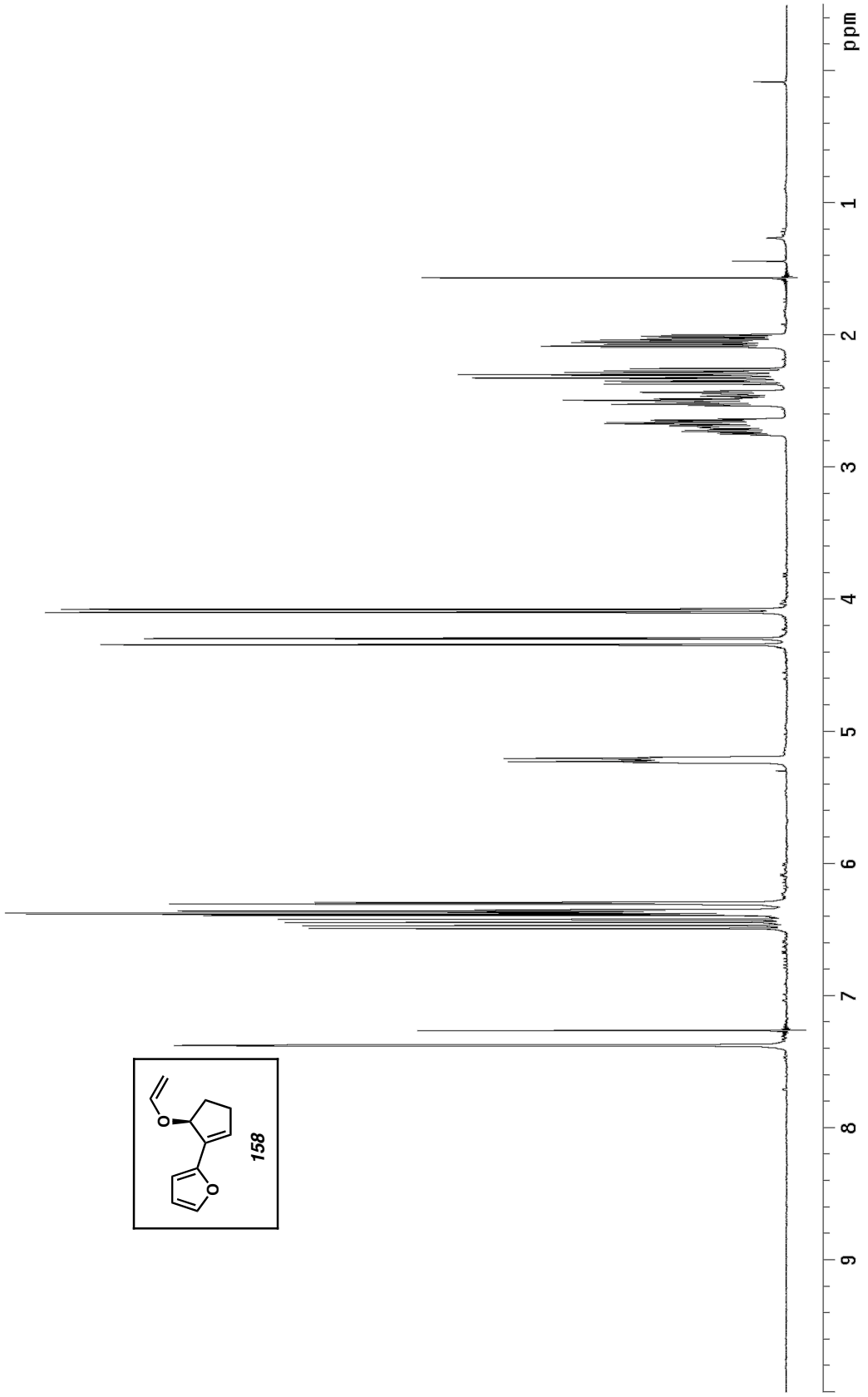

Figure A1.94 ^{1}H NMR (300 MHz, $CDCl_3$) of compound **158**.

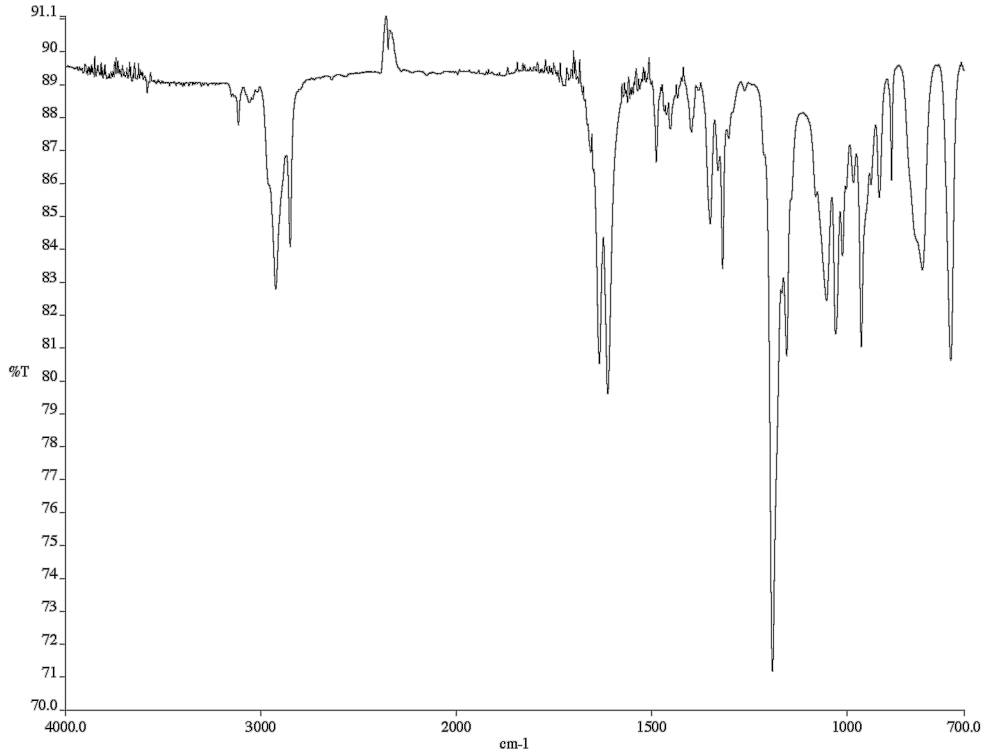

Figure A1.95 Infrared spectrum (thin film/NaCl) of compound **158**.

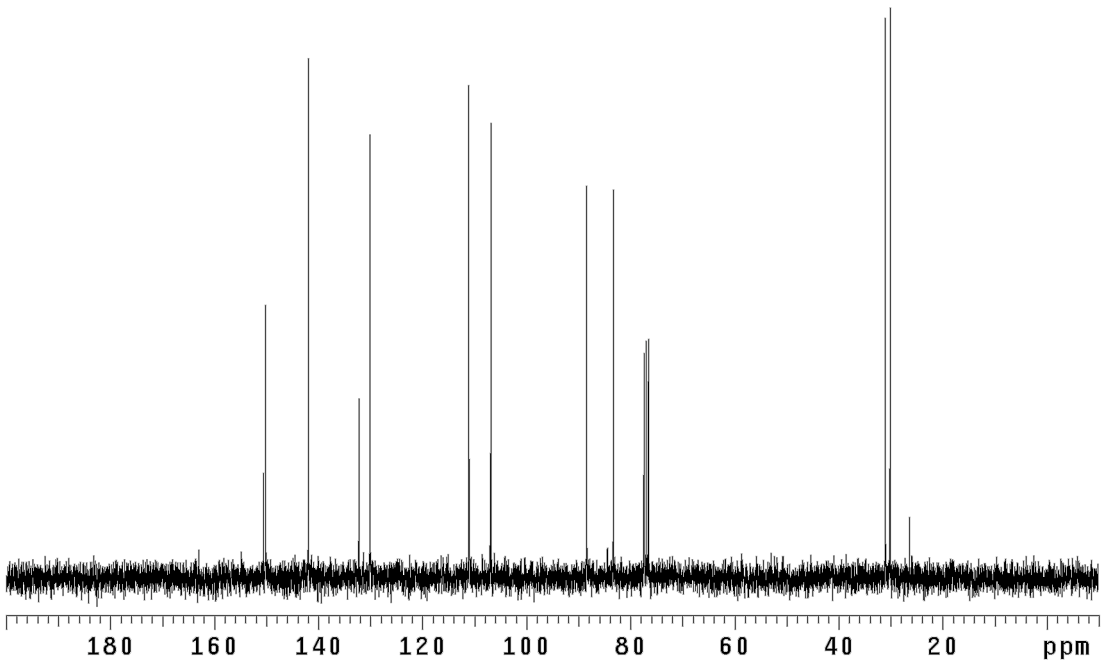

Figure A1.96 ^{13}C NMR (75 MHz, $CDCl_3$) of compound **158**.

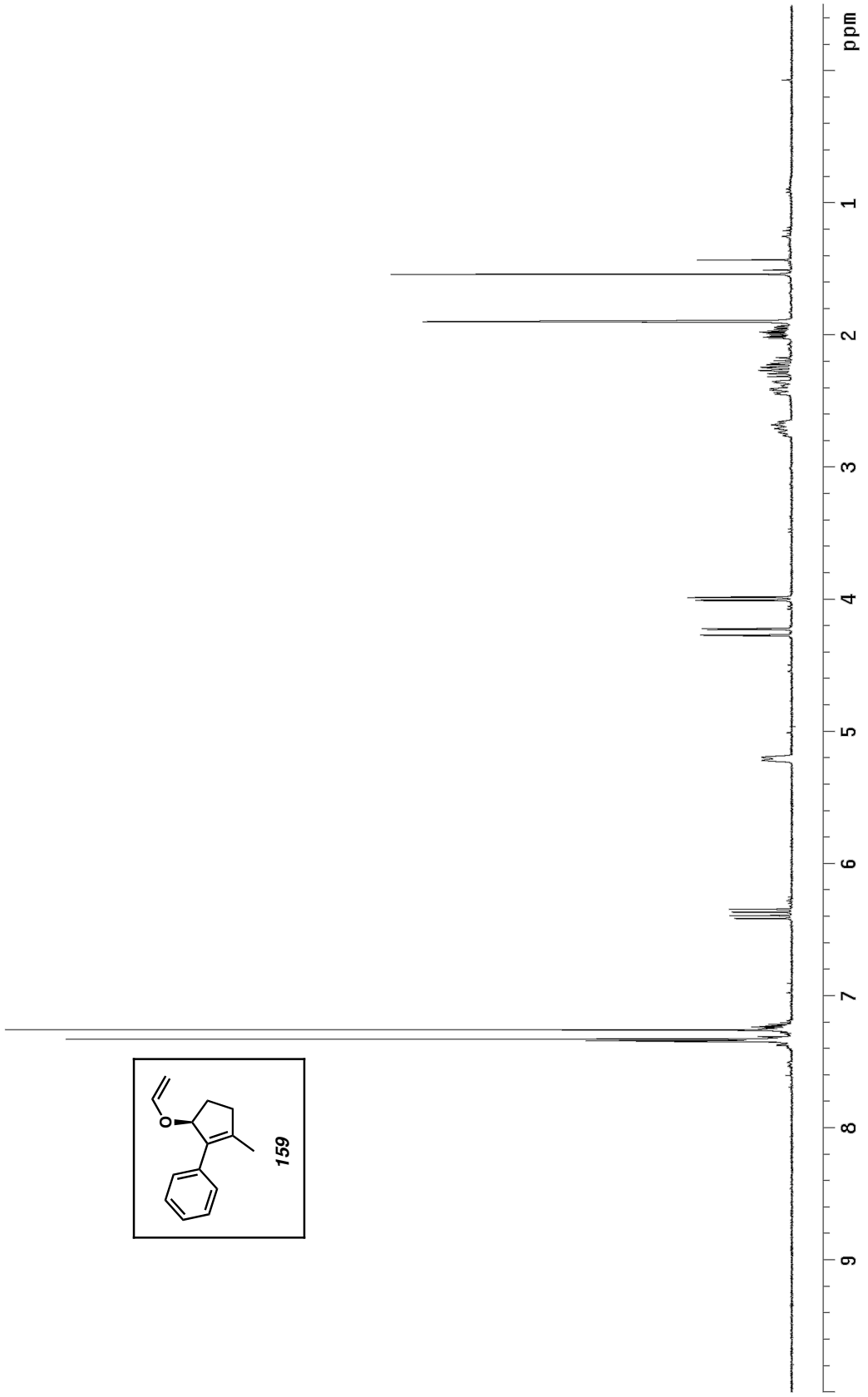

Figure A1.97 ^{1}H NMR (300 MHz, $CDCl_3$) of compound **159**.

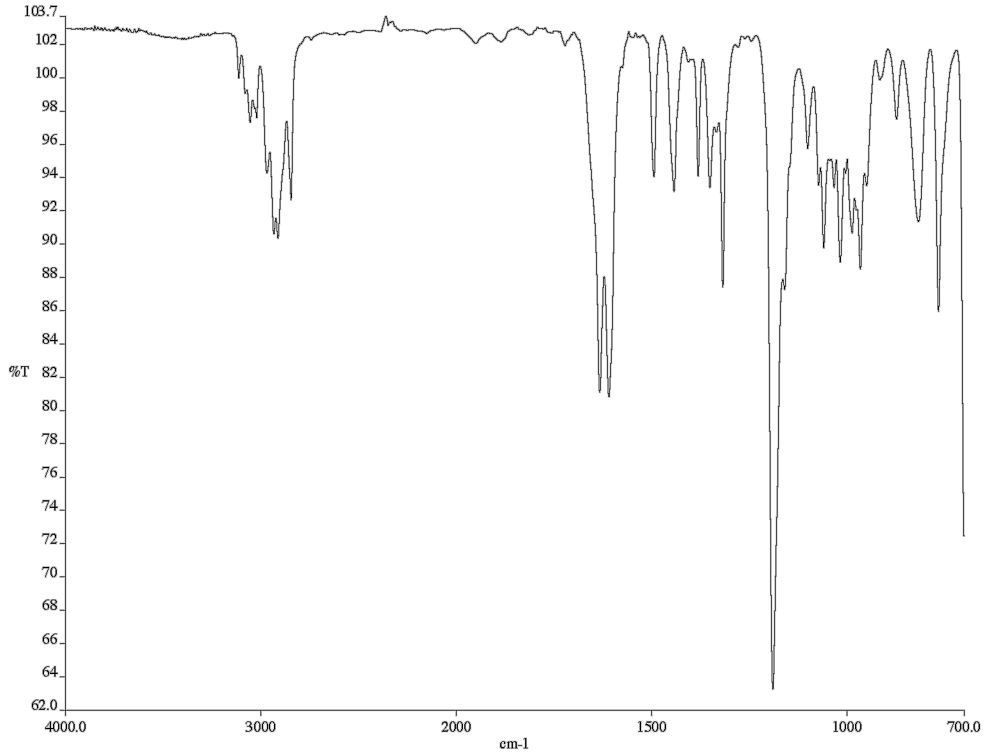

Figure A1.98 Infrared spectrum (thin film/NaCl) of compound **159**.

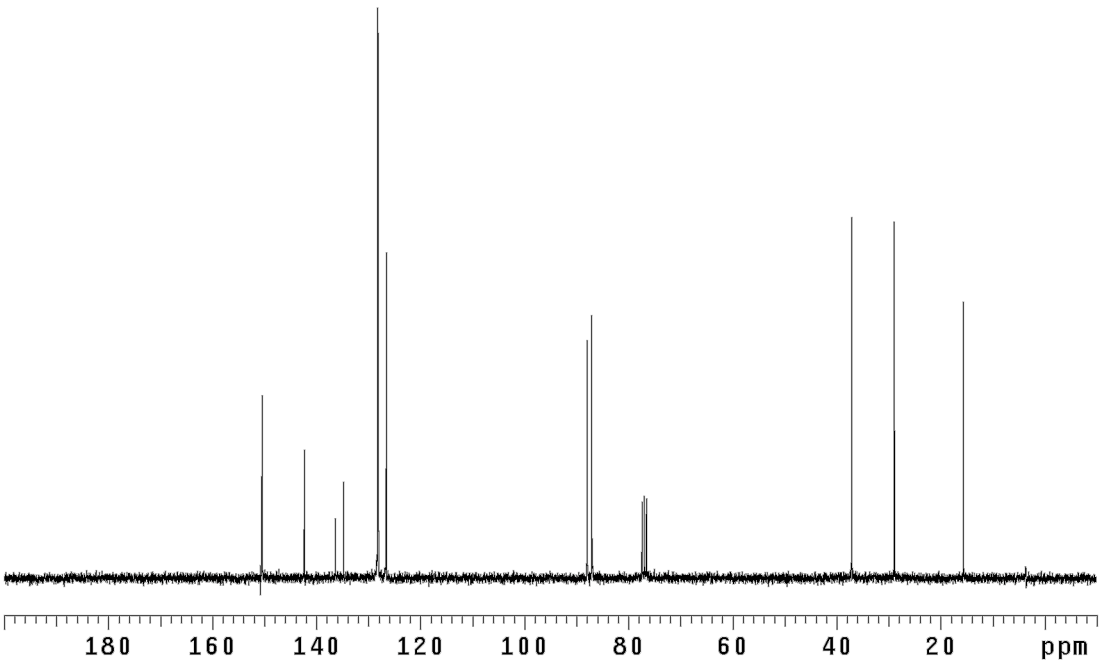

Figure A1.99 ^{13}C NMR (75 MHz, $CDCl_3$) of compound **159**.

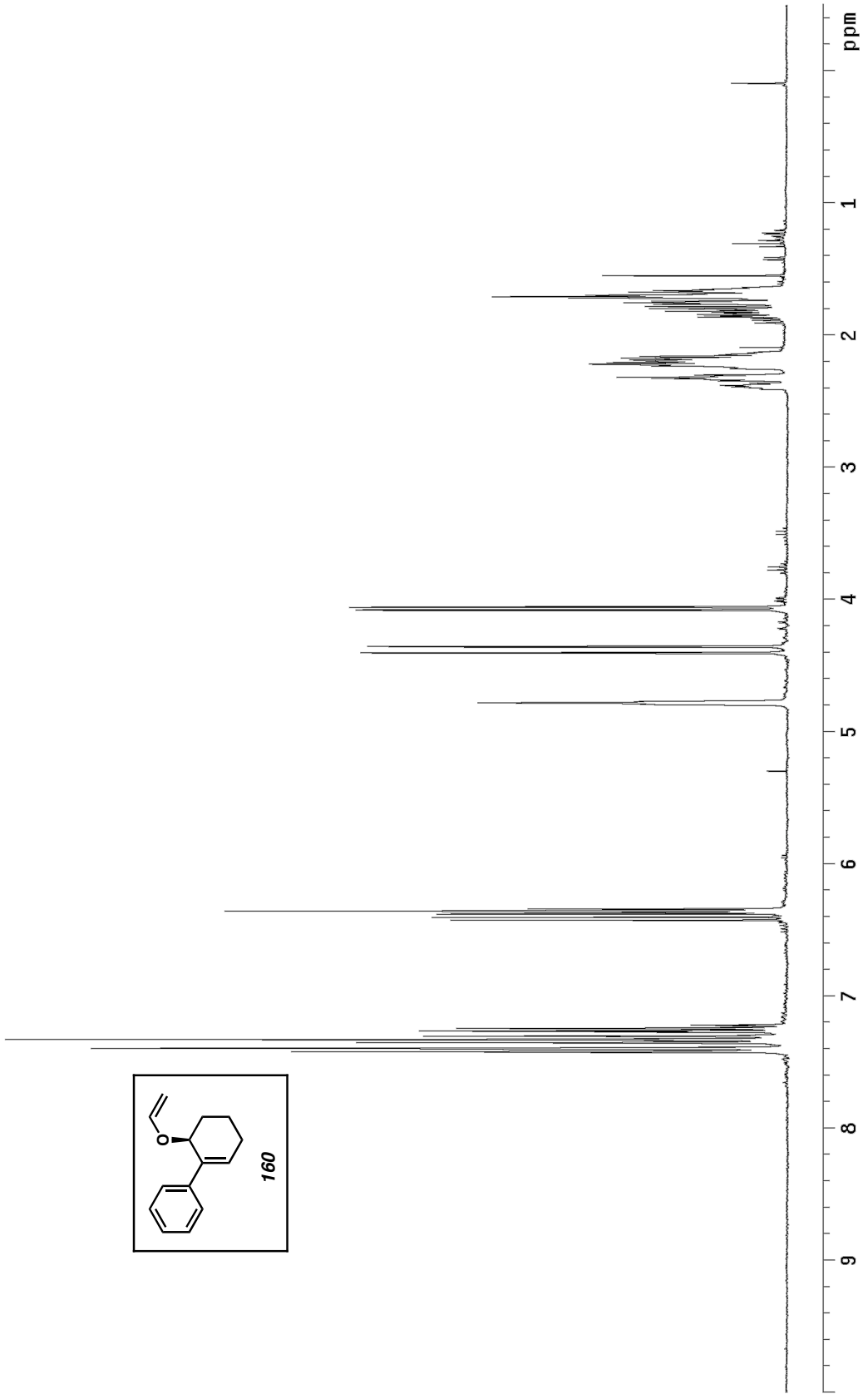

Figure A1.100 ^{1}H NMR (300 MHz, $CDCl_3$) of compound **160**.

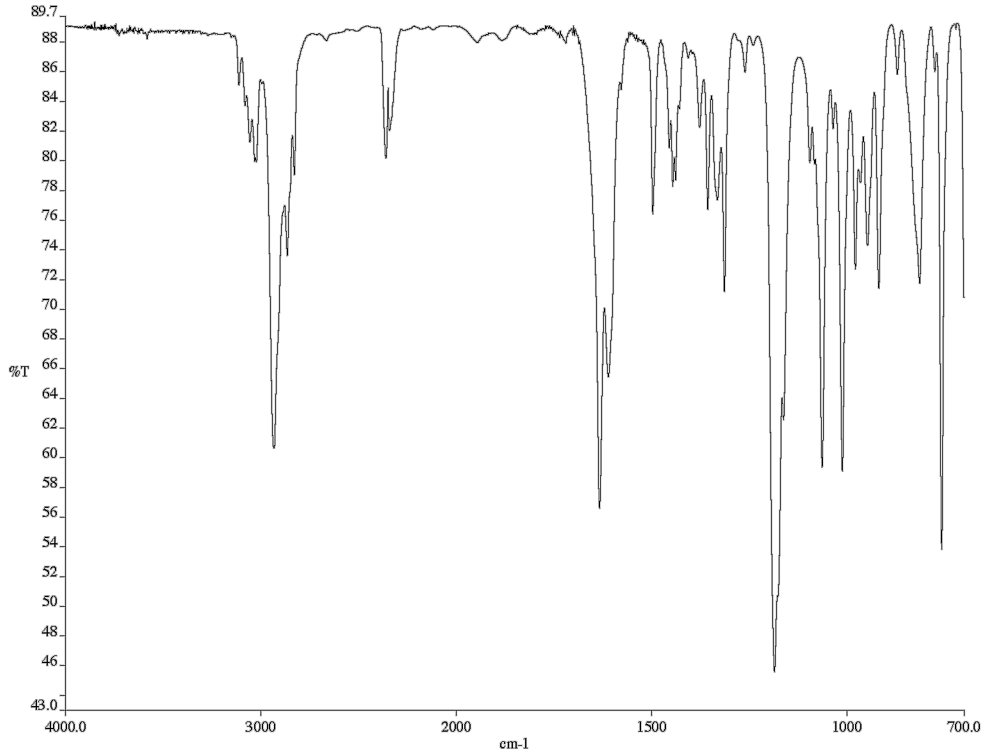

Figure A1.101 Infrared spectrum (thin film/NaCl) of compound **160**.

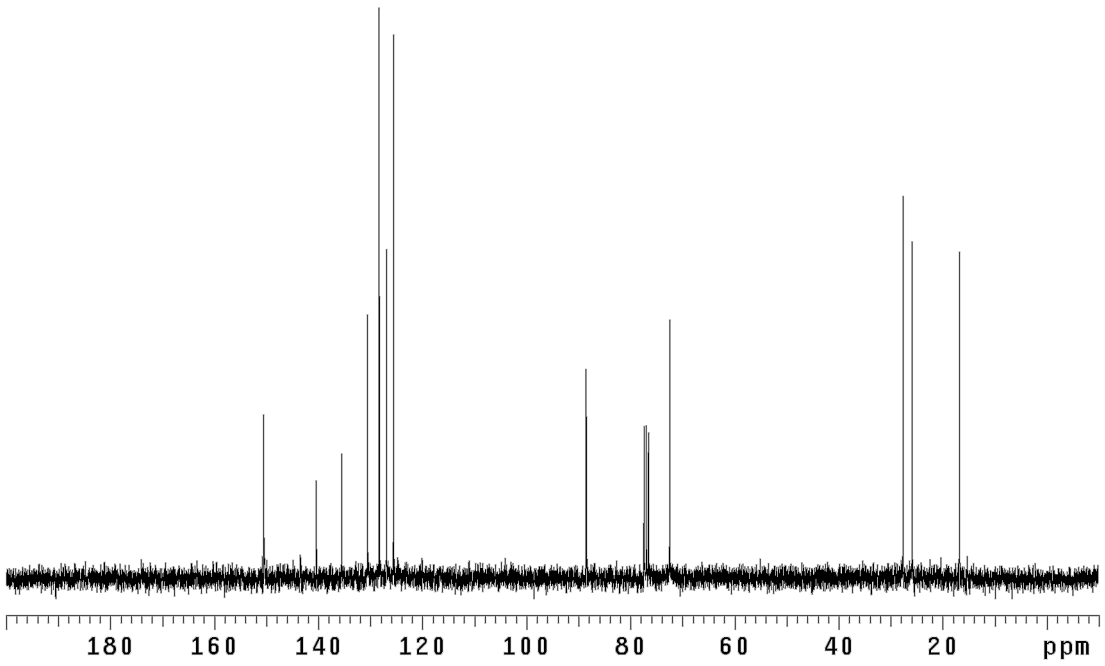

Figure A1.102 ^{13}C NMR (75 MHz, $CDCl_3$) of compound **160**.

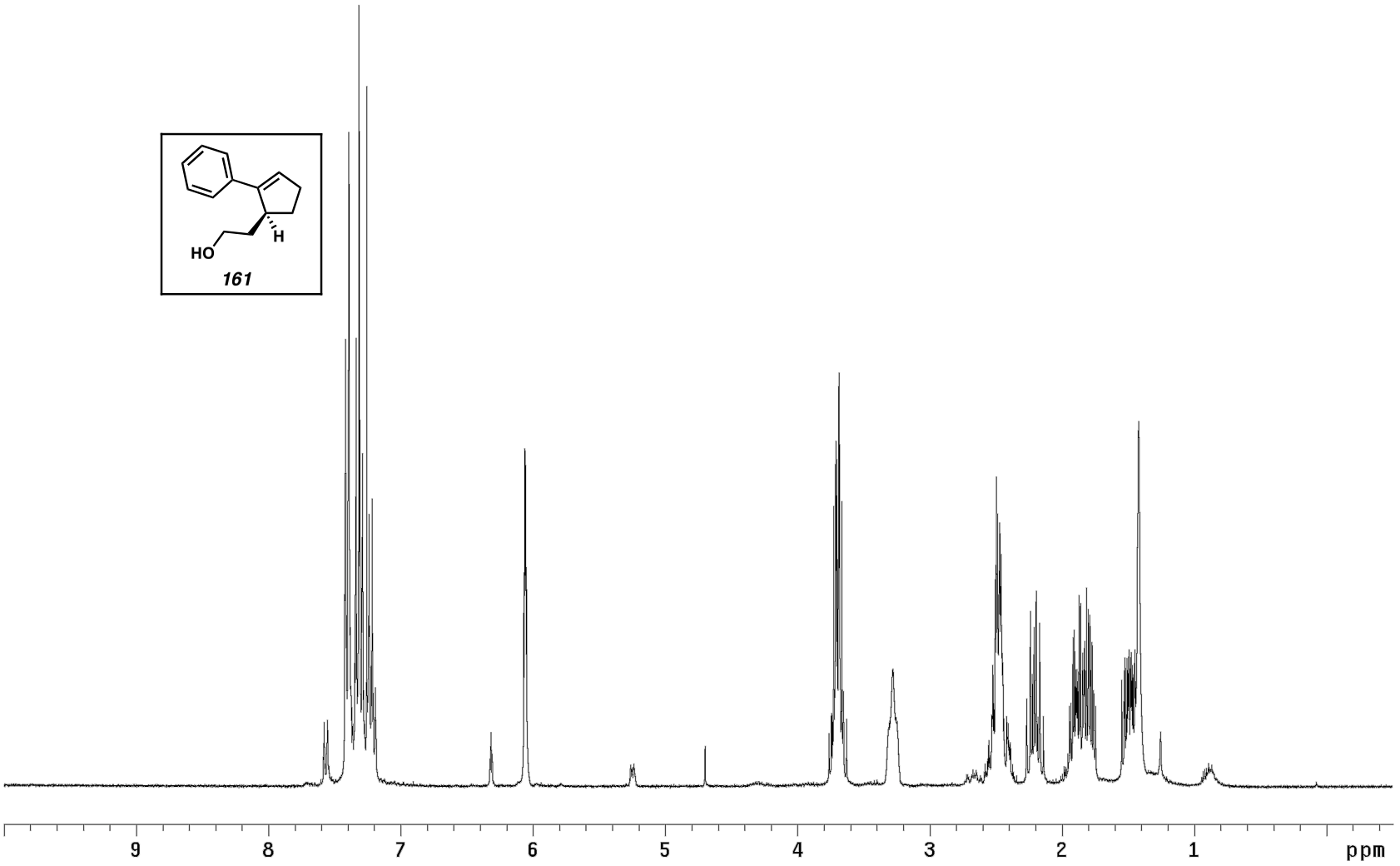

Figure A1.103 ^{1}H NMR (300 MHz, $CDCl_3$) of compound **161**.

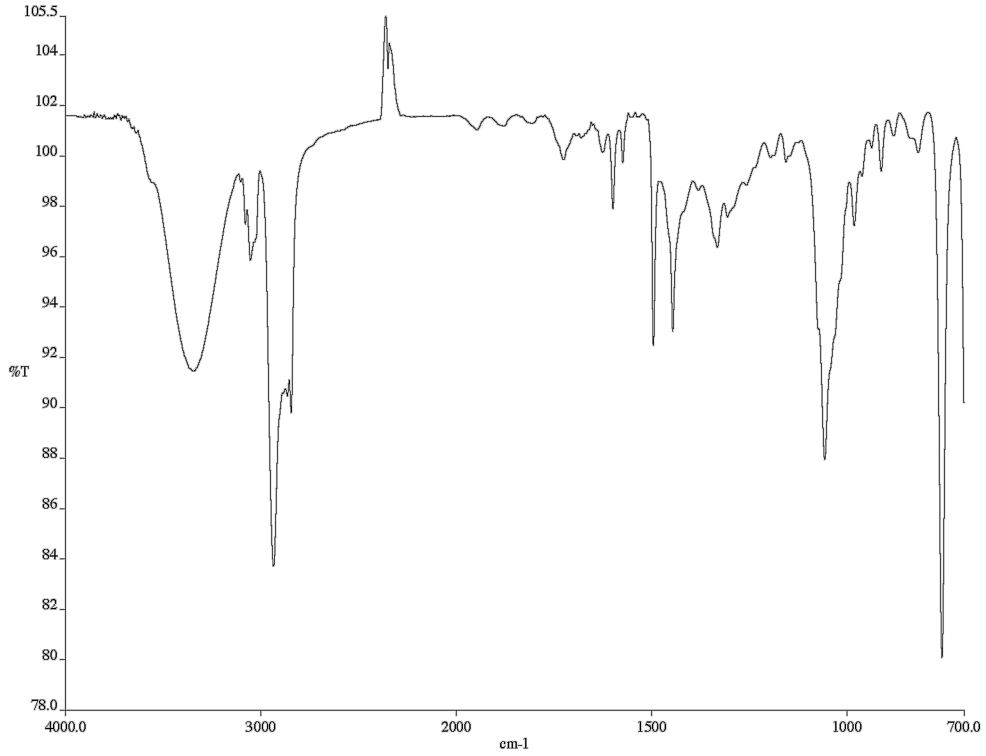

Figure A1.104 Infrared spectrum (thin film/NaCl) of compound **161**.

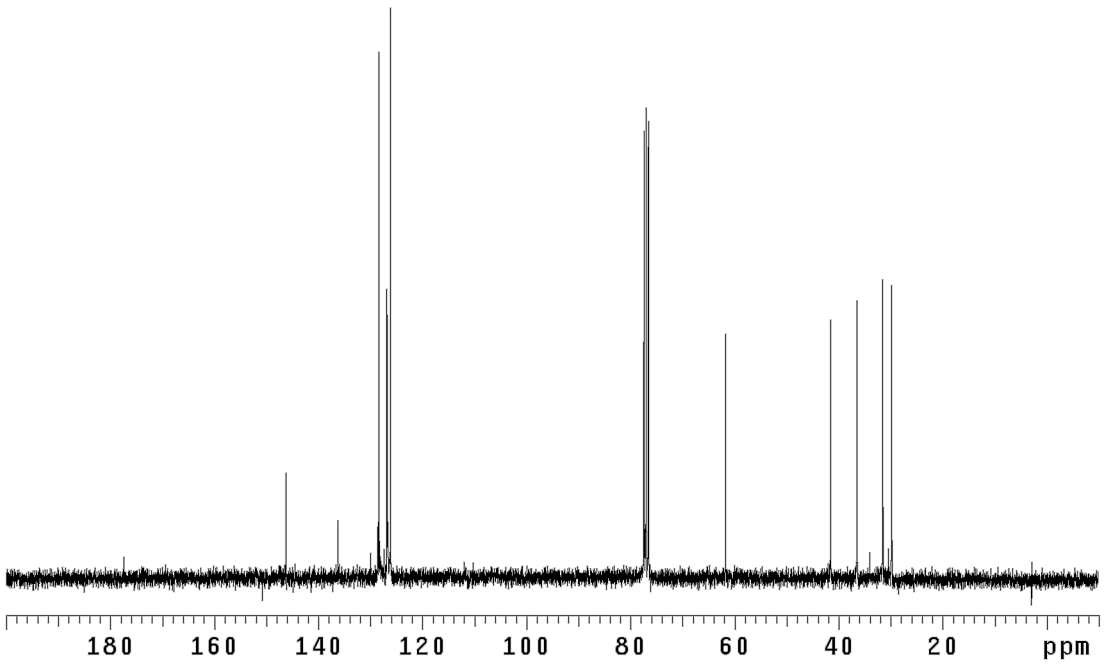

Figure A1.105 ^{13}C NMR (75 MHz, $CDCl_3$) of compound **161**.

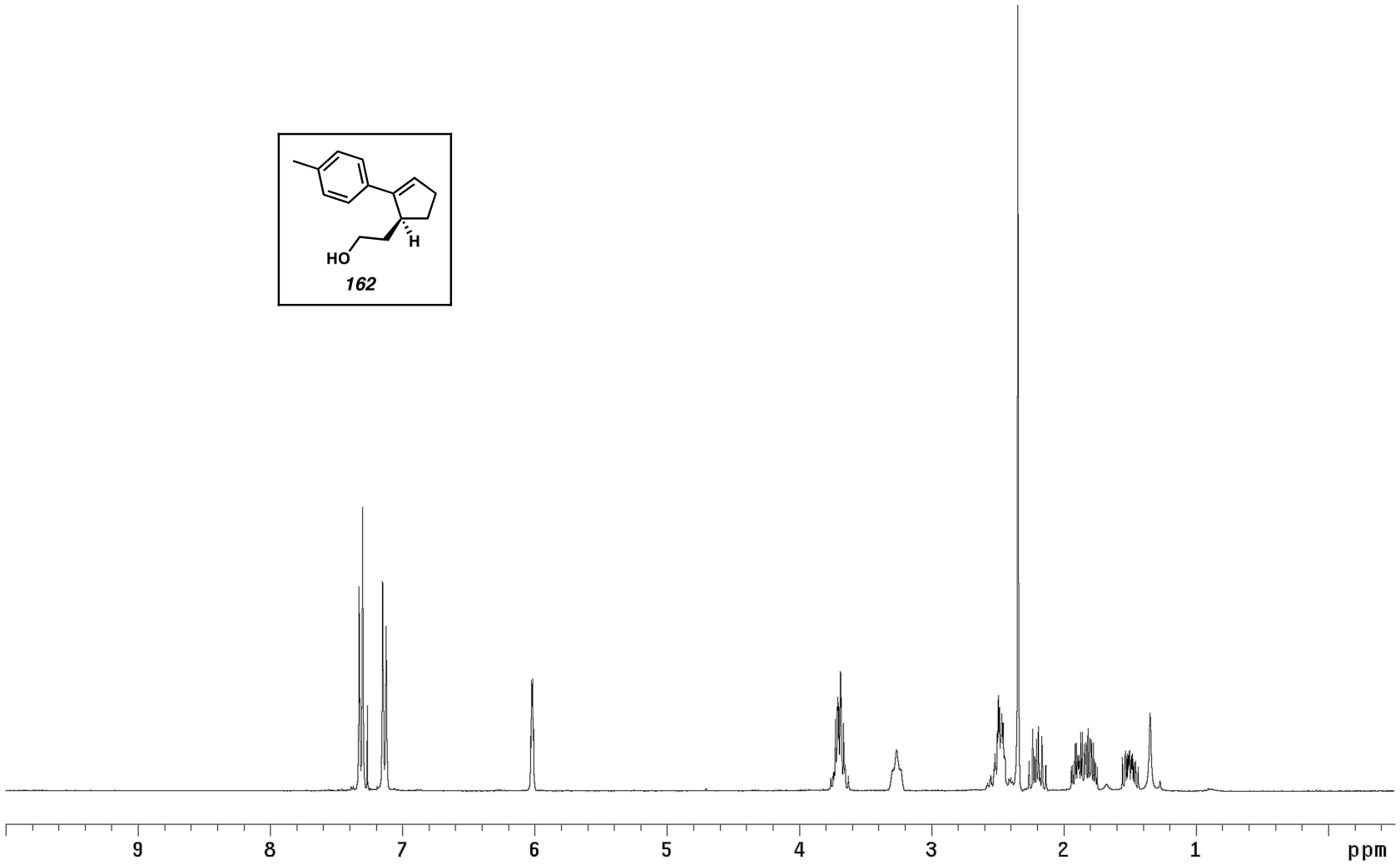

Figure A1.106 ^{1}H NMR (300 MHz, $CDCl_3$) of compound **162**.

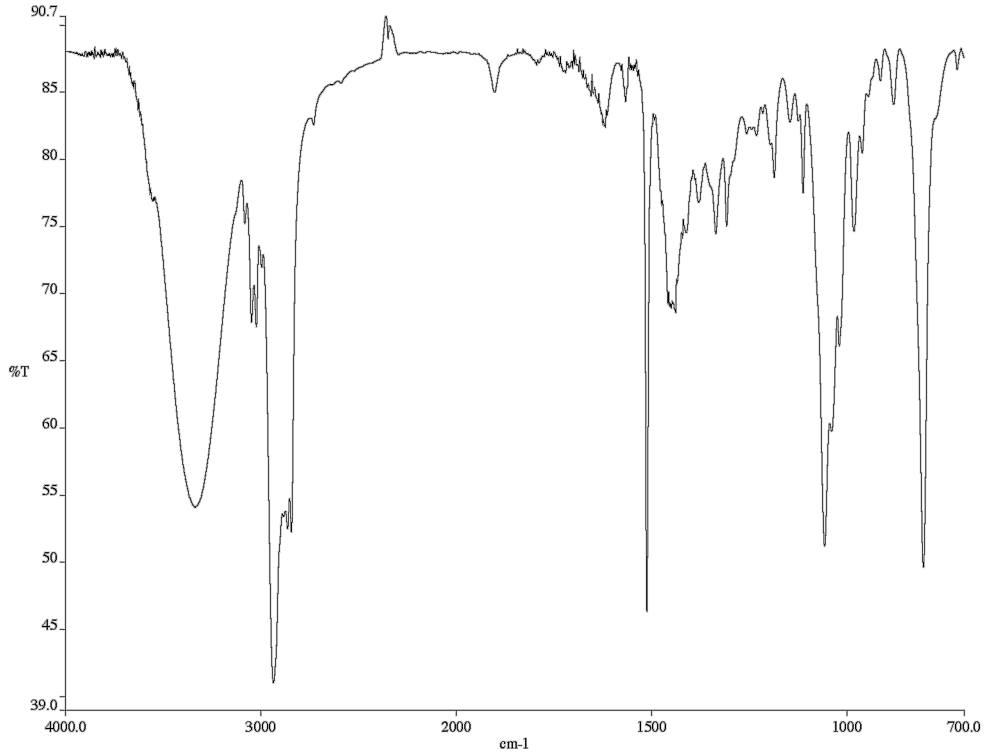

Figure A1.107 Infrared spectrum (thin film/NaCl) of compound **162**.

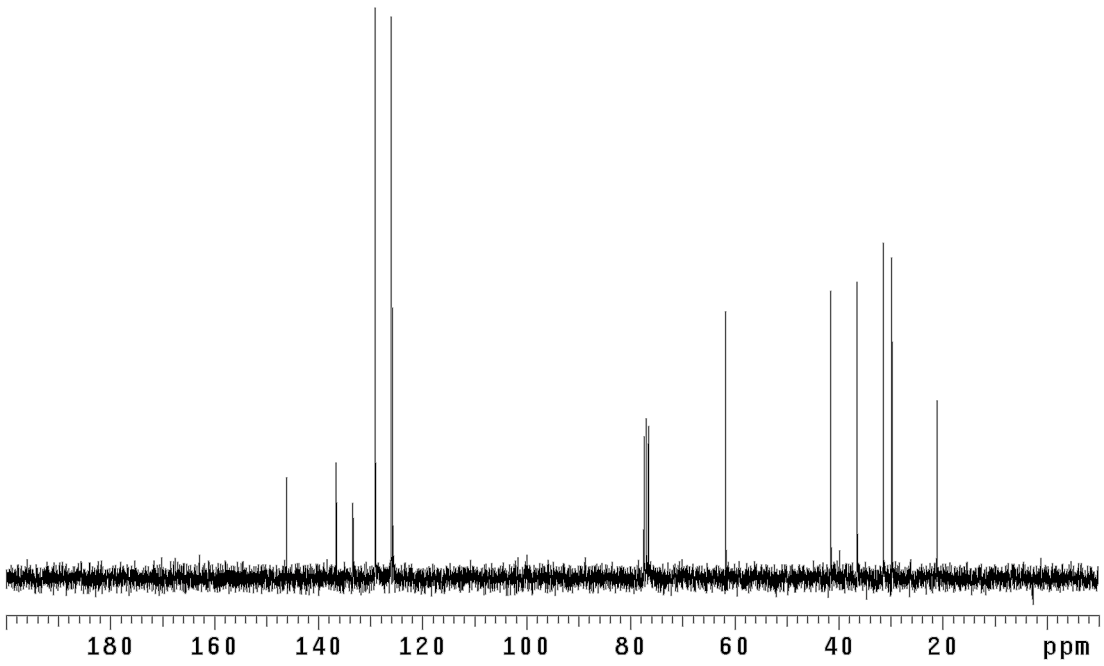

Figure A1.108 ^{13}C NMR (75 MHz, $CDCl_3$) of compound **162**.

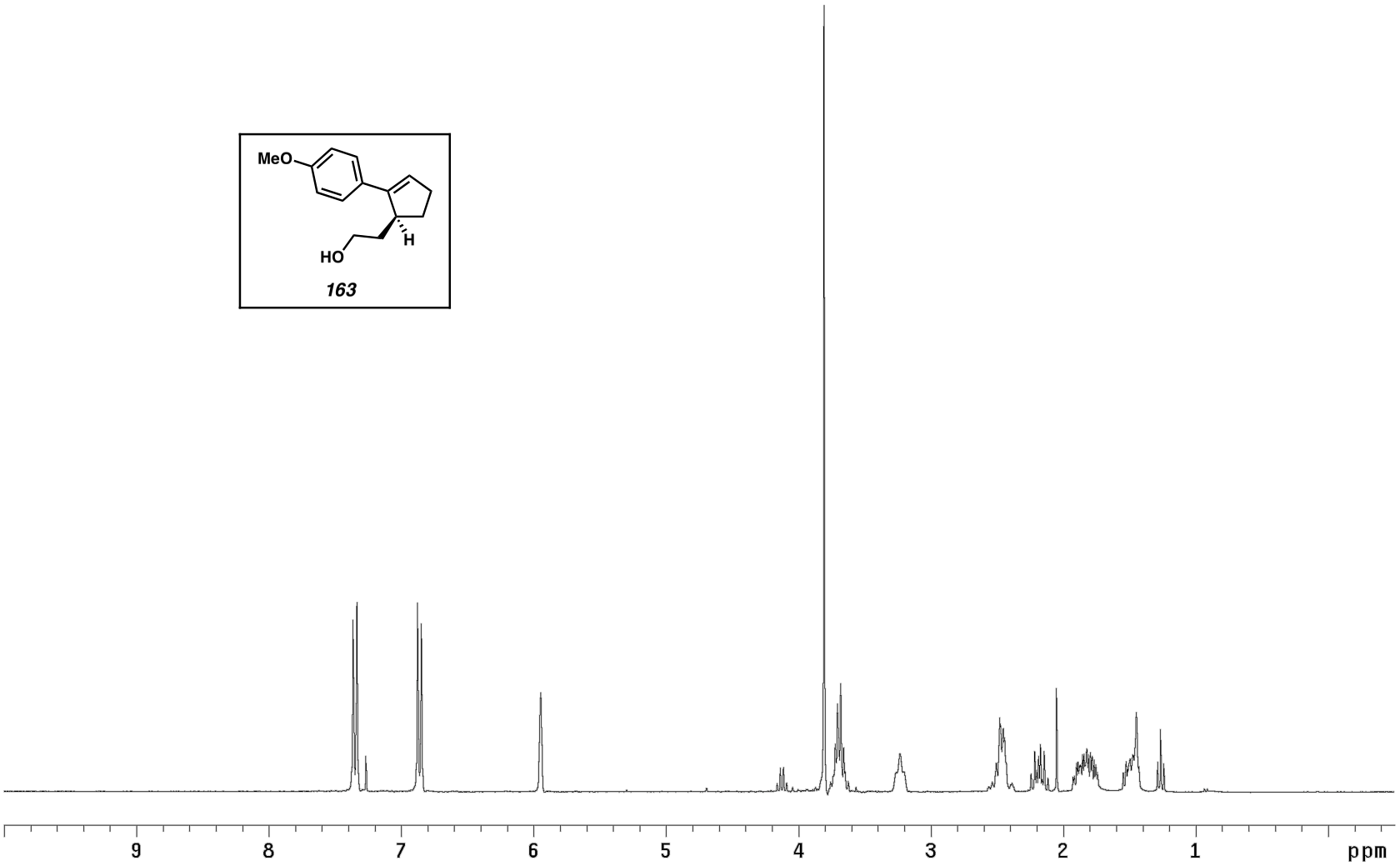

Figure A1.109 ^{1}H NMR (300 MHz, $CDCl_3$) of compound **163**.

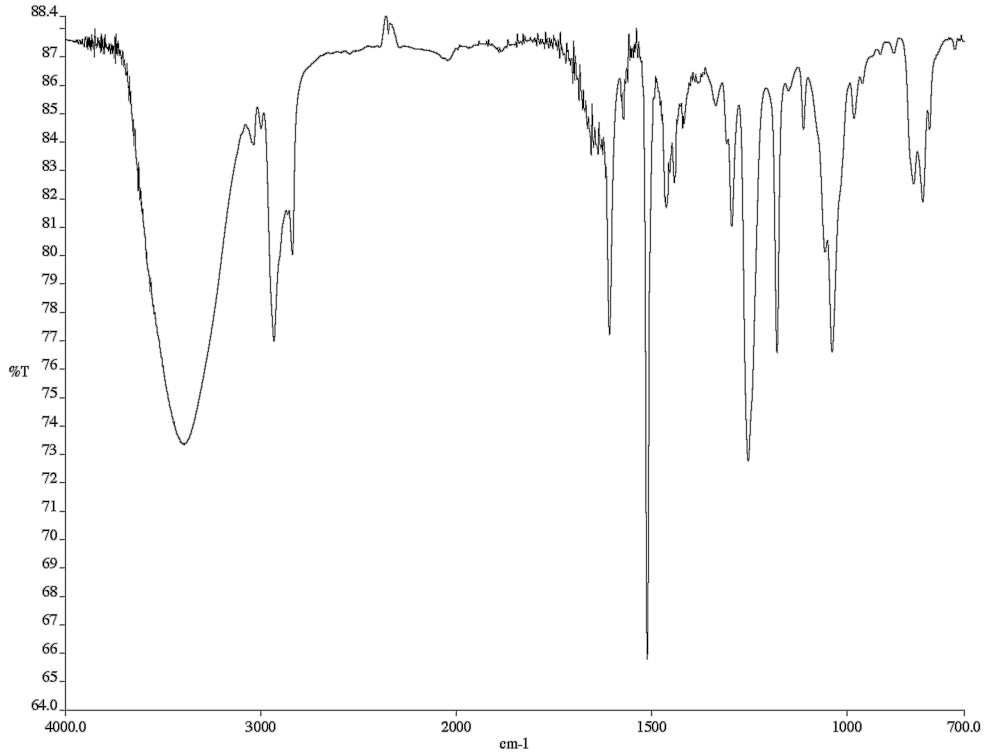

Figure A1.110 Infrared spectrum (thin film/NaCl) of compound **163**.

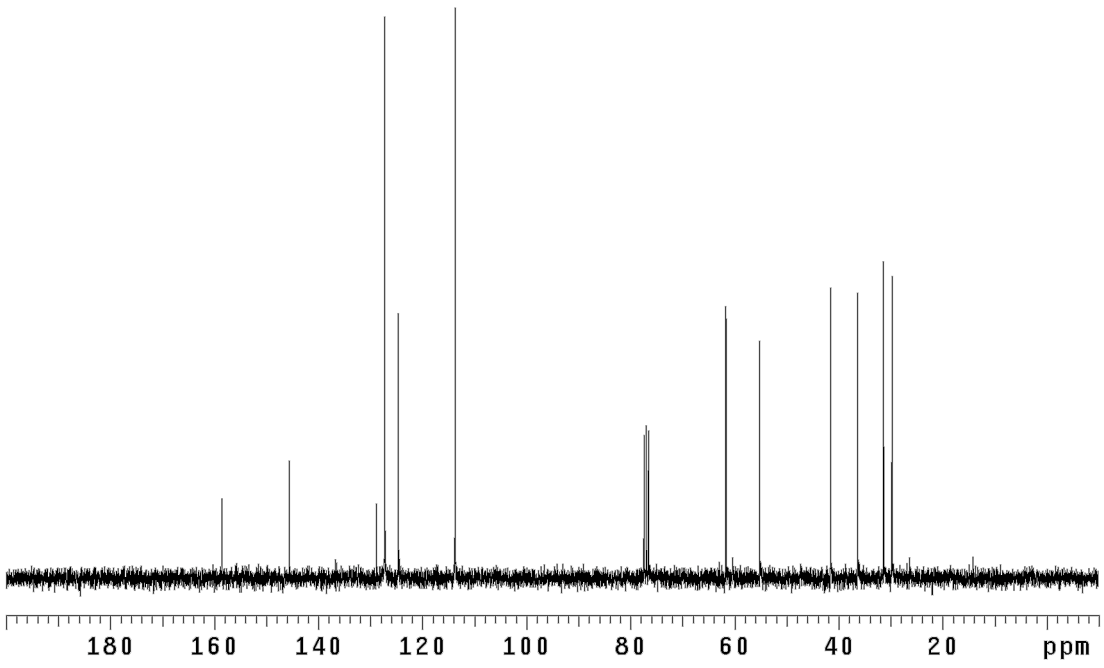

Figure A1.111 ^{13}C NMR (75 MHz, $CDCl_3$) of compound **163**.

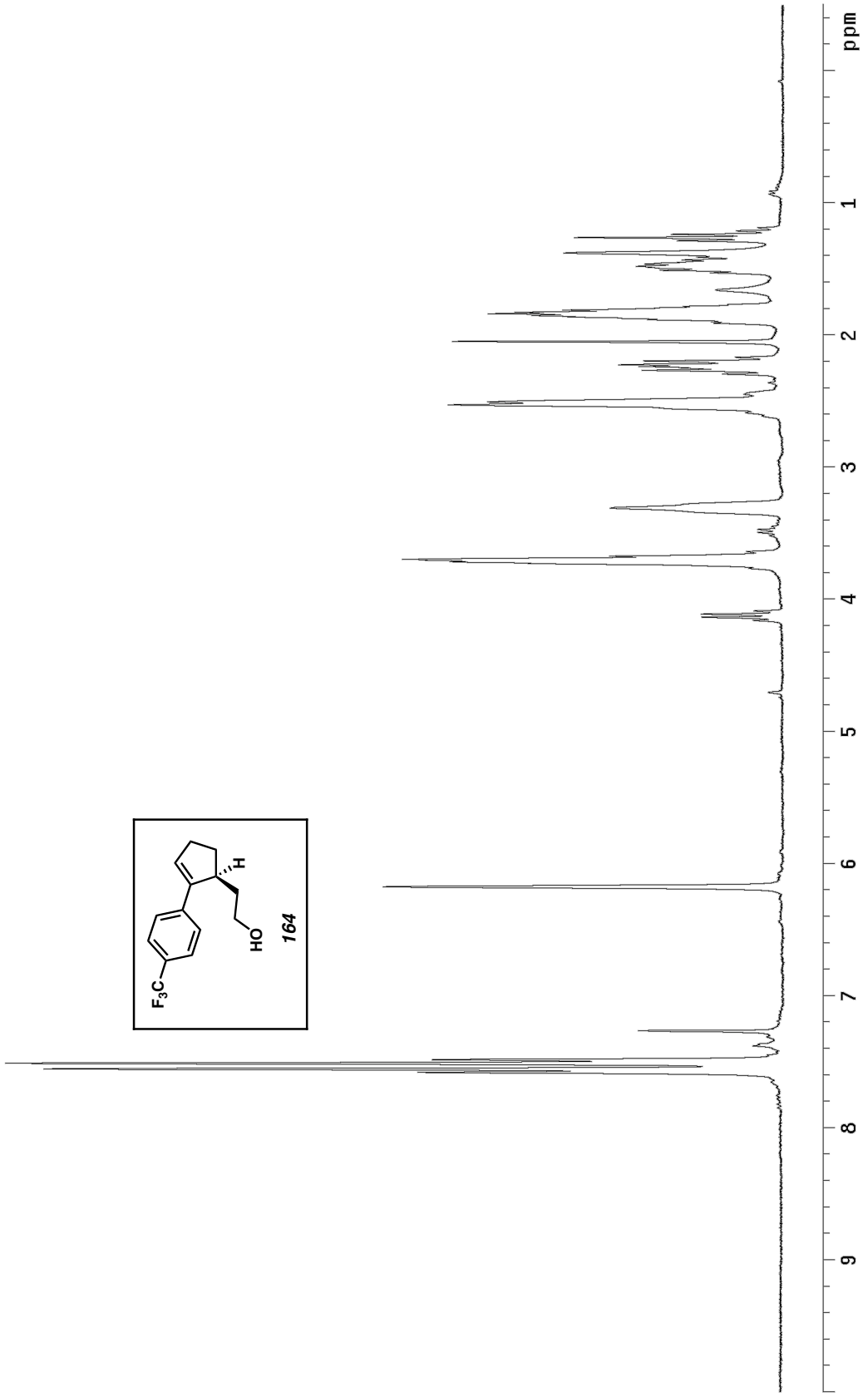

Figure A1.112 ^{1}H NMR (300 MHz, $CDCl_3$) of compound **164**.

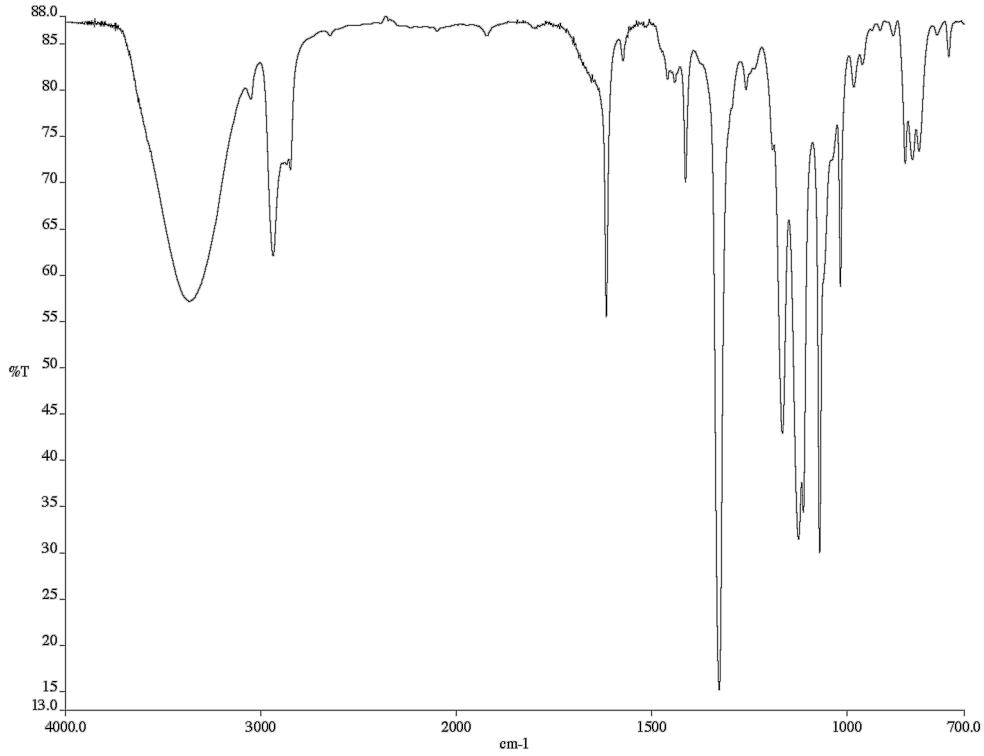

Figure A1.113 Infrared spectrum (thin film/NaCl) of compound **164**.

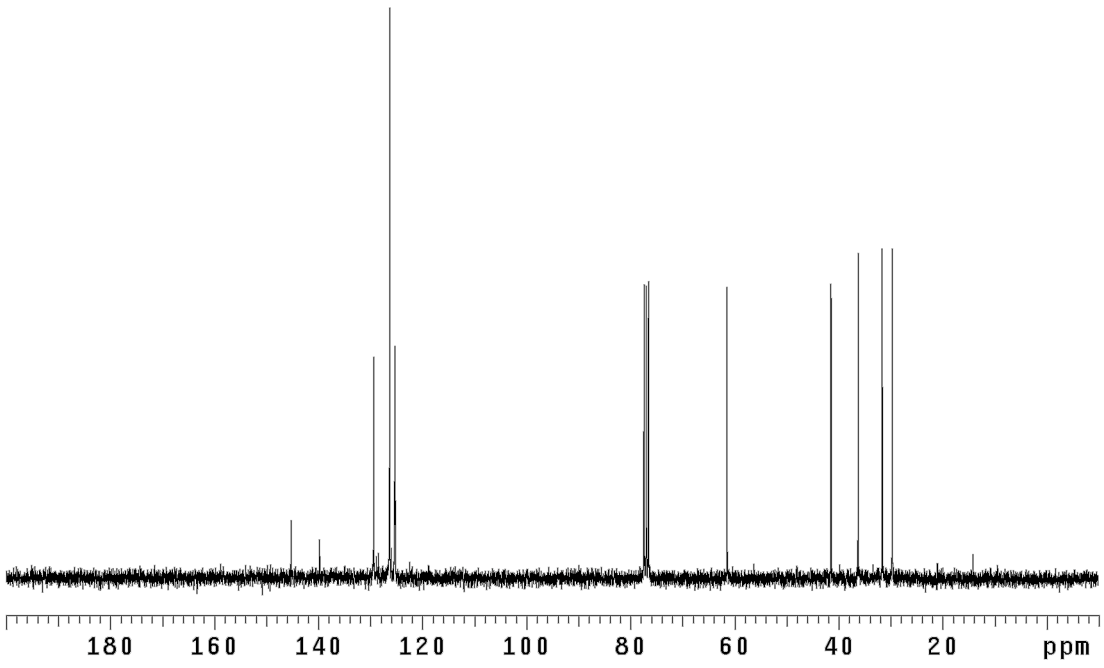

Figure A1.114 ^{13}C NMR (75 MHz, $CDCl_3$) of compound **164**.

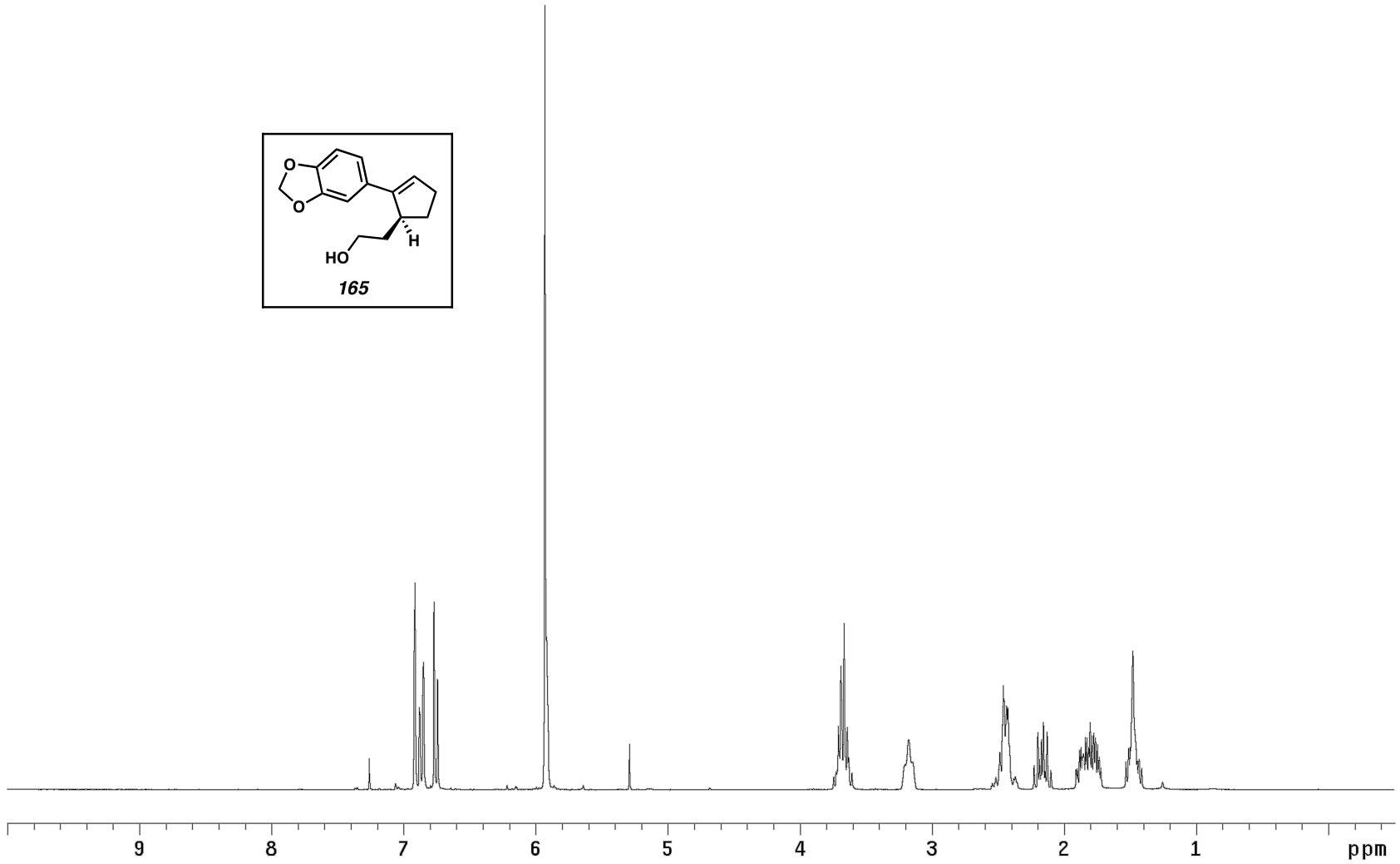

Figure A1.115 ^{1}H NMR (300 MHz, $CDCl_3$) of compound **165**.

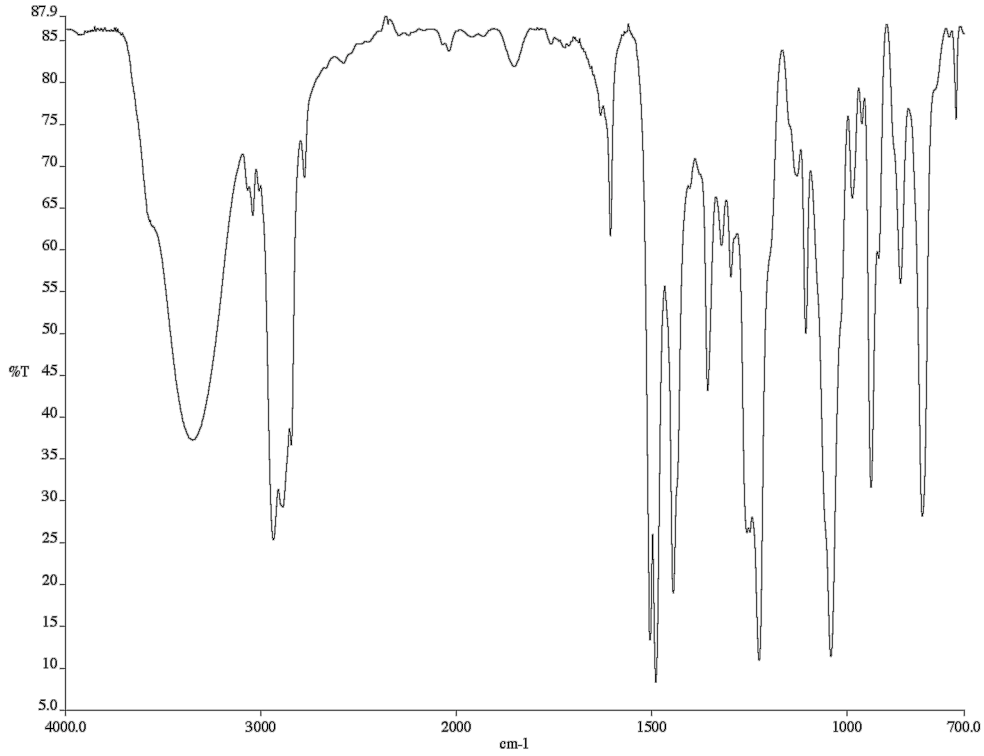

Figure A1.116 Infrared spectrum (thin film/NaCl) of compound **165**.

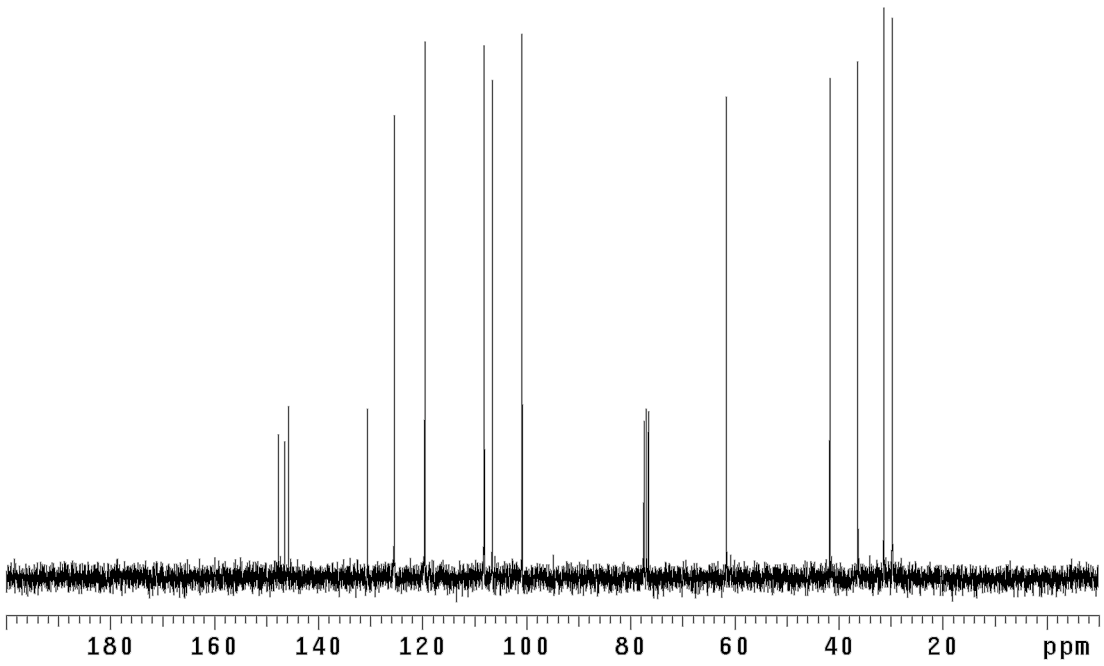

Figure A1.117 ^{13}C NMR (75 MHz, $CDCl_3$) of compound **165**.

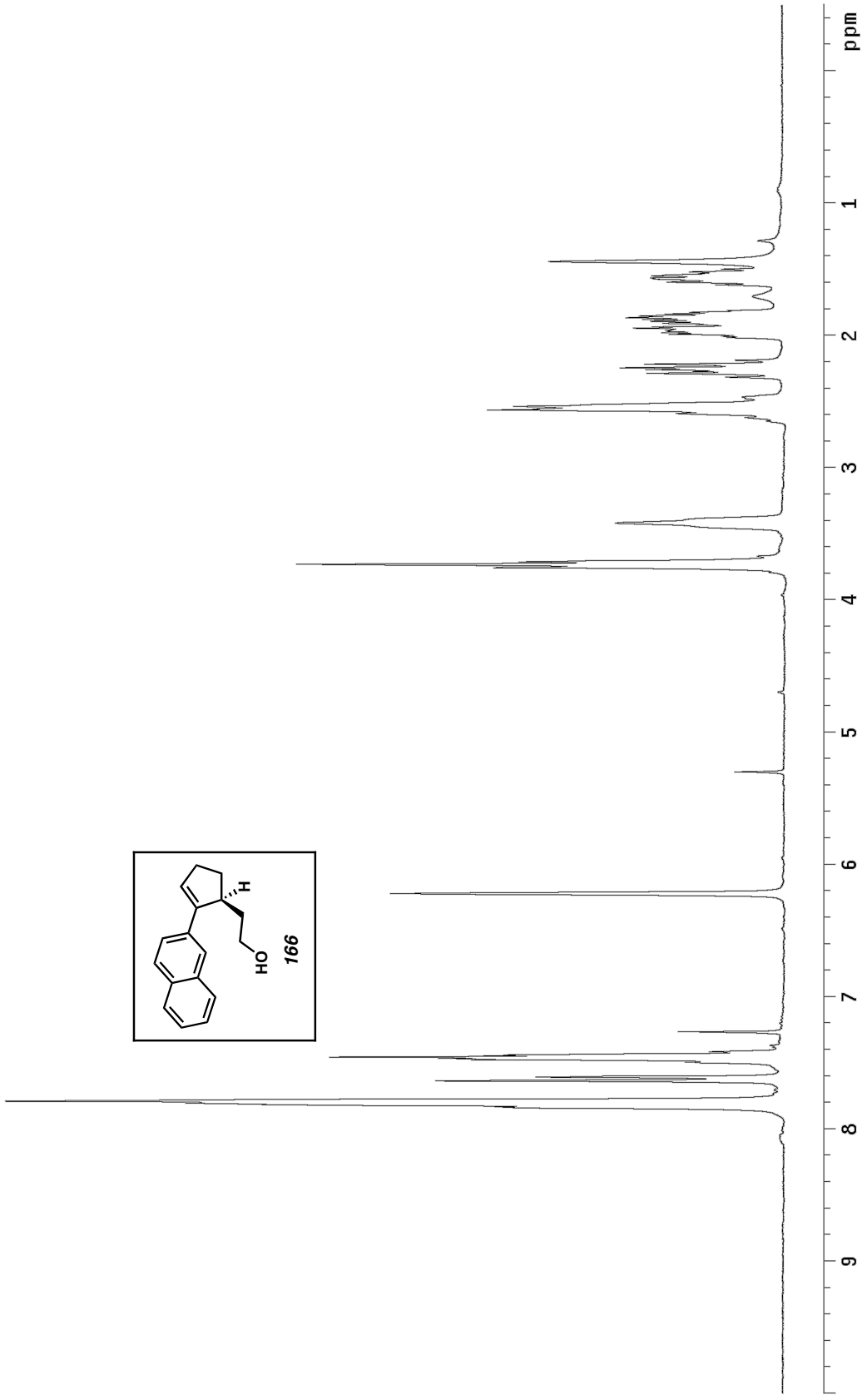

Figure A1.118 ^{1}H NMR (300 MHz, $CDCl_3$) of compound **166**.

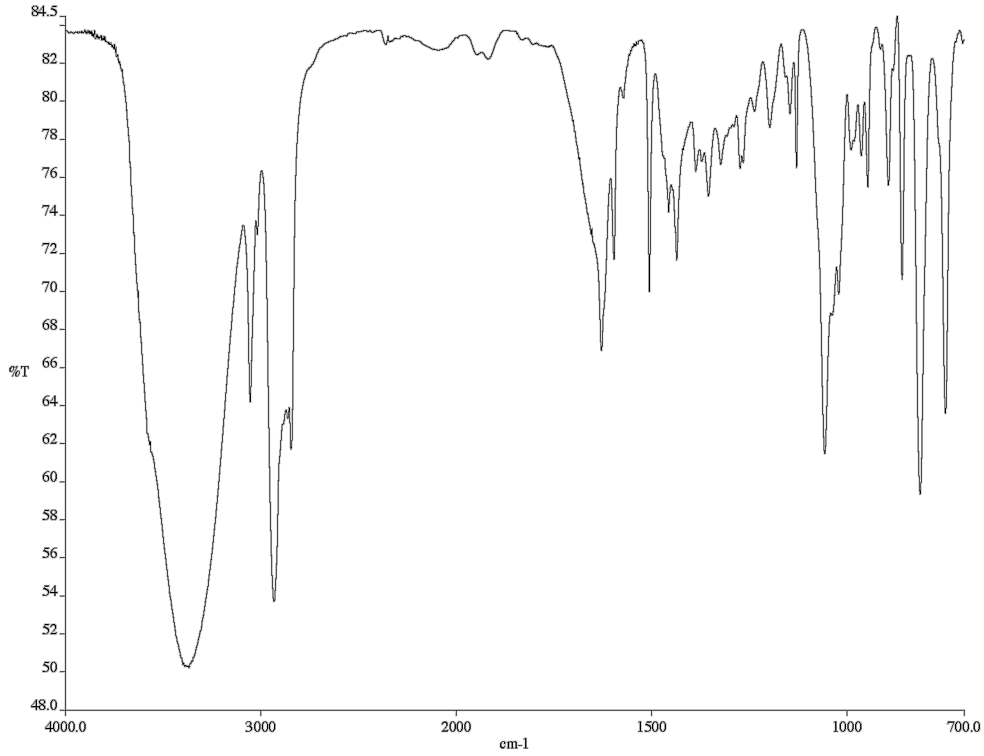

Figure A1.119 Infrared spectrum (thin film/NaCl) of compound **166**.

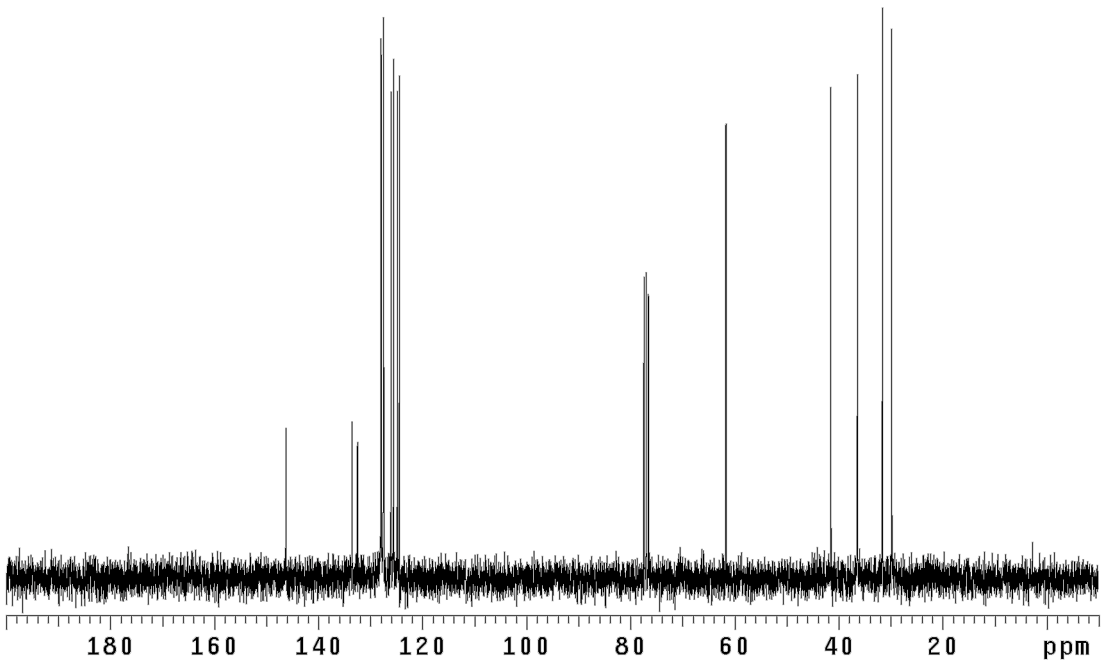

Figure A1.120 ^{13}C NMR (75 MHz, $CDCl_3$) of compound **166**.

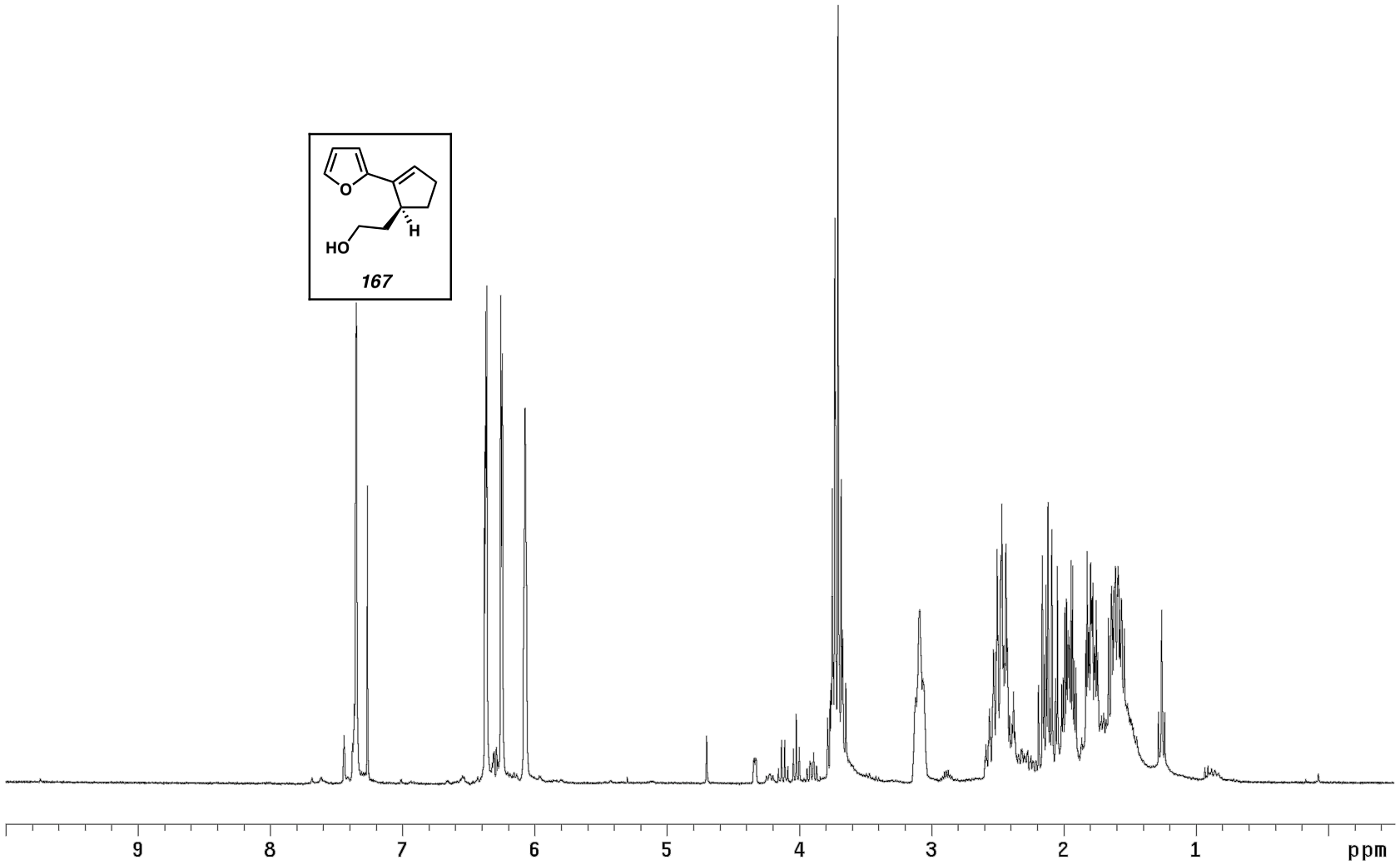

Figure A1.121 ^{1}H NMR (300 MHz, $CDCl_3$) of compound **167**.

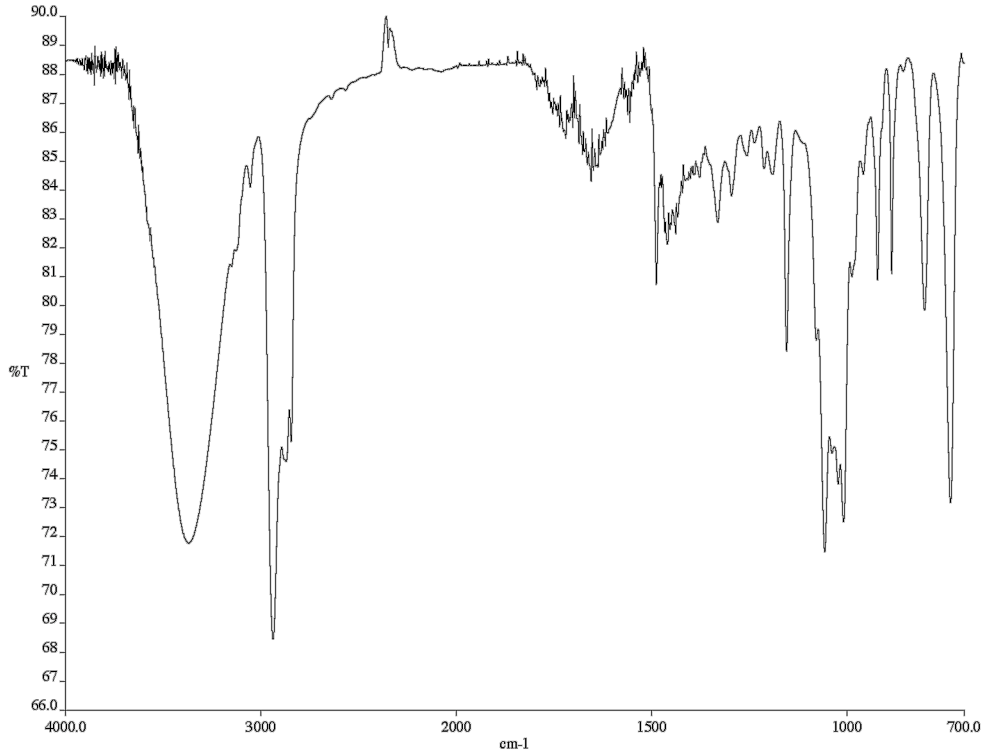

Figure A1.122 Infrared spectrum (thin film/NaCl) of compound **167**.

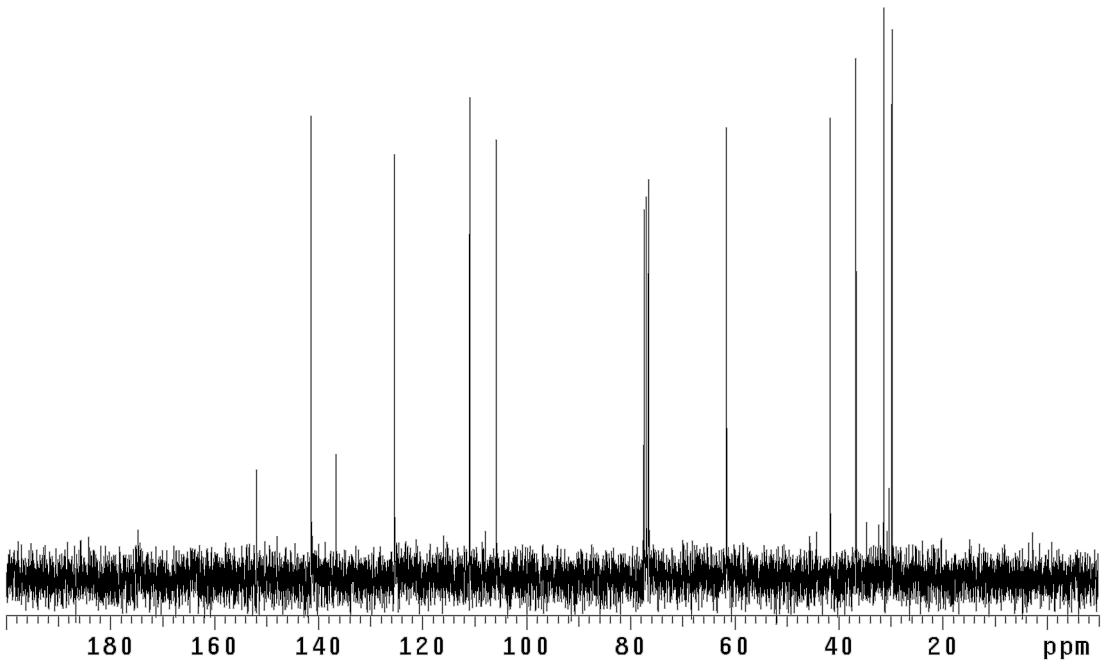

Figure A1.123 ^{13}C NMR (75 MHz, $CDCl_3$) of compound **167**.

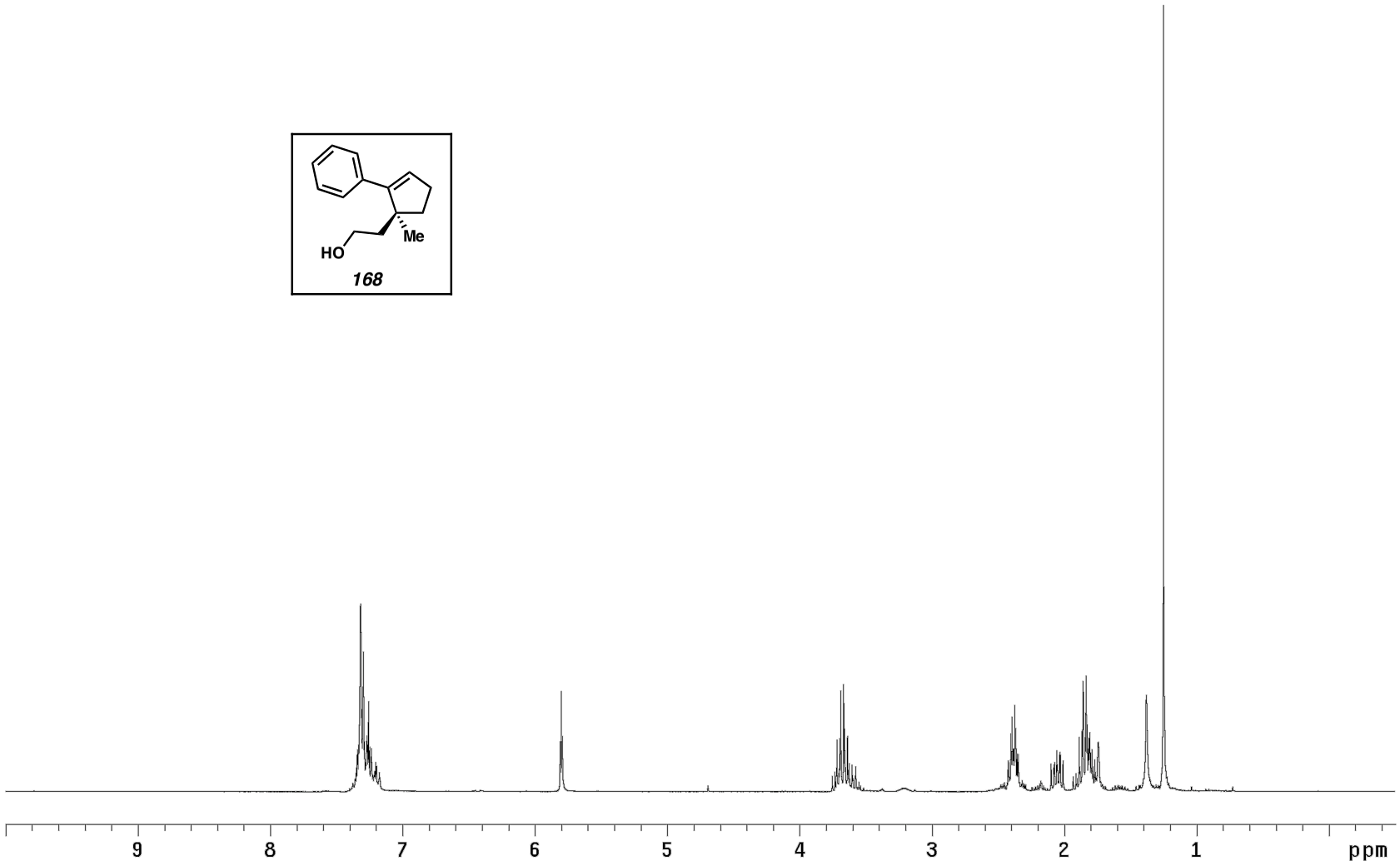

Figure A1.124 ^{1}H NMR (300 MHz, $CDCl_3$) of compound **168**.

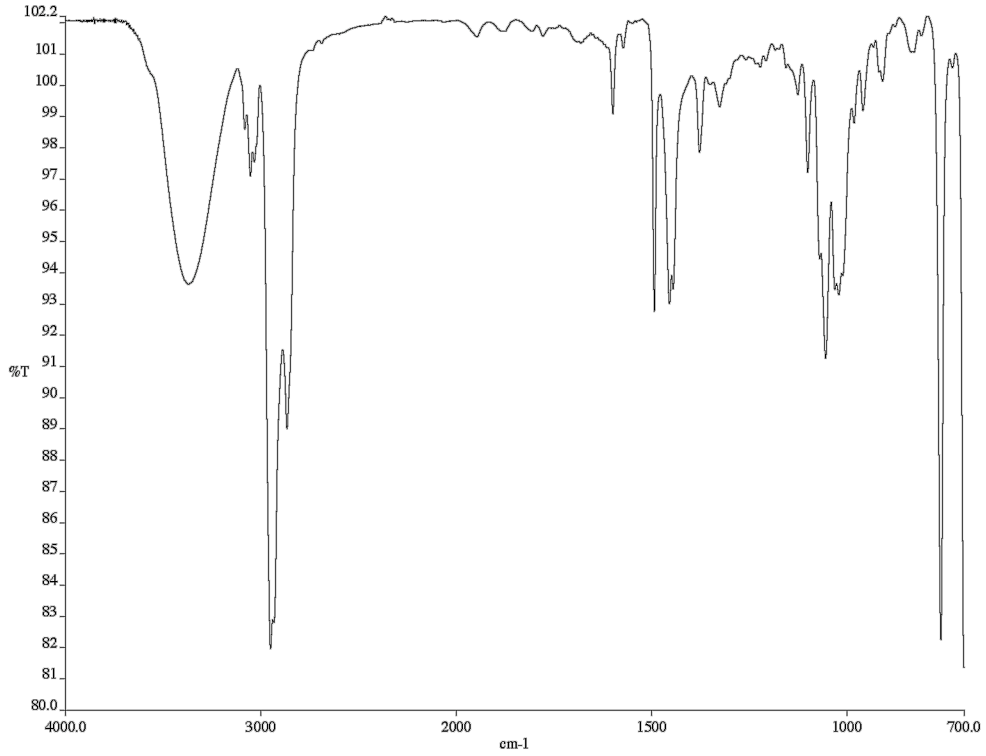

Figure A1.125 Infrared spectrum (thin film/NaCl) of compound **168**.

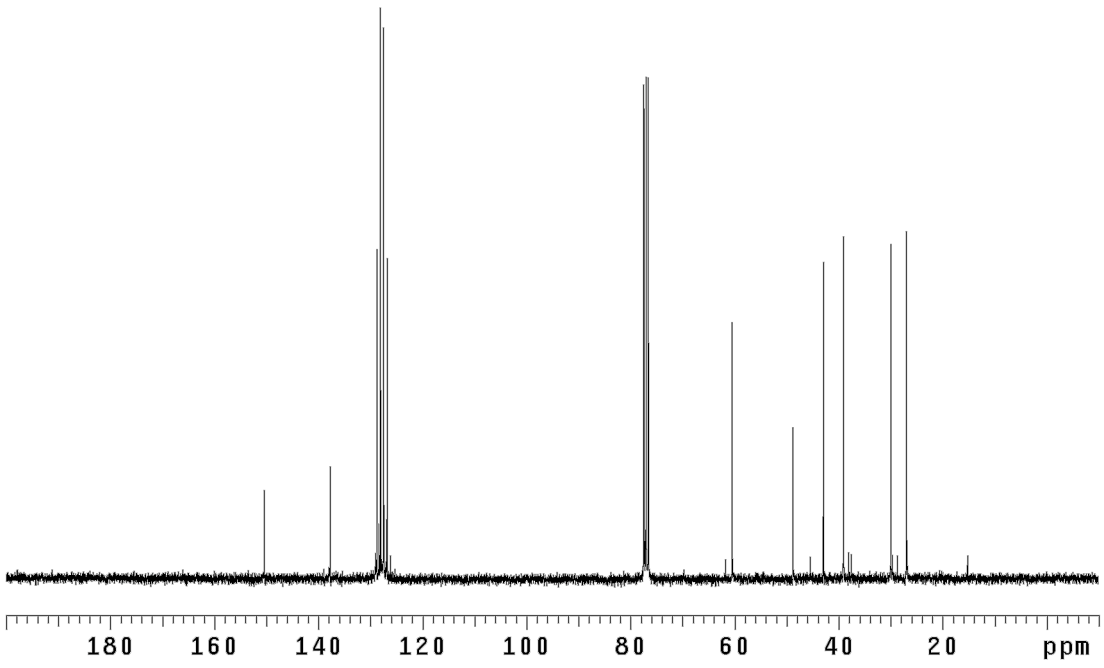

Figure A1.126 ^{13}C NMR (75 MHz, $CDCl_3$) of compound **168**.

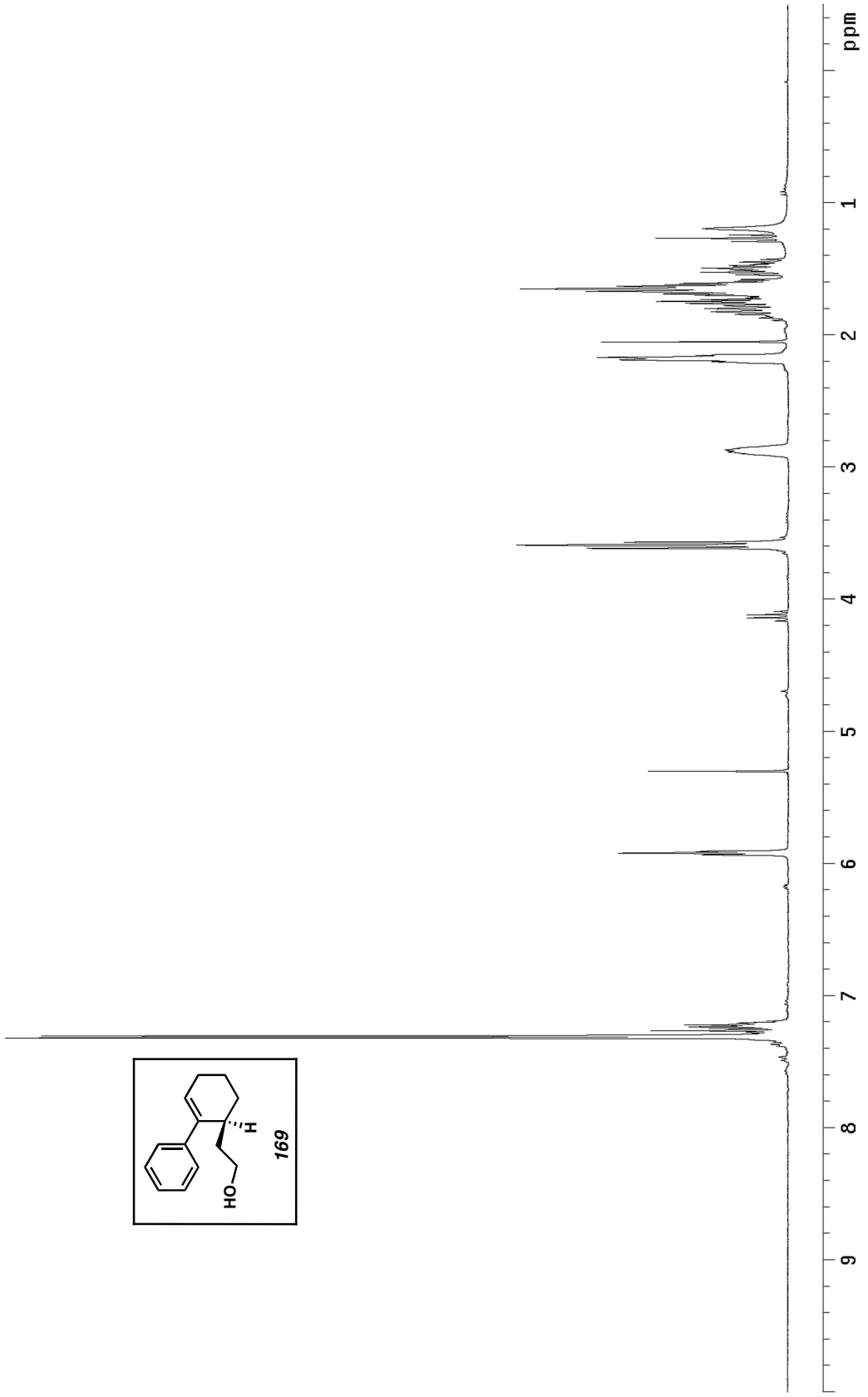

Figure A1.127 ^{1}H NMR (300 MHz, $CDCl_3$) of compound **169**.

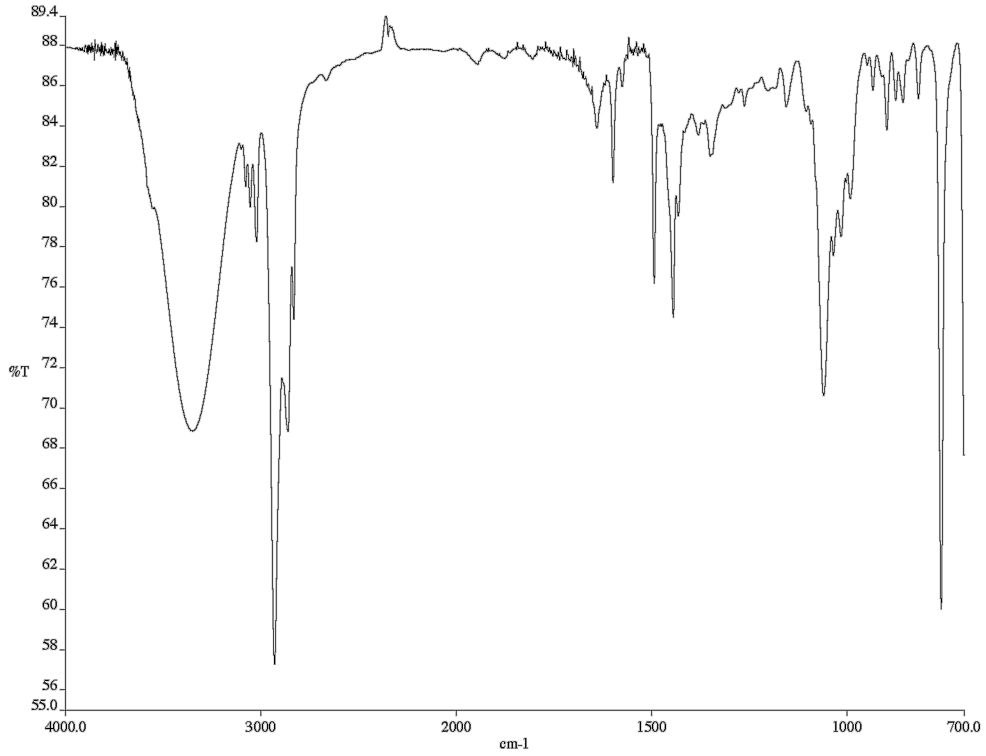

Figure A1.128 Infrared spectrum (thin film/NaCl) of compound **169**.

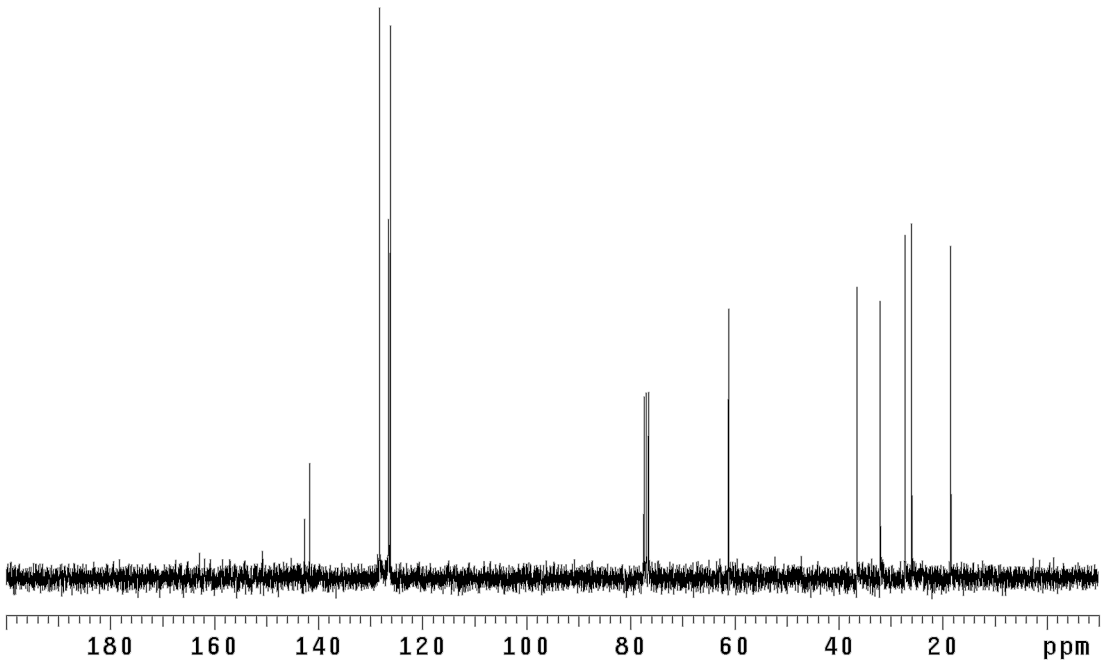

Figure A1.129 ^{13}C NMR (75 MHz, $CDCl_3$) of compound **169**.

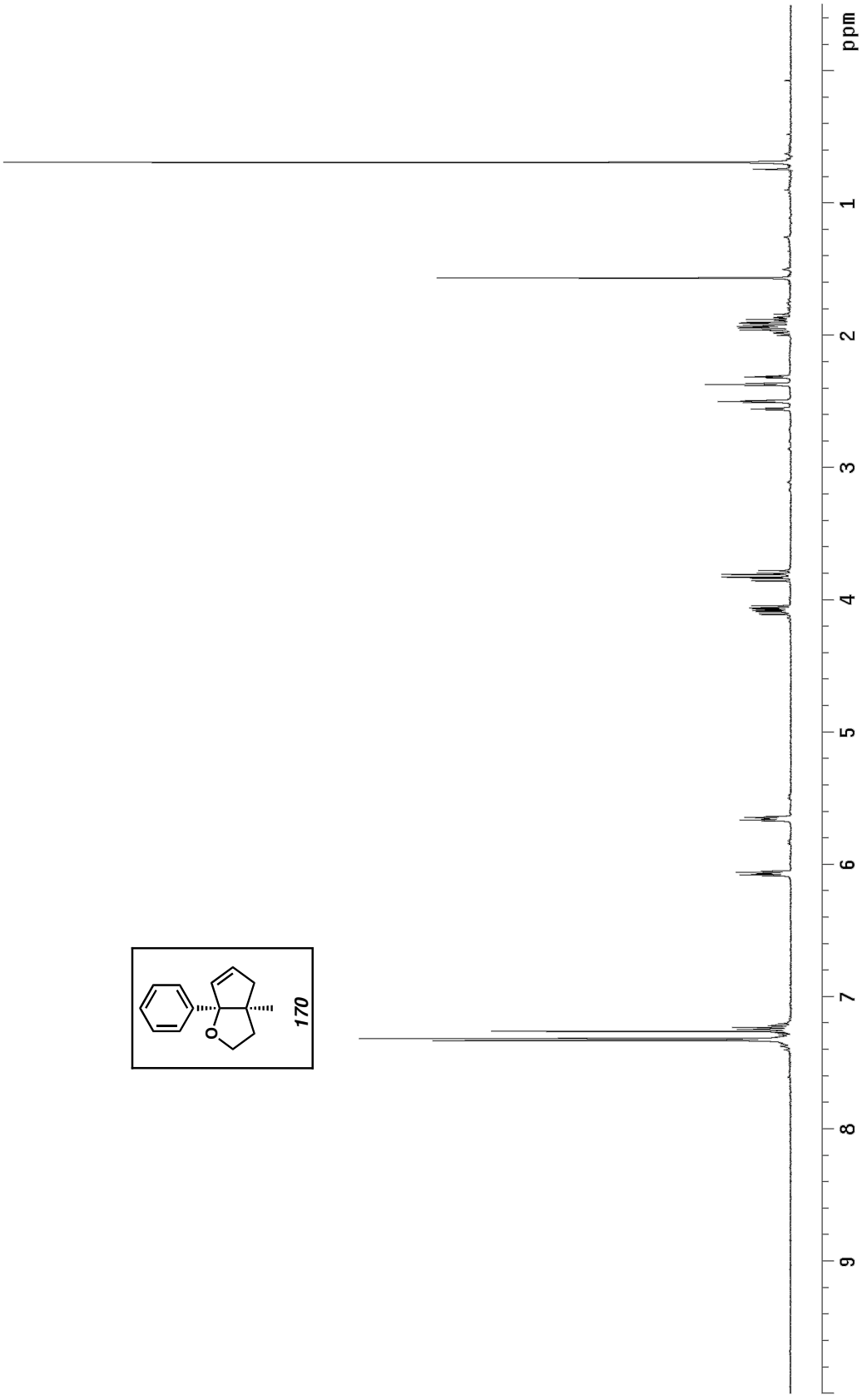

Figure A1.130 ^{1}H NMR (300 MHz, $CDCl_3$) of compound **170**.

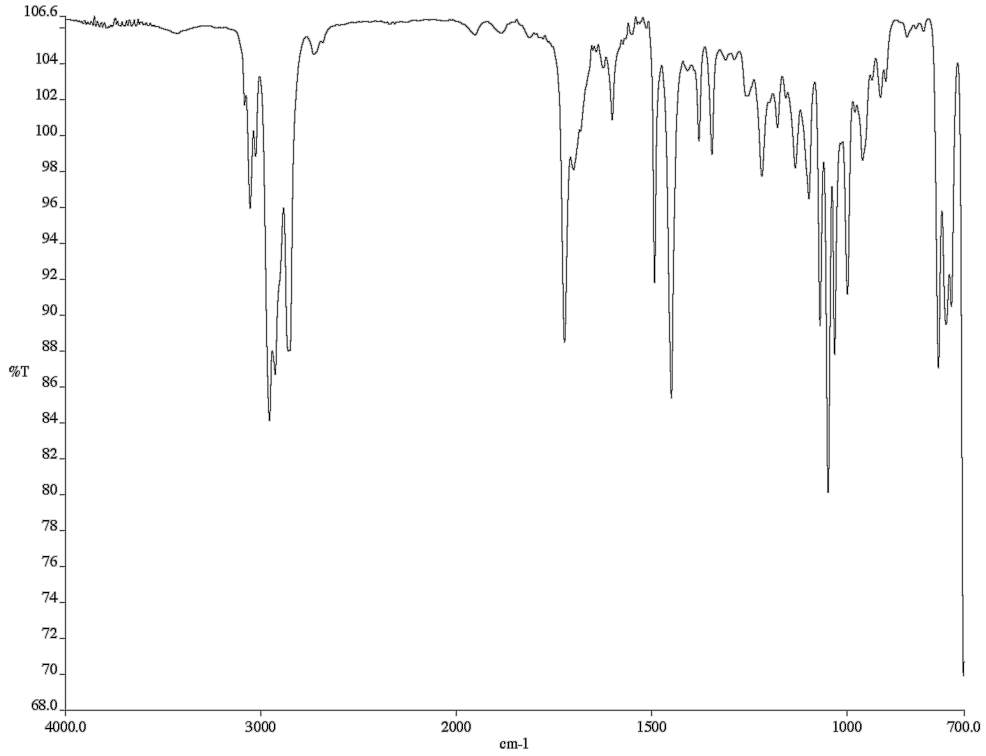

Figure A1.131 Infrared spectrum (thin film/NaCl) of compound **170**.

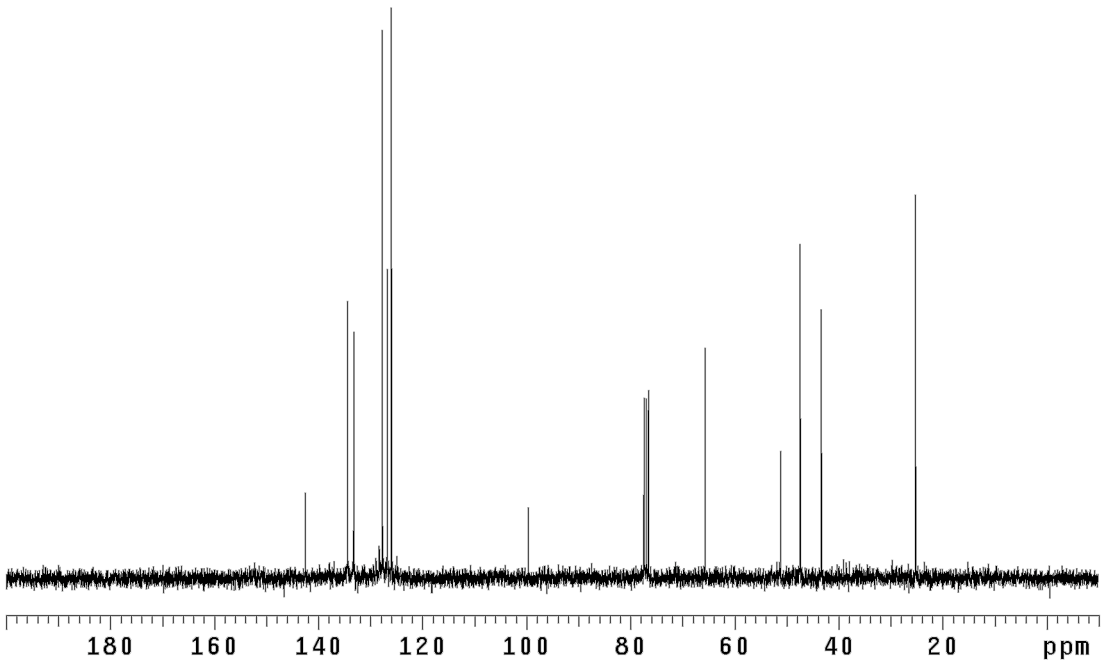

Figure A1.132 ^{13}C NMR (75 MHz, $CDCl_3$) of compound **170**.

CHAPTER 4

Advanced Catalyst Design in the Oxidative Kinetic Resolution

4.1 Background and Introduction

The development of improved catalysts for the oxidative kinetic resolution of secondary alcohols is critical to the enhanced utility of this process. Better catalysts provide more selective oxidations of a broader range of substrates in shorter reaction times, while maximizing the operational simplicity and safety of the transformation. Thus, the exploration of alternative systems for the aerobic enantioselective oxidation of secondary alcohols is of great value.[1]

Initial efforts in the area of enantioselective alcohol oxidation were based on the mild aerobic oxidation reported by Uemura.[2] Eric Ferreira, a graduate student in these laboratories, discovered that the use of the commercially available diamine (–)-sparteine (**28**) as a chiral additive with $Pd(OAc)_2$ under an atmosphere of molecular oxygen could provide kinetic resolution of (±)-1-phenylethanol ((±)-**25**), albeit in low conversion and with modest selectivity (Scheme 4.1.1).[3,4]

Scheme 4.1.1 Resolution with (–)-sparteine and $Pd(OAc)_2$.

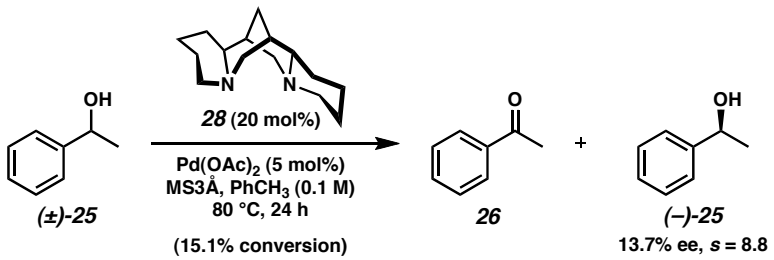

Catalyst modification was aided by an investigation of the mechanism for the oxidation, as proposed by Uemura (Scheme 4.1.2).[2b] Throughout the catalytic cycle, from initial alcohol coordination to form palladium alkoxide **228**, to subsequent β-

hydride elimination to form palladium hydride **229**, and to reaction with molecular oxygen to generate palladium peroxide **230**, counterion X is coordinated to the metal center. It was proposed that varying this counterion by changing the palladium catalyst precursor would have a marked effect on the reactivity and the selectivity of the system.

Scheme 4.1.2 Proposed mechanistic role of counterion.

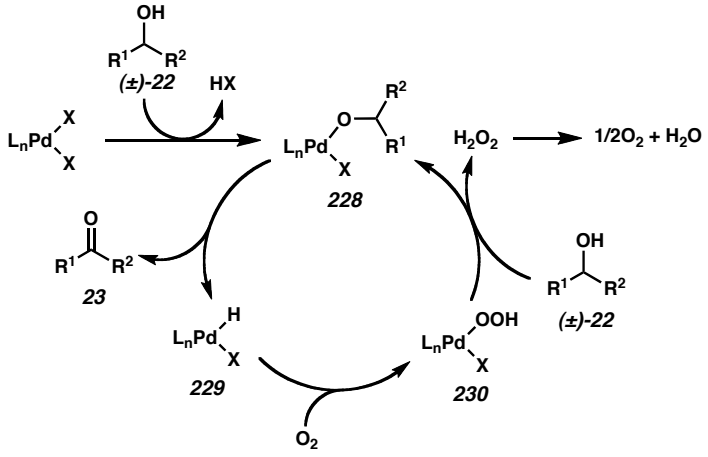

Indeed, this reaction displays a strong catalyst counterion dependence (Table 4.1.1). A palladium(0) precursor (entry 2), in which the counterion in presumed palladium(II) intermediates **228**, **229**, and **230** are not clear, provided reasonable levels of oxidation but decreased selectivity. Palladium precursors with chloride counterions (entries 3 and 4) led to more reactive and selective catalyst systems than those with acetate (entry 1), with $Pd(nbd)Cl_2$ emerging as the most effective palladium source. Interestingly, the use of a palladium bromide source (entry 5) led to rapid palladium aggregation and little oxidation.[5]

Table 4.1.1 Palladium source screen in toluene.

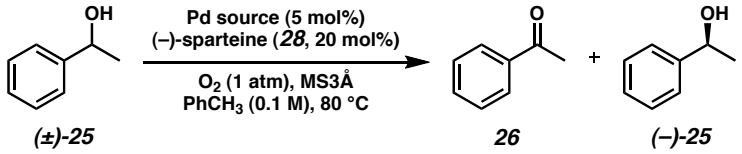

(±)-25 *26* *(–)-25*

entry	Pd source	time	conversion[a]	alcohol ee[b]	*s*
1	$Pd(OAc)_2$	24 h	15.1%	13.7%	8.8
2	$Pd_2(dba)_3$	55 h	66.2%	81.5%	5.7
3	$PdCl_2$	96 h	62.6%	98.0%	16
4	$Pd(nbd)Cl_2$	96 h	59.9%	98.7%	23
5[c]	$PdBr_2$	60 h	5.4%	5.0%	16

[a] Measured by GC. [b] Measured by chiral HPLC. [c] Pd black observed.

Theoretical calculations by the Goddard group confirmed the importance of the counterion for selectivity in the resolution.[6] The rate-limiting step in the catalytic cycle was found to be β-hydride elimination from the palladium alkoxide intermediate.[7] The counterion has a critical role imparting stereoselectivity to the process by occupying an open apical position in the β-hydride elimination transition state (Figure 4.1.1). Calculations correctly predicted the observed selectivity difference between larger chloride and smaller acetate counterions. Additionally, little selectivity (s = 1.5) was anticipated in the absence of a counterion.

Figure 4.1.1 Theoretical calculations on the enantioselective oxidation.

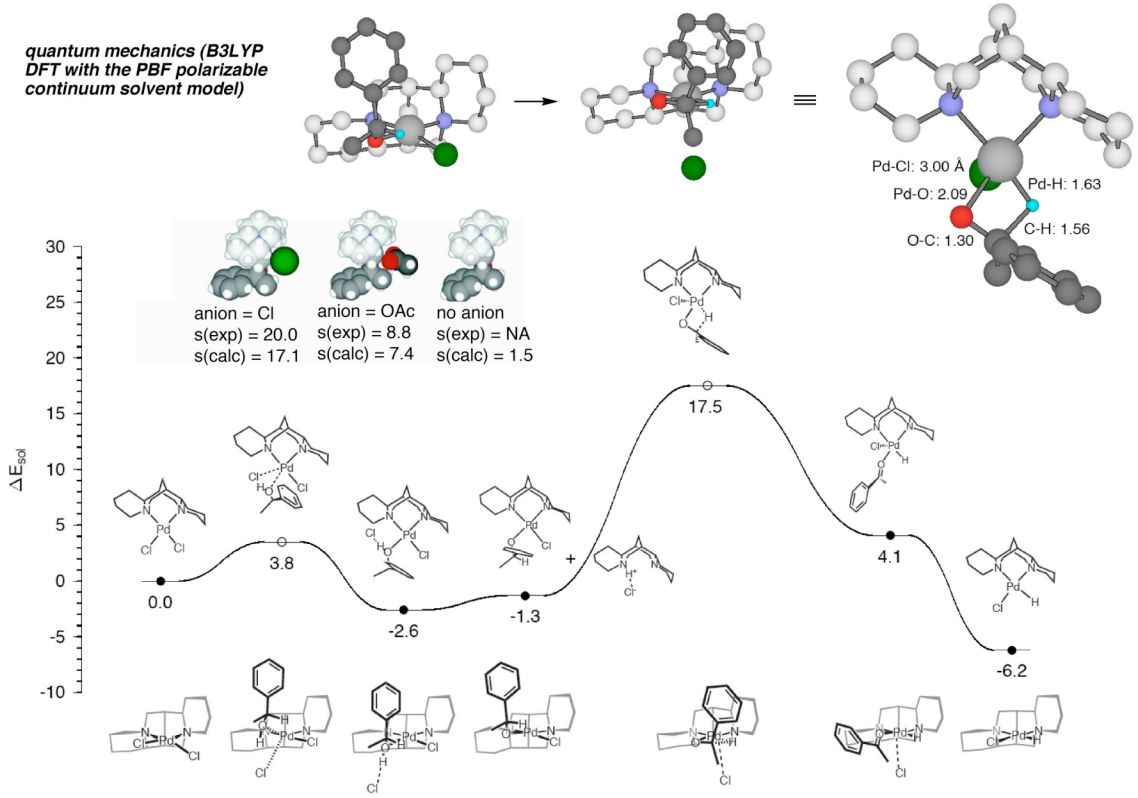

Further evidence demonstrating the key interaction between the counterion and sparteine ligand in imparting selectivity and reactivity was found in X-ray crystallographic analyses of palladium complexes relevant to the kinetic resolution. Crystallographic analysis of Pd(sparteine)Cl_2 (**66**), a catalyst precursor performing identically in the resolution to Pd(nbd)Cl_2 and 5 mol% (–)-sparteine (**28**), revealed a significant distortion in the square plane about the metal center (Figure 4.1.2).[8] The sum of the six angles around the metal center is only 705.99°, compared to 720° in an ideal square planar geometry. The majority of this deviation from planarity is due to chloride Cl2. Near the projecting N2 piperidine ring of the sterically crowded C_1 symmetric (–)-sparteine ligand, chloride Cl2 is deflected about 9.9° out of the plane of the metal

complex (180° – ∠N1–Pd–Cl2). This deformation is substantially larger than that for the less active kinetic resolution catalyst Pd(sparteine)$(OAc)_2$ (**231**, Figure 4.1.3), in which the sum of the six angles about the palladium center and acetate deflection are 711.36° and 5.4°, respectively.[9]

Figure 4.1.2 Structure of Pd(sparteine)Cl_2.

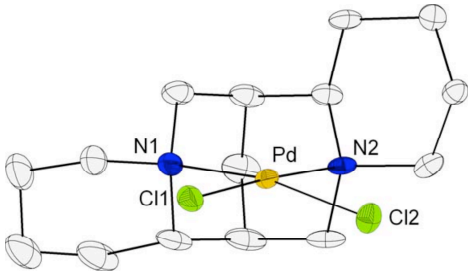

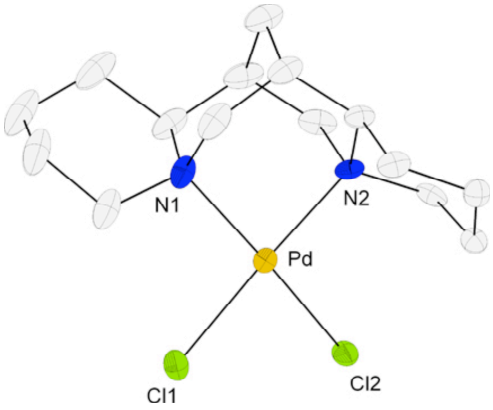

Select bond lengths (Å) and angles (°)			
Pd–N1	2.127(3)	N1–Pd–N2	87.51(10)°
Pd–N2	2.096(2)	Cl1–Pd–Cl2	83.09(3)°
Pd–Cl1	2.3161(9)	N2–Pd–Cl1	176.24(7)°
Pd–Cl2	2.3150(8)	N1–Pd–Cl2	170.06(8)°
		N1–Pd–Cl1	95.65(8)°
		N2–Pd–Cl2	93.44(7)°
		Σ ∠	705.99°

Figure 4.1.3 Structure of Pd(sparteine)$(OAc)_2$.

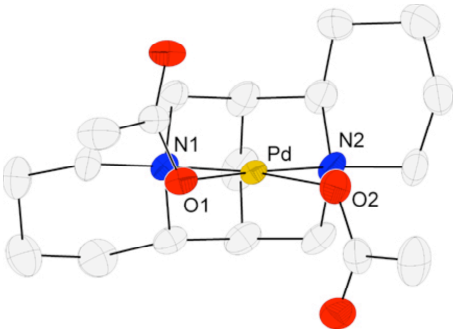

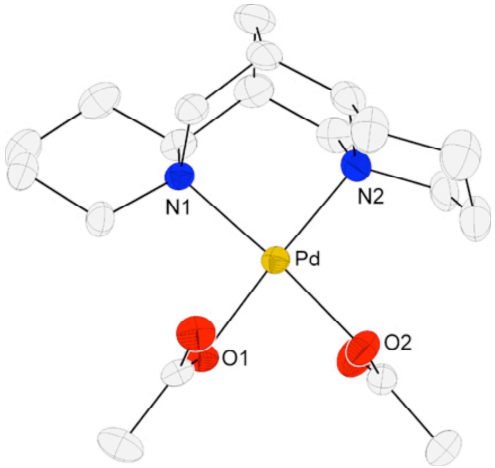

Select bond lengths (Å) and angles (°)			
Pd–N1	2.096(2)	N1–Pd–N2	88.41(8)°
Pd–N2	2.066(3)	O1–Pd–O2	82.58(9)°
Pd–O1	2.021(2)	N2–Pd–O1	176.83(10)°
Pd–O2	2.030(2)	N1–Pd–O2	174.65(9)°
		N1–Pd–O1	94.22(8)°
		N2–Pd–O2	94.67(9)°
		Σ ∠	711.36°

Raissa Trend, a graduate student in these laboratories, synthesized a number of palladium complexes to better understand the structural features and reactivity of Pd(sparteine)Cl_2 (**66**). Utilizing a trifluoromethyl derivative of (*R*)-1-phenylethanol ((+)-**25**), which is the faster reacting enantiomer in the oxidative kinetic resolution, she was able to prepare alkoxide **232** (Figure 4.1.4).[8] This complex is even more distorted from an ideal square plane than Pd(sparteine)Cl_2. The sum of the six bond angles around the metal center is 701.58°, and the chloride deflection is 15.4°. Interestingly, the benzylic C–H bond of the alkoxide aligned with the Pd-Cl bond. This orientation is expected to be similar to that required to displace the chloride ligand and form a β-agostic interaction between the benzylic C–H bond and the palladium center in the calculated transition state for β-hydride elimination. Presumably, β-hydride elimination does not occur because the electron-withdrawing trifluoromethyl group disfavors the formation of an actual β-agostic interaction in this complex.

Figure 4.1.4 Structure of palladium alkoxide **232**.

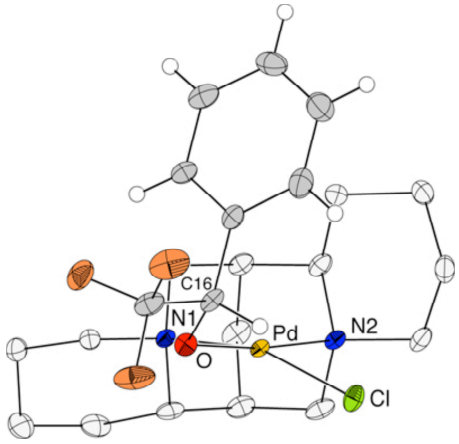

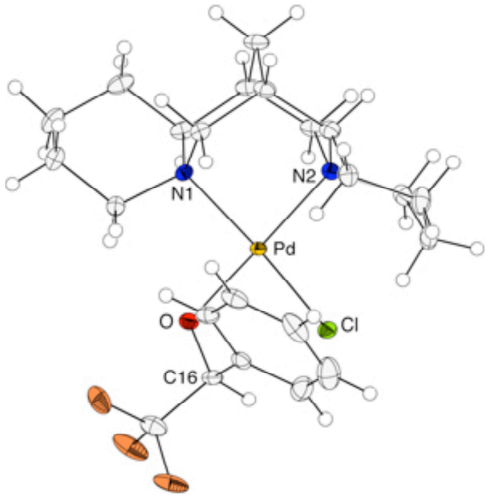

Select bond lengths (Å) and angles (°)			
Pd–N1	2.1243(17)	N1–Pd–N2	88.07(6)°
Pd–N2	2.0925(16)	O–Pd–Cl	87.71(4)°
Pd–O	2.0012(14)	N2–Pd–O	176.27(6)°
Pd–Cl	2.3316(5)	N1–Pd–Cl	164.59(5)°
		N1–Pd–O	89.78(6)°
		N2–Pd–Cl	95.16(4)°
		Σ ∠	701.58°

Based on crystallographic studies, as well as kinetic[7] and theoretical[6] work in this area, a model for reactivity and selectivity in the oxidative kinetic resolution was developed (Scheme 4.1.3, R^L = large substituent, R^S = small substituent).[8] When a racemic alcohol mixture is exposed to Pd(sparteine)Cl_2 (**66**), a diastereomeric mixture of palladium alkoxides **233** and **235** are formed. Complex **233**, formed with the faster reacting enantiomer of alcohol, proceeds through a β-hydride elimination transition state (**234**) similar to trifluoromethyl alkoxide **232**, in which the chloride counterion has been fully displaced into the apical position of the palladium complex. Subsequent β-hydride elimination leads to product ketone. Diastereomeric complex **235**, on the other hand, is unable to proceed through an intermediate similar to alkoxide **232** without destabilizing steric interactions between R^L and the chloride counterion. This unfavorable interaction

is even greater in transition state **238**. Alternatively for complex **235**, the C–H bond could approach the palladium center from the opposite side of the square plane, as in complex **237**. However, this geometry would be expected to lead to destabilizing interactions between R^L and one of the piperidine rings of the sparteine framework, as well as deflecting the chloride counterion into the other piperidine ring, which projects over the square plane of the complex. Thus, diastereomer **235** is reprotonated to form the resolved alcohol.

Scheme 4.1.3 Model for selectivity of the resolution.

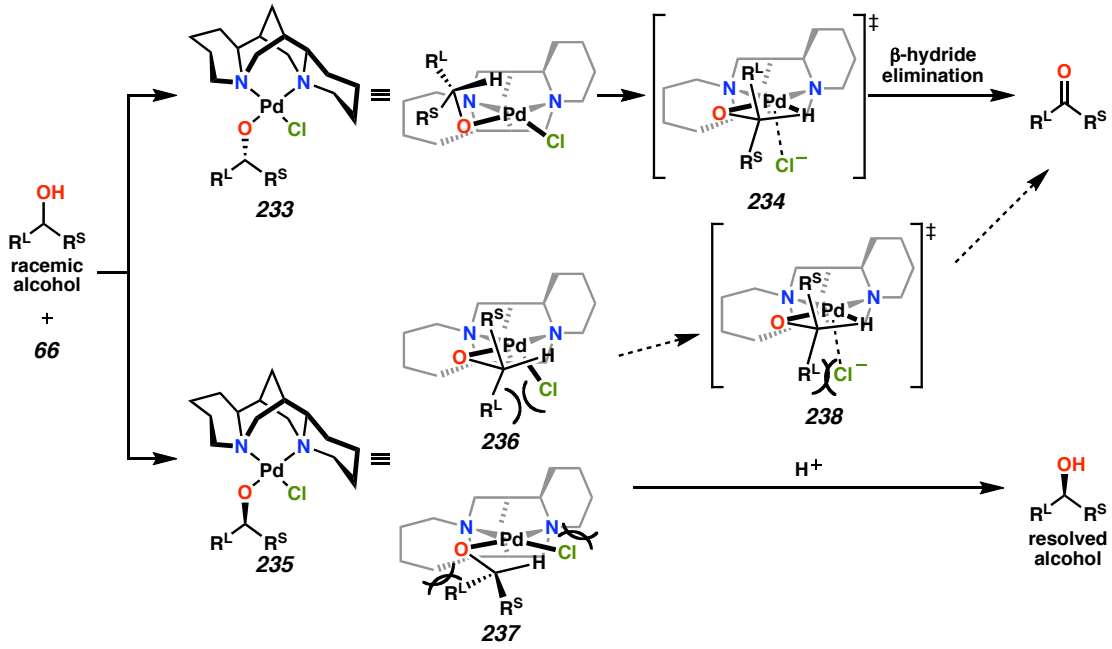

4.2 Counterion Studies in the Kinetic Resolution

4.2.1 Phenoxides

The previous computational and crystallographic studies have demonstrated the importance of the counterion for selectivity in the oxidation. However, the observed counterion distortion in a number of palladium complexes is intriguing. The greater the

counterion deflection in the complex, the more the geometry of the complex resembles that of the β-hydride elimination transition state. We reasoned that a complex with a greater counterion distortion might have a lower energy barrier to the rate-limiting β-hydride elimination, leading to increased rates of alcohol oxidation. Therefore, the interaction between the (–)-sparteine ligand and the counterion could be important for both selectivity and reactivity in the kinetic resolution. This hypothesis could explain why Pd(sparteine)Cl_2 (**66**) is both more selective and more reactive as a catalyst than Pd(sparteine)$(OAc)_2$ (**231**). Because of the critical role of counterion in the resolution, this area has been explored further to potentially provide even better catalysts for this useful transformation.

Jeffrey Bagdanoff, a graduate student in these laboratories, initiated a project utilizing salts of alcohols either resistant to β-hydride elimination or lacking β-hydrides completely as counterions in the resolution.[10] These counterions were expected to be easily modifiable, allowing for greater control of steric and electronic properties of the resulting palladium complex. Indeed, Jeffrey Bagdanoff was able to prepare and crystallize Pd(sparteine)$(OC_6F_5)_2$ (**239**) by simply stirring dichloride complex **66** with two equivalents of the sodium salt of pentafluorophenol (Figure 4.2.1). This complex exhibits a distorted square planar geometry, with the sum of the six bond angles around the palladium center and N1–Pd–O2 deflection of 710.98° and 7.5°, respectively. Based on our hypothesis, the bond angles observed suggested that this palladium complex would be less active in the oxidative kinetic resolution than Pd(sparteine)Cl_2 (**66**).

Figure 4.2.1 Structure of Pd(sparteine)(OC_6F_5)$_2$.

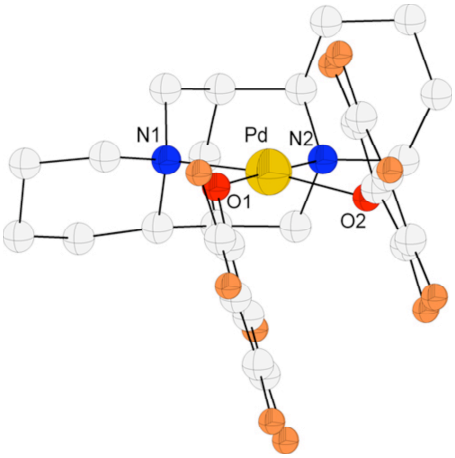

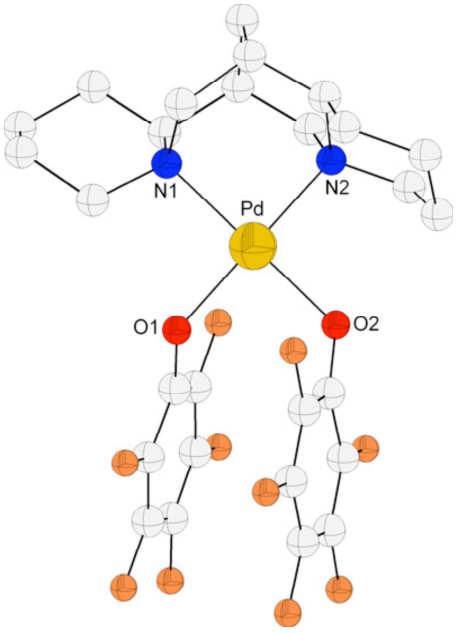

Select bond lengths (Å) and angles (°)			
Pd–N1	2.114(5)	N1–Pd–N2	88.5(2)°
Pd–N2	2.067(5)	O1–Pd–O2	88.96(16)°
Pd–O1	2.024(4)	N2–Pd–O1	178.6(2)°
Pd–O2	2.034(5)	N1–Pd–O2	172.50(19)°
		N1–Pd–O1	91.72(18)°
		N2–Pd–O2	90.7(2)°
		Σ ∠	710.98°

When generated in situ, Jeffrey Bagdanoff found that complex **239** was a poor catalyst for the enantioselective aerobic oxidation of (±)-1-phenylpropanol ((±)-**83**) (entry 3, Table 4.2.1). Indeed, use of the sodium salt of trifluoroethanol as the counterion also led to little oxidation (entry 2). Modest reactivity and selectivity was observed with sodium phenoxide (entry 4), although the control reaction without alkoxide was better (entry 1). Electron-rich phenoxides, however, provided much more promising results. Increased oxidation rates and selectivity were observed, leading to high enantiomeric excess of alcohol (–)-**83** (entries 5 and 6).

Table 4.2.1 Phenoxide screen with (±)-1-phenylpropanol.

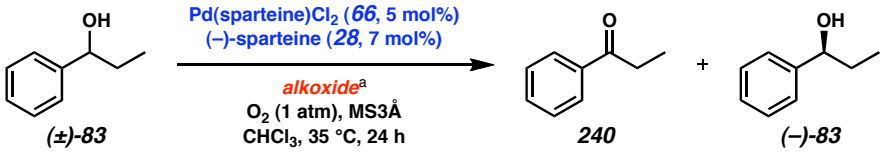

entry	alkoxide[b]	conversion[c]	alcohol ee[d]	*s*
1	none	36.5%	53.1%	27
2	$NaOCH_2CF_3$	1.2%	0.0%	–
3	$NaOC_6F_5$	3.1%	1.8%	3.6
4	NaOPh	22.8%	25.1%	16
5	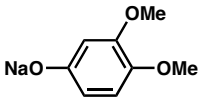	56.4%	97.3%	30
6	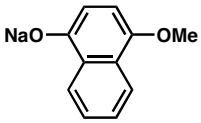	48.2%	83.6%	49

[a] Pd(sparteine)Cl_2 (**66**), (–)-sparteine (**28**), and alkoxide were sonicated in $CHCl_3$ 1 h prior to addition of (±)-**83**. [b] Prepared by treatment of the corresponding alcohol with Na (1 equiv) in toluene followed by concentration under reduced pressure. [c] Measured by GC. [d] Measured by chiral HPLC.

Further efforts in this area sought to build upon Jeffrey Bagdanoff's results with electron-rich phenoxides. Many of the corresponding phenols are commercially available. Furthermore, the sodium alkoxides are readily prepared by treatment of the phenol with metallic sodium in toluene, so a large number of phenoxides can be screened quickly. Generally, the more electron-rich phenoxides provide higher oxidation rates in the kinetic resolution of alcohol (±)-**25** (Table 4.2.2, entries 3-5) as compared to the previously reported conditions with cesium carbonate (entry 1).[11] Phenoxides with ortho substituents produce less active catalyst systems (entry 7), though these reactions still proceed to high alcohol enantiomeric excesses at prolonged reaction times. Addition of naphthoxides can lead to faster oxidation rates (entries 8 and 9) or slower rates with somewhat higher selectivity (entry 10).

Table 4.2.2 Phenoxide screen with (±)-1-phenylethanol.

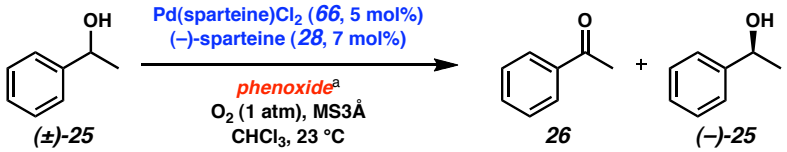

entry	phenoxide[b]	time	conversion[c]	alcohol ee[d]	*s*
1[e]	none	24 h	58.3%	97.8%	24
2	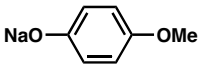	24 h	50.4%	85.7%	32
3	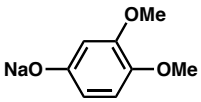	16 h	55.4%	94.0%	25
4	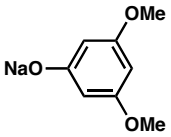	16 h	51.6%	87.6%	29
5	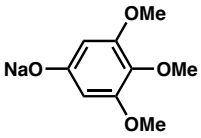	16 h	60.0%	99.5%	28
6	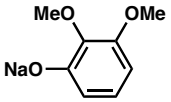	24 h	54.6%	93.5%	27
7	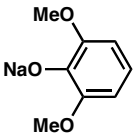	98 h	62.5%	98.1%	17
8	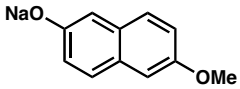	24 h	66.7%	>99.5%	>15
9	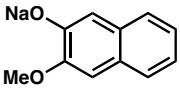	16 h	55.5%	95.0%	27
10	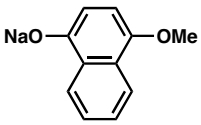	24 h	42.2%	64.8%	32

[a] Pd(sparteine)Cl_2 (**66**), (–)-sparteine (**28**), and alkoxide were stirred in $CHCl_3$ 1 h prior to addition of (±)-**25**. [b] Prepared by treatment of the corresponding phenol with Na (1 equiv) in toluene followed by concentration under reduced pressure. [c] Measured by GC. [d] Measured by chiral HPLC. [e] Cs_2CO_3 (40 mol%) was added.

While (±)-1-phenylethanol ((±)-**25**) was able to be resolved with a number of added phenoxides, a more challenging substrate for the enantioselective oxidation was sought in order to highlight the beneficial role of these additives. Alcohol (±)-**73** was a problematic substrate for the previously developed conditions, generally being resolved only at extended reaction times and with modest selectivity. Thus, phenoxides were explored in order to improve this resolution (Table 4.2.3). Many of the previously investigated phenoxides (entries 2-4, 6-8, 13, 14, and 18) lead to results that are not substantially different than those with cesium carbonate (entry 1). A number of other phenoxides (entries 5, 9-11, and 15) provide decreased oxidation rates. However, several naphthoxides (entries 12, 16, and 17) result in promising improvements in the selectivity of the kinetic resolution of this alcohol.

Table 4.2.3 Phenoxide screen with secondary alcohol (±)-**73**.

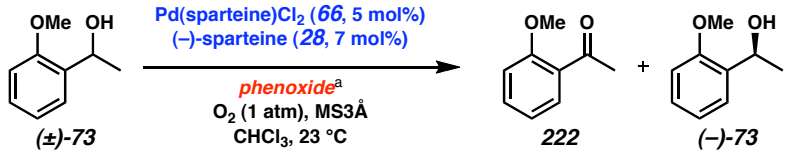

entry	phenoxide[b]	time	conversion[c]	alcohol ee[d]	*s*
1[e]	none	46 h	48.3%	66.0%	11
2	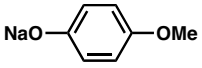	46 h	42.7%	52.3%	9.5
3	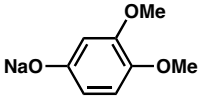	46 h	55.6%	82.6%	12
4		114 h	69.8%	99.1%	12
5	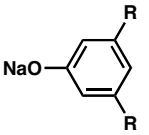 R = Me	114 h	45.2%	54.8%	8.5
6	R = OMe	46 h	50.4%	72.3%	13
7	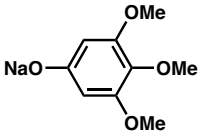	46 h	46.8%	63.6%	12
8	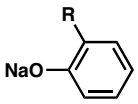 R = Me	46 h	48.8%	65.7%	11
9	R = Cl	118 h	39.3%	49.3%	12
10	R = OMe	118 h	46.8%	61.9%	11
11	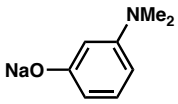	118 h	62.1%	92.8%	12
12	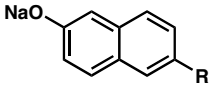 R = H	62 h	56.8%	88.8%	15
13	R = OMe	46 h	46.9%	65.1%	13
14	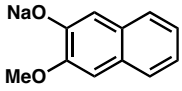	46 h	42.6%	56.7%	13
15	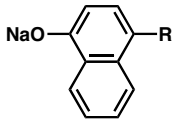 R = H	115 h	49.8%	67.8%	11
16	R = Cl	115 h	36.7%	50.2%	23
17	R = OMe	114 h	47.5%	73.9%	22
18	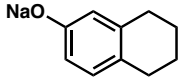	46 h	45.7%	58.6%	10

[a] Pd(sparteine)Cl_2 (**66**), (–)-sparteine (**28**), and alkoxide were stirred in $CHCl_3$ 1 h prior to addition of (±)-**73**. [b] Prepared by treatment of the corresponding phenol with Na (1 equiv) in toluene followed by concentration under reduced pressure. [c] Measured by GC. [d] Measured by chiral HPLC. [e] Cs_2CO_3 (40 mol%) was added.

The similar results for a wide range of phenoxides as additives in the kinetic resolution imply that instead of forming a discrete palladium phenoxide complex, the electron-rich phenoxides could just be acting as soluble bases. Some evidence indicating that palladium phenoxides are forming in situ include the isolation and crystallographic analysis of Pd(sparteine)(OC_6F_5)$_2$ (**239**) and the impact of steric effects on the rates of oxidation with some phenoxides (Table 4.2.3, entries 9, 10, and 15-17). Unfortunately, the isolation of palladium complexes with more electron-rich phenoxides that are active precatalysts in the oxidative kinetic resolution has been unsuccessful to date.

For further studies, two enantiomeric BINOL-derived phenoxides were prepared[12] and used as additives in the kinetic resolution (Table 4.2.4). While there is a difference in the initial oxidation rates of the resolutions, the outcomes of the resolutions are nearly identical, with selectivity factors of 20-21 in both cases. Either no palladium phenoxide complexes are formed in these reactions and the phenoxides are acting as soluble non-enantioselective bases, or the enantiomeric BINOL-derived phenoxides impart no chiral influence on the reaction when the two diastereomeric palladium phenoxide complexes are formed in situ.

Table 4.2.4 BINOL-derived phenoxides as additives.

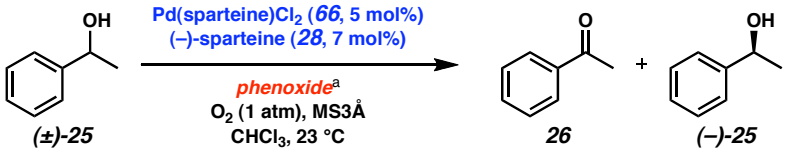

entry	phenoxide[b]	time	conversion[c]	alcohol ee[d]	*s*
1	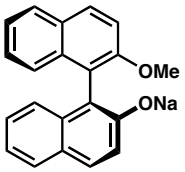	19 h	37.7%	51.3%	20
2		43 h	62.7%	>99%	>21
3	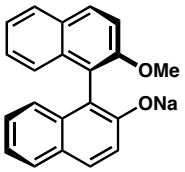	19 h	50.4%	80.4%	21
4		43 h	61.4%	>99%	>21

[a] Pd(sparteine)Cl_2 (**66**), (–)-sparteine (**28**), and alkoxide were stirred in $CHCl_3$ 1 h prior to addition of (±)-**25**. [b] Prepared by treatment of the corresponding phenol with Na (1 equiv) in toluene followed by concentration under reduced pressure. [c] Measured by GC. [d] Measured by chiral HPLC.

If a palladium bis-phenoxide complex is forming in situ, then the catalyst precursor should have little influence on the outcome of the resolution. To test this hypothesis, the sodium salt of 6-methoxy-2-naphthol was added to resolutions with a number of palladium precursors (Table 4.2.5). As described previously, reaction rate and selectivity are similar with Pd(sparteine)Cl_2 (**66**) and cesium carbonate or the naphthoxide (entries 1 and 2). However, in the case of Pd(sparteine)$(OAc)_2$ (**231**) or Pd(sparteine)$(TFA)_2$ (**241**),[13] which both display decreased selectivity with cesium carbonate (entries 3 and 5, respectively), a substantial improvement in the *s* factors is observed on addition of naphthoxide (entries 4 and 6). While the catalysts in these systems are still not as active as in the case of dichloride complex **66**, these results still demonstrate that phenoxides can have a large impact on the selectivity of the kinetic resolution. Because the selectivity is dictated by β-hydride elimination from a palladium

alkoxide complex, these results present strong evidence for the formation of palladium phenoxide complexes in situ.

Table 4.2.5 Counterion variation with phenoxides.

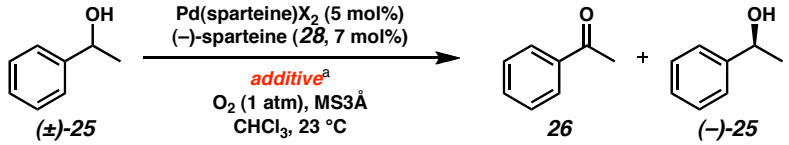

entry	X	additive[b]	time	conversion[c]	alcohol ee[d]	*s*
1	Cl	Cs_2CO_3 (40 mol%)	24 h	58.3%	97.8%	24
2	Cl	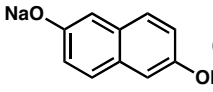 (10 mol%)	24 h	56.7%	97.6%	30
3	OAc	Cs_2CO_3 (40 mol%)	48 h	54.4%	72.8%	8.8
4	OAc	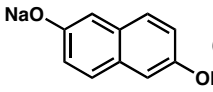 (10 mol%)	48 h	35.8%	50.2%	31
5	TFA	Cs_2CO_3 (40 mol%)	48 h	60.4%	85.0%	9.1
6	TFA	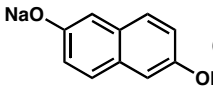 (10 mol%)	48 h	59.4%	95.0%	17

[a] Pd(sparteine)X_2, (–)-sparteine (**28**), and alkoxide were stirred in $CHCl_3$ 1 h prior to addition of (±)-**25**. [b] Phenoxide prepared by treatment of the phenol with Na (1 equiv) in toluene followed by concentration under reduced pressure. [c] Measured by GC. [d] Measured by chiral HPLC.

4.2.2 Bromide as Counterion in the Resolution

While phenoxides show promise in the oxidative kinetic resolution, other counterions have also been explored. Eric Ferreira had previously shown that $PdBr_2$ was not a good catalyst for alcohol oxidation at 80 °C (Table 4.1.1). The reaction rapidly darkened, indicating the aggregation of palladium(0). However, a crystal structure of Pd(sparteine)Br_2 (**242**) obtained by Raissa Trend led to a reinvestigation of bromide as a counterion.[1,14] As shown in Figure 4.2.2, the square plane of this complex is quite distorted. The sum of the six bond angles around the palladium center is 699.22°, largely

due to the 14.0° deflection of Br2 out of the plane. This much larger counterion distortion suggests that dibromide complex **242** could be a more active catalyst for the oxidative kinetic resolution than dichloride complex **66**.

Figure 4.2.2 Structure of Pd(sparteine)Br_2.

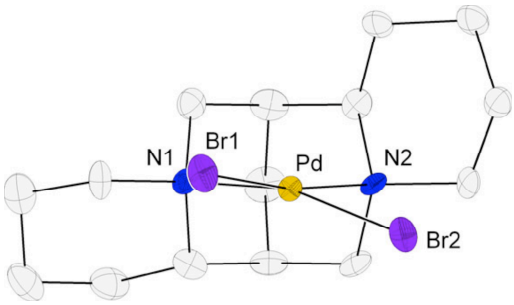

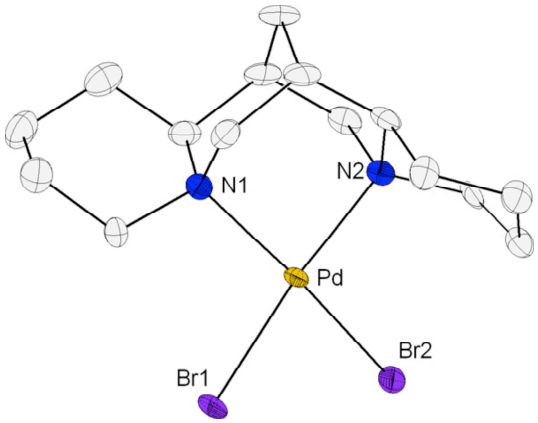

Select bond lengths (Å) and angles (°)			
Pd–N1	2.1510(18)	N1–Pd–N2	87.43(7)°
Pd–N2	2.1184(16)	Br1–Pd–Br2	84.155(10)°
Pd–Br1	2.4560(3)	N2–Pd–Br1	171.20(5)°
Pd–Br2	2.4474(3)	N1–Pd–Br2	165.96(5)°
		N1–Pd–Br1	96.25(5)°
		N2–Pd–Br2	94.22(5)°
		Σ ∠	699.22°

To more easily distinguish between the oxidation rates and selectivities of various catalysts, oxidations with the faster reacting enantiomer of 1-phenylethanol ((+)-**25**) were conducted (Table 4.2.6). In reactions conducted in chloroform at 23 °C, Pd(sparteine)Br_2 (**242**, entry 2) displays the highest reactivity, achieving 72.0% conversion to acetophenone (**26**) in only 4 h. Pd(sparteine)Cl_2 (**66**, entry 1) is significantly less active, providing 38.9% conversion. Several other palladium complexes (entries 3-5) have even lower rates of oxidation.

Table 4.2.6 Rate of oxidation of various palladium precatalysts.

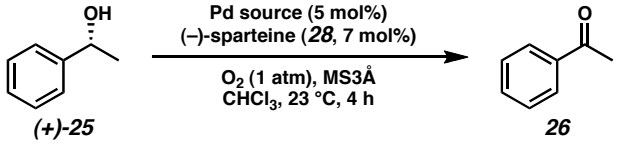

entry	Pd source	conversion[a]
1	Pd(sparteine)Cl_2 (***66***)	38.9%
2	Pd(sparteine)Br_2 (***242***)	72.0%
3	Pd(sparteine)I_2 (***243***)	17.5%
4	Pd(sparteine)$(OAc)_2$ (***231***)	7.8%
5	Pd(sparteine)$(TFA)_2$ (***241***)	30.3%

[a] Measured by GC.

In situ generation of the active catalyst with a number of palladium bromide sources and 12 mol% (–)-sparteine (**28**) was investigated (Table 4.2.7). $PdBr_2$ leads to a slower rate of oxidation (entry 1). The lower solubility of $PdBr_2$ may result in incomplete formation of Pd(sparteine)Br_2 in situ and therefore less of the active catalyst in solution. On the other hand, more soluble palladium bromide sources (entries 2-4) are viable as catalyst precursors and provide similar rates and only slightly decreased selectivity relative to the preformed complex (entry 5).

Table 4.2.7 Various dibromide precursors in the resolution.

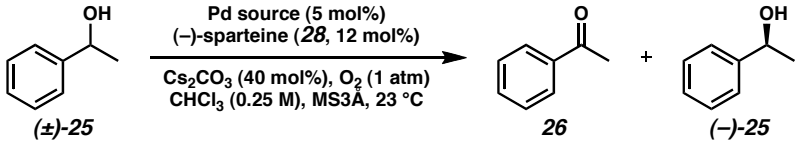

entry	Pd source	time	conversion[a]	alcohol ee[b]	*s*
1	$PdBr_2$	24 h	52.1%	88.1%	27
2	Pd$(CH_3CN)_2Br_2$ (***244***)	4.5 h	59.0%	97.6%	22
3	Pd(COD)Br_2 (***245***)	4.5 h	59.0%	97.3%	21
4	Pd(nbd)Br_2 (***246***)	4.5 h	48.2%	76.4%	23
5[c]	Pd(sparteine)Br_2 (***242***)	4 h	55.6%	95.6%	28

[a] Measured by GC. [b] Measured by chiral HPLC. [c] 7 mol% (–)-sparteine (**28**) added.

The optimal solvent for reactions with Pd(sparteine)Cl_2 (**66**) was chloroform,[11] so this solvent was chosen for the previous screens. However, a more thorough solvent investigation was undertaken at 23 °C (Table 4.2.8). Chlorinated solvents lead to the most rapid oxidations (entries 1-3). Dichloromethane has proven to be an even better solvent for high reaction rates. However, selectivity is decreased slightly with this solvent. Reactions in both acetone and 2-butanone (entries 5 and 6) display reasonable reaction rates and maintain the selectivity of reactions conducted in chloroform. Resolutions in tetrahydrofuran, *tert*-butyl alcohol, *p*-dioxane, and ethyl acetate (entries 9-12) exhibit excellent selectivity, but at the cost of prohibitively long reaction times. Toluene, a solvent successfully used previously in conditions with Pd(sparteine)Cl_2 (**66**), also performs well with Pd(sparteine)Br_2 (**242**). Though much slower than in chlorinated solvents or in acetone, oxidations are highly selective in toluene. Interestingly, *N*,*N*-dimethylformamide and acetonitrile (entries 4 and 7) support oxidations at comparable rates to acetone, but with substantially decreased selectivity. By and large, *s* factors are higher for solvents with lower dielectric constants. The more polar solvents could stabilize a larger counterion separation in the β-hydride elimination transition state, resulting in the observed decreased selectivity. The general trends in reactivity are harder to understand. Dielectric constants do not seem to account for the differences.[15] Catalyst solubility could be an important factor, as Pd(sparteine)Br_2 (**242**) is poorly soluble in most non-chlorinated solvents.

Table 4.2.8 Solvent screen with Pd(sparteine)Br_2.

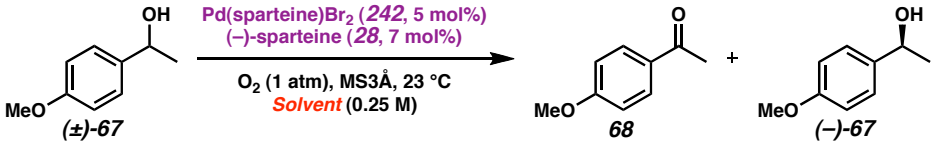

entry	solvent	dielectric constant	time	conversion[a]	alcohol ee[b]	*s*
1	CH_2Cl_2	8.93	2 h	61.5%	96.4%	15
2	DCE	10.42	4 h	56.6%	90.9%	17
3	***$CHCl_3$***	***4.81***	***4 h***	***55.2%***	***91.9%***	***22***
4	DMF	38.25	20 h	57.7%	73.0%	6.9
5	***acetone***	***21.01***	***30 h***	***55.9%***	***94.1%***	***23***
6	2-butanone	18.56	30 h	55.2%	91.6%	21
7	CH_3CN	36.64	30 h	54.7%	75.9%	10
8	***$PhCH_3$***	***2.38***	***50 h***	***52.1%***	***92.5%***	***41***
9	THF	7.52	144 h	54.8%	97.8%	41
10	*t*-BuOH	12.47	195 h	55.2%	96.8%	34
11	*p*-dioxane	2.22	120 h	38.1%	59.3%	98
12	EtOAc	6.08	144 h	39.3%	61.6%	76
13	H_2O:acetone (1:1)	80.10/21.01	72 h	19.8%	20.4%	13
14	$MeNO_2$	37.27	120 h	10.6%	–	–
15	pinacolone	12.73	48 h	2.8%	–	–
16	MTBE	–	48 h	1.3%	–	–

[a] Measured by GC. [b] Measured by chiral HPLC.

Optimization of conditions in toluene led to a number of useful resolution conditions (Table 4.2.9). Added cesium carbonate has a beneficial effect on oxidation rate in most resolutions with Pd(sparteine)Br_2 (**242**) in toluene (entries 3-5), as is the case with Pd(sparteine)Cl_2 (**66**) as catalyst. However, this exogenous base is slightly detrimental to the rate and selectivity of resolutions with dibromide complex **242** conducted at 23 °C (cf. entries 1 and 2). Presumably, the initial rate increase with added exogenous base is offset by formation of Pd(sparteine)(CO_3) (**69**), previously shown to be an inactive palladium complex generated under kinetic resolution conditions with

Pd(sparteine)Cl_2 (**66**).[16] Kinetic resolutions with dibromide complex **242** conducted at 60 °C under an atmosphere of molecular oxygen have exceptional rates (entry 3). As seen previously by Eric Ferreira (Table 4.1.1, entry 5), reactions conducted above 60 °C with Pd(sparteine)Br_2 (**242**) rapidly lose catalytic activity and become black, indicating palladium(0) aggregation. This system is also viable under ambient air atmosphere (entries 4 and 5). However, resolutions under ambient air in toluene must be conducted below 60 °C to prevent catalyst decomposition.

Table 4.2.9 Pd(sparteine)Br_2 conditions in toluene.

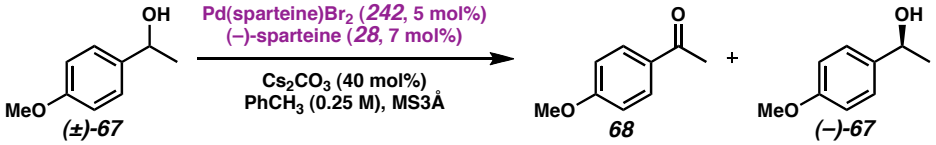

entry	temperature	oxidant (1 atm)	time	conversion[a]	alcohol ee[b]	*s*
1[c]	23 °C	O_2	50 h	52.1%	92.5%	41
2	23 °C	O_2	72 h	52.9%	88.6%	25
3	60 °C	O_2	3 h	52.4%	92.7%	39
4[d]	50 °C	air	4.5 h	57.0%	96.9%	26
5[d]	23 °C	air	50 h	54.8%	98.3%	44

[a] Measured by GC. [b] Measured by chiral HPLC. [c] No Cs_2CO_3. [d] Conducted with 15 mol% (–)-sparteine (**28**).

Conditions with Pd(sparteine)Br_2 (**242**) as catalyst in either toluene at 60 °C or chloroform at 23 °C are much more active in the oxidation of secondary alcohols than similar conditions with Pd(sparteine)Cl_2 (**66**). Thus, we looked to apply these more reactive systems to the kinetic resolution of alcohols that had proven challenging for our previous systems.[17] Table 4.2.10 displays a variety of secondary alcohols that require prolonged reaction times to reach even modest enantiomeric excesses. Several hindered benzylic alcohols (entries 1-3), enol ether **98** (entry 4), and non-activated alkyl alcohol

136 (entry 5) are slow to oxidize under conditions with Pd(sparteine)Cl_2 (**66**) in chloroform.

Table 4.2.10 Slow substrates with Pd(sparteine)Cl_2.

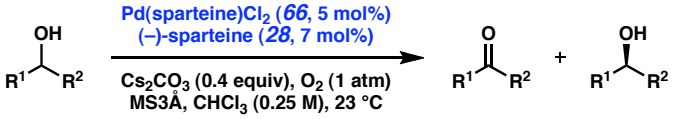

entry	alcohol, major enantiomer	time	conversion[a]	alcohol ee[b]	*s*
1	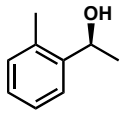 ***(–)-72***	63 h	40.1%	49.2%	11
2	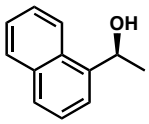 ***(–)-78***	97 h	51.2%	65.9%	8.5
3	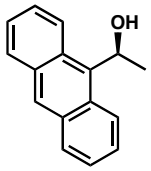 ***(–)-247***	48 h	21.8%	– [c]	–
4	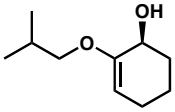 ***(S)-98***	74 h	52.2%	85.9%	23
5	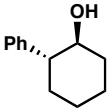 ***(+)-136***	93 h	38.2%	46.9%	12

[a] Measured by GC. [b] Measured by chiral HPLC. [c] Not determined.

When these alcohols are exposed to conditions with Pd(sparteine)Br_2 (**242**) in chloroform, on the other hand, successful resolutions are achieved (Table 4.2.11). Hindered benzylic alcohols (entries 6-10) are able to be resolved in reasonable times with increased selectivity relative to conditions with dichloride complex **66**. Even alkyl alcohol **136** (entries 12 and 13), which lacks an adjacent activating group such as an aromatic ring or alkene, can be resolved to high enantiomeric excess. Substrates that are

successfully resolved with Pd(sparteine)Cl_2 (**66**) can also be selectively oxidized with Pd(sparteine)Br_2 (**242**) (entries 1-5), but with substantially shorter reaction times. This catalyst system is sufficiently active to perform oxidations at temperatures below 23 °C too (entries 4 and 5). Finally, ambient air is competent as the terminal oxidant in these resolutions (entries 2, 7, 9, and 13), providing comparable rates and selectivities to reactions conducted under an atmosphere of molecular oxygen (entries 1, 6, 8, and 12).

Table 4.2.11 Substrate scope with Pd(sparteine)Br_2.

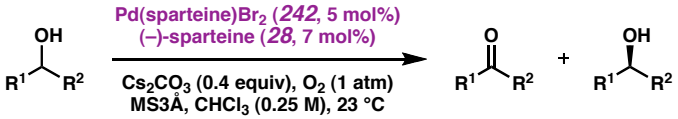

entry	alcohol, major enantiomer	time	conversion[a] (yield)[b]	alcohol ee[c]	*s*
1	 *(–)-25*	4 h	55.6% (43%)	95.6%	28
2[d]		5 h	55.3%	94.7%	27
3	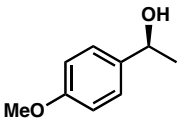 *(–)-67*	4 h	59.4% (41%)	95.4%	17
4[e]		8 h	59.3%	96.9%	20
5[f]	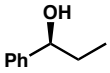 *(–)-83*	24 h	59.9%	97.8%	20
6	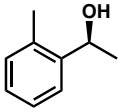 *(–)-72*	41 h	63.5% (35%)	97.1%	14
7[d]		30 h	63.4%	96.2%	13
8	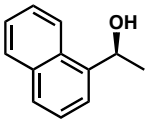 *(–)-78*	24 h	59.6% (40%)	92.5%	14
9[d]		21 h	64.9%	98.5%	15
10	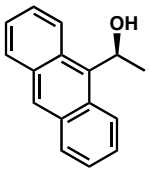 *(–)-247*	15 h	60.0%	91.2%	12
11	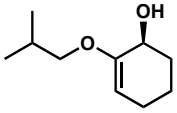 *(S)-98*	48 h	61.6%	97.0%	16
12	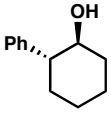 *(+)-136*	49 h	58.0% (40%)	90.6%	15
13[d]		45 h	57.7%	91.0%	15

[a] Measured by GC or ^{1}H NMR. [b] Isolated yield of enantioenriched alcohol. [c] Measured by chiral HPLC or GC. [d] Performed under ambient air. [e] Performed at 10 °C. [f] Performed at 4 °C.

4.3 Neutral Ligand Studies

4.3.1 Background and Early Results

In addition to exploring the counterion ligand for the palladium catalyst, we have also investigated the neutral ligand in the oxidative kinetic resolution. (–)-Sparteine (**28**)

emerged as the sole successful ligand in early studies by Eric Ferreira.[3] While the commercial availability of this diamine made it an attractive ligand for this process, the scarcity of its enantiomer (*ent*-(+)-**28**) was a major limitation to the broad utility of the method.[18] Thus, we sought an alternative chiral ligand for the resolution.[19]

Eric Ferreira and Jeffrey Bagdanoff explored a large number of potential ligands for the oxidative kinetic resolution (Figure 4.3.1). A range of bisoxazolines, bispidines, diamines, monoamines, and phosphines were examined. None of these compounds promoted significant enantioselective oxidation of secondary alcohols.[10]

Figure 4.3.1 Previously examined unsuccessful ligands.

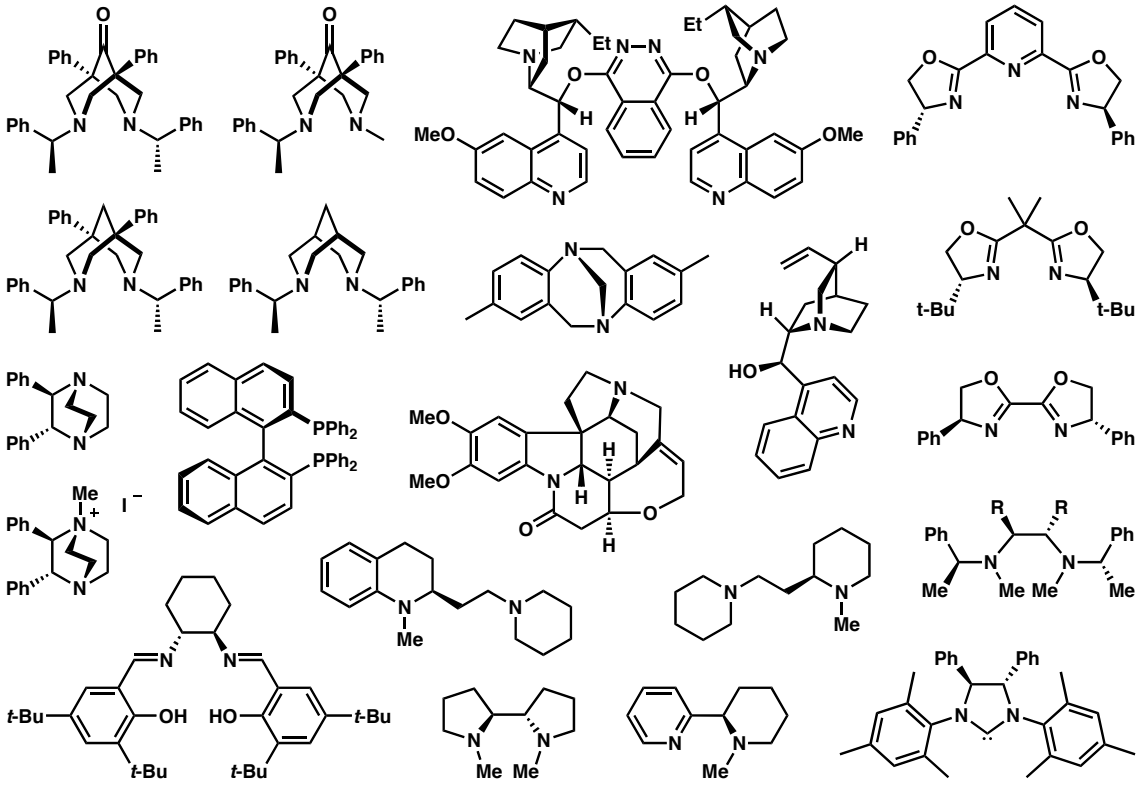

Our efforts built upon the lessons learned in these early experiments. Many common ligands, such as electron-rich phosphines, are unstable to the aerobic conditions

of the resolution. However, the system requires a sufficiently electron-rich ligand to strongly coordinate to the palladium center, promote enantioselective oxidation, and suppress palladium(0) aggregation. Monodentate ligands were anticipated to be too labile and unable to impart enough of a chiral influence on the kinetic resolution to be successful ligands.[20] Thus, diamines were targeted as oxidatively stable, bidentate ligands for the resolution. As seen in Figure 4.3.2, a variety of diamine motifs were investigated with $Pd(nbd)Cl_2$. Not only was there no kinetic resolution under aerobic conditions with any of the diamines, little non-enantioselective oxidation of secondary alcohols was observed.

Figure 4.3.2 Ligands not promoting oxidative kinetic resolution.

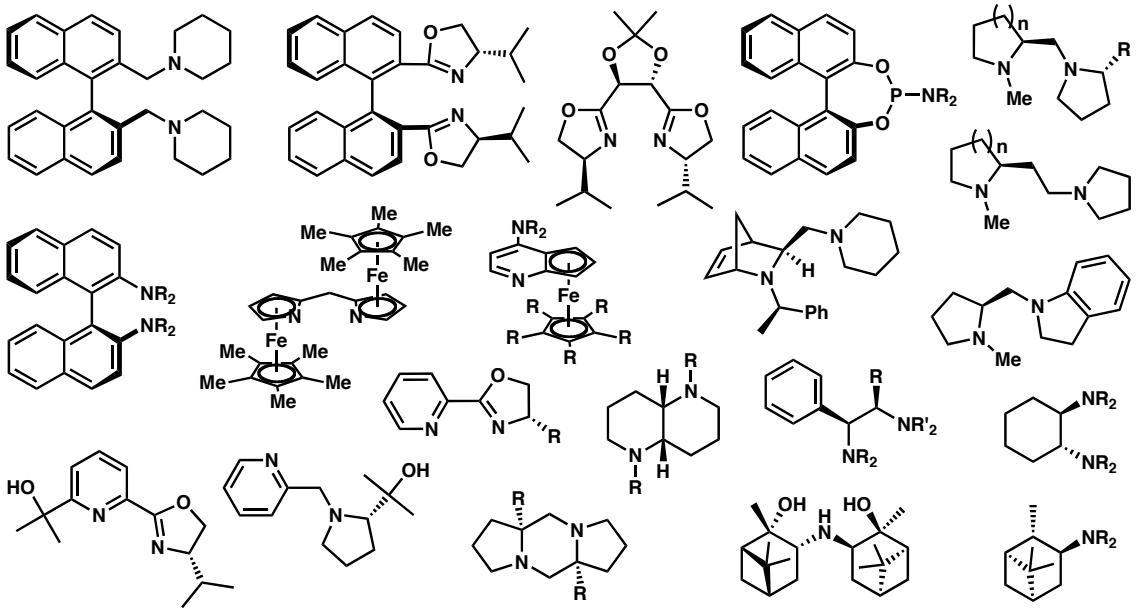

Inspiration for additional research was taken from rate studies performed by Jeffrey Bagdanoff (Table 4.3.1).[10] He evaluated a variety of diamines in the oxidation of (+)-1-phenylethanol ((+)-**25**). (–)-Sparteine (**28**) was a superior ligand for this reaction (entry 1). A number of linear diamines were largely ineffective (entries 2-4), as were

aromatic diamines (entries 7 and 8). Notably, only a diamine with a bispidine core similar to (–)-sparteine (**28**) promoted substantial alcohol oxidation (entry 9).

Table 4.3.1 Oxidation rates with various diamines.

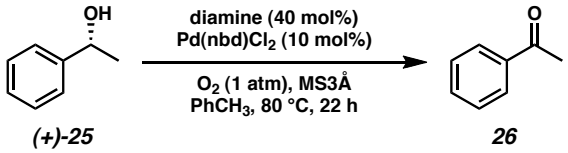

(+)-25 *26*

entry	diamine	conversion[a]	entry	diamine	conversion[a]
1	(–)-sparteine (***28***)	94.2%	6	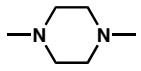	2.6%
2	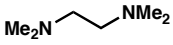	0.7%	7	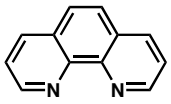	2.2%
3		8.8%			
4	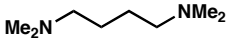	3.8%	8	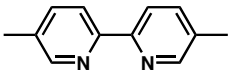	1.5%
5	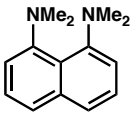	3.0%	9	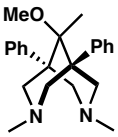	48.2%

[a] Measured by GC.

The successful oxidation with a bispidine led us to diamine **248**. O'Brien has demonstrated the ability of this diamine to act as a (+)-sparteine mimic in a number of processes (Scheme 4.3.1).[21] The enantioselective deprotonation of Boc-pyrrolidine (**249**) was accomplished by treatment with *sec*-butyllithium and diamine **248**. Subsequent trapping with chlorotrimethylsilane afforded silylpyrrolidine **250** in 90% ee.[22] The enantioselective deprotonation of cyclooctene oxide (**251**) provided alcohol **252** in 70% yield and a modest 62% ee. Finally, the deracemization of (±)-BINOL ((±)-**253**) was accomplished utilizing diamine **248** as a chiral promoter. Coordination of the diamine to copper(I) chloride, oxidation to a copper(II) species, coordination of diol (±)-**253**, thermal

equilibration, and treatment with concentrated hydrochloric acid liberated enantioenriched (+)-BINOL ((+)-**253**) in good yield and excellent enantiomeric excess.[21]

Scheme 4.3.1 Diamine **248** in asymmetric transformations.

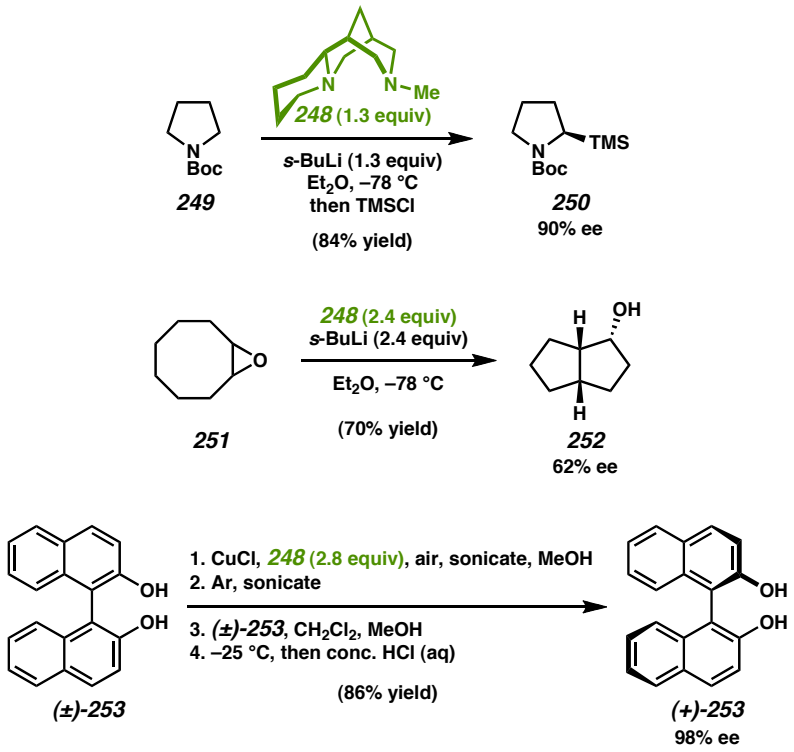

4.3.2 (–)-Cytisine-Based Diamines in the Oxidative Kinetic Resolution with $PdCl_2$

We anticipated that this diamine framework would be excellent for the kinetic resolution. Diamine **248** contains two coordinating, electron-rich tertiary amines that are stable to oxidation. Furthermore, as in the case of (–)-sparteine (**28**), this diamine contains a rigid bispidine core, which could provide a good chiral framework when coordinated to the palladium center.

A variety of potential ligands related to diamine **248** are readily prepared from (–)-cytisine (**254**). Substantial quantities of this alkaloid can be extracted from the seeds of the common decorative tree *Laburnum anagyroides*, the Golden Chain Tree.[23] From

this alkaloid, a number of known procedures can be followed to prepare diamines with a range of *N*-substitution. Acylation of the secondary amine of alkaloid **254** generates a number of amides in good to excellent yields (Scheme 4.3.2). Pyridone reduction with Adams' catalyst followed by exhaustive reduction with lithium aluminum hydride affords diamines **248** and **260**-**263**, with a variety of alkyl substituents.[23,24] Alternatively, reductive amination of (–)-cytisine (**254**) with acetone provides pyridone **264** in 95% yield. Two-step reduction yields diamine **265**.[25]

Scheme 4.3.2 Known syntheses of (–)-cytisine-based diamines.

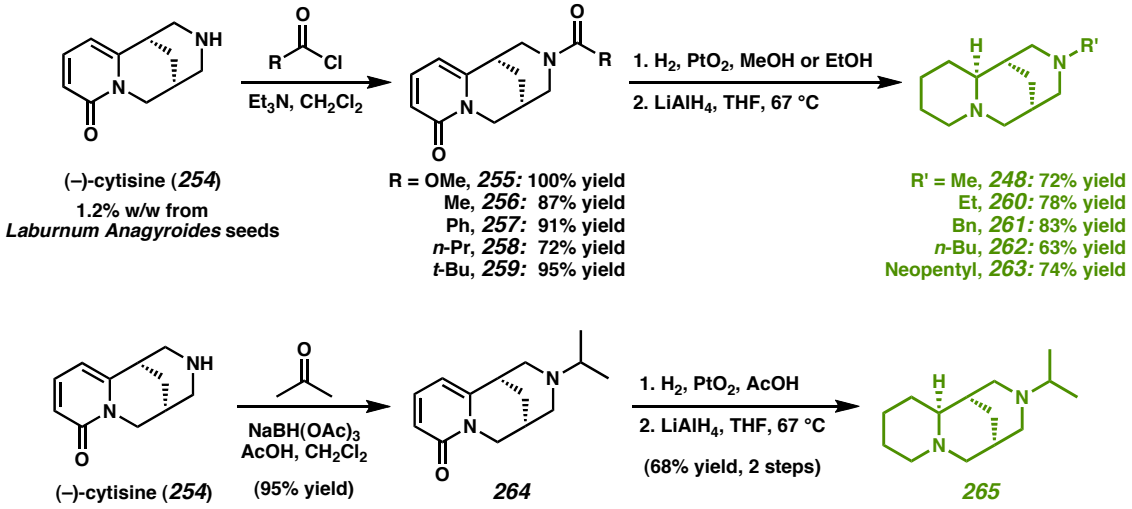

We also prepared several novel diamines (Scheme 4.3.3). Alkylation of (–)-cytisine (**254**) with isobutene oxide produces tertiary alcohol **266**.[26] Exhaustive reduction with hydrogen over Adams' catalyst and lithium aluminum hydride provides diamine **267**. Finally, hydrogenolysis of benzyl diamine **261** affords secondary amine **268**.

Scheme 4.3.3 Syntheses of novel diamines.

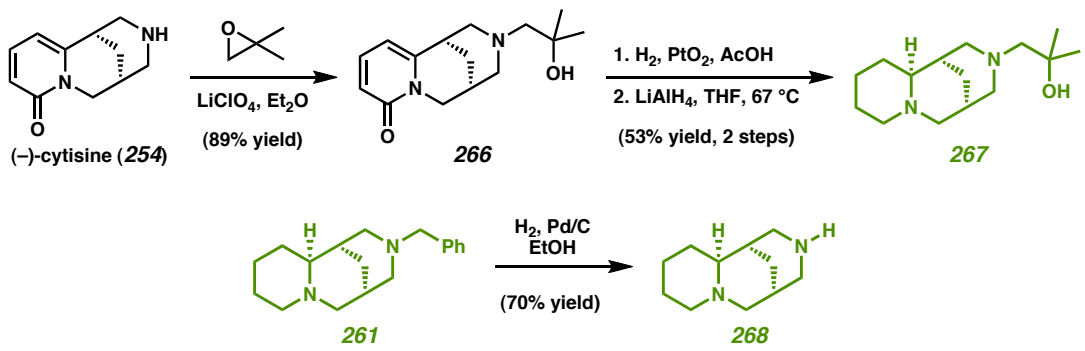

In order to assess the coordination of this structural framework to palladium salts, diamines **248** and **260** were exposed to Pd(nbd)Cl_2. Ligand exchange produces palladium complexes **269** and **270** in 83% and quantitative yields, respectively.

Scheme 4.3.4 Synthesis of dichloride complexes of diamines.

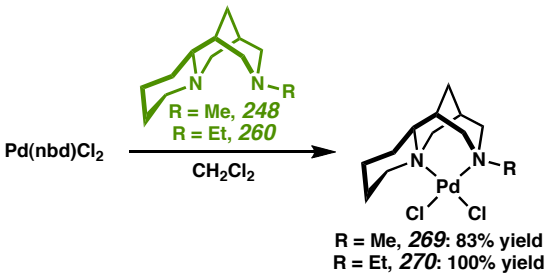

These metal complexes are readily crystallized by slow diffusion of heptane into a saturated chloroform solution. Subsequent X-ray crystallographic analysis confirms the structure of these dichloride complexes. The *N*-methyl derivative (**269**) is shown in Figure 4.3.3. This complex, like palladium complexes with (–)-sparteine (**28**), has a distorted square planar geometry, and the sum of the six bond angles around the palladium center is 704.67°. While (–)-sparteine complexes display a decreased N1–Pd–Cl2 angle, the projecting N1 piperidine ring of pseudo-enantiomeric diamine **248** results in a deflection of Cl1 of 11.9°. Because of the distortion of Cl1 instead of Cl2, we

predicted that this complex would have the opposite selectivity in the kinetic resolution, providing alcohols in the other enantiomeric series to those generated with (–)-sparteine (**28**).

Figure 4.3.3 Structure of *N*-methyl complex **269**.

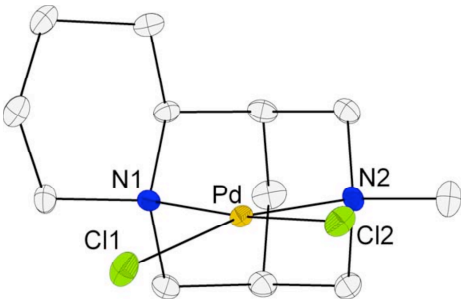

Select bond lengths (Å) and angles (°)			
Pd–N1	2.1116(14)	N1–Pd–N2	86.67(6)°
Pd–N2	2.1038(14)	Cl1–Pd–Cl2	84.895(18)°
Pd–Cl1	2.3197(4)	N2–Pd–Cl1	168.14(4)°
Pd–Cl2	2.3262(4)	N1–Pd–Cl2	175.64(4)°
		N1–Pd–Cl1	94.80(4)°
		N2–Pd–Cl2	94.52(4)°
		Σ ∠	704.67°

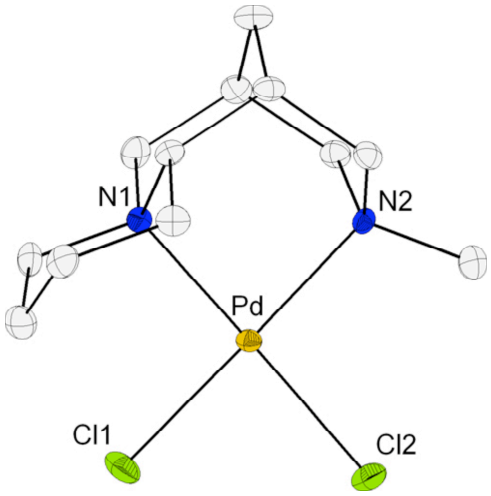

The structure of *N*-ethyl complex **270**, however, is contrary to what would be expected (Figure 4.3.4). It does still have a distorted square planar geometry about the metal center (sum of the six bond angles around the palladium center is 707.01°). However, Cl2 is deflected out of the plane by 8.8°, similar to Pd(sparteine)Cl_2 (**66**, see Figure 4.1.2), instead of displaying a Cl1 deformation as would be expected by a complex with a pseudo-enantiomeric diamine to (–)-sparteine. The cause of this geometric abnormality is still under investigation.

Figure 4.3.4 Structure of *N*-ethyl complex **270**.

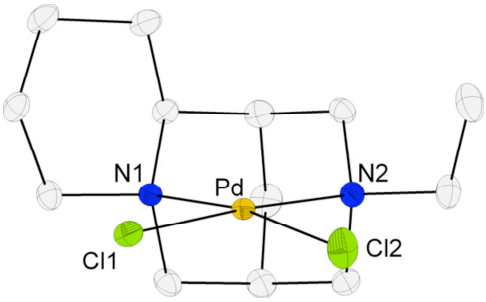

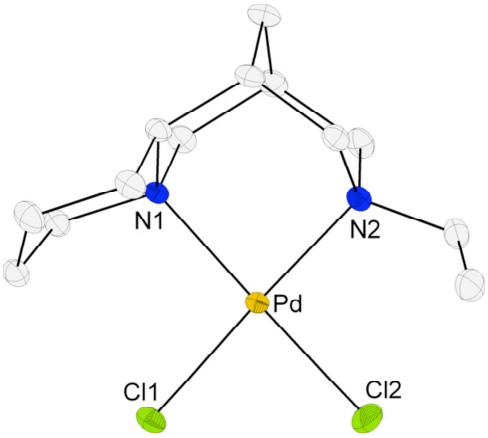

Select bond lengths (Å) and angles (°)			
Pd–N1	2.1294(16)	N1–Pd–N2	86.90(6)°
Pd–N2	2.1114(16)	Cl1–Pd–Cl2	83.73(2)°
Pd–Cl1	2.3254(5)	N2–Pd–Cl1	176.22(5)°
Pd–Cl2	2.3116(5)	N1–Pd–Cl2	171.22(4)°
		N1–Pd–Cl1	95.33(4)°
		N2–Pd–Cl2	93.61(5)°
		Σ ∠	707.01°

Next, these diamines were explored in oxidative kinetic resolutions (Table 4.3.2). For a variety of alkyl group substitutions, selectivity appears to decrease as the *N*-alkyl substituent increases in size (entries 2-6). Notably, *N*-ethyl diamine **260** (entry 3), whose palladium complex (**270**) exhibits the unexpected halide distortion, still provides the same major enantiomer of alcohol as *N*-methyl diamine **248** (entry 2). Both benzyl diamine **261** and secondary amine **268** were completely inactive (entries 7 and 8). Pentadeuterated diamine **271**,[27] a derivative of *N*-methyl diamine **248** postulated to be less prone to oxidation by β-hydride elimination, performs similarly to the undeuterated diamine (cf. entries 2 and 9). Interestingly, tertiary alcohol **267** gives the highest selectivity in the resolution of (±)-1-phenylethanol ((±)-**25**), though oxidations conducted with this ligand are extremely slow.

Table 4.3.2 Diamine substituent screen in the resolution.

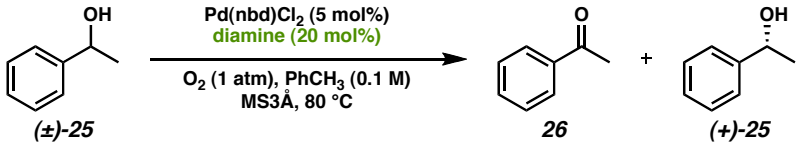

(±)-25 ***26*** ***(+)-25***

entry	diamine	time	conversion[a]	alcohol ee[b]	*s*
1	R = $CH_2C(OH)(CH_3)_2$: ***267***	76 h	27.3%	33.1%	22
2	= Me: ***248***	98 h	45.1%	53.8%	9.6
3	= Et: ***260***	29 h	61.2%	76.2%	7.0
4	= *n*-Bu: ***262***	48 h	54.8%	51.3%	4.0
5	= *i*-Pr: ***265***	145 h	28.4%	18.8%	3.4
6	= Neopentyl: ***263***	24 h	0.6%	–	–
7	= Bn: ***261***	24 h	0.0%	–	–
8	= H: ***268***	76 h	0.0%	–	–
9	***271***	115 h	52.4%	69.9%	9.1
10	(–)-sparteine (***28***)	96 h	59.9%	-98.7%	23

[a] Measured by GC. [b] Measured by chiral HPLC.

Further investigations with this class of ligands were pursued with diamines **248** and **260**. The increased reactivity of catalytic systems with the *N*-ethyl diamine (**260**) were useful for kinetic resolutions of a collection of alcohols in toluene (Table 4.3.3). Cyclohexenol (±)-**119** and cyclopentenol (±)-**111** are able to be resolved with a similar rate and selectivity with diamine **248** (entries 1 and 3) as with (–)-sparteine (entries 2 and 4). Methylcyclopentenol (±)-**120**, on the other hand, is not as efficiently resolved with this (+)-sparteine mimic. Generally, other secondary alcohols studied with this system have poor reactivity and selectivity compared to similar resolutions conducted with (–)-sparteine (**28**).

Table 4.3.3 *N*-Ethyl diamine resolution in toluene with $Pd(nbd)Cl_2$.

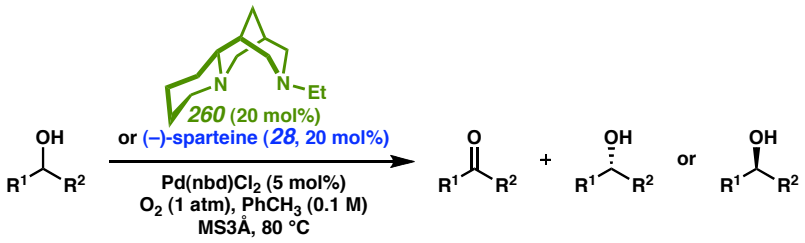

entry	alcohol, major enantiomer	diamine	time	conversion[a]	alcohol ee[b]	*s*
1	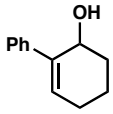 ***(R)-(+)-119***	N-Et diamine (***260***)	23 h	59.2%	98.2%	23
2	***(S)-(–)-119***	(–)-sparteine (***28***)	23 h	60.0%	99.3%	26
3	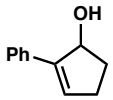 ***(R)-(–)-111***	N-Et diamine (***260***)	23 h	60.8%	99.4%	24
4	***(S)-(+)-111***	(–)-sparteine (***28***)	21 h	57.4%	99.0%	33
5	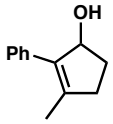 ***(R)-(+)-120***	N-Et diamine (***260***)	10 h	62.3%	98.8%	19
6	***(S)-(–)-120***	(–)-sparteine (***28***)	4 h	52.9%	99.0%	83

[a] Measured by GC. [b] Measured by chiral HPLC.

As is the case with resolutions involving (–)-sparteine, chloroform is an excellent solvent for enantioselective oxidations with *N*-methyl diamine **248**. In addition to the substrates able to be resolved with *N*-ethyl diamine **260** above (entries 1, 3, and 5), a benzylic alcohol (entry 7), and a cyclopropylcarbinyl alcohol (entry 9) are successfully resolved to high enantiomeric excesses. Somewhat lower selectivity is observed with this system compared to the analogous conditions with (–)-sparteine. More disconcerting is the substantially decreased reactivity seen with diamine **248**. Additional research involved improving the reactivity of catalysts derived from these diamines.

Table 4.3.4 *N*-Methyl diamine resolution in chloroform with $Pd(nbd)Cl_2$.

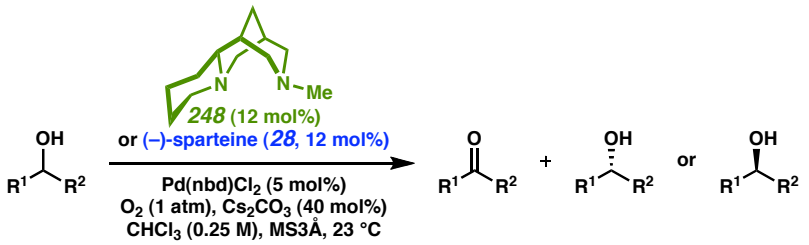

entry	alcohol, major enantiomer		diamine	time	conversion[a]	alcohol ee[b]	*s*
1	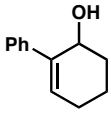	***(R)-(+)-119***	N-Me diamine (***248***)	60 h	59.3%	94.7%	17
2		***(S)-(–)-119***	(–)-sparteine (***28***)	24 h	55.4%	96.8%	33
3	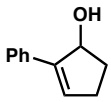	***(R)-(–)-111***	N-Me diamine (***248***)	36 h	59.1%	99.0%	27
4		***(S)-(+)-111***	(–)-sparteine (***28***)	11 h	58.4%	98.8%	28
5	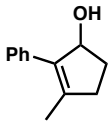	***(R)-(+)-120***	N-Me diamine (***248***)	24 h	68.1%	99.5%	14
6		***(S)-(–)-120***	(–)-sparteine (***28***)	9 h	57.9%	96.9%	23
7	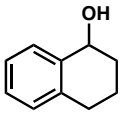	***(R)-(–)-82***	N-Me diamine (***248***)	48 h	61.8%	99.5%	23
8		***(S)-(+)-82***	(–)-sparteine (***28***)	24 h	58.0%	98.4%	28
9	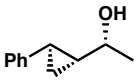	***(–)-126***	N-Me diamine (***248***)	107 h	50.3%	71.4%	12
10		***(+)-126***	(–)-sparteine (***28***)	25 h	58.6%	99.0%	28

[a] Measured by GC. [b] Measured by chiral HPLC.

The selectivity observed with diamine **248** is in line with the selectivity model proposed for the oxidative kinetic resolution with (–)-sparteine (Scheme 4.3.5).[8] For $Pd(sparteine)Cl_2$ (**66**), faster reacting alcohol (–)-**111** proceeds through intermediate **141** to undergo β-hydride elimination via transition state **142** to provide ketone **143**. Conversely for *N*-methyl complex **269**, alcohol (+)-**111** is the faster reacting enantiomer. Alcohol coordination generates intermediate palladium alkoxide **272**, which undergoes β-hydride elimination via transition state **273** to provide ketone **143** as well.

Scheme 4.3.5 Comparison of selectivity with different diamine ligands.

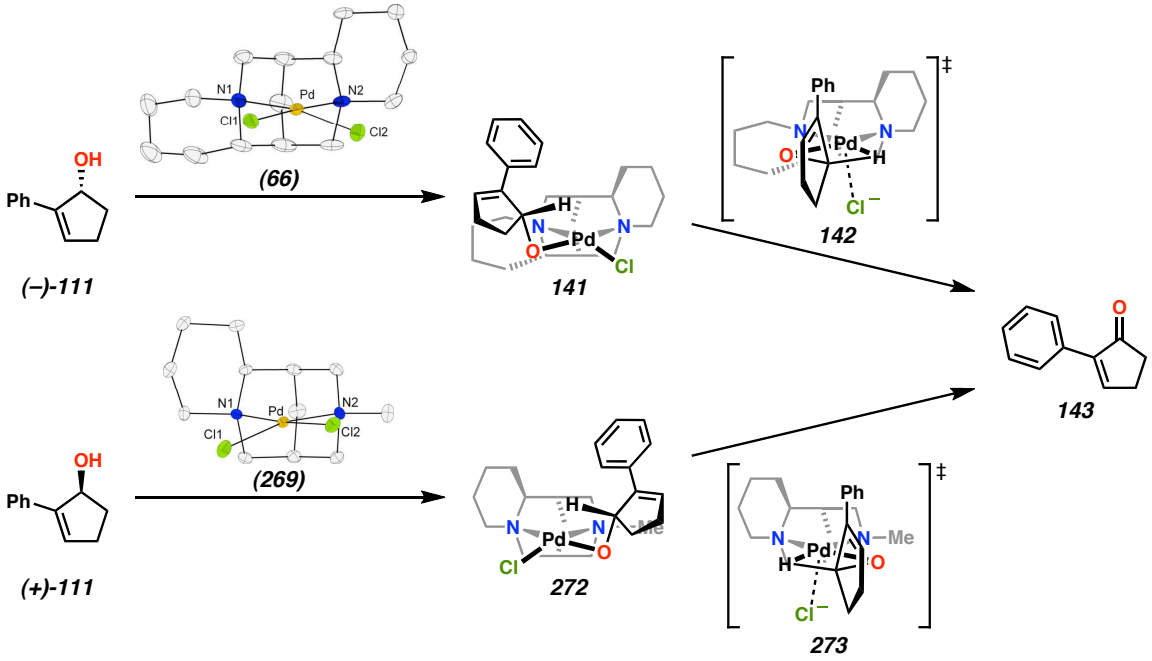

4.3.3 Alternative Diamine with $PdBr_2$ in the Oxidative Kinetic Resolution

The decreased reactivity of catalytic systems with the (–)-cytisine-based diamines led us to apply insights gained from the previous counterion studies to improve oxidation rates. Thus, dibromide complex **274** was prepared by treatment of dibromide precursor **244** with diamine **248** in dichloromethane (Scheme 4.3.6). This complex was recrystallized to provide crystals suitable for X-ray analysis (Figure 4.3.5), which reveals a distorted square planar geometry (sum of the six bond angles around palladium is 701.69°). The Br1 deflection is large (14.2°), but comparable with the deformation of Br2 of Pd(sparteine)Br_2 (**242**, 14.0°). Based on this larger deflection relative to dichloride complex **66** (11.9°), we anticipated that dibromide complex **274** would be a highly active catalyst for the oxidative kinetic resolution.

Scheme 4.3.6 Synthesis of dibromide complex **274**.

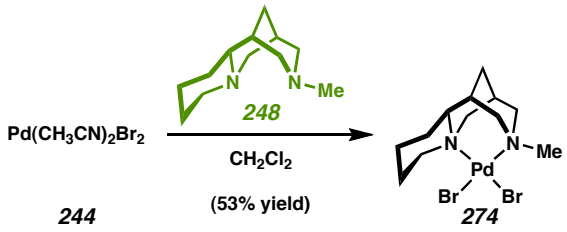

Figure 4.3.5 Structure of dibromide complex **274**.

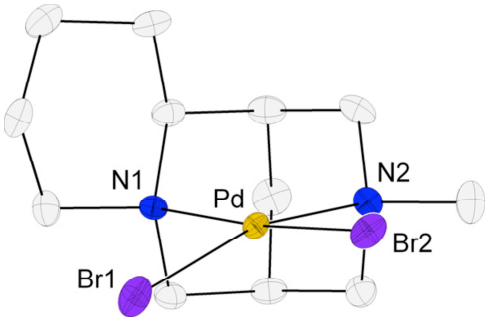

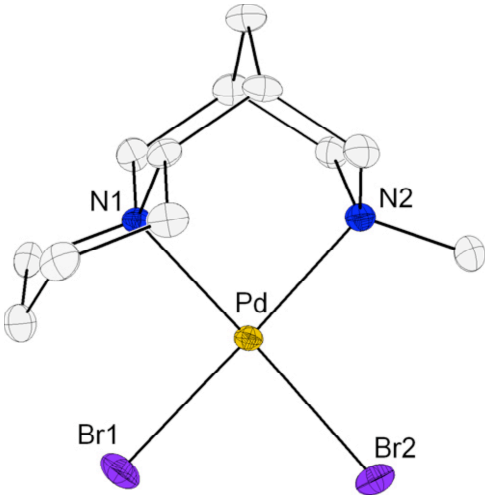

Select bond lengths (Å) and angles (°)			
Pd–N1	2.126(2)	N1–Pd–N2	86.46(8)°
Pd–N2	2.117(2)	Br1–Pd–Br2	84.449(12)°
Pd–Br1	2.4463(3)	N2–Pd–Br1	165.81(6)°
Pd–Br2	2.4513(3)	N1–Pd–Br2	174.56(6)°
		N1–Pd–Br1	95.17(6)°
		N2–Pd–Br2	95.24(6)°
		Σ ∠	701.69°

Diamine **248** was then explored in enantioselective oxidations of (±)-1-phenylethanol ((±)-**25**) with $Pd(CH_3CN)_2Br_2$ (**244**) as the dibromide catalyst precursor (Table 4.3.5). Analogous to the (–)-sparteine complexes, the catalyst derived from dibromide **244** is substantially more active than those derived from dichloride salts, while maintaining similar selectivity factors (cf. entries 1 and 4). An excess of diamine **248** is required to maintain viable catalysts (entries 4-7), though a large excess leads to some catalyst deactivation (entries 2 and 3). Use of the preformed dibromide complex (**274**) provides similar rates and selectivity (cf. entries 5 and 8). For operational simplicity, in

situ catalyst generation is preferred. Reactions maintained at 20 °C (entry 9) provide slightly improved selectivity and more consistent results than those at 23 °C (entry 5).

Table 4.3.5 Optimization of with *N*-methyl diamine and $PdBr_2$ sources.

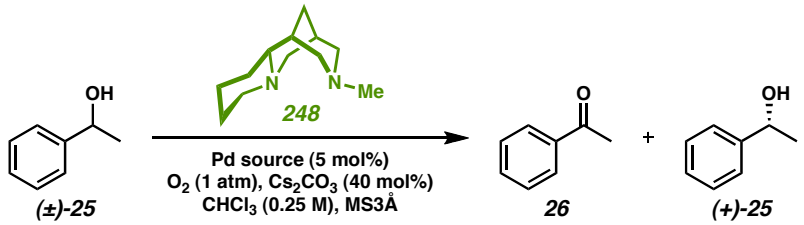

(±)-25 26 (+)-25

entry	Pd source	temperature	mol% diamine ***248***	time	conversion[a]	alcohol ee[b]	*s*
1	$Pd(nbd)Cl_2$	23 °C	12	41 h	29.9%	37.0%	20
2	$Pd(CH_3CN)_2Br_2$ (***244***)	23 °C	20	45 h	31.0%	38.9%	20
3	$Pd(CH_3CN)_2Br_2$ (***244***)	23 °C	15	35 h	39.9%	56.2%	21
4	$Pd(CH_3CN)_2Br_2$ (***244***)	23 °C	12	32 h	58.0%	96.1%	21
5	$Pd(CH_3CN)_2Br_2$ (***244***)	23 °C	10	35 h	55.5%	92.5%	22
6[c]	$Pd(CH_3CN)_2Br_2$ (***244***)	23 °C	7	24 h	41.6%	61.0%	24
7[c]	$Pd(CH_3CN)_2Br_2$ (***244***)	23 °C	5	35 h	19.3%	21.6%	24
8	$Pd(diamine)Br_2$ (***274***)	23 °C	5	41 h	56.1%	93.6%	22
9	$Pd(CH_3CN)_2Br_2$ (***244***)	20 °C	10	30 h	57.6%	97.1%	25

[a] Measured by GC. [b] Measured by chiral HPLC. [c] Pd black observed.

With optimized conditions in hand, we examined the scope of this transformation (Table 4.2.11). A number of benzylic alcohols are able to be resolved with good selectivity with this method (entries 1-5). Furthermore, allylic alcohols (entries 6-10), including several alcohols not successfully resolved with diamine **248** and $Pd(nbd)Cl_2$ (entries 9 and 10), are obtained with high enantiomeric excesses in shorter times. Cyclopropylcarbinyl alcohols containing three contiguous stereocenters are also resolved to high ee (entries 11 and 12). To further improve the practicality of the method, several resolutions were conducted under an atmosphere of ambient air. As seen in entries 2 and 4, kinetic resolutions under air perform nearly identically to those under an atmosphere of molecular oxygen (entries 1 and 3).

Table 4.3.6 Scope with dibromide catalysts of *N*-methyl diamine.

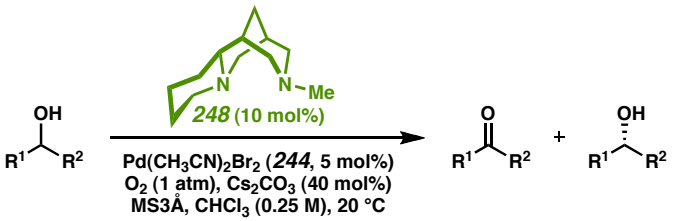

entry	alcohol, major enantiomer	time	conversion[a] (yield)[b]	alcohol ee[c]	*s*
1	 *(+)-25*	30 h	57.6% (40%)	97.1%	25
2[d]		34 h	57.9%	96.4%	22
3	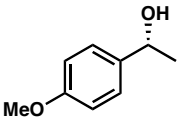 *(+)-67*	30 h	60.4%	97.7%	19
4[d]		34 h	61.2%	98.1%	19
5	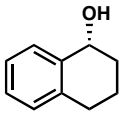 *(–)-82*	24 h	60.9% (38%)	90.2%	11
6	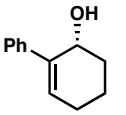 *(+)-119*	46 h	56.8% (43%)	90.7%	17
7	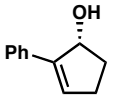 *(–)-111*	12 h	55.0%	94.1%	27
8	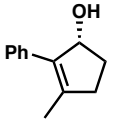 *(+)-120*	18 h	63.2%	94.4%	12
9	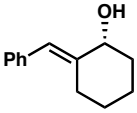 *(+)-105*	46 h	59.3% (39%)	90.6%	13
10	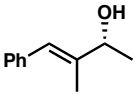 *(–)-104*	35 h	62.6%	92.0%	11
11	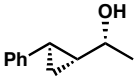 *(–)-126*	32 h	59.0% (40%)	90.2%	13
12	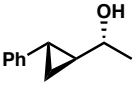 *(+)-128*	35 h	62.3%	90.0%	10

[a] Measured by GC or ^{1}H NMR. [b] Isolated yield of enantioenriched alcohol. [c] Measured by chiral HPLC. [d] Performed under ambient air.

4.4 Conclusion

Extensive counterion and neutral ligand studies have provided us with a thorough understanding of the factors that contribute to the reactivity and selectivity of the oxidative kinetic resolution of secondary alcohols. Solid-state X-ray crystallographic analysis proved vital to these studies, leading to many valuable insights. As a result, several greatly improved catalyst systems have been developed. Counterion investigations have led to the discovery of dibromide complexes of palladium with (–)-sparteine as highly active catalysts for the enantioselective aerobic oxidation of a broad range of substrates, including numerous examples of alcohols not resolved efficiently with previously developed Pd(sparteine)Cl_2 conditions. Broad surveys of neutral ligands have emphasized the unique ability of sparteine-like diamines to promote palladium-catalyzed oxidation, leading to diamines developed by O'Brien as excellent mimics of (+)-sparteine. These diamines have been employed successfully in the oxidative kinetic resolution, affording alcohols in the enantiomeric series opposite to that obtained with (–)-sparteine and greatly increasing the synthetic utility of this method.

4.5 Experimental Section

4.5.1 Materials and Methods

Pd(sparteine)Cl_2 (**66**),[8] Pd(sparteine)$(OAc)_2$ (**231**),[9] Pd(sparteine)$(TFA)_2$ (**241**),[13] Pd(sparteine)Br_2 (**242**),[1] Pd(COD)Br_2 (**245**), and Pd(nbd)Br_2 (**246**)[28] were prepared as previously reported. Palladium bromide was purchased from Strem Chemicals. (+)- And (–)-2'-methoxy-1,1'-binaphthyl-2-ol were prepared by the method of Xi.[12] (+)-1-Phenylethanol ((+)-**25**) was purchased from Acros Organics. (±)-(*E*)-3-Methyl-4-phenyl-3-buten-2-ol ((±)-**104**) was prepared by the method of West.[29] Diamines **248**,[22,23] **260**, **262**, **263**,[24] **261**, **265**,[25] and **271**[27] were prepared as previously described. Solvents were dried by passage through an activated alumina column under argon. Powdered 3Å molecular sieves were stored in a 120 °C drying oven until immediately prior to use. Other chemicals were prepared as described below, prepared as described in Chapter 3, or purchased from the Sigma-Aldrich Chemical Company and used as received. Unless stated otherwise, reactions were performed in flame-dried glassware sealed with rubber septa under a nitrogen atmosphere using dry, deoxygenated solvents. Liquids and solutions were transferred via syringe. Reaction temperatures were controlled using an IKAmag temperature modulator (heating) or a VWR 1160 refrigerated circulating bath (cooling). Thin-layer chromatography (TLC) was conducted with E. Merck silica gel 60 F254 pre-coated plates (0.25 mm) and visualized using a combination of UV at 254 nm, *p*-anisaldehyde, and potassium permanganate staining. ICN silica gel (particle size 32-63 μm) or SiliCycle Silia*Flash* P60 Academic silica gel (particle size 40-63 μm; pore diameter 60 Å) was used for flash column chromatography. Analytical achiral GC was performed on an Agilent 6850 GC with FID detector using an Agilent DB-WAX (30.0 m

x 0.25 mm) column at 1.0 mL/min He carrier gas flow. Chiral GC was performed on an Agilent 6850 GC with FID detector using a Chiraldex GTA column (30.0 m x 0.25 mm, purchased from Bodman Industries) at 1.0 mL/min He carrier gas flow. Analytical chiral HPLC was performed with an Agilent 1100 Series HPLC utilizing a Chiralpak AD, Chiralcel OD-H, Chiralcel OJ, or Chiralcel OB-H column (each is 4.6 mm x 25 cm) obtained from Daicel Chemical Industries, Ltd with visualization at 254 nm at 1.0 mL/min mobile phase. ^{1}H NMR spectra were recorded on a Varian Mercury 300 or 500 instrument (at 300 or 500 MHz, respectively) and are reported relative to Me_4Si (δ 0.0). Data for ^{1}H NMR spectra are reported in terms of chemical shift (δ ppm), multiplicity, coupling constant (Hz), and integration. ^{13}C NMR spectra were recorded on a Varian Mercury 300 or 500 instrument (at 75 or 126 MHz, respectively) and are reported relative to Me_4Si (δ 0.0). Data for ^{13}C NMR spectra are reported in terms of chemical shift (δ ppm). Melting points were determined on a Thomas-Hoover melting point apparatus and are uncorrected. Elemental analyses were carried out by Desert Analytics Laboratory, Tuscon, AZ. X-ray crystal structure analyses were obtained from the California Institute of Technology X-Ray Crystallography Laboratory. The absolute configurations of resolved alcohols were assigned based on comparisons of optical rotations to literature values or by analogy.

4.5.2 Preparation of Palladium Complexes and Diamines

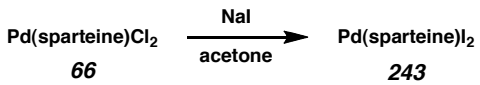

Diiodo(sparteine)palladium(II) (243). Sodium iodide (134 mg, 0.89 mmol, 2.1 equiv) was added to a suspension of complex **66** (175 mg, 0.43 mmol, 1.0 equiv) in

acetone (10 mL). The dark mixture was stirred at 23 °C for 30 min, after which the solvent was removed under reduced pressure. The solid was washed with copious amounts of H_2O followed by pentane to afford **243** as a dark purple solid: ^{1}H NMR (500 MHz, $CDCl_3$) δ 4.43 (app. dd, *J* = 12.5, 3.2 Hz, 1H), 4.33 (br. d, *J* = 11.7 Hz, 1H), 4.19 (ddd, *J* = 14.4, 13.1, 3.0 Hz, 1H), 3.92 (dt, *J* = 12.4, 2.4 Hz, 1H), 3.75-3.59 (comp. m, 2H), 2.97 (dd, *J* = 12.9, 3.4 Hz, 1H), 2.93-2.79 (comp. m, 2H), 2.54 (dd, *J* = 12.4, 3.1Hz, 1H), 2.17-1.37 (comp. m, 16H); ^{13}C NMR (126 MHz, $CDCl_3$) δ 72.2, 70.2, 66.5, 64.7, 63.8, 48.9, 35.0, 34.9, 29.5, 28.1, 27.3, 26.9, 24.3, 23.6, 21.8; IR (thin film/NaCl): 2935, 1440, 913, 728 cm^{-1}; HRMS-FAB (*m/z*): $[M]^+$ calcd for $[C_{15}H_{26}N_2I_2Pd]^+$, 593.9221; found, 593.9242.

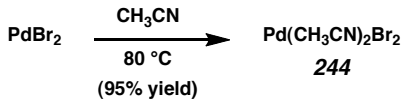

Dibromobis(acetonitrile)palladium(II) (244). Palladium bromide (532 mg, 2.0 mmol, 1.0 equiv) was added to acetonitrile (40 mL). The mixture was heated to 80 °C for 1.5 h. Once the solution became clear and orange-red, the reaction was cooled to 23 °C. The mixture was concentrated under reduced pressure to a volume of about 5 mL and then triturated with Et_2O (15 mL). The orange-red solid was filtered, washed with Et_2O (2 x 15 mL), and dried under vacuum to afford **244** (661 mg, 95% yield).

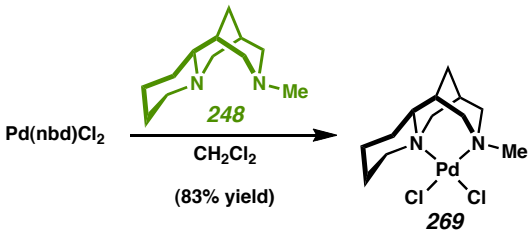

Dichloride Complex 269. To a solution of freshly distilled diamine **248**[23] (194 mg, 1.0 mmol, 1.0 equiv) in CH_2Cl_2 (20 mL) was added $Pd(nbd)Cl_2$ (269 mg, 1.0 mmol, 1.0 equiv). The reaction was allowed to stir 1 h. Then, the volatiles were removed under reduced pressure. The resulting solid was washed with pentane (3 x 5 mL) to afford **269** (310 mg, 83% yield) as a reddish-brown solid: mp 183-185 °C (dec.); ^{1}H NMR (300 MHz, $CDCl_3$) δ 4.30 (dq, *J* = 12.4, 1.7 Hz, 1H), 4.11 (dt, *J* = 12.8, 2.1 Hz, 1H), 3.95 (br. d, *J* = 12.0 Hz, 1H), 3.33 (dq, *J* = 13.0, 1.8 Hz, 1H), 3.10 (qd, *J* = 12.6, 3.6 Hz, 1H), 2.91-2.72 (m, 1H), 2.67 (s, 3H), 2.43 (dd, *J* = 12.6, 2.8 Hz, 1H), 2.38-2.27 (comp. m, 2H), 2.07 (dd, *J* = 13.1, 3.1 Hz, 1H), 2.04-1.94 (m, 1H), 1.91-1.73 (comp. m, 5H), 1.64-1.39 (comp. m, 3H); ^{13}C NMR (75 MHz, $CDCl_3$) δ 69.6, 64.7, 64.4, 64.1, 58.8, 57.0, 34.0, 32.8, 30.2, 29.3, 25.0, 24.2; IR (thin film/NaCl): 2953, 2856, 1454, 1009 cm^{-1}; HRMS-FAB (*m/z*): $[M-Cl]^+$ calcd for $[C_{12}H_{22}N_2ClPd]^+$, 337.0510; found, 337.0503; A single crystal suitable for X-ray analysis was grown by slow diffusion of heptane into a saturated $CHCl_3$ solution of **269**.

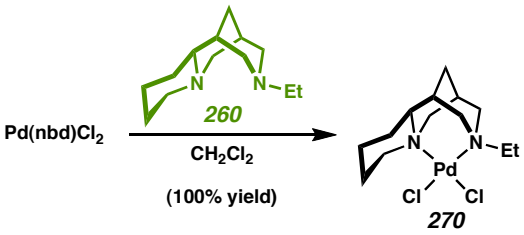

Dichloride Complex 270. To a solution of freshly distilled diamine **260** (208 mg, 1.0 mmol, 1.0 equiv) in CH_2Cl_2 (20 mL) was added Pd(nbd)Cl_2 (269 mg, 1.0 mmol, 1.0 equiv). The reaction was allowed to stir 1 h. Then, the volatiles were removed under reduced pressure. The resulting solid was washed with pentane (3 x 5 mL) and then hot filtered in $CHCl_3$ (200 mL). Heptane was layered over the filtrate, and the biphasic mixture was allowed to stand 4 d. The mixture was then filtered to afford **270** (386 mg, 100% yield) as an orange-brown solid: mp 177-179 °C (dec.); ^{1}H NMR (300 MHz, $CDCl_3$) δ 4.45 (app. d, *J* = 12.6 Hz, 1H), 4.34 (dt, *J* = 12.7, 2.1 Hz, 1H), 4.01 (br. d, *J* = 11.7 Hz, 1H), 3.77 (dq, *J* = 12.0, 6.9 Hz, 1H), 3.25 (app. d, *J* = 12.4 Hz, 1H), 2.84-2.63 (comp. m, 2H), 2.50-2.36 (comp. m, 3H), 2.09-1.70 (comp. m, 8H), 1.65-1.38 (comp. m, 3H), 1.32 (t, *J* = 6.9 Hz, 3H); ^{13}C NMR (75 MHz, $CDCl_3$) δ 69.0, 64.7, 64.1, 63.9, 61.1, 54.0, 33.5, 33.1, 30.2, 29.5, 25.0, 24.2, 12.7; IR (thin film/NaCl): 2856, 1460, 1033, 742 cm^{-1}; HRMS-FAB (*m*/*z*): $[M]^+$ calcd for $[C_{13}H_{24}N_2Cl_2Pd]^+$, 386.0356; found, 386.0338; A single crystal suitable for X-ray analysis was grown by slow diffusion of heptane into a saturated $CHCl_3$ solution of **270**.

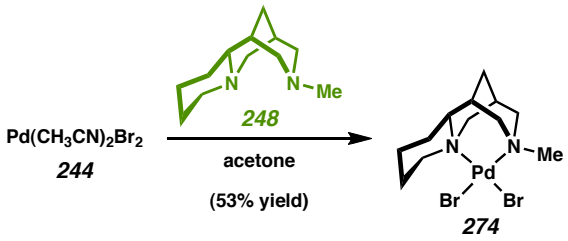

Dibromide Complex 274. To a solution of **244** (69.7 mg, 0.20 mmol, 1.0 equiv) in acetone (2 mL) was added a solution of freshly distilled diamine **248** (38.9 mg, 0.20 mmol, 1.0 equiv) in acetone (2 mL). The reaction was allowed to stir 1 h, after which Et_2O (4 mL) was layered over the mixture. The solid was filtered and washed with Et_2O (2 x 2 mL). 1,2-Dichloroethane (4 mL) was added to the solid, and the mixture was stirred vigorously for 4 h. After filtration of insoluble material, the filtrate was concentrated under reduced pressure to afford **274** (48.4 mg, 53% yield) as a brown solid: mp 197-199 °C (dec.); ^{1}H NMR (300 MHz, $CDCl_3$) δ 4.30 (dq, *J* = 13.0, 1.9 Hz, 1H), 4.15 (br. d, *J* = 12.1 Hz, 1H), 4.04 (dt, *J* = 12.6, 2.2 Hz, 1H), 3.30 (dq, *J* = 12.9, 1.8 Hz, 1H), 3.15 (qd, *J* = 12.3, 3.7 Hz, 1H), 2.95-2.76 (m, 1H), 2.87 (s, 3H), 2.59-2.50 (m, 1H), 2.43 (dd, *J* = 12.5, 2.8 Hz, 1H), 2.37-2.29 (m, 1H), 2.25 (dd, *J* = 13.0, 3.0 Hz, 1H), 2.05 (dd, *J* = 13.1, 3.2 Hz, 1H), 2.02-1.73 (comp. m, 5H), 1.64-1.41 (comp. m, 3H); ^{13}C NMR (75 MHz, $CDCl_3$) δ 69.7, 65.2, 64.7, 64.2, 59.8, 58.8, 34.1, 32.8, 30.1, 29.3, 25.8, 24.2; IR (thin film/NaCl): 2943, 1455, 1008 cm^{-1}; HRMS-FAB (*m*/*z*): $[M]^+$ calcd for $[C_{12}H_{22}Br_2N_2Pd]^+$, 459.9189; found, 459.9198. A single crystal suitable for X-ray analysis was grown by slow diffusion of hexanes into a saturated $CHCl_3$ solution of **274**.

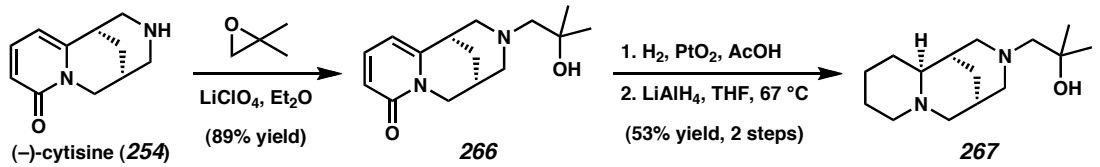

Diamine 267. To $LiClO_4$ (oven- and flame-dried, 4.26 g, 40 mmol, 10.0 equiv) was added Et_2O (8 mL). The mixture was stirred vigorously for 15 min, then isobutylene oxide (391 μL, 317 mg, 4.4 mmol, 1.1 equiv) and (–)-cytisine[23] (**254**, 761 mg, 4.0 mmol, 1.0 equiv) were added. After stirring the mixture vigorously for 50 h, the reaction was diluted with H_2O (30 mL). The biphasic mixture was extracted with CH_2Cl_2 (4 x 30 mL). The combined organic layers were dried over Na_2SO_4 and filtered. The filtrate was concentrated under reduced pressure to afford pyridone **266** (935 mg, 89% yield) as a tan solid: ^{1}H NMR (300 MHz, $CDCl_3$) δ 7.28 (dd, *J* = 9.1, 6.8 Hz, 1H), 6.44 (dd, *J* = 9.1, 1.3 Hz, 1H), 6.00 (dd, *J* = 6.8, 1.3 Hz, 1H), 4.17 (d, *J* = 15.5 Hz, 1H), 3.89 (dd, *J* = 15.5, 6.5 Hz, 1H), 3.04-2.93 (comp. m, 3H), 2.71-2.62 (comp. m, 2H), 2.42 (br. s, 1H), 2.21 (s, 2H), 1.95-1.86 (m, 1H), 1.82-1.72 (comp. m, 2H), 0.97 (s, 3H), 0.94 (s, 3H). The crude pyridone was used in the next step without further purification.

To crude pyridone **266** was added AcOH (glacial, 12 mL) and PtO_2 (81 mg, 0.36 mmol, 0.10 equiv). The reaction was then stirred under a balloon of H_2 (1 atm) for 48 h. The black mixture was filtered through Celite (MeOH eluent), and the filtrate was concentrated under reduced pressure. $PhCH_3$ (50 mL) was added, and the solution was concentrated under reduced pressure to effect azeotropic removal of traces of AcOH and afford the crude amide as a slightly yellow oil, which was used in the next step without further purification.

A solution of the crude amide in THF (16 mL) was cooled to 0 °C. $LiAlH_4$ (811 mg, 21.4 mmol, 6.0 equiv) was added in small portions. The mixture was heated to

reflux for 22 h, then cooled to 0 °C. Saturated aq Na_2SO_4 was added dropwise until bubbling ceased. The reaction was allowed to warm to 23 °C and stirred vigorously for 2 h. The mixture was diluted with CH_2Cl_2 (50 mL) and aq NaOH (10% w/v, 50 mL) and stirred 2 h. The mixture was then filtered, and the layers separated. The aqueous layer was extracted with CH_2Cl_2 (3 x 50 mL). The combined organic layers were dried over Na_2SO_4, filtered, and the filtrate concentrated under reduced pressure. Bulb-to-bulb distillation (0.2 torr, 170-190 °C) afforded diamine **267** (477 mg, 53% yield) as a colorless oil: ^{1}H NMR (500 MHz, $CDCl_3$) δ 5.73 (br. s, 1H), 3.05 (d, *J* = 11.1 Hz, 1H), 2.98 (d, *J* = 10.7 Hz, 1H), 2.89 (d, *J* = 11.3 Hz, 1H), 2.81-2.75 (m, 1H), 2.72 (dt, *J* = 10.7, 2.2 Hz, 1H), 2.61 (dd, *J* = 11.2, 2.5 Hz, 1H), 2.30-2.21 (comp. m, 3H), 1.81-1.50 (comp. m, 7H), 1.46-1.42 (m, 1H), 1.37-1.20 (comp. m, 3H), 1.18 (s, 3H), 1.16 (s, 3H); ^{13}C NMR (126 MHz, $CDCl_3$) δ 68.9, 66.7, 66.3, 60.8, 59.6, 57.4, 55.4, 36.0, 34.5, 31.3, 30.5, 29.9, 29.2, 25.9, 25.1; IR (thin film/NaCl) 3252, 2931, 2758, 1166 cm^{-1}; HRMS-FAB (*m/z*): $[M+H]^+$ calcd for $[C_{15}H_{29}N_2O]^+$, 253.2280; found 253.2280; $[\alpha]^{24}_D$ +27.1° (*c* 1.0, $CHCl_3$).

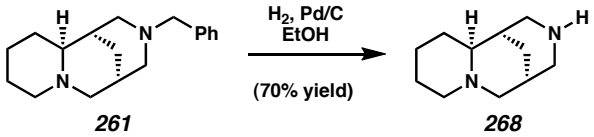

261 *268*

Diamine 268. To benzyl diamine **261**[25] (472 mg, 1.75 mmol, 1.0 equiv) was added EtOH (absolute, 8.8 mL) and then Pd/C (10% w/w, 186 mg, 0.18 mmol Pd, 0.10 equiv). The reaction was then stirred under a balloon of H_2 (1 atm) for 22 h. The mixture was then filtered through Celite (EtOH eluent). The filtrate was concentrated under reduced pressure and purified by bulb-to-bulb distillation (1-2 torr, 100-130 °C) to yield a colorless oil. To this oil was added Et_2O (10 mL), then HCl (2 M in Et_2O, 1.39 mL, 2.77

mmol, 1.6 equiv) dropwise. A white solid formed immediately. After stirring 30 min, the solid was collected by filtration, washed quickly with Et_2O (3 x 5 mL) and dissolved in CH_2Cl_2 (10 mL). NaOH (10% w/v aq, 10 mL) was added dropwise. The layers were separated, and the aqueous layer was extracted with CH_2Cl_2 (3 x 10 mL). The combined organic layers were dried over Na_2SO_4, filtered, and the filtrate concentrated under reduced pressure. Bulb-to-bulb distillation (1-2 torr, 110-125 °C) afforded diamine **268** (264 mg, 70% yield) as an oil, which solidified on standing to a white solid: ^{1}H NMR (500 MHz, $CDCl_3$) δ 3.22 (app. dt, *J* = 13.9, 2.3 Hz, 1H), 3.03 (br. d, *J* = 13.5 Hz, 1H), 2.94 (app. dt, *J* = 13.5, 2.5 Hz, 1H), 2.86 (dt, *J* = 11.0, 2.3 Hz, 1H), 2.76-2.70 (comp. m, 2H), 2.40 (dt, *J* = 11.0, 2.5 Hz, 1H), 2.11 (app. dt, *J* = 11.2, 2.6 Hz, 1H), 1.87 (dtd, *J* = 12.2, 3.1, 2.2 Hz, 1H), 1.80-1.66 (comp. m, 3H), 1.62-1.47 (comp. m, 4H), 1.43-1.37 (m, 1H), 1.34-1.24 (comp. m, 2H); ^{13}C NMR (126 MHz, $CDCl_3$) δ 66.4, 61.9, 57.5, 52.7, 48.5, 35.2, 34.7, 30.7, 30.3, 26.2, 24.9; IR (thin film/NaCl) 3387, 2930, 1654, 1442 cm^{-1}; HRMS-FAB (*m/z*): [M+H]$^+$ calcd for $[C_{11}H_{21}N_2]^+$, 181.1705; found 181.1703; $[\alpha]^{24}_D$ +21.51° (*c* 1.0, $CHCl_3$).

4.5.3 General Procedures

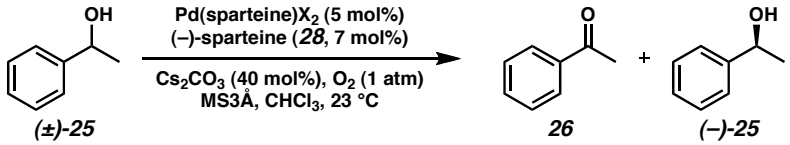

Kinetic Resolution Conditions with Pd(sparteine)X_2 and Cs_2CO_3 in $CHCl_3$ under O_2.[11] To an oven dried reaction tube with stir bar was added 3Å molecular sieves (250 mg). After cooling, Pd(sparteine)X_2 (0.025 mmol, 0.05 equiv), followed by $CHCl_3$ (1 mL)[30] and then (–)-sparteine (**28**, 8.0 μL, 0.035 mmol, 0.07 equiv) were added. The

reaction tube was cooled to –78 °C, then vacuum evacuated and purged with O_2 (3x). The reaction was allowed to warm to 23 °C and stirred vigorously under a balloon of O_2 (1 atm) for 15 min. Finely powdered Cs_2CO_3 (65.2 mg, 0.20 mmol, 0.40 equiv) was added, followed by a solution of (±)-1-phenylethanol ((±)-**25**, 60.3 μL, 0.50 mmol, 1.0 equiv) and tridecane (36.6 μL, 0.15 mmol, 0.30 equiv) in $CHCl_3$ (1 mL). The reaction was allowed to proceed under O_2 atmosphere at 23 °C. Aliquots were filtered through a small plug of silica gel (Et_2O eluent), evaporated, and analyzed by GC for conversion and chiral HPLC for alcohol ee. Purification of **26** and (–)-**25** was accomplished by direct chromatography of the crude reaction mixture.

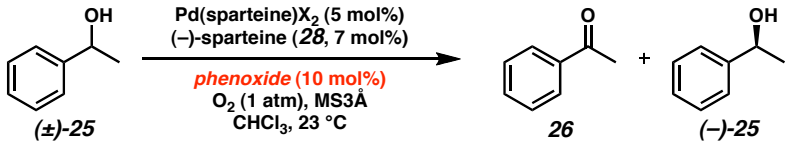

Kinetic Resolution Conditions with Pd(sparteine)X_2 and Phenoxides. To an oven dried reaction tube with stir bar was added 3Å molecular sieves (250 mg), Pd(sparteine)X_2 (0.025 mmol, 0.05 equiv), phenoxide[31] (0.05 mmol, 0.10 equiv), $CHCl_3$ (1 mL),[30] and **28** (8.0 μL, 0.035 mmol, 0.07 equiv). The reaction tube was cooled to –78 °C, then vacuum evacuated and purged with O_2 (3x). The reaction was allowed to warm to 23 °C and stirred vigorously under a balloon of O_2 (1 atm) for 1 h. A solution of (±)-**25** (60.3 μL, 0.50 mmol, 1.0 equiv) and tridecane (36.6 μL, 0.15 mmol, 0.30 equiv) in $CHCl_3$ (1 mL) was added. The reaction was allowed to proceed under O_2 atmosphere at 23 °C. Aliquots were filtered through a small plug of silica gel (Et_2O eluent), evaporated, and analyzed by GC for conversion and chiral HPLC for alcohol ee. Purification of **26** and (–)-**25** was accomplished by direct chromatography of the crude reaction mixture.

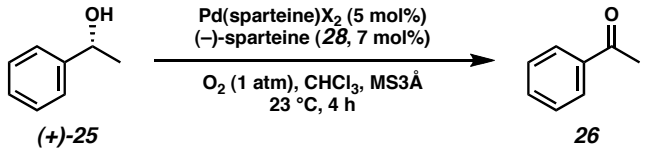

Single Enantiomer Rate Experiments with Various Pd(sparteine)X_2 Sources. To an oven dried reaction tube with stir bar was added 3Å molecular sieves (250 mg). After allowing the tube to cool, Pd(sparteine)X_2 (0.025 mmol, 0.05 equiv) was added, followed by $CHCl_3$ (1 mL)[30] and then **28** (8.0 μL, 0.035 mmol, 0.07 equiv). The reaction tube was cooled to –78 °C, then vacuum evacuated and purged with O_2 (3x). The reaction was allowed to warm to 23 °C and stirred vigorously under a balloon of O_2 (1 atm) for 15 min. A solution of (+)-**25** (60.4 μL, 0.50 mmol, 1.0 equiv) and tridecane (36.6 μL, 0.15 mmol, 0.30 equiv) in $CHCl_3$ (1 mL) was added. The reaction was allowed to proceed under O_2 atmosphere at 23 °C. Aliquots were filtered through a small plug of silica gel (Et_2O eluent), evaporated, and analyzed by GC for conversion to acetophenone (**26**).

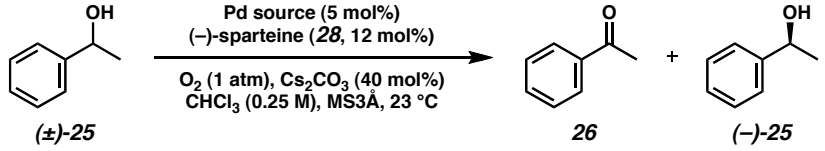

Screening of $PdBr_2$ Sources in $CHCl_3$. To an oven dried reaction tube with stir bar was added 3Å molecular sieves (250 mg). After allowing the tube to cool, the palladium source (0.025 mmol, 0.05 equiv) was added, followed by $CHCl_3$ (1 mL)[30] and then **28** (13.8 μL, 0.060 mmol, 0.12 equiv).[32] The reaction tube was cooled to –78 °C, then vacuum evacuated and purged with O_2 (3x). The reaction was allowed to warm to

23 °C and stirred vigorously under a balloon of O_2 (1 atm) for 15 min. Finely powdered Cs_2CO_3 (65.2 mg, 0.20 mmol, 0.40 equiv) was added, followed by a solution of (±)-**25** (60.3 μL, 0.50 mmol, 1.0 equiv) and tridecane (36.6 μL, 0.15 mmol, 0.30 equiv) in $CHCl_3$ (1 mL). The reaction was allowed to proceed under O_2 atmosphere at 23 °C. Aliquots were filtered through a small plug of silica gel (Et_2O eluent), evaporated, and analyzed by GC for conversion and chiral HPLC for alcohol ee.

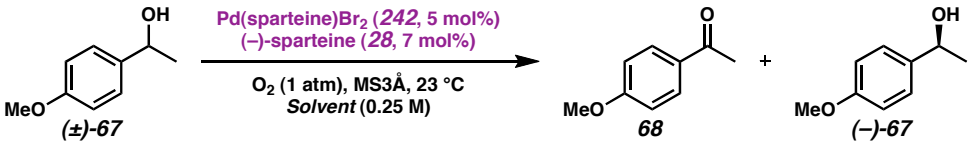

Solvent Screen with Pd(sparteine)Br_2. To an oven dried reaction tube with stir bar was added 3Å molecular sieves (250 mg). After allowing the tube to cool, Pd(sparteine)Br_2 (**242**, 12.5 mg, 0.025 mmol, 0.05 equiv) was added, followed by the solvent (1 mL) and then **28** (8.0 μL, 0.035 mmol, 0.07 equiv). The reaction tube was cooled to –78 °C, then vacuum evacuated and purged with O_2 (3x). The reaction was allowed to warm to 23 °C and stirred vigorously under a balloon of O_2 (1 atm) for 15 min. A solution of (±)-**67** (76.1 mg, 0.50 mmol, 1.0 equiv) and tridecane (36.6 μL, 0.15 mmol, 0.30 equiv) in the solvent (1 mL) was added. The reaction was allowed to proceed under O_2 atmosphere at 23 °C. Aliquots were filtered through a small plug of silica gel (Et_2O eluent), evaporated, and analyzed by GC for conversion and chiral HPLC for alcohol ee.

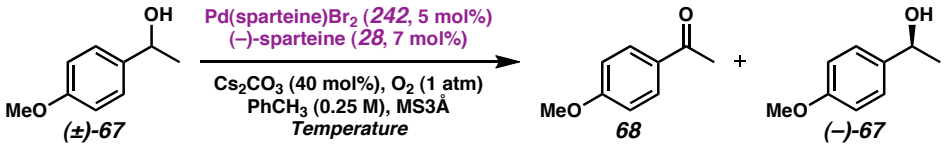

Kinetic Resolution Conditions with Pd(sparteine)Br_2 (242) and O_2 in $PhCH_3$. To an oven dried reaction tube with stir bar was added 3Å molecular sieves (250 mg). After allowing the tube to cool, Pd(sparteine)Br_2 (**242**, 12.5 mg, 0.025 mmol, 0.05 equiv) was added, followed by the $PhCH_3$ (1 mL) and then **28** (8.0 μL, 0.035 mmol, 0.07 equiv). The reaction tube was cooled to –78 °C, then vacuum evacuated and purged with O_2 (3x). The reaction was warmed to the appropriate temperature (23 or 60 °C) and stirred vigorously under a balloon of O_2 (1 atm) for 15 min. A solution of (±)-**67** (76.1 mg, 0.50 mmol, 1.0 equiv) and tridecane (36.6 μL, 0.15 mmol, 0.30 equiv) in $PhCH_3$ (1 mL) was added. The reaction was allowed to proceed under O_2 atmosphere at the appropriate temperature. Aliquots were filtered through a small plug of silica gel (Et_2O eluent), evaporated, and analyzed by GC for conversion and chiral HPLC for alcohol ee.

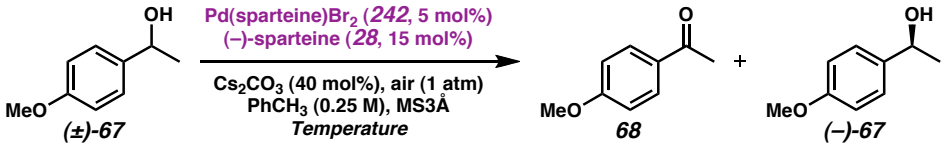

Kinetic Resolution Conditions with Pd(sparteine)Br_2 (242) and Air in $PhCH_3$. To an oven dried reaction tube with stir bar was added 3Å molecular sieves (250 mg). After allowing the tube to cool, Pd(sparteine)Br_2 (**242**, 12.5 mg, 0.025 mmol, 0.05 equiv) was added, followed by the $PhCH_3$ (1 mL) and then **28** (17.2 μL, 0.075 mmol, 0.15 equiv). A short (2-3 cm) tube containing Drierite was attached to the reaction tube. The reaction was warmed to the appropriate temperature (23 or 50 °C) and stirred vigorously

for 5 min. A solution of (±)-**67** (76.1 mg, 0.50 mmol, 1.0 equiv) and tridecane (36.6 μL, 0.15 mmol, 0.30 equiv) in $PhCH_3$ (1 mL) was added. The reaction was allowed to proceed under ambient air atmosphere at the appropriate temperature. Aliquots were filtered through a small plug of silica gel (Et_2O eluent), evaporated, and analyzed by GC for conversion and chiral HPLC for alcohol ee.

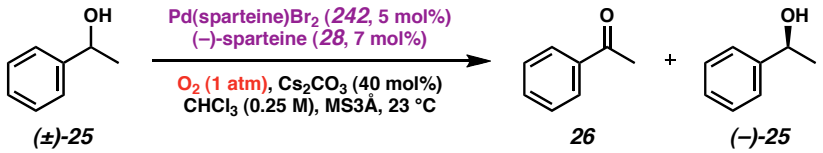

Kinetic Resolution Conditions with Pd(sparteine)Br_2 (242) and O_2 in $CHCl_3$. To an oven dried reaction tube with stir bar was added 3Å molecular sieves (250 mg). After allowing the tube to cool, **242** (12.5 mg, 0.025 mmol, 0.05 equiv) was added, followed by $CHCl_3$ (1 mL)[30] and then **28** (8.0 μL, 0.035 mmol, 0.07 equiv). The reaction tube was cooled to –78 °C, then vacuum evacuated and purged with O_2 (3x). The reaction was allowed to warm to 23 °C and stirred vigorously under a balloon of O_2 (1 atm) for 15 min. Finely powdered Cs_2CO_3 (65.2 mg, 0.20 mmol, 0.40 equiv) was added, followed by (±)-**25** (60.3 μL, 0.50 mmol, 1.0 equiv) and tridecane (36.6 μL, 0.15 mmol, 0.30 equiv) in $CHCl_3$ (1 mL). The reaction was allowed to proceed under O_2 atmosphere at 23 °C. Aliquots were filtered through a small plug of silica gel (Et_2O eluent), evaporated, and analyzed by GC for conversion and chiral HPLC for alcohol ee. Purification of the product ketone and enantioenriched secondary alcohol was accomplished by direct chromatography of the crude reaction mixture.

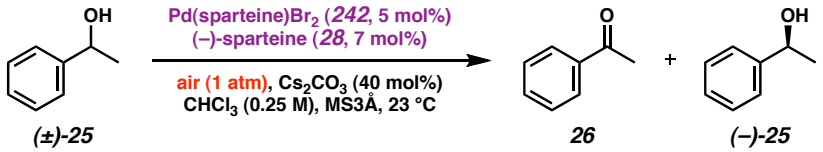

Kinetic Resolution Conditions with Pd(sparteine)Br_2 (242) and Air in $CHCl_3$. To an oven dried reaction tube with stir bar was added 3Å molecular sieves (250 mg). After allowing the tube to cool, **242** (12.5 mg, 0.025 mmol, 0.05 equiv) was added, followed by $CHCl_3$ (1 mL)[30] and then **28** (8.0 μL, 0.035 mmol, 0.07 equiv). A short (2-3 cm) tube containing Drierite was attached to the reaction tube. The reaction was stirred vigorously at 23 °C under a balloon of O_2 (1 atm) for 5 min. Finely powdered Cs_2CO_3 (65.2 mg, 0.20 mmol, 0.40 equiv) was added, followed by (±)-**25** (60.3 μL, 0.50 mmol, 1.0 equiv) and tridecane (36.6 μL, 0.15 mmol, 0.30 equiv) in $CHCl_3$ (1 mL). The reaction was allowed to proceed under ambient air atmosphere at 23 °C. Aliquots were filtered through a small plug of silica gel (Et_2O eluent), evaporated, and analyzed by GC for conversion and chiral HPLC for alcohol ee. Purification of the product ketone and enantioenriched secondary alcohol was accomplished by direct chromatography of the crude reaction mixture.

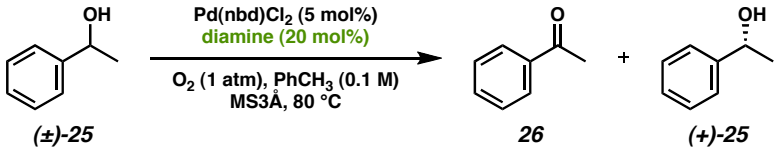

Kinetic Resolution Conditions With Diamines and Pd(nbd)Cl_2 in $PhCH_3$. To an oven dried reaction tube with stir bar was added 3Å molecular sieves (250 mg). After cooling, Pd(nbd)Cl_2 (6.7 mg, 0.025 mmol, 0.05 equiv) followed by toluene (2.5 mL) and then the diamine (0.10 mmol, 0.20 equiv) were added. The reaction tube was then cooled

to –78 °C, then vacuum evacuated and purged with O_2 (3x). Then, the tube was heated to 80 °C with vigorous stirring under a balloon of O_2 (1 atm) for 20 min. A solution of (±)-**25** (60.3 μL, 0.50 mmol, 1.0 equiv) and tridecane (36.6 μL, 0.15 mmol, 0.30 equiv) in toluene (2.5 mL) was added, and the reaction was allowed to proceed under O_2 atmosphere at 80 °C. Aliquots were filtered through a small plug of silica gel (Et_2O eluent), evaporated, and analyzed by GC for conversion and chiral HPLC for alcohol ee.

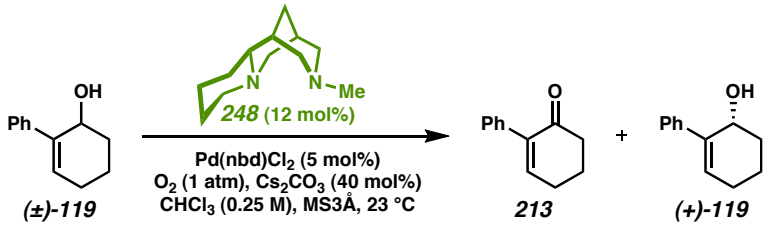

Kinetic Resolution Conditions With Diamine 248 and $Pd(nbd)Cl_2$ in $CHCl_3$. To an oven dried reaction tube with stir bar was added 3Å molecular sieves (250 mg). After allowing the tube to cool, $Pd(nbd)Cl_2$ (6.7 mg, 0.025 mmol, 0.05 equiv) was added, followed by $CHCl_3$ (1 mL)[30] and then freshly distilled diamine **248** (11.7 mg, 0.06 mmol, 0.12 equiv). The reaction tube was cooled to –78 °C, then vacuum evacuated and purged with O_2 (3x). The reaction was allowed to warm to 23 °C and stirred vigorously under a balloon of O_2 (1 atm) for 15 min. Finely powdered Cs_2CO_3 (65.2 mg, 0.20 mmol, 0.40 equiv) was added, followed by (±)-**119** (87.1 mg, 0.50 mmol, 1.0 equiv) and tridecane (36.6 μL, 0.15 mmol, 0.30 equiv) in $CHCl_3$ (1 mL). The reaction was allowed to proceed under O_2 atmosphere at 23 °C. Aliquots were filtered through a small plug of silica gel (Et_2O eluent), evaporated, and analyzed by GC for conversion and chiral HPLC for alcohol ee.

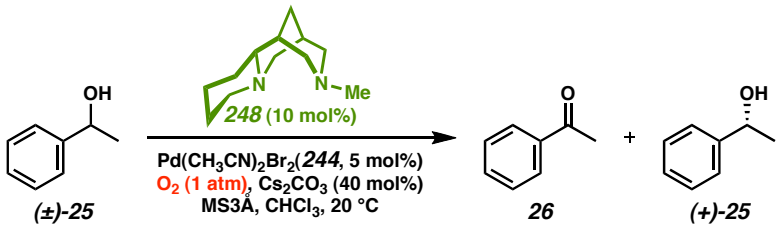

Kinetic Resolution Conditions with Pd(diamine)Br_2 and O_2. To an oven dried reaction tube with stir bar was added 3Å molecular sieves (250 mg). After allowing the tube to cool, **244** (8.7 mg, 0.025 mmol, 0.05 equiv) was added, followed by $CHCl_3$ (1 mL)[30] and then freshly distilled diamine **248** (9.7 mg, 0.050 mmol, 0.10 equiv). The reaction tube was cooled to –78 °C, then vacuum evacuated and purged with O_2 (3x). The reaction was warmed to 20 °C in a circulating bath and stirred vigorously under a balloon of O_2 (1 atm) for 15 min. Finely powdered Cs_2CO_3 (65.2 mg, 0.20 mmol, 0.40 equiv) was added, followed by (±)-**25** (60.3 μL, 0.50 mmol, 1.0 equiv) and tridecane (36.6 μL, 0.15 mmol, 0.30 equiv) in $CHCl_3$ (1 mL). The reaction was allowed to proceed under O_2 atmosphere at 20 °C. Aliquots were filtered through a small plug of silica gel (Et_2O eluent), evaporated, and analyzed by GC for conversion and chiral HPLC for alcohol ee. Purification of the product ketone and enantioenriched secondary alcohol was accomplished by direct chromatography of the crude reaction mixture.

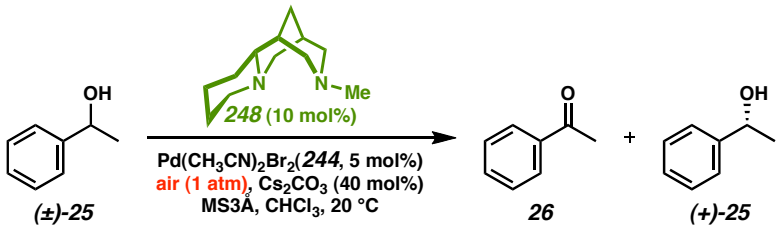

Kinetic Resolution Conditions with Pd(diamine)Br_2 and Air. To an oven dried reaction tube with stir bar was added 3Å molecular sieves (250 mg). After allowing

the tube to cool, **244** (8.7 mg, 0.025 mmol, 0.05 equiv) was added, followed by $CHCl_3$ (1 mL)[30] and then freshly distilled diamine **248** (9.7 mg, 0.050 mmol, 0.10 equiv). A short (2-3 cm) tube containing Drierite was attached to the reaction tube. The reaction was cooled to 20 °C in a circulating bath and stirred vigorously for 15 min. Finely powdered Cs_2CO_3 (65.2 mg, 0.20 mmol, 0.40 equiv) was added, followed by (±)-**25** (60.3 μL, 0.50 mmol, 1.0 equiv) and tridecane (36.6 μL, 0.15 mmol, 0.30 equiv) in $CHCl_3$ (1 mL). The reaction was allowed to proceed under ambient air atmosphere at 20 °C. Aliquots were filtered through a small plug of silica gel (Et_2O eluent), evaporated, and analyzed by GC for conversion and chiral HPLC for alcohol ee. Purification of the product ketone and enantioenriched secondary alcohol was accomplished by direct chromatography of the crude reaction mixture.

4.5.4 Preparative Resolution of Alcohols

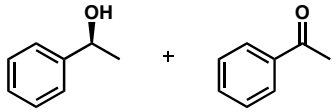

(–)-25 *26*

(–)-1-Phenylethanol ((–)-25, Table 4.2.11, entry 1). After 4 h (55.6% conversion), the crude reaction mixture was purified by flash chromatography (4:1 hexanes:Et_2O) to afford (–)-**25** (26.4 mg, 43% yield, 95.6% ee, s = 28) and **26** (28.5 mg, 47% yield, 91% total mass recovery).

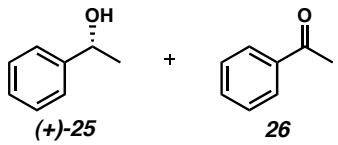

(+)-1-Phenylethanol ((+)-25, Table 4.3.6, entry 1). After 30 h (57.6% conversion), the crude reaction mixture was purified by flash chromatography (4:1 hexanes:Et_2O) to afford (+)-**25** (24.5 mg, 40% yield, 97.1% ee, *s* = 25) and **26** (30.8 mg, 51% yield, 91% total mass recovery).

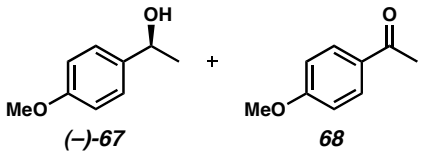

(–)-1-(4-Methoxyphenyl)ethanol ((–)-67, Table 4.2.11, entry 3). After 4 h (59.4% conversion), the crude reaction mixture was purified by flash chromatography (9:1→7:3 hexanes:EtOAc) to afford (–)-**67** (30.9 mg, 41% yield, 95.4% ee, *s* = 17) and **68** (43.3 mg, 58% yield, 98% total mass recovery).

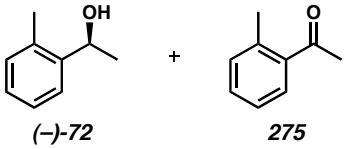

(–)-1-(2-Methylphenyl)ethanol ((–)-72, Table 4.2.11, entry 6). After 41 h (63.5% conversion), the crude reaction mixture was purified by flash chromatography (9:1→7:3 hexanes:EtOAc) to afford (–)-**72** (23.5 mg, 35% yield, 97.1% ee, *s* = 14) and **275** (33.2 mg, 50% yield, 84% total mass recovery).

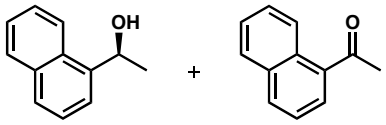

(–)-78 *276*

(–)-1-(1-Naphthyl)ethanol ((–)-78, Table 4.2.11, entry 8). After 24 h (59.6% conversion), the crude reaction mixture was purified by flash chromatography (9:1→7:3 hexanes:EtOAc) to afford (–)-**78** (34.2 mg, 40% yield, 92.5% ee, *s* = 14) and **276** (48.4 mg, 57% yield, 97% total mass recovery).

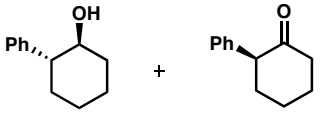

(+)-136 *(–)-277*

(+)-*trans*-2-Phenylcyclohexanol ((+)-136, Table 4.2.11, entry 12). After 49 h (58.0% conversion), the crude reaction mixture was purified by flash chromatography (19:1 hexanes:EtOAc) to afford (+)-**136** (34.9 mg, 40% yield, 90.6% ee, *s* = 15) and (–)-**277** (47.4 mg, 54% yield, 64.0% ee, 94% total mass recovery).

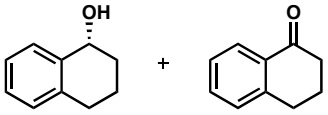

(–)-82 *278*

(–)-1-Tetralol ((–)-82, Table 4.3.6, entry 5). After 24 h (60.9% conversion), the crude reaction mixture was purified by flash chromatography (9:1→7:3 hexanes:EtOAc) to afford (–)-**82** (28.3 mg, 38% yield, 90.2% ee, *s* = 11) and **278** (39.0 mg, 53% yield, 92% total mass recovery).

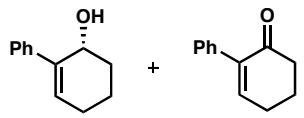

(+)-119 *213*

(+)-2-Phenylcyclohex-2-enol ((+)-119, Table 4.3.6, entry 6). After 46 h (56.8% conversion), the crude reaction mixture was purified by flash chromatography (19:1→4:1 hexanes:EtOAc) to afford (+)-**119** (37.6 mg, 43% yield, 90.7% ee, *s* = 17) and **213** (45.8 mg, 53% yield, 96% total mass recovery).

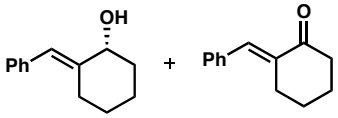

(+)-105 *279*

(+)-(*E*)-2-Benzylidenecyclohexanol ((+)-105, Table 4.3.6, entry 9). After 46 h (59.3% conversion), the crude reaction mixture was purified by flash chromatography (9:1 hexanes:EtOAc) to afford (+)-**105** (36.3 mg, 39% yield, 90.6% ee, *s* = 13) and **279** (51.2 mg, 55% yield, 94% total mass recovery).

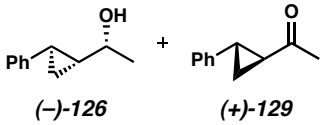

(–)-126 *(+)-129*

(–)-*syn*,*trans*-1-(2-Phenylcyclopropyl)ethanol ((–)-126, Table 4.3.6, entry 11). After 32 h (59.0% conversion), the crude reaction mixture was purified by flash chromatography (4:1 hexanes:EtOAc) to afford (–)-**126** (32.1 mg, 40% yield, 90.2% ee, *s* = 13) and (+)-**129** (42.3 mg, 53% yield, 64.1% ee, 92% total mass recovery).

4.5.5 Methods for Determination of Conversion

Conversion values for (±)-1-(9-anthacenyl)ethanol ((±)-**247**) were determined relative to product ketone by ^{1}H NMR of a reaction aliquot after filtration through a short plug of silica gel. All other conversions were determined by GC (Table 4.5.1 or Chapters 2 and 3) relative to tridecane as internal standard.

Table 4.5.1 Methods for determination of conversion.

entry	alcohol	ketone	GC conditions	alcohol retention time (min)	ketone retention time (min)
1	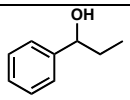 (±)-83	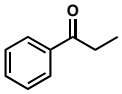 240	100 °C, 5 min; Ramp 13 °C/min	11.5	10.0
2	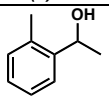 (±)-72	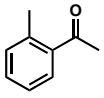 275	100 °C, 5 min; Ramp 13 °C/min	12.9	10.5
3	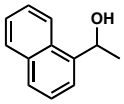 (±)-78	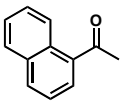 276	100 °C, 5 min; Ramp 13 °C/min to 240 °C 240 °C, 5 min	19.2	17.1
4	 (±)-136	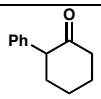 (±)-XX	100 °C, 5 min; Ramp 13 °C/min	14.2	14.9
5	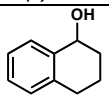 (±)-XX	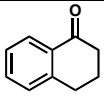 XX	100 °C, 5 min; Ramp 13 °C/min	14.5	13.6
6	 (±)-SI14	 (±)-277	100 °C, 5 min; Ramp 13 °C/min to 240 °C 240 °C, 5 min	15.8	16.1
7	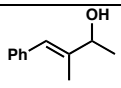 (±)-104	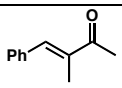 280	100 °C, 5 min; Ramp 13 °C/min	14.1	13.1

4.5.6 Methods for Determination of Enantiomeric Excess

Table 4.5.2 Methods for determination of enantiomeric excess.

entry	alcohol	ee assay and column	assay conditions	(*S*) enantiomer retention time (min)	(*R*) enantiomer retention time (min)
1	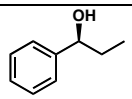 *(–)-83*	HPLC OD-H	3% EtOH/hexanes	17.6	12.0
2	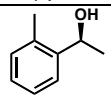 *(–)-72*	HPLC AD	3% EtOH/hexanes	13.1	11.2
3	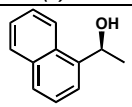 *(–)-78*	HPLC OD-H	8% EtOH/hexanes	12.6	18.4
4	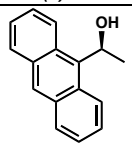 *(–)-247*	HPLC AD	5% EtOH/hexanes	17.6	27.9
5	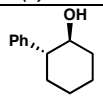 *(+)-136*	HPLC AD	4% EtOH/hexanes	28.1[a]	18.8
6	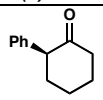 *(–)-277*	HPLC OB-H	3% EtOH/hexanes	18.1	23.2
7	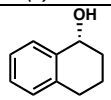 *(–)-82*	HPLC OB-H	3% *i*PrOH/hexanes	21.3	12.2
8	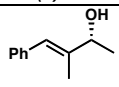 *(–)-104*	HPLC OD-H	3% *i*PrOH/hexanes	17.9	15.6

[a] Retention time for (*1S*, *2R*) enantiomer (shown).

4.6 Notes and References

(1) Portions of this chapter are reproduced in part from: Ebner, D. C.; Trend, R. M.; Genet, C.; McGrath, M. J.; O'Brien, P.; Stoltz, B. M. *Angew. Chem., Int. Ed.* **2008**, *47*, 6367-6370.

(2) (a) Nishimura, T.; Onoue, T.; Ohe, K.; Uemura, S. *Tetrahedron Lett.* **1998**, *39*, 6011-6014. (b) Nishimura, T.; Onoue, T.; Ohe, K.; Uemura, S. *J. Org. Chem.* **1999**, *64*, 6750-6755. (c) Nishimura, T.; Maeda, Y.; Kakiuchi, N.; Uemura, S. *J. Chem. Soc., Perkin Trans. 1* **2000**, 4301-4305. (d) Nishimura, T.; Uemura, S. *Synlett* **2004**, 201-216.

(3) Ferreira, E. M.; Stoltz, B. M. *J. Am. Chem. Soc.* **2001**, *123*, 7725-7726.

(4) The selectivity factor (*s*) was determined using the following equation: $s = \frac{\ln[(1-conv)(1-ee_{alc})]}{\ln[(1-conv)(1+ee_{alc})]}$, where ee_{alc} is the ee of the recovered alcohol and *conv* is the total conversion of alcohol to ketone, see: Kagan, H. B.; Fiaud, J. C. In *Topics in Stereochemistry*; Eliel, E. L., Ed.; Wiley & Sons: New York, 1988; Vol. 18, pp 249-330.

(5) Ferreira, E. M.; Stoltz, B. M. Unpublished results.

(6) Nielsen, R. J.; Keith, J. M.; Stoltz, B. M.; Goddard, W. A., III. *J. Am. Chem. Soc.* **2004**, *126*, 7967-7974.

(7) Kinetic studies performed by the Sigman group confirmed this finding, see: Mueller, J. A.; Jensen, D. R.; Sigman, M. S. *J. Am. Chem. Soc.* **2002**, *124*, 8202-8203.

(8) Trend, R. M.; Stoltz, B. M. *J. Am. Chem. Soc.* **2004**, *126*, 4482-4483.

(9) Mueller, J. A.; Sigman, M. S. *J. Am. Chem. Soc.* **2003**, *125*, 7005-7013.

(10) Bagdanoff, J. T. Development of the Enantioselective Oxidation of Secondary Alcohols and Natural Products Total Synthesis. Ph.D. Dissertation, California Institute of Technology, Pasadena, CA, 2005.

(11) Bagdanoff, J. T.; Stoltz, B. M. *Angew. Chem., Int. Ed.* **2004**, *43*, 353-357.

(12) Liu, H.; Liu, Y.; Zhu, C.; Liu, M.; Wang, C.; Chen, C.; Xi, F. *Synth. Met.* **1997**, *131*, 135-139.

(13) Trend, R. M.; Ramtohul, Y. K.; Ferreira, E. M.; Stoltz, B. M. *Angew. Chem., Int. Ed.* **2003**, *42*, 2892-2895.

(14) Raissa Trend also performed several preliminary oxidative kinetic resolutions utilizing Pd(sparteine)Br_2 (**242**) as catalyst in $CHCl_3$ and $PhCH_3$, obtaining results similar to Table 4.2.7, entry 5, and Table 4.2.9, entry 3, respectively.

(15) For dielectric constant tables, see: *CRC Handbook of Chemistry and Physics*, 76th ed.; Lide, D. R., Frederikse, H. P. R., Eds.; New York, 1995; Section 6, pp 159-192.

(16) Bagdanoff, J. T.; Ferreira, E. M.; Stoltz, B. M. *Org. Lett.* **2003**, *5*, 835-837.

(17) For a discussion of the limitations of conditions with Pd(sparteine)Cl_2 (**66**) in the oxidative kinetic resolution, see Chapter 3.

(18) For an asymmetric synthesis of (+)-sparteine, see: Smith, B. T.; Wendt, J. A.; Aubé, J. *Org. Lett.* **2002**, *4*, 2577-2579.

(19) Recently, similar palladium-catalyzed systems utilizing different ligands for enantioselective alcohol oxidation have been developed, see: (a) Jensen, D. R.; Sigman, M. S. *Org. Lett.* **2003**, *5*, 63-65. (b) Chen, T.; Jiang, J.-J.; Xu, Q.; Shi, M. *Org. Lett.* **2007**, *9*, 865-868. (c) Lesma, G.; Pilati, T.; Sacchetti, A.; Silvani, A. *Tetrahedron: Asymmetry* **2008**, *19*, 1363-1366.

(20) Several achiral, monodentate amines and Pd(nbd)Cl_2 did not provide active catalysts for the oxidation of (±)-1-phenylethanol ((±)-**25**), see Chapter 2.

(21) O'Brien, P. *Chem. Commun.* **2008**, 655-667.

(22) Dearden, M. J.; Firkin, C. R.; Hermet, J.-P. R.; O'Brien, P. *J. Am. Chem. Soc.* **2002**, *124*, 11870-11871.

(23) Dixon, A. J.; McGrath, M. J.; O'Brien, P. *Org. Synth.* **2006**, *83*, 141-154.

(24) Dearden, M. J.; McGrath, M. J.; O'Brien, P. *J. Org. Chem.* **2004**, *69*, 5789-5792.

(25) Johansson, M. J.; Schwartz, L.; Amedjkouh, M.; Kann, N. *Tetrahedron: Asymmetry* **2004**, *15*, 3531-3538.

(26) Heyari, A.; Mehrdad, M.; Maleki, A.; Ahmadi, N. *Synthesis* **2004**, 1563-1565.

(27) Genet, C.; McGrath, M. J.; O'Brien, P. *Org. Biomol. Chem.* **2006**, *4*, 1376-1382.

(28) Drew, D.; Doyle, J. R. *Inorg. Synth.* **1972**, Vol. XIII, 53-55.

(29) Grant, T. N.; West, F. G. *J. Am. Chem. Soc.* **2006**, *128*, 9348-9349.

(30) $CHCl_3$ stabilized with amylenes. $CHCl_3$ stabilized with EtOH must be distilled prior to use.

(31) Phenoxide was prepared by adding Na (1.0 equiv) to the appropriate phenol (1.05 equiv) in $PhCH_3$ (0.1 M). After the Na was consumed, the mixture was concentrated under reduced pressure and used without further purification.

(32) For conditions with Pd(sparteine)Br_2, 7 mol% (–)-sparteine (**28**) was added.

APPENDIX 2

Spectra Relevant to Chapter 4

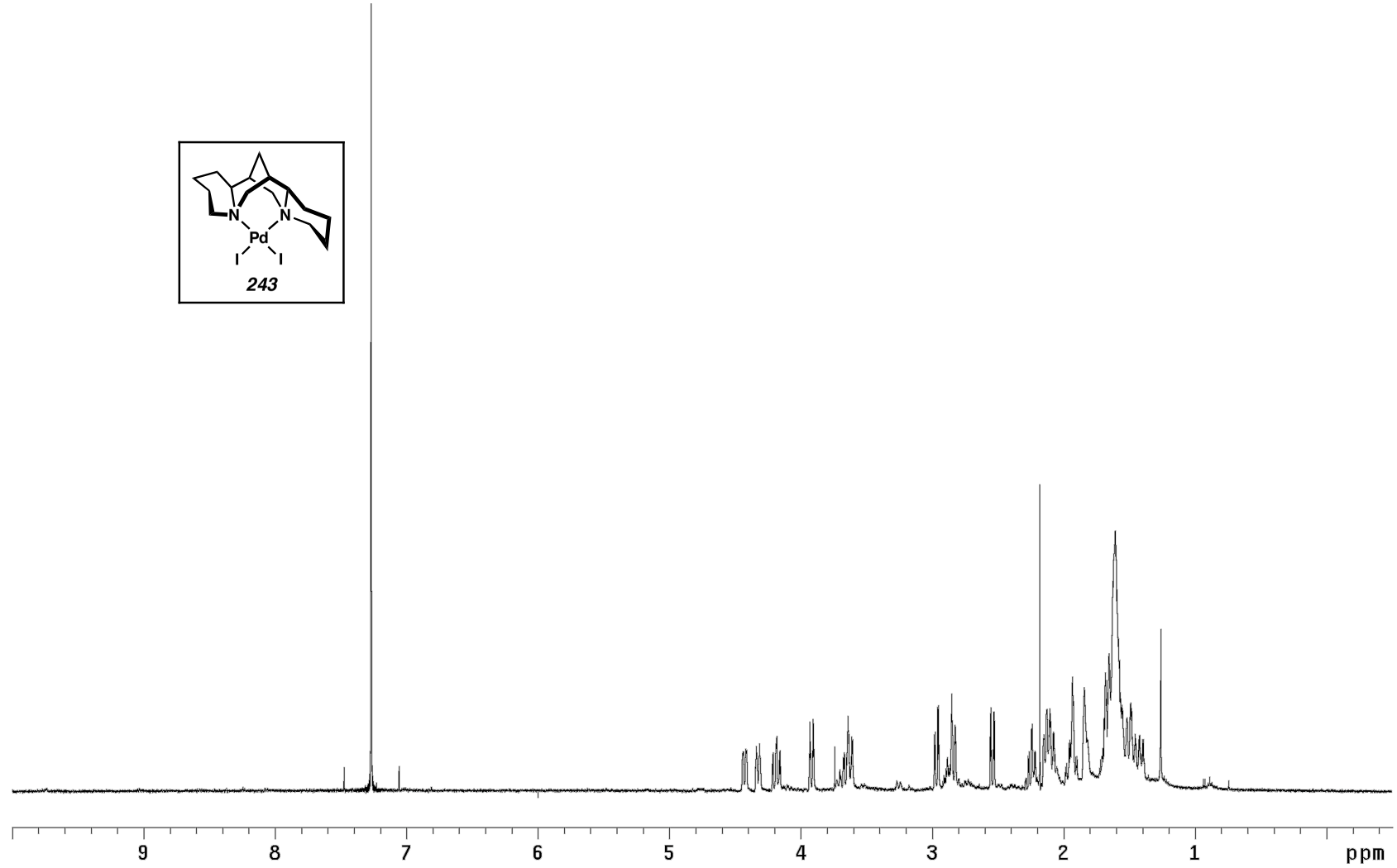

Figure A2.1 ^{1}H NMR (500 MHz, $CDCl_3$) of compound **243**.

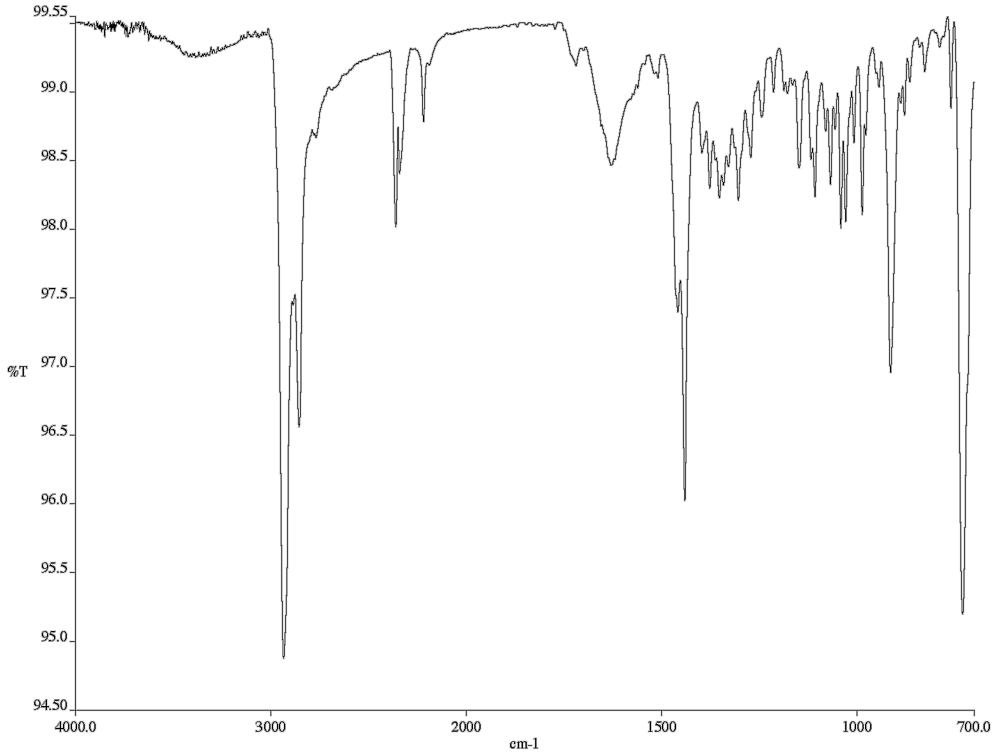

Figure A2.2 Infrared spectrum (thin film/NaCl) of compound **243**.

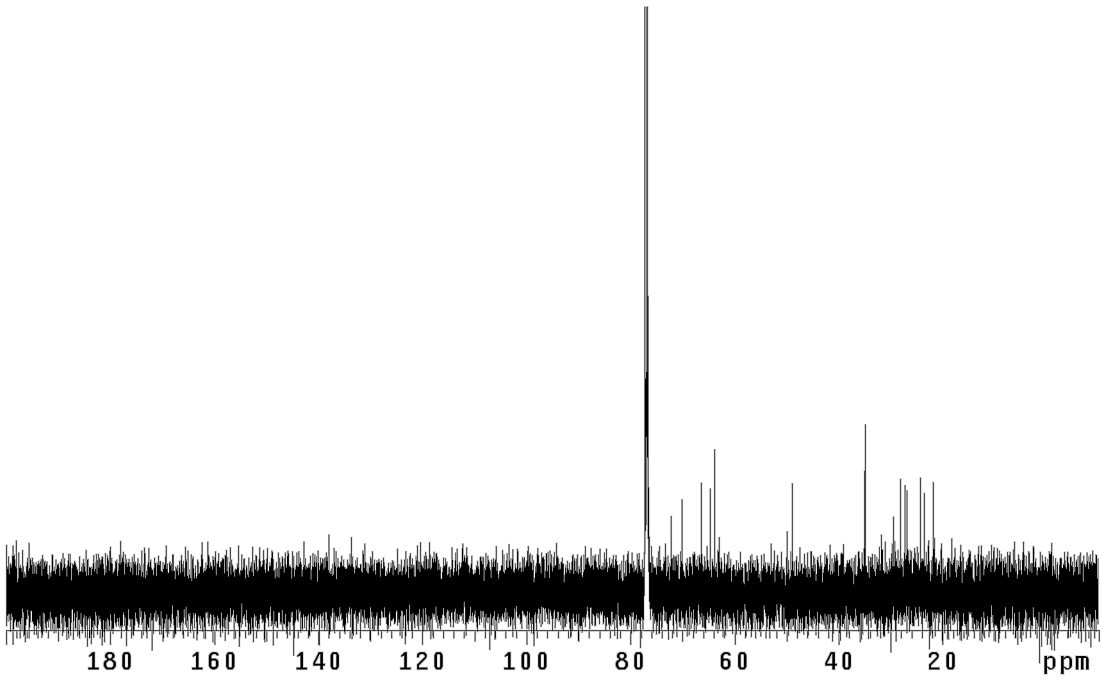

Figure A2.3 ^{13}C NMR (126 MHz, $CDCl_3$) of compound **243**.

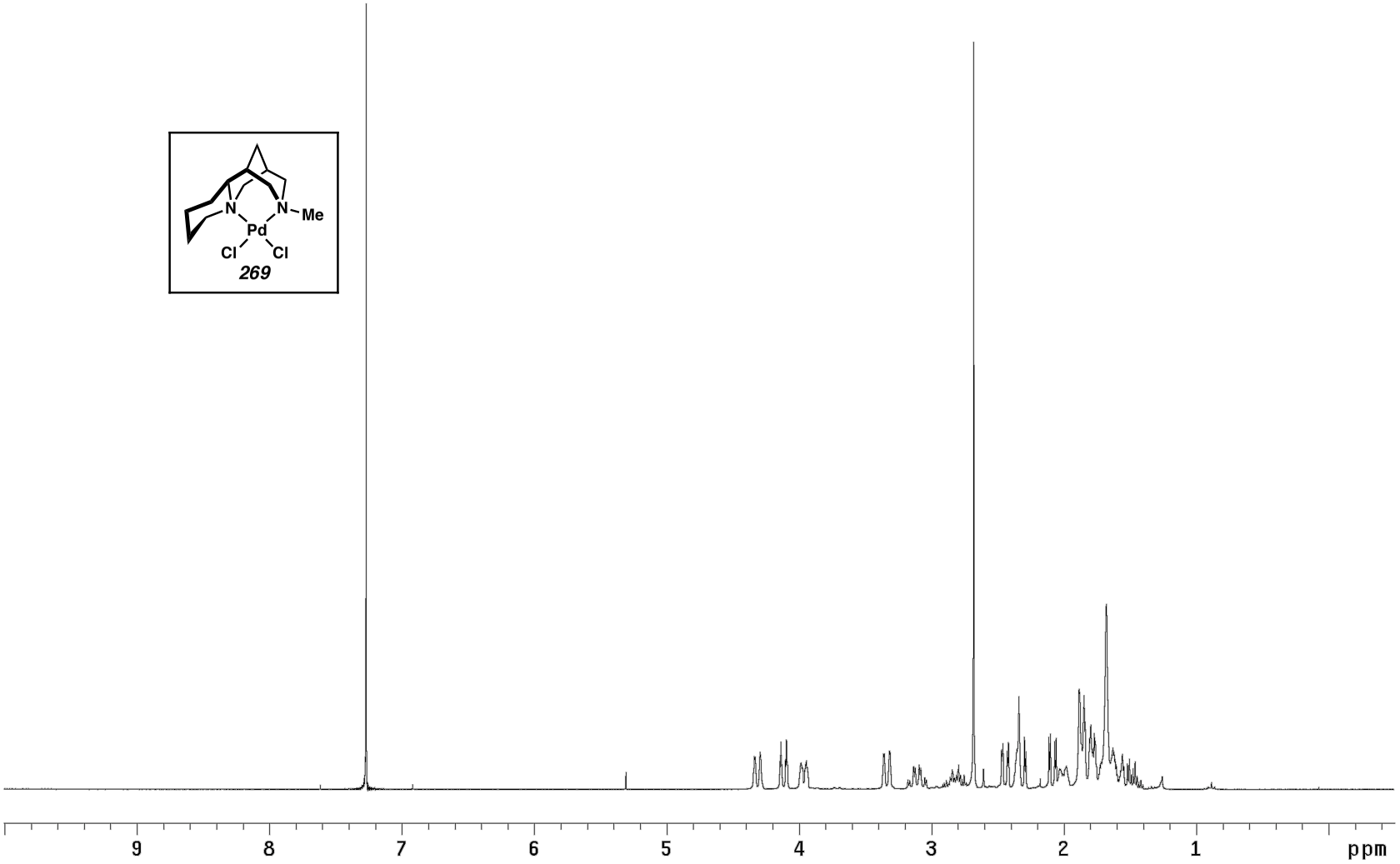

Figure A2.4 ^{1}H NMR (300 MHz, $CDCl_3$) of compound **269**.

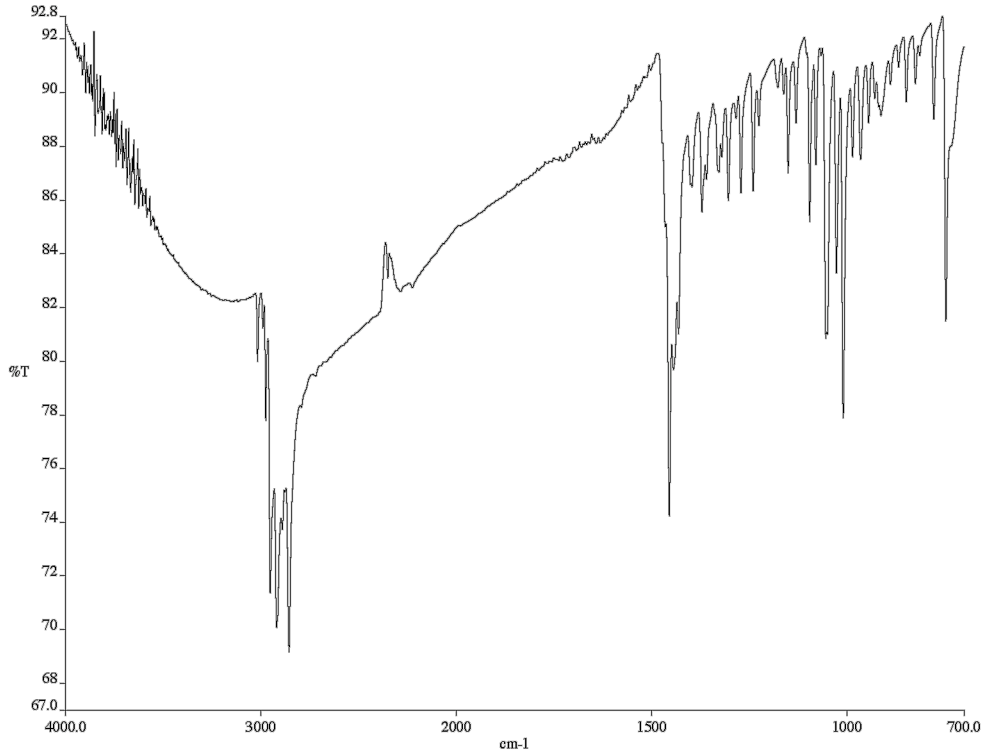

Figure A2.5 Infrared spectrum (thin film/NaCl) of compound **269**.

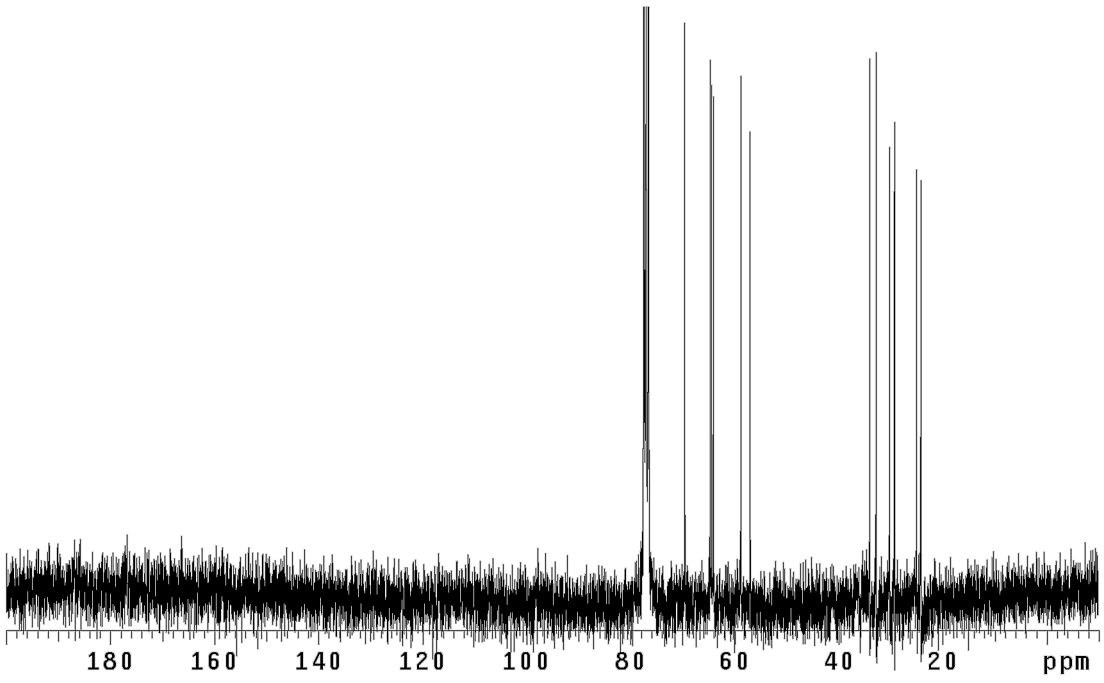

Figure A2.6 ^{13}C NMR (75 MHz, $CDCl_3$) of compound **269**.

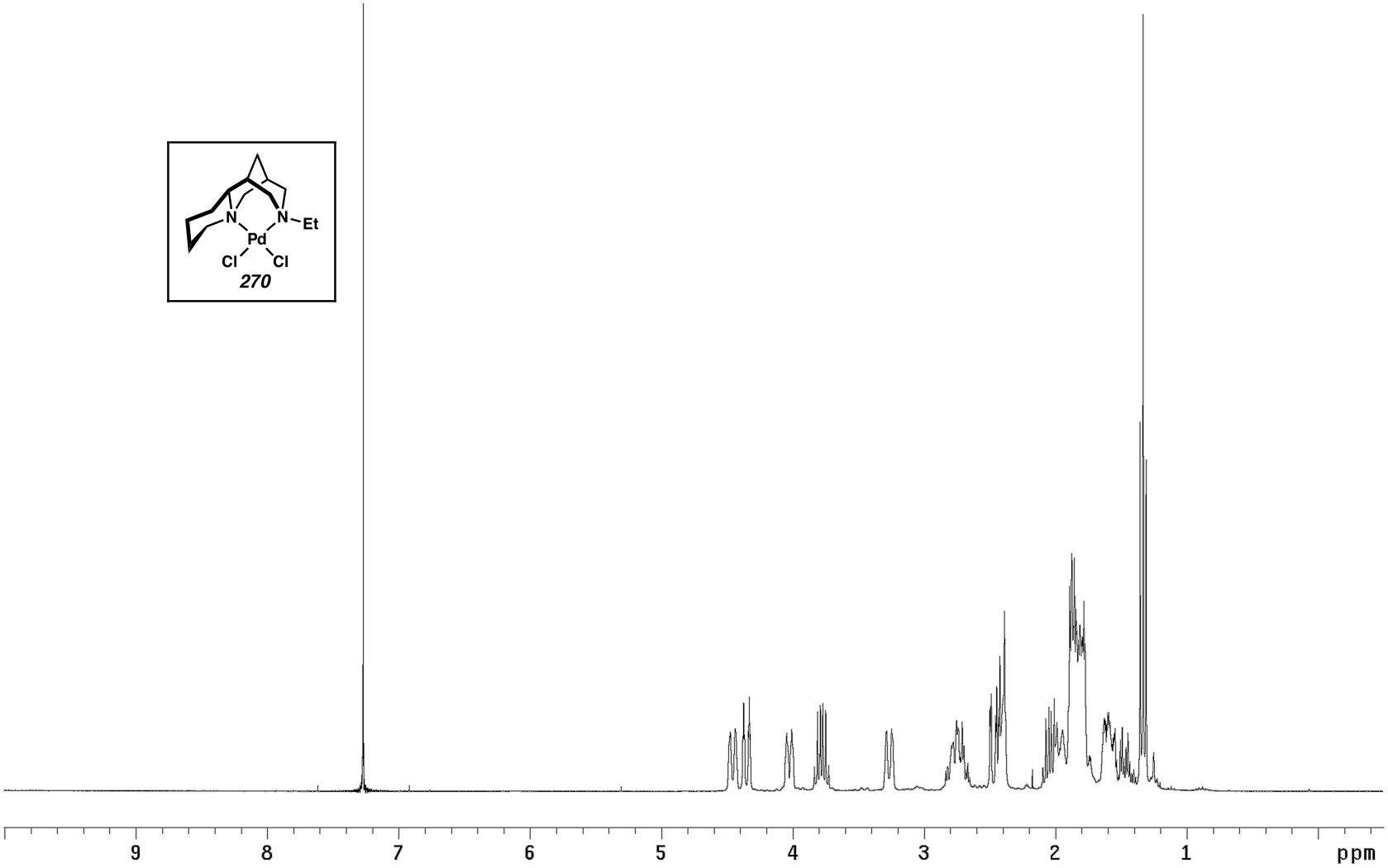

Figure A2.7 ^{1}H NMR (300 MHz, $CDCl_3$) of compound **270**.

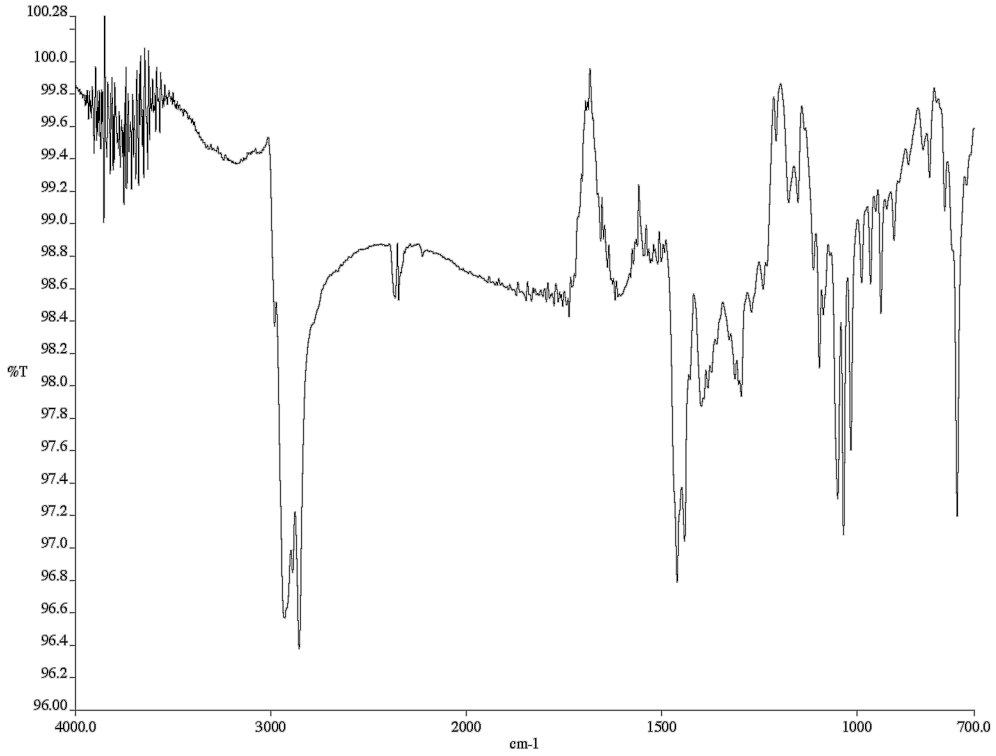

Figure A2.8 Infrared spectrum (thin film/NaCl) of compound **270**.

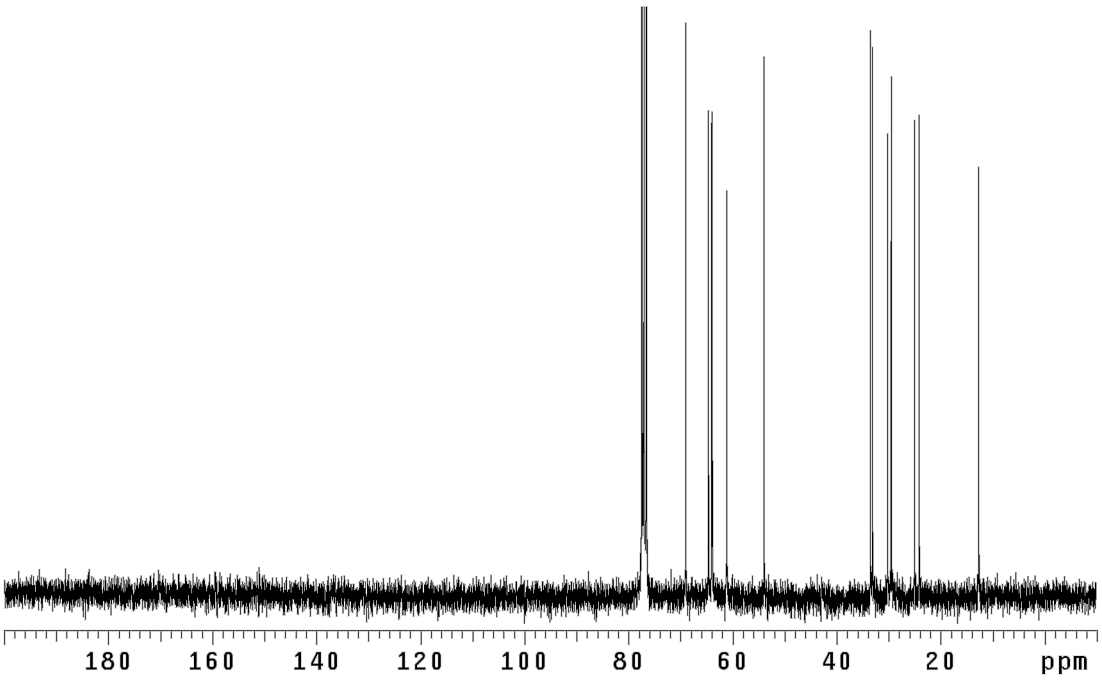

Figure A2.9 ^{13}C NMR (75 MHz, $CDCl_3$) of compound **270**.

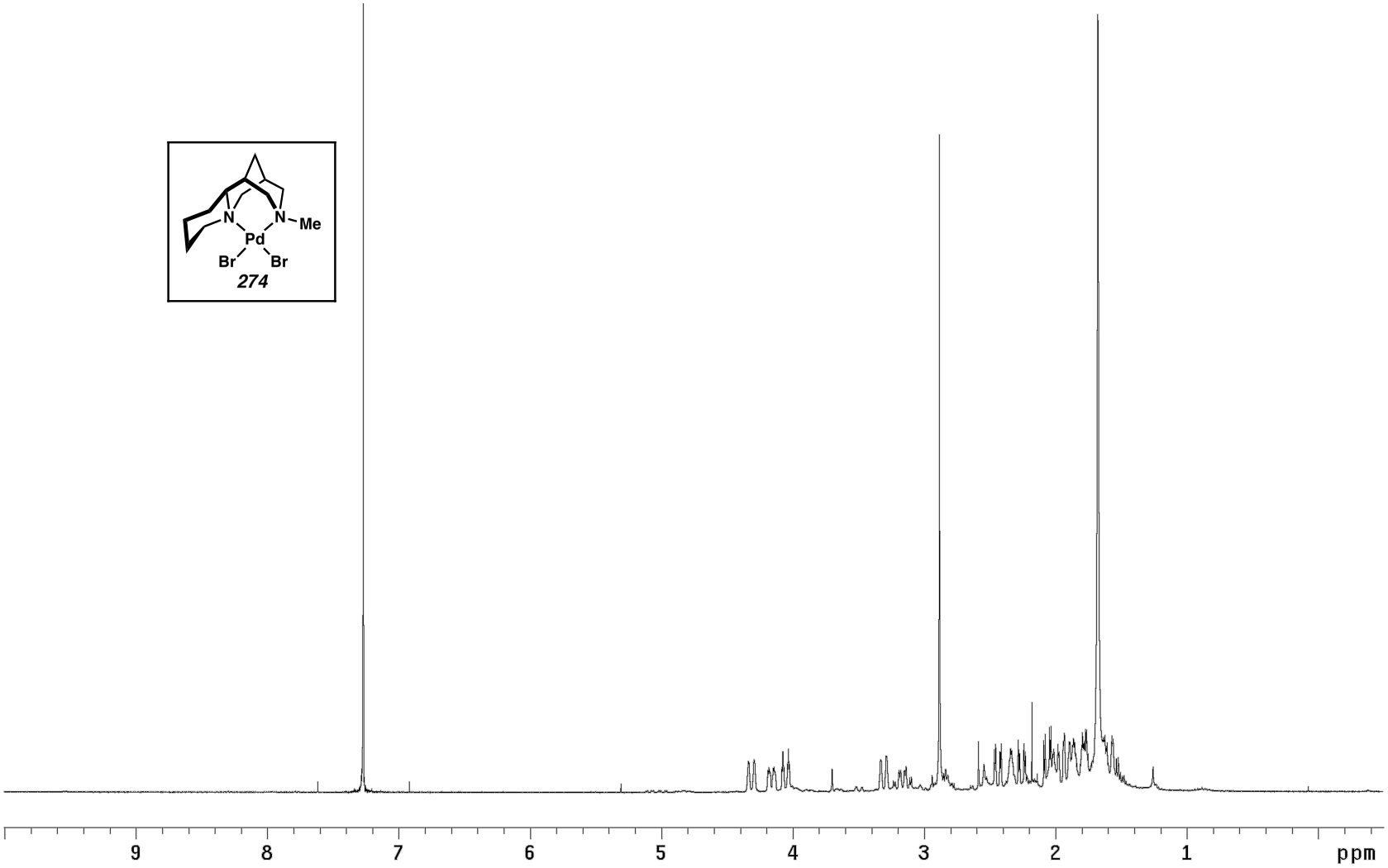

Figure A2.10 ^{1}H NMR (300 MHz, $CDCl_3$) of compound **274**.

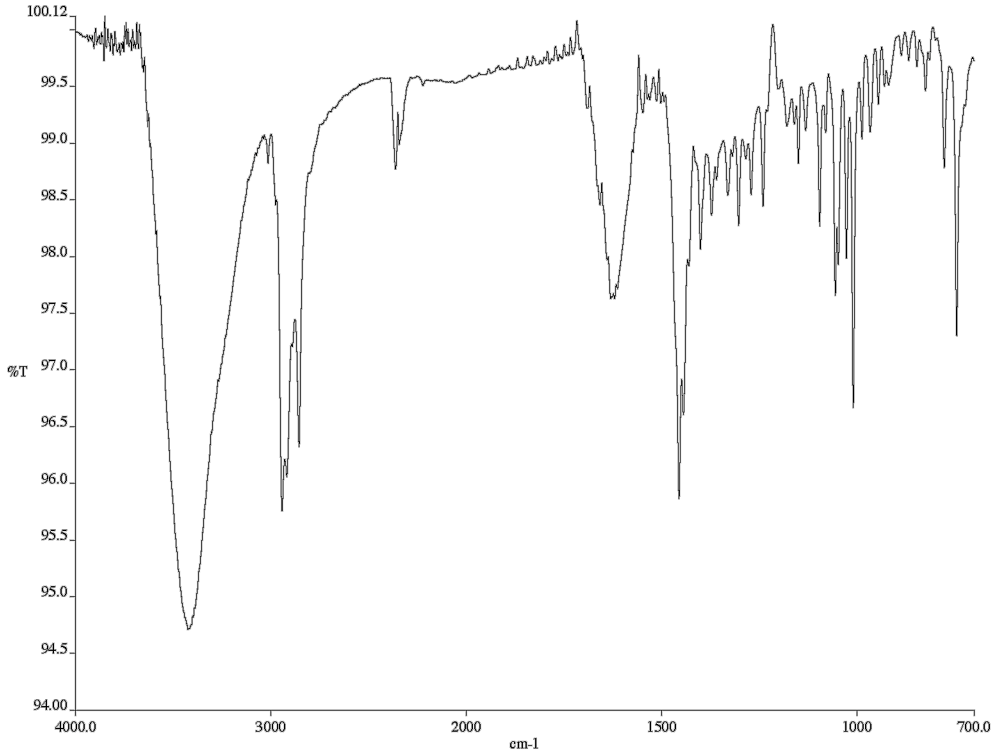

Figure A2.11 Infrared spectrum (thin film/NaCl) of compound **274**.

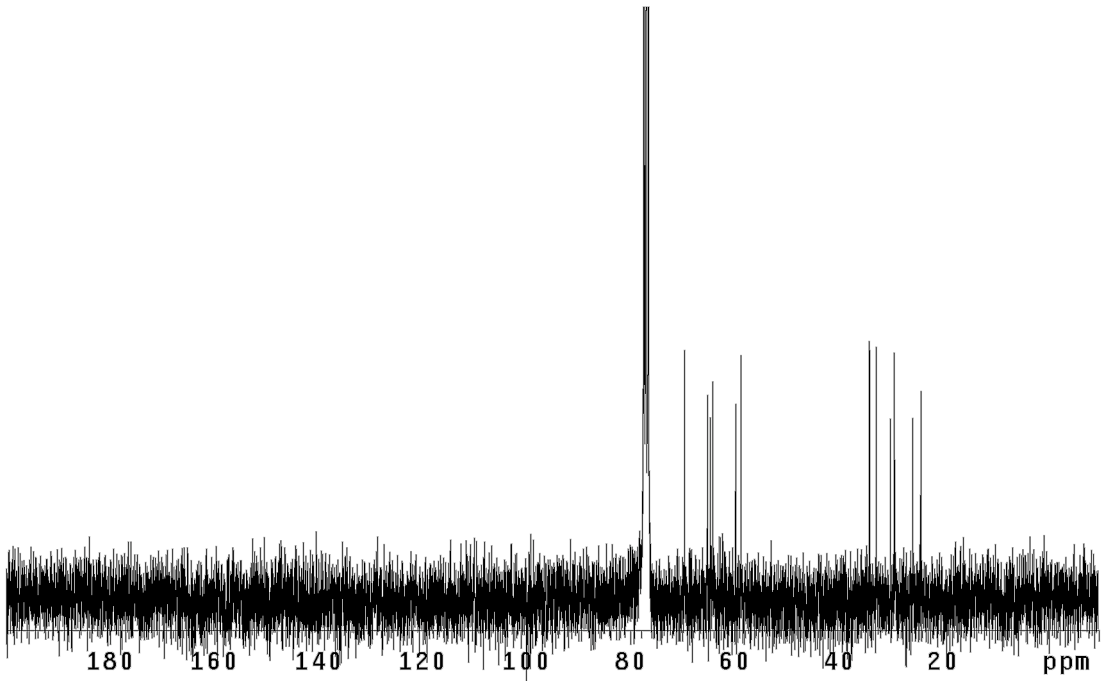

Figure A2.12 ^{13}C NMR (75 MHz, $CDCl_3$) of compound **274**.

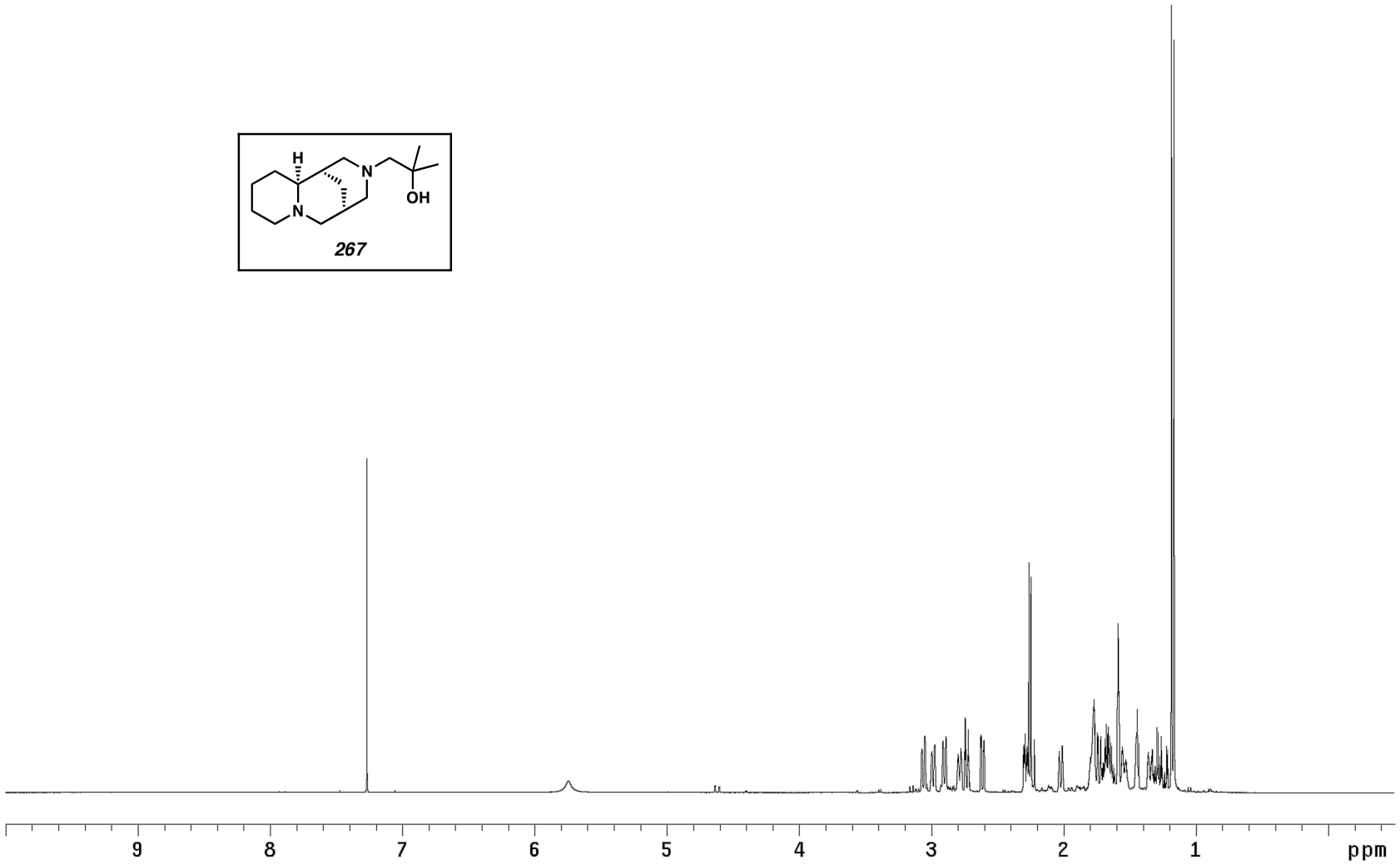

Figure A2.13 ^{1}H NMR (500 MHz, $CDCl_3$) of compound **267**.

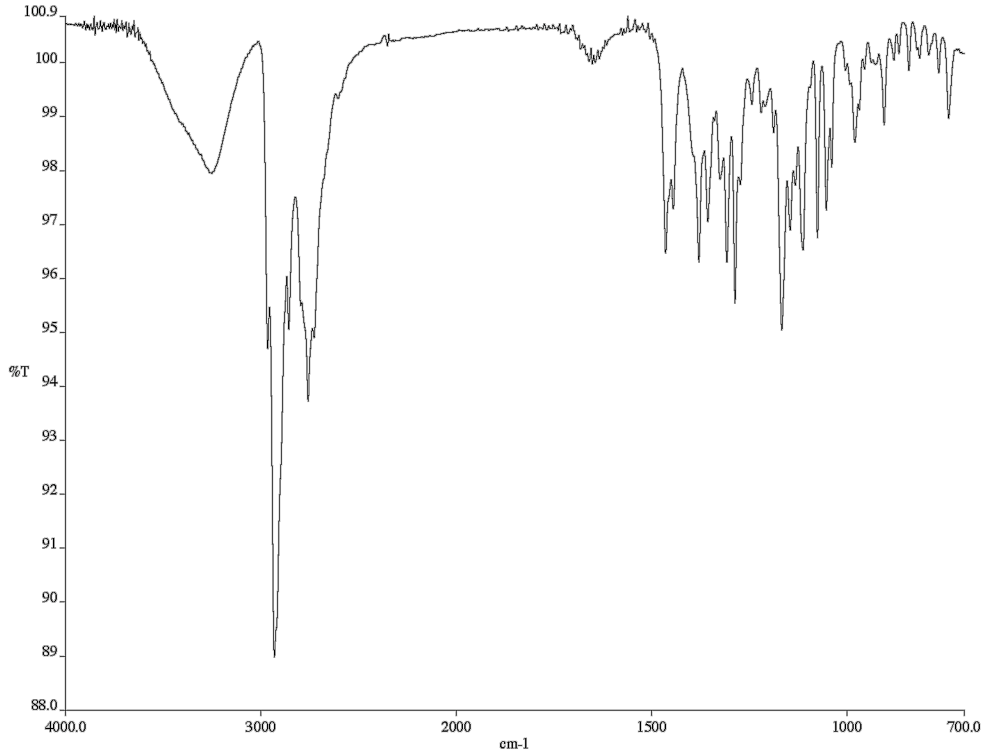

Figure A2.14 Infrared spectrum (thin film/NaCl) of compound **267**.

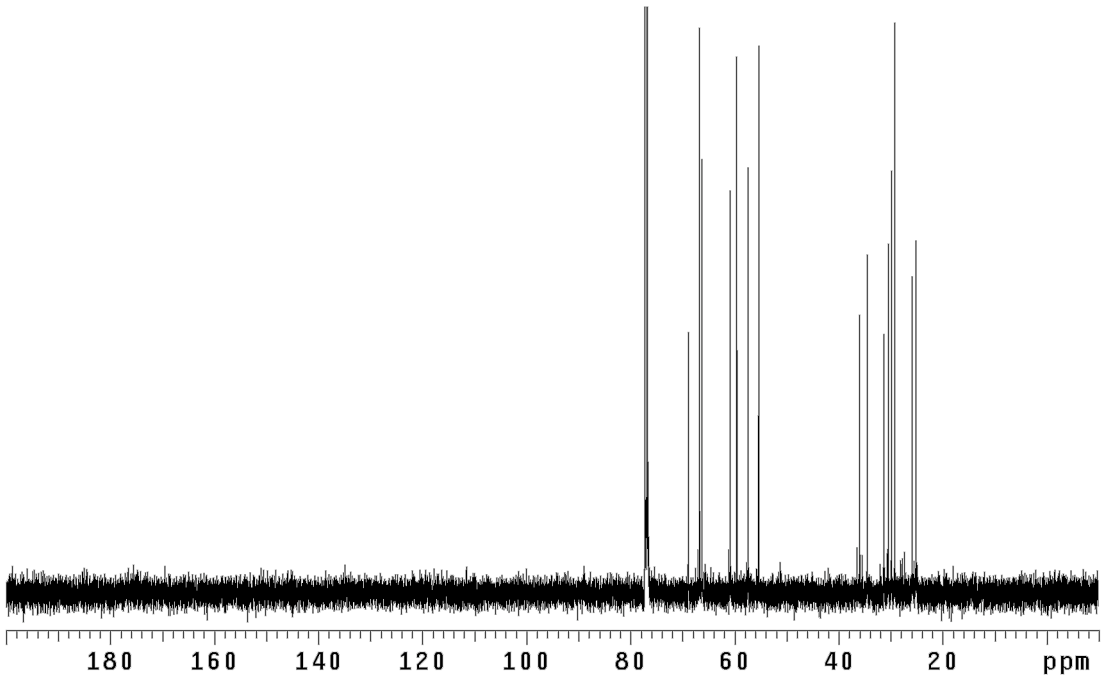

Figure A2.15 ^{13}C NMR (126 MHz, $CDCl_3$) of compound **267**.

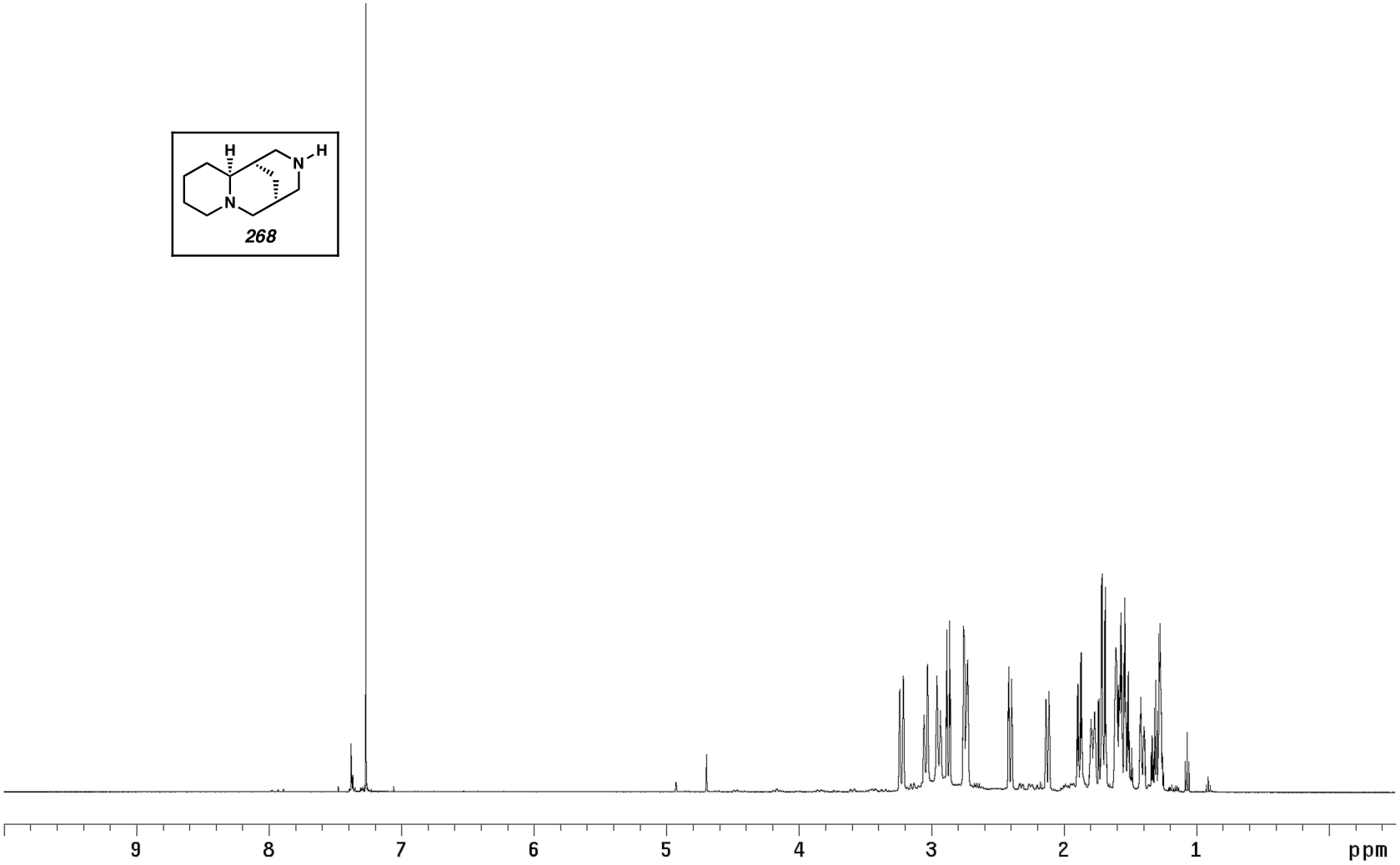

Figure A2.16 ^{1}H NMR (500 MHz, $CDCl_3$) of compound **268**.

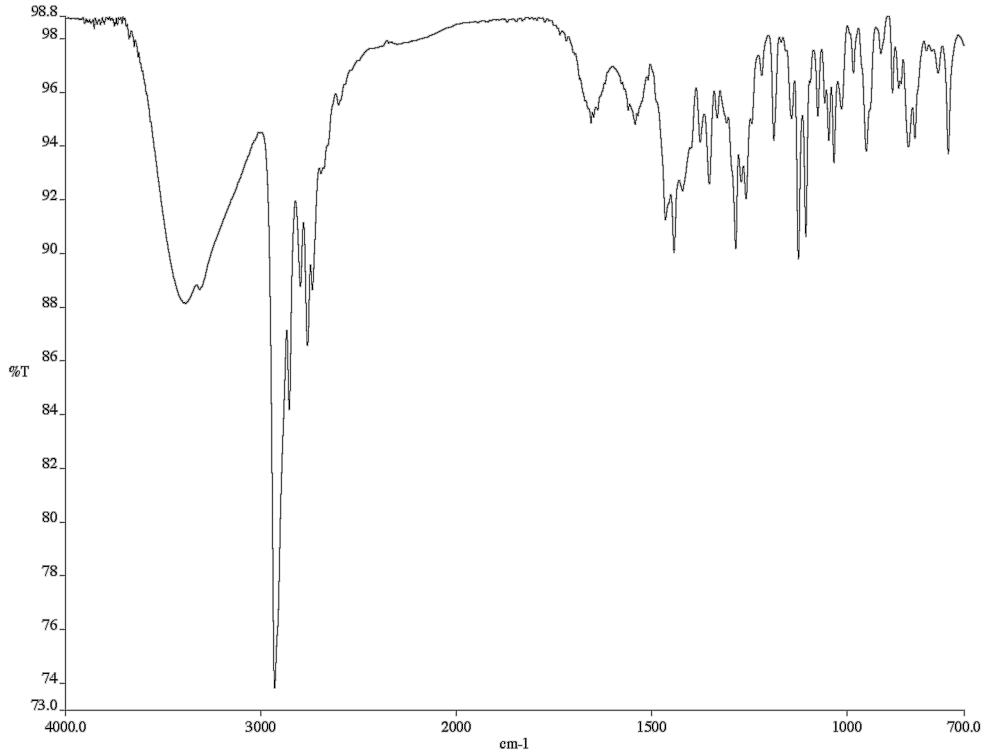

Figure A2.17 Infrared spectrum (thin film/NaCl) of compound **268**.

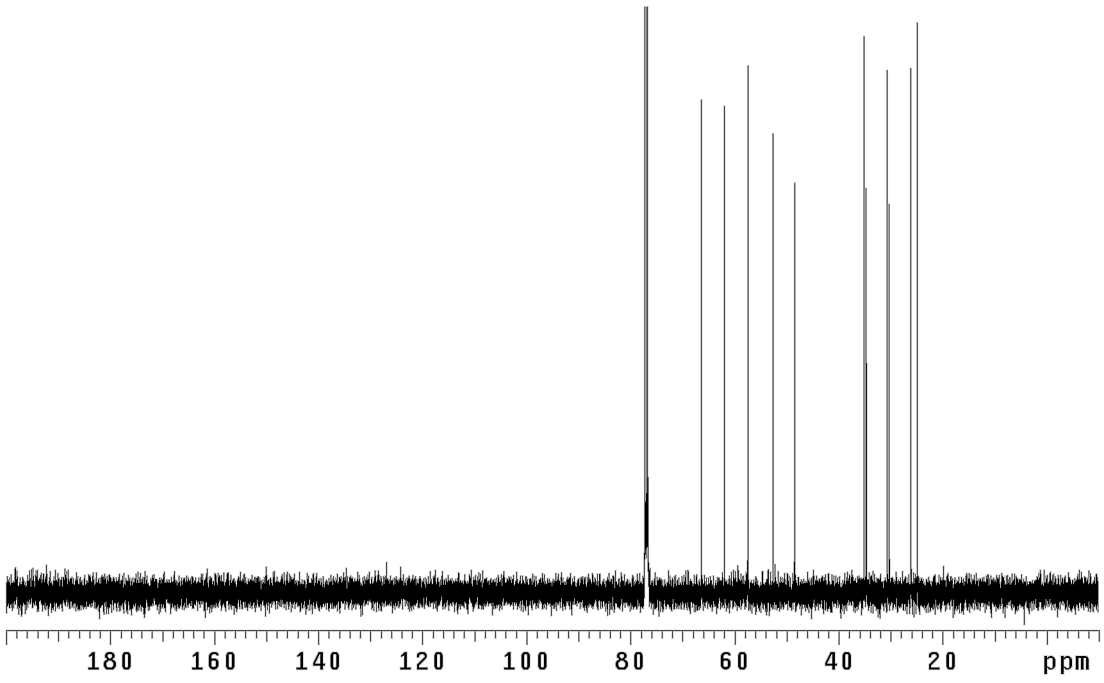

Figure A2.18 ^{13}C NMR (126 MHz, $CDCl_3$) of compound **268**.

APPENDIX 3

X-Ray Crystallographic Data Relevant to Chapter 4

A3.1 Pd(N-Me Diamine)Cl_2 (269)

Figure A3.1.1 Pd(N-Me Diamine)Cl_2 (**269**).[1]

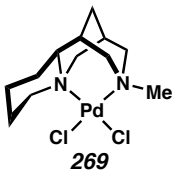

269

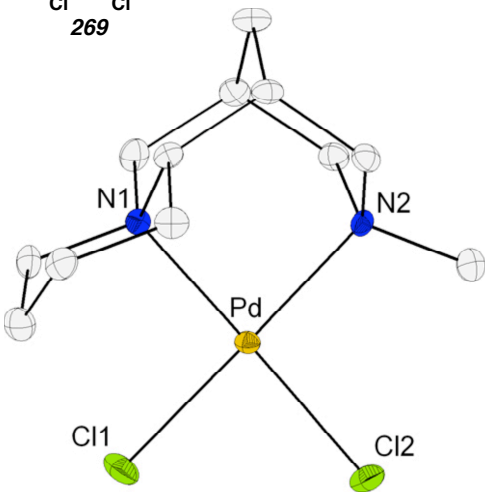

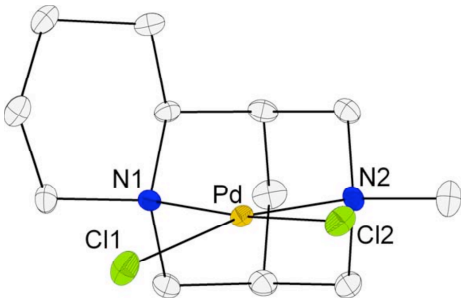

Select bond lengths (Å) and angles (°)			
Pd–N1	2.1116(14)	N1–Pd–N2	86.67(6)°
Pd–N2	2.1038(14)	Cl1–Pd–Cl2	84.895(18)°
Pd–Cl1	2.3197(4)	N2–Pd–Cl1	168.14(4)°
Pd–Cl2	2.3262(4)	N1–Pd–Cl2	175.64(4)°
		N1–Pd–Cl1	94.80(4)°
		N2–Pd–Cl2	94.52(4)°
		Σ ∠	704.67°

[1] Crystallographic data have been deposited at the CCDC, 12 Union Road, Cambridge CB2 1EZ, UK and copies can be obtained on request, free of charge, by quoting the publication citation and the deposition number 274539.

Table A3.1.1 Crystal data and structure refinement for DCE03 (CCDC 274539).

Empirical formula	$C_{12}H_{22}N_2Cl_2Pd$
Formula weight	371.62
Crystal Habit	Square
Crystal size	0.27 x 0.25 x 0.10 mm^3
Crystal color	Orange

Data Collection

Type of diffractometer	Bruker SMART 1000
Wavelength	0.71073 Å MoKα
Data Collection Temperature	100(2) K
θ range for 12945 reflections used in lattice determination	2.86 to 49.26°
Unit cell dimensions	a = 7.0251(3) Å b = 13.6041(5) Å β = 109.0170(10)° c = 7.5396(3) Å
Volume	681.23(5) $Å^3$
Z	2
Crystal system	Monoclinic
Space group	$P2_1$
Density (calculated)	1.812 Mg/m^3
F(000)	376
Data collection program	Bruker SMART v5.630
θ range for data collection	2.86 to 49.74°
Completeness to θ = 49.74°	93.9 %
Index ranges	$-14 \le h \le 11$, $-28 \le k \le 27$, $-14 \le l \le 15$
Data collection scan type	ω scans at 7 ϕ settings
Data reduction program	Bruker SAINT v6.45A
Reflections collected	23502
Independent reflections	11670 [R_{int}= 0.0389]
Absorption coefficient	1.734 mm^{-1}
Absorption correction	Face-indexed (SADABS)
Max. and min. transmission	0.8457 (1.000000) and 0.6517 (0.858406)

Structure Solution and Refinement

Structure solution program	Bruker XS v6.12
Primary solution method	Direct methods
Secondary solution method	Difference Fourier map
Hydrogen placement	Difference Fourier map
Structure refinement program	Bruker XL v6.12
Refinement method	Full matrix least-squares on F^2
Data / restraints / parameters	11670 / 1 / 242
Treatment of hydrogen atoms	Unrestrained
Goodness-of-fit on F^2	1.159
Final R indices [I>2σ(I), 10050 reflections]	R1 = 0.0348, *w*R2 = 0.0634
R indices (all data)	R1 = 0.0457, *w*R2 = 0.0669
Type of weighting scheme used	Sigma
Weighting scheme used	$w=1/\sigma^2(Fo^2)$
Max shift/error	0.001
Average shift/error	0.000
Absolute structure parameter	-0.015(17)
Largest diff. peak and hole	1.711 and -0.893 e.$Å^{-3}$

Special Refinement Details

Data were collected from two different crystals (DCE01 and DCE03) and data from both crystals provided high quality structures. The results from the second crystal (DCE03) are reported herein. The structure refined against data from the second crystal resulted in more uniform hydrogen parameters and a lower goodness-of-fit. The data set from the second crystal was nearly 10% more complete and the residual for the merging of equivalent reflections was lower.

Refinement of F^2 against ALL reflections. The weighted R-factor (*w*R) and goodness of fit (S) are based on F^2, conventional R-factors (R) are based on F, with F set to zero for negative F^2. The threshold expression of $F^2 > 2\sigma(F^2)$ is used only for calculating R-factors(gt) etc. and is not relevant to the choice of reflections for refinement. R-factors based on F^2 are statistically about twice as large as those based on F, and R-factors based on ALL data will be even larger.

All esds (except the esd in the dihedral angle between two l.s. planes) are estimated using the full covariance matrix. The cell esds are taken into account individually in the estimation of esds in distances, angles and torsion angles; correlations between esds in cell parameters are only used when they are defined by crystal symmetry. An approximate (isotropic) treatment of cell esds is used for estimating esds involving l.s. planes.

Figure A3.1.2 Pd(N-Me Diamine)Cl_2 (**269**).

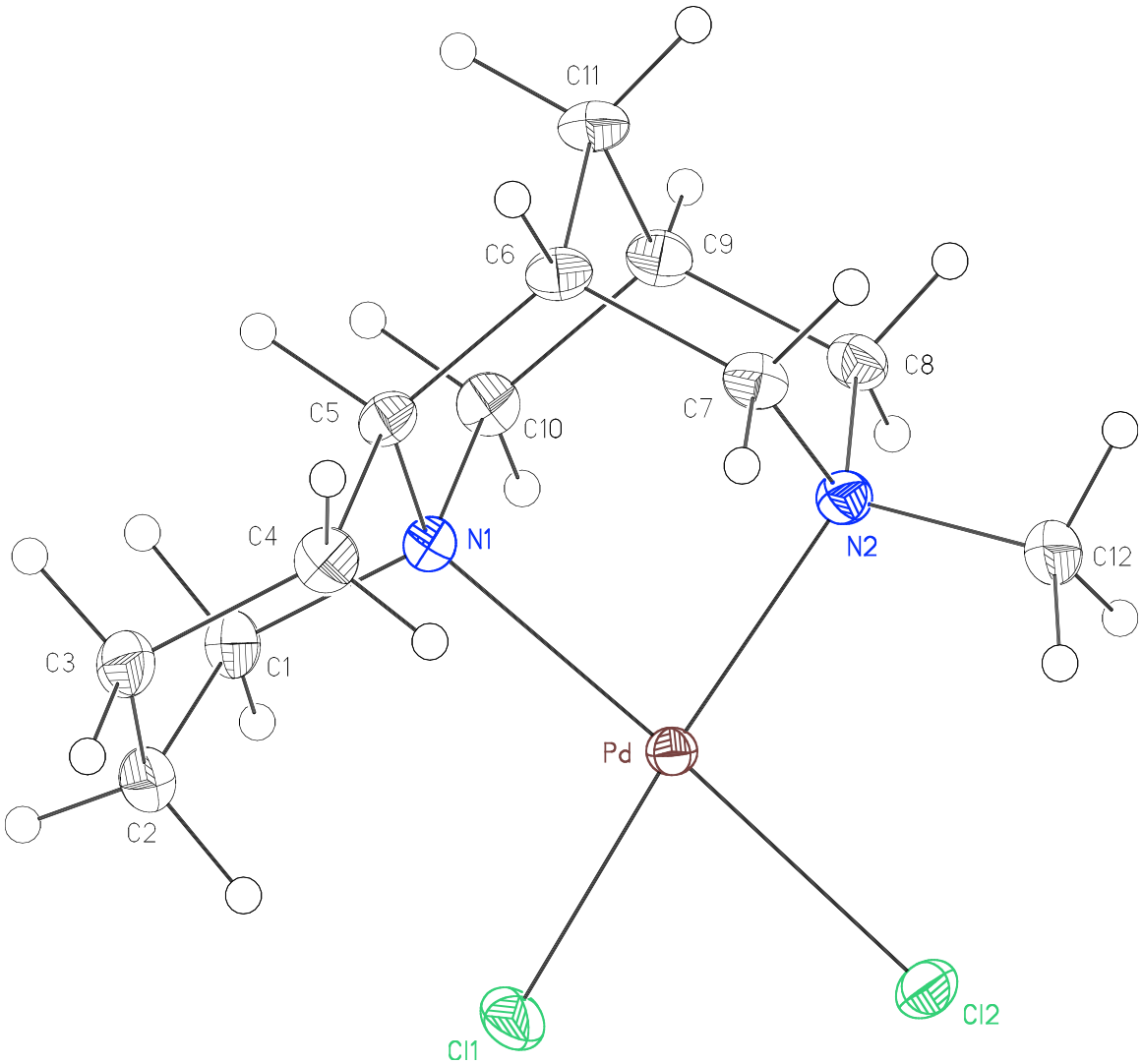

Figure A3.1.3 Unit cell of Pd(N-Me Diamine)Cl_2 (**269**).

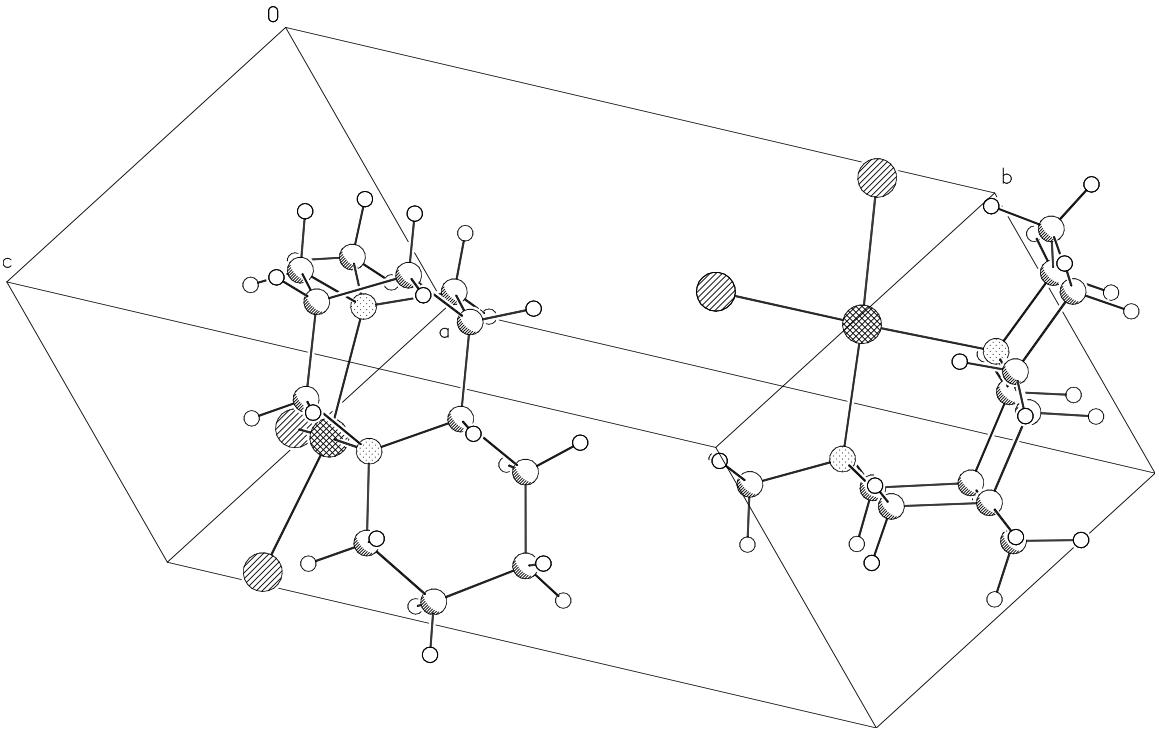

Figure A3.1.4 Stereo view of unit cell of Pd(N-Me Diamine)Cl_2 (**269**).

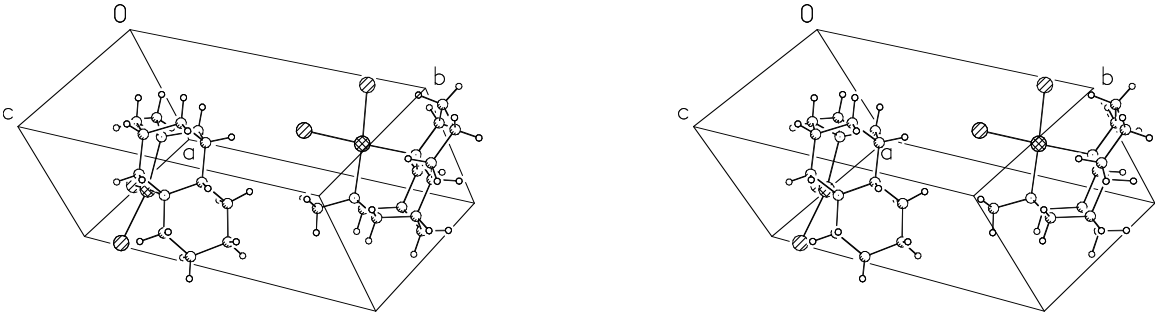

Table A3.1.2 Atomic coordinates (x 10^4) and equivalent isotropic displacement parameters ($Å^2$ x 10^3) for DCE03 (CCDC 274539). U(eq) is defined as the trace of the orthogonalized U^{ij} tensor.

	x	y	z	U_{eq}
Pd	4607(1)	7707(1)	1579(1)	12(1)
Cl(1)	2190(1)	7345(1)	-1278(1)	22(1)
Cl(2)	3137(1)	6436(1)	2738(1)	19(1)
N(1)	5775(2)	8934(1)	560(2)	13(1)
N(2)	7149(2)	7812(1)	4004(2)	14(1)
C(1)	4413(3)	9321(1)	-1293(3)	18(1)
C(2)	2473(3)	9778(1)	-1170(3)	20(1)
C(3)	2876(3)	10580(1)	318(3)	19(1)
C(4)	4301(3)	10173(1)	2169(3)	18(1)
C(5)	6231(3)	9805(1)	1889(2)	14(1)
C(6)	7912(3)	9599(1)	3719(2)	16(1)
C(7)	7432(3)	8795(1)	4916(3)	16(1)
C(8)	8913(3)	7580(1)	3341(2)	16(1)
C(9)	9359(3)	8386(1)	2135(3)	16(1)
C(10)	7675(3)	8583(1)	284(2)	16(1)
C(11)	9824(3)	9335(1)	3284(3)	18(1)
C(12)	7154(3)	7080(2)	5468(3)	21(1)

Table A3.1.3 Selected bond lengths [Å] and angles [°] for DCE03 (CCDC 274539).

Pd-N(2)	2.1038(14)	N(2)-Pd-N(1)	86.67(6)
Pd-N(1)	2.1116(14)	N(2)-Pd-Cl(1)	168.14(4)
Pd-Cl(1)	2.3197(4)	N(1)-Pd-Cl(1)	94.80(4)
Pd-Cl(2)	2.3262(4)	N(2)-Pd-Cl(2)	94.52(4)
		N(1)-Pd-Cl(2)	175.64(4)
		Cl(1)-Pd-Cl(2)	84.895(18)

Table A3.1.4 Bond lengths [Å] and angles [°] for DCE03 (CCDC 274539).

Pd-N(2)	2.1038(14)	C(5)-N(1)-C(1)	105.84(13)
Pd-N(1)	2.1116(14)	C(10)-N(1)-Pd	105.60(10)
Pd-Cl(1)	2.3197(4)	C(5)-N(1)-Pd	113.60(10)
Pd-Cl(2)	2.3262(4)	C(1)-N(1)-Pd	114.10(11)
N(1)-C(10)	1.495(2)	C(7)-N(2)-C(12)	106.97(14)
N(1)-C(5)	1.517(2)	C(7)-N(2)-C(8)	109.88(14)
N(1)-C(1)	1.508(2)	C(12)-N(2)-C(8)	107.55(14)
N(2)-C(7)	1.487(2)	C(7)-N(2)-Pd	114.23(11)
N(2)-C(12)	1.487(2)	C(12)-N(2)-Pd	113.32(12)
N(2)-C(8)	1.512(2)	C(8)-N(2)-Pd	104.69(10)
C(1)-C(2)	1.529(3)	N(1)-C(1)-C(2)	113.28(15)
C(1)-H(1A)	0.97(3)	N(1)-C(1)-H(1A)	106.5(18)
C(1)-H(1B)	0.97(3)	C(2)-C(1)-H(1A)	111.6(19)
C(2)-C(3)	1.523(3)	N(1)-C(1)-H(1B)	105.4(19)
C(2)-H(2A)	0.99(3)	C(2)-C(1)-H(1B)	111(2)
C(2)-H(2B)	0.93(3)	H(1A)-C(1)-H(1B)	108(3)
C(3)-C(4)	1.531(3)	C(1)-C(2)-C(3)	112.36(17)
C(3)-H(3A)	0.95(4)	C(1)-C(2)-H(2A)	105.6(18)
C(3)-H(3B)	0.94(3)	C(3)-C(2)-H(2A)	110.7(18)
C(4)-C(5)	1.523(2)	C(1)-C(2)-H(2B)	106.4(19)
C(4)-H(4A)	0.87(3)	C(3)-C(2)-H(2B)	110.4(18)
C(4)-H(4B)	0.96(3)	H(2A)-C(2)-H(2B)	111(3)
C(5)-C(6)	1.521(3)	C(4)-C(3)-C(2)	108.78(15)
C(5)-H(5)	1.06(2)	C(4)-C(3)-H(3A)	106(2)
C(6)-C(11)	1.525(3)	C(2)-C(3)-H(3A)	110(2)
C(6)-C(7)	1.524(3)	C(4)-C(3)-H(3B)	111.6(19)
C(6)-H(6)	1.02(3)	C(2)-C(3)-H(3B)	109.2(19)
C(7)-H(7A)	0.92(3)	H(3A)-C(3)-H(3B)	111(3)
C(7)-H(7B)	0.88(3)	C(3)-C(4)-C(5)	109.87(16)
C(8)-C(9)	1.521(3)	C(3)-C(4)-H(4A)	115(2)
C(8)-H(8A)	0.83(3)	C(5)-C(4)-H(4A)	102(2)
C(8)-H(8B)	0.91(3)	C(3)-C(4)-H(4B)	115.5(18)
C(9)-C(10)	1.530(3)	C(5)-C(4)-H(4B)	107(2)
C(9)-C(11)	1.529(3)	H(4A)-C(4)-H(4B)	106(3)
C(9)-H(9)	0.87(3)	N(1)-C(5)-C(6)	112.95(13)
C(10)-H(10A)	1.01(3)	N(1)-C(5)-C(4)	110.01(14)
C(10)-H(10B)	0.92(3)	C(6)-C(5)-C(4)	113.45(15)
C(11)-H(11A)	0.96(3)	N(1)-C(5)-H(5)	105.4(13)
C(11)-H(11B)	1.04(3)	C(6)-C(5)-H(5)	108.9(14)
C(12)-H(12A)	0.94(3)	C(4)-C(5)-H(5)	105.5(14)
C(12)-H(12B)	0.94(3)	C(5)-C(6)-C(11)	109.03(15)
C(12)-H(12C)	1.10(3)	C(5)-C(6)-C(7)	114.36(14)
		C(11)-C(6)-C(7)	109.79(15)
N(2)-Pd-N(1)	86.67(6)	C(5)-C(6)-H(6)	105.3(16)
N(2)-Pd-Cl(1)	168.14(4)	C(11)-C(6)-H(6)	112.0(17)
N(1)-Pd-Cl(1)	94.80(4)	C(7)-C(6)-H(6)	106.3(16)
N(2)-Pd-Cl(2)	94.52(4)	N(2)-C(7)-C(6)	113.18(14)
N(1)-Pd-Cl(2)	175.64(4)	N(2)-C(7)-H(7A)	107(2)
Cl(1)-Pd-Cl(2)	84.895(18)	C(6)-C(7)-H(7A)	111(2)
C(10)-N(1)-C(5)	109.60(13)	N(2)-C(7)-H(7B)	107.6(19)
C(10)-N(1)-C(1)	107.97(13)	C(6)-C(7)-H(7B)	112.5(19)

H(7A)-C(7)-H(7B)	105(3)	N(1)-C(10)-H(10B)	105.8(18)
N(2)-C(8)-C(9)	113.43(14)	C(9)-C(10)-H(10B)	112.2(17)
N(2)-C(8)-H(8A)	108(2)	H(10A)-C(10)-H(10B)	107(2)
C(9)-C(8)-H(8A)	108.2(19)	C(6)-C(11)-C(9)	106.27(14)
N(2)-C(8)-H(8B)	108.9(16)	C(6)-C(11)-H(11A)	112.8(18)
C(9)-C(8)-H(8B)	107.4(17)	C(9)-C(11)-H(11A)	110.4(18)
H(8A)-C(8)-H(8B)	111(3)	C(6)-C(11)-H(11B)	107.7(17)
C(8)-C(9)-C(10)	115.02(15)	C(9)-C(11)-H(11B)	111.7(16)
C(8)-C(9)-C(11)	108.50(15)	H(11A)-C(11)-H(11B)	108(3)
C(10)-C(9)-C(11)	109.15(15)	N(2)-C(12)-H(12A)	106.9(16)
C(8)-C(9)-H(9)	104.9(17)	N(2)-C(12)-H(12B)	110.7(17)
C(10)-C(9)-H(9)	106.0(17)	H(12A)-C(12)-H(12B)	109(2)
C(11)-C(9)-H(9)	113.3(18)	N(2)-C(12)-H(12C)	113.3(15)
N(1)-C(10)-C(9)	112.86(14)	H(12A)-C(12)-H(12C)	113(2)
N(1)-C(10)-H(10A)	110.0(18)	H(12B)-C(12)-H(12C)	105(2)
C(9)-C(10)-H(10A)	108.8(18)		

Table A3.1.5 Anisotropic displacement parameters ($Å^2$ x 10^4) for DCE03 (CCDC 274539). The anisotropic displacement factor exponent takes the form: $-2\pi^2$ [$h^2*a^2*U^{11}$ + ... + 2h*k*a*b*U^{12}]

	U^{11}	U^{22}	U^{33}	U^{23}	$U^{13\ 13}$	U^{12}
Pd	104(1)	108(1)	131(1)	-6(1)	32(1)	-3(1)
Cl(1)	202(2)	164(2)	215(2)	-19(1)	-45(2)	-12(1)
Cl(2)	158(2)	149(2)	265(2)	25(1)	87(2)	-11(1)
N(1)	133(5)	121(5)	128(5)	-3(3)	53(4)	3(3)
N(2)	131(4)	164(8)	137(5)	10(4)	44(4)	-14(4)
C(1)	200(7)	178(7)	149(7)	25(5)	55(6)	14(5)
C(2)	183(7)	170(7)	211(8)	31(5)	30(6)	17(5)
C(3)	185(7)	147(6)	244(8)	26(5)	69(6)	29(5)
C(4)	172(7)	166(6)	211(8)	-10(5)	95(6)	27(5)
C(5)	153(6)	118(5)	164(6)	-16(4)	68(5)	-14(4)
C(6)	146(6)	158(6)	167(7)	-45(5)	59(5)	-27(4)
C(7)	148(6)	191(7)	128(6)	-33(5)	48(5)	-10(5)
C(8)	123(5)	174(10)	179(6)	-1(5)	39(4)	14(4)
C(9)	125(6)	197(7)	186(7)	-13(5)	73(5)	6(4)
C(10)	161(6)	195(7)	157(7)	-8(5)	89(5)	15(5)
C(11)	127(6)	197(7)	223(8)	-30(5)	65(6)	-34(5)
C(12)	186(8)	233(8)	190(8)	62(6)	37(6)	-7(6)

Table A3.1.6 Hydrogen coordinates (x 10^4) and isotropic displacement parameters (Å^2 x 10^3) for DCE03 (CCDC 274539).

	x	y	z	U_{iso}
H(1A)	4140(50)	8770(20)	-2160(40)	23(7)
H(1B)	5210(50)	9800(30)	-1690(40)	30(9)
H(2A)	1700(50)	9230(20)	-860(40)	25(8)
H(2B)	1800(50)	10040(20)	-2350(40)	23(7)
H(3A)	3570(60)	11120(30)	-10(50)	43(10)
H(3B)	1650(50)	10790(20)	440(40)	24(7)
H(4A)	3880(50)	9650(20)	2580(40)	21(7)
H(4B)	4690(50)	10630(20)	3190(40)	21(7)
H(5)	6690(40)	10374(18)	1170(30)	8(5)
H(6)	8070(40)	10230(20)	4480(40)	17(6)
H(7A)	8450(50)	8730(20)	6050(40)	27(8)
H(7B)	6350(50)	8930(20)	5210(40)	18(7)
H(8A)	8660(40)	7070(20)	2710(40)	17(6)
H(8B)	10040(40)	7500(20)	4360(40)	16(6)
H(9)	10370(40)	8168(19)	1830(30)	11(6)
H(10A)	8170(50)	9080(20)	-460(40)	23(7)
H(10B)	7330(40)	8026(19)	-450(40)	16(6)
H(11A)	10960(50)	9240(20)	4390(40)	21(7)
H(11B)	10140(50)	9910(20)	2520(40)	18(7)
H(12A)	8380(40)	7152(19)	6440(30)	11(6)
H(12B)	7080(50)	6440(20)	4990(40)	15(7)
H(12C)	5840(50)	7140(20)	5950(40)	26(8)

A3.2 Pd(N-Et Diamine)Cl_2 (270)

Figure A3.2.1 Pd(N-Et Diamine)Cl_2 (**270**).[2]

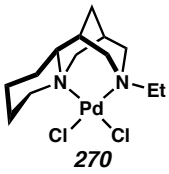

270

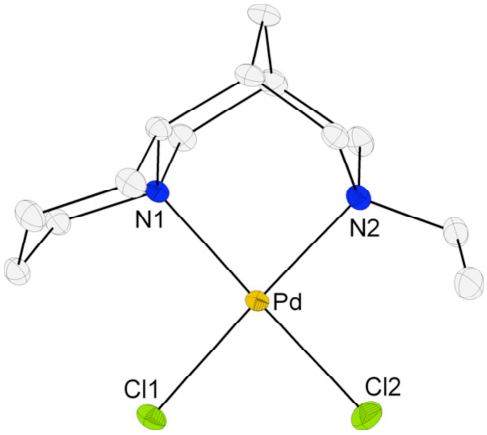

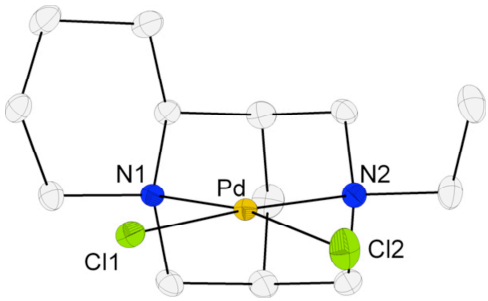

Select bond lengths (Å) and angles (°)			
Pd–N1	2.1294(16)	N1–Pd–N2	86.90(6)°
Pd–N2	2.1114(16)	Cl1–Pd–Cl2	83.73(2)°
Pd–Cl1	2.3254(5)	N2–Pd–Cl1	176.22(5)°
Pd–Cl2	2.3116(5)	N1–Pd–Cl2	171.22(4)°
		N1–Pd–Cl1	95.33(4)°
		N2–Pd–Cl2	93.61(5)°
		Σ ∠	707.01°

[2] Crystallographic data have been deposited at the CCDC, 12 Union Road, Cambridge CB2 1EZ, UK and copies can be obtained on request, free of charge, by quoting the publication citation and the deposition number 274867.

Table A3.2.1 Crystal data and structure refinement for DCE02 (CCDC 274867).

Empirical formula	$C_{13}H_{24}N_2Cl_2Pd \bullet CHCl_3$
Formula weight	505.01
Crystallization Solvent	Chloroform/heptane
Crystal Habit	Fragment
Crystal size	0.33 x 0.23 x 0.03 mm^3
Crystal color	Orange

Data Collection

Type of diffractometer	Bruker SMART 1000
Wavelength	0.71073 Å MoKα
Data Collection Temperature	100(2) K
θ range for 11657 reflections used in lattice determination	2.34 to 44.83°
Unit cell dimensions	a = 9.0343(3) Å b = 11.9016(4) Å β = 109.1540(10)° c = 9.2290(4) Å
Volume	937.39(6) $Å^3$
Z	2
Crystal system	Monoclinic
Space group	$P2_1$
Density (calculated)	1.789 Mg/m^3
F(000)	508
Data collection program	Bruker SMART v5.630
θ range for data collection	2.34 to 47.35°
Completeness to θ = 47.35°	94.5 %
Index ranges	$-18 \le h \le 18$, $-24 \le k \le 24$, $-18 \le l \le 16$
Data collection scan type	ω scans at 7 ϕ settings
Data reduction program	Bruker SAINT v6.45A
Reflections collected	29263
Independent reflections	14853 [R_{int}= 0.0447]
Absorption coefficient	1.700 mm^{-1}
Absorption correction	Face-indexed and (SADABS)
Max. and min. transmission	0.93080 (1.000000) and 0.61310 (0.877919)

Structure Solution and Refinement

Structure solution program	Bruker XS v6.12
Primary solution method	Direct methods
Secondary solution method	Difference Fourier map
Hydrogen placement	Difference Fourier map
Structure refinement program	Bruker XL v6.12
Refinement method	Full matrix least-squares on F^2
Data / restraints / parameters	14853 / 1 / 299
Treatment of hydrogen atoms	Unrestrained
Goodness-of-fit on F^2	1.076
Final R indices [I>2σ(I), 12280 reflections]	R1 = 0.0374, *w*R2 = 0.0699
R indices (all data)	R1 = 0.0532, *w*R2 = 0.0753
Type of weighting scheme used	Sigma
Weighting scheme used	$w=1/\sigma^2(Fo^2)$
Max shift/error	0.001
Average shift/error	0.000
Absolute structure determination	Anomalous dispersion
Absolute structure parameter	-0.005(16)
Largest diff. peak and hole	1.688 and -1.015 e.$Å^{-3}$

Special Refinement Details

Refinement of F^2 against ALL reflections. The weighted R-factor (*w*R) and goodness of fit (S) are based on F^2, conventional R-factors (R) are based on F, with F set to zero for negative F^2. The threshold expression of $F^2 > 2\sigma(F^2)$ is used only for calculating R-factors(gt) etc. and is not relevant to the choice of reflections for refinement. R-factors based on F^2 are statistically about twice as large as those based on F, and R-factors based on ALL data will be even larger.

All esds (except the esd in the dihedral angle between two l.s. planes) are estimated using the full covariance matrix. The cell esds are taken into account individually in the estimation of esds in distances, angles and torsion angles; correlations between esds in cell parameters are only used when they are defined by crystal symmetry. An approximate (isotropic) treatment of cell esds is used for estimating esds involving l.s. planes.

Figure A3.2.2 Pd(N-Et Diamine)Cl_2 (**270**).

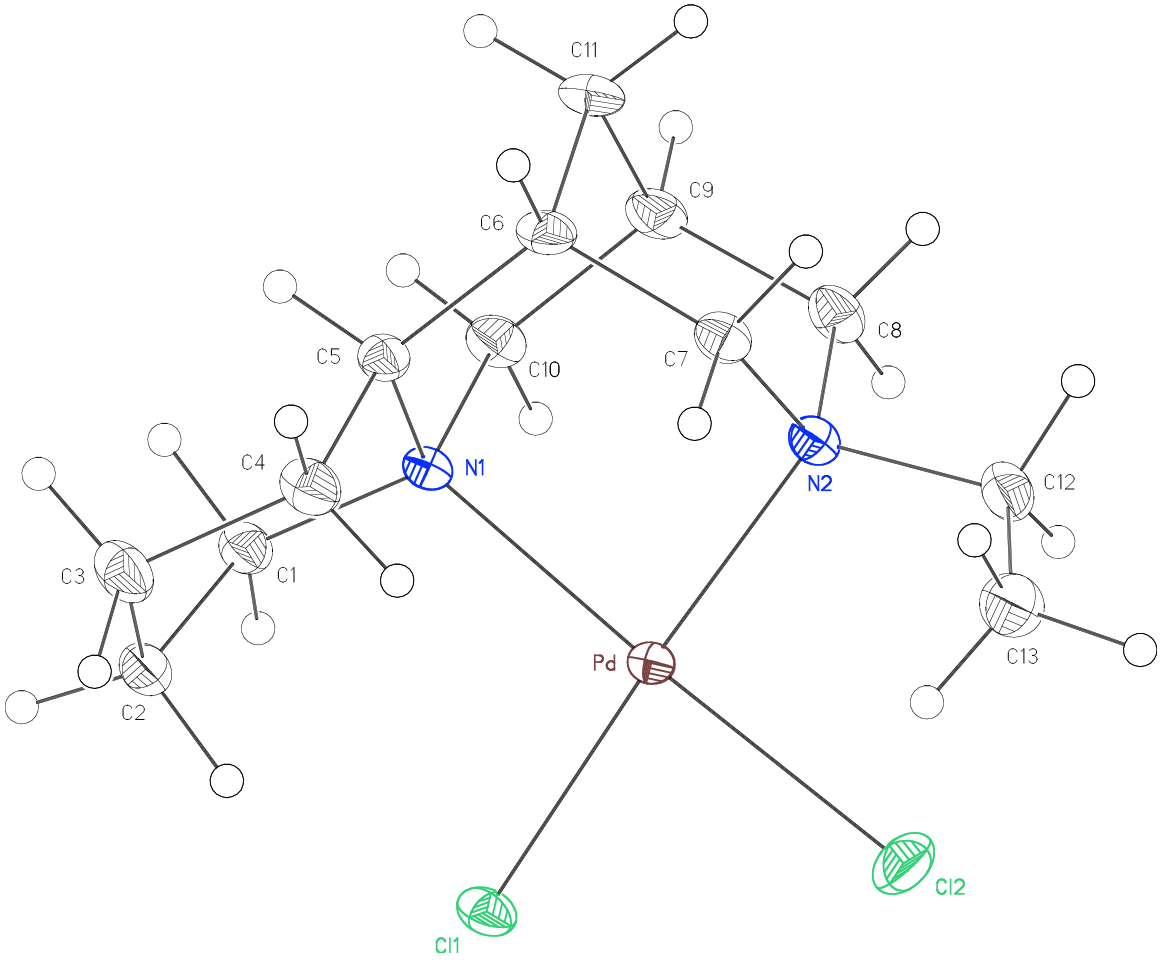

Figure A3.2.3 Unit cell of Pd(N-Et Diamine)Cl_2 (**270**).

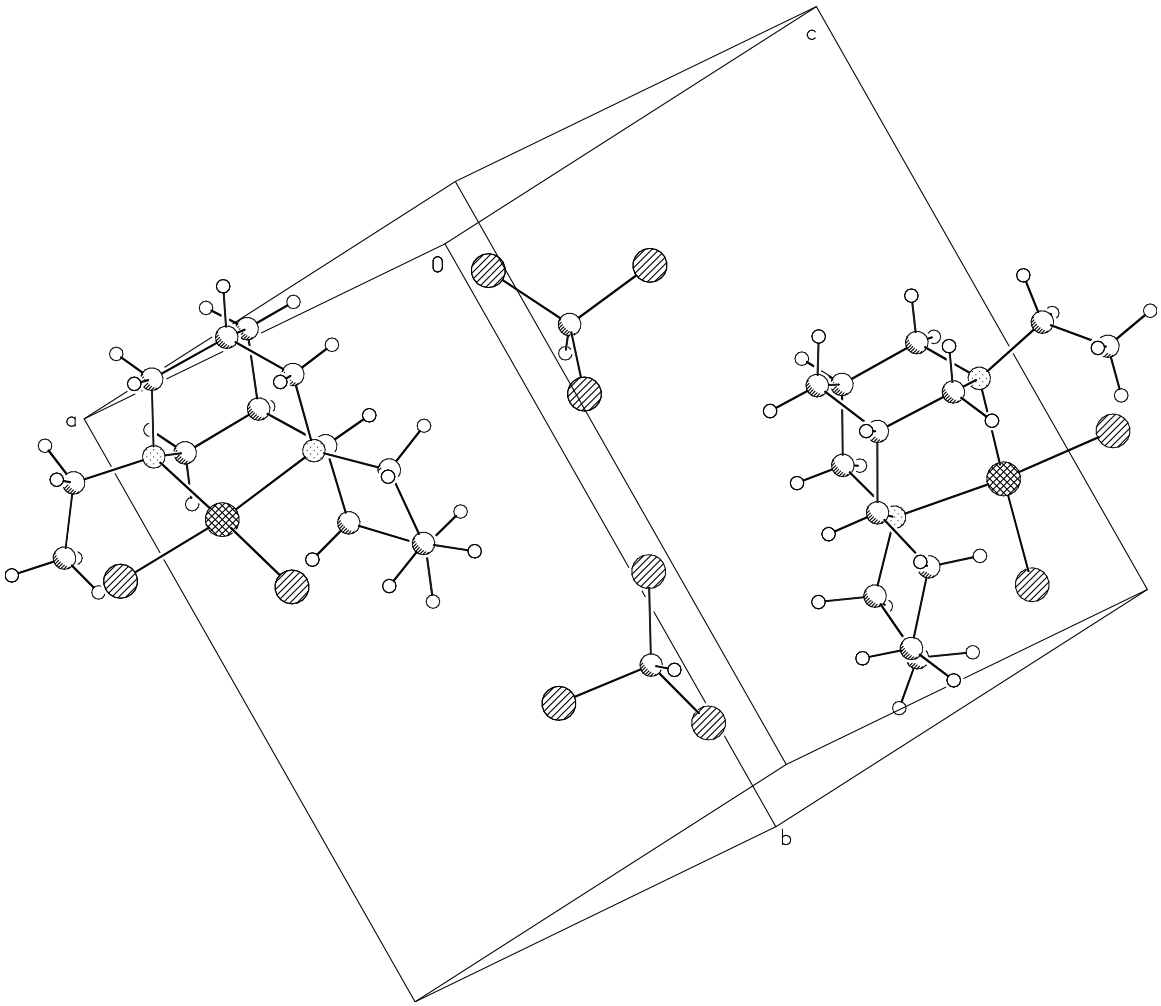

Figure A3.2.4 Stereo view of unit cell of Pd(N-Et Diamine)Cl_2 (**270**).

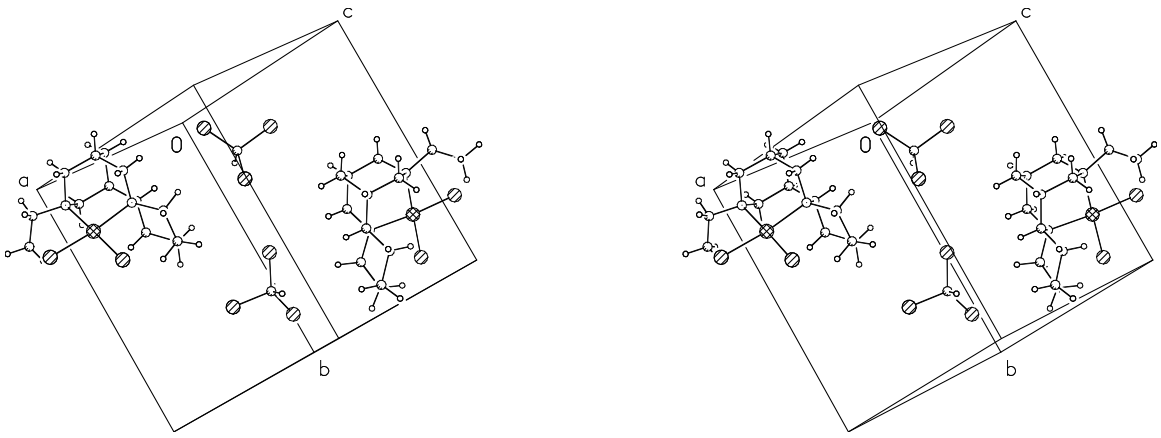

Table A3.2.2 Atomic coordinates (x 10^4) and equivalent isotropic displacement parameters ($Å^2$ x 10^3) for DCE02 (CCDC 274867). U(eq) is defined as the trace of the orthogonalized U^{ij} tensor.

	x	y	z	U_{eq}
Pd	-502(1)	7416(1)	7945(1)	11(1)
Cl(1)	-1611(1)	8902(1)	6313(1)	16(1)
Cl(2)	-2765(1)	7533(1)	8586(1)	25(1)
N(1)	1376(2)	7154(1)	7068(2)	11(1)
N(2)	359(2)	6015(1)	9376(2)	14(1)
C(1)	1487(2)	7997(2)	5899(2)	16(1)
C(2)	2061(2)	9155(2)	6567(3)	17(1)
C(3)	3579(2)	9095(2)	7934(3)	21(1)
C(4)	3431(2)	8198(2)	9058(3)	18(1)
C(5)	2985(2)	7074(2)	8246(2)	14(1)
C(6)	3144(2)	6060(2)	9299(2)	16(1)
C(7)	2074(2)	6097(2)	10273(2)	15(1)
C(8)	66(3)	5041(2)	8277(3)	17(1)
C(9)	1135(3)	5041(2)	7299(3)	17(1)
C(10)	941(2)	6055(2)	6231(2)	16(1)
C(11)	2840(3)	4977(2)	8351(3)	20(1)
C(12)	-472(3)	5756(2)	10498(3)	19(1)
C(13)	-169(3)	6607(2)	11797(3)	24(1)
Cl(3)	4429(1)	6076(1)	4377(1)	23(1)
Cl(4)	6571(1)	7160(1)	3071(1)	22(1)
Cl(5)	4005(1)	8432(1)	3477(1)	23(1)
C(14)	5387(2)	7339(2)	4248(2)	17(1)

Table A3.2.3 Selected bond lengths [Å] and angles [°] for DCE02 (CCDC 274867).

Pd-N(2)	2.1114(16)	N(2)-Pd-N(1)	86.90(6)
Pd-N(1)	2.1294(16)	N(2)-Pd-Cl(2)	93.61(5)
Pd-Cl(2)	2.3116(5)	N(1)-Pd-Cl(2)	171.22(4)
Pd-Cl(1)	2.3254(5)	N(2)-Pd-Cl(1)	176.22(5)
		N(1)-Pd-Cl(1)	95.33(4)
		Cl(2)-Pd-Cl(1)	83.73(2)

Table A3.2.4 Bond lengths [Å] and angles [°] for DCE02 (CCDC 274867).

Pd-N(2)	2.1114(16)	N(2)-Pd-Cl(2)	93.61(5)
Pd-N(1)	2.1294(16)	N(1)-Pd-Cl(2)	171.22(4)
Pd-Cl(2)	2.3116(5)	N(2)-Pd-Cl(1)	176.22(5)
Pd-Cl(1)	2.3254(5)	N(1)-Pd-Cl(1)	95.33(4)
N(1)-C(1)	1.500(2)	Cl(2)-Pd-Cl(1)	83.73(2)
N(1)-C(10)	1.505(2)	C(1)-N(1)-C(10)	106.28(15)
N(1)-C(5)	1.505(2)	C(1)-N(1)-C(5)	106.58(14)
N(2)-C(12)	1.497(3)	C(10)-N(1)-C(5)	110.07(14)
N(2)-C(7)	1.501(2)	C(1)-N(1)-Pd	115.17(11)
N(2)-C(8)	1.505(2)	C(10)-N(1)-Pd	102.45(11)
C(1)-C(2)	1.530(3)	C(5)-N(1)-Pd	115.83(12)
C(1)-H(1A)	0.99(4)	C(12)-N(2)-C(7)	107.03(16)
C(1)-H(1B)	1.01(3)	C(12)-N(2)-C(8)	106.85(15)
C(2)-C(3)	1.531(3)	C(7)-N(2)-C(8)	110.09(15)
C(2)-H(2A)	0.98(4)	C(12)-N(2)-Pd	115.45(12)
C(2)-H(2B)	1.01(3)	C(7)-N(2)-Pd	113.31(11)
C(3)-C(4)	1.524(3)	C(8)-N(2)-Pd	103.87(12)
C(3)-H(3A)	1.04(4)	N(1)-C(1)-C(2)	113.96(17)
C(3)-H(3B)	0.93(4)	N(1)-C(1)-H(1A)	114(2)
C(4)-C(5)	1.522(3)	C(2)-C(1)-H(1A)	105(2)
C(4)-H(4A)	0.89(4)	N(1)-C(1)-H(1B)	107.1(18)
C(4)-H(4B)	0.94(4)	C(2)-C(1)-H(1B)	111.0(19)
C(5)-C(6)	1.527(3)	H(1A)-C(1)-H(1B)	106(3)
C(5)-H(5)	0.94(3)	C(1)-C(2)-C(3)	112.56(16)
C(6)-C(7)	1.521(3)	C(1)-C(2)-H(2A)	111(2)
C(6)-C(11)	1.531(3)	C(3)-C(2)-H(2A)	109(3)
C(6)-H(6)	0.94(4)	C(1)-C(2)-H(2B)	107.5(19)
C(7)-H(7A)	0.93(3)	C(3)-C(2)-H(2B)	105.6(18)
C(7)-H(7B)	0.99(3)	H(2A)-C(2)-H(2B)	111(3)
C(8)-C(9)	1.523(3)	C(4)-C(3)-C(2)	109.83(16)
C(8)-H(8A)	0.92(4)	C(4)-C(3)-H(3A)	105(2)
C(8)-H(8B)	0.91(5)	C(2)-C(3)-H(3A)	108(2)
C(9)-C(11)	1.530(3)	C(4)-C(3)-H(3B)	107(3)
C(9)-C(10)	1.531(3)	C(2)-C(3)-H(3B)	111(2)
C(9)-H(9)	0.97(3)	H(3A)-C(3)-H(3B)	116(3)
C(10)-H(10A)	0.87(4)	C(5)-C(4)-C(3)	110.40(19)
C(10)-H(10B)	0.94(3)	C(5)-C(4)-H(4A)	109(2)
C(11)-H(11A)	0.93(4)	C(3)-C(4)-H(4A)	108(2)
C(11)-H(11B)	0.95(4)	C(5)-C(4)-H(4B)	111(2)
C(12)-C(13)	1.525(3)	C(3)-C(4)-H(4B)	110(2)
C(12)-H(12A)	0.95(4)	H(4A)-C(4)-H(4B)	108(3)
C(12)-H(12B)	0.90(3)	N(1)-C(5)-C(4)	109.69(14)
C(13)-H(13A)	0.98(4)	N(1)-C(5)-C(6)	112.15(14)
C(13)-H(13B)	0.98(4)	C(4)-C(5)-C(6)	115.27(17)
C(13)-H(13C)	0.93(5)	N(1)-C(5)-H(5)	102(2)
Cl(3)-C(14)	1.758(2)	C(4)-C(5)-H(5)	106(2)
Cl(4)-C(14)	1.7694(19)	C(6)-C(5)-H(5)	111(2)
Cl(5)-C(14)	1.781(2)	C(7)-C(6)-C(5)	114.08(15)
C(14)-H(14)	0.92(3)	C(7)-C(6)-C(11)	109.43(16)
		C(5)-C(6)-C(11)	109.85(17)
N(2)-Pd-N(1)	86.90(6)	C(7)-C(6)-H(6)	105(2)

C(5)-C(6)-H(6)	110(2)	H(10A)-C(10)-H(10B)	112(3)
C(11)-C(6)-H(6)	109(2)	C(9)-C(11)-C(6)	105.96(15)
N(2)-C(7)-C(6)	114.39(16)	C(9)-C(11)-H(11A)	109(3)
N(2)-C(7)-H(7A)	110(2)	C(6)-C(11)-H(11A)	107(2)
C(6)-C(7)-H(7A)	107.1(19)	C(9)-C(11)-H(11B)	109(2)
N(2)-C(7)-H(7B)	110.3(18)	C(6)-C(11)-H(11B)	109(2)
C(6)-C(7)-H(7B)	109.5(18)	H(11A)-C(11)-H(11B)	116(3)
H(7A)-C(7)-H(7B)	105(2)	N(2)-C(12)-C(13)	113.94(18)
N(2)-C(8)-C(9)	113.15(15)	N(2)-C(12)-H(12A)	109(2)
N(2)-C(8)-H(8A)	108(2)	C(13)-C(12)-H(12A)	108(2)
C(9)-C(8)-H(8A)	114(2)	N(2)-C(12)-H(12B)	102.9(17)
N(2)-C(8)-H(8B)	105(3)	C(13)-C(12)-H(12B)	117.9(17)
C(9)-C(8)-H(8B)	109(3)	H(12A)-C(12)-H(12B)	104(3)
H(8A)-C(8)-H(8B)	108(4)	C(12)-C(13)-H(13A)	117(2)
C(8)-C(9)-C(11)	109.05(18)	C(12)-C(13)-H(13B)	109(2)
C(8)-C(9)-C(10)	114.87(16)	H(13A)-C(13)-H(13B)	106(3)
C(11)-C(9)-C(10)	109.07(17)	C(12)-C(13)-H(13C)	109(2)
C(8)-C(9)-H(9)	112(2)	H(13A)-C(13)-H(13C)	105(3)
C(11)-C(9)-H(9)	105(2)	H(13B)-C(13)-H(13C)	112(3)
C(10)-C(9)-H(9)	106.2(19)	Cl(3)-C(14)-Cl(4)	110.45(12)
N(1)-C(10)-C(9)	113.56(16)	Cl(3)-C(14)-Cl(5)	110.80(10)
N(1)-C(10)-H(10A)	108(2)	Cl(4)-C(14)-Cl(5)	109.16(11)
C(9)-C(10)-H(10A)	107(2)	Cl(3)-C(14)-H(14)	113.4(17)
N(1)-C(10)-H(10B)	106(2)	Cl(4)-C(14)-H(14)	110.2(16)
C(9)-C(10)-H(10B)	110(2)	Cl(5)-C(14)-H(14)	102.5(17)

Table A3.2.5 Anisotropic displacement parameters ($Å^2$ x 10^4) for DCE02 (CCDC 274867). The anisotropic displacement factor exponent takes the form: $-2\pi^2 [h^2*a^2*U^{11} + ... + 2h*k*a*b*U^{12}]$

	U^{11}	U^{22}	U^{33}	U^{23}	U^{13}	U^{12}
Pd	103(1)	96(1)	111(1)	-4(1)	24(1)	5(1)
Cl(1)	136(2)	127(1)	184(2)	24(1)	7(1)	15(1)
Cl(2)	167(2)	337(3)	288(2)	91(2)	120(2)	80(2)
N(1)	127(5)	93(4)	115(6)	-1(4)	30(4)	7(3)
N(2)	159(6)	113(5)	135(7)	3(5)	46(5)	3(4)
C(1)	187(7)	144(6)	154(8)	22(6)	63(6)	17(5)
C(2)	166(7)	131(6)	210(9)	28(6)	60(6)	-1(5)
C(3)	177(7)	151(6)	274(11)	34(7)	31(7)	-34(6)
C(4)	152(7)	151(6)	214(9)	2(6)	15(6)	-18(5)
C(5)	110(5)	133(5)	153(7)	19(5)	22(5)	11(4)
C(6)	132(6)	140(6)	180(8)	19(6)	20(5)	39(5)
C(7)	168(6)	140(6)	125(7)	7(6)	25(5)	11(5)
C(8)	222(8)	113(6)	176(9)	-22(6)	60(6)	-32(5)
C(9)	242(8)	109(6)	166(8)	-28(6)	72(6)	12(5)
C(10)	226(8)	129(6)	124(7)	-23(6)	56(6)	10(5)
C(11)	226(8)	117(6)	253(10)	6(6)	88(7)	60(6)
C(12)	254(9)	156(6)	200(9)	33(7)	112(7)	3(6)
C(13)	348(11)	225(8)	206(10)	19(8)	153(9)	40(8)
Cl(3)	244(2)	163(2)	285(3)	30(2)	92(2)	-26(2)
Cl(4)	218(2)	203(2)	264(2)	-37(2)	117(2)	-5(1)
Cl(5)	248(2)	166(2)	289(3)	18(2)	123(2)	30(2)
C(14)	168(5)	154(7)	180(7)	-12(7)	62(5)	-19(6)

Table A3.2.6 Hydrogen coordinates (x 10^4) and isotropic displacement parameters (Å^2 x 10^3) for DCE02 (CCDC 274867).

	x	y	z	U_{iso}
H(1A)	480(50)	8140(30)	5080(40)	26(9)
H(1B)	2210(40)	7670(30)	5370(30)	19(8)
H(2A)	2230(50)	9650(30)	5800(50)	36(11)
H(2B)	1250(40)	9470(30)	6980(30)	13(7)
H(3A)	3710(50)	9850(30)	8530(40)	28(9)
H(3B)	4420(50)	8890(40)	7620(40)	34(10)
H(4A)	4350(50)	8130(30)	9790(50)	31(10)
H(4B)	2700(50)	8420(30)	9530(40)	26(9)
H(5)	3620(40)	6990(30)	7620(40)	26(9)
H(6)	4160(50)	6040(30)	10010(40)	28(9)
H(7A)	2360(40)	5510(20)	10960(40)	11(7)
H(7B)	2290(40)	6790(20)	10910(30)	11(7)
H(8A)	-980(50)	5030(30)	7720(40)	28(9)
H(8B)	270(50)	4420(40)	8880(50)	39(11)
H(9)	980(40)	4380(30)	6650(40)	14(7)
H(10A)	1560(40)	5950(30)	5690(40)	24(8)
H(10B)	-110(40)	6120(30)	5610(40)	18(8)
H(11A)	2950(50)	4380(30)	9030(40)	31(10)
H(11B)	3510(40)	4970(30)	7740(40)	22(8)
H(12A)	-150(50)	5040(30)	10940(50)	29(10)
H(12B)	-1460(30)	5650(20)	9890(30)	5(6)
H(13A)	890(40)	6620(30)	12550(40)	21(8)
H(13B)	-870(50)	6450(40)	12390(50)	34(10)
H(13C)	-310(40)	7320(40)	11380(40)	36(10)
H(14)	5980(30)	7630(20)	5190(30)	7(6)

A3.3 Pd(N-Me Diamine)Br_2 (274)

Figure A3.3.1 Pd(N-Me Diamine)Br_2 (**274**).[3,4]

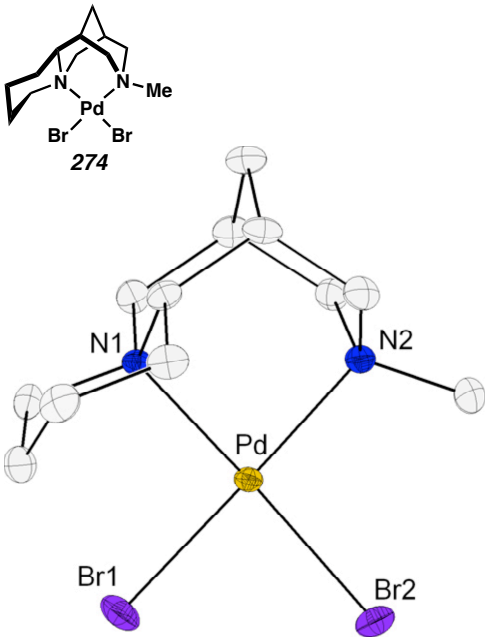

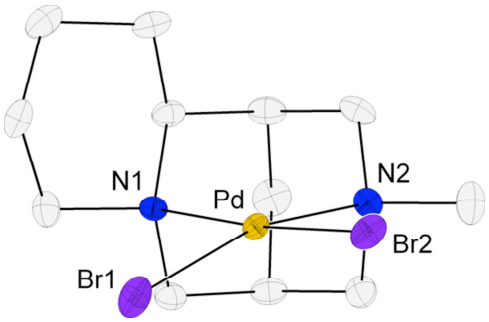

Select bond lengths (Å) and angles (°)			
Pd–N1	2.126(2)	N1–Pd–N2	86.46(8)°
Pd–N2	2.117(2)	Br1–Pd–Br2	84.449(12)°
Pd–Br1	2.4463(3)	N2–Pd–Br1	165.81(6)°
Pd–Br2	2.4513(3)	N1–Pd–Br2	174.56(6)°
		N1–Pd–Br1	95.17(6)°
		N2–Pd–Br2	95.24(6)°
		Σ ∠	701.69°

[3] The numbering in Figure A3.3.1 differs from that in the X-ray crystallographic report.

[4] Crystallographic data have been deposited at the CCDC, 12 Union Road, Cambridge CB2 1EZ, UK and copies can be obtained on request, free of charge, by quoting the publication citation and the deposition number 639648.

Table A3.3.1 Crystal data and structure refinement for DCE04 (CCDC 639648).

Empirical formula	$C_{12}H_{22}N_2Br_2Pd$
Formula weight	460.54
Crystallization Solvent	Chloroform/hexanes
Crystal Habit	Fragment
Crystal size	0.36 x 0.12 x 0.08 mm^3
Crystal color	Brown

Data Collection

Type of diffractometer	Bruker SMART 1000
Wavelength	0.71073 Å MoKα
Data Collection Temperature	100(2) K
θ range for 13773 reflections used in lattice determination	2.84 to 42.48°
Unit cell dimensions	a = 7.0987(2) Å b = 13.9562(3) Å β = 107.4540(10)° c = 7.5296(2) Å
Volume	711.62(3) $Å^3$
Z	2
Crystal system	Monoclinic
Space group	$P2_1$
Density (calculated)	2.149 Mg/m^3
F(000)	448
Data collection program	Bruker SMART v5.630
θ range for data collection	2.84 to 42.48°
Completeness to θ = 42.48°	94.4 %
Index ranges	$-13 \le h \le 13$, $-26 \le k \le 26$, $-14 \le l \le 14$
Data collection scan type	ω scans at 9 ϕ settings
Data reduction program	Bruker SAINT v6.45A
Reflections collected	23293
Independent reflections	8669 [R_{int}= 0.0533]
Absorption coefficient	6.900 mm^{-1}
Absorption correction	Semi-empirical from equivalents
Max. and min. transmission	0.7480 and 0.2324

Structure Solution and Refinement

Structure solution program	Bruker XS v6.12
Primary solution method	Direct methods
Secondary solution method	Difference Fourier map
Hydrogen placement	Geometric positions
Structure refinement program	Bruker XL v6.12
Refinement method	Full matrix least-squares on F^2
Data / restraints / parameters	8669 / 1 / 155
Treatment of hydrogen atoms	Riding
Goodness-of-fit on F^2	0.991
Final R indices [I>2σ(I), 7491 reflections]	R1 = 0.0348, *w*R2 = 0.0686
R indices (all data)	R1 = 0.0445, *w*R2 = 0.0719
Type of weighting scheme used	Sigma
Weighting scheme used	$w=1/\sigma^2(Fo^2)$
Max shift/error	0.001
Average shift/error	0.000
Absolute structure determination	Anomalous differences
Absolute structure parameter	0.039(5)
Largest diff. peak and hole	2.583 and -0.963 e.$Å^{-3}$

Special Refinement Details

All difference Fourier peaks larger than one electron lie within 1Å of either Pd or Br.

Refinement of F^2 against ALL reflections. The weighted R-factor (*w*R) and goodness of fit (S) are based on F^2, conventional R-factors (R) are based on F, with F set to zero for negative F^2. The threshold expression of $F^2 > 2\sigma(F^2)$ is used only for calculating R-factors(gt) etc. and is not relevant to the choice of reflections for refinement. R-factors based on F^2 are statistically about twice as large as those based on F, and R-factors based on ALL data will be even larger.

All esds (except the esd in the dihedral angle between two l.s. planes) are estimated using the full covariance matrix. The cell esds are taken into account individually in the estimation of esds in distances, angles and torsion angles; correlations between esds in cell parameters are only used when they are defined by crystal symmetry. An approximate (isotropic) treatment of cell esds is used for estimating esds involving l.s. planes.

Figure A3.3.2 Pd(N-Me Diamine)Br_2 (**274**).

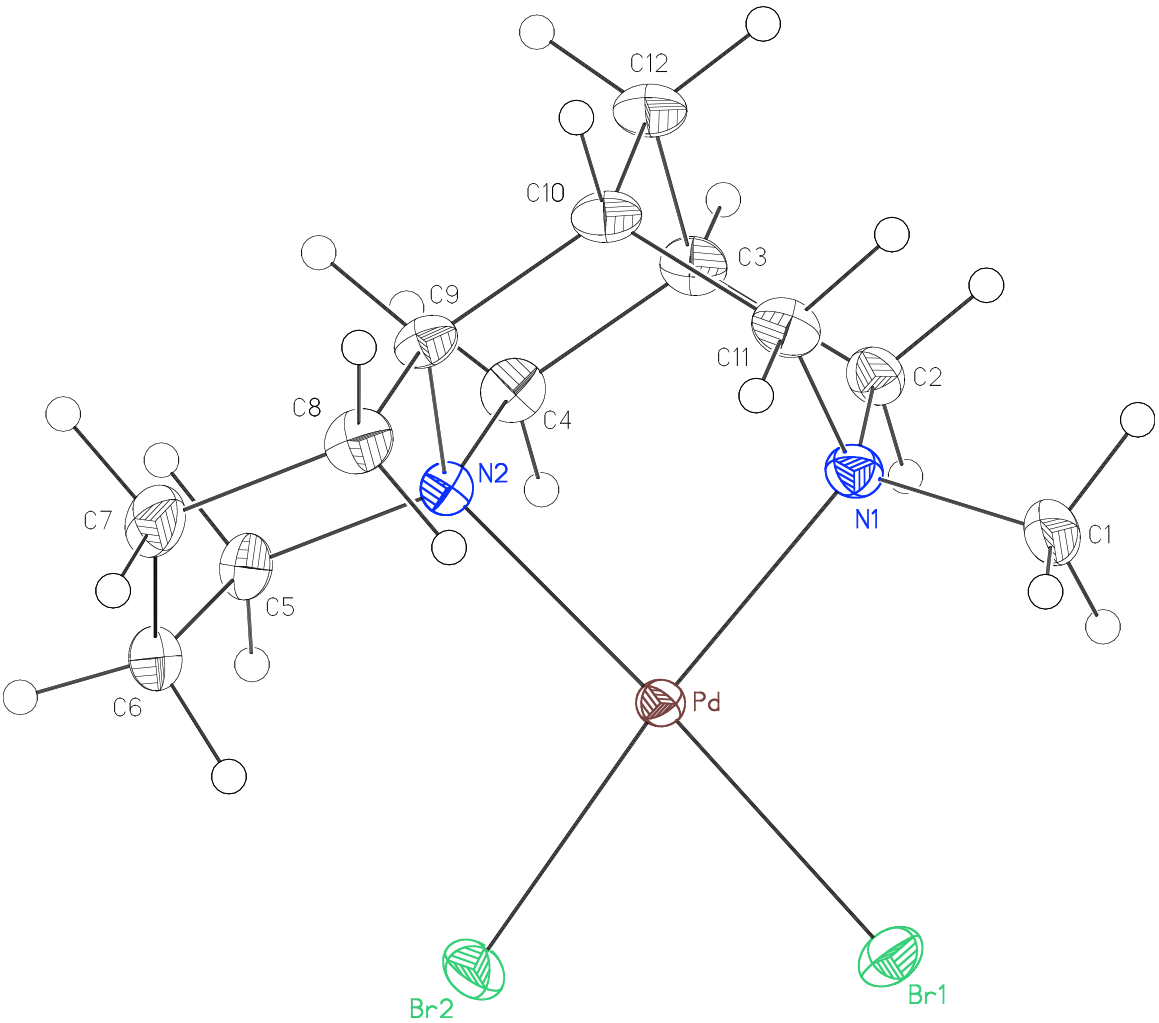

Table A3.3.2 Atomic coordinates (x 10^4) and equivalent isotropic displacement parameters ($Å^2$ x 10^3) for DCE04 (CCDC 639648). U(eq) is defined as the trace of the orthogonalized U^{ij} tensor.

	x	y	z	U_{eq}
Pd	4434(1)	7358(1)	6449(1)	12(1)
Br(1)	2842(1)	6044(1)	7616(1)	20(1)
Br(2)	2121(1)	6941(1)	3422(1)	25(1)
N(1)	6883(3)	7466(2)	8877(3)	16(1)
N(2)	5599(3)	8584(2)	5468(3)	13(1)
C(1)	6893(4)	6742(2)	10329(4)	23(1)
C(2)	8636(4)	7247(2)	8200(3)	17(1)
C(3)	9104(4)	8050(2)	7009(4)	18(1)
C(4)	7496(4)	8248(2)	5183(4)	18(1)
C(5)	4314(4)	8974(2)	3645(4)	19(1)
C(6)	2377(4)	9409(2)	3784(4)	21(1)
C(7)	2732(5)	10167(2)	5296(4)	23(1)
C(8)	4074(4)	9759(2)	7107(4)	20(1)
C(9)	5998(4)	9417(2)	6811(4)	16(1)
C(10)	7627(4)	9213(2)	8624(4)	18(1)
C(11)	7135(4)	8421(2)	9805(4)	19(1)
C(12)	9530(4)	8964(2)	8174(4)	21(1)

Table A3.3.3 Selected bond lengths [Å] and angles [°] for DCE04 (CCDC 639648).

Pd-N(2)	2.126(2)	N(2)-Pd-N(1)	86.46(8)
Pd-N(1)	2.117(2)	N(2)-Pd-Br(2)	95.17(6)
Pd-Br(2)	2.4463(3)	N(1)-Pd-Br(2)	165.81(6)
Pd-Br(1)	2.4513(3)	N(2)-Pd-Br(1)	174.56(6)
		N(1)-Pd-Br(1)	95.24(6)
		Br(2)-Pd-Br(1)	84.449(12)

Table A3.3.4 Bond lengths [Å] and angles [°] for DCE04 (CCDC 639648).

Pd-N(2)	2.126(2)	C(11)-N(1)-C(2)	110.1(2)
Pd-N(1)	2.117(2)	C(1)-N(1)-C(2)	106.7(2)
Pd-Br(2)	2.4463(3)	C(11)-N(1)-Pd	114.87(16)
Pd-Br(1)	2.4513(3)	C(1)-N(1)-Pd	114.09(17)
N(1)-C(11)	1.490(3)	C(2)-N(1)-Pd	103.91(14)
N(1)-C(1)	1.487(4)	C(5)-N(2)-C(4)	107.84(19)
N(1)-C(2)	1.511(3)	C(5)-N(2)-C(9)	105.8(2)
N(2)-C(5)	1.504(3)	C(4)-N(2)-C(9)	109.9(2)
N(2)-C(4)	1.501(3)	C(5)-N(2)-Pd	114.59(16)
N(2)-C(9)	1.511(3)	C(4)-N(2)-Pd	104.94(16)
C(2)-C(3)	1.532(4)	C(9)-N(2)-Pd	113.69(15)
C(3)-C(12)	1.525(4)	N(1)-C(2)-C(3)	113.2(2)
C(3)-C(4)	1.526(4)	C(12)-C(3)-C(4)	109.4(2)
C(5)-C(6)	1.535(4)	C(12)-C(3)-C(2)	108.4(2)
C(6)-C(7)	1.519(4)	C(4)-C(3)-C(2)	115.1(2)
C(7)-C(8)	1.521(4)	N(2)-C(4)-C(3)	112.8(2)
C(8)-C(9)	1.525(4)	N(2)-C(5)-C(6)	113.0(2)
C(9)-C(10)	1.528(4)	C(7)-C(6)-C(5)	112.1(2)
C(10)-C(11)	1.524(4)	C(8)-C(7)-C(6)	109.3(2)
C(10)-C(12)	1.528(4)	C(7)-C(8)-C(9)	109.5(2)
		N(2)-C(9)-C(8)	110.0(2)
N(2)-Pd-N(1)	86.46(8)	N(2)-C(9)-C(10)	113.2(2)
N(2)-Pd-Br(2)	95.17(6)	C(8)-C(9)-C(10)	113.5(2)
N(1)-Pd-Br(2)	165.81(6)	C(11)-C(10)-C(12)	109.7(2)
N(2)-Pd-Br(1)	174.56(6)	C(11)-C(10)-C(9)	114.3(2)
N(1)-Pd-Br(1)	95.24(6)	C(12)-C(10)-C(9)	109.1(2)
Br(2)-Pd-Br(1)	84.449(12)	N(1)-C(11)-C(10)	113.1(2)
C(11)-N(1)-C(1)	106.8(2)	C(3)-C(12)-C(10)	106.4(2)

Table A3.3.5 Anisotropic displacement parameters ($Å^2$ x 10^4) for DCE04 (CCDC 639648). The anisotropic displacement factor exponent takes the form: $-2\pi^2$ [$h^2*a^2*U^{11}$ + ... + $2h*k*a*b*U^{12}$]

	U	U^{22}	U^{33}	U^{23}	U^{13}	U^{12}
Pd	110(1)	111(1)	137(1)	-2(1)	27(1)	1(1)
Br(1)	175(1)	151(1)	305(1)	29(1)	103(1)	-6(1)
Br(2)	254(1)	174(1)	236(1)	-17(1)	-78(1)	-10(1)
N(1)	138(7)	183(10)	148(7)	4(7)	43(7)	-14(7)
N(2)	141(8)	135(8)	123(7)	-6(6)	52(7)	3(7)
C(1)	207(12)	280(13)	187(11)	76(10)	17(10)	-13(10)
C(2)	140(9)	188(11)	180(9)	6(8)	44(8)	15(8)
C(3)	133(9)	208(11)	212(11)	-20(9)	84(9)	13(8)
C(4)	186(10)	201(10)	179(10)	-14(9)	106(9)	11(9)
C(5)	224(12)	191(11)	163(10)	45(8)	61(9)	7(9)
C(6)	195(11)	178(11)	237(12)	49(9)	21(10)	24(9)
C(7)	225(12)	158(10)	316(14)	40(10)	89(12)	56(10)
C(8)	189(11)	160(10)	275(12)	-28(9)	100(10)	34(9)
C(9)	157(10)	121(9)	210(10)	-29(8)	89(9)	-8(8)
C(10)	176(10)	164(10)	198(10)	-66(8)	65(9)	-34(9)
C(11)	195(11)	221(11)	139(9)	-56(8)	52(9)	-12(9)
C(12)	148(10)	238(12)	259(13)	-22(10)	68(10)	-44(9)

CHAPTER 5

A Convergent Total Synthesis of (+)-Amurensinine and Formal Synthesis of (–)-Amurensinine via Oxidative Kinetic Resolution[†]

5.1 Background and Introduction

5.1.1 Isopavine Natural Products

The isopavines are a class of natural products originally isolated from plants in the family Papaveraceae (Figure 5.1.1).[1,2] These alkaloids have a characteristic tetrahydroisoquinoline core structure consisting of a doubly benzannulated azabicyclo[3.2.2]nonane. The isopavines and non-natural analogues have displayed important biological activity for the treatment of neurological disorders such as Parkinson's disease, Down's syndrome, Alzheimer's disease, amyotrophic lateral sclerosis, and Huntington's chorea.[3]

Figure 5.1.1 Representative isopavine natural products.

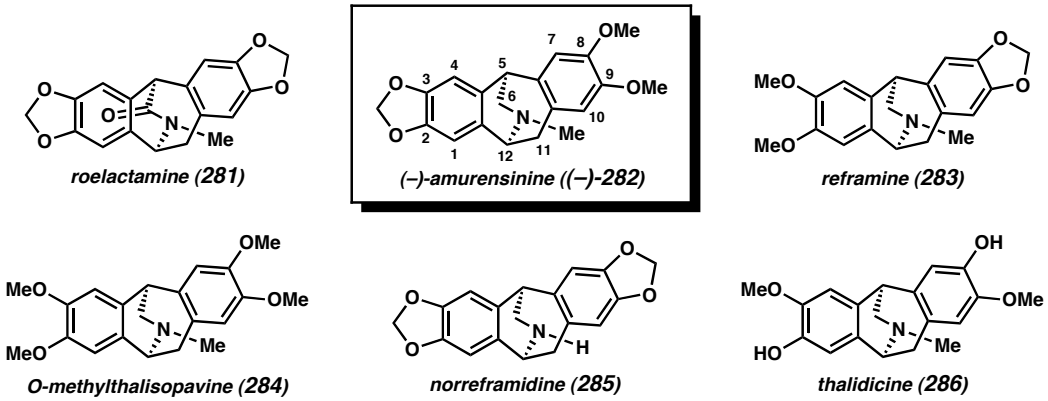

[†] This work was performed in collaboration with Uttam K. Tambar (Ph.D. 2005), a graduate student in the Stoltz group at California Institute of Technology.

5.1.2 Previous Isopavine Syntheses

Despite the potential medicinal applications of the isopavines and related non-natural structures, relatively few total syntheses of these natural products have been reported. The majority of these syntheses involve intramolecular acid-promoted cyclizations to form the azabicyclo[3.2.2]nonane core of the isopavines (Scheme 5.1.1).[4] Enantioselective syntheses have been even rarer. Badía and Domínguez reported the only enantioselective synthesis of (–)-amurensinine ((–)-**282**), based on a chiral auxiliary and acid-promoted cyclization approach (Scheme 5.1.2).[5] Recently, a number of non-natural isopavine analogues have been prepared by [1,2]- and [2,3]-Stevens rearrangements.[6]

Scheme 5.1.1 Classical approach to isopavine synthesis.

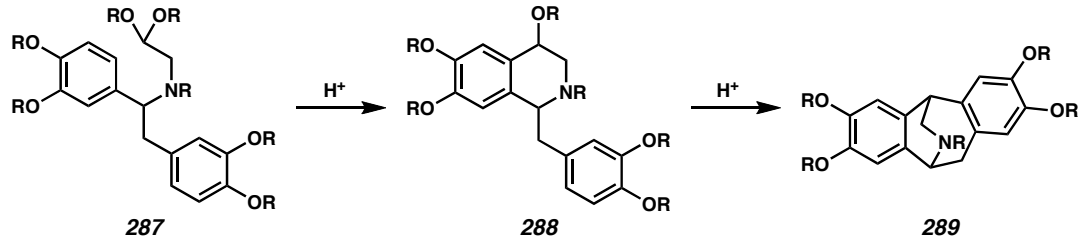

Scheme 5.1.2 Auxiliary-based synthesis of (–)-amurensinine.

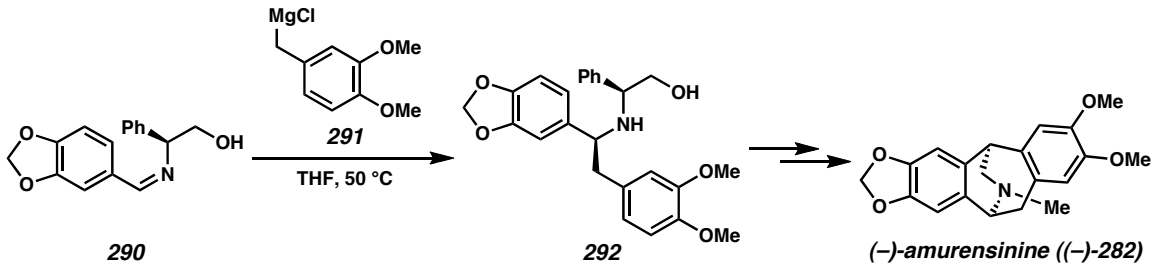

5.1.3 Retrosynthetic Analysis of Amurensinine

We looked to develop a novel approach to the isopavine core and utilize our oxidative kinetic resolution methodology to provide a catalytic enantioselective synthesis of (+)-amurensinine. Our approach to the isopavines, and specifically to amurensinine, is depicted in Scheme 5.1.3.[7] The tertiary amine of the natural product could be obtained from amide (+)-**293**. Disconnection of the bridging amide reveals hydroxyester **294**. This benzylic alcohol potentially could be resolved utilizing our oxidative kinetic resolution methodology, providing access to an enantioselective synthesis. Hydroxyester **294** could be derived from ketoester (±)-**295**, which we envisioned arising from arylsilyl triflate **296** and β-ketoester **298** via aryne insertion methodology developed in our laboratories.[8] Arylsilyl triflate **296** could be readily prepared from sesamol (**297**), and β-ketoester **298** could be derived from homoveratric acid (**299**).

Scheme 5.1.3 Retrosynthesis of (+)-amurensinine.

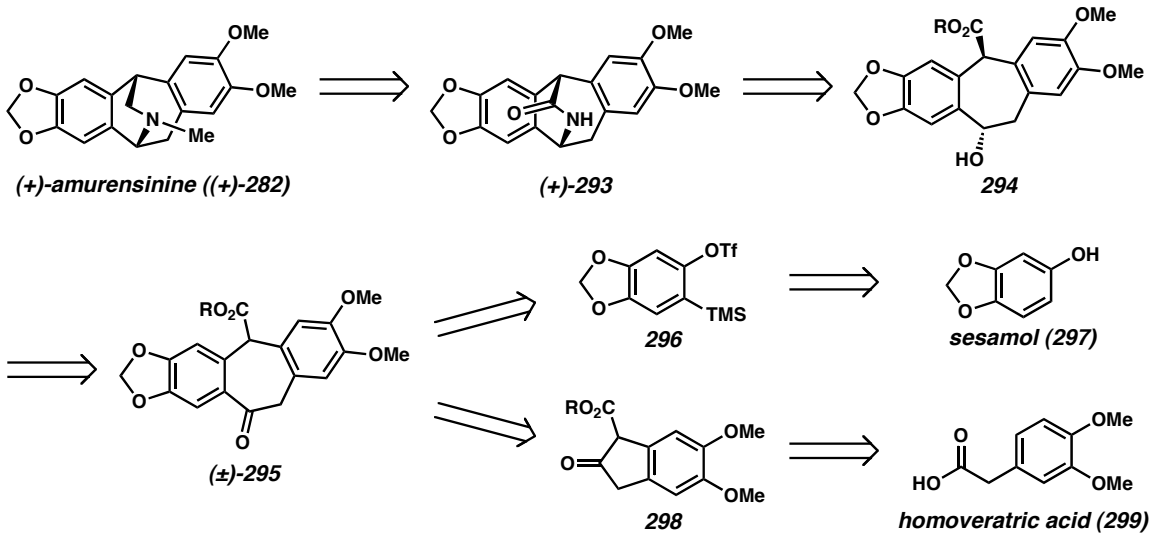

5.2 Total Synthesis of (+)-Amurensinine

5.2.1 Initial Route

The synthesis of amurensinine commenced with benzylation and bromination of sesamol (**297**, Scheme 5.2.1).[9] Lithiation of aryl bromide **300** followed by trapping of the aryl anion with chlorotrimethylsilane afforded arylsilane **301**. Benzyl group removal and reaction of the resulting phenol with triflic anhydride provided arylsilyl triflate **296** in good overall yield from sesamol (**297**).

Scheme 5.2.1 Synthesis of aryne precursor **296**.

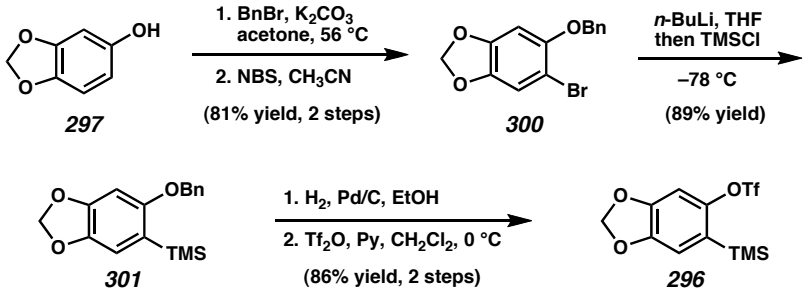

The β-ketoester coupling partner (**304**) was synthesized starting from homoveratric acid (**299**). Acid chloride formation and treatment with Meldrum's acid, followed by acidic aqueous washing and heating in absolute ethanol afforded β-ketoester **302** in excellent yield (Scheme 5.2.2). Ketoester **302** was diazotized with *p*-ABSA to produce diazoketoester **303**. A highly regioselective rhodium(II)-catalyzed C–H insertion generated the desired β-ketoester **304** in 96% yield.[10]

Scheme 5.2.2 Synthesis of β-ketoester **304**.

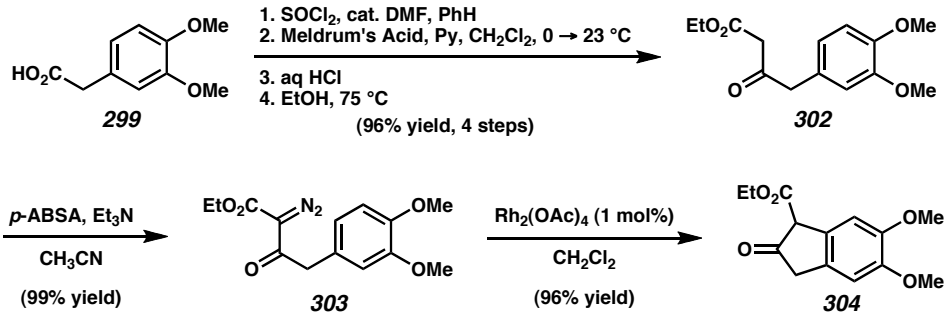

The feasibility of the key bond-forming aryne insertion reaction was then investigated. Treatment of β-ketoester **304** with arylsilyl triflate **296** under standard aryne generation conditions with cesium fluoride in dry acetonitrile[11] formed aryne **305**, which then underwent a formal [2+2] cycloaddition with cesium enolate **306** (Scheme 5.2.3). Retro-aldol reaction then opened the cyclobutene to provide observed ketoester (±)-**308**. Importantly, in a single step from readily available precursors, the entire carbocyclic framework of amurensinine was produced, including all of the carbons present in the natural product.

Scheme 5.2.3 Aryne insertion.

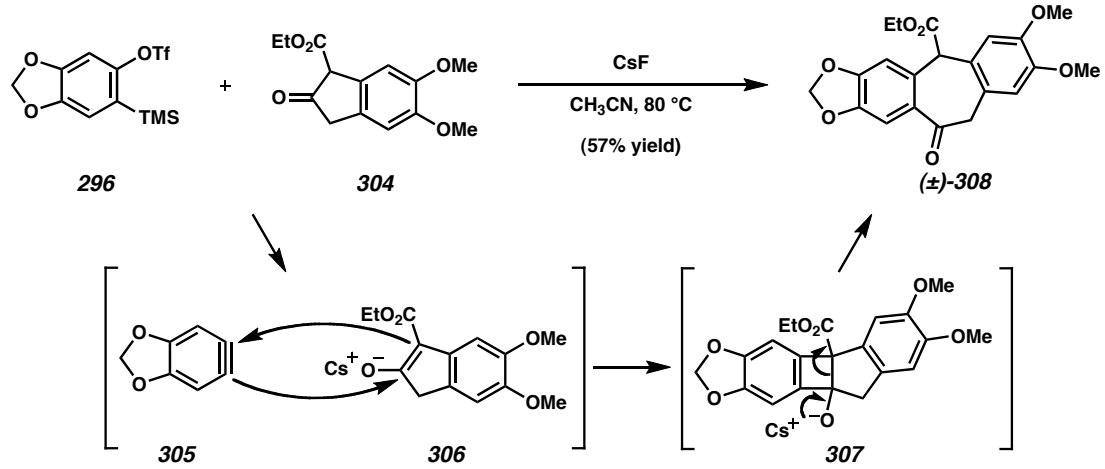

Selective reduction of the ketone of (±)-**308** with L-Selectride generated hydroxyester (±)-**309**. While a variety of other reduction protocols gave mixtures of products, a single diastereomer was observed in this transformation. The excellent observed selectivity potentially is due to preferential equatorial delivery of hydride from the bulky Selectride reagent to the ketone.

Scheme 5.2.4 Diastereoselective ketone reduction of hydroxyester (±)-**308**.

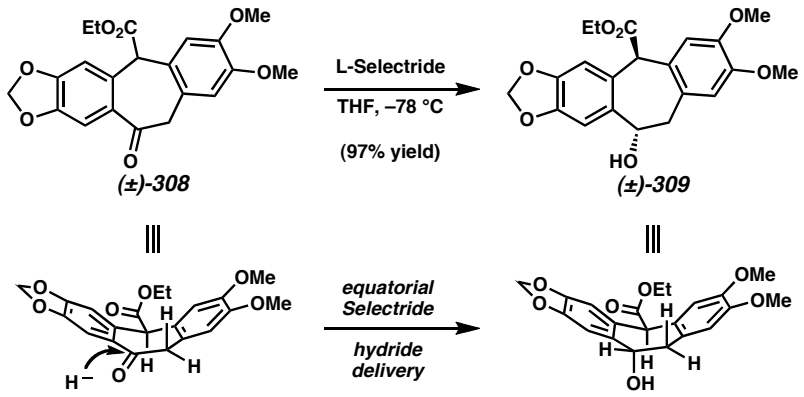

Next, we looked to apply our oxidative kinetic resolution methodology to this hydroxyester.[12] Conditions at 23 °C in chloroform proved best for the resolution of this alcohol, promoting good rate and selectivity[13] under modified conditions with elevated catalyst loadings (Scheme 5.2.5). While overall mass recovery from the resolution was moderate, substantial quantities of enantioenriched hydroxyester (–)-**309** could be accessed from this reaction.

Scheme 5.2.5 Resolution of hydroxyester (±)-**309**.

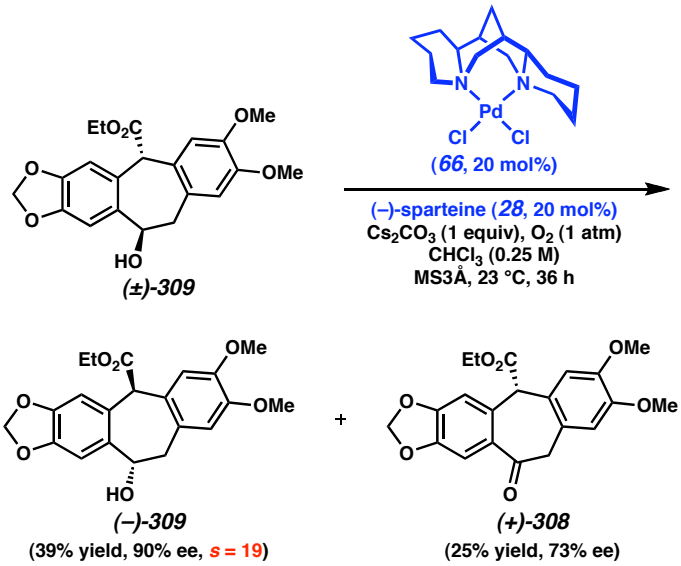

Installation of the amine required for amurensinine proved challenging. Mitsunobu protocols with many common *N*-nucleophiles led either to no reaction or elimination to form a stilbene system. Installation of an azide was achieved by treatment of hydroxyester (–)-**309** with DPPA in a procedure developed specifically for electron-rich benzylic alcohols by Thompson (Scheme 5.2.6).[14] After reduction of the resulting azide, lactam (+)-**293** was formed directly. Amide reduction and reductive methylation afforded amurensinine ((+)-**282**) in 17% yield over 4 steps.

Scheme 5.2.6 Initial route to complete (+)-amurensinine.

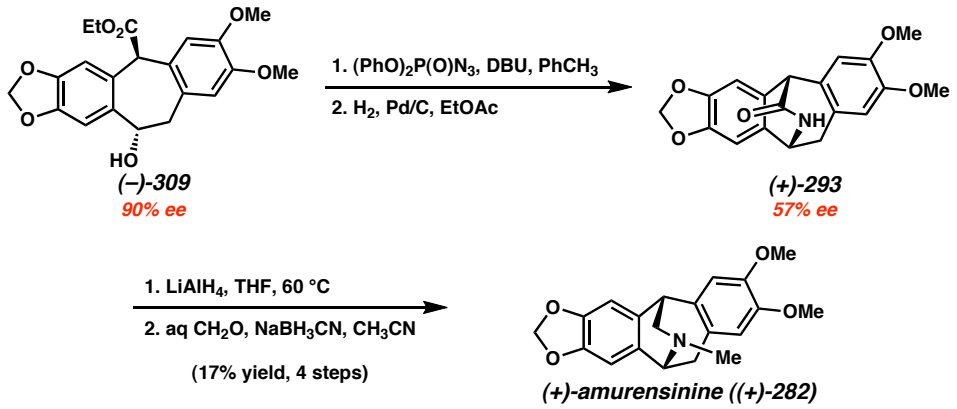

The low yield for this four-step sequence, primarily due to the production of a number of side products, was problematic. Even more disconcerting, lactam (+)-**293** was produced in only 57% ee. This partial racemization required two stereocenters to be inverted in the azide installation reaction, C(5) and C(12),[15] potentially by an intermediate such as **311** (Scheme 5.2.7). Achiral intermediate **311** could lead to four possible azidoester products (±)-*cis*-**312** and (±)-*trans*-**312**, only two of which have the necessary cis configuration for cyclization subsequent to the azide reduction. Furthermore, rearomatization of achiral ester **311** would produce one of the observed byproducts, stilbene (±)-**313**.

Scheme 5.2.7 Possible racemization mechanism.

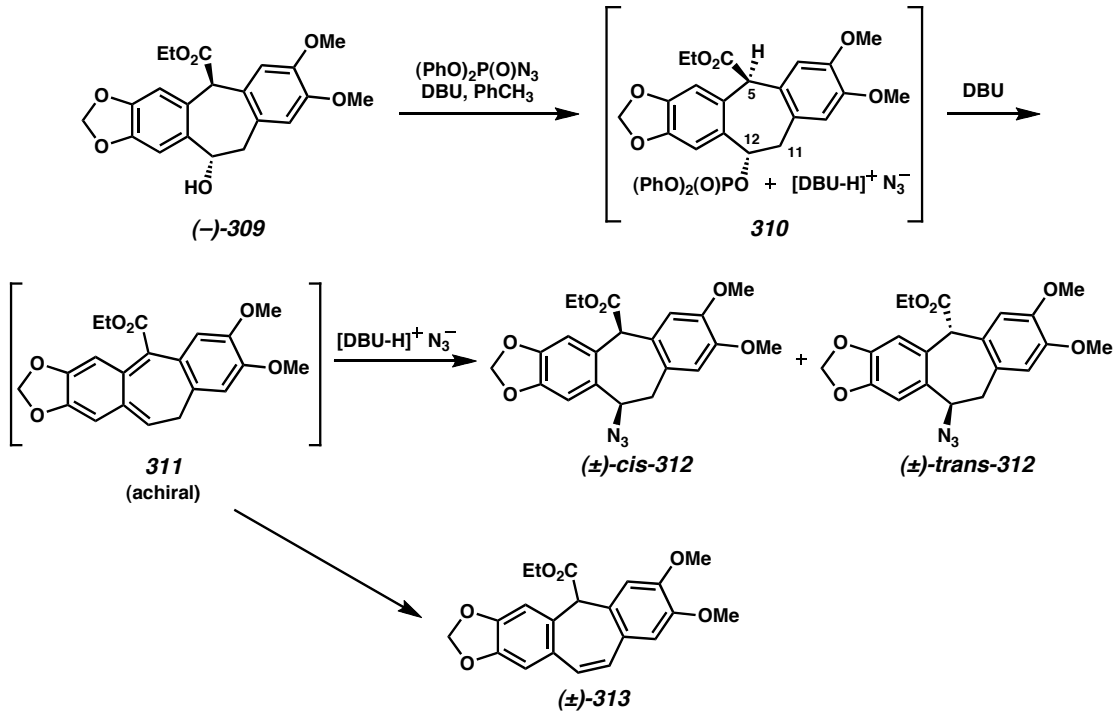

Alternatively, the inversion of the two stereocenters could be independent. Epimerization of C(5) could accompany competing S_N1 and S_N2 displacements at C(12) by azide. To demonstrate the propensity of C(5) toward epimerization, hydroxyester (±)-**309** was exposed to DBU without DPPA. Lactone (±)-**314** was generated, presumably via epimerization followed by base-promoted lactonization.

Scheme 5.2.8 Lactonization by epimerization of hydroxyester (±)-**309**.

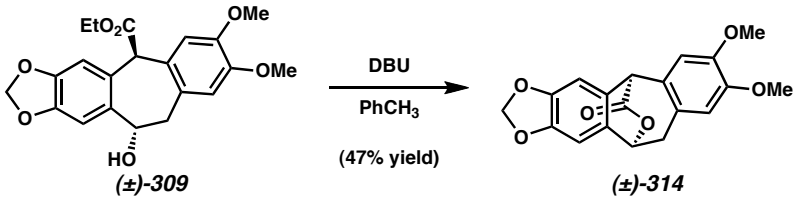

5.2.2 Alternate End Sequence

To circumvent the issues associated with epimerization of C(5), an alternate route to amurensinine was devised. Protection of the benzylic alcohol of hydroxyester (–)-**309** as a silyl ether, ester reduction to the primary alcohol, alcohol acetylation, and silyl ether cleavage afforded hydroxyacetate (–)-**315** in 71% overall yield. This benzylic alcohol was anticipated to be much less prone to epimerization at C(5). Indeed, treatment of hydroxyacetate (–)-**315** with DPPA and DBU afforded a 73% yield of azidoacetate (–)-**316**. Importantly, azidoacetate (–)-**316** of 88% ee was obtained from hydroxyester (–)-**309** of 88% ee, demonstrating that the stereochemistry of C(5) was maintained. Furthermore, clean inversion was observed in the azide displacement, indicating no competing S_N1 processes. Azidoacetate (–)-**316** was next transformed to lactam (+)-**293** by a five-step sequence. Acetate cleavage, two-step oxidation, and esterification with diazomethane afforded an azidoester, which was reduced to generate lactam (+)-**293** in 55% yield over five steps. Reduction and amine methylation provided (+)-amurensinine ((+)-**282**).

Scheme 5.2.9 Long route to complete (+)-amurensinine.

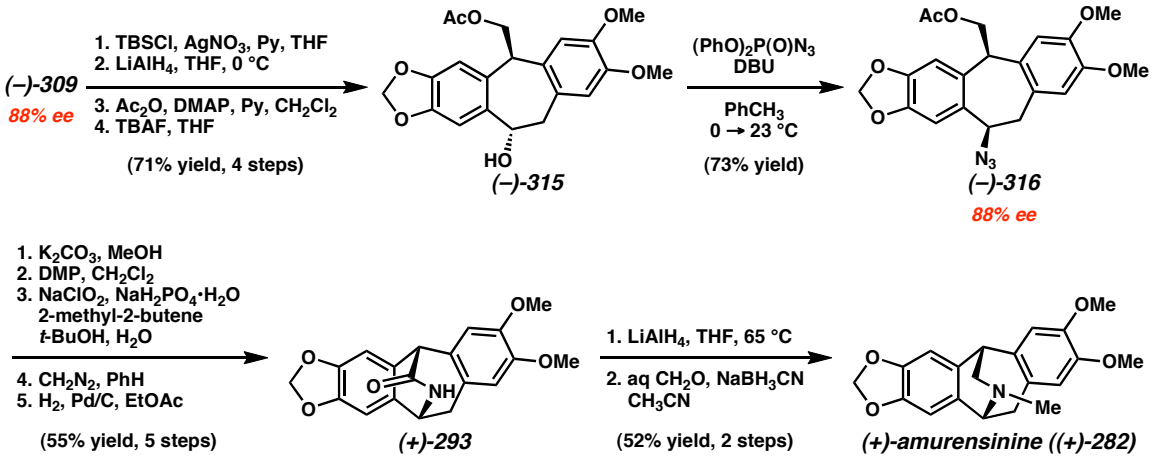

5.2.3 Final Route to (+)-Amurensinine

Further improvements of the synthesis were investigated. While the racemization issues in the azide displacement had been addressed, the route was much longer. Furthermore, the oxidative kinetic resolution proved to be a problematic step in the sequence. In addition to poor mass recovery, this reaction rarely provided enantioenriched hydroxyester (–)-**309** in over 90% ee. Thus, an alternate oxidative kinetic resolution substrate was pursued.

To this end, hydroxyester (±)-**309** was reduced with lithium aluminum hydride to afford a diol, which was selectively silylated on the primary alcohol to yield hydroxysilane (±)-**317** (Scheme 5.2.10). This selective procedure was a substantial improvement over the previous four-step procedure involving protection/deprotection to obtain hydroxyacetate (–)-**315**, while still decreasing the acidity of C(5) from hydroxyester (–)-**309**. Gratifyingly, oxidative kinetic resolution of this alcohol proved highly selective, providing enantioenriched hydroxysilane (–)-**317** in high ee with excellent mass recovery. Reactions conducted under ambient air atmosphere instead of pure oxygen provided comparable results.

Scheme 5.2.10 Hydroxysilane (±)-**317** oxidative kinetic resolution.

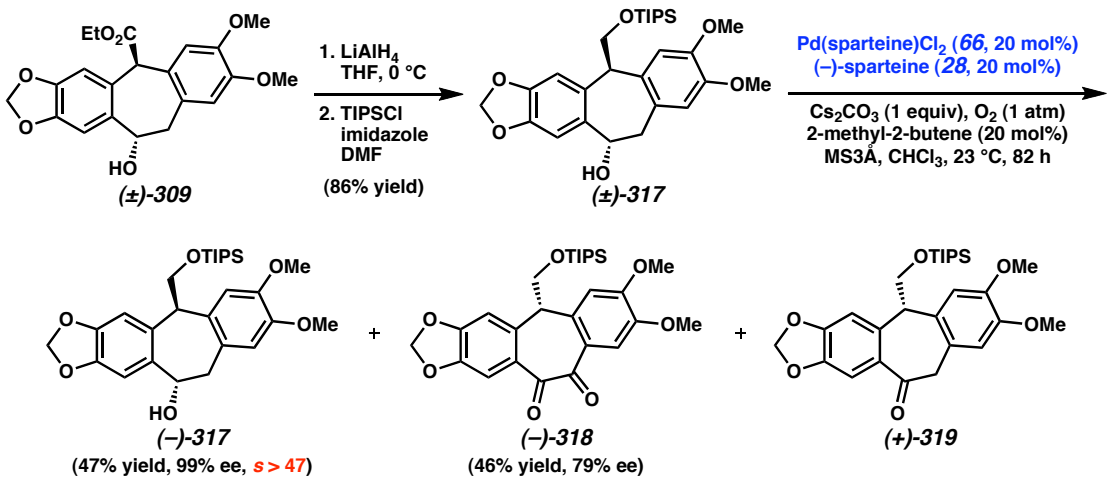

Interestingly, resolutions allowed to proceed to high ee of (–)-**317** did not afford any expected ketosilane (+)-**319**. Instead, diketosilane (–)-**318** was formed in good yield and enantiomeric excess. Monitoring the reactions by TLC and ^{1}H NMR demonstrated that ketosilane (+)-**319** was being generated; however, it slowly underwent further oxidation to the diketosilane. In fact, isolated samples of ketosilane **319** slowly oxidized to diketosilane **318** in C_6D_6. Handling of this ketosilane under argon delayed this decomposition. We hypothesized that ketosilane (+)-**319** was reacting with molecular oxygen in situ via a radical pathway to lead to the diketosilane. This theory was supported by experiments with non-enantioselective oxidations. Treatment of hydroxysilane (±)-**317** with Dess-Martin periodinane cleanly provided ketosilane (±)-**319** (Scheme 5.2.11). However, conditions with MnO_2, an oxidant thought to react with alcohols via radical pathways, and palladium(II) with molecular oxygen both formed diketosilane (±)-**318**. Thus, various radical inhibitors were added to kinetic resolutions of hydroxysilane (±)-**317**. While BHT had little effect, tetracyanoethylene led to little alcohol oxidation. 2-Methyl-2-butene also did not suppress ketosilane overoxidation;

however, incorporation of even catalytic quantities provided improved mass recovery in the kinetic resolution. Efforts to elucidate the role of 2-methyl-2-butene in the resolution are ongoing.

Scheme 5.2.11 Non-enantioselective oxidations of hydroxysilane (±)-**317**.

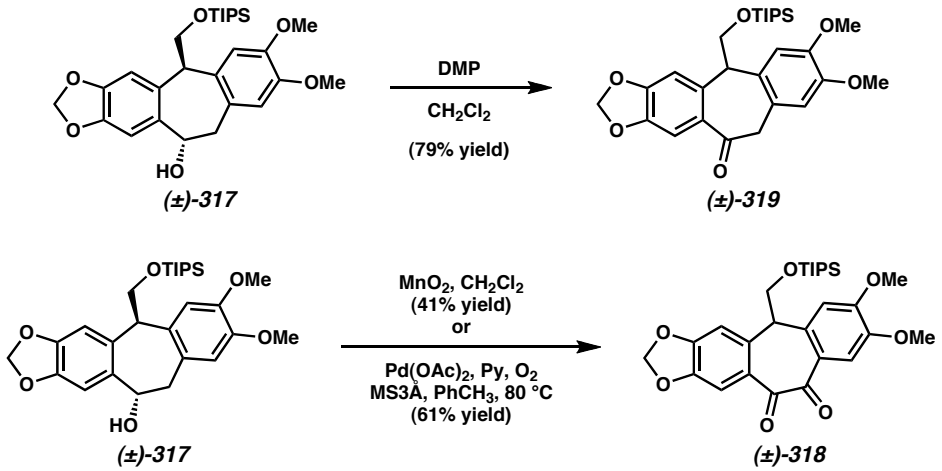

Ongoing catalyst development studies in the oxidative kinetic resolution led to the discovery of Pd(sparteine)Br_2 (**242**) as a catalyst promoting more rapid oxidation with comparable selectivity for a range of secondary alcohol substrates as compared to Pd(sparteine)Cl_2 (**66**).[16] This effect was also explored in the context of the total synthesis of amurensinine. Hydroxysilane (±)-**317** was exposed to modified conditions with dibromide complex **242** in chloroform at 23 °C. Much more rapid resolution was observed, even at decreased catalyst loadings relative to Pd(sparteine)Cl_2 conditions. While these conditions did not completely suppress overoxidation of ketosilane (+)-**319** to diketosilane (–)-**318**, significant quantities of the ketosilane at moderate ee were obtained. Most importantly, hydroxysilane (–)-**317** was produced in 98% ee and in excellent yield.

Scheme 5.2.12 Rate enhancement with Pd(sparteine)Br_2.

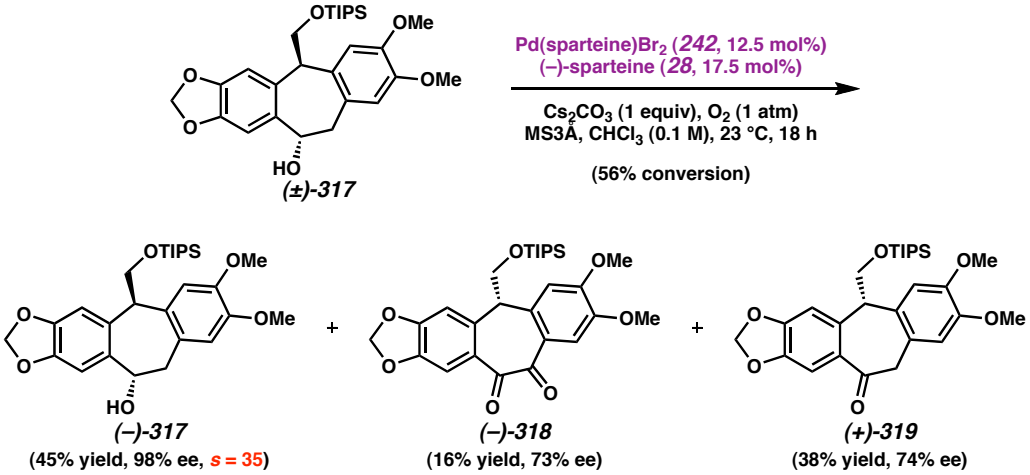

Having substantial quantities of highly enantioenriched alcohol (–)-**317**, we next sought to install the necessary nitrogen of the natural product. Use of Thompson's conditions[14] followed by exposure to TBAF to effect desilylation provided azidoalcohol (–)-**320** (Scheme 5.2.13). Gratifyingly, this azide was obtained with clean inversion in 99% ee. Two-step oxidation provided an intermediate azidoacid. Azide reduction led directly to bridged amide (+)-**293** in 99% ee, without requiring intermediate esterification. Reduction and methylation as before afforded (+)-amurensinine ((+)-**282**).

Scheme 5.2.13 Final route to complete (+)-amurensinine.

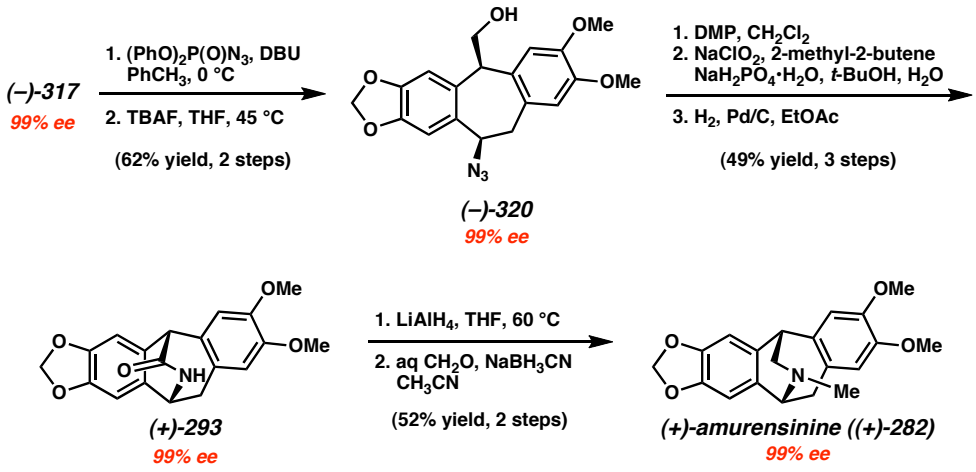

5.3 Formal Synthesis of (–)-Amurensinine

5.3.1 Enantioenriched Ketosilane Reduction

With the completion of the total synthesis of the non-natural enantiomer of amurensinine, efforts were undertaken to access natural (–)-amurensinine ((–)-**282**). When the enantiomer of alcohol desired is opposite to that produced in an enantioselective process, a Mitsunobu inversion protocol is a common method to obtain the desired stereochemistry. However, inversion of the benzylic alcohol stereocenter of hydroxysilane (–)-**317** would provide a diastereomer and not the desired enantiomeric alcohol (+)-**317** due to the C(5) stereocenter. Because this stereochemical information is preserved in the stereoablative oxidative kinetic resolution,[17] ketosilane (+)-**319** has the stereochemistry at C(5) needed for natural enantiomer (–)-**282**.

Thus, an enantiodivergent approach to both enantiomers of amurensinine based on the oxidative kinetic resolution was envisioned. Enantioenriched hydroxysilane (–)-**317** was transformed into non-natural (+)-amurensinine, while (–)-amurensinine could potentially be derived from the oxidation product, ketosilane (+)-**319**. In the event, reduction of ketosilane (+)-**319** with L-Selectride proceeded selectively to desired hydroxysilane (+)-**317**, constituting a formal total synthesis of (+)-amurensinine via the route described for hydroxysilane (–)-**317** (Scheme 5.3.1). However, the low yield for this transformation, the instability of ketosilane (+)-**319** to oxidation, and the moderate enantiomeric excess of the ketone made this route unfeasible for accessing (–)-amurensinine ((–)-**282**).

Scheme 5.3.1 Diastereoselective ketosilane reduction.

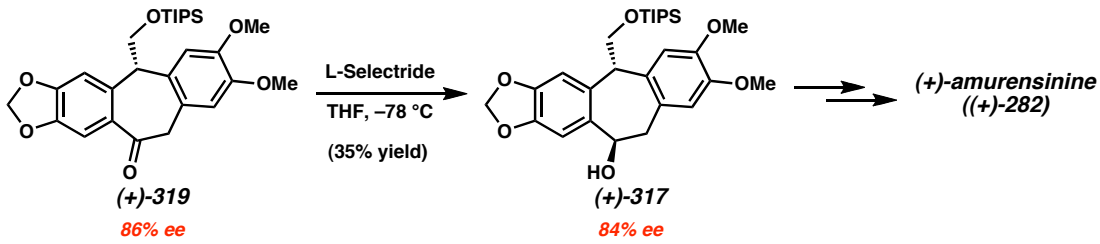

5.3.2 Preparation of Enantioenriched Hydroxysilane by Resolution

An alternate approach to a formal synthesis of (–)-amurensinine would involve the production of hydroxysilane (+)-**317** directly from the oxidative kinetic resolution. Oxidation of the opposite enantiomer of the alcohol would require the (+)-enantiomer of the chiral ligand, sparteine (**28**). While the use of diamine *ent*-(+)-**28** in the oxidation is impractical due to its inaccessibility,[18] recent developments in the use of alternate ligands in the palladium-catalyzed resolution have demonstrated the utility of diamine **248** as a (+)-sparteine surrogate.[16]

In the oxidative kinetic resolution of hydroxysilane (±)-**317**, diamine **248** proved to be a competent ligand for selective oxidation with a dibromide complex. At 23 °C in chloroform under an atmosphere of molecular oxygen, hydroxysilane (+)-**317** was recovered in high ee with good yield and excellent corresponding selectivity (Scheme 5.3.2). Ketosilane (–)-**319** and diketosilane (+)-**318** could also be obtained from the resolutions in modest enantiomeric excess. Additionally, these resolutions could be conducted with ambient air as oxidant with no detrimental effects (Scheme 5.3.3). This resolution of (±)-**317** constitutes a formal synthesis of (–)-amurensinine ((–)-**282**).

Scheme 5.3.2 Resolution with diamine **248** under O_2.

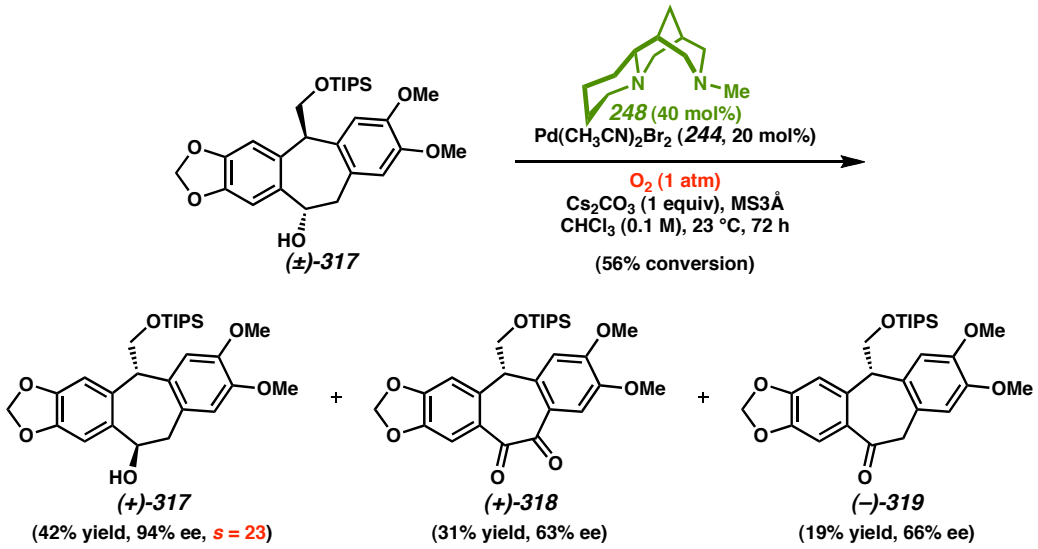

Scheme 5.3.3 Resolution with diamine **248** under ambient air.

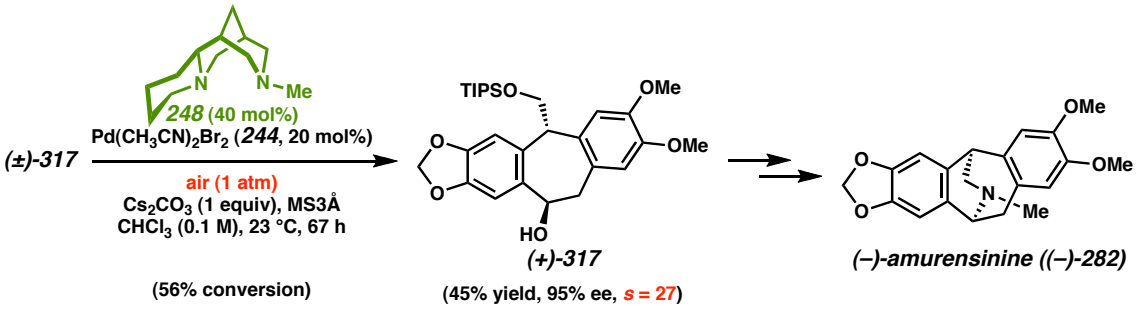

5.4 Conclusion

A novel route to both enantiomers of amurensinine has been developed. The core of the natural product has been constructed in a rapid and convergent manner by aryne insertion methodology developed in these laboratories. A highly selective oxidative kinetic resolution with (–)-sparteine (**28**) has provided an enantioenriched alcohol intermediate in high enantiomeric excess. Synthetic investigations have led to a stereocontrolled method for incorporation of the amine found in the natural product, leading to a highly enantio- and diastereoselective synthesis of (+)-amurensinine.[7]

Further efforts based on recent advances in the oxidative kinetic resolution utilizing alternate diamine **248** have provided a formal total synthesis of (–)-amurensinine.[16b] These syntheses are readily amenable to modifications to provide other members of the isopavine family of natural products, as well as non-natural derivatives. Finally, the described approaches to amurensinine establish the aryne insertion and oxidative kinetic resolution methodologies as highly applicable and flexible tools for modern synthesis.

5.5 Experimental Section

5.5.1 Materials and Methods

Unless stated otherwise, reactions were performed in flame-dried glassware sealed with rubber septa under a nitrogen atmosphere using dry, deoxygenated solvents. Commercially obtained reagents were purchased from the Sigma-Aldrich Chemical Company, Milwaukee, WI and were used as received. Pyridine, Et_3N, and TMSCl were distilled over CaH_2. Solvents were dried by passage through an activated alumina column under argon. Liquids and solutions were transferred via syringe. Powdered 3Å activated molecular sieves were stored in a 120 °C drying oven until immediately prior to use. Reaction temperatures were controlled using an IKAmag temperature modulator. Thin-layer chromatography (TLC) was conducted with E. Merck silica gel 60 F254 pre-coated plates (0.25 or 0.5 mm) and visualized using a combination of UV, anisaldehyde, ceric ammonium molybdate, and potassium permanganate staining. ICN silica gel (particle size 32-63 μm) or SiliCycle Silia*Flash* P60 Academic silica gel (particle size 40-63 μm; pore diameter 60 Å) was used for flash column chromatography. Analytical chiral HPLC was performed with an Agilent 1100 Series HPLC utilizing a Chiralpak AD, Chiralcel OD-H, or Chiralcel OJ column (each is 4.6 mm x 25 cm) obtained from Daicel Chemical Industries, Ltd. with visualization at 254 nm. Semi-preparative achiral HPLC was performed on a Waters 600 system with a 15-20 μm particle size Waters μPorasil column with peak detection at 254 nm. ^{1}H NMR spectra were recorded on a Varian Mercury 300 (at 300 MHz) or a Varian Inova 500 (at 500 MHz) and are reported relative to Me_4Si (δ 0.0). Data for ^{1}H NMR spectra are reported as follows: chemical shift (δ ppm), multiplicity, coupling constant (Hz), and integration. ^{13}C NMR spectra were

recorded on a Varian Mercury 300 (at 75 MHz) or Varian Inova 500 (at 126 MHz) and are reported relative to Me_4Si (δ 0.0). Data for ^{13}C NMR spectra are reported in terms of chemical shift. ^{19}F NMR spectra were recorded on a Varian Mercury 300 instrument (at 282 MHz) and are reported relative to external F_3CCO_2H standard (δ –76.53). Data for ^{19}F NMR spectra are reported in terms of chemical shift (δ ppm). Optical rotations were measured with a Jasco P-1010 polarimeter at 589 nm using a 100 mm path-length cell. IR spectra were recorded on a Perkin Elmer Paragon 1000 or Spectrum BX II spectrometer and are reported in terms of frequency of absorption (cm^{-1}). UV-Vis spectra were collected on an Agilent 8453 UV-Vis spectrometer and are reported in terms of wavelength of absorption (nm). High resolution mass spectra were obtained from the California Institute of Technology Mass Spectral Facility.

5.5.2 Preparative Procedures

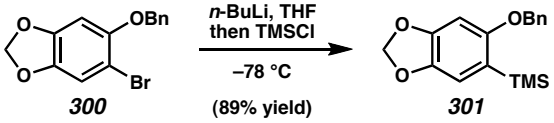

300 *301*

Arylsilane 301. A solution of aryl bromide **300**[9] (325 mg, 1.06 mmol, 1.0 equiv) in THF (3.5 mL) was cooled to –78 °C. *n*-Butyllithium (2.5 M in hexanes, 634 μL, 1.59 mmol, 1.5 equiv) was added dropwise. After 15 min, TMSCl (200 μL, 1.59 mmol, 1.5 equiv) was added dropwise at –78 °C. After 5 min, the reaction mixture was allowed to warm to 23 °C and stirred for 15 min. Saturated aq NH_4Cl (5 mL) was added, and the mixture was extracted with Et_2O (3 x 5 mL). The combined organic layers were dried over Na_2SO_4 and filtered. The filtrate was concentrated under reduced pressure. Purification by flash chromatography (10:1 hexanes:EtOAc eluent) provided arylsilane **301** (282 mg, 89% yield) as a clear oil: R_f 0.57 (3:1 hexanes:EtOAc); ^1H NMR (300

MHz, $CDCl_3$): δ 7.45-7.29 (comp. m, 5H), 6.85 (s, 1H), 6.53 (s, 1H), 5.91 (s, 2H), 5.01 (s, 2H), 0.23 (s, 9H); ^{13}C NMR (75 MHz, $CDCl_3$): δ 159.2, 149.6, 141.5, 137.3, 128.7, 128.0, 127.5, 119.3, 113.7, 101.3, 95.2, 71.0, -0.5; IR (thin film/NaCl): 2953, 2894, 1606, 1502, 1473, 1410, 1386, 1243, 1177, 1042 cm^{-1}; HRMS-EI (*m*/*z*): $[M]^+$ calcd for $[C_{17}H_{20}O_3Si]^+$, 300.1182; found, 300.1187.

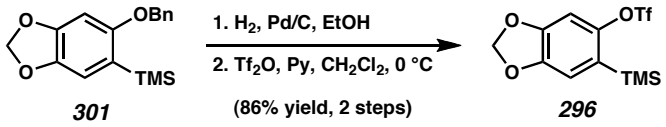

301 *296*

Arylsilyl Triflate 296. To a solution of arylsilane **301** (4.90 g, 16.3 mmol, 1.0 equiv) in absolute EtOH (300 mL) was added Pd/C (10% w/w, 1.74 g, 1.63 mmol Pd, 0.10 equiv). The reaction was wrapped in aluminum foil to exclude light. The reaction was allowed to proceed under a balloon of H_2 (1 atm) for 12 h. The mixture was then filtered in the dark over Celite (Et_2O eluent). The filtrate was evaporated under reduced pressure to afford a crude phenol, which was used in the next step without further purification.

A solution of the crude phenol in CH_2Cl_2 (95 mL) was cooled to 0 °C in the dark. Pyridine (3.26 mL, 40.4 mmol, 2.5 equiv) was added. A solution of Tf_2O (4.07 mL, 24.2 mmol, 1.5 equiv) in CH_2Cl_2 (65 mL) was added dropwise by addition funnel over 30 min. After allowing the reaction to stir 2.5 h in the dark at 0 °C, saturated aq $NaHCO_3$ (150 mL) was added. The layers were separated, and the aqueous layer was extracted with CH_2Cl_2 (3 x 150 mL). The organic layers were combined, dried over Na_2SO_4, and filtered. The filtrate was concentrated under reduced pressure and purified by flash chromatography (97:3 hexanes:CH_2Cl_2 eluent) to provide arylsilyl triflate **296** (4.80 g,

86% yield over 2 steps) as a clear oil: R_f 0.54 (3:1 hexanes:EtOAc); ^{1}H NMR (500 MHz, $CDCl_3$): δ 6.88 (s, 1H), 6.84 (s, 1H), 6.03 (s, 2H), 0.33 (s, 9H); ^{13}C NMR (126 MHz, $CDCl_3$): δ 149.7, 148.8, 147.1, 125.1, 113.4, 113.4, 102.6, 102.5, -0.5; ^{19}F NMR (282 MHz, $CDCl_3$) δ -74.63; IR (thin film/NaCl): 2960, 2903, 1479, 1422, 1247, 1216, 1141, 984, 843 cm^{-1}; HRMS-EI (*m/z*): $[M]^+$ calcd for $[C_{11}H_{13}O_5F_3SiS]^+$, 342.0205; found, 342.0211.

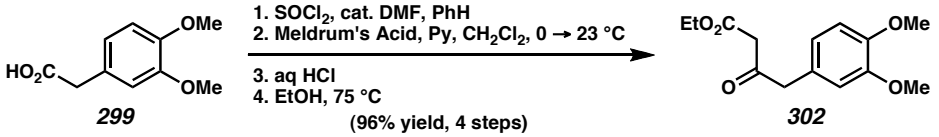

β-Ketoester 302. To a solution of homoveratric acid (**299**, 1.0 g, 5.1 mmol, 1.0 equiv) in benzene (5 mL) was added thionyl chloride (741 μL, 10.2 mmol, 2.0 equiv) and DMF (40 μL, 0.52 mmol, 0.1 equiv). After stirring for 3 h, the reaction mixture was concentrated under reduced pressure to afford the crude acid chloride.

The resulting crude acid chloride was then dissolved in CH_2Cl_2 (10 mL) and cooled to 0 °C. To this solution was added pyridine (825 μL, 10.2 mmol, 2.0 equiv) and Meldrum's acid (735 mg, 5.1 mmol, 1.0 equiv). After stirring at 0 °C for 2 min, the mixture was stirred at 23 °C for 8 h. The reaction was then washed with aq HCl (10% w/v, 10 mL) followed by H_2O (10 mL). The organic layer was dried over $MgSO_4$ and filtered, and the filtrate was concentrated under reduced pressure to afford the crude β-ketoacid.

The crude β-ketoacid was dissolved in absolute EtOH (10 mL) and refluxed at 75 °C. After 11 h, the reaction mixture was cooled to 23 °C and concentrated under reduced pressure. Purification by flash chromatography (5:1→3:1→1:1 hexanes:EtOAc eluent)

provided β-ketoester **302** (1.31 g, 96% yield over 4 steps) as a clear oil. The characterization data matched the data reported in the literature.[19]

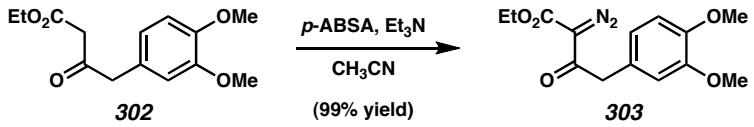

Diazoketoester 303. To a cooled (0 °C) solution of β-ketoester **302** (445 mg, 1.67 mmol, 1.0 equiv) in acetonitrile (8 mL) was added *p*-ABSA (441 mg, 1.84 mmol, 1.1 equiv) and Et_3N (698 μL, 5.01 mmol, 3.0 equiv). After stirring at 0 °C for 1 min, the mixture was stirred at 23 °C for 90 min. Then, the reaction was washed with aq NaOH (10% w/v, 10 mL). The aqueous layer was then extracted with Et_2O (3 x 10 mL). The organic layers were combined, dried over $MgSO_4$, and filtered. The filtrate was concentrated under reduced pressure and purified by flash chromatography (4:1 hexanes:EtOAc eluent) to provide diazoketoester **303** (487 mg, 99% yield) as a clear oil: R_f 0.50 (1:1 hexanes:EtOAc); ^{1}H NMR (300 MHz, C_6D_6): δ 7.00-6.94 (comp. m, 2H), 6.62 (d, J = 8.0 Hz, 1H), 4.12 (s, 2H), 3.89 (q, J = 7.1 Hz, 2H), 3.51 (s, 3H), 3.43 (s, 3H), 0.89 (t, J = 7.2 Hz, 3H); ^{13}C NMR (75 MHz, C_6D_6): δ 190.1, 161.4, 150.4, 149.7, 127.5, 122.7, 114.5, 112.7, 75.8, 61.6, 56.0, 55.9, 45.7, 14.5; IR (thin film/NaCl): 2938, 2836, 2136, 1714, 1650, 1515, 1263, 1029 cm^{-1}; HRMS-EI (*m*/*z*): $[M]^+$ calcd for $[C_{14}H_{16}N_2O_5]^+$, 292.1059; found, 292.1070.

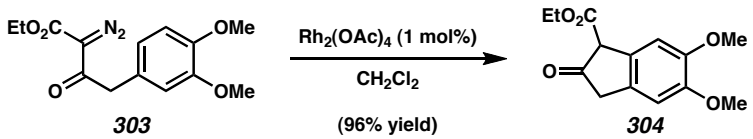

β-Ketoester 304. A flask equipped with an addition funnel and an N_2 inlet was charged with $Rh_2(OAc)_4$ (138 mg, 0.31 mmol, 0.01 equiv) and CH_2Cl_2 (140 mL). A solution of diazoketoester **303** (9.12 g, 31.2 mmol, 1.0 equiv) in CH_2Cl_2 (100 mL) was added dropwise over 90 min via an addition funnel. After stirring for 2.5 h at 23 °C, the reaction mixture was concentrated under reduced pressure. Purification by flash chromatography (7:3→1:1 hexanes:EtOAc eluent) provided β-ketoester **304** (7.88 g, 96% yield) as a white solid: R_f 0.52 (1:1 hexanes:EtOAc); mp 117 °C; ^{1}H NMR (300 MHz, $CDCl_3$): δ 10.85 (s, 1H), 7.23 (s, 1H), 6.92 (s, 1H), 4.42 (q, J = 7.1 Hz, 2H), 3.91 (s, 3H), 3.87 (s, 3H), 3.52 (d, J = 0.8 Hz, 2H), 1.45 (t, J = 7.2 Hz, 3H); ^{13}C NMR (75 MHz, $CDCl_3$): δ 180.1, 148.7, 146.3, 132.6, 125.1, 108.6, 105.2, 105.2, 105.0, 60.7, 56.6, 56.2, 37.8, 14.6; IR (thin film/NaCl): 2976, 2833, 1650, 1602, 1494, 1469, 1305 cm^{-1}; HRMS-FAB (*m/z*): $[M]^+$ calcd for $[C_{14}H_{16}O_5]^+$, 264.0998; found, 264.1003.

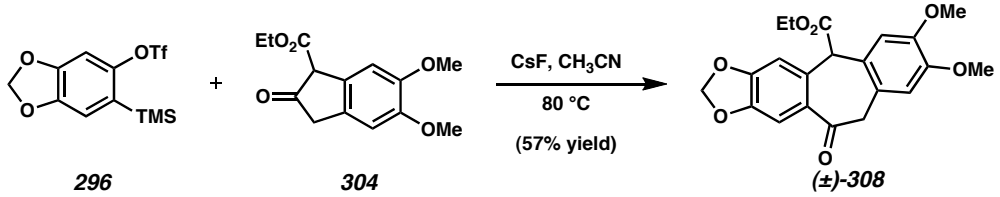

Ketoester (±)-308. To a solution of arylsilyl triflate **296** (898 mg, 2.62 mmol, 1.7 equiv) in acetonitrile (9 mL) was added β-ketoester **304** (415 mg, 1.57 mmol, 1.0 equiv) and cesium fluoride (715 mg, 4.71 mmol, 3.0 equiv). The reaction was quickly immersed in an 80 °C oil bath and allowed to reflux until arylsilyl triflate **296** was consumed (determined by TLC, 2 h). The reaction mixture was then cooled to 23 °C and washed

with saturated aq NaCl (15 mL). The aqueous layer was back-extracted with Et_2O (3 x 15 mL). The organic layers were combined, dried over Na_2SO_4, and filtered, and the filtrate was concentrated under reduced pressure. Purification by flash chromatography (1:1 hexanes:EtOAc eluent) provided ketoester (±)-**308** (348 mg, 57% yield) as a clear oil: R_f 0.23 (1:1 hexanes:EtOAc); ^{1}H NMR (300 MHz, C_6D_6): δ 8.03 (s, 1H), 6.67 (s, 1H), 6.53 (s, 1H), 6.44 (s, 1H), 5.13 (d, J = 1.3 Hz, 1H), 5.10 (d, J = 1.3 Hz, 1H), 4.59 (d, J = 15.4 Hz, 1H), 4.54 (s, 1H), 3.90 (dq, J = 7.1, 2.0 Hz, 2H), 3.83 (d, J = 15.3 Hz, 1H), 3.41 (s, 3H), 3.24 (s, 3H), 0.84 (t, J = 7.1 Hz, 3H); ^{13}C NMR (75 MHz, C_6D_6): δ 192.4, 171.4, 151.7, 150.2, 149.1, 148.5, 137.1, 130.6, 130.5, 125.9, 115.6, 114.9, 111.4, 110.8, 102.1, 61.9, 59.7, 56.3, 55.9, 50.0, 14.4; IR (thin film/NaCl): 2908, 1727, 1663, 1616, 1518, 1506, 1485, 1254 cm^{-1}; HRMS-EI (m/z): [M]$^+$ calcd for $[C_{21}H_{20}O_7]^+$, 384.1209; found, 384.1212.

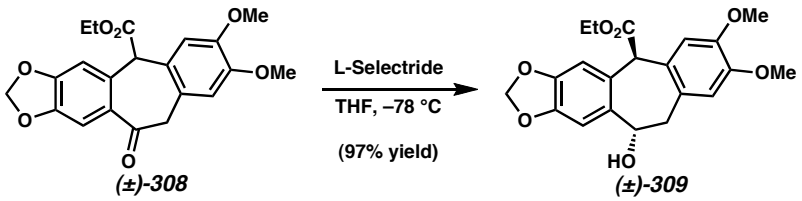

Hydroxyester (±)-309. To a solution of ketoester (±)-**308** (52.9 mg, 0.138 mmol, 1.0 equiv) in THF (1.5 mL) at –78 °C was added dropwise L-Selectride (1.0 M in THF, 200 μL, 0.206 mmol, 1.5 equiv). The resulting solution was stirred for 25 min at –78 °C and then quenched with saturated aq NH_4Cl (5 mL). After warming to 23 °C and stirring 25 min, the mixture was extracted with Et_2O (4 x 5 mL). The organics were combined, dried over Na_2SO_4, and filtered. The filtrate was concentrated under reduced pressure and purified by flash chromatography (1:1 hexanes:EtOAc eluent) to provide

hydroxyester (±)-**309** (51.4 mg, 97% yield) as a yellow solid: R_f 0.33 (1:1 hexanes:EtOAc); ^{1}H NMR (500 MHz, $CDCl_3$): δ 6.99 (s, 1H), 6.77 (s, 1H), 6.72 (s, 1H), 6.69 (s, 1H), 5.94 (d, *J* = 1.5 Hz, 1H), 5.92 (d, *J* = 1.0 Hz, 1H), 5.02-4.96 (m, 1H), 4.59 (s, 1H), 4.13 (q, *J* = 7.2 Hz, 2H), 3.88 (s, 3H), 3.87 (s, 3H), 3.50 (dd, *J* = 15.1, 2.4 Hz, 1H), 2.93 (dd, *J* = 15.1, 6.8 Hz, 1H), 1.73 (d, *J* = 8.3 Hz, 1H), 1.17 (t, *J* = 7.1 Hz, 3H); ^{13}C NMR (126 MHz, $CDCl_3$): δ 172.6, 148.4, 147.6, 147.6, 146.9, 135.2, 129.6, 128.0, 127.3, 114.9, 114.5, 111.3, 110.7, 101.4, 69.4, 61.8, 58.5, 56.2, 56.1, 39.6, 14.3; IR (thin film/NaCl): 3500, 2937, 1725, 1610, 1520, 1486, 1244 cm^{-1}; HRMS-EI (*m/z*): $[M]^+$ calcd for $[C_{21}H_{22}O_7]^+$, 386.1366; found, 386.1366.

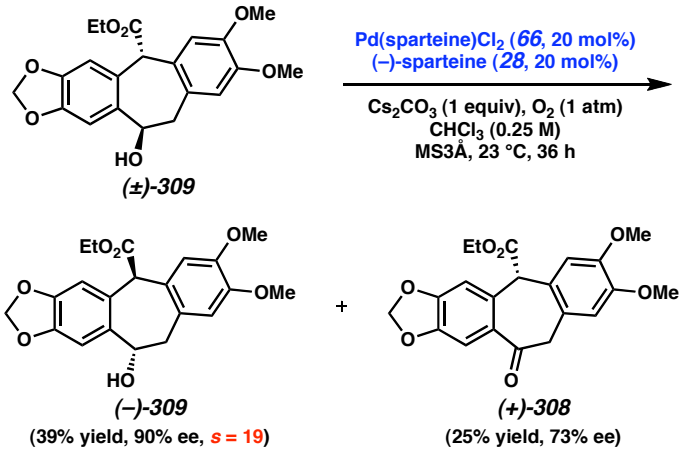

Kinetic Resolution of Hydroxyester (±)-309: Hydroxyester (–)-309. To a 1 dram vial with stir bar was added oven-dried powdered 3Å molecular sieves (190 mg). After cooling, Pd(sparteine)Cl_2[20] (**66**, 31.5 mg, 0.076 mmol, 0.20 equiv) followed by $CHCl_3$ (750 μL)[21] and (–)-sparteine (**28**, 17.6 μL, 0.076 mmol, 0.20 equiv) were added. The mixture was then cooled to –78 °C and alternately evacuated and backfilled with O_2 (3 ×). After allowing the mixture to warm to 23 °C, powdered anhydrous Cs_2CO_3 (124.5 mg, 0.38 mmol, 1.0 equiv) followed by a solution of hydroxyester (±)-**309** (147.7 mg,

0.38 mmol, 1.0 equiv) in $CHCl_3$ (750 μL) were added, and the reaction was stirred vigorously under a balloon of O_2 for 36 h. The reaction mixture was then filtered through a short plug of silica gel (EtOAc eluent) and evaporated under reduced pressure. Purification by flash chromatography (3:1 hexanes:EtOAc eluent) afforded hydroxyester (–)-**309** (56.8 mg, 39% yield) and ketoester (+)-**308** (36.6 mg, 25% yield). Hydroxyester (–)-**309** was found to be 90.4% ee by chiral HPLC (AD column, 0.55 mL/min, 60% EtOH/hexanes, major peak 16.3 min, minor peak 26.7 min); $[\alpha]^{25}_D$ –64.3° (*c* 0.78, $CHCl_3$, 87.9% ee). Ketoester (+)-**308** was found to be 73.0% ee by chiral HPLC (AD column, 0.55 mL/min, 60% EtOH/hexanes, major peak 46.6 min, minor peak 20.5 min); $[\alpha]^{25}_D$ +19.9° (*c* 0.47, $CHCl_3$, 84.8% ee).

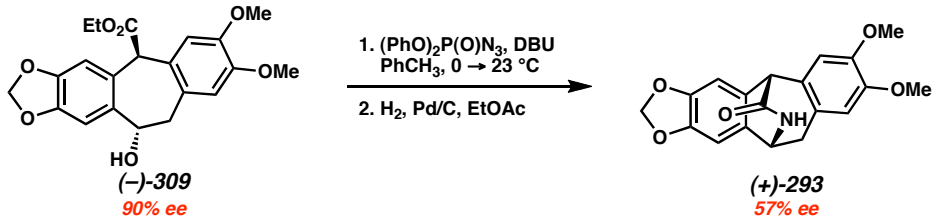

Lactam (+)-293. To a solution of hydroxyester (–)-**309** (9.7 mg, 0.025 mmol, 1.0 equiv) in toluene (500 μL) at 0 °C was added DPPA (27 μL, 0.126 mmol, 5.0 equiv) and DBU (19 μL, 0.126 mmol, 5.0 equiv). The resulting solution was stirred for 30 min at 0 °C and then stirred at 23 °C for 12 h. The reaction was then quenched with H_2O (3 mL) and extracted with Et_2O (3 x 3 mL). The combined organics were dried over Na_2SO_4 and filtered, and the filtrate was concentrated under reduced pressure. The crude azide was passed through a short pad of silica gel (EtOAc eluent), concentrated under reduced pressure, and used in the next step without further purification.

To a solution of the azide in EtOAc (1.5 mL) was added Pd/C (10% w/w, 15 mg, 0.014 mmol Pd, 0.56 equiv). The reaction flask was placed under a balloon of H_2 (1 atm) and stirred at 23 °C for 9 h. The reaction mixture was then passed through a short pad of Celite (Et_2O eluent) and concentrated under reduced pressure. Lactam (+)-**293** was used in the next step without further purification: R_f 0.46 (9:1 $CHCl_3$:MeOH); ^{1}H NMR (500 MHz, $CDCl_3$): δ 6.75 (s, 1H), 6.74 (s, 1H), 6.72 (s, 1H), 6.55-6.52 (m, 1H), 6.49 (s, 1H), 5.94 (d, J = 1.5 Hz, 1H), 5.88 (d, J = 1.5 Hz, 1H), 4.58-4.54 (m, 1H), 4.21 (d, J = 2.0 Hz, 1H), 3.88 (s, 3H), 3.78 (s, 3H), 3.28 (dd, J = 16.8, 4.6 Hz, 1H), 3.07 (dd, J = 17.1, 2.4 Hz, 1H); ^{13}C NMR (126 MHz, $CDCl_3$): δ 175.4, 148.8, 147.6, 147.2, 146.7, 134.1, 130.0, 128.1, 125.2, 114.7, 112.1, 106.7, 105.6, 101.4, 56.7, 56.2, 56.1, 53.6, 36.9; IR (thin film/NaCl): 3221, 2916, 1680, 1517, 1485, 1465, 1246 cm^{-1}; HRMS-FAB (m/z): $[M+H]^+$ calcd for $[C_{19}H_{18}NO_5]^+$, 340.1185; found, 340.1181. Lactam (+)-**293** was found to be 57.0% ee by chiral HPLC (OD-H column, 1.0 mL/min, 15% EtOH/hexanes, major peak 29.0 min, minor peak 45.1 min).

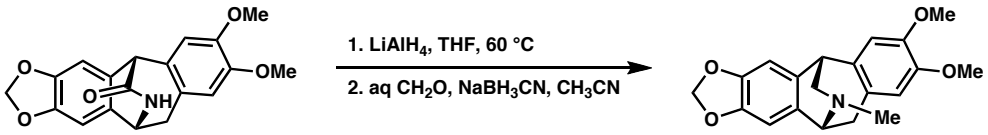

(+)-293
57% ee

(+)-amurensinine ((+)-282)

(+)-Amurensinine ((+)-282). To a solution of crude lactam (+)-**293** in THF (1 mL) was added lithium aluminum hydride (30 mg, 0.0751 mmol, 3.0 equiv). The resulting solution was stirred for 8 h at 60 °C. The reaction mixture was then cooled to 0 °C and sequentially quenched with H_2O (30 μL), aq NaOH (15% w/v, 30 μL), and H_2O (90 μL). The slurry was stirred at 23 °C for 25 min, passed through a short pad of Celite

(Et_2O eluent), and concentrated under reduced pressure to afford the crude secondary amine, which was used in the next step without further purification.

To a solution of the crude secondary amine in acetonitrile (1 mL) was added $NaBH_3CN$ (10.0 mg, 0.159 mmol, 6.4 equiv) and aq formaldehyde (37% w/w, 50 μL, 0.67 mmol, 26.9 equiv). After stirring at 23 °C for 2 h, the reaction mixture was washed with H_2O (2 mL). The aqueous layer was back-extracted with CH_2Cl_2 (3 x 3 mL). The organics were combined, dried over Na_2SO_4, and filtered. The filtrate was concentrated under reduced pressure and purified by preparative TLC (0.25 mm, 9:1 $CHCl_3$:MeOH eluent) to provide (+)-amurensinine ((+)-**282**, 1.5 mg, 17% yield over 4 steps) as a colorless thin film: R_f 0.18 (9:1 $CHCl_3$:MeOH); ^{1}H NMR (300 MHz, $CDCl_3$): δ 6.72 (s, 1H), 6.71 (s, 1H), 6.62 (s, 1H), 6.52 (s, 1H), 5.91 (d, J = 1.4 Hz, 1H), 5.85 (d, J = 1.4 Hz, 1H), 3.86 (s, 3H), 3.84 (dd, J = 3.7, 3.7 Hz, 1H), 3.77 (s, 3H), 3.62 (dd, J = 4.5, 1.5 Hz, 1H), 3.53 (dd, J = 10.4, 1.6 Hz, 1H), 3.48 (dd, J = 17.0, 4.1 Hz, 1H), 2.90 (dd, J = 17.3, 3.5 Hz, 1H), 2.83 (dd, J = 10.6, 4.6 Hz, 1H), 2.48 (s, 3H); ^{13}C NMR (75 MHz, $CDCl_3$): δ 147.7, 146.6, 146.3, 145.9, 135.1, 134.5, 131.2, 126.5, 114.2, 111.1, 107.2, 106.1, 100.6, 62.5, 59.9, 56.0, 55.9, 46.0, 45.3, 38.2; IR (thin film/NaCl): 2916, 2848, 1607, 1517, 1482, 1249 cm^{-1}; HRMS-EI (m/z): $[M]^+$ calcd for $[C_{20}H_{21}NO_4]^+$, 339.1471; found, 339.1469; UV-Vis λ_{max} 294 nm, shoulders at 232 and 250 nm, λ_{min} at 263 nm; $[\alpha]^{25}_D$ +82.8° (c 0.035, CH_2Cl_2) [lit.[22] $[\alpha]^{20}_D$ –145.0° (c 1.0, CH_2Cl_2)].

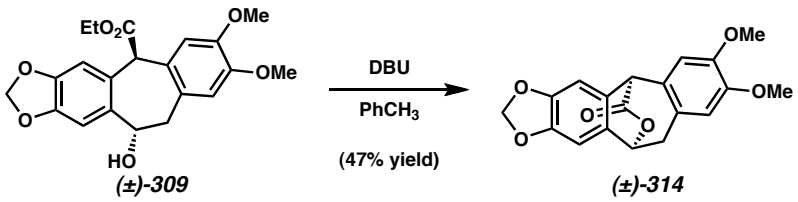

Lactone (±)-314. To a solution of hydroxyester (±)-**309** (11.6 mg, 0.030 mmol, 1.0 equiv) in $PhCH_3$ (1 mL) was added DBU (44.9 μL, 45.7 mg, 0.30 mmol, 10.0 equiv). After 20 h, the reaction mixture was diluted with H_2O (2 mL) and extracted with EtOAc (3 x 3 mL). The organic layers were combined, dried over Na_2SO_4, and filtered. The filtrate was concentrated under reduced pressure and purified by flash chromatography (3:2 hexanes:EtOAc) to afford lactone (±)-**314** (4.8 mg, 47% yield) as a foamy white solid: R_f 0.33 (1:1 hexanes:EtOAc); ^{1}H NMR (300 MHz, $CDCl_3$) δ 6.77 (s, 1H), 6.73 (s, 1H), 6.72 (s, 1H), 6.52 (s, 1H), 5.97 (d, J = 1.4 Hz, 1H), 5.91 (d, J = 1.4 Hz, 1H), 5.55 (dd, J = 4.5, 2.4 Hz, 1H), 4.43 (s, 1H), 3.89 (s, 3H), 3.79 (s, 3H), 3.59 (dd, J = 17.8, 4.5 Hz, 1H), 3.15 (dd, J = 17.9, 2.4 Hz, 1H); ^{13}C NMR (126 MHz, $CDCl_3$) δ 171.9, 149.0, 148.0, 147.8, 147.1, 132.1, 127.1, 126.4, 124.3, 113.9, 111.4, 106.1, 105.6, 101.4, 78.7, 56.0, 55.9, 54.0, 35.8; IR (thin film/NaCl) 2904, 1746, 1519, 1252 cm^{-1}; HRMS-EI (*m/z*): $[M]^+$ calcd for $[C_{19}H_{16}O_6]^+$, 340.0947; found, 340.0941.

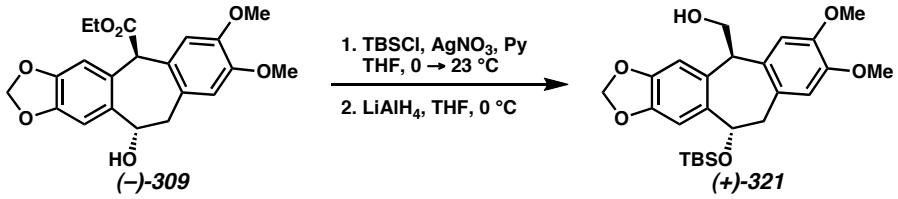

Hydroxysilane (+)-321. A solution of hydroxyester (–)-**309** (375.2 mg, 0.97 mmol, 1.0 equiv) in THF (19 mL) was cooled to 0 °C. $AgNO_3$ (660 mg, 3.89 mmol, 4.0 equiv), pyridine (628 μL, 7.76 mmol, 8.0 equiv), and then TBSCl (585 mg, 3.89 mmol,

4.0 equiv) were added. The cloudy mixture was allowed to warm to 23 °C and stirred 14 h. The mixture was filtered through a short plug of Celite (Et_2O eluent). The filtrate was washed with H_2O (40 mL). The aqueous layer was extracted with Et_2O (3 x 40 mL). The organic layers were combined, dried over Na_2SO_4, and filtered. The filtrate was concentrated under reduced pressure to afford the crude silylester, which was used in the next step without further purification.

A solution of the crude silylester in THF (19 mL) was cooled to 0 °C. Lithium aluminum hydride (184 mg, 4.85 mmol, 5.0 equiv) was added. The mixture was allowed to stir at 0 °C for 30 min. H_2O (200 μL), then aq NaOH (10% w/v, 200 μL), then H_2O (400 μL) were sequentially added. The mixture was allowed to warm to 23 °C and stir 30 min before filtration through a short plug of Celite (Et_2O eluent). The filtrate was concentrated under reduced pressure and purified by flash chromatography (3:1 hexanes:EtOAc eluent) to afford hydroxysilane (+)-**321** as a white foam: R_f 0.20 (1:1 hexanes:EtOAc); ^{1}H NMR (300 MHz, C_6D_6) δ 7.53 (s, 1H), 6.72 (s, 1H), 6.61 (s, 1H), 6.44 (s, 1H), 5.53 (dd, J = 10.2, 2.4 Hz, 1H), 5.39 (app. s, 1H), 5.37 (app. s, 1H), 4.11-3.84 (comp. m, 4H), 3.47 (s, 3H), 3.39 (s, 3H), 3.31-3.08 (comp. m, 2H), 0.98 (s, 9H), 0.12 (s, 3H), 0.09 (s, 3H); ^{13}C NMR (75 MHz, C_6D_6) δ 148.7, 148.2, 147.4, 146.6, 138.4, 129.6, 129.2, 128.7, 116.0, 115.4, 111.7, 106.2, 100.9, 70.1, 67.8, 57.5, 55.7, 55.5, 44.3, 26.0, 18.4, -4.8, -4.8; IR (thin film/NaCl) 3512, 2930, 1521, 1484, 1040 cm^{-1}; HRMS-FAB (m/z): [M-H]$^+$ calcd for $[C_{25}H_{33}O_6Si]^+$, 457.2046; found, 457.2049. Hydroxysilane (+)-**321** was found to be 86.8% ee by chiral HPLC (AD column, 1.0 mL/min, 10% EtOH/hexanes, major peak 8.1 min, minor peak 12.1 min); $[\alpha]^{25}_D$ +66.9° (c 0.71, C_6H_6).

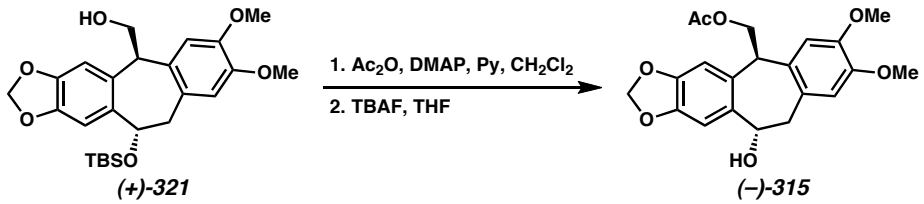

(+)-321 *(–)-315*

Hydroxyacetate (–)-315. To a solution of hydroxysilane (+)-**321** in CH_2Cl_2 (12 mL) was added pyridine (672 μL, 8.3 mmol, 10.0 equiv), DMAP (101 mg, 0.83 mmol, 1.0 equiv), and acetic anhydride (785 μL, 8.3 mmol, 10.0 equiv). After 5 min, saturated aq NaCl (15 mL) was added. The layers were separated, and the aqueous layer was extracted with CH_2Cl_2 (3 x 15 mL). The organic layers were combined, dried over Na_2SO_4, and filtered. The filtrate was evaporated under reduced pressure. Heptane (200 mL) was added, followed by concentration under reduced pressure. Then, $PhCH_3$ (100 mL) was added, and the solution was concentrated under reduced pressure to azeotrope excess reagents. The crude silylacetate was used in the next step without further purification.

To a solution of crude silylacetate in THF (8 mL) was added TBAF (1.0 M in THF, 2.40 mL, 2.40 mmol, 3.0 equiv). After 10 min, the reaction was diluted with EtOAc (50 mL), washed with H_2O (2 x 10 mL) and saturated aq NaCl (10 mL), dried over Na_2SO_4, and filtered. The filtrate was concentrated under reduced pressure and purified by flash chromatography (3:2 hexanes:EtOAc) to afford hydroxyacetate (–)-**315** (219 mg, 71% yield over 4 steps) as a white foam: R_f 0.19 (1:1 hexanes:EtOAc); ^{1}H NMR (300 MHz, C_6D_6) δ 7.13 (s, 1H), 6.70 (s, 1H), 6.62 (s, 1H), 6.46 (s, 1H), 5.36-5.32 (comp. m, 2H), 4.87 (d, J = 7.5 Hz, 1H), 4.60-4.46 (comp. m, 2H), 4.15 (t, J = 8.1 Hz, 1H), 3.46 (s, 3H), 3.37 (s, 3H), 3.27 (dd, J = 15.2, 8.1 Hz, 1H), 2.86 (dd, J = 15.3, 8.1 Hz, 1H), 1.59 (s, 3H); ^{13}C NMR (75 MHz, C_6D_6) δ 170.4, 149.5, 148.8, 147.9, 147.4, 137.2,

130.5, 130.2, 128.9, 116.4, 116.0, 111.5, 110.4, 101.5, 70.2, 67.6, 56.2, 55.9, 53.3, 41.8, 20.8; IR (thin film/NaCl) 3506, 2935, 1736, 1487, 1242, 1038 cm^{-1}; $[\alpha]^{25}_{D}$ –11.9° (*c* 1.14, C_6H_6).

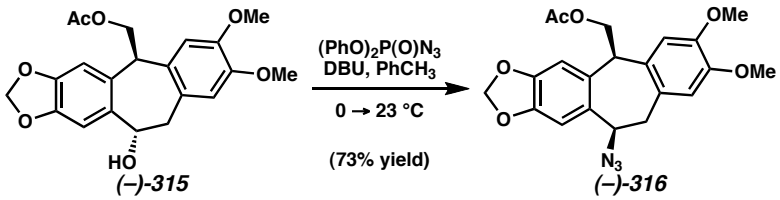

Azidoacetate (–)-316. A solution of hydroxyacetate (–)-**315** (101.8 mg, 0.26 mmol, 1.0 equiv) in $PhCH_3$ (5.2 mL) was cooled to 0 °C. DPPA (118 μL, 0.55 mmol, 7.5 equiv) and DBU (82 μL, 0.55 mmol, 7.5 equiv) were added. The reaction was stirred and allowed to warm to 23 °C. After 15 h, H_2O (15 mL) was added. The mixture was extracted with Et_2O (3 x 20 mL). The organics were combined, dried over Na_2SO_4, and filtered. The filtrate was concentrated under reduced pressure and purified by flash chromatography (4:1→7:3 hexanes:EtOAc) to afford azidoacetate (–)-**316** (79.5 mg of (–)-**316**, 73% yield of (–)-**316**, contaminated with trace byproducts) as a colorless oil. Further purification by preparative HPLC (1:0→4:1 hexanes:EtOAc) provided an analytically pure sample of azidoacetate (–)-**316**: R_f 0.64 (2:3 hexanes:EtOAc); ^{1}H NMR (300 MHz, C_6D_6) δ 7.00 (s, 1H), 6.67 (s, 1H), 6.56 (s, 1H), 6.37 (s, 1H), 5.29 (dd, *J* = 1.4, 0.6 Hz, 1H), 5.24 (dd, *J* = 1.4, 0.5 Hz, 1H), 4.76 (dd, *J* = 11.0, 8.2 Hz, 1H), 4.62 (dd, *J* = 11.0, 7.6 Hz, 1H), 4.27 (dd, *J* = 10.7, 4.8 Hz, 1H), 4.16 (t, *J* = 7.9 Hz, 1H), 3.42 (s, 3H), 3.39 (s, 3H), 3.28 (dd, *J* = 14.6, 10.9 Hz, 1H), 2.89 (dd, *J* = 15.0, 4.8 Hz, 1H), 1.59 (s, 3H); ^{13}C NMR (75 MHz, C_6D_6) δ 170.4, 149.6, 149.2, 148.0, 147.8, 132.7, 131.9, 131.1, 128.9, 115.4, 113.8, 110.7, 110.2, 101.7, 66.9, 62.9, 56.2, 56.1, 50.1, 38.5, 20.8; IR (thin

film/NaCl) 2934, 2099, 1737, 1236 cm^{-1}; HRMS-EI (*m/z*): $[M]^+$ calcd for $[C_{21}H_{21}N_3O_6]^+$, 411.1430; found, 411.1423. Azidoacetate (–)-**316** was found to be 88.3% ee by chiral HPLC (AD column, 1.0 mL/min, 10% EtOH/hexanes, major peak 45.2 min, minor peak 41.4 min); $[\alpha]^{25}_D$ –58.8° (*c* 0.61, C_6H_6).

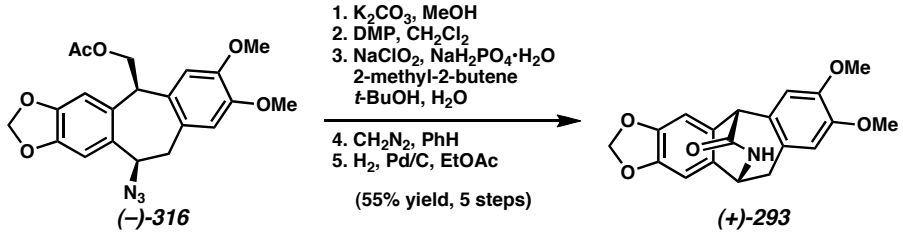

Lactam (+)-293. To a solution of azidoacetate (–)-**316** (20.0 mg, 0.049 mmol, 1.0 equiv) in MeOH (2 mL) was added K_2CO_3 (67 mg, 0.49 mmol, 10.0 equiv). After 25 min, the reaction was diluted with saturated aq NH_4Cl (5 mL) and H_2O (5 mL). The mixture was then extracted with EtOAc (3 x 10 mL). The organics were combined, dried over Na_2SO_4, and filtered. The filtrate was concentrated under reduced pressure to afford a crude azidoalcohol, which was used in the next step without further purification.

To a solution of crude azidoalcohol in CH_2Cl_2 (2 mL) was added Dess-Martin periodinane[23] (62.0 mg, 0.15 mmol, 3.0 equiv). After 2 h, the mixture was filtered through a short plug of Celite (CH_2Cl_2 eluent). The filtrate was concentrated under reduced pressure to afford a crude azidoaldehyde, which was used in the next step without further purification.

To a solution of crude azidoaldehyde in *t*-BuOH (1.6 mL) was added 2-methyl-2-butene (154 μL, 1.45 mmol, 30.0 equiv) followed by a solution of $NaClO_2$ (technical grade [80%], 22.0 mg, 0.24 mmol, 5.0 equiv) and $NaH_2PO_4 \bullet H_2O$ (53.0 mg, 0.39 mmol, 8.0 equiv) in H_2O (800 μL). After stirring vigorously for 2 h, the mixture was diluted

with saturated aq NaCl (4 mL) and extracted with EtOAc (4 x 4 mL). The organics were combined, dried over Na_2SO_4, and filtered. The filtrate was concentrated under reduced pressure to afford a crude azidoacid, which was used in the next step without further purification.

To a solution of crude azidoacid in PhH (3 mL) was added CH_2N_2 (0.2 M in Et_2O, 2 mL) until yellow color persisted. After 5 min, the reaction was concentrated under reduced pressure and purified by preparative TLC (0.5 mm, 3:2 hexanes:EtOAc eluent) to afford an azidoester, which was used in the next step without further purification.

To a solution of azidoester in EtOAc (4.7 mL) was added Pd/C (10% w/w, 50 mg, 0.049 mmol Pd, 1.0 equiv). The reaction flask was placed under a balloon of H_2 (1 atm) and stirred at 23 °C for 15 h. The reaction mixture was then filtered through a short plug of Celite (EtOAc eluent), concentrated under reduced pressure, and purified by preparative TLC (0.25 mm, 9:1 $CHCl_3$:MeOH) to afford lactam (+)-**293** (9.1 mg, 55% yield over 5 steps).

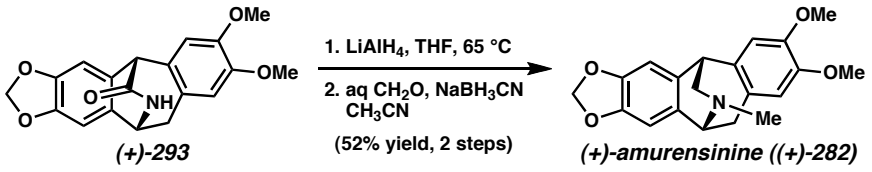

(+)-Amurensinine ((+)-282). To a solution of lactam (+)-**293** (9.8 mg, 0.029 mmol, 1.0 equiv) in THF (1 mL) was added lithium aluminum hydride (11.0 mg, 0.29 mmol, 10.0 equiv) at 0 °C. The reaction was then heated to 65 °C for 4 h. The mixture was cooled to 0 °C and diluted with CH_2Cl_2 (1 mL). H_2O (100 μL), aq NaOH (10% w/v, 100 μL), and H_2O (200 μL) were added sequentially dropwise. The biphasic mixture was warmed to 23 °C and stirred vigorously for 1 h. The reaction was then filtered through a

short plug of Celite (CH_2Cl_2 eluent) to remove suspended solids. After dilution with H_2O (2 mL) and aq NaOH (10% w/v, 2 mL), the biphasic mixture was extracted with CH_2Cl_2 (5 x 5 mL). The organic layers were combined, dried over Na_2SO_4, and filtered. The filtrate was concentrated under reduced pressure to afford the crude secondary amine, which was carried on to the next step without further purification.

To a solution of crude secondary amine in acetonitrile (1 mL) was added sodium cyanoborohydride (24.7 mg, 0.40 mmol, 13.8 equiv) followed by aq formaldehyde (37% w/w, 110 μL, 1.48 mmol, 51.0 equiv). After stirring for 5.5 h at 23 °C, the reaction was diluted with H_2O (2 mL) and extracted with CH_2Cl_2 (4 x 2 mL). The organic layers were combined, dried over Na_2SO_4, and filtered. The filtrate was concentrated under reduced pressure and purified by preparative TLC (0.25 mm, 19:1 $CHCl_3$:MeOH eluent) to afford (+)-amurensinine ((+)-**282**, 5.1 mg, 52% yield over 2 steps) as a colorless thin film.

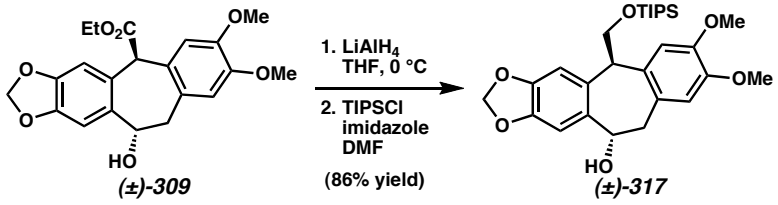

Hydroxysilane (±)-317. To a solution of hydroxyester (±)-**309** (76.6 mg, 0.20 mmol, 1.0 equiv) in THF (4 mL) was added lithium aluminum hydride (37.6 mg, 0.99 mmol, 5.0 equiv) at 0 °C. After 30 min, the reaction was quenched at 0 °C by slow addition of EtOAc (5 mL) followed by aq sodium potassium tartrate (10% w/v, 5 mL). After warming to 23 °C and stirring vigorously for 1 h, the biphasic mixture was diluted with H_2O (10 mL) and extracted with EtOAc (4 x 20 mL). The organic layers were combined, dried over Na_2SO_4, and filtered. The filtrate was concentrated under reduced

pressure to afford a crude diol, which was carried on to the next step without further purification. Diol: R_f 0.12 (2:3 hexanes:EtOAc); ^{1}H NMR (300 MHz, C_6D_6): δ 7.10 (s, 1H), 6.69 (s, 1H), 6.56 (s, 1H), 6.49 (s, 1H), 5.36 (dd, *J* = 1.4, 0.5 Hz, 1H), 5.34 (dd, *J* = 1.4, 0.6 Hz, 1H), 4.82 (br d, *J* = 6.8 Hz, 1H), 3.86-3.78 (comp. m, 3H), 4.15 (s, 1H), 3.44 (s, 3H), 3.40 (s, 3H), 3.21 (dd, *J* = 15.0, 2.6 Hz, 1H), 2.83 (dd, *J* = 15.0, 7.9 Hz, 1H), 1.37 (br s, 1H), 1.03 (br s, 1H).

To a solution of crude diol in DMF (4 mL) was added imidazole (40.5 mg, 0.60 mmol, 3.0 equiv) then tri-isopropylchlorosilane (63.7 μL, 0.30 mmol, 1.5 equiv). After stirring 12 h at 23 °C, the solution was quenched by addition of H_2O (20 mL). The mixture was then extracted with EtOAc (4 x 30 mL). The organic layers were combined, dried over Na_2SO_4, and filtered. The filtrate was concentrated under reduced pressure and purified by flash chromatography (2:3 hexanes:Et_2O eluent) to provide hydroxysilane (±)-**317** (85.8 mg, 86% yield over 2 steps) as a white solid: R_f 0.28 (3:2 hexanes:EtOAc); ^{1}H NMR (300 MHz, C_6D_6): δ 7.11 (s, 1H), 6.86 (s, 1H), 6.74 (s, 1H), 6.55 (s, 1H), 5.37 (d, *J* = 1.3 Hz, 1H), 5.34 (d, *J* = 1.3 Hz, 1H), 4.93 (ddd, *J* = 7.9, 7.9, 1.9 Hz, 1H), 4.18-4.15 (comp. m, 2H), 4.09 (dd, *J* = 15.5, 8.1 Hz, 1H), 3.53 (s, 3H), 3.41 (s, 3H), 3.41 (dd, *J* = 14.8, 2.2 Hz, 1H), 2.91 (dd, *J* = 14.9, 7.6 Hz, 1H), 1.36 (d, *J* = 8.4 Hz, 1H), 1.01 (comp. m, 21H); ^{13}C NMR (75 MHz, C_6D_6): δ 149.0, 148.5, 147.3, 147.1, 136.4, 132.0, 131.3, 116.6, 116.3, 112.2, 110.5, 101.1, 70.4, 68.2, 57.9, 55.9, 55.7, 41.5, 18.2, 12.3; IR (thin film/NaCl): 2941, 2865, 1520, 1487, 1240, 1098, 1041 cm^{-1}; HRMS-FAB (*m*/*z*): $[M]^+$ calcd for $[C_{28}H_{40}O_6Si]^+$, 500.2594; found, 500.2598.

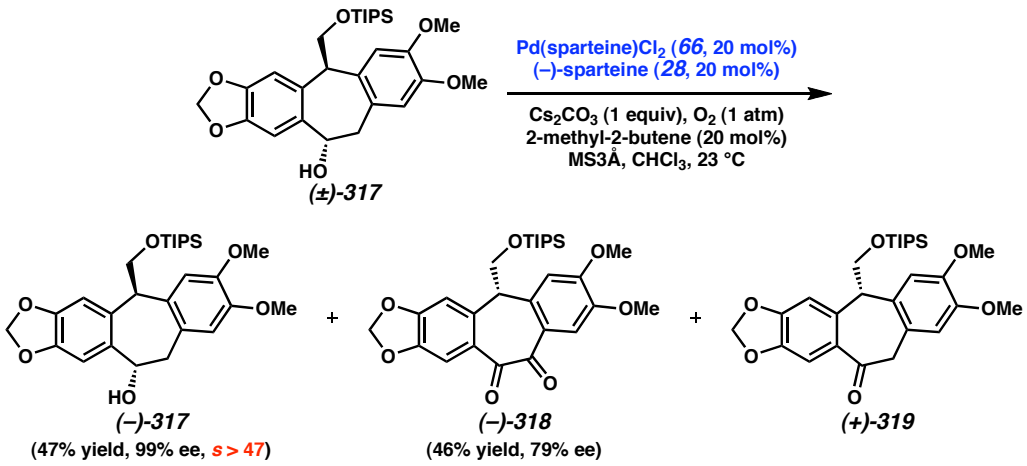

Oxidative Kinetic Resolution of Hydroxysilane (±)-317: Hydroxysilane (–)-317. To a 1 dram vial with stir bar was added oven-dried powdered 3Å molecular sieves (50 mg), Pd(sparteine)Cl_2 (**66**, 8.2 mg, 0.02 mmol, 0.20 equiv), $CHCl_3$ (0.5 mL),[21] and (–)-sparteine (**28**, 4.6 μL, 0.02 mmol, 0.20 equiv). The mixture was cooled to –78 °C and alternately evacuated and backfilled with O_2 (3x). After allowing the mixture to warm to 23 °C, powdered anhydrous Cs_2CO_3 (32.6 mg, 0.10 mmol, 1.0 equiv), 2-methyl-2-butene (2.1 μL, 0.02 mmol, 0.20 equiv), and a solution of hydroxysilane (±)-**317** (50.1 mg, 0.10 mmol, 1.0 equiv) in $CHCl_3$ (0.5 mL) were added. The reaction was stirred vigorously under a balloon of O_2 for 82 h. The reaction mixture was filtered through a short plug of silica gel (EtOAc eluent) and evaporated under reduced pressure. Purification by preparative TLC (0.5 mm, 3:2 hexanes:EtOAc eluent) afforded hydroxysilane (–)-**317** (23.7 mg, 47% yield) and diketosilane (–)-**318** (23.4 mg). Hydroxysilane (–)-**317** was found to be >99% ee by chiral HPLC (AD column, 1.0 mL/min, 5% EtOH/hexanes, major peak 13.0 min, minor peak 21.0 min); $[\alpha]^{25}_{D}$ –24.4° (*c* 0.86, C_6H_6, >99% ee). Reactions stopped earlier than 82 h afforded another product in addition to hydroxysilane (–)-**317** and diketosilane (–)-**318**. This compound was revealed to be ketosilane (+)-**319**, which gradually oxidized to the diketone in the presence of O_2.

Diketosilane (–)-318. R_f 0.35 (3:2 hexanes:EtOAc); ^{1}H NMR (300 MHz, C_6D_6): δ 7.61 (s, 1H), 7.58 (s, 1H), 6.59 (s, 1H), 6.48 (s, 1H), 5.16 (s, 2H), 3.97 (d, J = 5.9 Hz, 2H), 3.79 (t, J = 5.7 Hz, 1H), 3.39 (s, 3H), 3.26 (s, 3H), 0.94 (comp. m, 21H); ^{13}C NMR (75 MHz, C_6D_6): δ 186.8, 185.8, 153.6, 151.6, 149.6, 147.9, 138.8, 136.8, 131.0, 114.5, 112.9, 111.5, 109.9, 101.9, 71.9, 58.9, 55.3, 18.1, 12.2; IR (thin film/NaCl): 2942, 2866, 1659, 1597, 1517, 1485, 1251 cm^{-1}; HRMS-FAB (*m*/*z*): $[M+H]^+$ calcd for $[C_{28}H_{37}O_7Si]^+$, 513.2309; found, 513.2313. Diketosilane (–)-**318** was found to be 79.1% ee by chiral HPLC (AD column, 1.0 mL/min, 5% EtOH/hexanes, major peak 63.8 min, minor peak 24.7 min). The kinetic resolution therefore has a selectivity factor $s > 47$.[13] $[\alpha]^{25}_D$ –39.9º (*c* 1.21, C_6H_6, 73.9% ee).

Ketosilane (+)-319. R_f 0.50 (3:2 hexanes:EtOAc); ^{1}H NMR (300 MHz, C_6D_6): δ 8.03 (s, 1H), 6.82 (s, 1H), 6.71 (s, 1H), 6.48 (s, 1H), 5.21 (d, J = 1.4 Hz, 1H), 5.17 (d, J = 1.2 Hz, 1H), 4.42 (d, J = 14.5 Hz, 1H), 4.37-4.26 (m, 2H), 4.24-4.13 (m, 1H), 3.83 (d, J = 14.9 Hz, 1H), 3.49 (s, 3H), 3.29 (s, 3H), 1.00 (comp. m, 21H); ^{13}C NMR (75 MHz, C_6D_6): δ 192.8, 151.3, 149.5, 148.7, 147.6, 139.9, 132.1, 130.8, 125.1, 115.2, 114.6, 110.9, 110.2, 101.7, 65.8, 56.0, 55.6, 50.3, 18.2, 12.2; IR (thin film/NaCl): 2941, 2865, 1665, 1516, 1484, 1102 cm^{-1}; HRMS-FAB (*m*/*z*): $[M]^+$ calcd for $[C_{28}H_{38}O_6Si]^+$, 498.2438; found, 498.2433. Ketosilane (+)-**319** was found to be 76.8% ee by chiral HPLC (AD column, 1.0 mL/min, 5% EtOH/hexanes, major peak 20.6 min, minor peak 10.7 min); $[\alpha]^{25}_D$ +10.6º (*c* 0.65, C_6H_6, 76.8% ee).

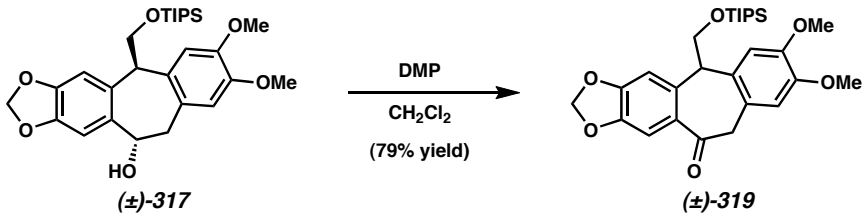

(±)-317 *(±)-319*

Ketosilane (±)-319 by Dess-Martin Periodinane Oxidation. To a solution of hydroxysilane (±)-**317** (10.0 mg, 0.020 mmol, 1.0 equiv) in CH_2Cl_2 (0.5 mL) was added Dess-Martin periodinane (25.4 mg, 0.060 mmol, 3.0 equiv). After 5 min, the reaction was diluted with Et_2O (2 mL) and filtered through a short plug of Celite (Et_2O eluent). The filtrate was concentrated under reduced pressure and purified by preparative TLC (0.25 mm, 7:3 hexanes:EtOAc eluent) to afford ketosilane (±)-**319** (7.9 mg, 79% yield) as a colorless oil.

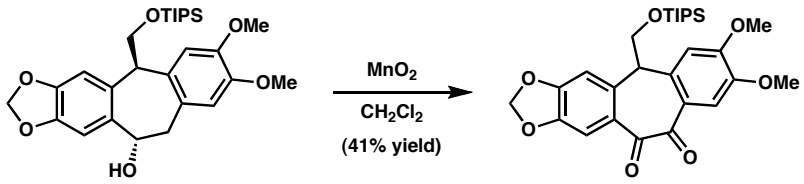

(±)-317 *(±)-318*

Diketosilane (±)-318 by MnO_2 Oxidation. To a solution of hydroxysilane (±)-**317** (13.2 mg, 0.026 mmol, 1.0 equiv) in CH_2Cl_2 (1 mL) was added MnO_2 (activated, 22.9 mg, 0.26 mmol, 10.0 equiv). After 19 h, more MnO_2 (45.8 mg, 0.52 mmol, 20.0 equiv) was added. After 115 h, the reaction was filtered through a short plug of Celite (CH_2Cl_2 eluent). The filtrate was concentrated under reduced pressure and purified by preparative TLC (0.25 mm, 7:3 hexanes:EtOAc eluent) to afford diketosilane (±)-**318** (5.4 mg, 41% yield) as a yellow solid.

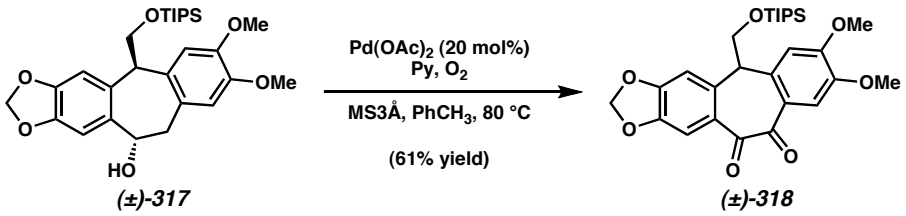

(±)-317 *(±)-318*

Diketosilane (±)-318 by Pd-catalyzed Aerobic Oxidation. Palladium acetate (1.8 mg, 0.008 mmol, 0.20 equiv), oven-dried 3Å molecular sieves (20 mg), $PhCH_3$ (0.5 mL), and pyridine (2.6 μL, 0.032 mmol, 0.80 equiv) were allowed to stir at 80 °C under O_2 atmosphere (balloon) for 10 min. Hydroxysilane (±)-**317** (20.0 mg, 0.040 mmol, 1.0 equiv) was added, and the reaction was allowed to stir at 80 °C under O_2 atmosphere for 23 h. After cooling to 23 °C, the mixture was diluted with EtOAc (2 mL) and filtered through a short plug of Celite (EtOAc eluent). The filtrate was concentrated under reduced pressure and purified by preparative TLC (0.25 mm, 3:2 hexanes:EtOAc eluent) to afford diketosilane (±)-**318** (12.1 mg, 61% yield) as a yellow solid.

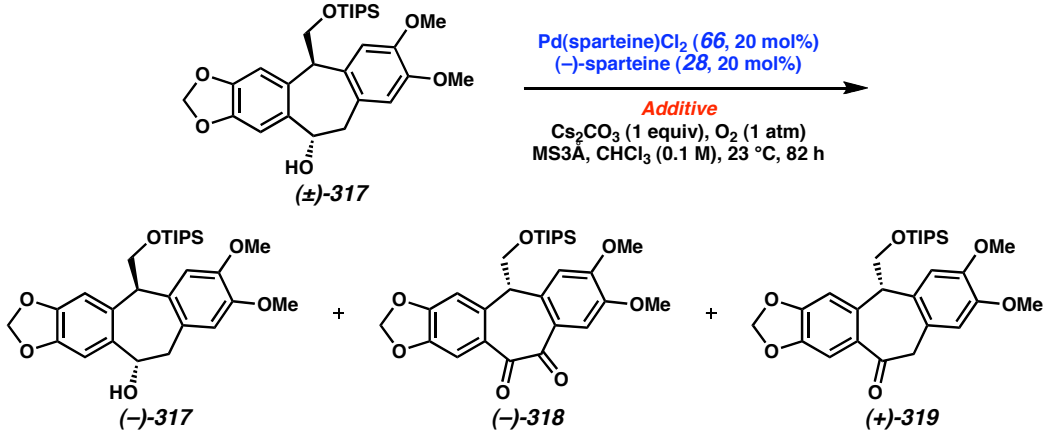

(±)-317 *(–)-317* *(–)-318* *(+)-319*

Radical Inhibitor Screen in the Oxidative Kinetic Resolution of Hydroxysilane (±)-317: Hydroxysilane (–)-317. To a 1 dram vial with stir bar was added oven-dried powdered 3Å molecular sieves (50 mg), Pd(sparteine)Cl_2 (**66**, 8.2 mg, 0.02 mmol, 0.20 equiv), $CHCl_3$ (0.5 mL),[21] and (–)-sparteine (**28**, 4.6 μL, 0.02 mmol,

0.20 equiv). The mixture was cooled to –78 °C and alternately evacuated and backfilled with O_2 (3x). After allowing the mixture to warm to 23 °C, powdered anhydrous Cs_2CO_3 (32.6 mg, 0.10 mmol, 1.0 equiv), the appropriate additive (0.020 mmol, 0.20 equiv), and a solution of hydroxysilane (±)-**317** (50.1 mg, 0.10 mmol, 1.0 equiv) in $CHCl_3$ (0.5 mL) were added. The reaction was stirred vigorously under a balloon of O_2 for 82 h. The reaction mixture was filtered through a short plug of silica gel (EtOAc eluent) and evaporated under reduced pressure. Purification by preparative TLC (0.25 mm, 3:2 hexanes:EtOAc eluent) afforded hydroxysilane (–)-**317**, diketosilane (–)-**318**, and ketosilane (+)-**319**, as shown in Table 5.5.1.

Table 5.5.1 Radical inhibitor screening.

additive	hydroxysilane % yield (ee)	diketosilane % yield (ee)	ketosilane % yield (ee)	% conversion[a]	*s*[b]
none[c]	36 (97)	28 (83)	19 (76)	54	44
BHT	47 (95)	49 (82)	--[d]	54	36
tetracyanoethylene	92 (< 5)	8 (--)	--[d]	8	--
2-methyl-2-butene	47 (99)	46 (79)	--[d]	56	47

[a] % Conversion determined relative to hydroxysilane ee and diketosilane ee, see ref 13. [b] Selectivity factor (*s*) determined according to ref 13. [c] Reaction run for 72 h. [d] No ketosilane recovered.

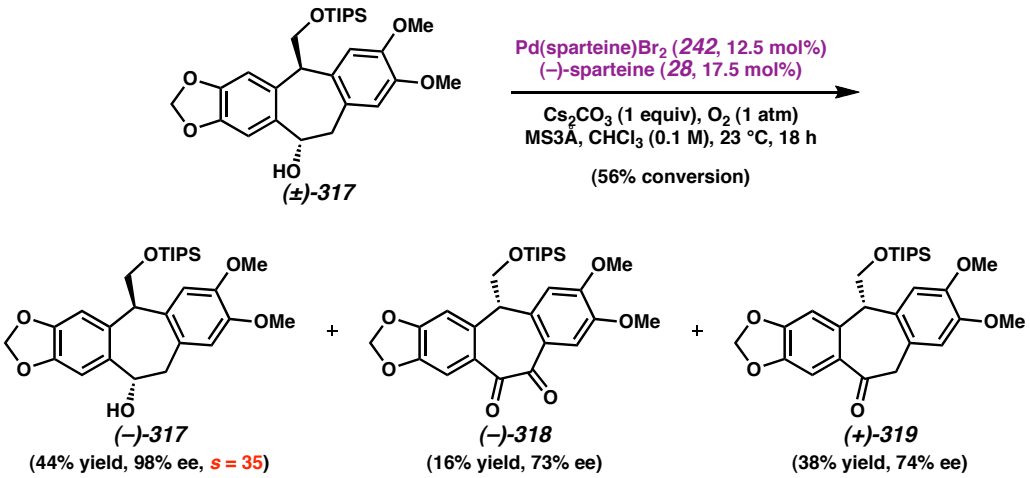

Oxidative Kinetic Resolution of Hydroxysilane (±)-317 with Dibromide Complex 242: Hydroxysilane (–)-317. To a 1 dram vial with stir bar was added oven-dried powdered 3Å molecular sieves (125 mg), Pd(sparteine)Br_2[16] (**242**, 6.3 mg, 0.0125 mmol, 0.125 equiv), $CHCl_3$ (0.5 mL),[21] and (–)-sparteine (**28**, 4.0 μL, 0.0175 mmol, 0.175 equiv). The mixture was cooled to –78 °C and alternately evacuated and backfilled with O_2 (3x). After allowing the mixture to warm to 23 °C, powdered anhydrous Cs_2CO_3 (32.6 mg, 0.10 mmol, 1.0 equiv) and a solution of hydroxysilane (±)-**317** (50.1 mg, 0.10 mmol, 1.0 equiv) and 1,4-bis(trimethylsilyl)benzene (internal ^{1}H NMR standard, 4.4 mg, 0.020 mmol, 0.20 equiv) in $CHCl_3$ (0.5 mL) were added. The reaction was stirred vigorously under a balloon of O_2 for 18 h. The reaction mixture was filtered through a short plug of silica gel (EtOAc eluent) and evaporated under reduced pressure. Conversion was determined to be 55.8% based on ^{1}H NMR of remaining starting hydroxysilane relative to internal standard. Purification by flash chromatography (7:3→1:1 hexanes:Et_2O eluent) afforded hydroxysilane (–)-**317** (22.7 mg, 45% yield, 98.0% ee, s = 35), diketosilane (–)-**318** (8.3 mg, 73.3% ee), and ketosilane (+)-**319** (19.0 mg, 73.7% ee).

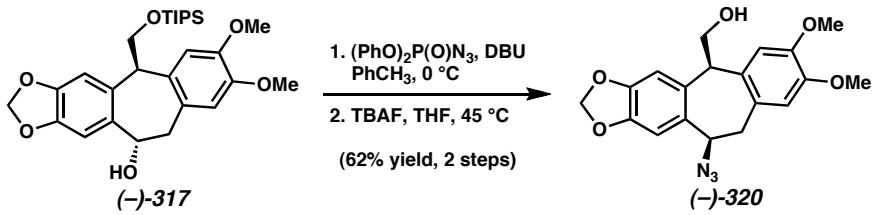

(–)-317 *(–)-320*

Azidoalcohol (–)-320. To a solution of hydroxysilane (–)-**317** (100.1 mg, 0.20 mmol, 1.0 equiv) in $PhCH_3$ (5 mL) was added DBU (179 μL, 1.20 mmol, 6.0 equiv) followed by DPPA (259 μL, 1.20 mmol, 6.0 equiv) at 0 °C. After stirring 6 h at 0 °C, the reaction was quenched by addition of H_2O (25 mL). The mixture was then extracted with Et_2O (3 x 30 mL). The organic layers were combined, dried over Na_2SO_4, and filtered. The filtrate was concentrated under reduced pressure to afford a crude azidosilane, which was carried on to the next step without further purification.

To a solution of crude azidosilane in THF (2 mL) was added TBAF (1.0 M in THF, 2.0 mL, 2.0 mmol, 10.0 equiv). The reaction was warmed to 45 °C for 5 h. The solution was allowed to cool to 23 °C and diluted with EtOAc (40 mL). The solution was washed with H_2O (3 x 20 mL) and saturated aq NaCl (20 mL), dried over Na_2SO_4, and filtered. The filtrate was concentrated under reduced pressure and purified by flash chromatography (7:3 hexanes:EtOAc eluent) followed by preparative TLC (0.5 mm, 1:1 hexanes:EtOAc eluent) to afford azidoalcohol (–)-**320** (45.9 mg, 62% yield over 2 steps) as a white foam: R_f 0.44 (2:3 hexanes:EtOAc); ^{1}H NMR (300 MHz, C_6D_6): δ 7.03 (s, 1H), 6.67 (s, 1H), 6.54 (s, 1H), 6.40 (s, 1H), 5.31 (d, J = 1.4 Hz, 1H), 5.27 (d, J = 1.3 Hz, 1H), 4.27 (dd, J = 10.8, 4.6 Hz, 1H), 4.04-3.90 (comp. m, 2H), 3.86 (dd, J = 14.6, 7.3 Hz, 1H), 3.43 (s, 3H), 3.41 (s, 3H), 3.28 (dd, J = 14.7, 11.0 Hz, 1H), 2.87 (dd, J = 14.7, 4.7 Hz, 1H), 1.10 (br s, 1H); ^{13}C NMR (75 MHz, C_6D_6): δ 149.1, 148.8, 147.6, 147.3, 133.1,

132.5, 130.6, 115.1, 114.2, 110.5, 110.4, 101.3, 66.3, 62.8, 55.9, 55.9, 54.4, 38.2; IR (thin film/NaCl): 3492, 2935, 2099, 1517, 1487, 1236 cm^{-1}; HRMS-FAB (*m*/*z*): $[M]^+$ calcd for $[C_{19}H_{19}N_3O_5]^+$, 369.1325; found, 369.1328. Azidoalcohol (–)-**320** was found to be >99% ee by chiral HPLC (AD column, 1.0 mL/min, 30% EtOH/hexanes, major peak 17.0 min, minor peak 15.3 min); $[\alpha]^{28}_D$ –70.8° (*c* 0.91, CH_2Cl_2).

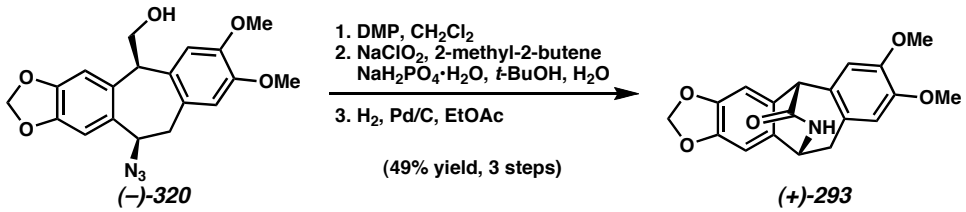

(–)-320 *(+)-293*

Lactam (+)-293. To a solution of azidoalcohol (–)-**320** (10.6 mg, 0.029 mmol, 1.0 equiv) in CH_2Cl_2 (1 mL) was added Dess-Martin periodinane (24.3 mg, 0.057 mmol, 2.0 equiv) at 0 °C. After 30 min, the mixture was diluted with Et_2O (3 mL) and filtered through a plug of Celite (Et_2O eluent). Concentration under reduced pressure afforded crude azidoaldehyde, which was used in the next step without further purification: R_f 0.77 (2:3 hexanes:EtOAc); ^{1}H NMR (300 MHz, C_6D_6): δ 9.63 (s, 1H), 6.83 (s, 1H), 6.43 (s, 1H), 6.38 (s, 1H), 6.32 (s, 1H), 5.30 (d, *J* = 1.3 Hz, 1H), 5.23 (d, *J* = 1.3 Hz, 1H), 4.00 (dd, *J* = 10.6, 4.2 Hz, 1H), 3.84 (s, 1H), 3.42 (s, 3H), 3.40 (s, 3H), 3.12 (dd, *J* = 15.0, 10.7 Hz, 1H), 2.67 (dd, *J* = 15.0, 4.1 Hz, 1H).

To a solution of crude azidoaldehyde in *t*-BuOH (1 mL) was added 2-methyl-2-butene (182 μL, 1.71 mmol, 59.0 equiv) followed by a solution of $NaClO_2$ (technical grade [80%], 32.4 mg, 0.29 mmol, 10.0 equiv) and NaH_2PO_4•H_2O (63.1 mg, 0.46 mmol, 15.9 equiv) in H_2O (1 mL). The biphasic mixture was stirred vigorously for 90 min. After diluting with saturated aq NaCl (4 mL), the mixture was extracted with EtOAc (5 x

4 mL). The organic layers were combined, dried over Na_2SO_4, and filtered. The filtrate was concentrated under reduced pressure to afford the crude azidoacid, which was used in the next step without purification: R_f 0.40 (9:1 $CHCl_3$:MeOH); ^{1}H NMR (300 MHz, C_6D_6): δ 6.89 (s, 1H), 6.53 (s, 1H), 6.51 (s, 1H), 6.35 (s, 1H), 5.26 (d, J = 1.4 Hz, 1H), 5.17 (d, J = 1.3 Hz, 1H), 4.32 (s, 1H), 4.07 (dd, J = 12.0, 5.2 Hz, 1H), 3.67 (dd, J = 14.4, 12.0, 1H), 3.40 (s, 3H), 3.38 (s, 3H), 2.78 (dd, J = 14.4, 5.1 Hz, 1H).

To a solution of crude azidoacid in EtOAc (1 mL) was added Pd/C (10% w/w, 30.4 mg, 0.029 mmol Pd, 1.0 equiv). The suspension was stirred under a balloon of H_2 (1 atm) for 12 h, after which it was filtered through a plug of Celite (MeOH eluent). Concentration under reduced pressure followed by purification by preparative TLC (0.25 mm, EtOAc eluent) afforded lactam (+)-**293** (4.8 mg, 49% yield over 3 steps) as a white solid. Lactam (+)-**293** was found to be >99% ee by chiral HPLC; $[\alpha]^{26}_D$ +3.0º (*c* 0.89, CH_2Cl_2).

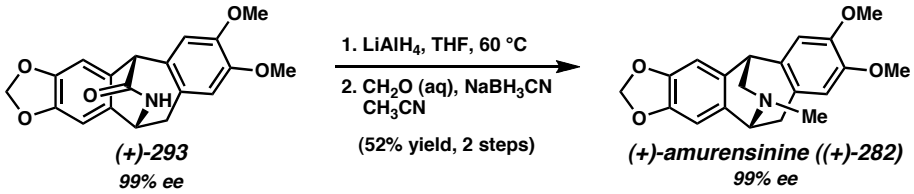

(+)-Amurensinine ((+)-282). To a solution of lactam (+)-**293** (9.8 mg, 0.029 mmol, 1.0 equiv) in THF (1 mL) was added lithium aluminum hydride (11.0 mg, 0.29 mmol, 10.0 equiv) at 0 °C. The reaction was then heated to 65 °C for 4 h. The mixture was cooled to 0 °C and diluted with CH_2Cl_2 (1 mL). H_2O (100 μL), aq NaOH (10% w/v, 100 μL), and H_2O (200 μL) were added sequentially dropwise. The biphasic mixture was warmed to 23 °C and stirred vigorously for 1 h. The reaction was then filtered through a

short plug of Celite (CH_2Cl_2 eluent) to remove suspended solids. After dilution with H_2O (2 mL) and aq NaOH (10% w/v, 2 mL), the biphasic mixture was extracted with CH_2Cl_2 (5 x 5 mL). The organic layers were combined, dried over Na_2SO_4, and filtered. The filtrate was concentrated under reduced pressure to afford the crude secondary amine, which was carried on to the next step without further purification.

To a solution of crude secondary amine in acetonitrile (1 mL) was added sodium cyanoborohydride (24.7 mg, 0.40 mmol, 13.8 equiv) followed by aq formaldehyde (37% w/w, 110 μL, 1.48 mmol, 51.0 equiv). After stirring for 5.5 h at 23 °C, the reaction was diluted with H_2O (2 mL) and extracted with CH_2Cl_2 (4 x 2 mL). The organic layers were combined, dried over Na_2SO_4, and filtered. The filtrate was concentrated under reduced pressure and purified by preparative TLC (0.25 mm, 19:1 $CHCl_3$:MeOH eluent) to afford (+)-amurensinine ((+)-**282**, 5.1 mg, 52% yield over 2 steps) as a colorless thin film. (+)-Amurensinine was found to be 99.0% ee by chiral HPLC (OJ column, 0.8 mL/min, 30% EtOH/hexanes, major peak 28.2 min, minor peak 20.5 min); $[\alpha]^{25}_D$ +125.8° (*c* 0.49, CH_2Cl_2).

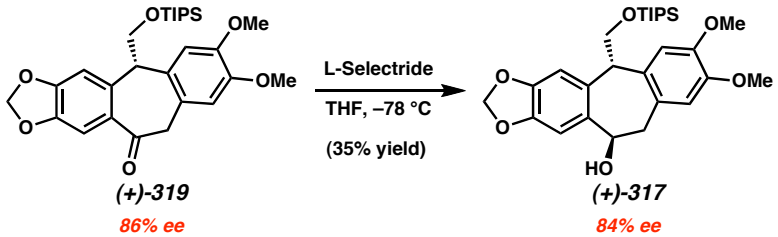

Hydroxysilane (+)-317. A solution of ketosilane (+)-**319** (12.7 mg, 0.025 mmol, 1.0 equiv, 85.9% ee by HPLC) in THF (0.5 mL) was cooled to –78 °C. L-Selectride (1.0 M in THF, 204 μL, 0.20 mmol, 8.0 equiv) was added dropwise. After stirring 15 min at –78 °C, saturated aq NH_4Cl (1 mL) was added. The mixture was allowed to warm to 23

°C and was diluted with H_2O (1 mL). The mixture was extracted with EtOAc (4 x 2 mL). The organic layers were combined, dried over Na_2SO_4, and filtered. The filtrate was concentrated under reduced pressure and purified by preparative TLC (0.25 mm, 3:2 hexanes:EtOAc eluent) to afford hydroxysilane (+)-**317** (4.5 mg, 35% yield, 83.7% ee by HPLC).

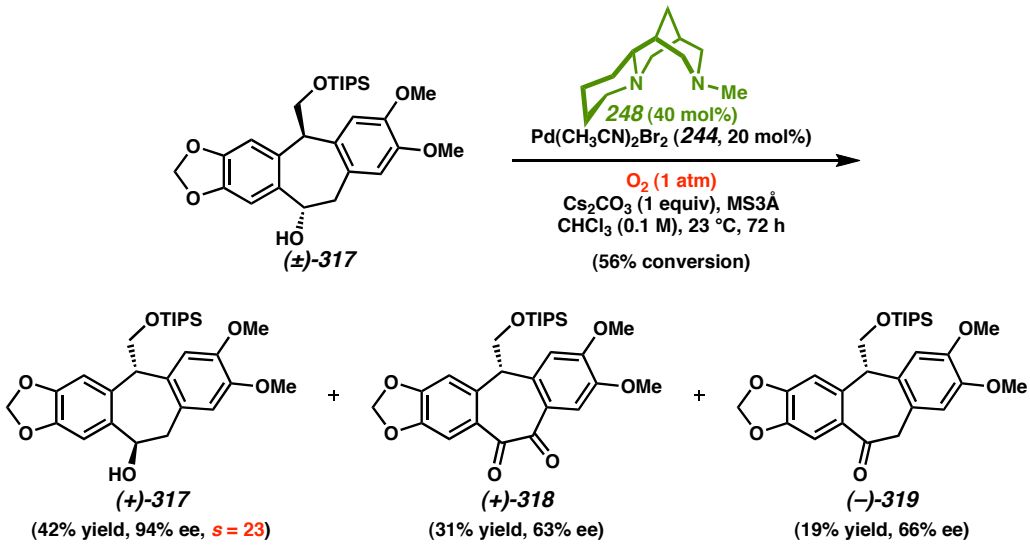

Oxidative Kinetic Resolution of Hydroxysilane (±)-317 with $Pd(CH_3CN)_2Br_2$ (244), Diamine 248, and O_2: Hydroxysilane (+)-317. To a 1 dram vial with stir bar was added oven-dried powdered 3Å molecular sieves (125 mg), $Pd(CH_3CN)_2Br_2$[16] (**244**, 7.0 mg, 0.020 mmol, 0.20 equiv), $CHCl_3$ (0.5 mL),[21] and diamine **248**[24] (7.8 mg, 0.040 mmol, 0.40 equiv). The mixture was cooled to –78 °C and alternately evacuated and backfilled with O_2 (3x). After allowing the mixture to warm to 23 °C, powdered anhydrous Cs_2CO_3 (32.6 mg, 0.10 mmol, 1.0 equiv) and a solution of hydroxysilane (±)-**317** (50.1 mg, 0.10 mmol, 1.0 equiv) and 1,4-bis(trimethylsilyl)benzene (internal ^1H NMR standard, 4.4 mg, 0.020 mmol, 0.20 equiv) in $CHCl_3$ (0.5 mL) were added. The reaction was stirred vigorously under a balloon of O_2 for 72 h. The reaction mixture was filtered through a

short plug of silica gel (EtOAc eluent) and evaporated under reduced pressure. Conversion was determined to be 56.3% based on ^{1}H NMR of remaining starting hydroxysilane relative to internal standard. Purification by flash chromatography (7:3→1:1 hexanes:Et_2O eluent) afforded hydroxysilane (+)-**317** (20.9 mg, 42% yield, 94.3% ee, *s* = 23), diketosilane (+)-**318** (16.0 mg, 62.9% ee), and ketosilane (–)-**319** (9.5 mg, 65.8% ee).

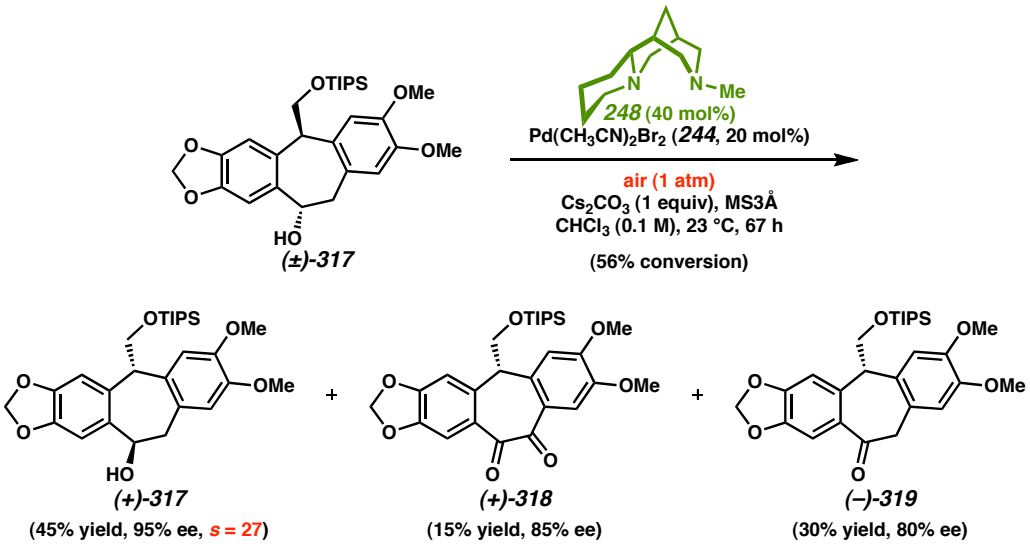

Oxidative Kinetic Resolution of Hydroxysilane (±)-317 with $Pd(CH_3CN)_2Br_2$ (244), Diamine 248, and Air: Hydroxysilane (+)-317. To a 1 dram vial with stir bar was added oven-dried powdered 3Å molecular sieves (125 mg), $Pd(CH_3CN)_2Br_2$ (**244**, 7.0 mg, 0.020 mmol, 0.20 equiv), $CHCl_3$ (0.5 mL),[21] and diamine **248** (7.8 mg, 0.040 mmol, 0.40 equiv). Powdered anhydrous Cs_2CO_3 (32.6 mg, 0.10 mmol, 1.0 equiv) and a solution of hydroxysilane (±)-**317** (50.1 mg, 0.10 mmol, 1.0 equiv) and 1,4-bis(trimethylsilyl)benzene (internal ^{1}H NMR standard, 4.4 mg, 0.020 mmol, 0.20 equiv) in $CHCl_3$ (0.5 mL) were added. The reaction was stirred vigorously open to air for 67 h. The reaction mixture was filtered through a short plug of silica gel (EtOAc eluent) and

evaporated under reduced pressure. Conversion was determined to be 55.6% based on ^{1}H NMR of remaining starting hydroxysilane relative to internal standard. Purification by flash chromatography (7:3→1:1 hexanes:Et_2O eluent) followed by preparative TLC (0.25 mm, 3:2 hexanes:EtOAc eluent) afforded hydroxysilane (+)-**317** (22.4 mg, 45% yield, 95.3% ee, *s* = 27), diketosilane (+)-**318** (7.5 mg, 84.8% ee), and ketosilane (–)-**319** (15.0 mg, 80.3% ee).

5.6 Notes and References

(1) Gözler, B.; Lantz, M. S.; Shamma, M. *J. Nat. Prod.* **1983**, *46*, 293-309.

(2) For the isolation of amurensinine, see: Maturová, M.; Pavlásková, D.; Santavy, F. *Planta Medica* **1966**, *14*, 22-41.

(3) For discussions on the biological activity of the isopavine alkaloids, see: (a) Weber, E.; Keana, J.; Barmettler, P. PCT Int. Appl. WO 9012575, 1990; *Chem. Abstr.* **1991**, *115*, 106019w. (b) Childers, W. E., Jr.; Abou-Gharbia, M. A. U.S. Patent 4,940,789, 1990; *Chem. Abstr.* **1990**, *113*, 191190w.

(4) For selected syntheses of isopavine alkaloids, see: (a) Gözler, B. Pavine and Isopavine Alkaloids. In *The Alkaloids*; Brossi, A., Ed.; Academic Press: New York, 1987; Vol. 31, pp 343-356. (b) Shinohara, T.; Takeda, A.; Toda, J.; Sano, T. *Heterocycles* **1998**, *48*, 981-992. (c) Gottlieb, L.; Meyers, A. I. *J. Org. Chem.* **1990**, *55*, 5659-5662. (d) Hanessian, S.; Mauduit, M. *Angew. Chem., Int. Ed.* **2001**, *40*, 3810-3813. (e) Dragoli, D. R.; Burdett, M. T.; Ellman, J. A. *J. Am. Chem. Soc.* **2001**, *123*, 10127-10128.

(5) Carrillo, L.; Badía, D.; Domínguez, E.; Vicario, J. L.; Tellitu, I. *J. Org. Chem.* **1997**, *62*, 6716-6721.

(6) Hanessian, S.; Talbot, C.; Saravanan, P. *Synthesis* **2006**, 723-734.

(7) Portions of this chapter are reproduced in part from: (a) Tambar, U. K.; Ebner, D. C.; Stoltz, B. M. *J. Am. Chem. Soc.* **2006**, *128*, 11752-11753. (b) Krishnan, S.;

Ramtohul, Y. K.; Bagdanoff, J. T.; Ebner, D. C.; Tambar, U. K.; Stoltz, B. M. *J. Am. Chem. Soc.* in press.

(8) Tambar, U. K.; Stoltz, B. M. *J. Am. Chem. Soc.* **2005**, *127*, 5340-5341.

(9) Witiak, D. T.; Kim, S. K.; Tehim, A. K.; Sternitzke, K. D.; McCreery, R. L.; Kim, S. U.; Feller, D. R.; Romstedt, K. J.; Kamanna, V. S.; Newman, H. A. I. *J. Med. Chem.* **1988**, *31*, 1437-1445.

(10) (a) Wenkert, E.; Davis, L. L.; Mylari, B. L.; Solomon, M. F.; Da Silva, R. R.; Shulman, S.; Warnet, R. J.; Ceccherelli, P.; Curini, M.; Pellicciari, R. *J. Org. Chem.* **1982**, *47*, 3242-3247. (b) Taber, D. F.; Petty, E. H. *J. Org. Chem.* **1982**, *47*, 4808-4809. (c) Taber, D. F.; Ruckle, R. E., Jr. *J. Am. Chem. Soc.* **1986**, *108*, 7686-7693.

(11) Himeshima, Y.; Sonoda, T.; Kobayashi, H. *Chem. Lett.* **1983**, 1211-1214.

(12) For a discussion of the Pd-catalyzed aerobic oxidative kinetic resolution of secondary alcohols, see Chapter 2.

(13) The selectivity factor (*s*) was determined using the following equations: $\frac{ee_{alc}}{ee_{ket}} = \frac{conv}{1-conv}$ and $s = \frac{\ln[(1-conv)(1-ee_{alc})]}{\ln[(1-conv)(1+ee_{alc})]}$, where ee_{alc} is the ee of the recovered alcohol, ee_{ket} is the ee of the product ketone, and $conv$ is the total conversion of alcohol to ketone, see: Kagan, H. B.; Fiaud, J. C. In *Topics in*

Stereochemistry; Eliel, E. L., Ed.; Wiley & Sons: New York, 1988; Vol. 18, pp 249-330.

(14) Thompson, A. S.; Humphrey, G. R.; DeMarco, A. M.; Mathre, D. J.; Grabowski, E. J. J. *J. Org. Chem.* **1993**, *58*, 5886-5888.

(15) Isopavine numbering convention, see ref 1.

(16) For a discussion of the effect of dibromide complex **242** in the oxidative kinetic resolution of alcohols, see: (a) Chapter 4. (b) Ebner, D. C.; Trend, R. M.; Genet, C.; McGrath, M. J.; O'Brien, P.; Stoltz, B. M. *Angew. Chem., Int. Ed.* **2008**, *47*, 6367-6370.

(17) Mohr, J. T.; Ebner, D. C.; Stoltz, B. M. *Org. Biomol. Chem.* **2007**, *5*, 3571-3576.

(18) For an asymmetric synthesis of (+)-sparteine, see: Smith, B. T.; Wendt, J. A.; Aubé, J. *Org. Lett.* **2002**, *4*, 2577-2579.

(19) Capozzi, G.; Roelens, S.; Talami, S. *J. Org. Chem.* **1993**, *58*, 7932-7936.

(20) Trend, R. M.; Stoltz, B. M. *J. Am. Chem. Soc.* **2004**, *126*, 4482-4483.

(21) $CHCl_3$ was stabilized with amylenes. $CHCl_3$ stabilized with EtOH must be distilled prior to use.

(22) Carrillo, L.; Badía, D.; Domínguez, E.; Vicario, J. L.; Tellitu, I. *J. Org. Chem.* **1997**, *62*, 6716-6721.

(23) Dess, D. B.; Martin, J. C. *J. Org. Chem.* **1983**, *48*, 4155-4156.

(24) Dixon, A. J.; McGrath, M. J.; O'Brien, P. *Org. Synth.* **2006**, *83*, 141-154.

APPENDIX 4

Synthetic Summary for (+)-Amurensinine

Scheme A4.1 Synthesis of silyl triflate **296**.

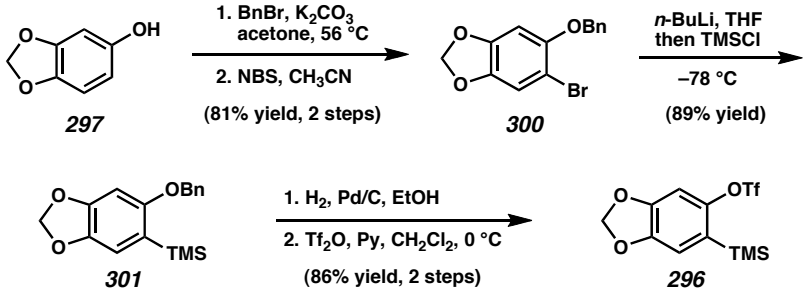

Scheme A4.2 Synthesis of β-ketoester **304**.

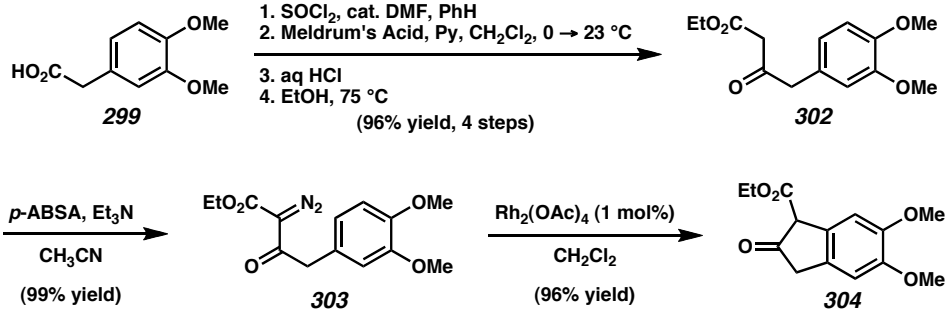

Scheme A4.3 Synthesis of (+)-amurensinine ((+)-**282**).

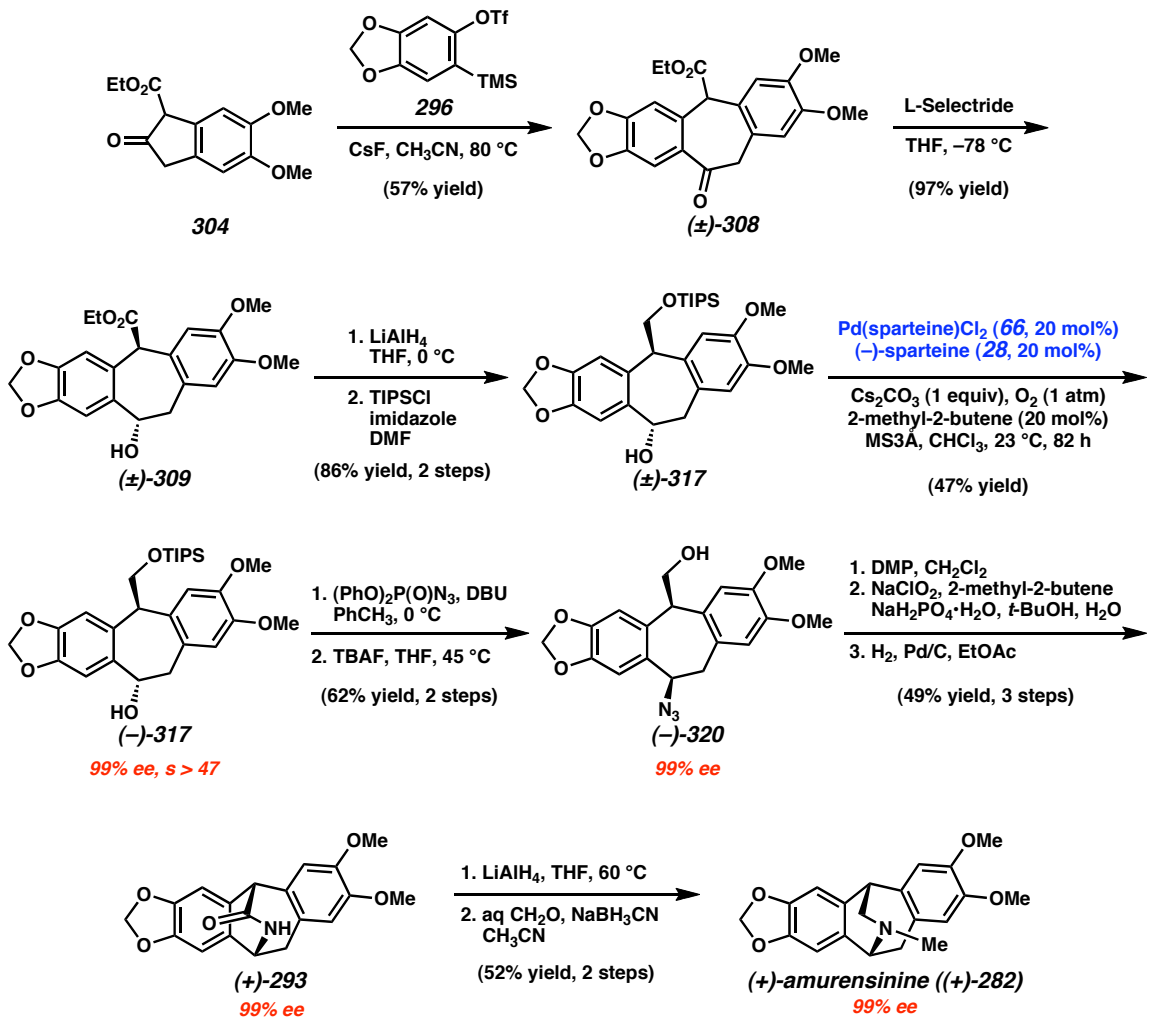

APPENDIX 5

Spectra Relevant to Chapter 5

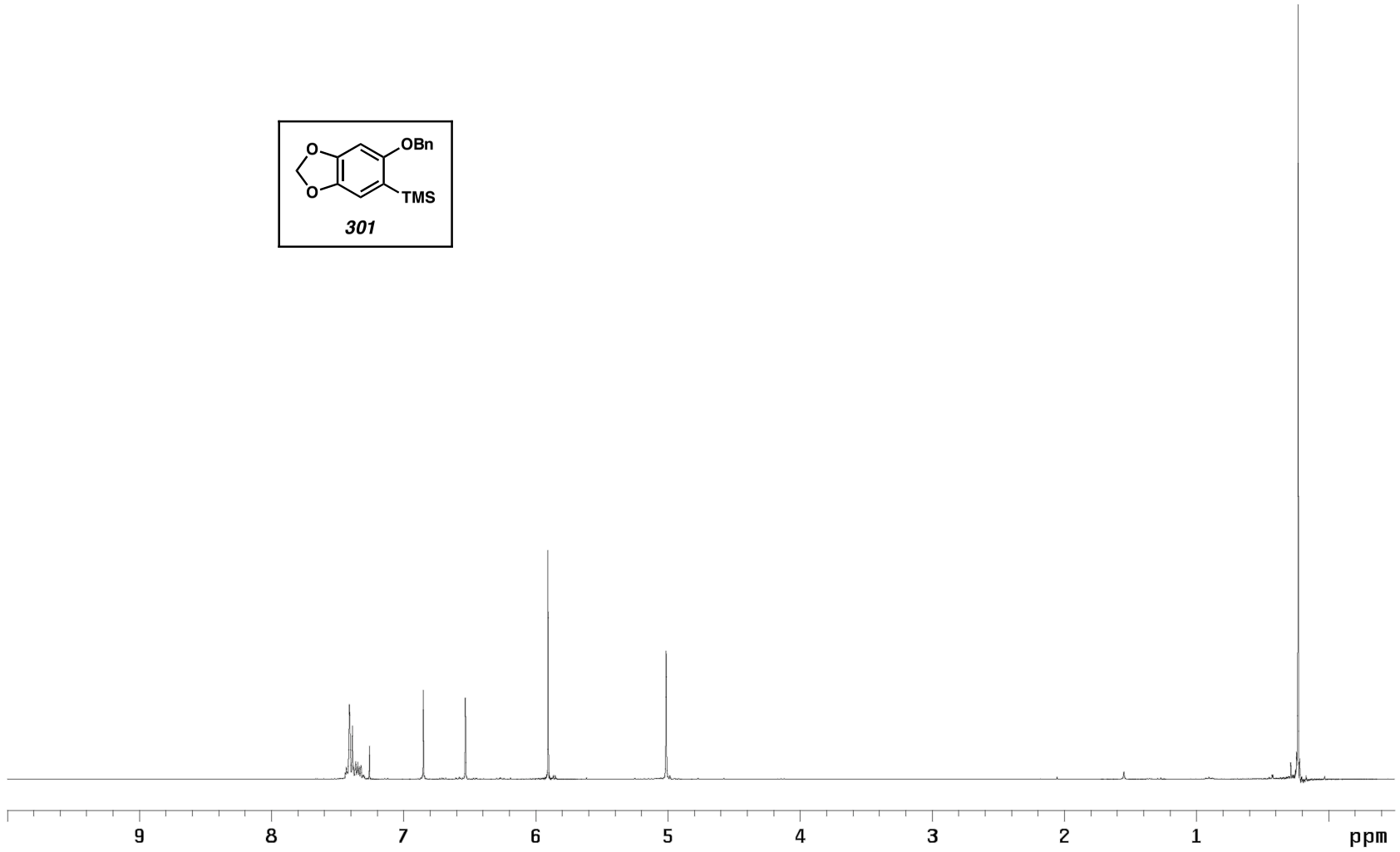

Figure A5.1 ^{1}H NMR (300 MHz, $CDCl_3$) of compound **301**.

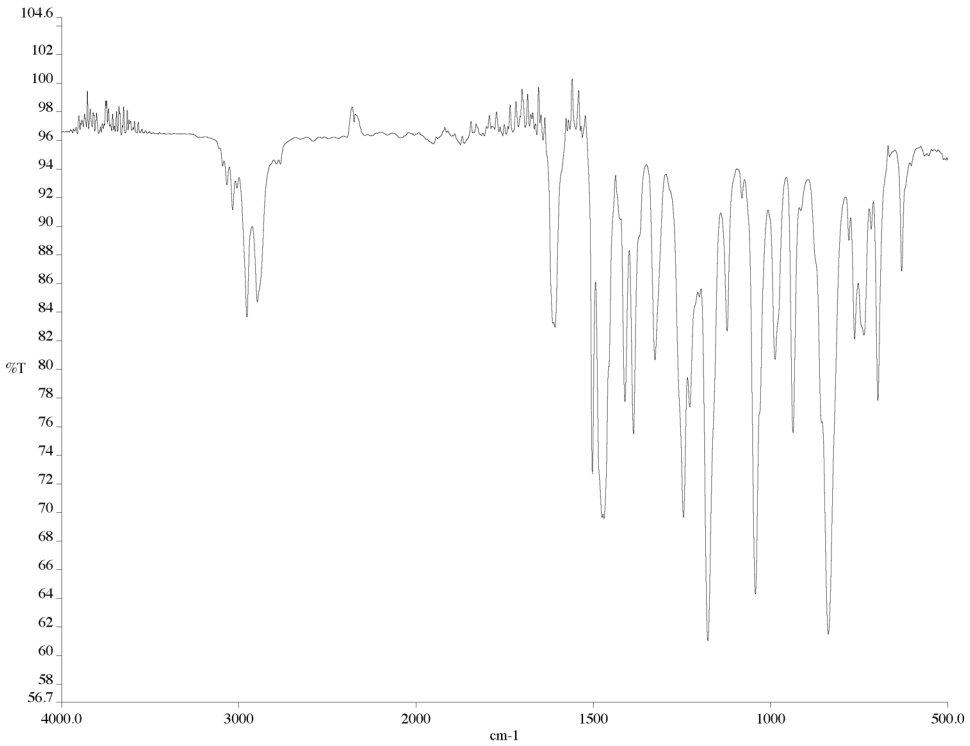

Figure A5.2 Infrared spectrum (thin film/NaCl) of compound **301**.

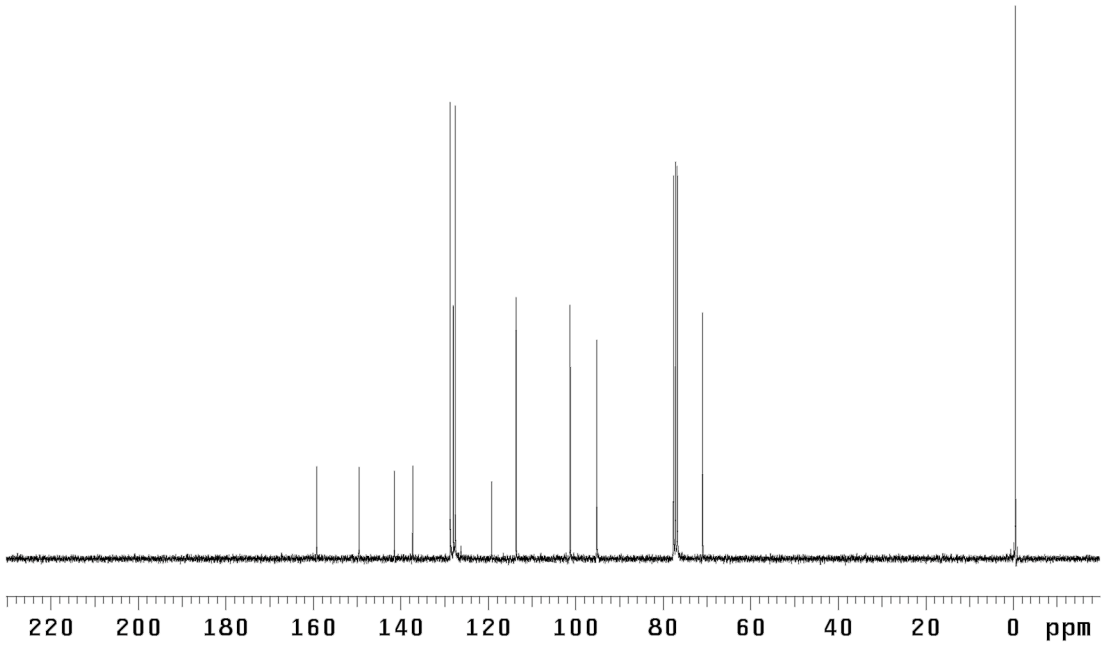

Figure A5.3 ^{13}C NMR (75 MHz, $CDCl_3$) of compound **301**.

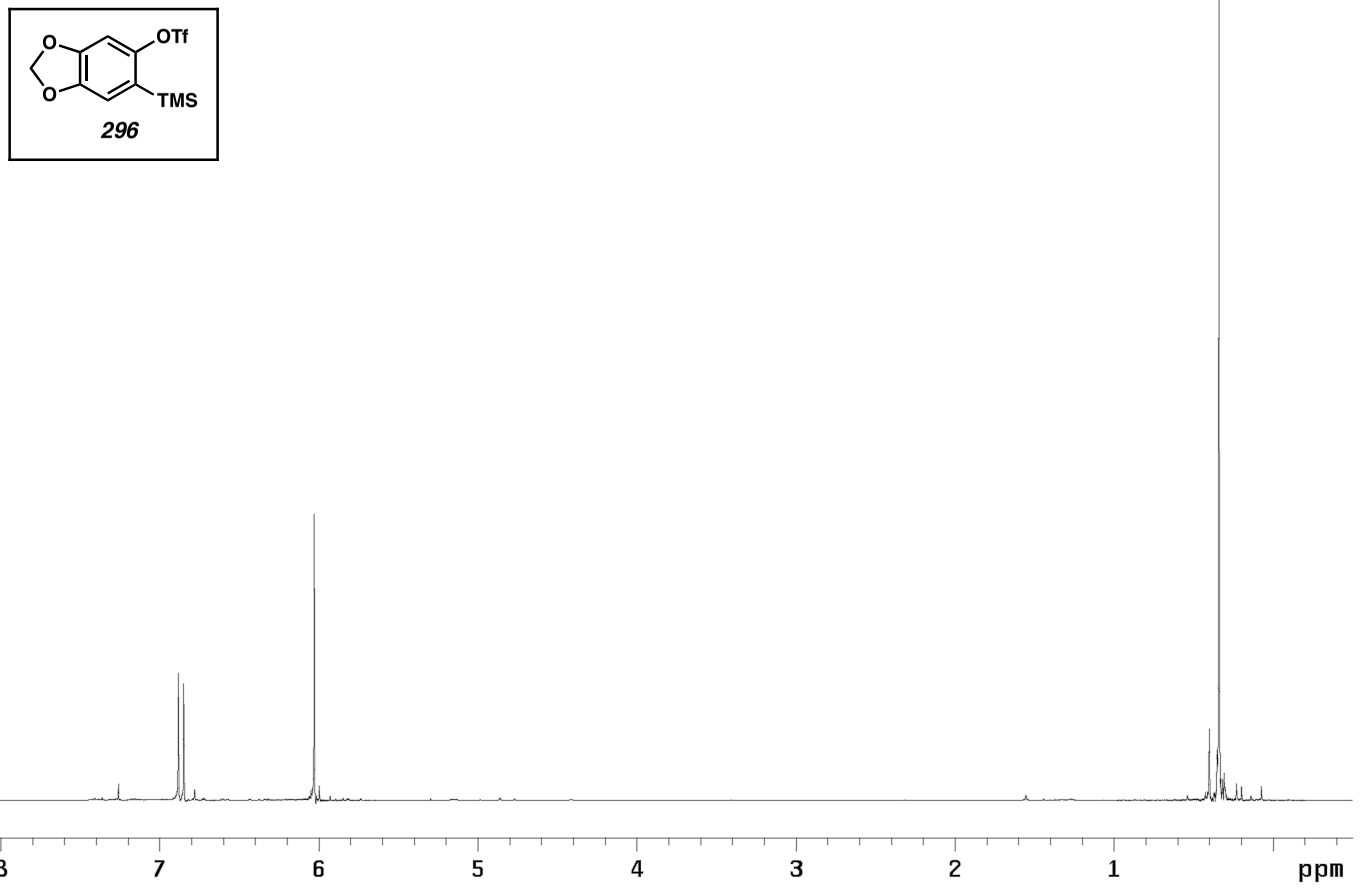

Figure A5.4 ^{1}H NMR (500 MHz, $CDCl_3$) of compound **296**.

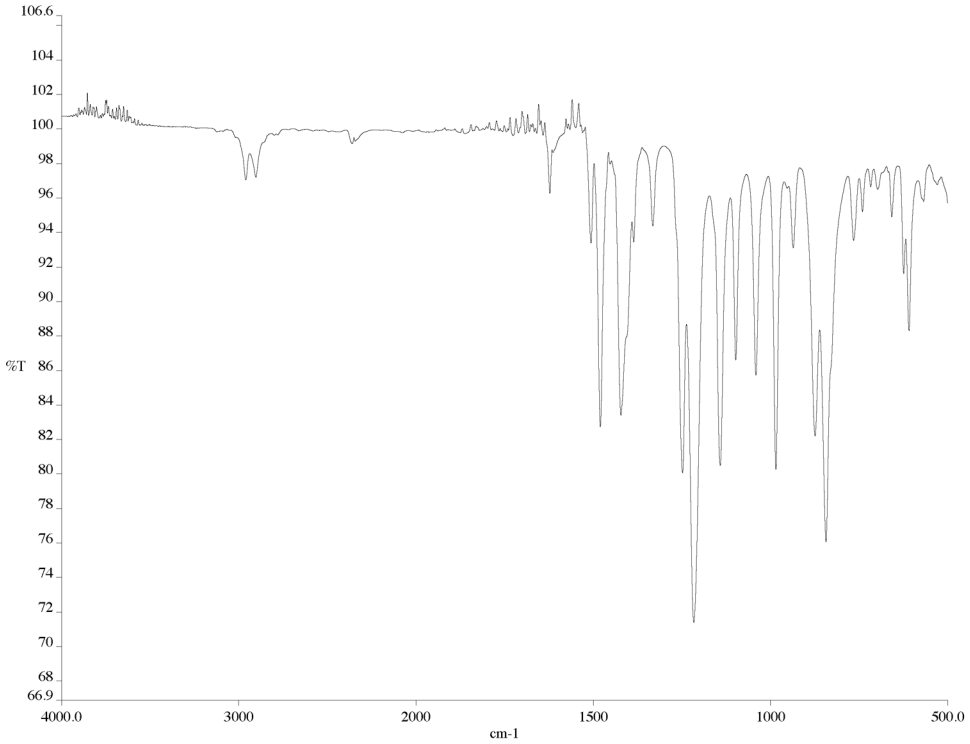

Figure A5.5 Infrared spectrum (thin film/NaCl) of compound **296**.

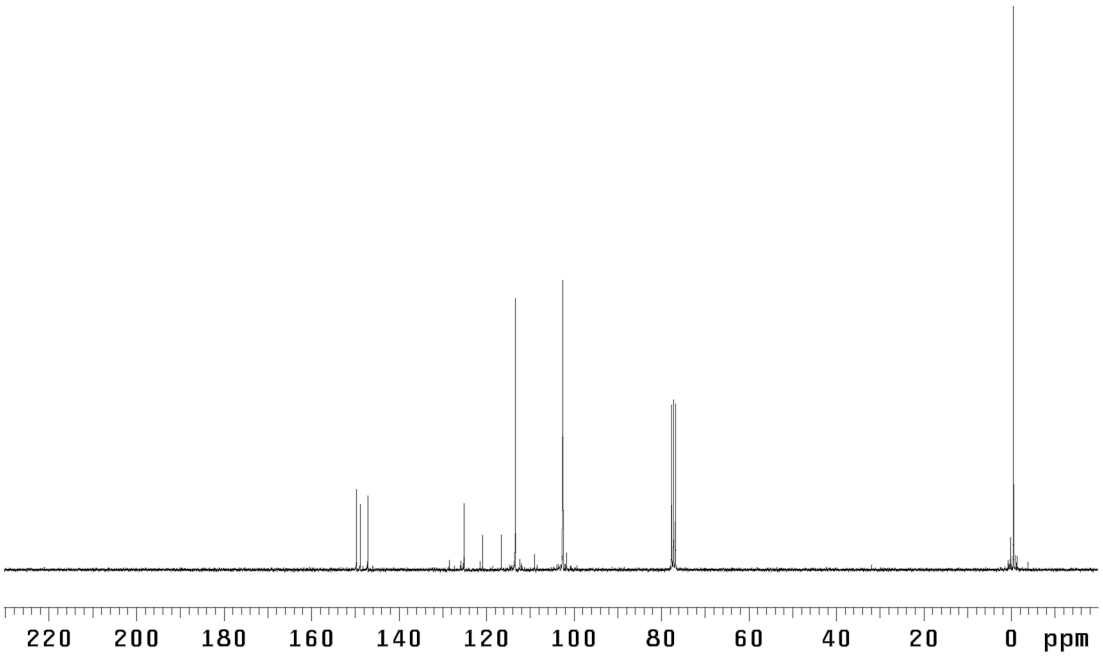

Figure A5.6 ^{13}C NMR (125 MHz, $CDCl_3$) of compound **296**.

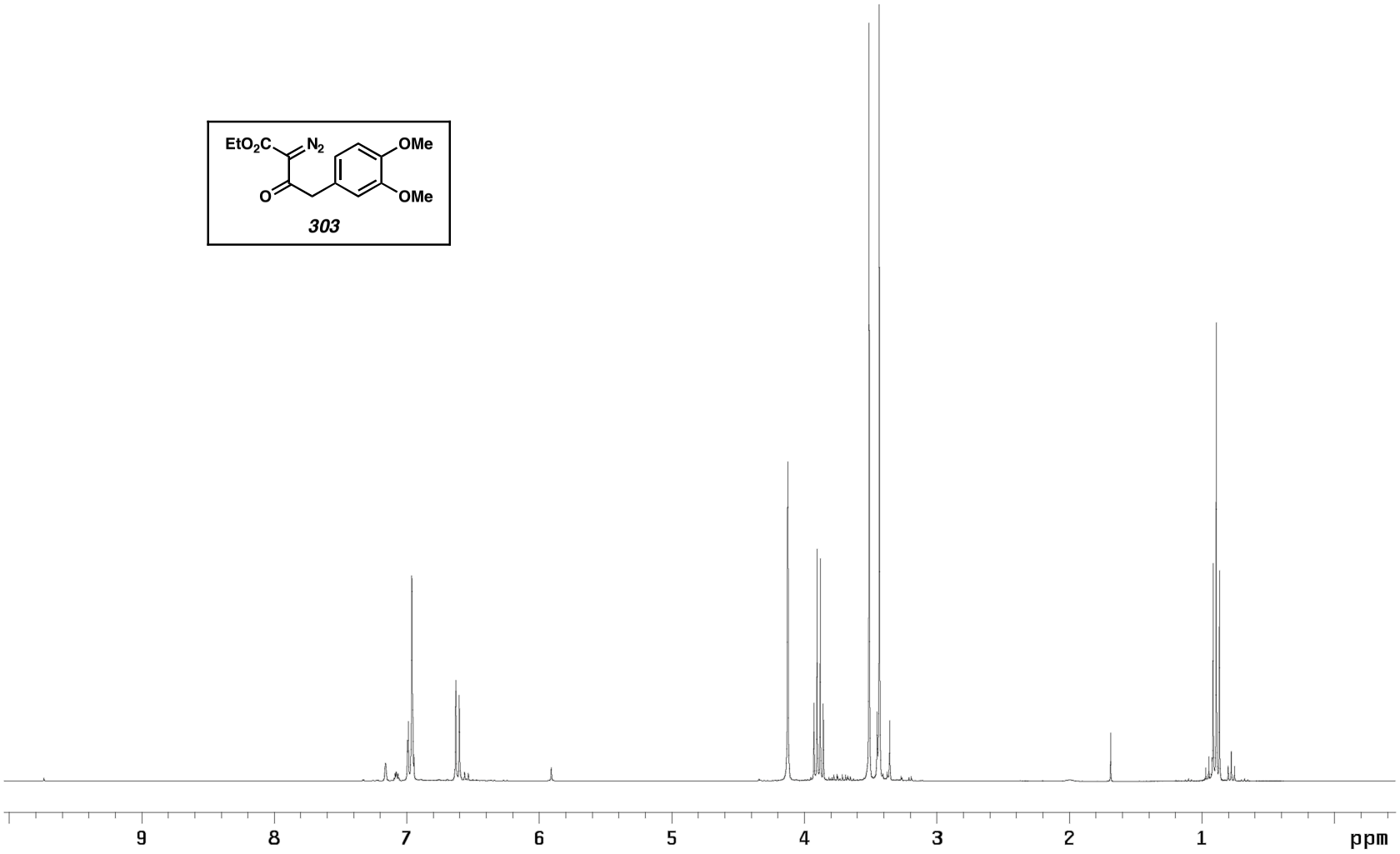

Figure A5.7 ^{1}H NMR (300 MHz, C_6D_6) of compound **303**.

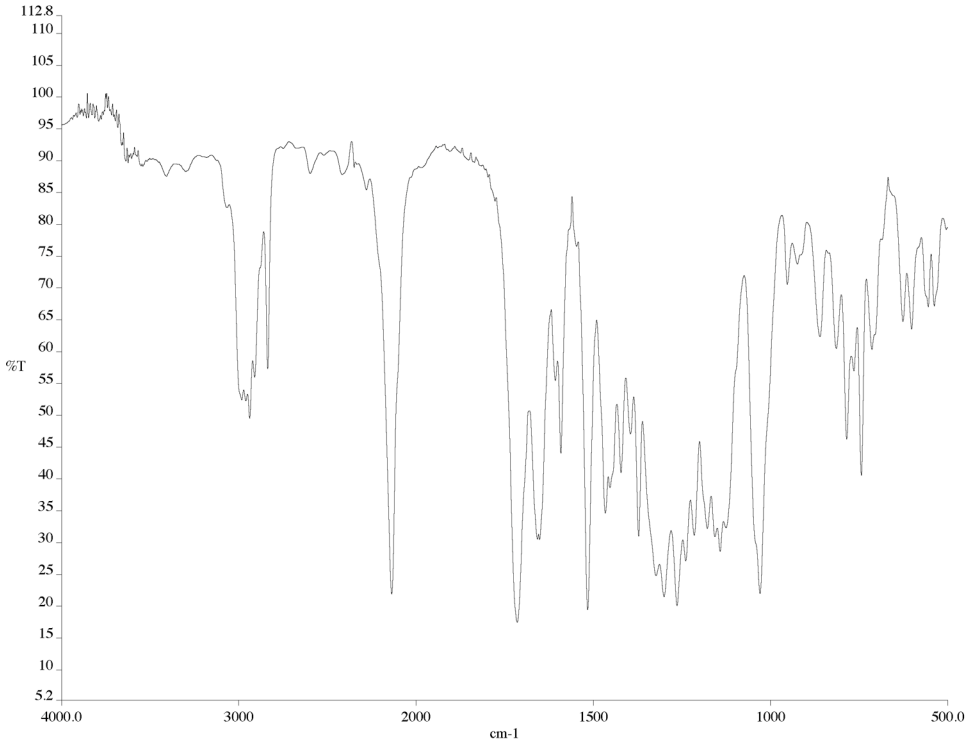

Figure A5.8 Infrared spectrum (thin film/NaCl) of compound **303**.

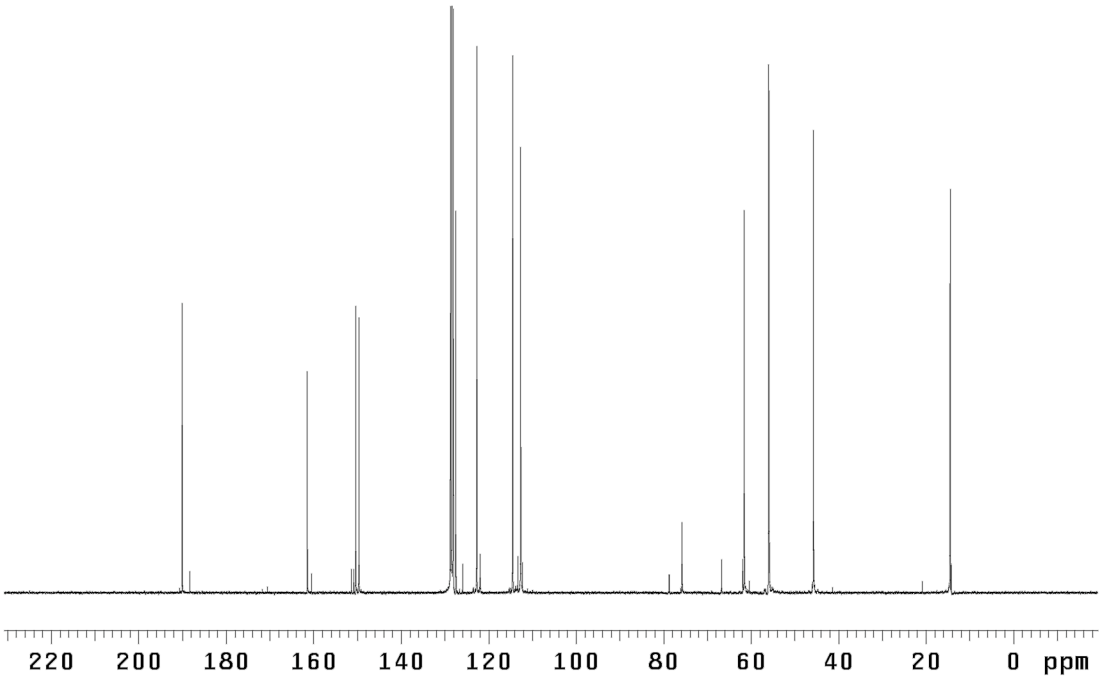

Figure A5.9 ^{13}C NMR (75 MHz, C_6D_6) of compound **303**.

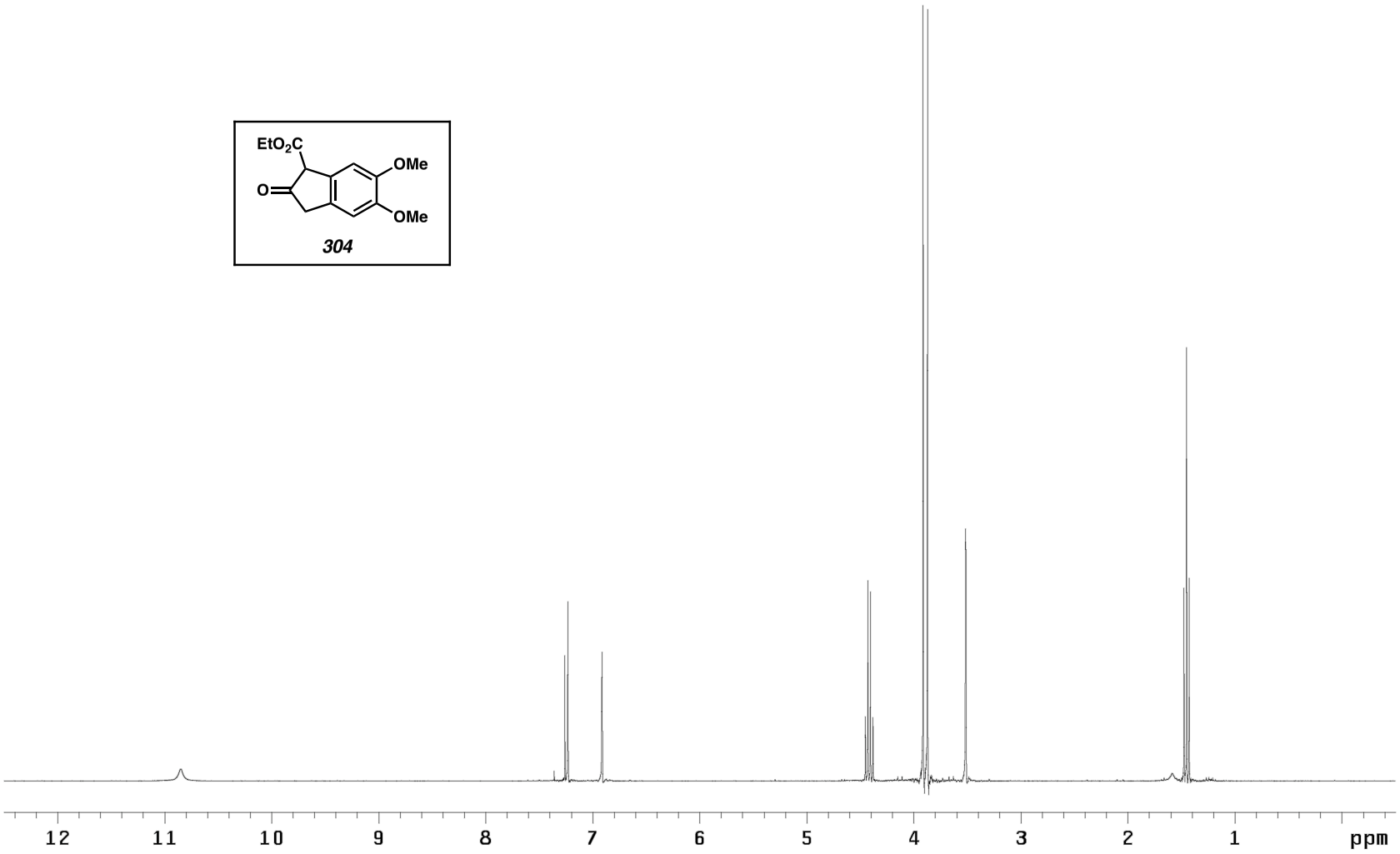

Figure A5.10 ^{1}H NMR (300 MHz, $CDCl_3$) of compound **304**.

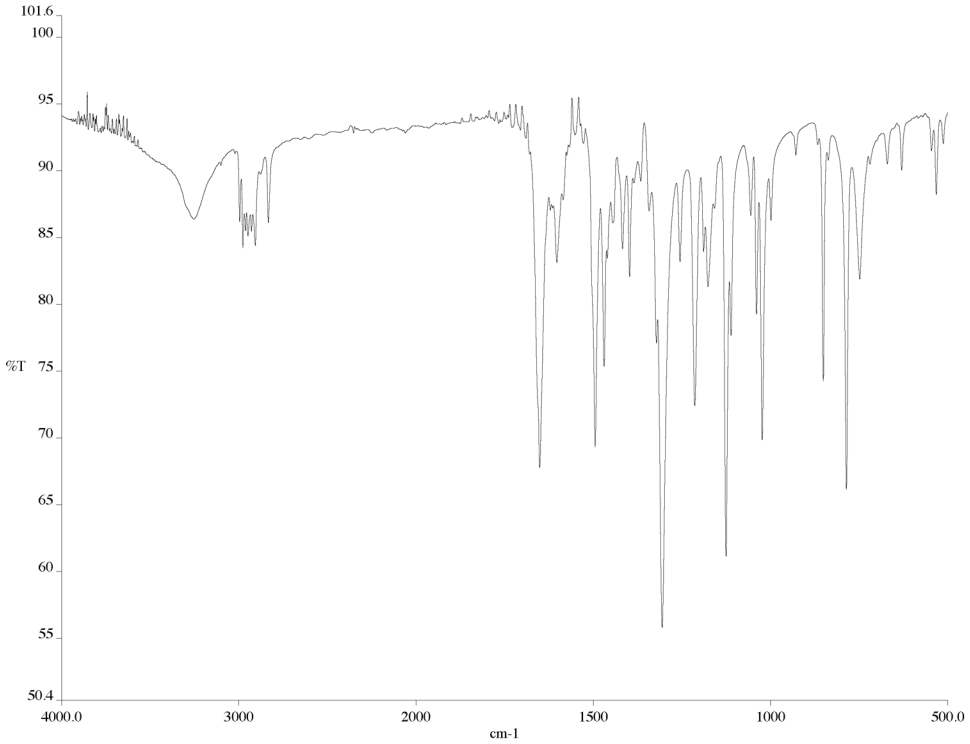

Figure A5.11 Infrared spectrum (thin film/NaCl) of compound **304**.

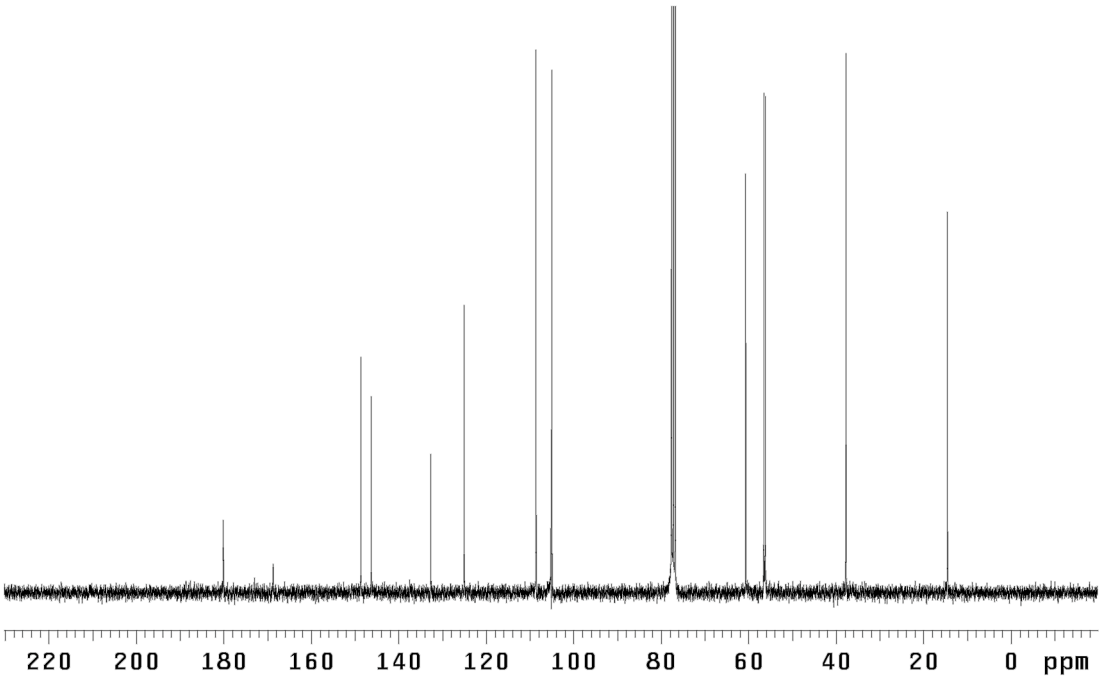

Figure A5.12 ^{13}C NMR (75 MHz, $CDCl_3$) of compound **304**.

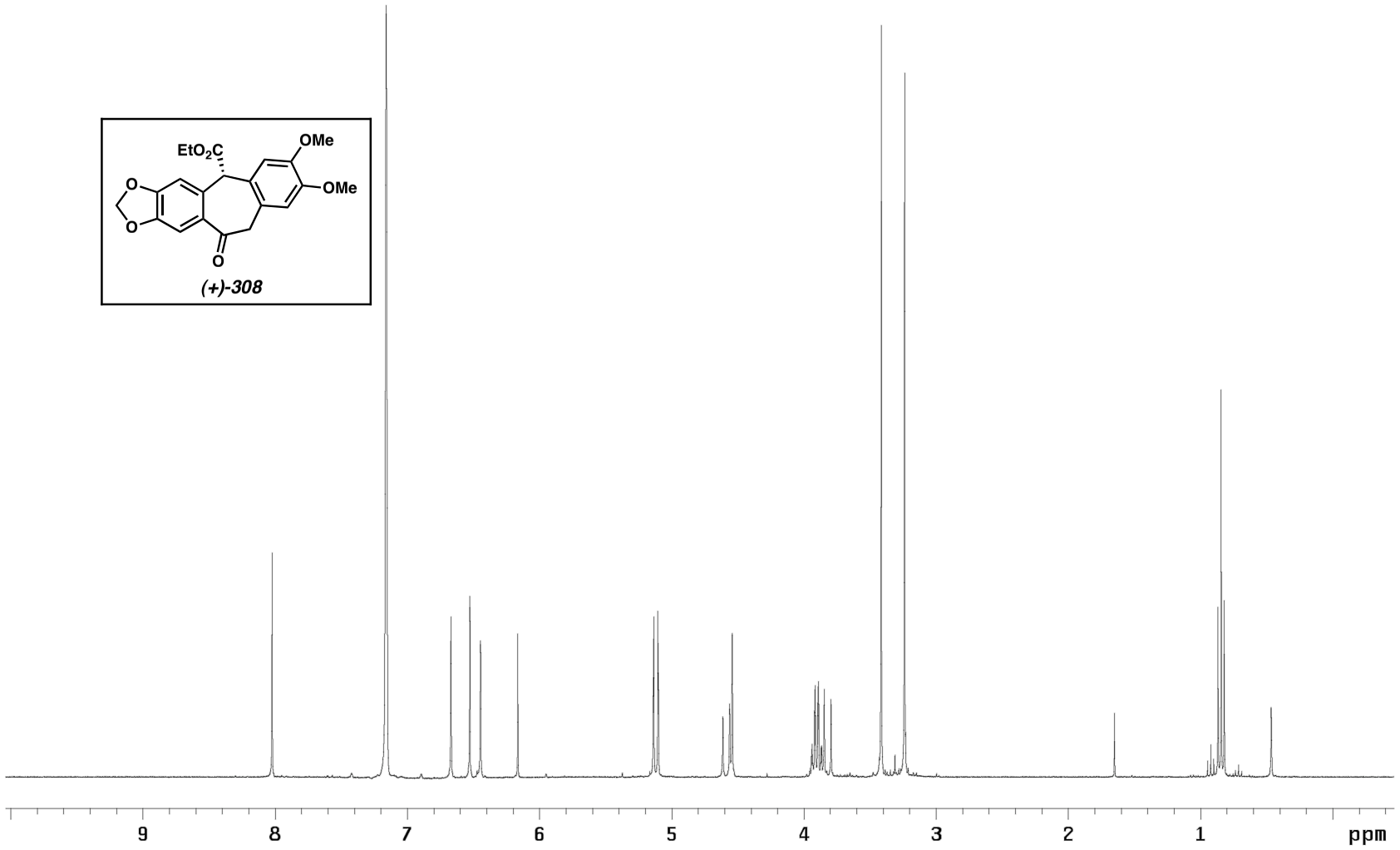

Figure A5.13 ^{1}H NMR (300 MHz, C_6D_6) of compound (+)-**308**.

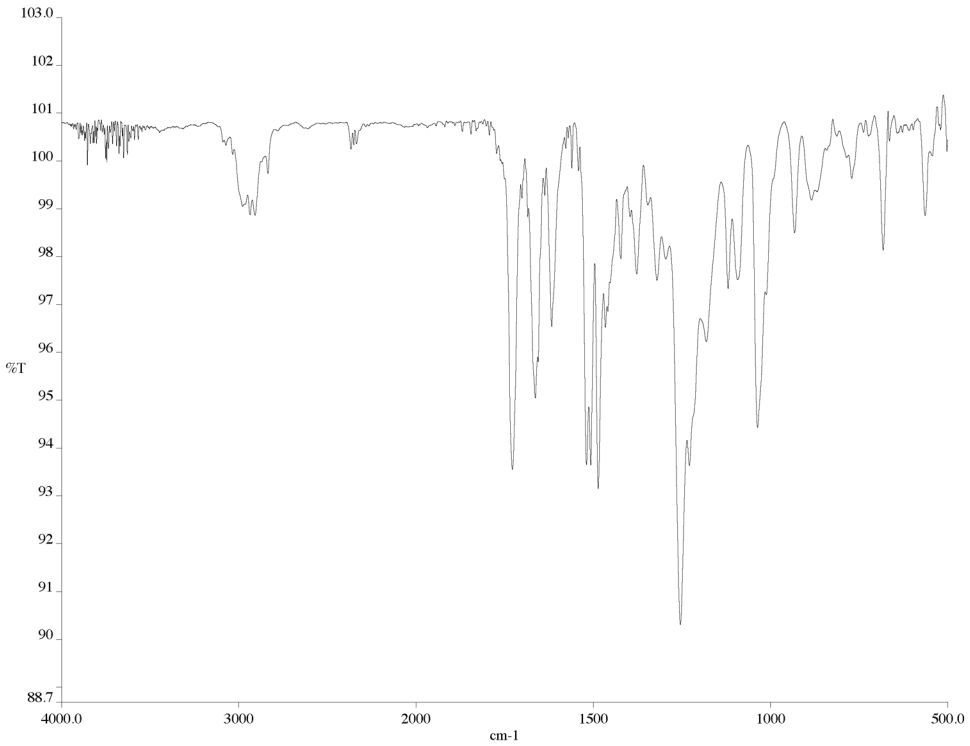

Figure A5.14 Infrared spectrum (thin film/NaCl) of compound (+)-**308**.

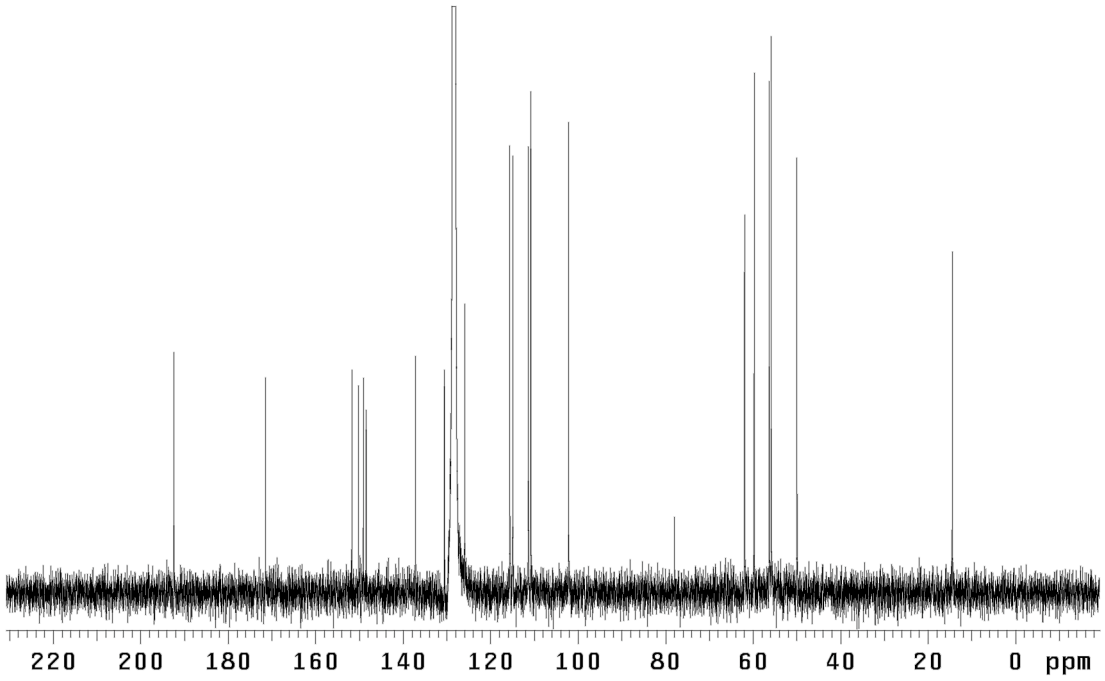

Figure A5.15 ^{13}C NMR (75 MHz, C_6D_6) of compound (+)-**308**.

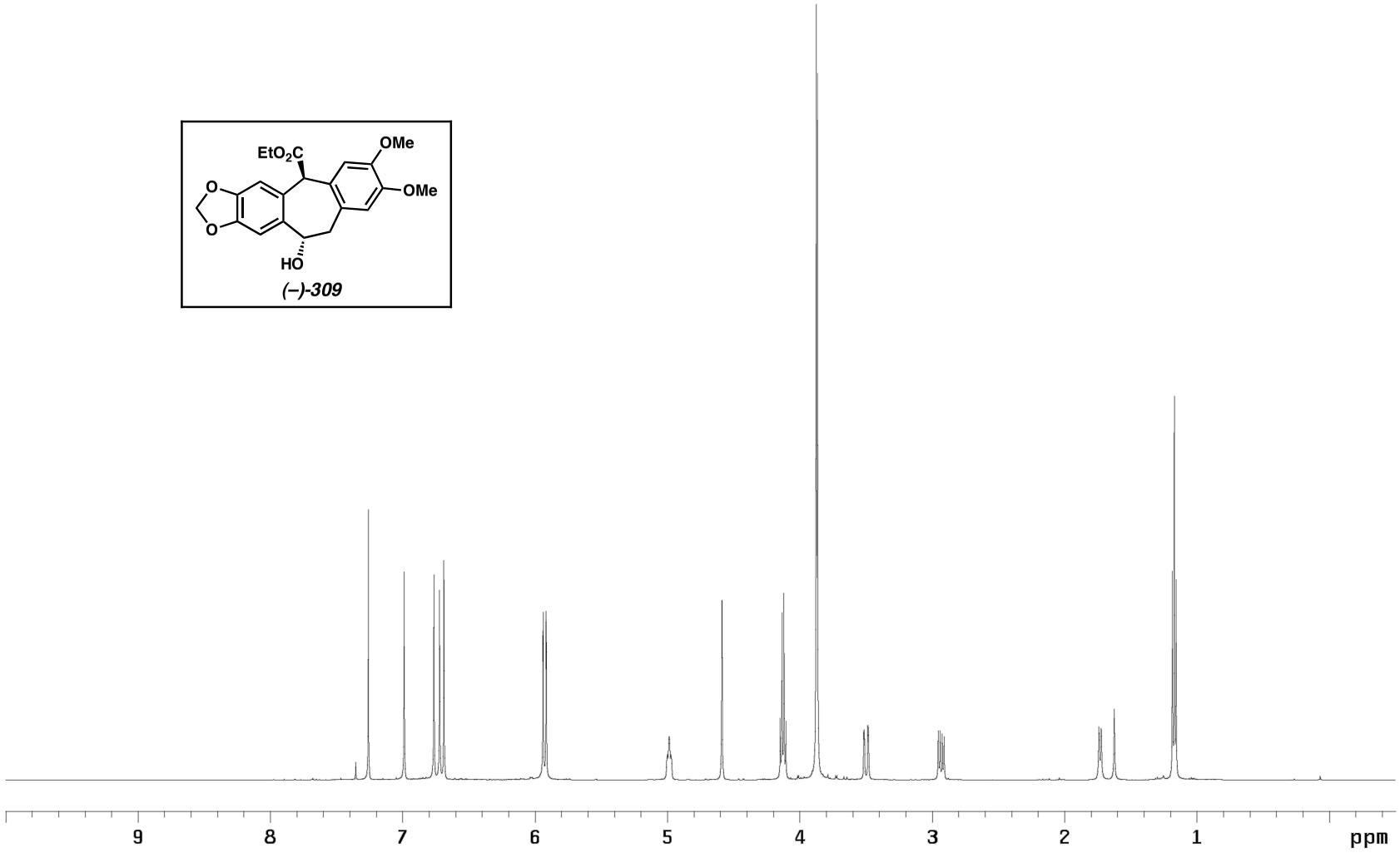

Figure A5.16 ^{1}H NMR (500 MHz, $CDCl_3$) of compound (–)-**309**.

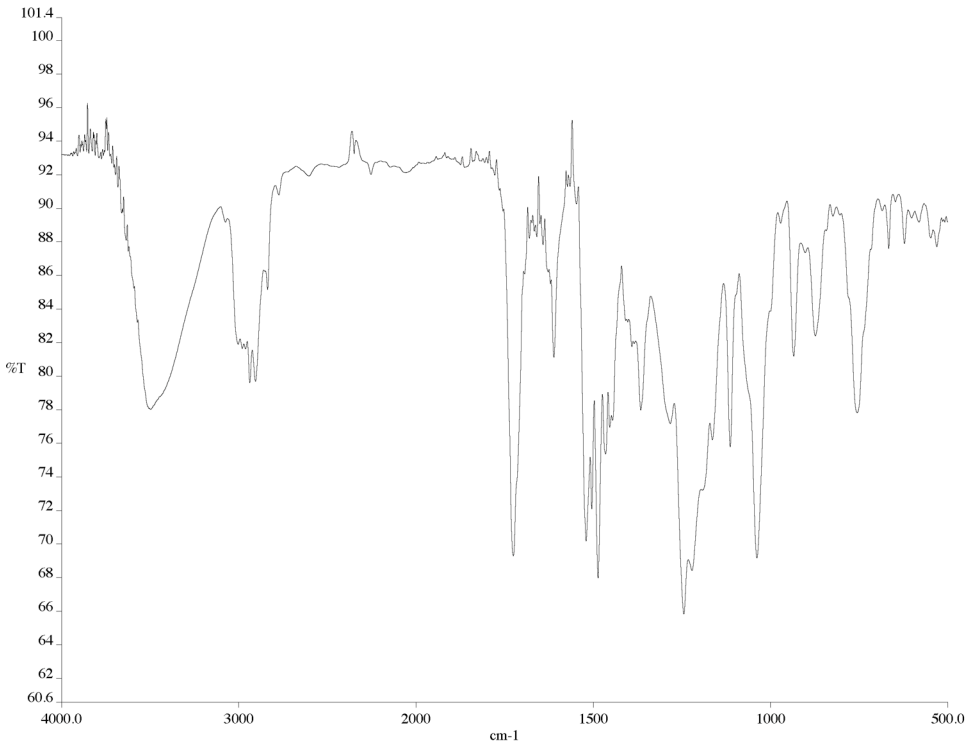

Figure A5.17 Infrared spectrum (thin film/NaCl) of compound (–)-**309**.

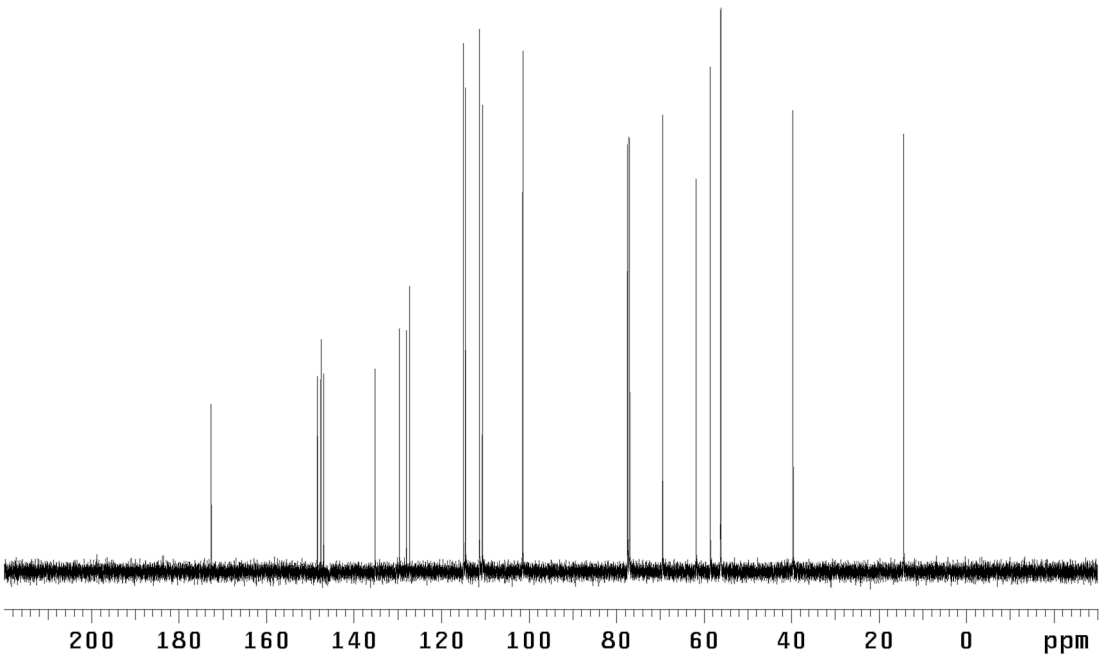

Figure A5.18 ^{13}C NMR (125 MHz, $CDCl_3$) of compound (–)-**309**.

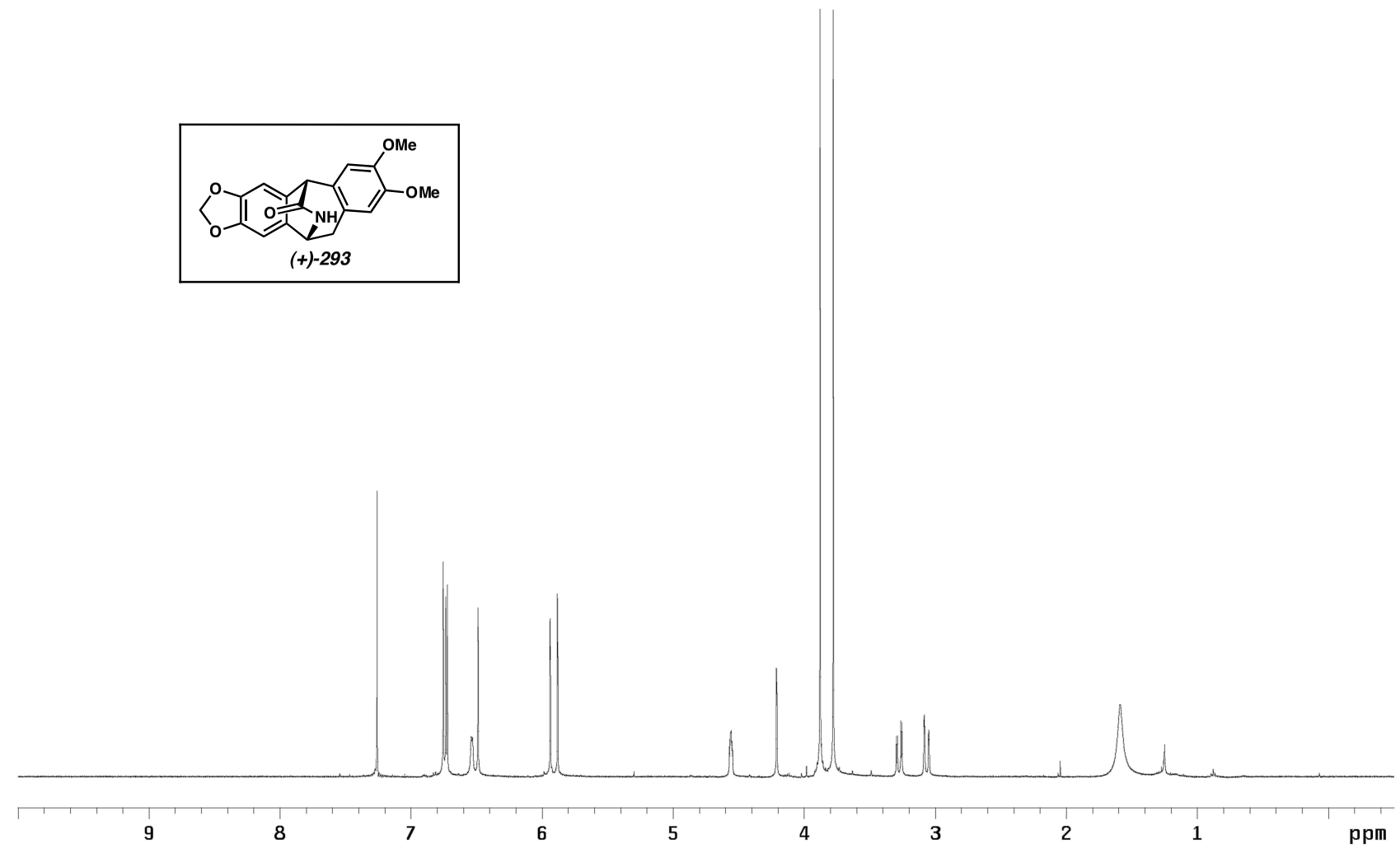

Figure A5.19 ^{1}H NMR (500 MHz, $CDCl_3$) of compound (+)-**293**.

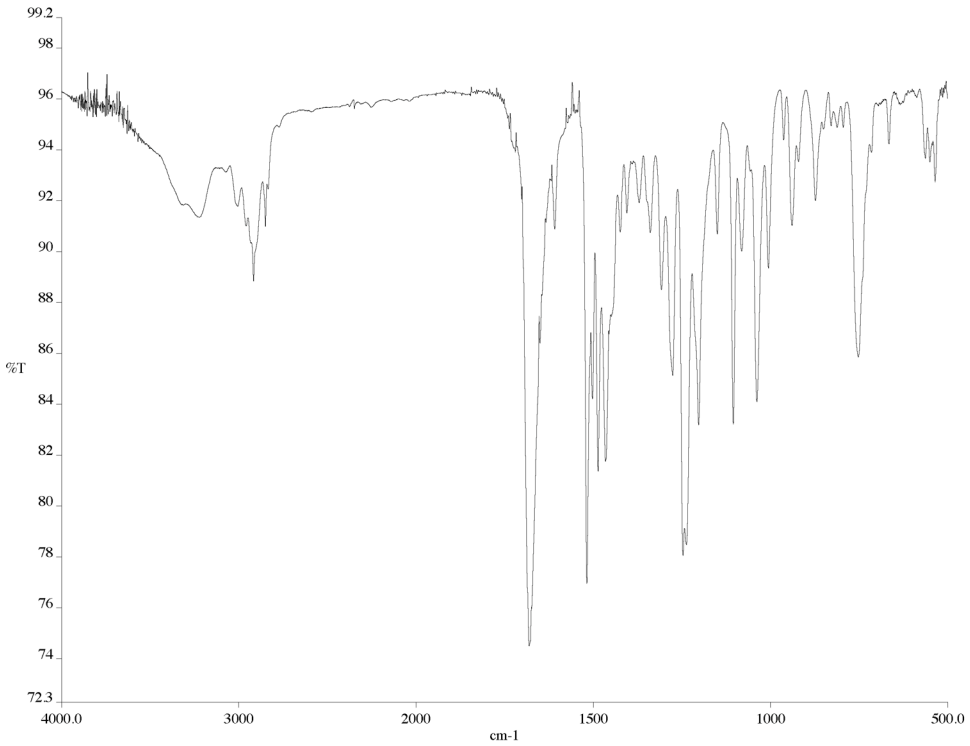

Figure A5.20 Infrared spectrum (thin film/NaCl) of compound (+)-**293**.

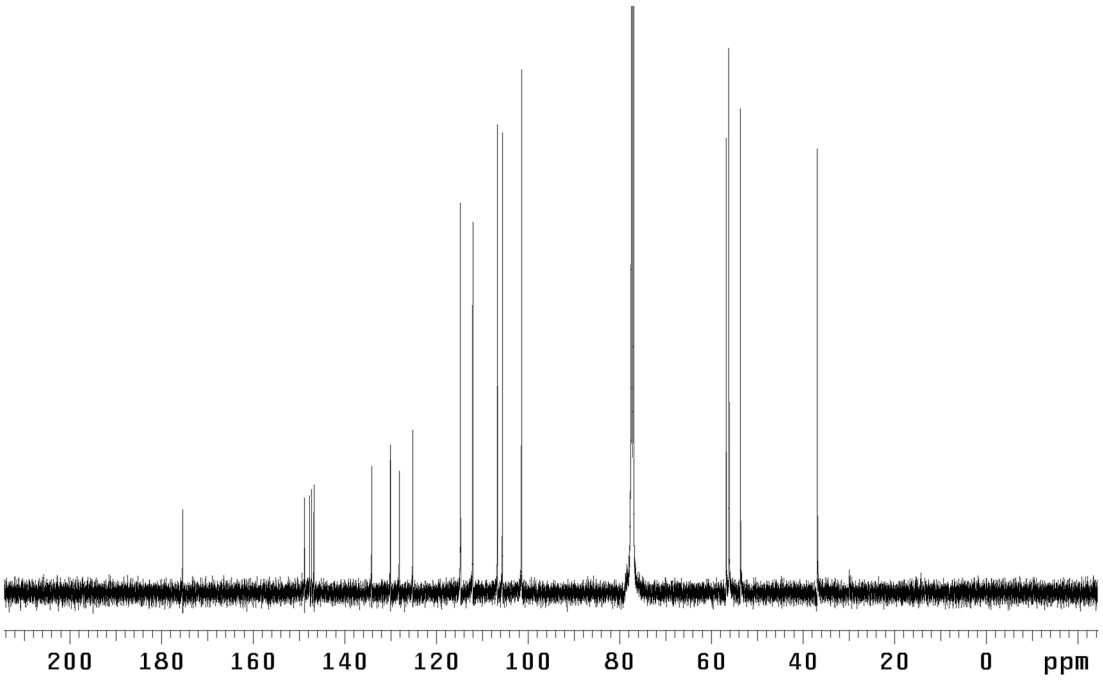

Figure A5.21 ^{13}C NMR (125 MHz, $CDCl_3$) of compound (+)-**293**.

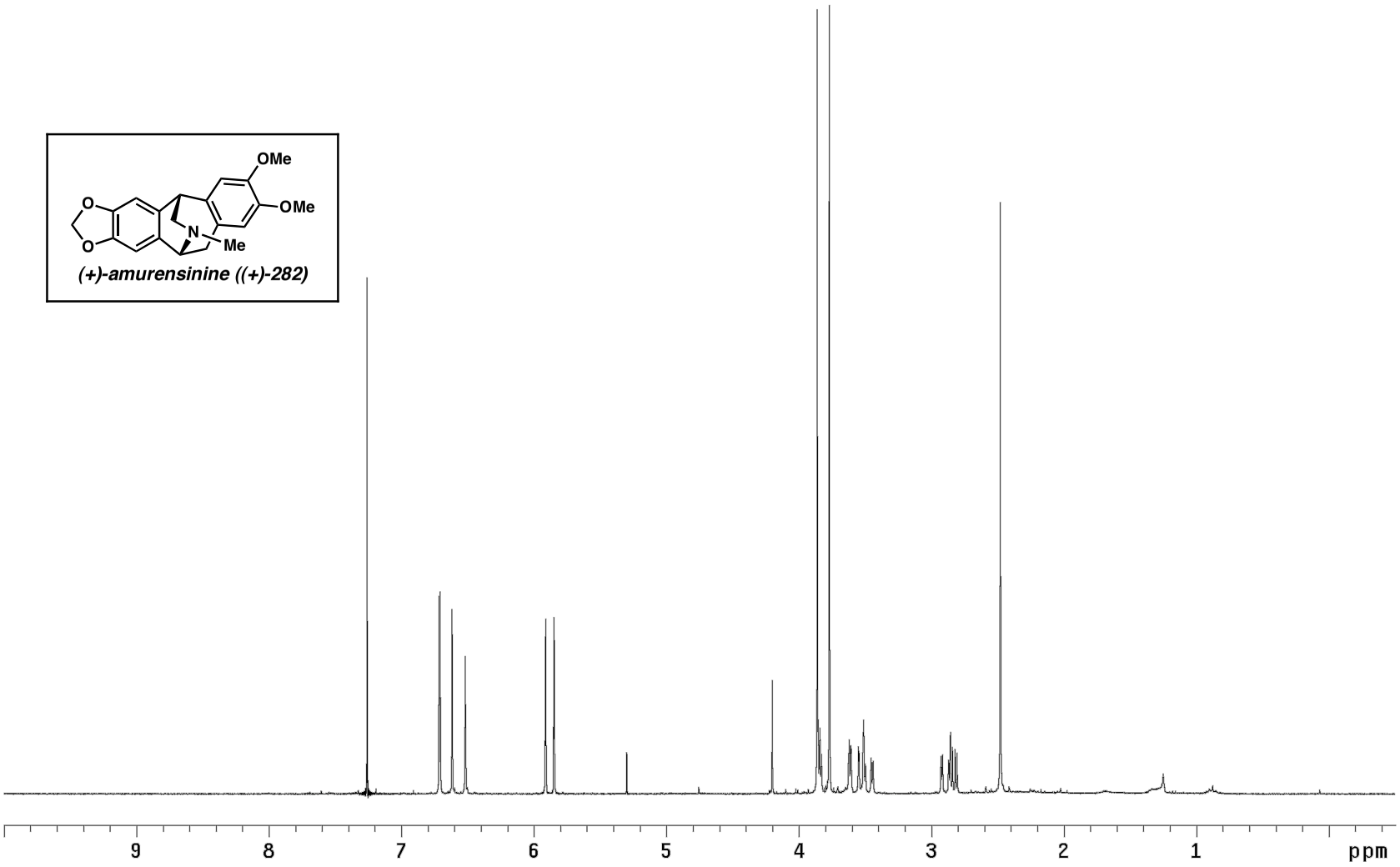

Figure A5.22 ^{1}H NMR (300 MHz, $CDCl_3$) of compound (+)-**282**.

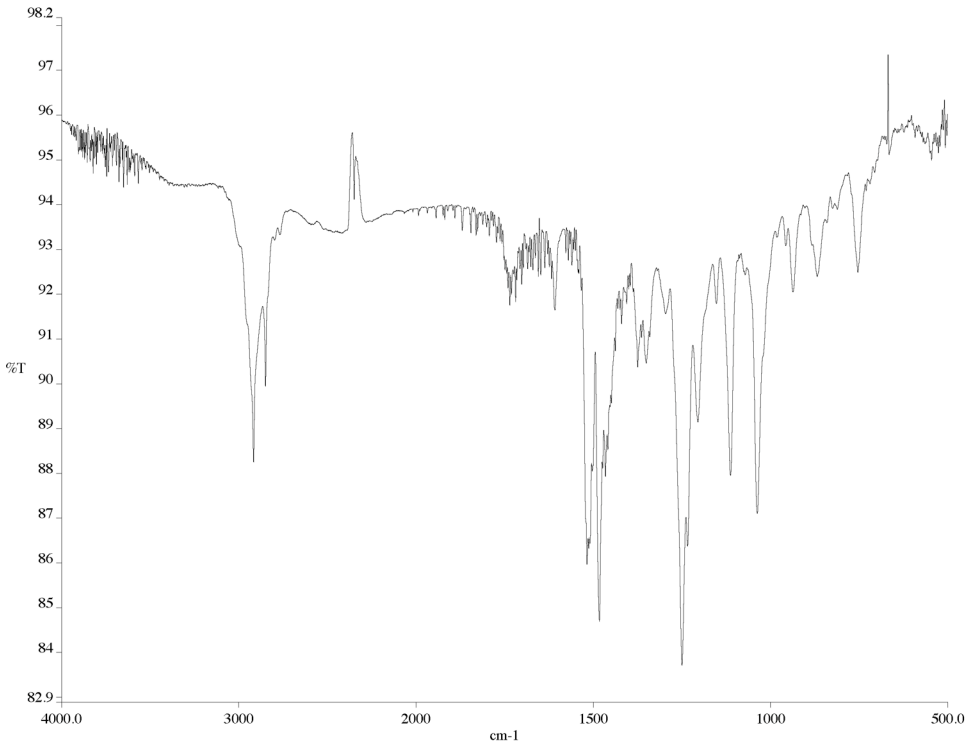

Figure A5.23 Infrared spectrum (thin film/NaCl) of compound (+)-**282**.

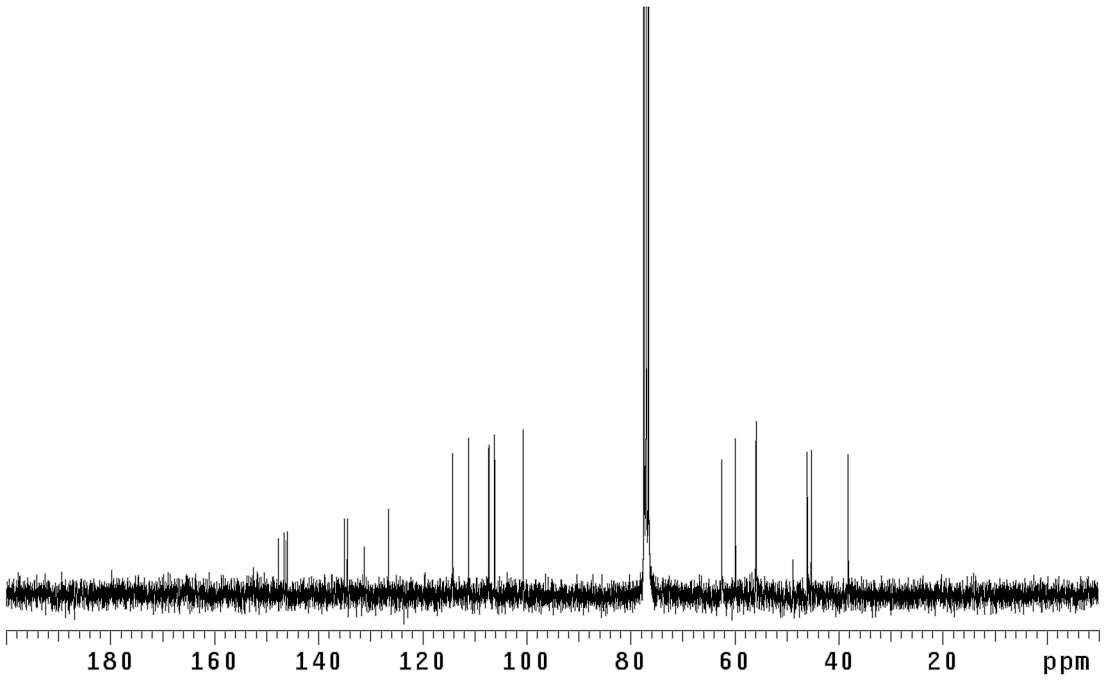

Figure A5.24 ^{13}C NMR (75 MHz, $CDCl_3$) of compound (+)-**282**.

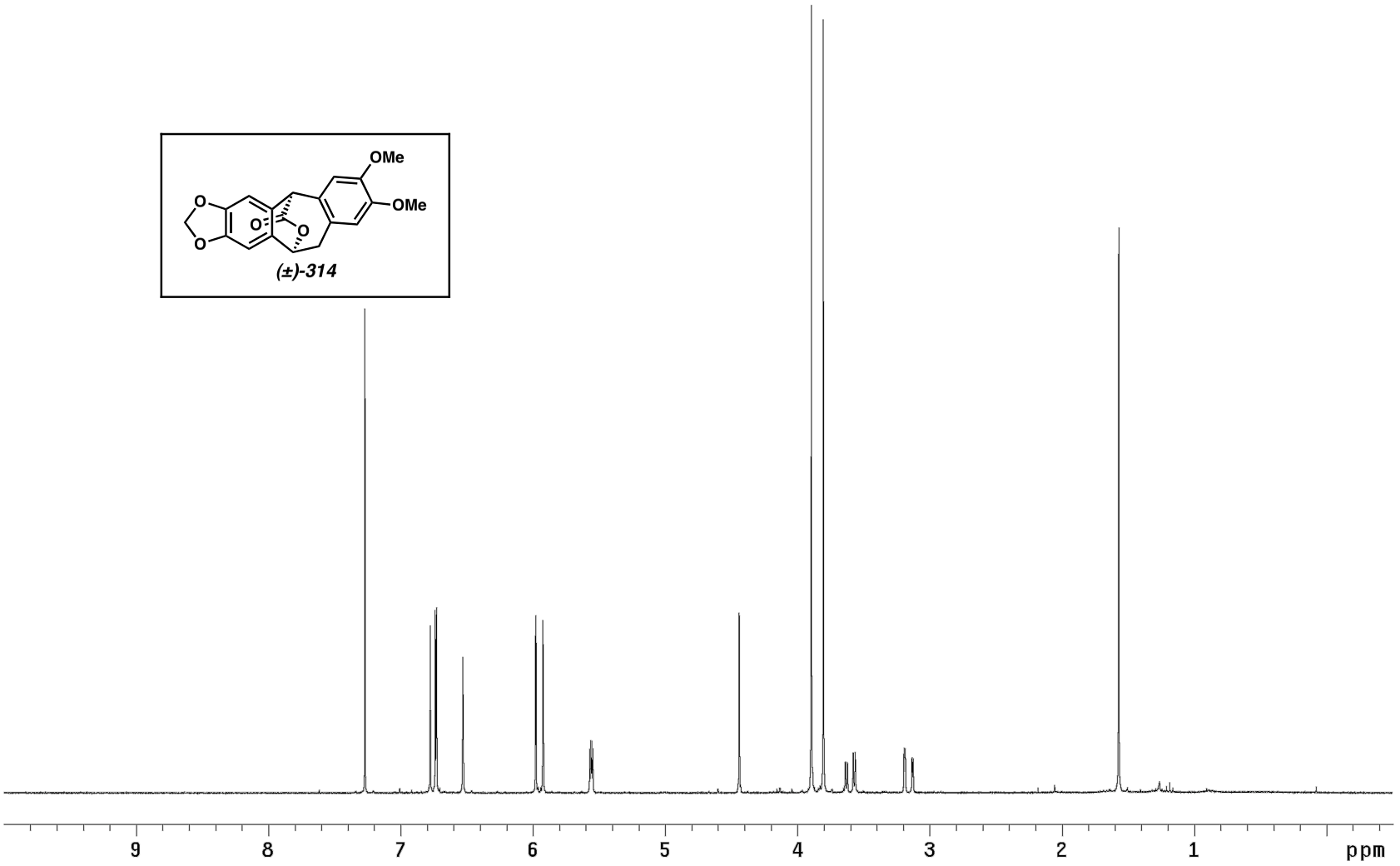

Figure A5.25 ^{1}H NMR (300 MHz, $CDCl_3$) of compound (±)-**314**.

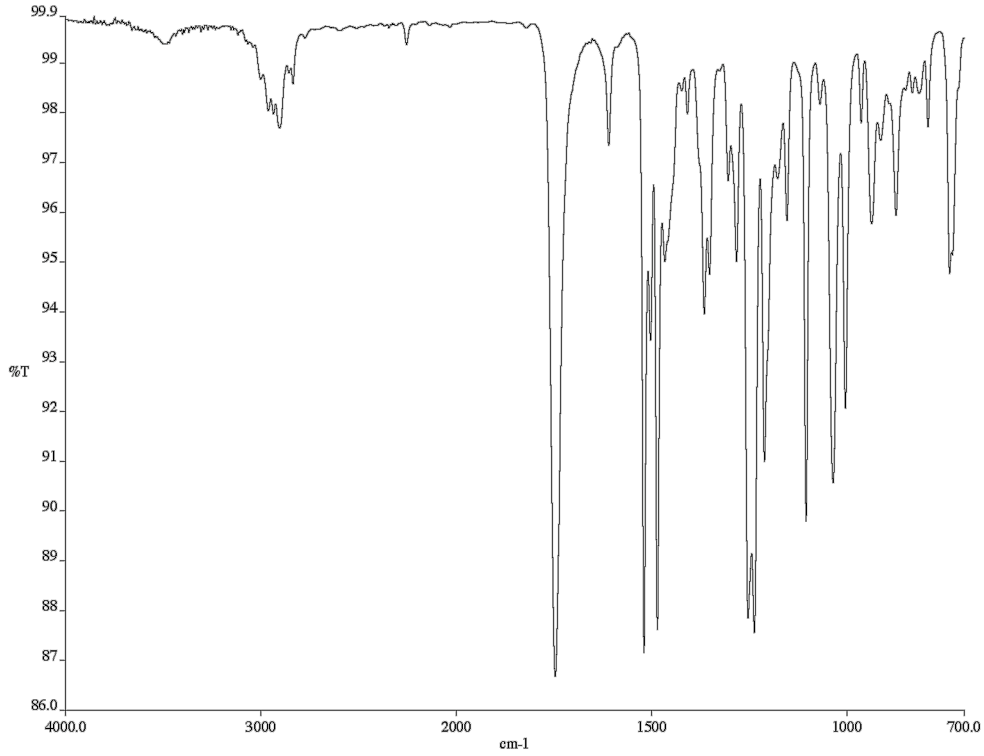

Figure A5.26 Infrared spectrum (thin film/NaCl) of compound (±)-**314**.

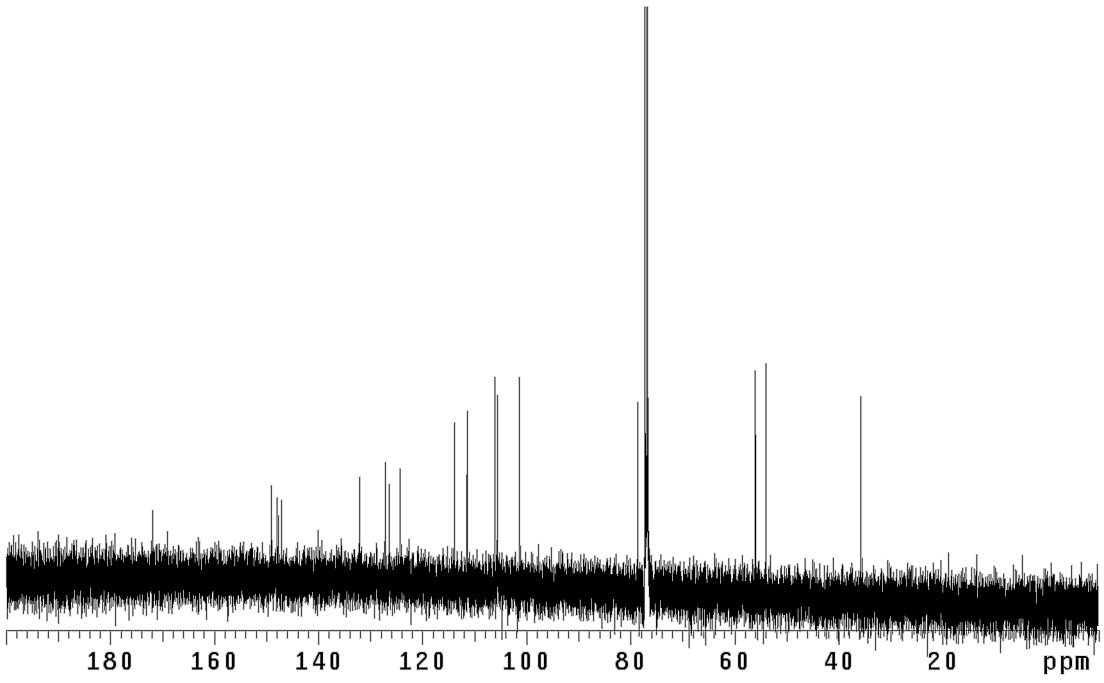

Figure A5.27 ^{13}C NMR (126 MHz, $CDCl_3$) of compound (±)-**314**.

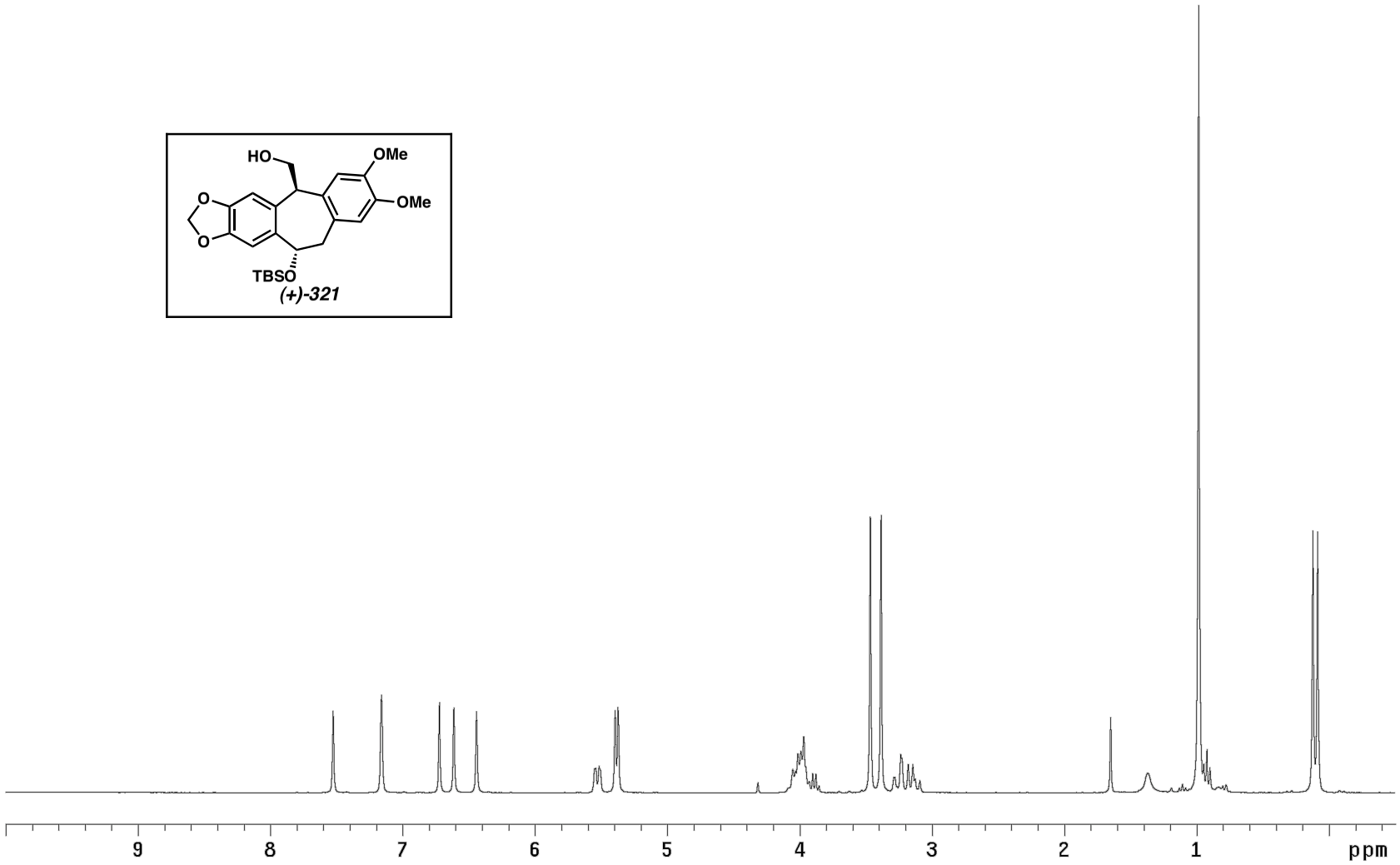

Figure A5.28 ^{1}H NMR (300 MHz, C_6D_6) of compound (+)-**321**.

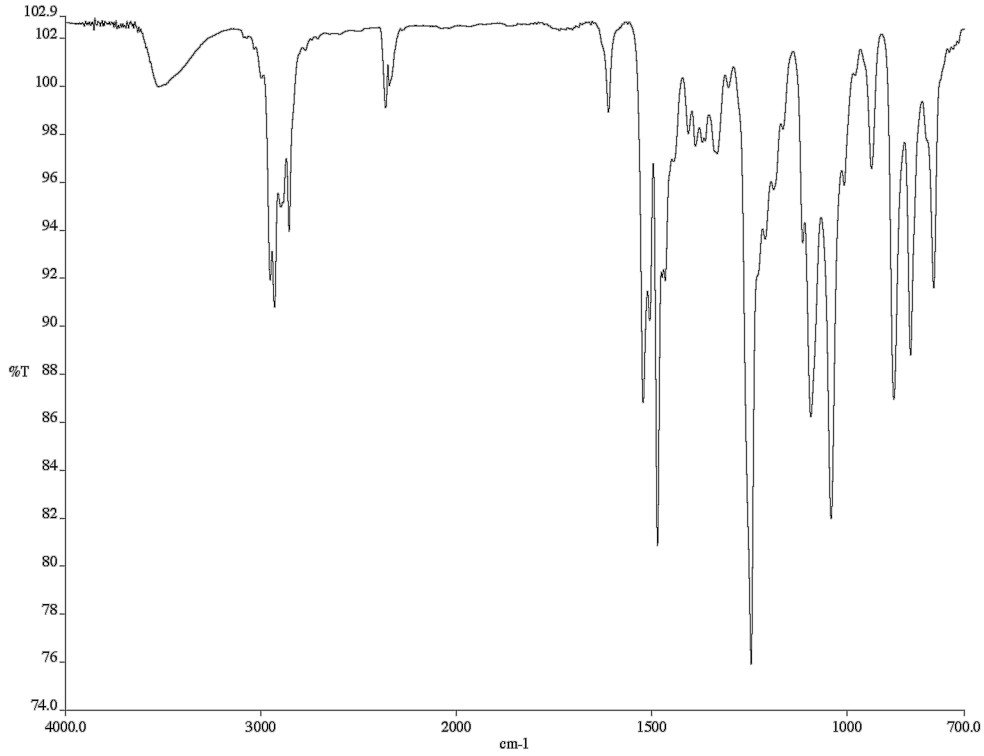

Figure A5.29 Infrared spectrum (thin film/NaCl) of compound (+)-**321**.

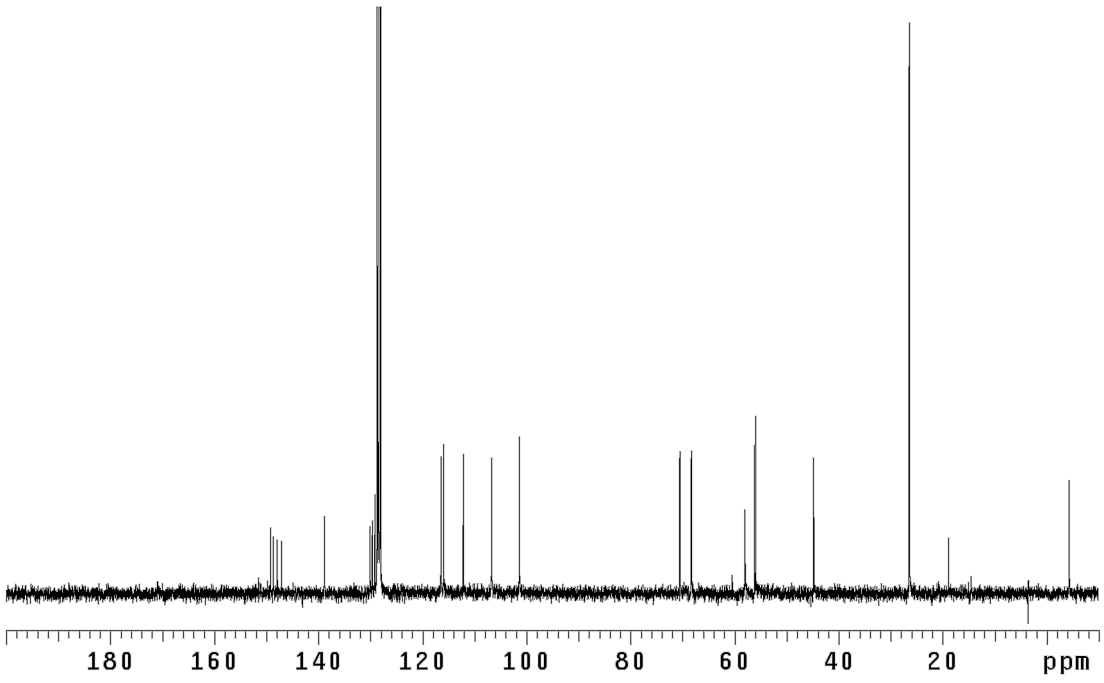

Figure A5.30 ^{13}C NMR (75 MHz, C_6D_6) of compound (+)-**321**.

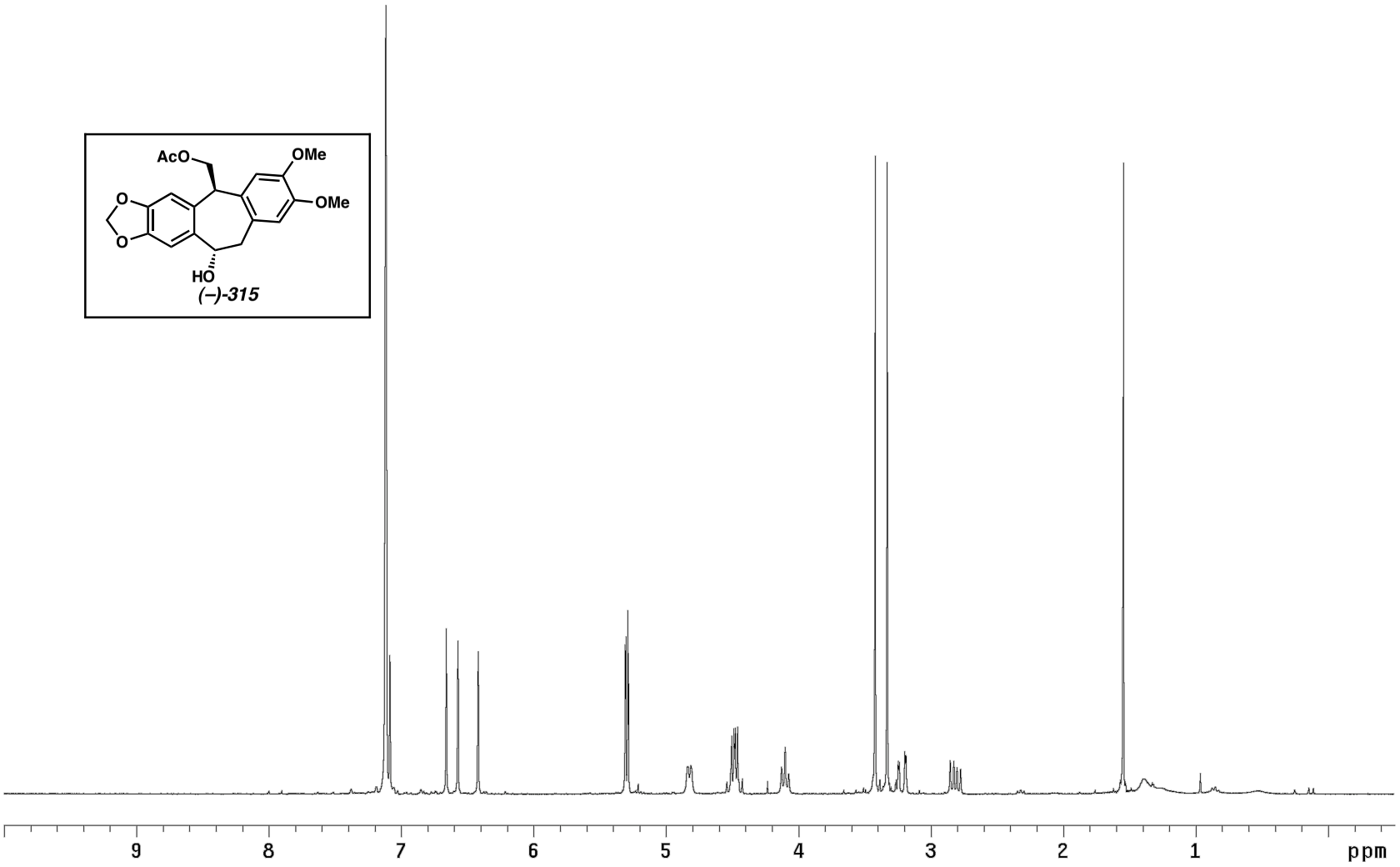

Figure A5.31 ^{1}H NMR (300 MHz, C_6D_6) of compound (–)-**315**.

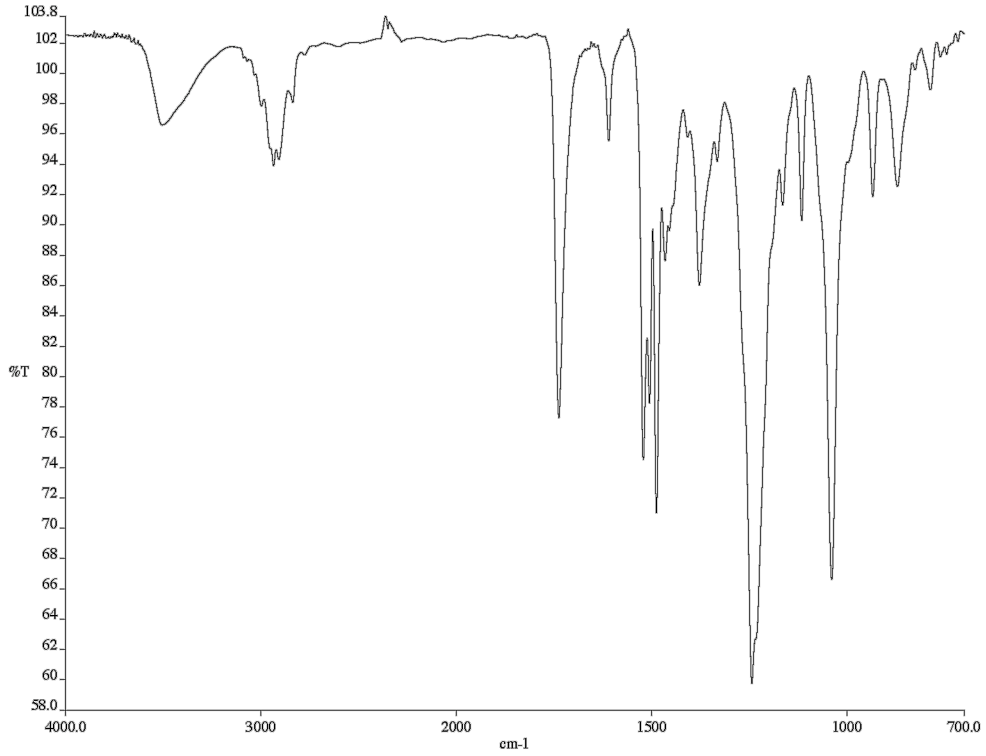

Figure A5.32 Infrared spectrum (thin film/NaCl) of compound (–)-**315**.

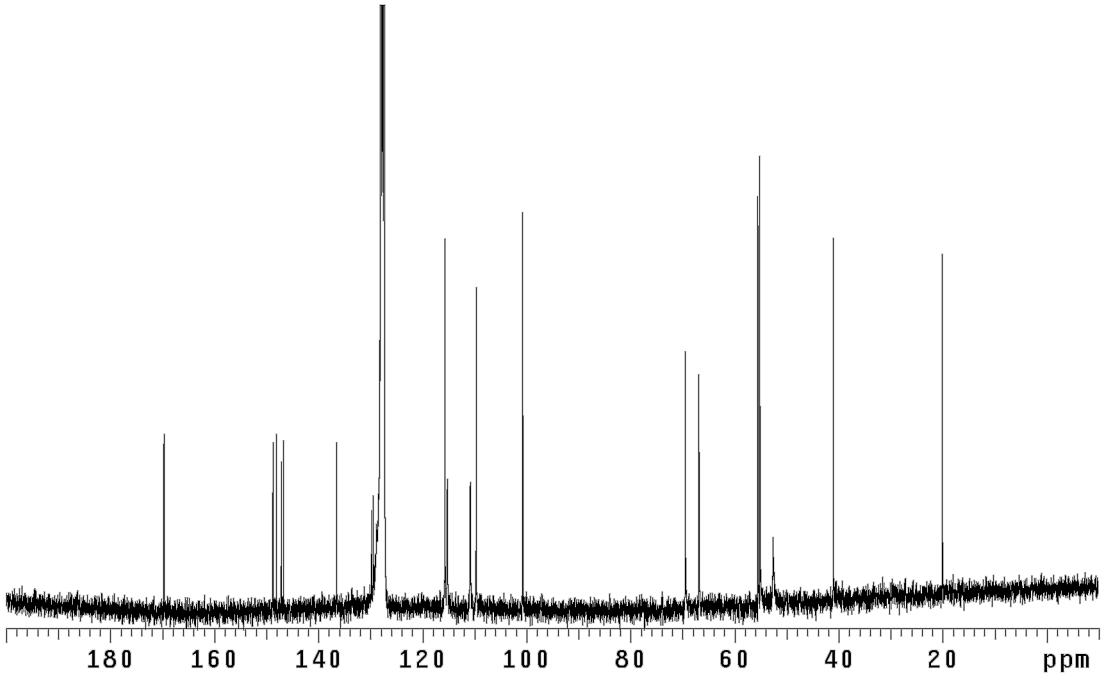

Figure A5.33 ^{13}C NMR (75 MHz, C_6D_6) of compound (–)-**315**.

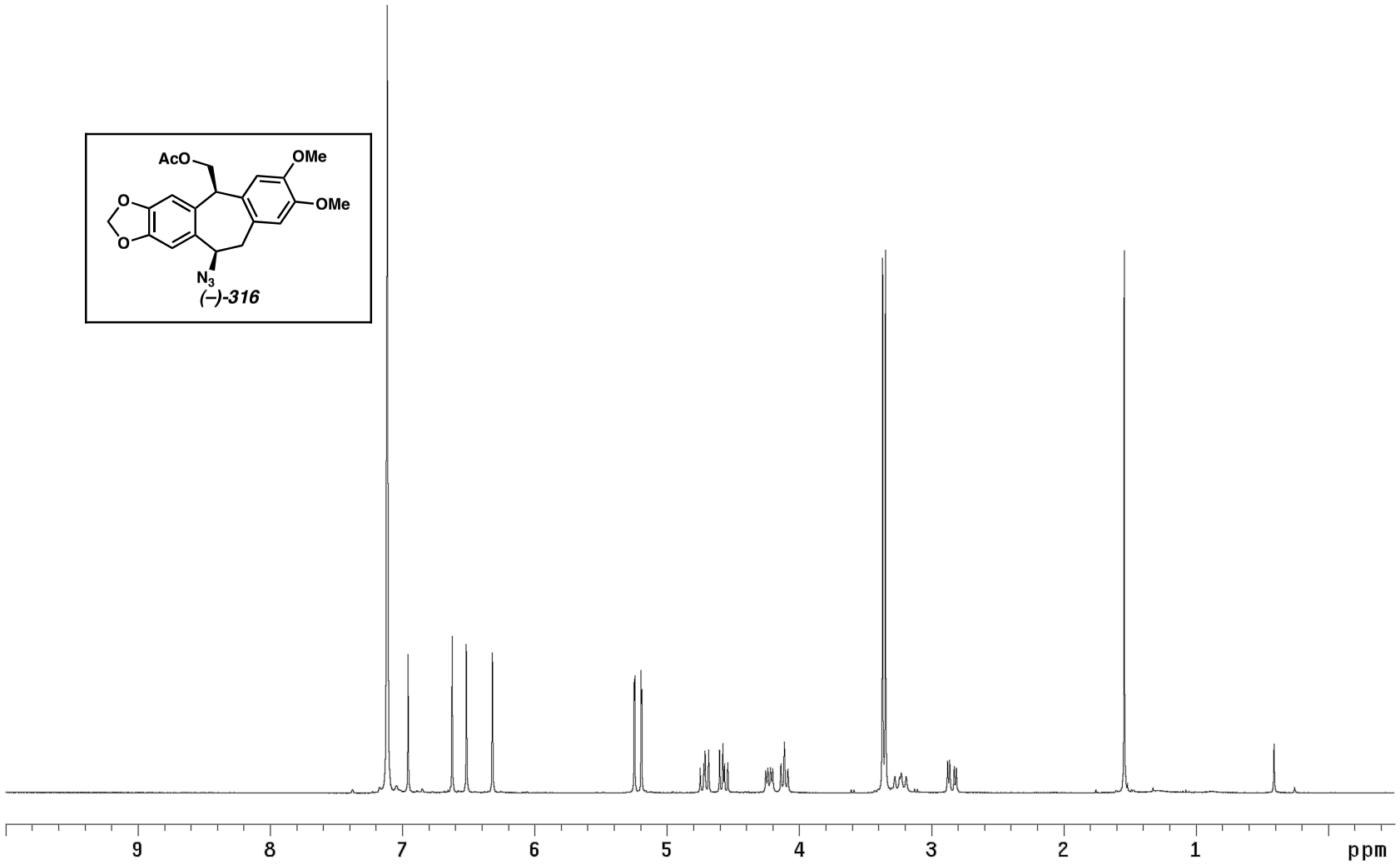

Figure A5.34 ^{1}H NMR (300 MHz, C_6D_6) of compound (–)-**316**.

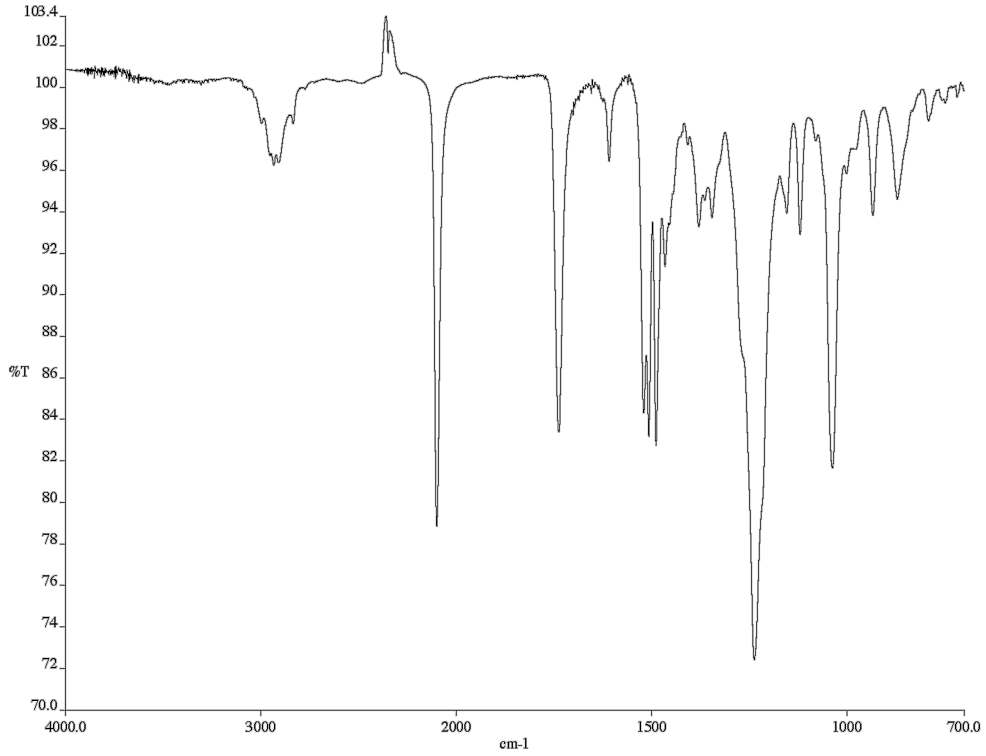

Figure A5.35 Infrared spectrum (thin film/NaCl) of compound (–)-**316**.

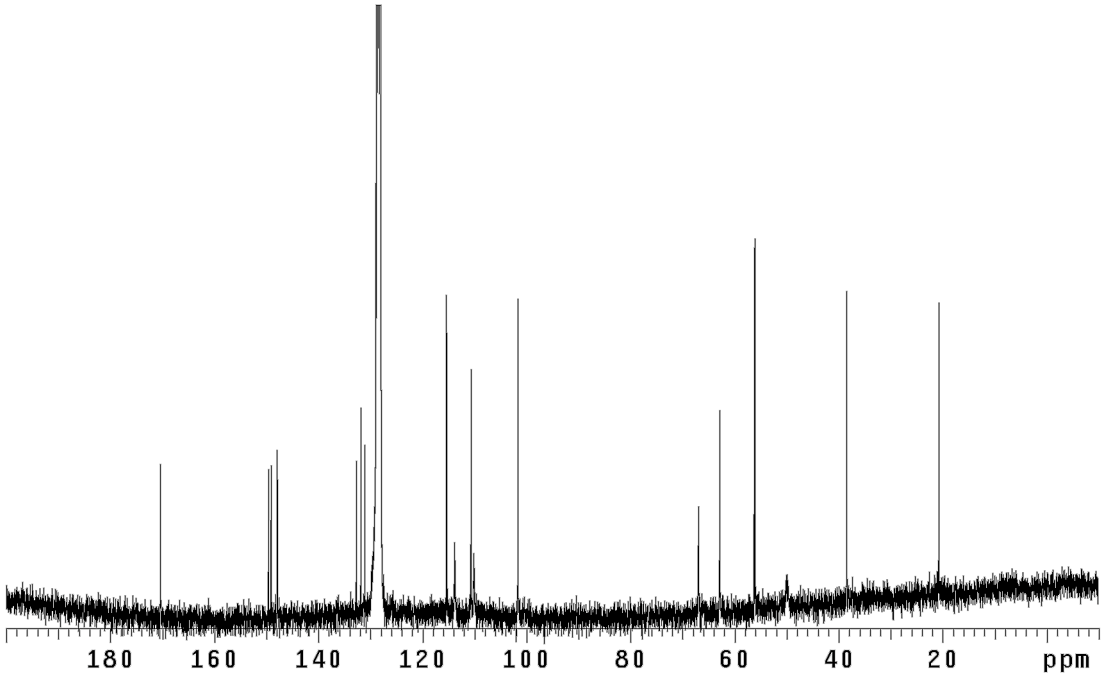

Figure A5.36 ^{13}C NMR (75 MHz, C_6D_6) of compound (–)-**316**.

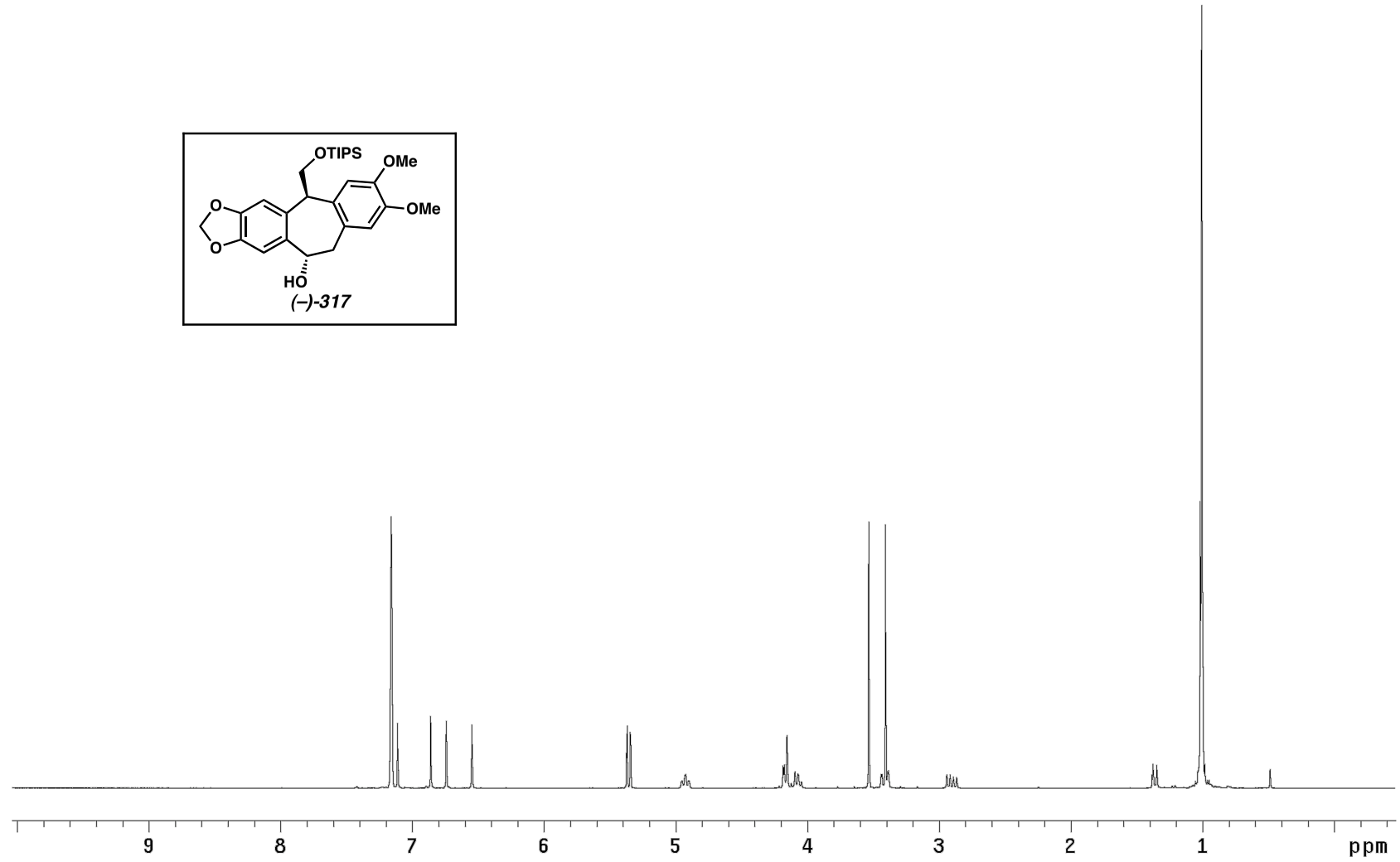

Figure A5.37 ^{1}H NMR (300 MHz, C_6D_6) of compound (–)-**317**.

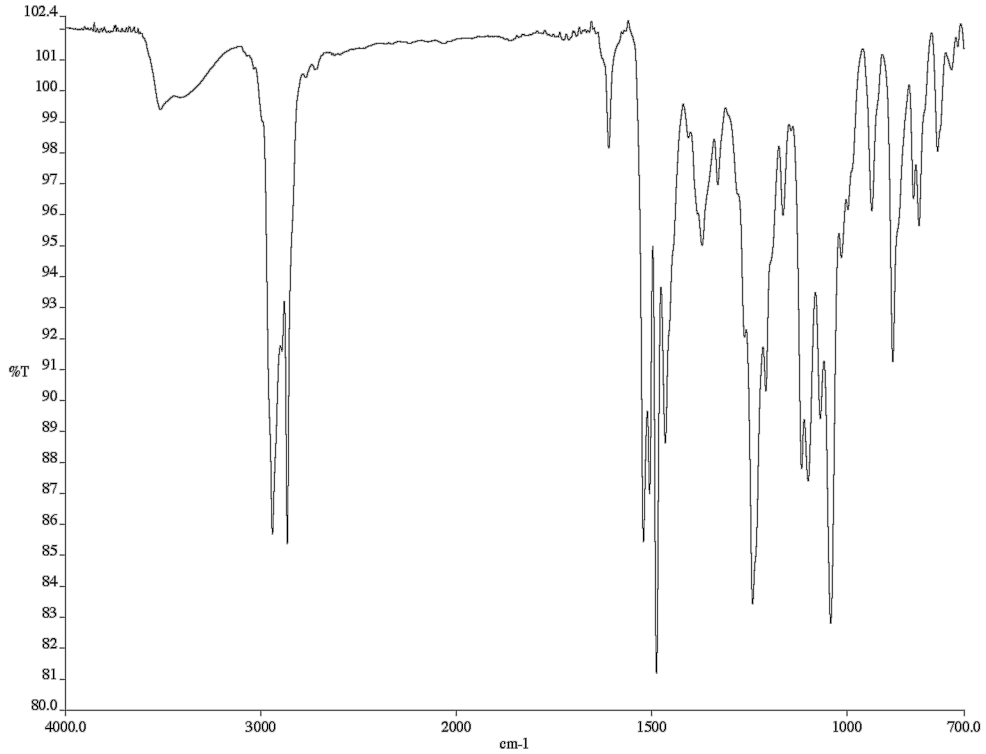

Figure A5.38 Infrared spectrum (thin film/NaCl) of compound (–)-**317**.

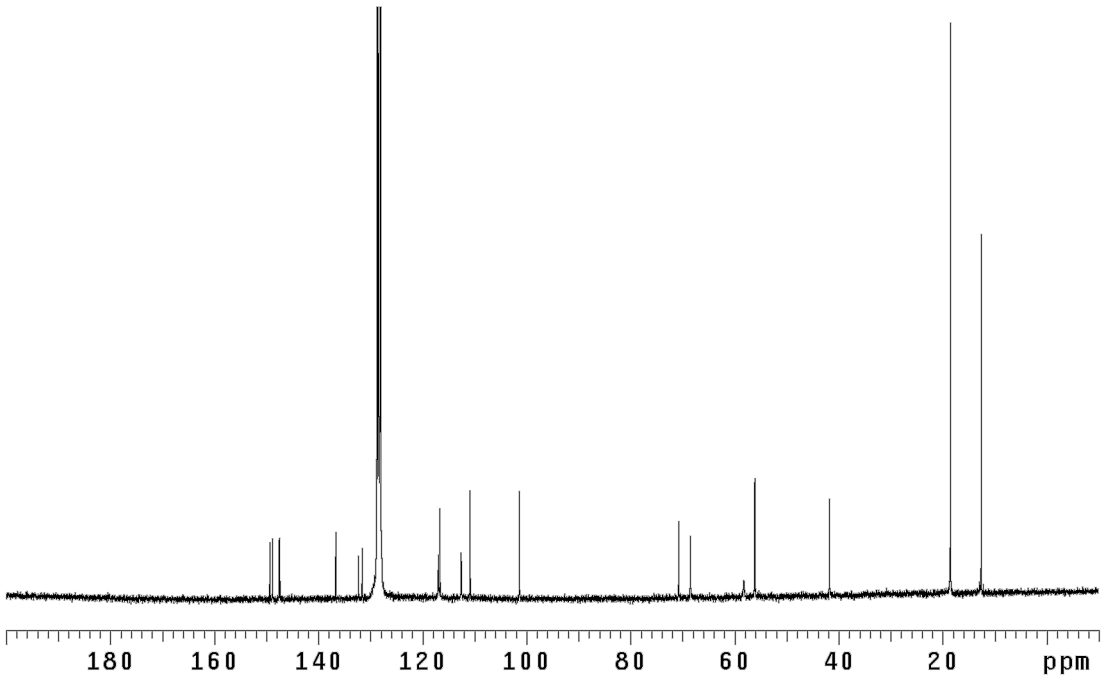

Figure A5.39 ^{13}C NMR (75 MHz, C_6D_6) of compound (–)-**317**.

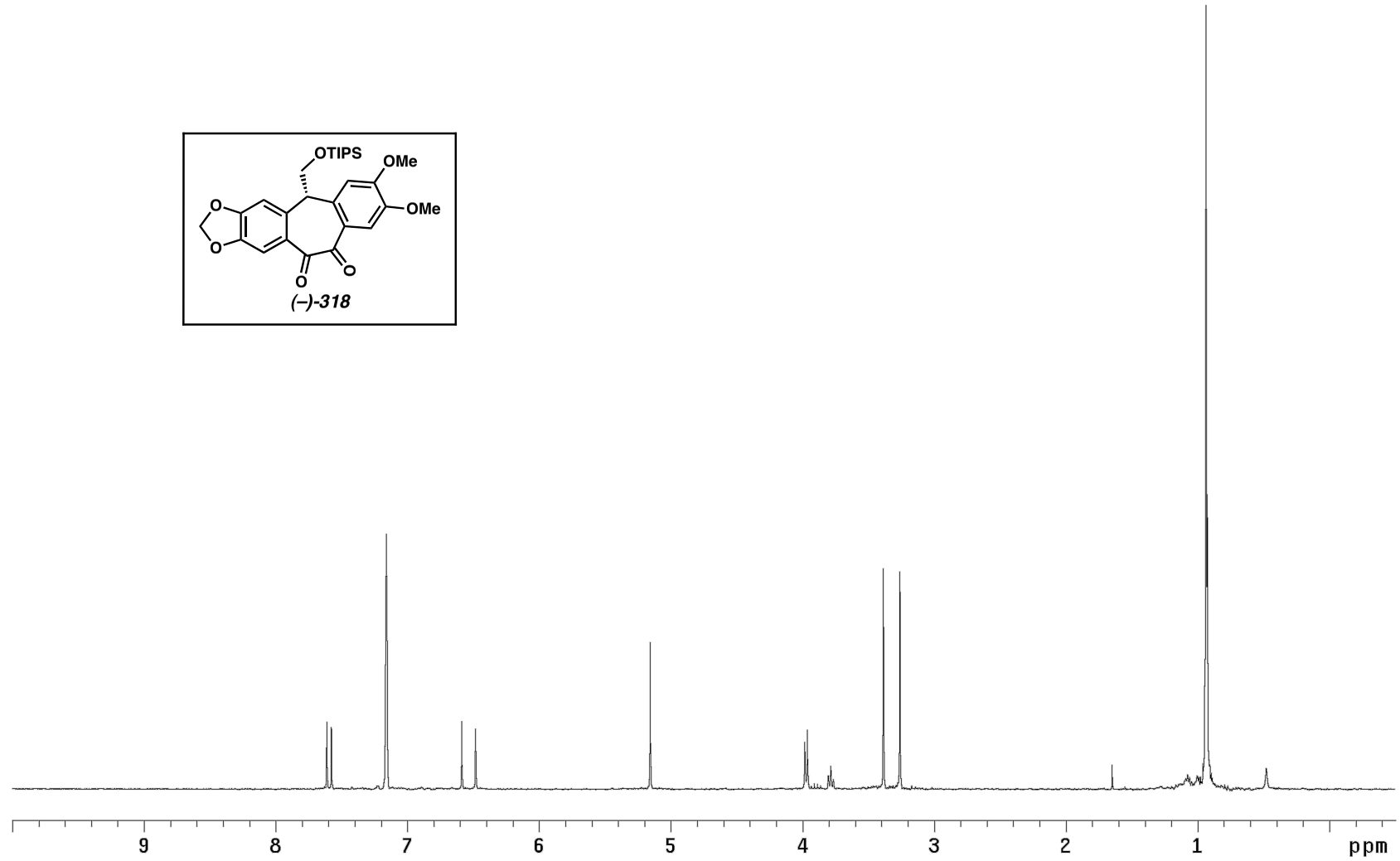

Figure A5.40 ^{1}H NMR (300 MHz, C_6D_6) of compound (–)-**318**.

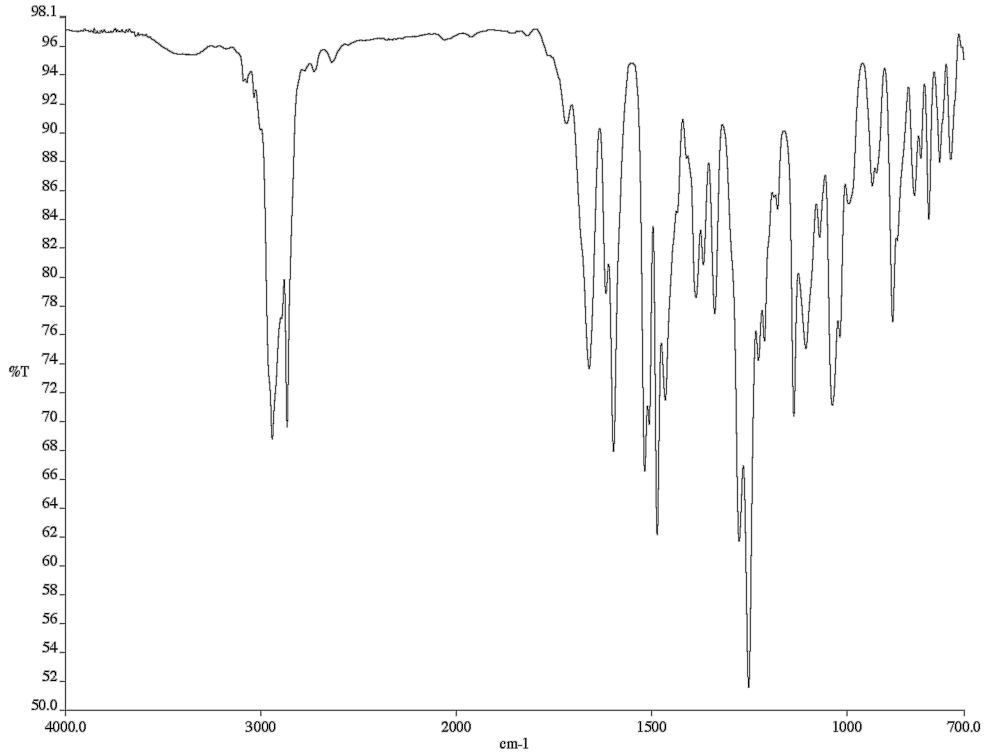

Figure A5.41 Infrared spectrum (thin film/NaCl) of compound (–)-**318**.

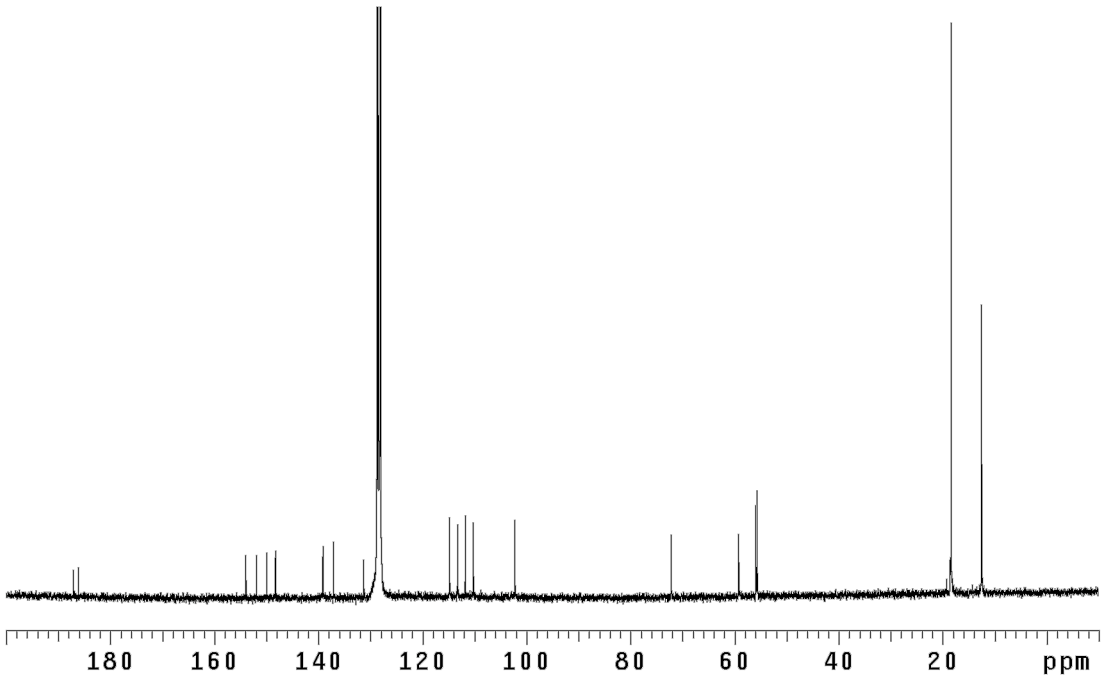

Figure A5.42 ^{13}C NMR (75 MHz, C_6D_6) of compound (–)-**318**.

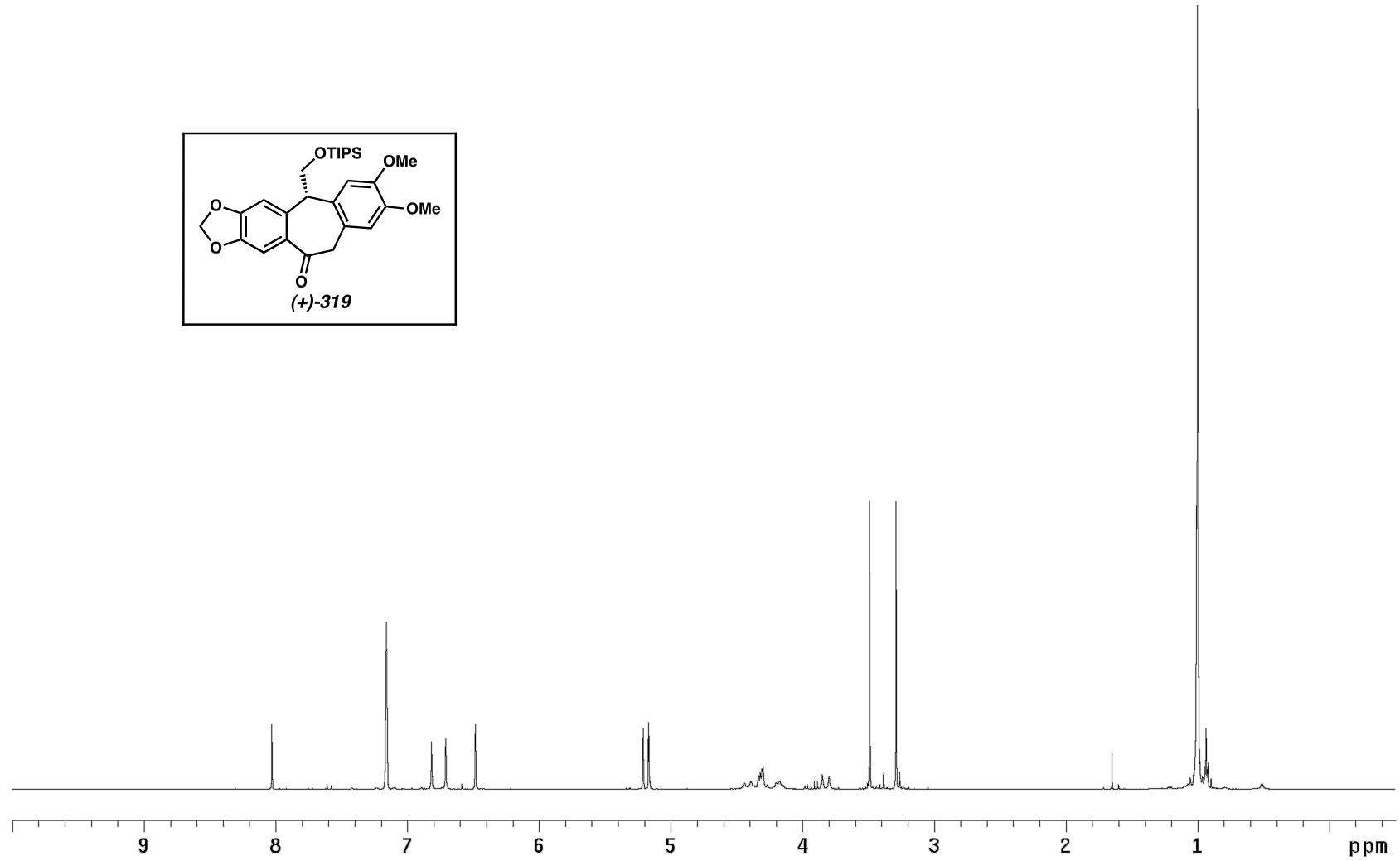

Figure A5.43 ^{1}H NMR (300 MHz, C_6D_6) of compound (+)-**319**.

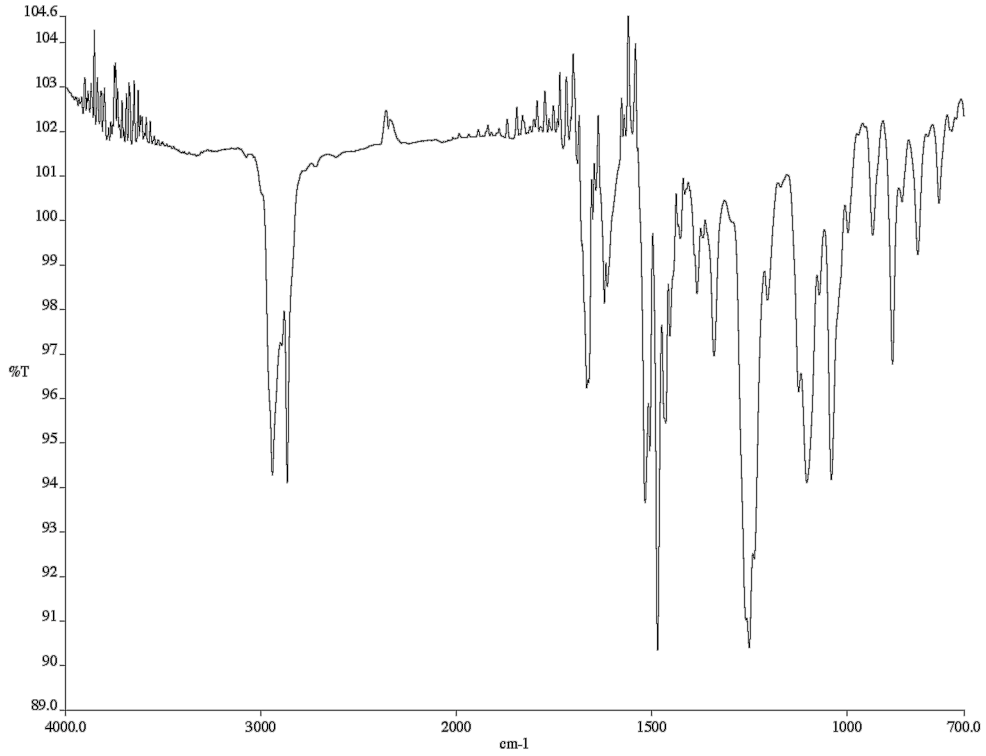

Figure A5.44 Infrared spectrum (thin film/NaCl) of compound (+)-**319**.

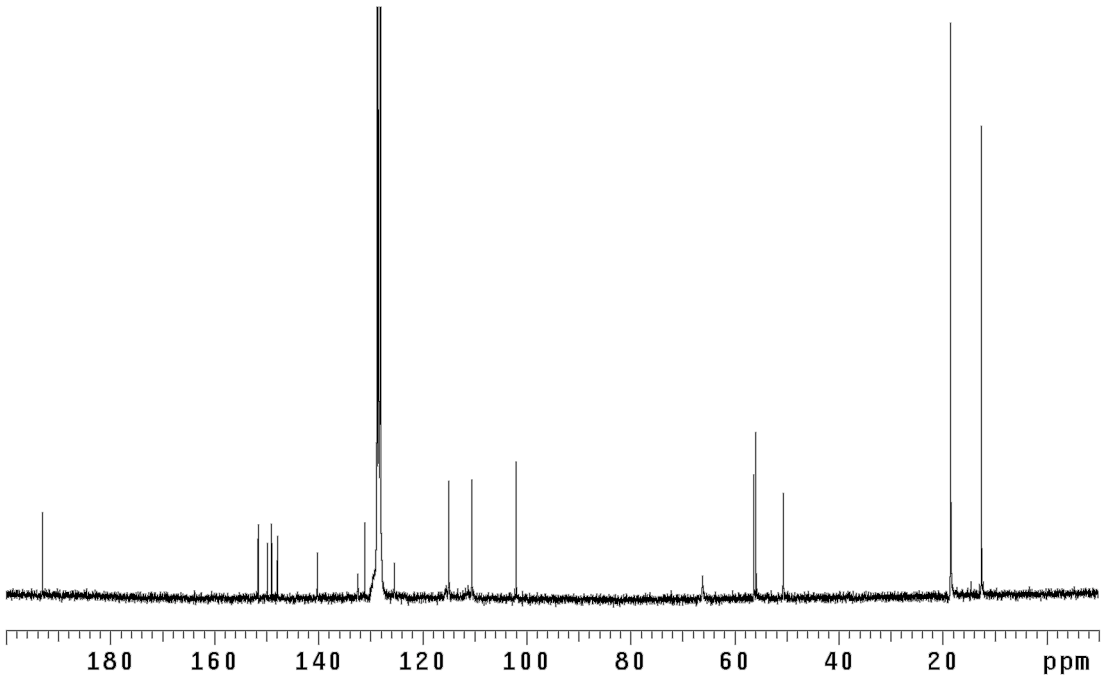

Figure A5.45 ^{13}C NMR (75 MHz, C_6D_6) of compound (+)-**319**.

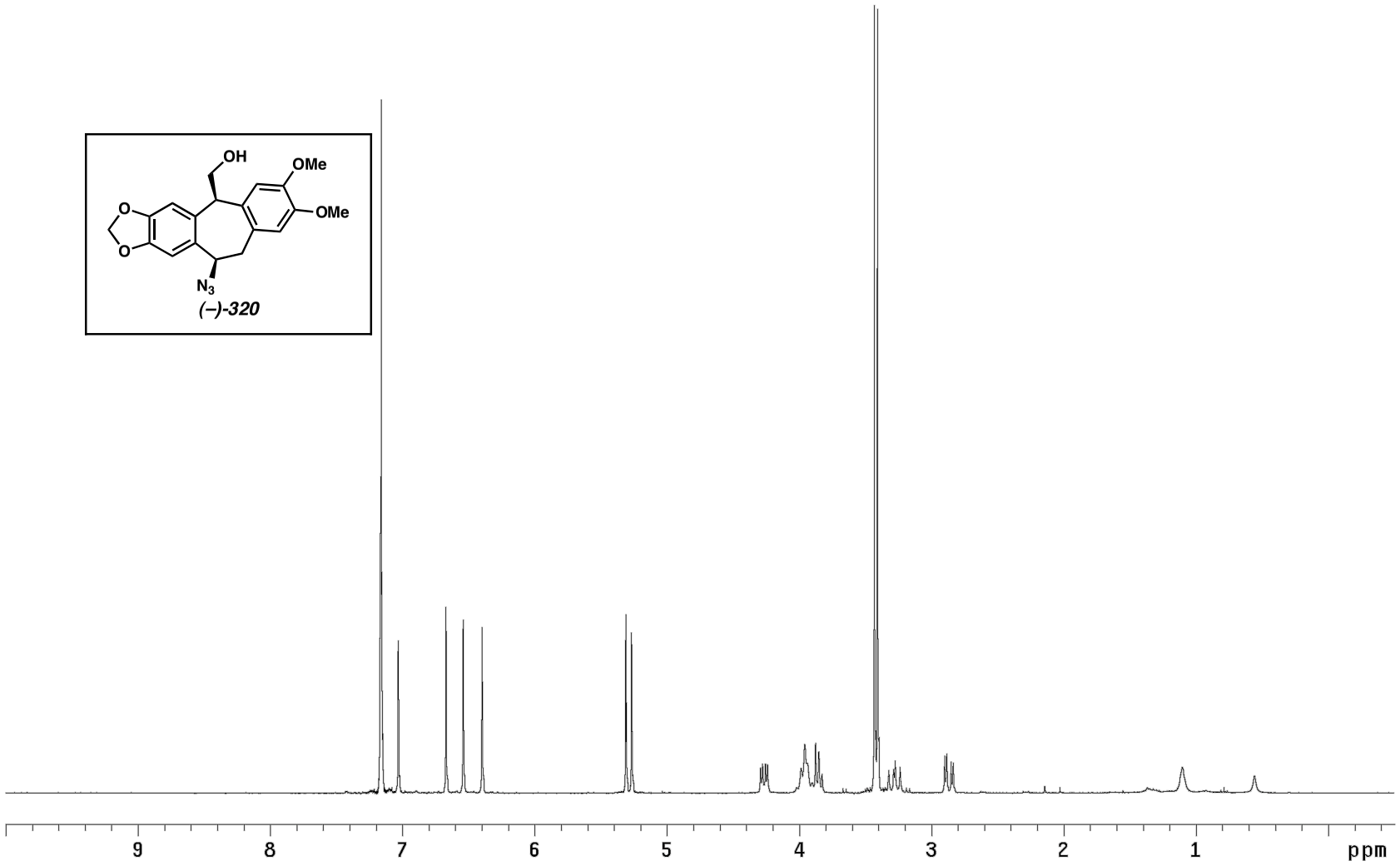

Figure A5.46 ^{1}H NMR (300 MHz, C_6D_6) of compound (–)-**320**.

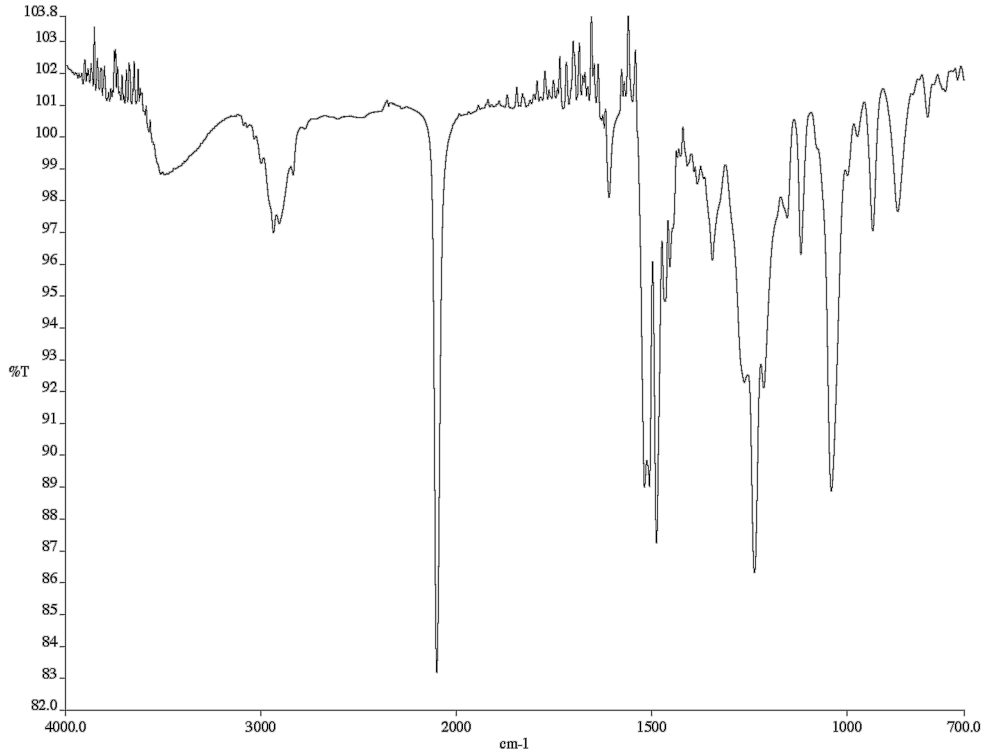

Figure A5.47 Infrared spectrum (thin film/NaCl) of compound (–)-**320**.

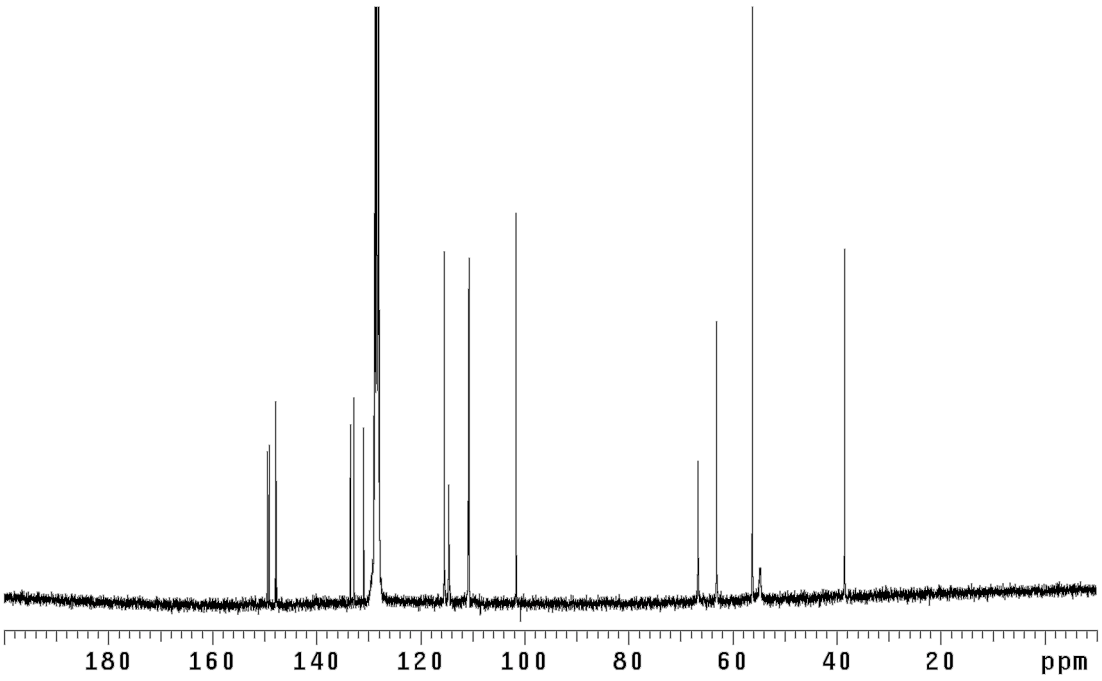

Figure A5.48 ^{13}C NMR (75 MHz, C_6D_6) of compound (–)-**320**.

APPENDIX 6

The Development of a Scaleable Acyl-Alkylation of Arynes and Application to the Construction of 1,3-Dihydroxynaphthalenes[†]

A6.1 Background and Introduction

The study of arynes has a rich history in physical organic chemistry. The application of these structures in complex molecule synthesis has, however, been hampered by the harsh conditions for their generation and their high reactivity with a wide variety of organic functionalities. Recent advances in the formation of arynes from readily available precursors have increased the synthetic utility of these reactive intermediates, allowing a broader range of reactions to be developed.[1]

In 1983, Kobayashi reported a mild method for the formation of arynes by the fluoride-mediated elimination of *ortho*-silyl aryltriflates (Scheme A6.1.1).[2] These conditions obviate the need for strongly basic conditions or high reaction temperatures to cleanly generate aryne intermediates.

Scheme A6.1.1 Kobayashi's aryne preparation.

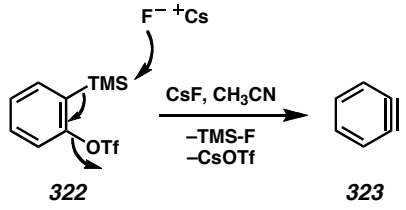

Based on this procedure, we recently developed the acyl-alkylation of arynes.[3,4] Treatment of *ortho*-silyl aryltriflates with CsF and β-ketoesters produced *ortho*-substituted ketoesters in good to excellent yields (Scheme A6.1.2). This reaction is

[†] This work was performed in collaboration with Uttam K. Tambar (Ph.D. 2005), a graduate student in the Stoltz group at California Institute of Technology.

believed to involve initial fluoride-induced aryne formation (**323**). Subsequent formal [2+2] cycloaddition and fragmentation with the cesium enolate of the β-ketoester (**325**) provides the observed product (**327**).

Scheme A6.1.2 Aryne insertion and possible mechanism.

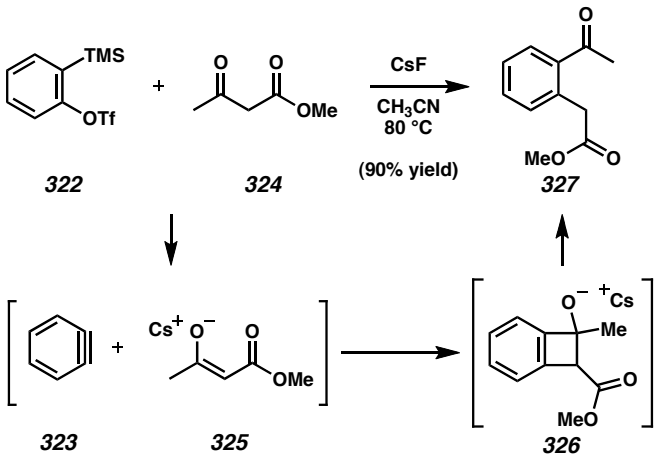

Functionality on the aryne, as well as variation of the β-ketoester, is well tolerated. Furthermore, acyl-alkylation with cyclic β-ketoesters affords ring-expansion products for the construction of a variety of benzannulated ring structures (Scheme A6.1.3). In the next section, we describe a scaleable aryne insertion protocol that allows access to multi-gram quantities of these ketoesters. The synthetic value of these intermediates is demonstrated by their further transformation to 1,3-dihydroxynaphthalenes.

Scheme A6.1.3 Ring expansion by aryne insertion.

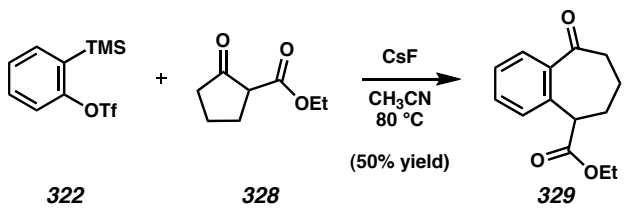

A6.2 The Development of a Scaleable Aryne Insertion into β-Ketoesters

Initial efforts to produce multi-gram amounts of methyl 2-(2-acetylphenyl)acetate (**327**) involved direct application of the previously developed conditions (Scheme A6.2.1). Purification by silica gel chromatography provided 5.9 g of acetate **327** in 76% yield. However, this material was contaminated with substantial quantities of an unknown byproduct. Repeated crystallization of this material from hexanes or pentane produced reasonably clean acetate **327**. Preparative thin-layer chromatography of the crystallization filtrate provided a pure sample of the byproduct, which was identified as over-arylation product phenylacetate **330**. Unfortunately, the purification of acetate **327** was not reproducible on large scale.

Scheme A6.2.1 Initial procedure with byproduct.

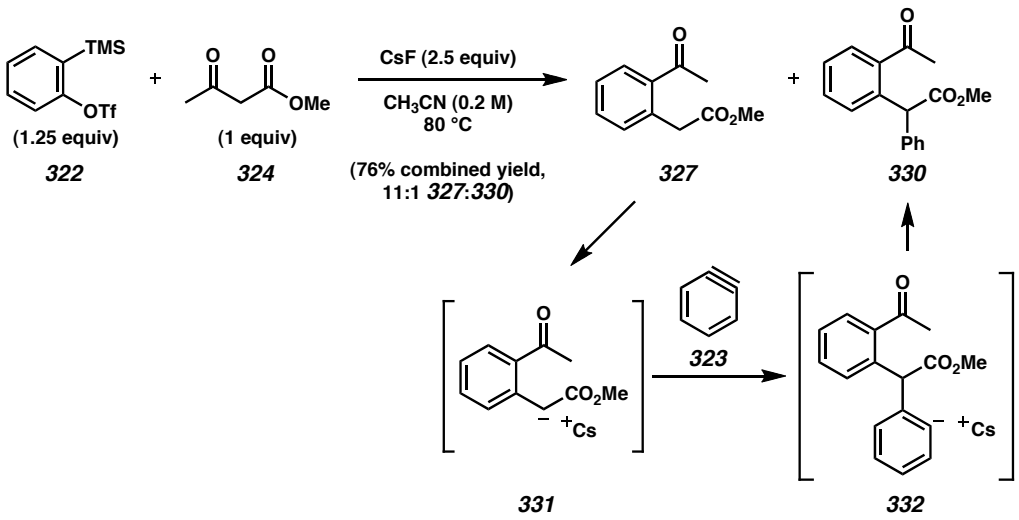

Phenylacetate **330** was expected to arise from α-arylation of desired product **327** by excess benzyne present in the reaction. Thus, we anticipated that fewer equivalents of benzyne precursor **322** would suppress this over-arylation product. Indeed, improved

ratios of **327** relative to **330** were observed, but at the expense of yield, particularly on larger scale (Table A6.2.1).

Table A6.2.1 Screen of reagent ratios in the aryne insertion.

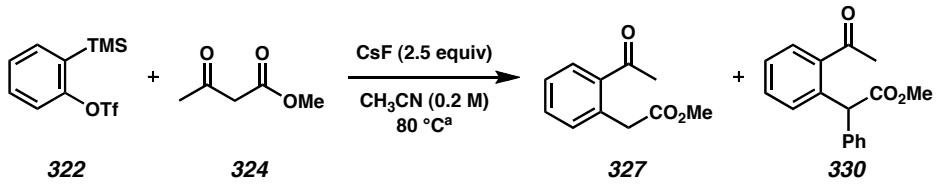

322 ***324*** ***327*** ***330***

entry	equiv ***322***	equiv ***324***	yield[b]	***327***:***330*** ratio[c]
1	1.1	1.0	85%	8:1
2	1.0	1.0	76%	11:1
3	1.0	1.25	82%	12.5:1
4	1.0	2.0	67%	1:0
5[d]	1.0	2.0	58%	99:1

[a] Performed on 0.4 mmol scale, unless otherwise noted. [b] Isolated yield of mixture of **327** and **330**. [c] Ratio determined by ^{1}H NMR. [d] Performed on 2.0 mmol scale.

Ultimately, the initially reported conditions were reinvestigated for this transformation. Again, purification procedures based on recrystallization proved difficult to reproduce. However, distillation under vacuum proved to be a simple and scaleable procedure for obtaining acetate **327** pure in 65% yield (Scheme A6.2.2).

Scheme A6.2.2 Final large scale aryne insertion.

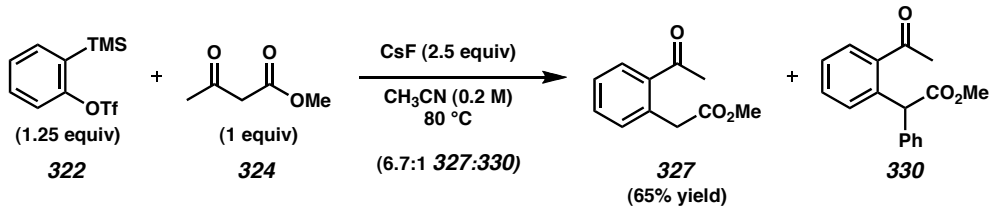

A6.3 Application to the Construction of 1,3-Dihydroxynaphthalenes

With pure acetate **327** and phenylacetate **330** in hand, further transformations to 1,3-dihydroxynaphthalenes were investigated. Reactions involving acetate **327** were

complicated by the instability of the desired 1,3-dihydroxynaphthalene (**333**) to oxygen under basic conditions. Thus, initial attempts to isolate diol **333** resulted in formation of the natural dye lawsone (**335**), presumably due to molecular oxygen exposure during reaction quenching (Scheme A6.3.1). Careful quenching of reactions with degassed HCl allowed isolation of the desired hydroxynaphthalenes **333** and **334** in excellent yields.

Scheme A6.3.1 Base-promoted dihydroxynaphthalene formation.

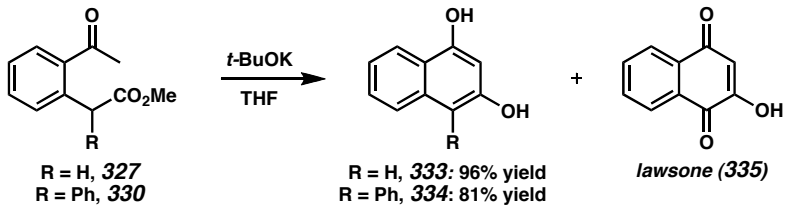

A6.4 Conclusion

A scaleable methodology for the insertion of arynes into C-C bonds of β-ketoesters has been developed. This procedure allows the preparation of methyl 2-acetylphenylacetate (**327**) in good yield and excellent purity. The transformation of this acetate, as well as the byproduct phenylacetate **330**, to 1,3-dihydroxynaphthalenes has also been demonstrated. These efforts illuminate the utility of this aryne insertion methodology in complex molecule synthesis.

A6.5 Experimental Section

A6.5.1 Materials and Methods

Unless stated otherwise, reactions were performed in flame-dried glassware sealed with rubber septa under a nitrogen atmosphere using dry, deoxygenated solvents. Chemicals were purchased from the Sigma-Aldrich Chemical Company, Milwaukee, WI and were used as received. 2-(Trimethylsilyl)phenyl trifluoromethanesulfonate could also be prepared by the method of Peña and coworkers.[5] Solvents were dried by passage through an activated alumina column under argon. Liquids and solutions were transferred via syringe. Reaction temperatures were controlled using an IKAmag temperature modulator. Thin-layer chromatography (TLC) was conducted with E. Merck silica gel 60 F254 pre-coated plates (0.25 mm) and visualized using a combination of UV at 254 nm, *p*-anisaldehyde, and potassium permanganate staining. ICN silica gel (particle size 32-63 μm) or SiliCycle Silia*Flash* P60 Academic silica gel (particle size 40-63 μm; pore diameter 60 Å) was used for flash column chromatography. Bulb-to-bulb distillations were performed with a Büchi Glass Oven B-585 Kugelrohr. ^{1}H NMR spectra were recorded on a Varian Mercury 300 instrument (at 300 MHz) and are reported relative to Me_4Si (δ 0.0). Data for ^{1}H NMR spectra are reported in terms of chemical shift (δ ppm), multiplicity, coupling constant (Hz), and integration. ^{13}C NMR spectra were recorded on a Varian Mercury 300 instrument (at 75 MHz) and are reported relative to Me_4Si (δ 0.0). Data for ^{13}C NMR spectra are reported in terms of chemical shift (δ ppm). IR spectra were recorded on a Perkin Elmer Paragon 1000 or Spectrum BX II spectrometer and are reported in terms of frequency of absorption (cm^{-1}). Melting points were determined on a Thomas-Hoover melting point apparatus and are

uncorrected. High resolution mass spectra were obtained from the California Institute of Technology Mass Spectral Facility.

A6.5.2 Preparative Procedures

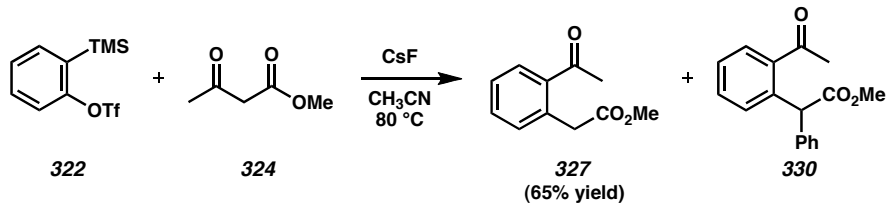

322 *324* *327* (65% yield) *330*

Methyl 2-(2-Acetylphenyl)acetate (327) and Methyl 2-Phenyl-2-(2-acetylphenyl)acetate (330). To a solution of methyl acetoacetate (**324**, 5.59 mL, 6.01 g, 51.8 mmol, 1.0 equiv) and 2-trimethylsilylphenyl trifluoromethanesulfonate (**322**, 15.7 mL, 19.31 g, 64.7 mmol, 1.25 equiv) in CH_3CN (260 mL) was added anhydrous CsF (19.66 g, 129.4 mmol, 2.5 equiv). The reaction mixture was submerged in an 80 °C oil bath and allowed to reflux for 30 min. After cooling to 23 °C, saturated aq NaCl (200 mL) was added. The phases were separated, and the aqueous phase was extracted with Et_2O (3 x 200 mL). The combined organic phases were dried over Na_2SO_4 and filtered. The filtrate was concentrated under reduced pressure and purified by flash chromatography (9:1→4:1→2:1 hexanes:EtOAc) to provide a mixture of **327** and **330** (8.00 g, 87:13 ratio) as an off-white solid. Bulb-to-bulb distillation (1-2 torr, 159-165 °C) afforded **327** (6.49 g, 65% yield, 98.4:1.6 **327**:**330** ratio) as a white crystalline solid. The characterization data matched the data in the literature:[6] R_f 0.46 (3:1 hexanes:EtOAc); mp 53-55 °C (lit.[7] mp 57-59 °C); ^{1}H NMR (300 MHz, $CDCl_3$) δ 7.79 (dd, J = 7.6, 1.5 Hz, 1H), 7.47-7.33 (comp. m, 2H), 7.24-7.20 (m, 1H), 3.91 (s, 2H), 3.66 (s, 3H), 2.56 (s, 3H); ^{13}C NMR (75 MHz, $CDCl_3$) δ 201.3, 172.0, 137.1, 134.4, 132.8, 132.1, 130.1, 127.5, 51.9, 40.2, 28.8; IR (thin film/NaCl) 3001, 2952, 1739, 1683 cm^{-1};

HRMS-EI (*m*/*z*): $[M]^+$ calcd for $[C_{11}H_{12}O_3]^+$, 192.0787; found 192.0787. The distillation residue was found to be mainly **330** (1.36 g, 10% yield, 89:11 **330**:**327** ratio) as a viscous amber oil, which solidified upon standing. An analytically pure sample of **330** was obtained by preparative TLC (3:2 hexanes:Et_2O). The characterization data matched the data in the literature:[8] R_f 0.46 (3:1 hexanes:EtOAc); ^{1}H NMR (300 MHz, $CDCl_3$) δ 7.77-7.73 (m, 1H), 7.40-7.25 (comp. m, 5H), 7.25-7.18 (comp. m, 2H), 7.09-7.04 (m, 1H), 5.76 (s, 1H), 3.71 (s, 3H), 2.56 (s, 3H); ^{13}C NMR (75 MHz, $CDCl_3$) δ 202.0, 173.3, 138.7, 138.1, 137.1, 131.8, 130.6, 129.6, 129.3, 128.7, 127.3, 127.0, 53.7, 52.2, 29.3; IR (thin film/NaCl) 1735, 1681, 1254, 1201, 1161 cm^{-1}; HRMS-EI (*m*/*z*): $[M]^+$ calcd for $[C_{17}H_{16}O_3]^+$, 268.1100; found 268.1105.

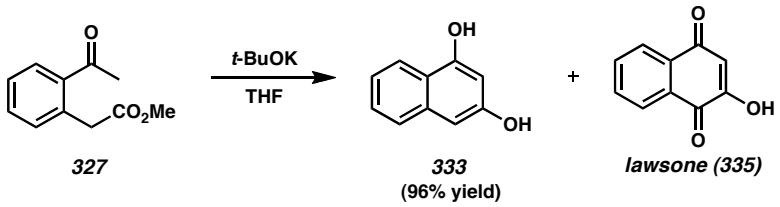

1,3-Dihydroxynaphthalene (333). To a solution of potassium *tert*-butoxide (112.2 mg, 1.0 mmol, 2.0 equiv) in THF (4 mL) was added dropwise a solution of ester **327** (96.1 mg, 0.50 mmol, 1.0 equiv) in THF (1 mL). After 5 min, the reaction was complete by TLC analysis. 1 N aq HCl (degassed with argon, 5 mL) then saturated aq NaCl (2.5 mL) was added. Use of non-degassed HCl resulted in formation of substantial quantities of lawsone (**335**). The mixture was extracted with $CHCl_3$ (3 x 8 mL). The organic phases were dried over Na_2SO_4 and filtered. The filtrate was concentrated under reduced pressure to afford **333** (77.0 mg, 96% yield) as a tan solid. The characterization data matched that for a commercially available sample.

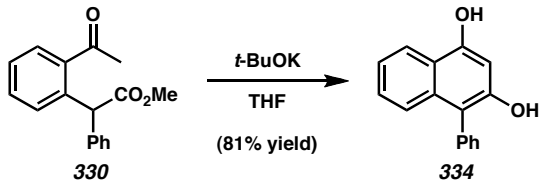

1,3-Dihydroxy-4-phenylnaphthalene (334). To a solution of potassium *tert*-butoxide (112.2 mg, 1.0 mmol, 2.0 equiv) in THF (4 mL) was added dropwise a solution of ester **330** (134.2 mg, 0.50 mmol, 1.0 equiv) in THF (1 mL). After 5 min, the reaction was complete by TLC analysis. 1 N aq HCl (degassed with argon, 5 mL) then saturated aq NaCl (2.5 mL) was added. The mixture was extracted with $CHCl_3$ (3 x 8 mL). The organic phases were dried over Na_2SO_4 and filtered. The filtrate was concentrated under reduced pressure and purified by flash chromatography (3:1 hexanes:EtOAc) to afford **334** as a brown oil contaminated with EtOAc. Et_2O (1 mL) then pentane (4 mL) was added to this oil. The resulting solution was concentrated under reduced pressure to afford **334** (contaminated with Et_2O, 7:2 **334**:Et_2O by ^1H NMR, 104.8 mg total, 96.2 mg **334**, 81% yield) as an off-white foamy solid: R_f 0.24 (7:3 hexanes:EtOAc); ^1H NMR (300 MHz, $CDCl_3$) δ 8.17-8.11 (m, 1H), 7.61-7.54 (comp. m, 2H), 7.52-7.45 (m, 1H), 7.43-7.29 (comp. m, 5H), 6.65 (s, 1H), 5.42 (s, 1H), 5.13 (s, 1H); ^{13}C NMR (75 MHz, $CDCl_3$) δ 152.4, 150.3, 134.1, 131.6, 129.7, 128.3, 127.2, 124.5, 122.7, 121.7, 120.1, 114.3, 108.2, 100.2; IR (thin film/NaCl) 3399, 1628, 1596, 1387, 765, 706 cm^{-1}; HRMS-FAB (*m/z*): $[M]^+$ calcd for $[C_{16}H_{12}O_2]^+$, 236.0837; found 236.0833.

A6.6 Notes and References

(1) Pellissier, H.; Santelli, M. *Tetrahedron* **2003**, *59*, 701-730.

(2) Himeshima, Y.; Sonoda, T.; Kobayashi, H. *Chem. Lett.* **1983**, 1211-1214.

(3) Tambar, U. K.; Stoltz, B. M. *J. Am. Chem. Soc.* **2005**, *127*, 5340-5341.

(4) Subsequent to our report, similar aryne insertions into C-C bonds were disclosed, see: (a) Yoshida, H.; Watanabe, M.; Ohshita, J.; Kunai, A. *Chem. Commun.* **2005**, 3292-3294. (b) Yoshida, H.; Watanabe, M.; Ohshita, F.; Kunai, A. *Tetrahedron Lett.* **2005**, *46*, 6729-6731. (c) Yoshida, H.; Watanabe, M.; Morishita, T.; Ohshita, J.; Kunai, A. *Chem. Commun.* **2007**, 1505-1507. (d) Huang, X.; Xue, J. *J. Org. Chem.* **2007**, *72*, 3965-3968.

(5) Peña, D.; Cobas, A.; Pérez, D.; Guitián, E. *Synthesis* **2002**, 1454-1458.

(6) Cruces, J.; Estevez, J. C.; Castedo, L.; Estevez, R. J. *Tetrahedron Lett.* **2001**, *42*, 4825-4828.

(7) Halford, J. O.; Raiford, R. W., Jr.; Weissmann, B. *J. Org. Chem.* **1961**, *26*, 1898-1901.

(8) Breslow, R.; Kivelevich, D. *J. Org. Chem.* **1961**, *26*, 679-681.

APPENDIX 7

Spectra Relevant to Appendix 6

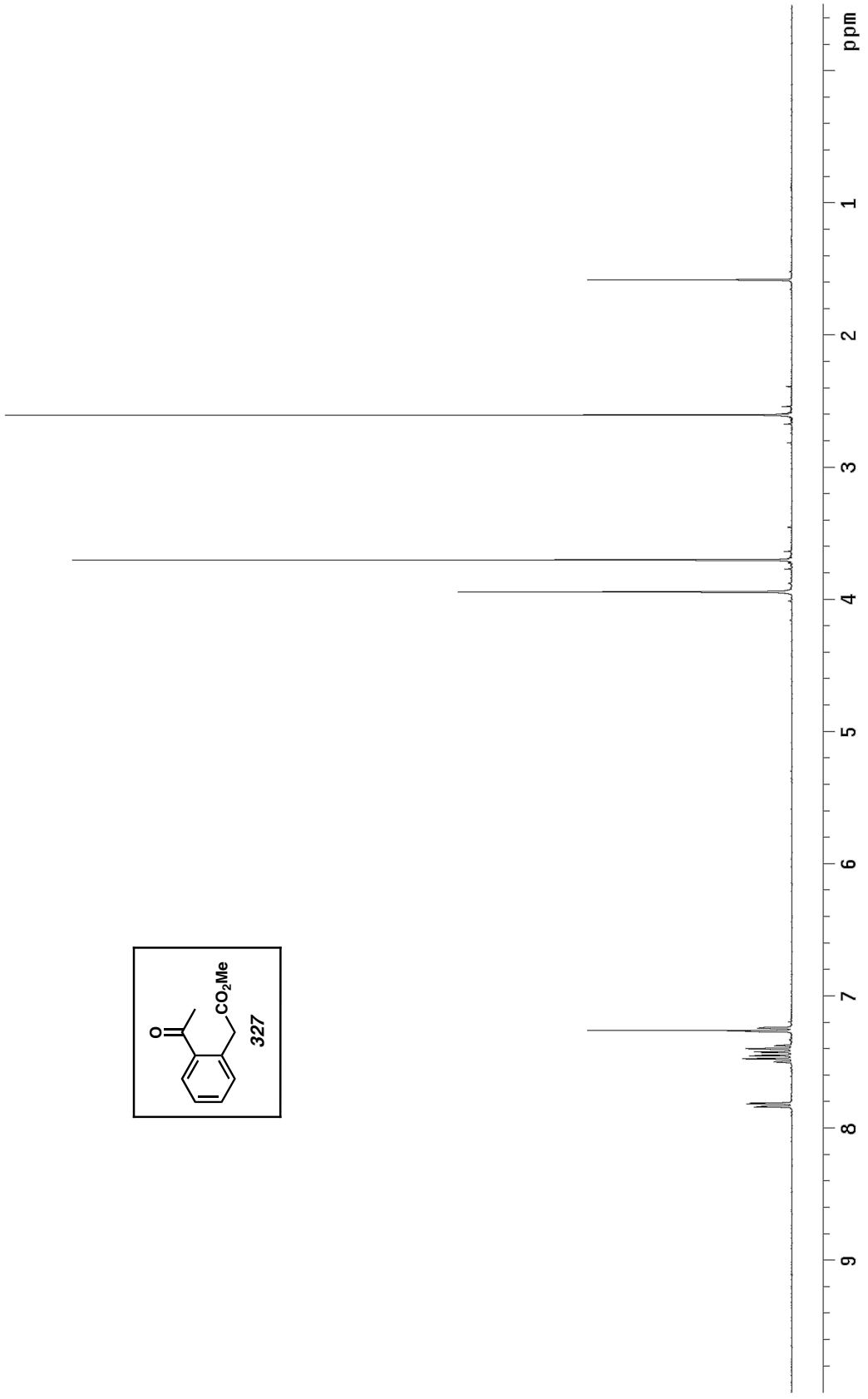

Figure A7.1 ^{1}H NMR (300 MHz, $CDCl_3$) of compound **327**.

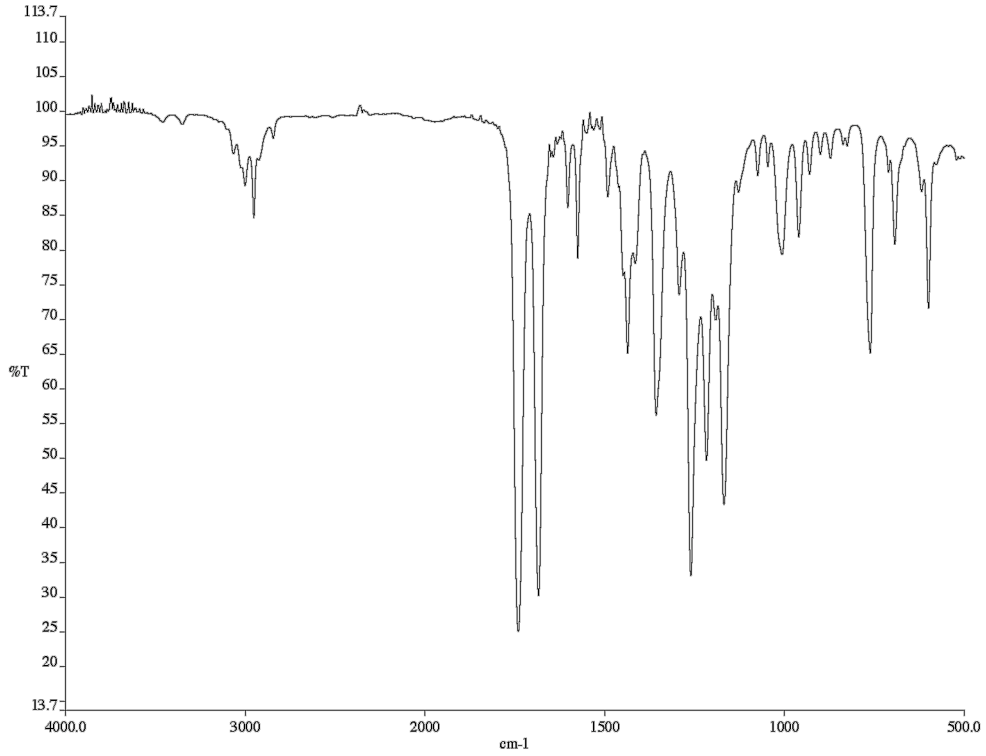

Figure A7.2 Infrared spectrum (thin film/NaCl) of compound **327**.

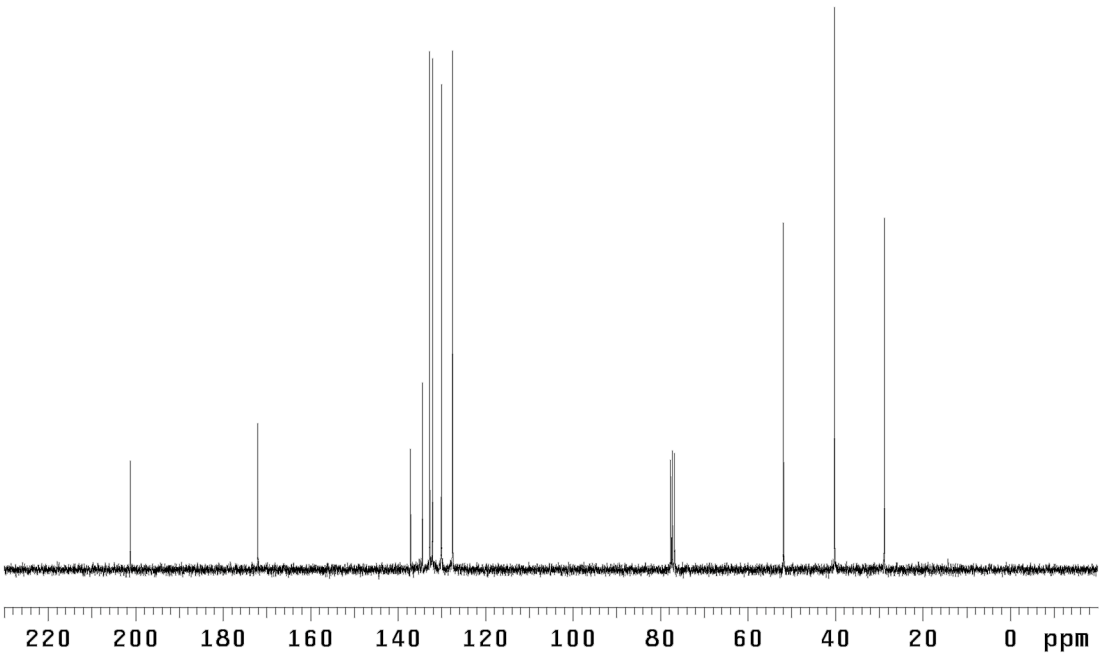

Figure A7.3 ^{13}C NMR (75 MHz, $CDCl_3$) of compound **327**.

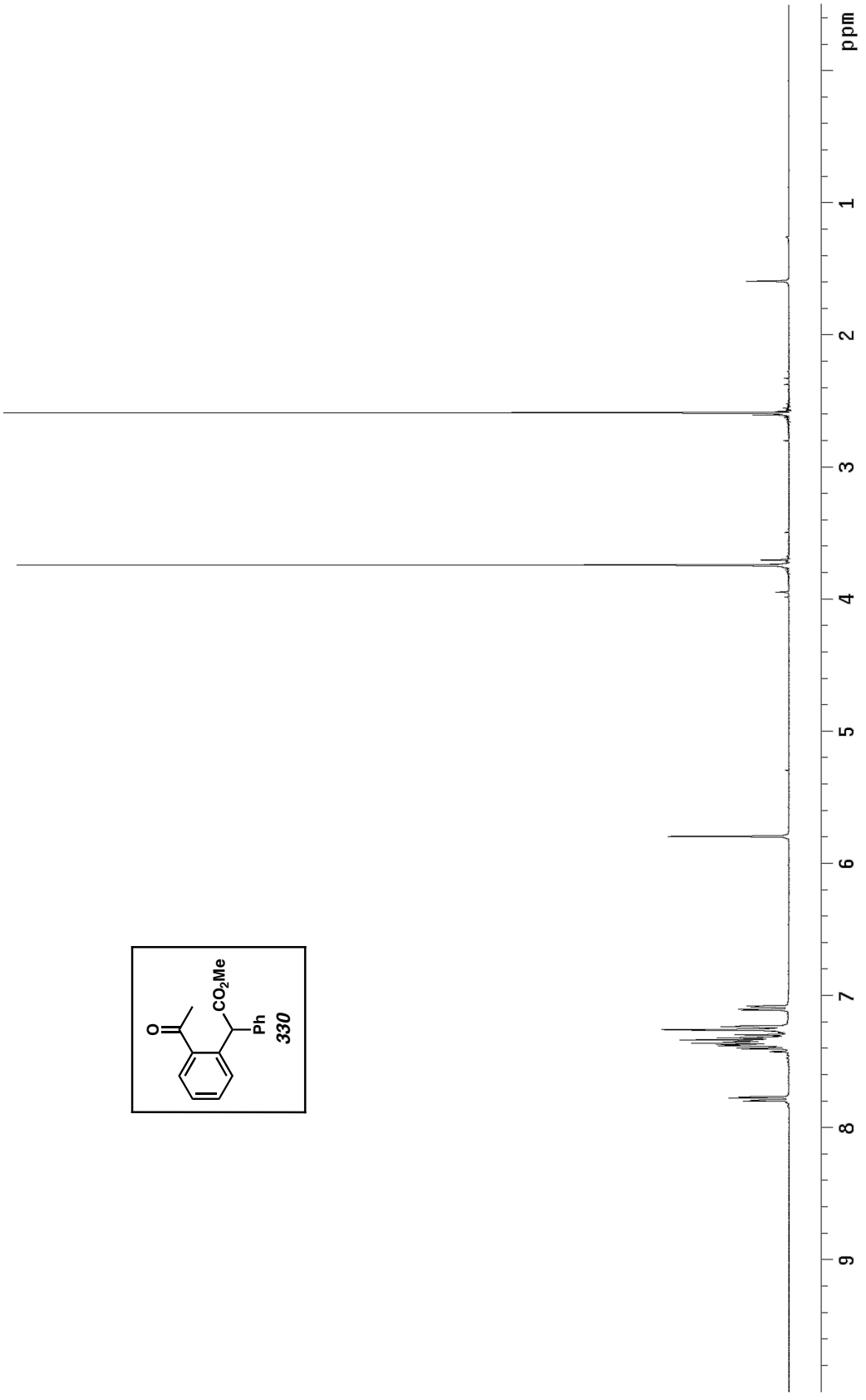

Figure A7.4 ^{1}H NMR (300 MHz, $CDCl_3$) of compound **330**.

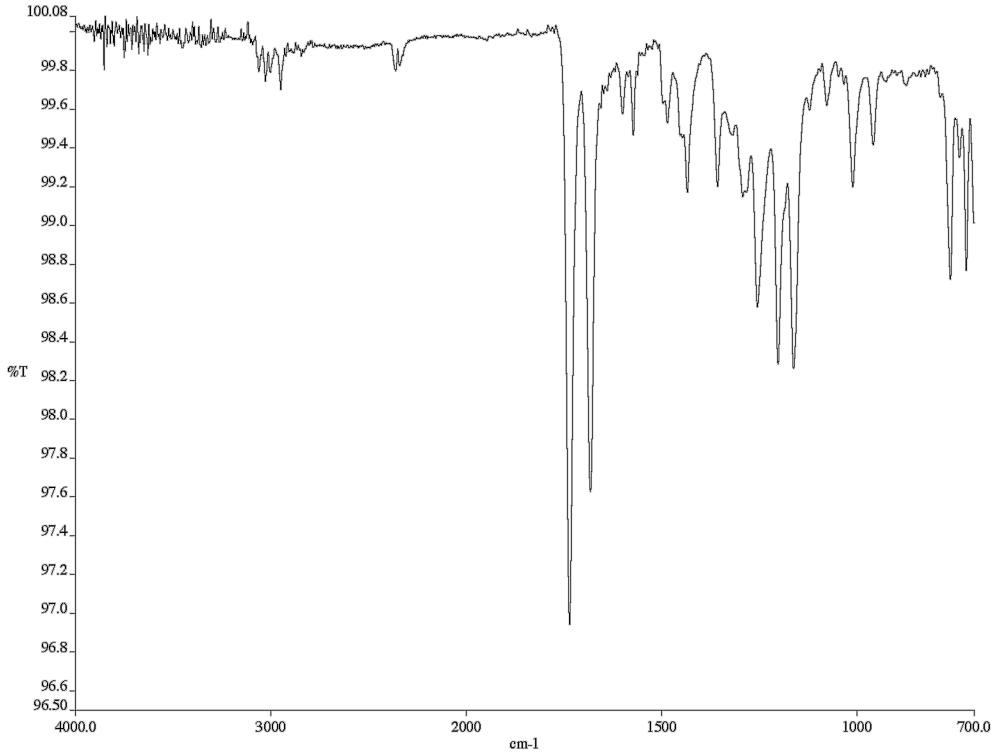

Figure A7.5 Infrared spectrum (thin film/NaCl) of compound **330**.

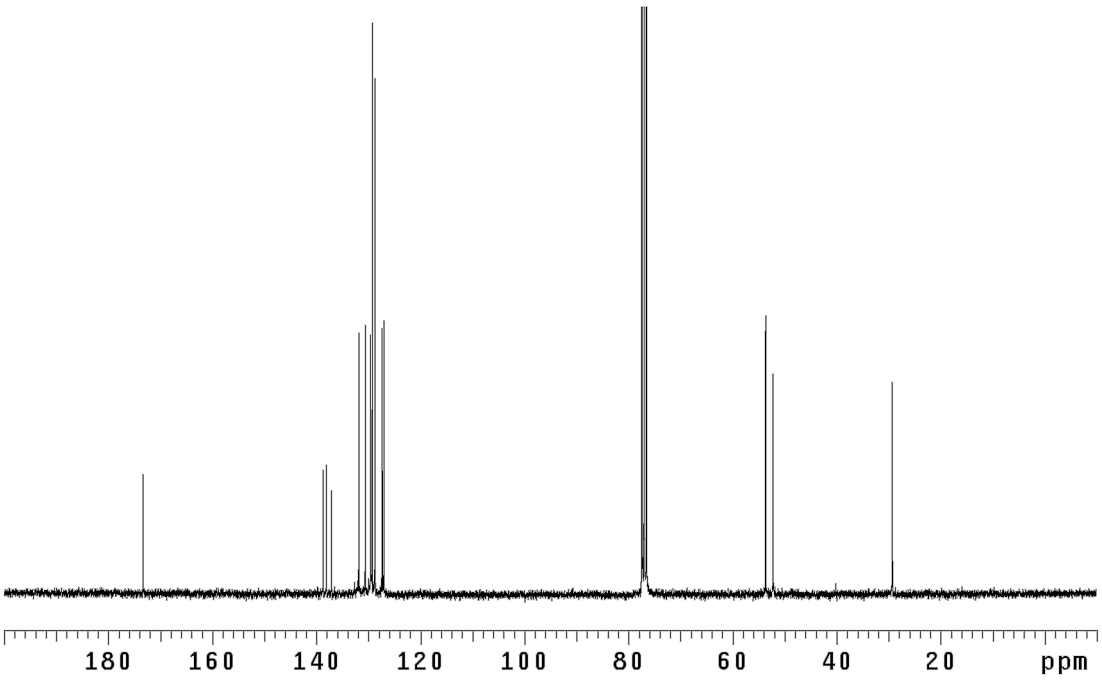

Figure A7.6 ^{13}C NMR (75 MHz, $CDCl_3$) of compound **330**.

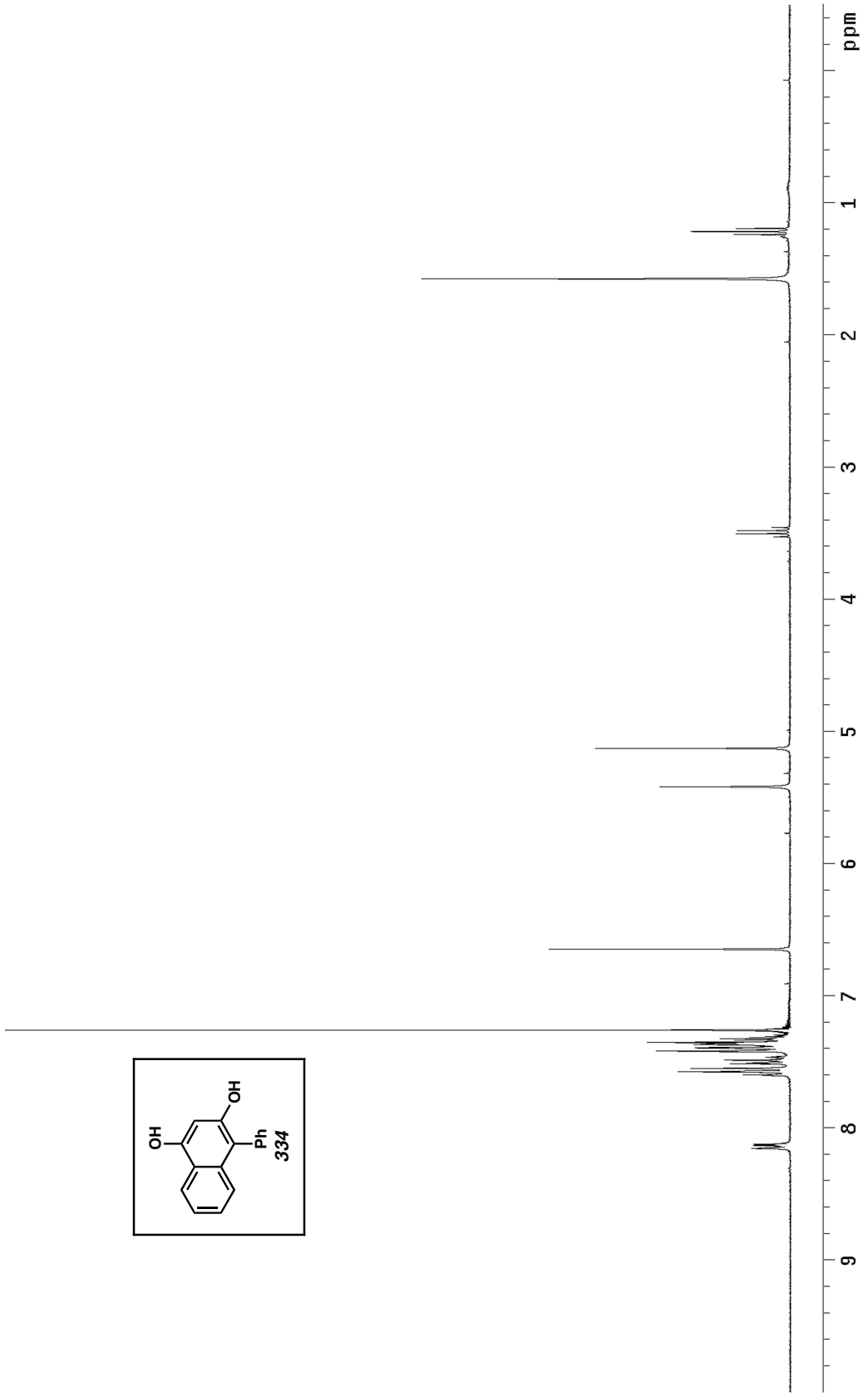

Figure A7.7 ^{1}H NMR (300 MHz, $CDCl_3$) of compound **334**.

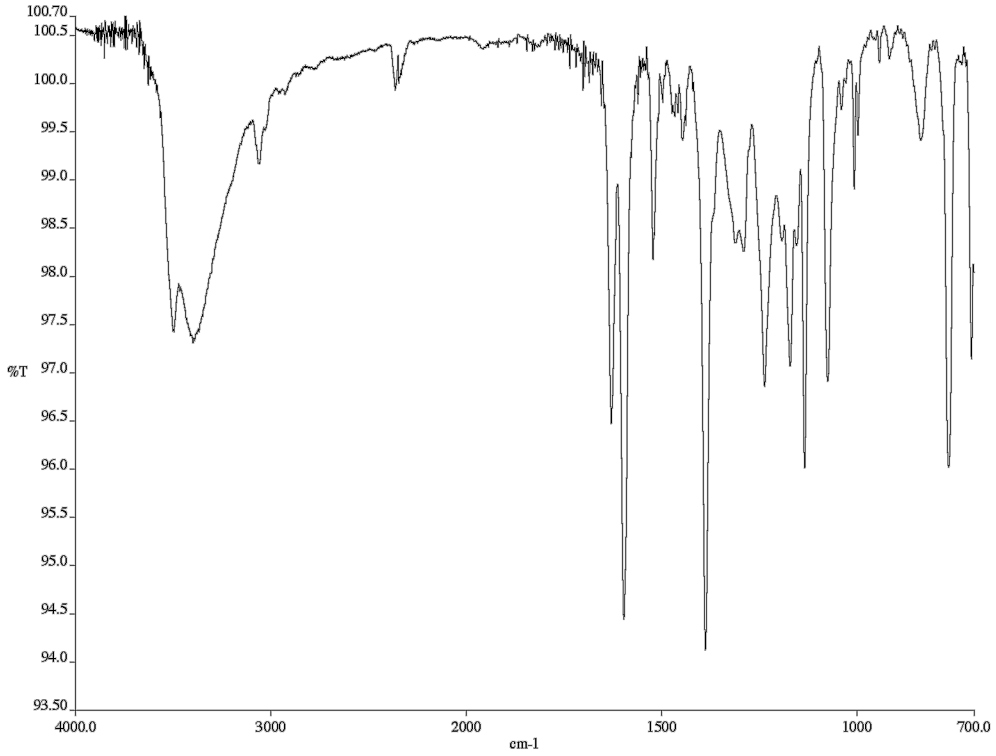

Figure A7.8 Infrared spectrum (thin film/NaCl) of compound **334**.

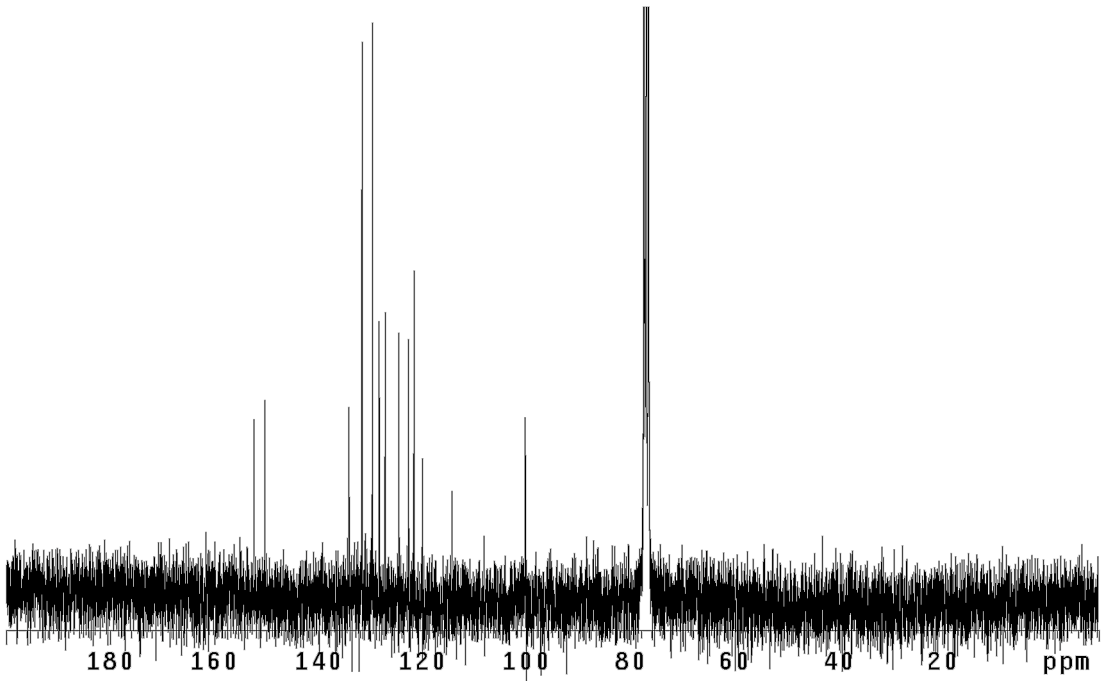

Figure A7.9 ^{13}C NMR (75 MHz, $CDCl_3$) of compound **334**.

APPENDIX 8

Notebook Cross-Reference

The following notebook cross-reference has been included to facilitate access to the original spectroscopic data obtained for the compounds presented in this thesis. For each compound, both hardcopy and electronic characterization folders have been created that contain copies of the original ^{1}H NMR, ^{13}C NMR, and IR spectra. All notebooks and spectral data are stored in the Stoltz archives.

Table A8.1 Compounds Appearing in Chapter 3: Scope and Applications of the Oxidative Kinetic Resolution of Secondary Alcohols.

Compound	^{1}H NMR	^{13}C NMR	IR
(–)-**74**	JTB-IX-071b1H	JTB-IX-071b13C	JTB-IX-071b
(–)-**76**	DCE-XVI-041c1H	DCE-XVI-041c13C	DCE-XVI-041b
(–)-**96**	DCE-VI-171b	DCE-VI-065g	DCE-VI-065a
(*S*)-**102**	DCE-V-221c	DCE-V-221e	DCE-V-221a
(+)-**111**	DCE-I-199e	DCE-I-199f	DCE-I-199
(+)-**112**	DCE-V-047b	DCE-V-047c	DCE-V-047a
(+)-**113**	DCE-V-127g	DCE-V-041c	DCE-V-041a
202	DCE-XVI-239d1H	DCE-XVI-239d13C	DCE-XVI-239a
203	DCE-V-125e	DCE-IV-253e	DCE-IV-253b
(+)-**114**	DCE-V-051b	DCE-V-051d	DCE-V-051a
205	DCE-IV-269g	DCE-IV-269h	DCE-IV-269a
(+)-**115**	DCE-V-067c	DCE-V-067d	DCE-V-067a
207	DCE-V-129a	DCE-V-077c	DCE-V-077a
(+)-**116**	DCE-V-081a	DCE-V-081d	DCE-V-081a
209	DCE-V-093a	DCE-V-093d	DCE-V-093a
(+)-**117**	DCE-V-095a	DCE-V-095b	DCE-V-095a
212	DCE-V-053d	DCE-V-053e	DCE-V-053a
(+)-**118**	DCE-VI-097b	DCE-V-059c	DCE-V-059a
(–)-**120**	DCE-XIII-083a	DCE-III-077c	DCE-III-077a
216	DCE-VI-277a	DCE-VI-277c	DCE-VI-277b
(–)-**122**	DCE-VI-277b	DCE-III-113c	DCE-III-113a
217	DCE-VI-293a	DCE-VI-293c	DCE-VI-293b
(–)-**123**	DCE-VI-293b	DCE-III-175b	DCE-III-175a
221	DCE-XV-237c	DCE-VIII-125d	DCE-VIII-125a
(–)-**124**	DCE-VIII-137f	DCE-VIII-137g	DCE-VIII-137a
152	ZN-V-135-1	ZN-V-135-1C	ZN-V-135-1
153	ZN-IV-127	ZN-IV-127c	ZN-IV-127

Compound	^{1}H NMR	^{13}C NMR	IR
154	ZN-IV-129	ZN-IV-129c	ZN-IV-129
155	ZN-IV-141	ZN-IV-141c	ZN-IV-141
156	ZN-IV-137	ZN-IV-137c	ZN-IV-137
157	ZN-IV-227	ZN-IV-139c	ZNIV139
158	ZN-IV-135	ZN-IV-135c	ZN-IV-135
159	DCE-XIII-101a	ZN-II-241-1C	ZN-II-269-1
160	ZN-IV-131	ZN-IV-131C	ZN-IV-131
161	ZN-V-175	ZN-V-175C	ZN-V-175
162	ZN-IV-191	ZN-IV-191C	ZNIV191
163	ZN-IV-193	ZN-IV-193c	ZNIV193
164	ZN-IV-203	ZN-IV-203C	ZNIV203
165	ZN-IV-199	ZN-IV-199C	ZNIV199
166	ZN-IV-201	ZN-IV-201C	ZNIV201
167	ZN-IV-197	ZN-IV-197C	ZNIV197
168	ZN-V-169	ZN-III-177.0603	ZN-V-169
169	ZN-IV-195	ZN-IV-195C	ZNIV195
170	DCE-XIII-135b	DCE-XIII-153b	DCE-XIII-139a

Table A8.2 Compounds Appearing in Chapter 4: Catalyst Development in the Oxidative Kinetic Resolution.

Compound	^{1}H NMR	^{13}C NMR	IR
243	RMT-XIV-301b	RMT-XIV-301b	RMT-XIV-301a
269	DCE-IX-235c	DCE-IX-235d	DCE-IX-235b
270	DCE-IX-237c	DCE-IX-237c	DCE-IX-237d
274	DCE-XIV-235c	DCE-XIV-235c	DCE-XIV-235a
267	DCE-XIII-253g	DCE-XIII-253g	DCE-XIII-253a
268	DCE-XIII-303d	DCE-XIII-303d	DCE-XIII-303a

Table A8.3 Compounds Appearing in Chapter 5: A Convergent Total Synthesis of (+)-Amurensinine and Formal Synthesis of (–)-Amurensinine via Oxidative Kinetic Resolution.

Compound	^{1}H NMR	^{13}C NMR	IR
301	UKTXIX-213	UKTXIX-213	UKTXIX-213
296	UKTXIX-219	UKTXIX-219	UKTXIX-189
303	UKTXXI-37	UKTXXI-37	UKTXXI-37
304	UKTXXI-213	UKTXXI-213	UKTXXI-213
(+)-**308**	UKTXXI-227	UKTXXI-227	UKTXXI-227
(–)-**309**	UKTXXI-87	UKTXXI-87	UKTXXI-87
(+)-**293**	UKTXXI-185	UKTXXI-185	UKTXXI-185
(+)-**282**	DCE-XI-125c	DCE-XI-125d	UKTXXI-149
(±)-**314**	DCE-XVII-279c	DCE-XVII-279d	DCE-XVII-279a
(+)-**321**	DCE-X-223e	DCE-X-223f	DCE-XI-093a
(–)-**315**	DCE-X-181d	DCE-X-281f	DCE-X-281b
(–)-**316**	DCE-X-301s	DCE-X-301r	DCE-X-301a
(–)-**317**	DCE-XI-261b	DCE-XI-261c	DCE-XI-261a
(–)-**318**	DCE-XII-107d	DCEXI-293c	DCE-XI-245b
(+)-**319**	DCE-XII-027b	DCE-XII-027c	DCE-XII-027b
(–)-**320**	DCE-XII-049f	DCE-XII-049g	DCE-XII-049a

Table A8.4 Compounds Appearing in Appendix 6: The Development of a Scaleable Acyl-Alkylation of Arynes and Application to the Construction of 1,3-Dihydroxynaphthalenes.

Compound	^{1}H NMR	^{13}C NMR	IR
327	DCE-XII-299e	UKTXIX-51	UKTXIX-51
330	DCE-XII-299k	DCE-XII-299k	DCE-XII-299c
334	DCE-XVI-267h	DCE-XVI-267h	DCE-XVI-267a

COMPREHENSIVE BIBLIOGRAPHY

Aït-Mohand, S.; Hénin, F.; Muzart, J. *Tetrahedron Lett.* **1995**, *36*, 2473-2476.

Ali, I. S.; Sudalai, A. *Tetrahedron Lett.* **2002**, *43*, 5435-5436.

Ansell, M. F.; Ducker, J. W. *J. Chem. Soc.* **1959**, 329-331.

Arends, I. W. C. E.; ten Brink, G.-J.; Sheldon, R. A. *J. Mol. Catal. A: Chem.* **2006**, *251*, 246-254.

Arita, S.; Koike, T.; Kayaki, Y.; Ikariya, T. *Angew. Chem., Int. Ed.* **2008**, *47*, 2447-2449.

Asymmetric Oxidation Reactions; Katsuki, T., Ed.; Practical Approach in Chemistry Series; Oxford Press: New York, 2001.

Bagdanoff, J. T. Development of the Enantioselective Oxidation of Secondary Alcohols and Natural Products Total Synthesis. Ph.D. Dissertation, California Institute of Technology, Pasadena, CA, 2005.

Bagdanoff, J. T.; Ferreira, E. M.; Stoltz, B. M. *Org. Lett.* **2003**, *5*, 835-837.

Bagdanoff, J. T.; Stoltz, B. M. *Angew. Chem., Int. Ed.* **2004**, *43*, 353-357.

Baker, L.; Minehan, T. *J. Org. Chem.* **2004**, *69*, 3957-3960.

Barluenga, J.; Bernad, P. L., Jr.; Concellón, J. M.; Piñera-Nicolás, A.; García-Granda, S. *J. Org. Chem.* **1997**, *62*, 6870-6875.

Begley, M. J.; Ladlow, M.; Pattenden, G. *J. Chem. Soc., Perkin Trans. 1* **1988**, 1095-1106.

Bellemin-Laponnaz, S.; Tweddell, J.; Ruble, J. C.; Breitling, F. M.; Fu, G. C. *Chem. Commun.* **2000**, 1009-1010.

Bhupathy, M.; McNamara, J. M.; Sidler, D. R.; Volante, R. P.; Bergan, J. J. (Merck & Co., Inc.). World Patent 95/18107, 1995.

Bhupathy, M.; McNamara, J. M.; Sidler, D. R.; Volante, R. P.; Bergan, J. J. (Merck & Co., Inc.). U. S. Patent 5,614,632, 1997.

Billimoria, J. D. *J. Chem. Soc.* **1955**, 1126-1129.

Birch, A. J.; Slobbe, J. *Aust. J. Chem.* **1977**, *30*, 1045-1049.

Blackburn, T. F.; Schwartz, J. *J. Chem. Soc., Chem. Commun.* **1977**, 157-158.

Boller, T. M.; Murphy, J. M.; Hapke, M.; Ishiyama, T.; Miyaura, N.; Hartwig, J. F. *J. Am. Chem. Soc.* **2005**, *127*, 14263-14278.

Bolm, C.; Hildebrand, J. P.; Muñiz, K. Recent Advances in Asymmetric Dihydroxylation and Aminohydroxylation. In *Catalytic Asymmetric Synthesis,* 2nd ed.; Ojima, I., Ed.; Wiley & Sons: New York, 2000; Chapter 6E, pp 399-428.

Breslow, R.; Kivelevich, D. *J. Org. Chem.* **1961**, *26*, 679-681.

Bunnelle, W. H.; Isbell, T. A. *J. Org. Chem.* **1992**, *57*, 729-740.

Capozzi, G.; Roelens, S.; Talami, S. *J. Org. Chem.* **1993**, *58*, 7932-7936.

Carlier, P. R.; Mungall, W. S.; Schröder, G.; Sharpless, K. B. *J. Am. Chem. Soc*. **1988**, *110*, 2978-2979.

Carrillo, L.; Badía, D.; Domínguez, E.; Vicario, J. L.; Tellitu, I. *J. Org. Chem*. **1997**, *62*, 6716-6721.

Caspi, D. D.; Ebner, D. C.; Bagdanoff, J. T.; Stoltz, B. M. *Adv. Synth. Catal*. **2004**, *346*, 185-189.

Chandrasekhar, S.; Kulkarni, G. *Tetrahedron: Asymmetry* **2002**, *13*, 615-619.

Charette, A. B.; Lacasse, M.-C. *Org. Lett*. **2002**, *4*, 3351-3353.

Charette, A. B.; Lebel, H. *J. Org. Chem*. **1995**, *60*, 2966-2967.

Charette, A. B.; Lebel, H.; Gagnon, A. *Tetrahedron* **1999**, *55*, 8845-8856.

Charette, A. B.; Molinaro, C.; Brochu, C. *J. Am. Chem. Soc*. **2001**, *123*, 12160-12167.

Chen, C.-T.; Bettigeri, S.; Weng, S.-S.; Pawar, V. D.; Lin, Y.-H.; Liu, C.-Y.; Lee, W.-Z. *J. Org. Chem*. **2007**, *72*, 8175-8185.

Chen, T.; Jiang, J.-J.; Xu, Q.; Shi, M. *Org. Lett*. **2007**, *9*, 865-868.

Childers, W. E., Jr.; Abou-Gharbia, M. A. U.S. Patent 4,940,789, 1990; *Chem. Abstr*. **1990**, *113*, 191190w.

Chisholm, M. H.; Drake, S. R.; Naiini, A. A.; Streib, W. E. *Polyhedron* **1991**, *10*, 337-345.

Comprehensive Biological Catalysis; Sinnott, M., Ed.; Academic Press: San Diego, CA, 1998; Vol. 1-3.

Comprehensive Organic Synthesis; Trost, B. M. Fleming, I., Eds.; Pergamon: Oxford, U.K., 1991.

Correa, J.; Mainero, R. M. *J. Org. Chem.* **1969**, *34*, 2192-2195.

CRC Handbook of Chemistry and Physics, 76th ed.; Lide, D. R., Frederikse, H. P. R., Eds.; New York, 1995; Section 8, p 43.

CRC Handbook of Chemistry and Physics, 76th ed.; Lide, D. R., Frederikse, H. P. R., Eds.; New York, 1995; Section 6, pp 159-192.

Crow, W. D. *Aust. J. Chem.* **1959**, *12*, 474-482.

Cruces, J.; Estevez, J. C.; Castedo, L.; Estevez, R. J. *Tetrahedron Lett.* **2001**, *42*, 4825-4828.

Dang, H.-S.; Davies, A. G.; Davison, I. G. E.; Schiesser, C. H. *J. Org. Chem.* **1990**, *55*, 1432-1438.

de Graauw, C. F.; Peters, J. A.; van Bekkum, H.; Huskens, J. *Synthesis* **1994**, 1007-1017.

Dearden, M. J.; Firkin, C. R.; Hermet, J.-P. R.; O'Brien, P. *J. Am. Chem. Soc.* **2002**, *124*, 11870-11871.

Dearden, M. J.; McGrath, M. J.; O'Brien, P. *J. Org. Chem.* **2004**, *69*, 5789-5792.

DePuy, C. H.; Breitbeil, F. W.; DeBruin, K. R. *J. Am. Chem. Soc.* **1966**, *88*, 3347-3354.

Desai, R. C.; Cicala, P.; Meurer, L. C.; Finke, P. E. *Tetrahedron Lett.* **2002**, *43*, 4569-4570.

Dess, D. B.; Martin, J. C. *J. Org. Chem.* **1983**, *48*, 4155-4156.

Dixon, A. J.; McGrath, M. J.; O'Brien, P. *Org. Synth.* **2006**, *83*, 141-154.

Dounay, A. B.; Overman, L. E. *Chem. Rev.* **2003**, *103*, 2945-2963.

Dragoli, D. R.; Burdett, M. T.; Ellman, J. A. *J. Am. Chem. Soc.* **2001**, *123*, 10127-10128.

Drew, D.; Doyle, J. R. *Inorg. Synth.* **1972**, Vol. XIII, 53-55.

Ebner, D. C.; Novák, Z.; Stoltz, B. M. *Synlett* **2006**, 3533-3539.

Ebner, D. C.; Trend, R. M.; Genet, C.; McGrath, M. J.; O'Brien, P.; Stoltz, B. M. *Angew. Chem., Int. Ed.* **2008**, *47*, 6367-6370.

Felpin, F. X. *J. Org. Chem.* **2005**, *70*, 8575-8578.

Ferreira, E. M.; Stoltz, B. M. *J. Am. Chem. Soc.* **2001**, *123*, 7725-7726.

Ferreira, E. M.; Stoltz, B. M. *J. Am. Chem. Soc.* **2003**, *125*, 9578-9579.

Ferreira, E. M.; Zhang, H.; Stoltz, B. M. *Tetrahedron* **2008**, *64*, 5987-6001.

Fischer, F.; Pfleiderer, G. *Z. Anorg. Allg. Chem.* **1922**, *124*, 61-69.

Fogliato, G.; Fronza, G.; Fuganti, C.; Lanati, S.; Rallo, R.; Rigoni, R.; Servi, S. *Tetrahedron* **1995**, *51*, 10231-10240.

Fürstner, A.; Seidel, G. *Org. Lett.* **2002**, *4*, 541-543.

Garg, N. K.; Caspi, D. D.; Stoltz, B. M. *J. Am. Chem. Soc.* **2004**, *126*, 9552-9553.

Garg, N. K.; Caspi, D. D.; Stoltz, B. M. *J. Am. Chem. Soc.* **2005**, *127*, 5970-5978.

Garg, N. K.; Caspi, D. D.; Stoltz, B. M. *Synlett* **2006**, 3081-3087.

Garg, N. K.; Sarpong, R.; Stoltz, B. M. *J. Am. Chem. Soc.* **2002**, *124*, 13179-13184.

Genet, C.; McGrath, M. J.; O'Brien, P. *Org. Biomol. Chem.* **2006**, *4*, 1376-1382.

Gómez-Bengoa, E.; Noheda, P.; Echavarren, A. M. *Tetrahedron Lett.* **1994**, *35*, 7097-7098.

Gottlieb, L.; Meyers, A. I. *J. Org. Chem.* **1990**, *55*, 5659-5662.

Gözler, B. Pavine and Isopavine Alkaloids. In *The Alkaloids*; Brossi, A., Ed.; Academic Press: New York, 1987; Vol. 31, pp 343-356.

Gözler, B.; Lantz, M. S.; Shamma, M. *J. Nat. Prod.* **1983**, *46*, 293-309.

Graening, T.; Schmalz, H.-G. *Angew. Chem., Int. Ed.* **2003**, *42*, 2580-2584.

Graetz, B.; Rychnovsky, S.; Leu, W.-H.; Farmer, P.; Lin, R. *Tetrahedron: Asymmetry* **2005**, *16*, 3584-3598.

Grant, T. N.; West, F. G. *J. Am. Chem. Soc.* **2006**, *128*, 9348-9349.

Grau-Martinez, A.; Curran, D. P. *Tetrahedron* **1997**, *53*, 5679-5698.

Green, R. D. *Hydrogen Bonding by C–H Groups*; John Wiley & Sons: New York, 1974.

Gross, Z.; Ini, S. *Org. Lett.* **1999**, *1*, 2077-2080.

Halford, J. O.; Raiford, R. W., Jr.; Weissmann, B. *J. Org. Chem.* **1961**, *26*, 1898-1901.

Hallman, K.; Moberg, C. *Adv. Synth. Catal.* **2001**, *343*, 260-263.

Hamada, T.; Irie, R.; Mihara, J.; Hamachi, K.; Katsuki, T. *Tetrahedron* **1998**, *54*, 10017-10028.

Hamashima, Y.; Sodeoka, M. *Synlett* **2006**, 1467-1478.

Hanessian, S.; Mauduit, M. *Angew. Chem., Int. Ed.* **2001**, *40*, 3810-3813.

Hanessian, S.; Talbot, C.; Saravanan, P. *Synthesis* **2006**, 723-734.

Hansson, S.; Heumann, A.; Rein, T.; Åkermark, B. *J. Org. Chem.* **1990**, *55*, 975-984.

Harada, T.; Kagamihara, Y.; Tanaka, S.; Sakamoto, K.; Oku, A. *J. Org. Chem.* **1992**, *57*, 1637-1639.

Hashiguchi, S.; Fujii, A.; Haack, K.-J.; Matsumura, K.; Ikariya, T.; Noyori, R. *Angew. Chem., Int. Ed. Engl.* **1997**, *36*, 288-289.

Hayashi, T. *J. Organomet. Chem.* **1999**, *576*, 195-202.

Helmchen, G. *J. Organomet. Chem.* **1999**, *576*, 203-214.

Hewett, C. L. *J. Chem. Soc.* **1936**, 50-52.

Heyari, A.; Mehrdad, M.; Maleki, A.; Ahmadi, N. *Synthesis* **2004**, 1563-1565.

Hii, K. K. *Pure Appl. Chem.* **2006**, *78*, 341-349.

Himeshima, Y.; Sonoda, T.; Kobayashi, H. *Chem. Lett.* **1983**, 1211-1214.

Huang, X.; Xue, J. *J. Org. Chem.* **2007**, *72*, 3965-3968.

Hudlicky, M. *Oxidations in Organic Chemistry*; ACS Monograph Series; American Chemical Society: Washington, DC, 1990.

Ikemoto, N.; Schreiber, S. L. *J. Am. Chem. Soc.* **1990**, *112*, 9657-9659.

Ireland, R. E.; Mueller, R. H.; Willard, A. K. *J. Am. Chem. Soc.* **1976**, *98*, 2868-2877.

Ishii, Y.; Suzuki, K.; Ikariya, T.; Saburi, M.; Yoshikawa, S. *J. Org. Chem.* **1986**, *51*, 2822-2824.

Ito, S.; Kasai, M.; Ziffer, H.; Silverton, J. V. *Can. J. Chem.* **1987**, *65*, 574-582.

Iwasawa, T.; Tokunaga, M.; Obora, Y.; Tsuji, Y. *J. Am. Chem. Soc.* **2004**, *126*, 6554-6555.

Jacobsen, E. N. Aziridination. In *Comprehensive Asymmetric Catalysis*; Jacobsen, E. N., Pfaltz, A., Yamamoto, H., Eds.; Springer-Verlag: Berlin, 1999; Vol. 2, Chapter 17, pp 607-618.

Jacobsen, E. N.; Wu, M. H. Epoxidation of Alkenes Other than Allylic Alcohols. In *Comprehensive Asymmetric Catalysis*; Jacobsen, E. N., Pfaltz, A., Yamamoto, H., Eds.; Springer-Verlag: Berlin, 1999; Vol. 2, Chapter 18.2, pp 649-677.

Jarvo, E. R.; Copeland, G. T.; Papaioannou, N.; Bonitatebus, P. J., Jr.; Miller, S. J. *J. Am. Chem. Soc.* **1999**, *121*, 11638-11643.

Jensen, D. R.; Pugsley, J. S.; Sigman, M. S. *J. Am. Chem. Soc.* **2001**, *123*, 7475-7476.

Jensen, D. R.; Schultz, M. J.; Mueller, J. A.; Sigman, M. S. *Angew. Chem., Int. Ed.* **2003**, *42*, 3810-3813.

Jensen, D. R.; Sigman, M. S. *Org. Lett.* **2003**, *5*, 63-65.

Johansson, M. J.; Schwartz, L.; Amedjkouh, M.; Kann, N. *Tetrahedron: Asymmetry* **2004**, *15*, 3531-3538.

Johnson, R. A.; Sharpless, K. B. Catalytic Asymmetric Dihydroxylation–Discovery and Development. In *Catalytic Asymmetric Synthesis,* 2nd ed.; Ojima, I., Ed.; Wiley & Sons: New York, 2000; Chapter 6D, pp 357-398.

Johnson, R. A.; Sharpless, K. B. Catalytic Asymmetric Epoxidation of Allylic Alcohols. In *Catalytic Asymmetric Synthesis,* 2nd ed.; Ojima, I., Ed.; Wiley & Sons: New York, 2000; Chapter 6A, pp 231-280.

Johnson, W. S.; Werthemann, L.; Bartlett, W. R.; Brocksom, T. J.; Li, T.-t.; Faulkner, D. J.; Petersen, M. R. *J. Am. Chem. Soc.* **1970**, *92*, 741-743.

Kagan, H. B.; Fiaud, J. C. In *Topics in Stereochemistry*; Eliel, E. L., Ed.; Wiley & Sons: New York, 1988; Vol. 18, pp 249-330.

Kantam, M. L.; Ramani, T.; Chakrapani, L.; Choudary, B. M. *J. Mol. Catal. A: Chem.* **2007**, *274*, 11-15.

Kashiwagi, Y.; Kurashima, F.; Kikuchi, C.; Anzai, J.-i.; Osa, T.; Bobbitt, J. M. *Tetrahedron Lett.* **1999**, *40*, 6469-6472.

Kashiwagi, Y.; Yanagisawa, Y.; Kurashima, F.; Anzai, J.-i.; Osa, T.; Bobbitt, J. M. *Chem. Commun.* **1996**, 2745-2746.

Katsuki, T. Asymmetric Epoxidation of Unfunctionalized Olefins and Related Reactions. In *Catalytic Asymmetric Synthesis,* 2nd ed.; Ojima, I., Ed.; Wiley & Sons: New York, 2000; Chapter 6B, pp 287-326.

Katsuki, T. Epoxidation of Allylic Alcohols. In *Comprehensive Asymmetric Catalysis*; Jacobsen, E. N., Pfaltz, A., Yamamoto, H., Eds.; Springer-Verlag: Berlin, 1999; Vol. 2, Chapter 18.1, pp 621-648.

Kawabata, T.; Nagato, M.; Takasu, K.; Fuji, K. *J. Am. Chem. Soc.* **1997**, *119*, 3169-3170.

Kawabata, T.; Yamamoto, K.; Momose, Y.; Yoshida, H.; Nagaoka, Y.; Fuji, K. *Chem. Commun.* **2001**, 2700-2701.

Keith, J. M.; Goddard, W. A., III.; Oxgaard, J. *J. Am. Chem. Soc.* **2007**, *129*, 10361-10369.

Keith, J. M.; Larrow, J. F.; Jacobsen, E. N. *Adv. Synth. Catal.* **2001**, *343*, 5-26.

Keith, J. M.; Nielsen, R. J.; Oxgaard, J.; Goddard, W. A., III. *J. Am. Chem. Soc.* **2005**, *127*, 13172-13179.

King, A. O.; Corley, E. G.; Anderson, R. K.; Larsen, R. D.; Verhoeven, T. R.; Reider, P. J.; Xiang, Y. B.; Belley, M.; Leblanc, Y.; Labelle, M.; Prasit, P.; Zamboni, R. J. *J. Org. Chem.* **1993**, *58*, 3731-3735.

Kitamura, M.; Kasahara, I.; Manabe, K.; Noyori, R.; Takaya, H. *J. Org. Chem.* **1988**, *53*, 708-710.

Koenig, T. M.; Mitchell, D. *Tetrahedron Lett.* **1994**, *35*, 1339-1342.

Konnick, M. M.; Guzei, I. A.; Stahl, S. S. *J. Am. Chem. Soc.* **2004**, *126*, 10212-10213.

Kraus, G. A.; Frazier, K. *J. Org. Chem.* **1980**, *45*, 2579-2581.

Krishnan, S.; Ramtohul, Y. K.; Bagdanoff, J. T.; Ebner, D. C.; Tambar, U. K.; Stoltz, B. M. *J. Am. Chem. Soc.* in press.

Kuethe, J. T.; Wong, A.; Wu, J.; Davies, I. W.; Dormer, P. G.; Welch, C. J.; Hillier, M. C.; Hughes, D. L.; Reider, P. J. *J. Org. Chem.* **2002**, *67*, 5993-6000.

Kumar, A.; Ner, D. H.; Dike, S. *Ind. J. Chem. B* **1992**, *31*, 803-809.

Kumar, A.; Ner, D. H.; Dike, S. Y. *Tetrahedron Lett.* **1991**, *32*, 1901-1904.

Kureshy, R. I.; Ahmad, I.; Pathak, K.; Khan, N.-u. H.; Abdi, S. H. R.; Prathap, J. K.; Jasra, R. V. *Chirality* **2007**, *19*, 352-357.

Kuroboshi, M.; Yoshihisa, H.; Cortona, M. N.; Kawakami, Y.; Gao, Z.; Tanaka, H. *Tetrahedron Lett.* **2000**, *41*, 8131-8135.

Landis, C. R.; Morales, C. M.; Stahl, S. S. *J. Am. Chem. Soc.* **2004**, *126*, 16302-16303.

Larock, R. C. *Comprehensive Organic Transformations*; Wiley & Sons: New York, 1999; pp 1234-1248.

Larsen, R. D.; Corley, E. G.; King, A. O.; Carroll, J. D.; Davis, P.; Verhoeven, T. R.; Reider, P. J.; Labelle, M; Gauthier, J. Y.; Xiang, Y. B.; Zamboni, R. J. *J. Org. Chem.* **1996**, *61*, 3398-3405.

Lesma, G.; Pilati, T.; Sacchetti, A.; Silvani, A. *Tetrahedron: Asymmetry* **2008**, *19*, 1363-1366.

Li, Y.-Y.; Zhang, X.-Q.; Dong, Z.-R.; Shen, W.-Y.; Chen, G.; Gao, J.-X. *Org. Lett.* **2006**, *8*, 5565-5567.

Li, Z.; Tang, Z. H.; Hu, X. X.; Xia, C. G. *Chem.–Eur. J.* **2005**, *11*, 1210-1216.

Little, R. D.; Brown, L. M.; Masjedizadeh, M. R. *J. Am. Chem. Soc.* **1992**, *114*, 3071-3075.

Liu, H.; Liu, Y.; Zhu, C.; Liu, M.; Wang, C.; Chen, C.; Xi, F. *Synth. Met.* **1997**, *131*, 135-139.

Liu, Q.; Ferreira, E. M.; Stoltz, B. M. *J. Org. Chem.* **2007**, *72*, 7352-7358.

Lloyd, W. G. *J. Org. Chem.* **1967**, *32*, 2816-2819.

Luche, J. L.; Gemal, A. L. *J. Chem. Soc., Chem. Commun.* **1978**, 601-602.

Luzzio, F. A. *Org. React.* **1998**, *53*, 1-221.

Mandal, S. K.; Jensen, D. R.; Pugsley, J. S.; Sigman, M. S. *J. Org. Chem.* **2003**, *68*, 4600-4603.

Mandal, S. K.; Sigman, M. S. *J. Org. Chem.* **2003**, *68*, 7535-7537.

Markó, I. E.; Svendsen, J. S. Dihydroxylation of Carbon-Carbon Double Bonds. In *Comprehensive Asymmetric Catalysis*; Jacobsen, E. N., Pfaltz, A., Yamamoto, H., Eds.; Springer-Verlag: Berlin, 1999; Vol. 2, Chapter 20, pp 713-787.

Marrero, J.; Rodríguez, A. D.; Baran, P.; Raptis, R. G.; Sánchez, J. A.; Ortega-Barria, E.; Capson, T. L. *Org. Lett.* **2004**, *6*, 1661-1664.

Martin, V. S.; Woodard, S. S.; Katsuki, T.; Yamada, Y.; Ikeda, M.; Sharpless, K. B. *J. Am. Chem. Soc.* **1981**, *103*, 6237-6240.

Masutani, K.; Uchida, T.; Irie, R.; Katsuki, T. *Tetrahedron Lett.* **2000**, *41*, 5119-5123.

Maturová, M.; Pavlásková, D.; Santavy, F. *Planta Medica* **1966**, *14*, 22-41.

Meyers, C.; Maes, B. U. W.; Loones, K. T. J.; Bal, G.; Lemiere, G. L. F.; Dommisse, R. A. *J. Org. Chem.* **2004**, *69*, 6010-6017.

Miller, S. J.; Copeland, G. T.; Papaioannou, N.; Horstmann, T. E.; Ruel, E. M. *J. Am. Chem. Soc.* **1998**, *120*, 1629-1630.

Mitchell, D.; Koenig, T. M. *Synth. Commun.* **1995**, *25*, 1231-1238.

Mohr, J. T.; Ebner, D. C.; Stoltz, B. M. *Org. Biomol. Chem.* **2007**, *5*, 3571-3576.

Mueller, J. A.; Cowell, A.; Chandler, B. D.; Sigman, M. S. *J. Am. Chem. Soc.* **2005**, *127*, 14817-14824.

Mueller, J. A.; Goller, C. P.; Sigman, M. S. *J. Am. Chem. Soc.* **2004**, *126*, 9724-9734.

Mueller, J. A.; Jensen, D. R.; Sigman, M. S. *J. Am. Chem. Soc.* **2002**, *124*, 8202-8203.

Mueller, J. A.; Sigman, M. S. *J. Am. Chem. Soc.* **2003**, *125*, 7005-7013.

Murata, M.; Oyama, T.; Watanabe, S.; Masuda, Y. *J. Org. Chem.* **2000**, *65*, 164-168.

Murphy, J. A.; Scott, K. A.; Sinclair, R. S.; Martin, C. G.; Kennedy, A. R.; Lewis, N. *J. Chem. Soc., Perkin Trans. 1* **2000**, 2395-2408.

Muzart, J. *Tetrahedron* **2003**, *59*, 5789-5816.

Nakamura, Y.; Egami, H.; Matsumoto, K.; Uchida, T.; Katsuki, T. *Tetrahedron* **2007**, *63*, 6383-6387.

Negishi, E.-i.; Tan, Z.; Liou, S.-Y.; Liao, B. *Tetrahedron* **2000**, *56*, 10197-10207.

Nielsen, R. J.; Goddard, W. A., III. *J. Am. Chem. Soc.* **2006**, *128*, 9651-9660.

Nielsen, R. J.; Keith, J. M.; Stoltz, B. M.; Goddard, W. A., III. *J. Am. Chem. Soc.* **2004**, *126*, 7967-7974.

Nishibayashi, Y.; Takei, I.; Uemura, S.; Hidai, M. *Organometallics* **1999**, *18*, 2291-2293.

Nishibayashi, Y.; Yamauchi, A.; Onodera, G.; Uemura, S. *J. Org. Chem.* **2003**, *68*, 5875-5880.

Nishimura, T.; Maeda, Y.; Kakiuchi, N.; Uemura, S. *J. Chem. Soc., Perkin Trans. 1* **2000**, 4301-4305.

Nishimura, T.; Onoue, T.; Ohe, K.; Uemura, S. *J. Org. Chem.* **1999**, *64*, 6750-6755.

Nishimura, T.; Onoue, T.; Ohe, K.; Uemura, S. *Tetrahedron Lett.* **1998**, *39*, 6011-6014.

Nishimura, T.; Uemura, S. *Synlett* **2004**, 201-216.

O'Brien, P. *Chem. Commun.* **2008**, 655-667.

Ohkubo, K.; Hirata, K.; Yoshinaga, K.; Okada, M. *Chem. Lett.* **1976**, 183-184.

Onomura, O.; Arimoto, H.; Matsumura, Y.; Demizu, Y. *Tetrahedron Lett.* **2007**, *48*, 8668-8672.

Paavola, S.; Zetterberg, K.; Privalov, T.; Csöregh, I.; Moberg, C. *Adv. Synth. Catal.* **2004**, *346*, 237-244.

Padwa, A.; Blacklock, T. J.; Getman, D.; Hatanaka, N.; Loza, R. *J. Org. Chem.* **1978**, *43*, 1481-1492.

Pathak, K.; Ahmad, I.; Abdi, S. H. R.; Kureshy, R. I.; Khan, N.-u. H.; Jasra, R. V. *J. Mol. Catal. A: Chem.* **2007**, *274*, 120-126.

Pattenden, G.; Whybrow, D. *J. Chem. Soc., Perkin Trans. 1* **1981**, 3147-3149.

Pawar, V. D.; Bettigeri, S.; Weng, S.-S.; Kao, J.-Q.; Chen, C.-T. *J. Am. Chem. Soc.* **2006**, *128*, 6308-6309.

Pellissier, H.; Santelli, M. *Tetrahedron* **2003**, *59*, 701-730.

Peña, D.; Cobas, A.; Pérez, D.; Guitián, E. *Synthesis* **2002**, 1454-1458.

Peterson, K. P.; Larock, R. C. *J. Org. Chem.* **1998**, *63*, 3185-3189.

Popp, B. V.; Stahl, S. S. *J. Am. Chem. Soc.* **2007**, *129*, 4410-4422.

Poss, C. S.; Rychnovsky, S. D.; Schreiber, S. L. *J. Am. Chem. Soc.* **1993**, *115*, 3360-3361.

Poss, C. S.; Schreiber, S. L. *Acc. Chem. Res.* **1994**, *27*, 9-17.

Pour, M; Spulák, M; Balsánek, V.; Kunes, J.; Kubanová, P.; Buchta, V. *Bioorg. Med. Chem.* **2003**, *11*, 2843-2866.

Privalov, T.; Linde, C.; Zetterberg, K.; Moberg, C. *Organometallics* **2005**, *24*, 885-893.

Radosevich, A. T.; Chan, V. S.; Shih, H.-W.; Toste, F. D. *Angew. Chem., Int. Ed.* **2008**, *47*, 3755-3758.

Radosevich, A. T.; Musich, C.; Toste, F. D. *J. Am. Chem. Soc.* **2005**, *127*, 1090-1091.

RajanBabu, T. V. *Chem. Rev.* **2003**, *103*, 2845-2860.

Ruble, J. C.; Fu, G. C. *J. Org. Chem.* **1996**, *61*, 7230-7231.

Ruble, J. C.; Latham, H. A.; Fu, G. C. *J. Am. Chem. Soc.* **1997**, *119*, 1492-1493.

Ruble, J. C.; Tweddell, J.; Fu, G. C. *J. Org. Chem.* **1998**, *63*, 2794-2795.

Ruel, F. S.; Braun, M. P.; Johnson, W. S. *Organic Syntheses*; Wiley & Sons: New York, 2004; Collect. Vol. X, pp 467-471.

Rychnovsky, S. D.; McLernon, T. L.; Rajapakse, H. *J. Org. Chem.* **1996**, *61*, 1194-1195.

Sahoo, S.; Kumar, P.; Lefebvre, F.; Halligudi, S. B. *Tetrahedron Lett.* **2008**, *49*, 4865-4868.

Sano, T.; Imai, K.; Ohashi, K.; Oriyama, T. *Chem. Lett.* **1999**, 265-266.

Sayyed, I. A.; Kumar, N. S. C. R.; Sudalai, A. *Indian J. Chem., Sect. B* **2005**, *44B*, 1533-1535.

Schick, H.; Mahrwald, R. *Synthesis* **1990**, 592-595.

Schreiber, S. L.; Goulet, M. T.; Schulte, G. *J. Am. Chem. Soc.* **1987**, *109*, 4718-4720.

Schreiber, S. L.; Sammakia, T.; Uehling, D. E. *J. Org. Chem.* **1989**, *54*, 15-16.

Schultz, M. J.; Adler, R. S.; Zierkiewicz, W.; Privalov, T.; Sigman, M. S. *J. Am. Chem. Soc.* **2005**, *127*, 8499-8507.

Schultz, M. J.; Park, C. C.; Sigman, M. S. *Chem. Commun.* **2002**, 3034-3035.

Sekar, G.; Nishiyama, H. *J. Am. Chem. Soc.* **2001**, *123*, 3603-3604.

Sheldon, R. A.; Arends, I. W. C. E.; ten Brink, G.-J.; Dijksman, A. *Acc. Chem. Res.* **2002**, *35*, 774-781.

Shimizu, H.; Nakata, K.; Katsuki, T. *Chem. Lett.* **2002**, 1080-1081.

Shinohara, T.; Takeda, A.; Toda, J.; Sano, T. *Heterocycles* **1998**, *48*, 981-992.

Sigman, M. S.; Jensen, D. R. *Acc. Chem. Res.* **2006**, *39*, 221-229.

Sigman, M. S.; Schultz, M. J. *Org. Biomol. Chem.* **2004**, *2*, 2551-2554.

Smith, B. T.; Wendt, J. A.; Aubé, J. *Org. Lett.* **2002**, *4*, 2577-2579.

Sodeoka, M.; Hamashima, Y. *Bull. Chem. Soc. Jpn.* **2005**, *78*, 941-956.

Sodeoka, M.; Hamashima, Y. *Pure Appl. Chem.* **2006**, *78*, 477-494.

Sodeoka, M.; Shibasaki, M. *Pure Appl. Chem.* **1998**, *70*, 411-414.

Stahl, S. S. *Angew. Chem., Int. Ed.* **2004**, *43*, 3400-3420.

Stahl, S. S.; Thorman, J. L.; Nelson, R. C.; Kozee, M. A. *J. Am. Chem. Soc.* **2001**, *123*, 7188-7189.

Steinhoff, B. A.; Fix, S. R.; Stahl, S. S. *J. Am. Chem. Soc.* **2002**, *124*, 766-767.

Steinhoff, B. A.; Guzei, I. A.; Stahl, S. S. *J. Am. Chem. Soc.* **2004**, *126*, 11268-11278.

Steinhoff, B. A.; King, A. E.; Stahl, S. S. *J. Org. Chem.* **2006**, *71*, 1861-1868.

Steinhoff, B. A.; Stahl, S. S. *J. Am. Chem. Soc.* **2006**, *128*, 4348-4355.

Steinhoff, B. A.; Stahl, S. S. *Org. Lett.* **2002**, *4*, 4179-4181.

Steinke, N.; Frey, W.; Baro, A.; Laschat, S.; Drees, C.; Nimtz, M.; Hägele, C.; Giesselmann, F. *Chem.–Eur. J.* **2006**, *12*, 1026-1035.

Stoltz, B. M. *Chem. Lett.* **2004**, *33*, 362-367.

Stoltz, B. M.; Ebner, D. C. Kinetic Resolution by Enantioselective Aerobic Oxidation of Alcohols. In *Handbook of C–H Transformation*, Dyker, G., Ed.; Wiley-VCH: New York, 2005; Vol. 2, pp 393-401.

Sun, W.; Wang, H.; Xia, C.; Li, J.; Zhao, P. *Angew. Chem., Int. Ed.* **2003**, *42*, 1042-1044.

Sun, W.; Wu, X.; Xia, C. *Helv. Chim. Acta* **2007**, *90*, 623-626.

Taber, D. F.; Petty, E. H. *J. Org. Chem.* **1982**, *47*, 4808-4809.

Taber, D. F.; Ruckle, R. E., Jr. *J. Am. Chem. Soc.* **1986**, *108*, 7686-7693.

Tambar, U. K.; Ebner, D. C.; Stoltz, B. M. *J. Am. Chem. Soc.* **2006**, *128*, 11752-11753.

Tambar, U. K.; Stoltz, B. M. *J. Am. Chem. Soc.* **2005**, *127*, 5340-5341.

Tao, B.; Ruble, J. C.; Hoic, D. A.; Fu, G. C. *J. Am. Chem. Soc.* **1999**, *121*, 5091-5092.

Taylor, M. S.; Jacobsen, E. N. *Angew. Chem., Int. Ed.* **2006**, *45*, 1520-1543.

ten Brink, G.-J.; Arends, I. W. C. E.; Hoogenraad, M.; Verspui, G.; Sheldon, R. A. *Adv. Synth. Catal.* **2003**, *345*, 497-505.

ten Brink, G.-J.; Arends, I. W. C. E.; Hoogenraad, M.; Verspui, G.; Sheldon, R. A. *Adv. Synth. Catal.* **2003**, *345*, 1341-1352.

ten Brink, G.-J.; Arends, I. W. C. E.; Sheldon, R. A. *Adv. Synth. Catal.* **2002**, *344*, 355-369.

ten Brink, G.-J.; Arends, I. W. C. E.; Sheldon, R. A. *Science* **2000**, *287*, 1636-1639.

Thakur, V. V.; Sudalai, A. *Indian J. Chem., Sect. B* **2005**, *44B*, 557-562.

Thompson, A. S.; Humphrey, G. R.; DeMarco, A. M.; Mathre, D. J.; Grabowski, E. J. J. *J. Org. Chem.* **1993**, *58*, 5886-5888.

Tidwell, T. T. *Org. React.* **1990**, *39*, 297-572.

Tietze, L. F.; Ila, H.; Bell, H. P. *Chem. Rev.* **2004**, *104*, 3453-3516.

Trend, R. M.; Ramtohul, Y. K.; Ferreira, E. M.; Stoltz, B. M. *Angew. Chem., Int. Ed.* **2003**, *42*, 2892-2895.

Trend, R. M.; Ramtohul, Y. K.; Stoltz, B. M. *J. Am. Chem. Soc.* **2005**, *127*, 17778-17788.

Trend, R. M.; Stoltz, B. M. *J. Am. Chem. Soc.* **2004**, *126*, 4482-4483.

Trost, B. M. *Chem. Pharm. Bull.* **2002**, *50*, 1-14.

Trost, B. M. *J. Org. Chem.* **2004**, *69*, 5813-5837.

Trost, B. M.; Van Vranken, D. L. *Chem. Rev.* **1996**, *96*, 395-422.

Vedejs, E.; Daugulis, O. *J. Am. Chem. Soc.* **2003**, *125*, 4166-4173.

Vedejs, E.; Daugulis, O.; Diver, S. T. *J. Org. Chem.* **1996**, *61*, 430-431.

Vedejs, E.; Daugulis, O.; MacKay, J. A.; Rozners, E. *Synlett* **2001**, 1499-1505.

Vedejs, E.; Jure, M. *Angew. Chem., Int. Ed.* **2005**, *44*, 3974-4001.

Weber, E.; Keana, J.; Barmettler, P. PCT Int. Appl. WO 9012575, 1990; *Chem. Abstr.* **1991**, *115*, 106019w.

Wen, X.; Ojima, I. Chapter 6A Addendum–1999. In *Catalytic Asymmetric Synthesis,* 2nd ed.; Ojima, I., Ed.; Wiley & Sons: New York, 2000; Chapter 6A, pp 281-286.

Weng, S.-S.; Shen, M.-W.; Kao, J.-Q.; Munot, Y. S.; Chen, C.-T. *Proc. Natl. Acad. Sci. U.S.A.* **2006**, *103*, 3522-3527.

Wenkert, E.; Davis, L. L.; Mylari, B. L.; Solomon, M. F.; Da Silva, R. R.; Shulman, S.; Warnet, R. J.; Ceccherelli, P.; Curini, M.; Pellicciari, R. *J. Org. Chem.* **1982**, *47*, 3242-3247.

Witiak, D. T.; Kim, S. K.; Tehim, A. K.; Sternitzke, K. D.; McCreery, R. L.; Kim, S. U.; Feller, D. R.; Romstedt, K. J.; Kamanna, V. S.; Newman, H. A. I. *J. Med. Chem.* **1988**, *31*, 1437-1445.

Wong, C.-H.; Whitesides, G. M. *Enzymes in Synthetic Organic Chemistry*; Pergamon: Oxford, U.K., 1994.

Yoshida, H.; Watanabe, M.; Morishita, T.; Ohshita, J.; Kunai, A. *Chem. Commun.* **2007**, 1505-1507.

Yoshida, H.; Watanabe, M.; Ohshita, F.; Kunai, A. *Tetrahedron Lett.* **2005**, *46*, 6729-6731.

Yoshida, H.; Watanabe, M.; Ohshita, J.; Kunai, A. *Chem. Commun.* **2005**, 3292-3294.

Yun, J.; Buchwald, S. L. *J. Am. Chem. Soc.* **1999**, *121*, 5640-5644.

Zhang, H.; Ferreira, E. M.; Stoltz, B. M. *Angew. Chem., Int. Ed.* **2004**, *43*, 6144-6148.

Zhang, L.; Nadzan, A. M.; Heyman, R. A.; Love, D. L.; Mais, D. E.; Croston, G.; Lamph, W. W.; Boehm, M. F. *J. Med. Chem.* **1996**, *39*, 2659-2663.

Zierkiewicz, W.; Privalov, T. *Organometallics* **2005**, *24*, 6019-6028.

ABOUT THE AUTHOR

David C. Ebner was born on June 26, 1980 in Stillwater, Minnesota to Stephen and Coleen Ebner. He spent his childhood years with his younger sister, Stephanie, in Cottage Grove, Minnesota. In 1989, the family moved to West Lakeland Township. Dave attended Stillwater Area High School, where his interest in math and science developed. Mr. Symalla, his highly entertaining AP Physics teacher, made science exciting by encouraging independent work and a number of scientific construction projects. He managed to convince Dave that physics was the right field to pursue.

In 1998, he began undergraduate studies at the University of St. Thomas in St. Paul, Minnesota. After taking an outstanding general chemistry course taught by Professor Lynn Hartshorn, Dave developed a new passion and never took another physics course. (Sorry, Mr. Symalla!) After his freshman year, Dave started research in the labs of Professor J. Thomas Ippoliti in organic chemistry. With no previous organic coursework, the learning curve was steep, but Dave enjoyed it so much he continued on in Dr. Ippoliti's labs throughout his undergraduate studies. In 2002, Dave graduated with a B.S. in chemistry, along with a B.A. in mathematics (just for fun).

In 2002, Dave left the snowy winters and humid summers of Minnesota for sunny Pasadena, California. He joined the laboratories of Professor Brian M. Stoltz at the California Institute of Technology, completing his thesis on the palladium-catalyzed enantioselective oxidation of secondary alcohols in 2008. Dave will pursue postdoctoral studies with Professor Erik J. Sorensen at Princeton in October of 2008.